

haematologica

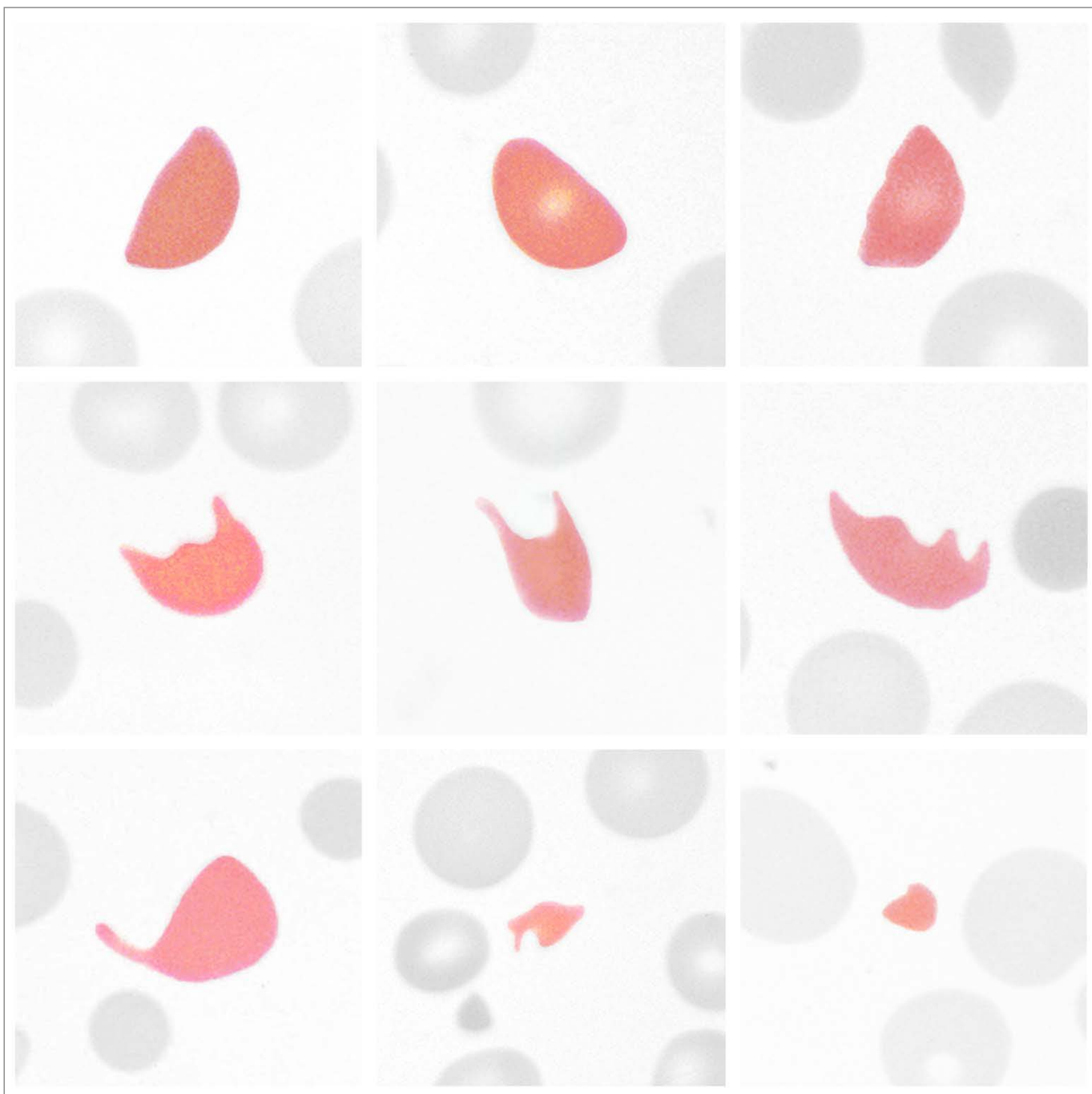
Journal of the Ferrata Storti Foundation



VOL.

107

SEPTEMBER 2022



Reasons for publishing in



Much cited Journal

 Impact Factor 2020: 9.94

 CiteScore 2021: 11.8

Fast review process

 Submission → 1st decision: 13 days

Fast publication

 Papers issued just after acceptance

Low publication cost

 The publisher is a Non-Profit Foundation that keeps the cost for authors as low as possible

baematologica

Journal of the Ferrata- Storti Foundation

Editor-in-Chief

Jacob M. Rowe (Jerusalem)

Deputy Editors

Carlo Balduini (Pavia), Jerry Radich (Seattle)

Associate Editors

Hélène Cavé (Paris), Monika Engelhardt (Freiburg), Steve Lane (Brisbane), Pier Mannuccio Mannucci (Milan), Pavan Reddy (Ann Arbor), David C. Rees (London), Francesco Rodeghiero (Vicenza), Gilles Salles (New York), Kerry Savage (Vancouver), Aaron Schimmer (Toronto), Richard F. Schlenk (Heidelberg), Sonali Smith (Chicago)

Statistical Consultant

Catherine Klersy (Pavia)

Editorial Board

Walter Ageno (Varese), Sarit Assouline (Montreal), Andrea Bacigalupo (Roma), Taman Bakchoul (Tübingen), Pablo Bartolucci (Créteil), Katherine Borden (Montreal), Marco Cattaneo (Milan), Corey Cutler (Boston), Kate Cwynarski (London), Mary Eapen (Milwaukee), Francesca Gay (Torino), Ajay Gopal (Seattle), Alex Herrera (Duarte), Shai Izraeli (Ramat Gan), Martin Kaiser (London), Marina Konopleva (Houston), Johanna A. Kremer Hovinga (Bern), Nicolaus Kröger (Hamburg), Austin Kulasekararaj (London), Shaji Kumar (Rochester), Ann LaCasce (Boston), Anthony R. Mato (New York), Matthew J. Maurer (Rochester), Neha Mehta-Shah (St. Louis), Alison Moskowitz (New York), Yishai Ofran (Haifa), Farhad Ravandi (Houston), John W. Semple (Lund), Liran Shlush (Toronto), Sara Tasian (Philadelphia), Pieter van Vlieberghe (Ghent), Ofir Wolach (Haifa), Loic Ysebaert (Toulouse)

Managing Director

Antonio Majocchi (Pavia)

Editorial Office

Lorella Ripari (Office & Peer Review Manager), Simona Giri (Production & Marketing Manager), Paola Cariati (Graphic Designer), Giulia Carlini (Graphic Designer), Igor Poletti (Graphic Designer), Marta Fossati (Peer Review), Diana Serena Ravera (Peer Review), Laura Sterza (Account Administrator)

Assistant Editors

Britta Dost (English Editor), Rachel Stenner (English Editor), Bertie Vitry (English Editor), Massimo Senna (Information technology), Idoya Lahortiga (Graphic artist)

Brief information on Haematologica

Haematologica (print edition, pISSN 0390-6078, eISSN 1592-8721) publishes peer-reviewed papers on all areas of experimental and clinical hematology. The journal is owned by a non-profit organization, the Ferrata Storti Foundation, and serves the scientific community following the recommendations of the World Association of Medical Editors (www.wame.org) and the International Committee of Medical Journal Editors (www.icmje.org).

Haematologica publishes Editorials, Original articles, Review articles, Perspective articles, Editorials, Guideline articles, Letters to the Editor, Case reports & Case series and Comments. Manuscripts should be prepared according to our guidelines (www.haematologica.org/information-for-authors), and the Uniform Requirements for Manuscripts Submitted to Biomedical Journals, prepared by the International Committee of Medical Journal Editors (www.icmje.org).

Manuscripts should be submitted online at <http://www.haematologica.org/>.

Conflict of interests. According to the International Committee of Medical Journal Editors (<http://www.icmje.org/#conflicts>), “Public trust in the peer review process and the credibility of published articles depend in part on how well conflict of interest is handled during writing, peer review, and editorial decision making”. The ad hoc journal’s policy is reported in detail at www.haematologica.org/content/policies.

Transfer of Copyright and Permission to Reproduce Parts of Published Papers. Authors will grant copyright of their articles to the Ferrata Storti Foundation. No formal permission will be required to reproduce parts (tables or illustrations) of published papers, provided the source is quoted appropriately and reproduction has no commercial intent. Reproductions with commercial intent will require written permission and payment of royalties.

Subscription. Detailed information about subscriptions is available at www.haematologica.org. Haematologica is an open access journal and access to the online journal is free. For subscriptions to the printed issue of the journal, please contact: Haematologica Office, via Giuseppe Belli 4, 27100 Pavia, Italy (phone +39.0382.27129, fax +39.0382.394705, E-mail: info@haematologica.org).

Rates of the printed edition for the year 2022 are as following:

Institutional: Euro 700

Personal: Euro 170

Advertisements. Contact the Advertising Manager, Haematologica Office, via Giuseppe Belli 4, 27100 Pavia, Italy (phone +39.0382.27129, fax +39.0382.394705, e-mail: marketing@haematologica.org).

Disclaimer. Whilst every effort is made by the publishers and the editorial board to see that no inaccurate or misleading data, opinion or statement appears in this journal, they wish to make it clear that the data and opinions appearing in the articles or advertisements herein are the responsibility of the contributor or advisor concerned. Accordingly, the publisher, the editorial board and their respective employees, officers and agents accept no liability whatsoever for the consequences of any inaccurate or misleading data, opinion or statement. Whilst all due care is taken to ensure that drug doses and other quantities are presented accurately, readers are advised that new methods and techniques involving drug usage, and described within this journal, should only be followed in conjunction with the drug manufacturer’s own published literature.

Direttore responsabile: Prof. Carlo Balduini; Autorizzazione del Tribunale di Pavia n. 63 del 5 marzo 1955.

Printing: Press Up, zona Via Cassia Km 36, 300 Zona Ind.le Settevene - 01036 Nepi (VT)



Associated with USPI, Unione Stampa Periodica Italiana.

Premiato per l'alto valore culturale dal Ministero dei Beni Culturali ed Ambientali

Table of Contents

Volume 107, Issue 9: September 2022

About the Cover

- 2008** **Images from the Haematologica Atlas of Hematologic Cytology: schistocytes in thrombotic microangiopathies**
Carlo L. Balduini
<https://doi.org/10.3324/haematol.2022.281543>

Landmark Papers in Hematology

- 2009** **The beginnings of molecular medicine**
David C. Rees
<https://doi.org/10.3324/haematol.2022.281711>

Editorials

- 2011** **How to keep the factor VIII/von Willebrand factor complex in the circulation**
Cécile V. Denis and Peter J. Lenting
<https://doi.org/10.3324/haematol.2021.280222>
- 2014** **To be, or not 3B**
Joo Y. Song
<https://doi.org/10.3324/haematol.2021.280263>
- 2016** **Novel-agent combination therapies in chronic lymphocytic leukemia: the law of relative contributions**
Anthony R. Mato and Lindsey E. Roeker
<https://doi.org/10.3324/haematol.2021.280217>

Review Articles

- 2018** **Diagnosis of immune thrombocytopenia, including secondary forms, and selection of second-line treatment**
James B. Bussel and Christine A. Garcia
<https://doi.org/10.3324/haematol.2021.279513>
- 2037** **IgM monoclonal gammopathies of clinical significance: diagnosis and management**
Jahanzaib Khwaja *et al.*
<https://doi.org/10.3324/haematol.2022.280953>

Articles

- 2051** **Acute Lymphoblastic Leukemia**
Genetic and genomic analysis of acute lymphoblastic leukemia in older adults reveals a distinct profile of abnormalities: analysis of 210 patients from the UKALL14 and UKALL60+ clinical trials
Thomas Creasey *et al.*
<https://doi.org/10.3324/haematol.2021.279177>

- 2064** Acute Lymphoblastic Leukemia
Outcome of relapsed or refractory acute B-lymphoblastic leukemia patients and *BCR-ABL*-positive blast cell crisis of B-lymphoid lineage with extramedullary disease receiving inotuzumab ozogamicin
Sabine Kayser *et al.*
<https://doi.org/10.3324/haematol.2021.280433>
- 2072** Acute Lymphoblastic Leukemia
High tumor burden before blinatumomab has a negative impact on the outcome of adult patients with B-cell precursor acute lymphoblastic leukemia. A real-world study by the GRAALL
Aurélie Cabannes-Hamy *et al.*
<https://doi.org/10.3324/haematol.2021.280078>
- 2081** Bone Marrow Failure
Syndromes predisposing to leukemia are a major cause of inherited cytopenias in children
Oded Gilad *et al.*
<https://doi.org/10.3324/haematol.2021.280116>
- 2096** Cell Therapy & Immunotherapy
Increased visceral fat distribution and body composition impact cytokine release syndrome onset and severity after CD19 chimeric antigen receptor T-cell therapy in advanced B-cell malignancies
David M. Cordas dos Santos *et al.*
<https://doi.org/10.3324/haematol.2021.280189>
- 2108** Chronic Lymphocytic Leukemia
First-line treatment of chronic lymphocytic leukemia with ibrutinib plus obinutuzumab *versus* chlorambucil plus obinutuzumab: final analysis of the randomized, phase III iLLUMINATE trial
Carol Moreno *et al.*
<https://doi.org/10.3324/haematol.2021.279012>
- 2121** Hemostasis
The von Willebrand factor A-1 domain binding aptamer BT200 elevates plasma levels of von Willebrand factor and factor VIII: a first-in-human trial
Katarina D. Kovacevic *et al.*
<https://doi.org/10.3324/haematol.2021.279948>
- 2133** Hemostasis
The impact of aberrant von Willebrand factor-GPIb α interaction on megakaryopoiesis and platelets in humanized type 2B von Willebrand disease model mouse
Sachiko Kanaji *et al.*
<https://doi.org/10.3324/haematol.2021.280561>
- 2144** Non-Hodgkin Lymphoma
Follicular lymphoma grade 3B and diffuse large B-cell lymphoma present a histopathological and molecular continuum lacking features of progression/ transformation
Karoline Koch *et al.*
<https://doi.org/10.3324/haematol.2021.279351>
- 2154** Non-Hodgkin Lymphoma
A pilot study of the use of dynamic analysis of cell-free DNA from aqueous humor and vitreous fluid for the diagnosis and treatment monitoring of vitreoretinal lymphomas
Xiaoxiao Wang *et al.*
<https://doi.org/10.3324/haematol.2021.279908>
- 2163** Non-Hodgkin Lymphoma
Humoral immune depression following autologous stem cell transplantation is a marker of prolonged response duration in patients with mantle cell lymphoma
Louise Bouard *et al.*
<https://doi.org/10.3324/haematol.2021.279561>
- 2173** Non-Hodgkin Lymphoma
Rituximab in addition to LMB-based chemotherapy regimen in children and adolescents with primary mediastinal large B-cell lymphoma: results of the French LMB2001 prospective study
Marie Emilie Dourthe *et al.*
<https://doi.org/10.3324/haematol.2021.280257>

- 2183** Plasma Cell Disorders
Extracellular vesicles mediate the communication between multiple myeloma and bone marrow microenvironment in a NOTCH dependent way
Domenica Giannandrea *et al.*
<https://doi.org/10.3324/haematol.2021.279716>
- 2195** Platelet Biology & its Disorders
Antiplatelet antibody predicts platelet desialylation and apoptosis in immune thrombocytopenia
Shiyong Silvia Zheng *et al.*
<https://doi.org/10.3324/haematol.2021.279751>
- 2206** Platelet Biology & its Disorders
Specific inhibition of the transporter MRP4/ABCC4 affects multiple signaling pathways and thrombus formation in human platelets
Robert Wolf *et al.*
<https://doi.org/10.3324/haematol.2021.279761>

Letters to the Editor

- 2218** **Deregulated JAK3 mediates growth advantage and hemophagocytosis in extranodal nasal-type natural killer/T-cell lymphoma**
Adrien Picod *et al.*
<https://doi.org/10.3324/haematol.2021.280349>
- 2226** **β adrenergic signaling regulates hematopoietic stem and progenitor cell commitment and therapy sensitivity in multiple myeloma**
Remya Nair *et al.*
<https://doi.org/10.3324/haematol.2022.280907>
- 2232** **Pure erythroid leukemia is characterized by biallelic TP53 inactivation and abnormal p53 expression patterns in *de novo* and secondary cases**
Hong Fang *et al.*
<https://doi.org/10.3324/haematol.2021.280487>
- 2238** **The gut microbiome in patients with chronic lymphocytic leukemia**
Tereza Faitová *et al.*
<https://doi.org/10.3324/haematol.2021.280455>
- 2244** **A validated clinical-genetic score for assessing the risk of thrombosis in patients with COVID-19 receiving thromboprophylaxis**
José Manuel Soria *et al.*
<https://doi.org/10.3324/haematol.2022.281068>
- 2249** **ETV6-related thrombocytopenia: dominant negative effect of mutations as common pathogenic mechanism**
Michela Faleschini *et al.*
<https://doi.org/10.3324/haematol.2022.280729>
- 2255** **Profound and sustained response with next-generation ALK inhibitors in patients with relapsed or progressive ALK-positive anaplastic large cell lymphoma with central nervous system involvement**
Charlotte Rigaud *et al.*
<https://doi.org/10.3324/haematol.2021.280081>
- 2261** **Autologous stem cell transplantation in an older adult population**
Kateryna Fedorov *et al.*
<https://doi.org/10.3324/haematol.2022.281020>

- 2266** **Cytomegalovirus proteins, maternal pregnancy cytokines, and their impact on neonatal immune cytokine profiles and acute lymphoblastic leukemogenesis in children**
Joseph L. Wiemels *et al.*
<https://doi.org/10.3324/haematol.2022.280826>
- 2271** **Inducing synthetic lethality for selective targeting of acute myeloid leukemia cells harboring *STAG2* mutations**
Agatheeswaran Subramaniam *et al.*
[doi:10.3324/haematol.2021.280303](https://doi.org/10.3324/haematol.2021.280303)
- 2276** **Prolonged remission with pembrolizumab and radiation therapy in a patient with multisystem Langerhans cell sarcoma**
Saurabh Zanwar *et al.*
<https://doi.org/10.3324/haematol.2022.280948>
- 2280** **Hereditary anemia caused by multilocus inheritance of *PIEZO1*, *SLC4A1* and *ABCB6* mutations: a diagnostic and therapeutic challenge**
Barbara Eleni Rosato *et al.*
<https://doi.org/10.3324/haematol.2022.280799>

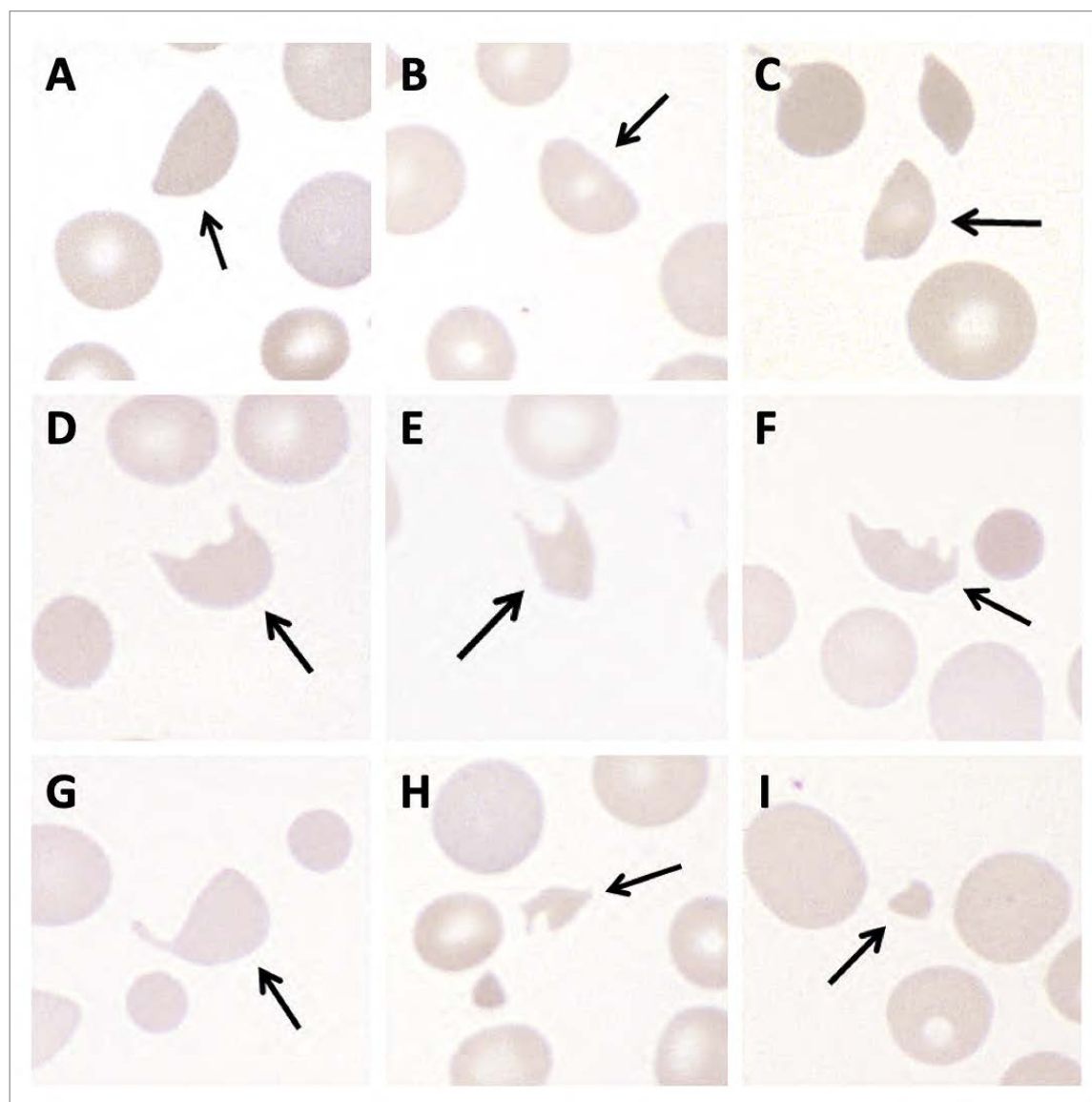
Images from the Haematologica Atlas of Hematologic Cytology: schistocytes in thrombotic microangiopathies

Carlo L. Balduini

Ferrata-Storti Foundation, Pavia, Italy

E-mail: carlo.balduini@unipv.it

<https://doi.org/10.3324/haematol.2022.281543>



The presence of schistocytes is a constant feature of patients with thrombotic microangiopathies. The highest concentrations of schistocytes are observed in thrombotic thrombocytopenic purpura in which they represent 1-18% of red blood cells. Lower concentrations can be observed in other thrombotic microangiopathies as well as in subjects with mechanical heart valves or other intravascular devices and in chronic renal diseases. Helmet cells (A-C, arrow) are erythrocytes with an amputated zone highlighted by a straight border as a result of a crash on a fibrin strand. The missing cell portion corresponds to the fragments of erythrocytes shown in (H) and (I). Keratocytes (cells with horns) (D-F, arrows) are characterized by two or three spicules separated by concave segments of membrane and have been formed by rupture of peripheral pseudovacua and subsequent fusion of the cell membrane. Fragments of erythrocytes with bizarre shapes escape a precise classification (G-I). In (F) and (G) you can also recognize microspherocytes, which are a secondary manifestation of fragmentation and should be included within the schistocyte count only in the presence of the shape abnormalities described in (A-F).¹

Disclosures

No conflicts of interest to disclose.

References

1. Balduini CL. Thrombotic microangiopathies. *Haematologica*. 2020;105(Suppl 1):270-275.

The beginnings of molecular medicine

David C. Rees

Department of Haematological Medicine, King's College Hospital and King's College London, UK

E-mail: david.rees@kcl.ac.uk

<https://doi.org/10.3324/haematol.2022.281711>



TITLE	Globin synthesis in thalassaemia: an in vitro study.
AUTHORS	Weatherall DJ, Clegg JB, Naughton MA.
JOURNAL	Nature. 1965;208(5015):1061-1065. DOI: 10.1038/2081061a0 PMID: 5870556

Thalassemia was first described in the 1920s by Thomas Cooley and Pearl Lee in Detroit. They described four children with massive hepatosplenomegaly, anemia, jaundice and marked bony abnormalities, including enlargement of cranial and facial bones.¹ It initially seemed more likely that this was a disease of bones than blood, as more clinical descriptions gradually emerged from the Mediterranean and Asia, where this seemed to be a common problem. In parallel with advances in genetics, red cell biology, and hemoglobin analysis, it became apparent that thalassaemia was inherited in an autosomal recessive manner, with mild red cell abnormalities typically present in both parents. Protein sequencing had shown that some hemoglobinopathies, most notably sickle cell disease, were caused by structural abnormalities of the globin

chains, whereas others had no detectable globin abnormalities, and were referred to as thalassaemia syndromes. It was suspected that thalassaemia was caused by quantitative defects of globin chain synthesis, but there was no direct evidence of this until Weatherall *et al.* published their landmark paper.² The authors were able to assess the relative rates of globin chain synthesis by incubating reticulocytes with radiolabeled leucine, and measuring the rate of leucine incorporation over different time periods. In this way, they showed that the rates of β and α globin synthesis were matched in normal reticulocytes, whereas there were quantitative deficits of β and α globin in the respective types of thalassaemia. This discovery was the beginning of the molecular understanding of thalassaemia, and led to an exponential increase in the under-

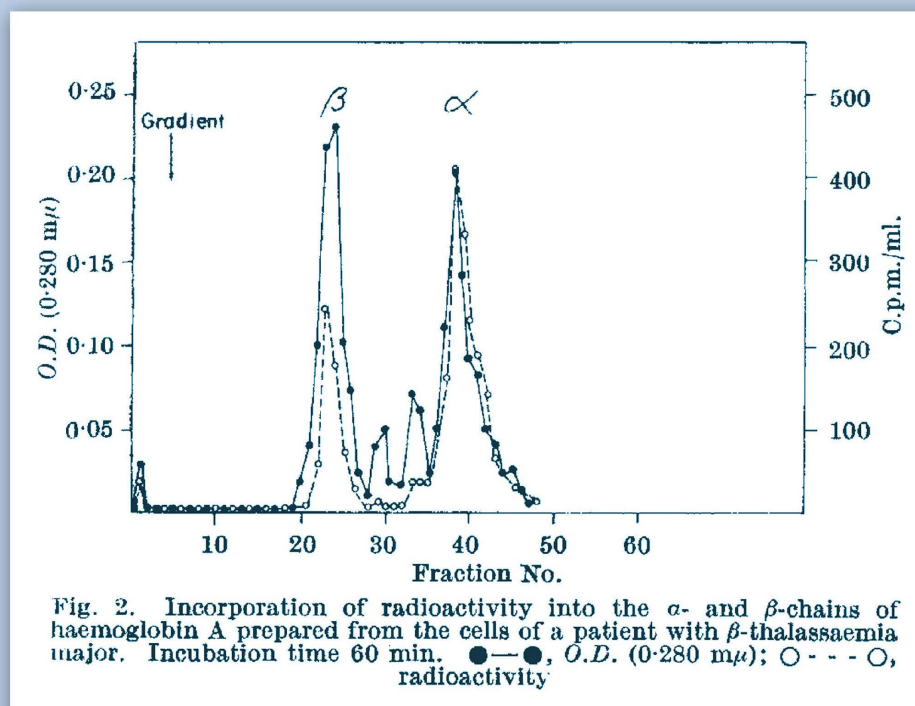


Figure 1. Rates of globin synthesis in reticulocytes from a patient with β -thalassaemia major. Incorporation of radioactivity into globin chains after reticulocytes from a patient with β -thalassaemia major had been incubated for 60 minutes with ¹⁴C-leucine. The solid line shows the amount of total protein, which is approximately the same for both β and α globin chains. The dotted line shows the rate of synthesis of new globin chains over the 60 minutes of the incubation, with significantly less synthesis of β globin compared to α globin.

standing of its pathophysiology, including an appreciation of ineffective erythropoiesis, and that the cellular pathology resulted from an excess of the unaffected globin chain rather than a deficiency of the protein from the mutated gene. This technique of globin chain synthesis was refined slightly over the years, but remained essentially the same. It was central to many of the discoveries concerning transcriptional and translational control of the globin genes, which in turn acted as paradigms for molecular biology in general. In particular, globin chain synthesis was used to identify the significance of many variants identified in the globin genes, and was only really replaced when quantitation of messenger RNA became routine in the 1990s. Similarly, it was used in the routine diagnosis of hemoglobinopathies until the 1980s, and in particular was used in the early prenatal diagnosis of he-

moglobinopathies from fetal blood samples.³

This landmark paper arose primarily from the interaction between a very astute hematologist, David Weatherall, who had identified an important question, and a very skilled protein chemist, John Clegg, who knew how to answer it. Together they went on to write 200 papers together, including more than 20 published in *Nature*. This interaction was one of the driving forces behind the development of molecular medicine, with the establishment of the Institute of Molecular Medicine (later the Weatherall Institute of Molecular Medicine) in Oxford, and the spawning of numerous clinical and laboratory scientists across the world.

Disclosures

No conflicts of interest to disclose.

References

1. Cooley TB, Lee P. A series of cases of splenomegaly in children with anemia and peculiar bone changes. *Trans Am Pediatr Soc.* 1925;37:29-30.
2. Weatherall DJ, Clegg JB, Naughton MA. Globin synthesis in thalassaemia: an in vitro study. *Nature.* 1965;208(5015):1061-1065.
3. Fairweather DV, Modell B, Berdoukas V, et al. Antenatal diagnosis of thalassaemia major. *Br Med J.* 1978;1(6109):350-353.

How to keep the factor VIII/von Willebrand factor complex in the circulation

Cécile V. Denis and Peter J. Lenting

Laboratory for Hemostasis, Inflammation & Thrombosis (HITH), Unité Mixte de Recherche (UMR)-1176, Institut National de la Santé et de la Recherche Médicale (Inserm), Université Paris-Saclay, Le Kremlin-Bicêtre, France

E-mail: cecile.denis@inserm.fr

<https://doi.org/10.3324/haematol.2021.280222>

von Willebrand disease and hemophilia A: current treatments

von Willebrand factor (VWF) and factor VIII (FVIII) make an enigmatic duo that is present in the circulation as a tightly bound complex.¹ Their individual roles in hemostasis have been well-established, and functional deficiency of either the former or the latter protein is associated with severe bleeding complications, known as von Willebrand disease (VWD) and hemophilia A, respectively. Over the last several decades, the clinical management of the severe forms of these disorders predominantly relied on replacement therapy using concentrates enriched in VWF, FVIII or both. In contrast, the moderate and mild variants of VWD and hemophilia A benefited from using desmopressin, a vasopressin 2-receptor agonist that stimulates the rapid release of endothelial VWF and FVIII.^{2,3} Despite its numerous advantages (such as ease of administration, low costs, no risk of inhibitor development or of transmissible disease), desmopressin also has a number of limitations. Post-treatment increases of VWF and FVIII are transient and limited by the natural short half-life (about 12 h) of the FVIII/VWF complex, and repetitive use of desmopressin results in a diminished responsiveness (tachyphylaxis) due to exhaustion of the VWF storage organelles.^{2,4} Furthermore, desmopressin has variable effectiveness in VWD-type 2A and 2M as well as in hemophilia A, and it is contraindicated for VWD-type 2B as it may worsen the thrombocytopenia in these patients.^{2,5} It is worth noting that desmopressin is foremost an anti-diuretic, and the desmopressin-induced secretion of VWF from storage organelles is actually an off-target effect. Finally, desmopressin use is associated with some side effects (transient headaches, facial flushing, hypotension, hyponatremia and mild tachycardia), although these are generally mild and well-tolerated.^{6,7}

Increasing endogenous von Willebrand factor and factor VIII levels

While the abovementioned treatment options are satisfactory to some extent, treatment still needs to be optimized. With regard to severe hemophilia A, new approaches have been approved for the clinic (e.g., extended half-life variants of FVIII, emicizumab) or are in advanced clinical development (e.g., fitusiran, concizumab,

marstacimab, efanesoctocog alfa, valoctocogene roxaparvovec). In contrast, few novel strategies are emerging or even appearing on the visible horizon with regard to VWD or mild hemophilia A. Interestingly, the majority of patients with VWD or mild/moderate hemophilia A could already benefit from an increase in endogenous levels of the VWF/FVIII complex, as is evident from the successful use of desmopressin. It could thus be worthwhile designing approaches that aim to increase endogenous FVIII and VWF levels in a more sustainable manner compared to desmopressin. A first approach was described already 20 years ago: treatment with interleukin-11 was associated with an increase in VWF in both mouse and canine models.^{8,9} The underlying mechanism seemed to be related to an upregulation of VWF mRNA in response to interleukin-11.⁹ However, follow-up phase II clinical studies were somewhat disappointing, as treatment with interleukin-11 was associated with only a modest rise in VWF plasma levels (1.1-1.5 fold).^{10,11}

The anti-von Willebrand factor aptamer BT200

In this issue of *Haematologica*, Kovacevic and colleagues present a new strategy that is associated with increased VWF/FVIII levels, centered around the aptamer BT200.¹² Originally, the authors developed BT200 as an antithrombotic agent to interfere with the platelet-binding activity of VWF.¹³ BT200 is a short hairpin-structured oligonucleotide consisting of the methylated nucleobases adenine, cytosine, guanine and uracil, and is an optimized derivative from the previously described aptamer ARC1779.¹⁴ Both BT200 and ARC1779 have in common that they specifically bind to the A1 domain of VWF, thereby interfering with the binding of VWF to its platelet-receptor glycoprotein Iba α (GpIba α).¹³ Preclinical studies in primates demonstrated that the improved BT200 aptamer is not only highly efficient (inhibition of VWF A1 domain activity: IC₅₀ = 70-180 nM), but also has an excellent bioavailability following subcutaneous injection (>77%) and a long half-life (>100 h) due to its pegylated character.¹³ Studies using blood samples of stroke patients further confirmed that BT200 has a potent antithrombotic activity.¹⁵

Initial studies using ARC1779 revealed that this molecule led to an increase of VWF levels in patients with VWD-

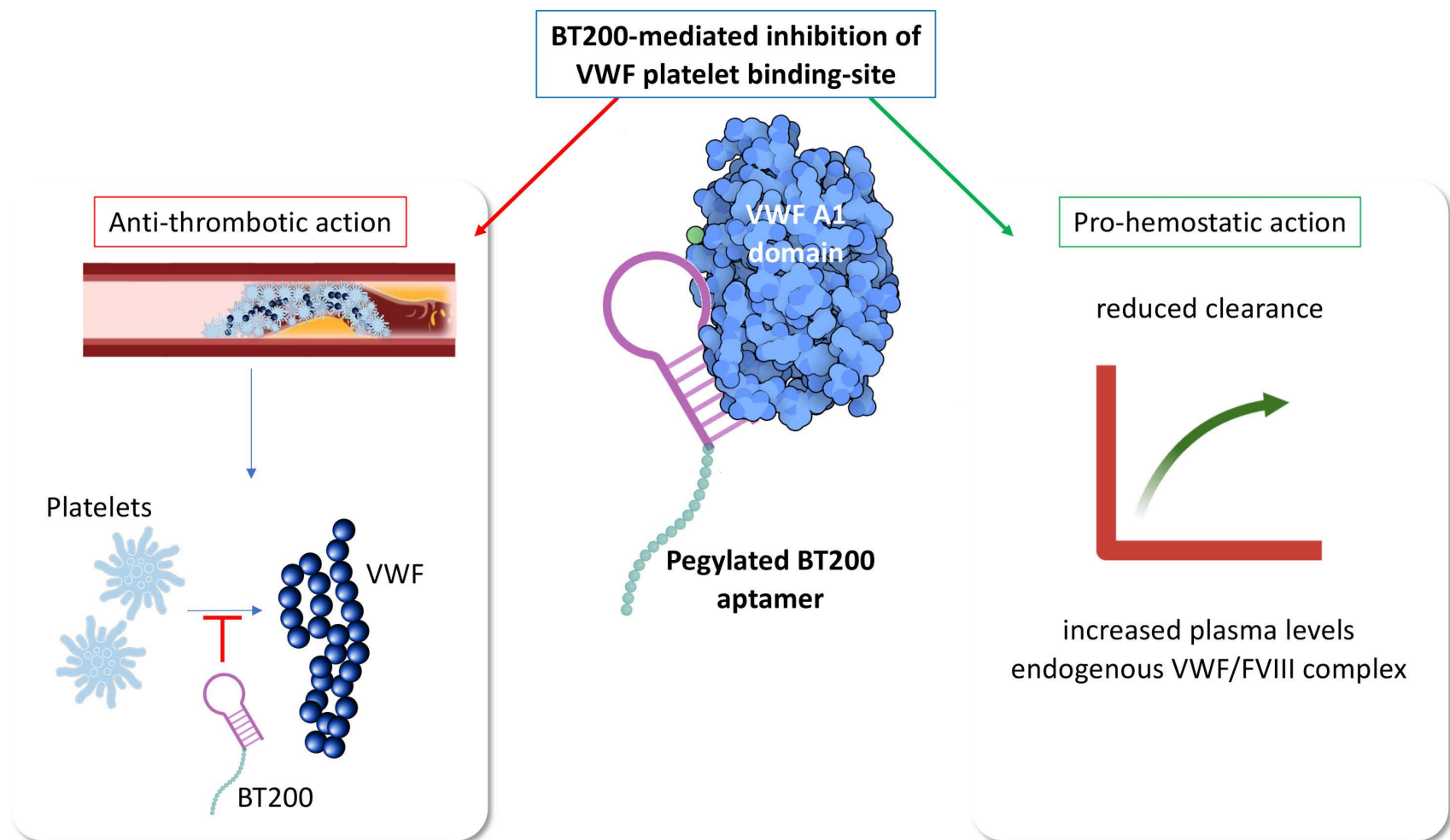


Figure 1. Mode of action of BT200. BT200 is a pegylated aptamer that binds with high affinity to the platelet-binding site within the von Willebrand factor (VWF) A1 domain. It was previously shown that BT200 interferes with VWF-dependent thrombus formation, which endows the molecule with efficient antithrombotic activity.¹³ In their study, Kovacevic and colleagues now demonstrate that BT200 also delays clearance of the VWF/factor VIII (FVIII) complex, resulting in transient increases in plasma levels of both proteins. This approach could thus be a strategy to increase endogenous VWF/FVIII levels in patients with mild/moderate forms of von Willebrand disease and hemophilia A.

type 2B.¹⁶ These results prompted the investigators to initiate a larger first-in-human prospective phase I study using the improved BT200 variant, the outcomes of which are reported in this issue of *Haematologica*.¹² In a single-dose bioavailability study, participants received 0.18 to 36 mg BT200 subcutaneously. This resulted in a dose-dependent increase in BT200 plasma concentrations, with maximal levels being around 3 µg/mL after 168 h when the highest dose was given. Increasing doses were associated with a dose-dependent occupation of the VWF A1 domain, with 75%-90% of A1 domains being occupied at doses between 12 and 24 mg. Maximal occupation was observed between 1 and 4 days after injection, after which free A1 domains gradually re-appeared and returned to normal levels 2 weeks after the injection. Interestingly, the administration of BT200 at these doses was associated with 3- to 4-fold increases in VWF antigen levels. However, VWF antigen levels peaked between 7 and 14 days after injection, somewhat later compared to maximal occupation of the A1 domains. Concurrent to the increase of VWF antigen, there was also a 2.5-fold increase in FVIII activity. Of note, FVIII levels could be further increased via the administration of desmopressin, indicating that the mechanisms by which FVIII levels are increased by BT200 and

desmopressin are different. Indeed, BT200 appears to act by prolonging the half-life of VWF rather than modifying its synthesis or secretion. As such, its mode of action is fundamentally different from that of desmopressin or interleukin-11.

In view of this listing of impressive data, it seems conceivable that BT200 is an attractive candidate to ameliorate endogenous levels of the FVWF/FVIII complex. Of course, these data are derived from an initial phase I study, and several issues would require additional investigations. For instance, BT200 is designed to interfere with VWF activity, and data presented in the *Online Supplementary Material* show that doses inducing the highest increase in VWF/FVIII levels were also associated with prolonged closure times in the platelet function analyzer assay and provoked reduced platelet aggregation activity, at least during (part of) the first week.¹² It is therefore going to be key to find the optimal dosing that allows increased FVIII and VWF levels, without compromising the patient's hemostatic potential. It should be noted that in the case that the activity of BT200 needs to be neutralized, the authors have already developed an efficient reversal agent, i.e., a complementary aptamer designated BT101, which specifically binds BT200 with high affinity.¹⁷ It is interesting to speculate further on the clinical ap-

plication of this molecule: designed as an antithrombotic agent, which could be used for VWF-dependent thrombotic complications (arterial thrombosis, thrombotic thrombocytopenic purpura); it may now also find a use in the treatment of bleeding disorders such as mild/moderate hemophilia A and certain types of VWD (Figure 1). It is unusual to find both features in a single molecule!

In conclusion, Kovacevic *et al.* present an elegant ap-

proach to improve endogenous VWF and FVIII levels through a single subcutaneous administration of BT200. We look forward to seeing additional clinical data.

Disclosures

No conflicts of interest to disclose.

Contributions

CVD and PJJ wrote the manuscript.

References

- Pipe SW, Montgomery RR, Pratt KP, Lenting PJ, Lillicrap D. Life in the shadow of a dominant partner: the FVIII-VWF association and its clinical implications for hemophilia A. *Blood*. 2016;128(16):2007-2016.
- Federici AB. The use of desmopressin in von Willebrand disease: the experience of the first 30 years (1977-2007). *Haemophilia*. 2008;14(Suppl 1):5-14.
- Franchini M, Zaffanello M, Lippi G. The use of desmopressin in mild hemophilia A. *Blood Coagul Fibrinolysis*. 2010;21(7):615-619.
- Mannucci PM, Bettega D, Cattaneo M. Patterns of development of tachyphylaxis in patients with haemophilia and von Willebrand disease after repeated doses of desmopressin (DDAVP). *Br J Haematol*. 1992;82(1):87-93.
- Castaman G, Tosetto A, Rodeghiero F. Reduced von Willebrand factor survival in von Willebrand disease: pathophysiologic and clinical relevance. *J Thromb Haemost*. 2009;7 (Suppl 1):71-74.
- Miesbach W, Krekeler S, Duck O, et al. Clinical assessment of efficacy and safety of DDAVP. *Hamostaseologie*. 2010;30(Suppl 1):S172-175.
- Stoof SC, Cnossen MH, de Maat MP, Leebeek FW, Kruip MJ. Side effects of desmopressin in patients with bleeding disorders. *Haemophilia*. 2016;22(1):39-45.
- Denis CV, Kwack K, Saffaripour S, et al. Interleukin 11 significantly increases plasma von Willebrand factor and factor VIII in wild type and von Willebrand disease mouse models. *Blood*. 2001;97(2):465-472.
- Olsen EH, McCain AS, Merricks EP, et al. Comparative response of plasma VWF in dogs to up-regulation of VWF mRNA by interleukin-11 versus Weibel-Palade body release by desmopressin (DDAVP). *Blood*. 2003;102(2):436-441.
- Ragni MV, Jankowitz RC, Jaworski K, Merricks EP, Kloos MT, Nichols TC. Phase II prospective open-label trial of recombinant interleukin-11 in women with mild von Willebrand disease and refractory menorrhagia. *Thromb Haemost*. 2011;106(4):641-645.
- Ragni MV, Novelli EM, Murshed A, Merricks EP, Kloos MT, Nichols TC. Phase II prospective open-label trial of recombinant interleukin-11 in desmopressin-unresponsive von Willebrand disease and mild or moderate haemophilia A. *Thromb Haemost*. 2013;109(2):248-254.
- Kovacevic KD, Grafeneder J, Schörghofer C, et al. The von Willebrand factor A-1 domain binding aptamer BT200 elevates plasma levels of von Willebrand factor and factor VIII: a first-in-human trial. *Haematologica*. 2017;102(9):2121-2132.
- Zhu S, Gilbert JC, Hatala P, et al. The development and characterization of a long acting anti-thrombotic von Willebrand factor (VWF) aptamer. *J Thromb Haemost*. 2020;18(5):1113-1123.
- Gilbert JC, DeFeo-Fraulini T, Hutabarat RM, et al. First-in-human evaluation of anti von Willebrand factor therapeutic aptamer ARC1779 in healthy volunteers. *Circulation*. 2007;116(23):2678-2686.
- Kovacevic KD, Greisenegger S, Langer A, et al. The aptamer BT200 blocks von Willebrand factor and platelet function in blood of stroke patients. *Sci Rep*. 2021;11(1):3092.
- Jilma-Stohlawetz P, Knobl P, Gilbert JC, Jilma B. The anti-von Willebrand factor aptamer ARC1779 increases von Willebrand factor levels and platelet counts in patients with type 2B von Willebrand disease. *Thromb Haemost*. 2012;108(2):284-290.
- Zhu S, Gilbert JC, Liang Z, et al. Potent and rapid reversal of the von Willebrand factor inhibitor aptamer BT200. *J Thromb Haemost*. 2020;18(7):1695-1704.

To be, or not 3B

Joo Y. Song

Department of Pathology, City of Hope National Medical Center, Duarte, CA, USA

E-mail: josong@coh.org

doi:10.3324/haematol.2021.280263

Although follicular lymphoma (FL) is the most common, indolent non-Hodgkin B-cell lymphoma, grade 3B (FL3B) only accounts for 5-10% of cases of FL and is characterized by follicles consisting exclusively of centroblasts.¹ Approximately half of the cases of FL3B also show a low-grade component (grade 1-2) or diffuse large B-cell lymphoma (DLBCL).² Most consider FL3B to be aggressive and treat these cases as DLBCL with intense immunochemotherapy such as rituximab plus cyclophosphamide, doxorubicin, vincristine and prednisone (R-CHOP). However, there are limited data on these cases from molecular and therapeutic standpoints since these cases are often excluded from clinical trials.

In this issue of *Haematologica*, Koch and colleagues³ help to shed light on this rare and aggressive disease by analyzing cases of FL3B alone and FL3B together with DLBCL using a targeted sequencing panel and taking care to exclude cases of pediatric FL and cases with the *IRF4* translocation.⁴ The authors observed that 88% (14/16) of the cases of composite FL3B and DLBCL showed mutational variants shared by the FL3B component and DLBCL after macrodissection of these areas. In addition, the majority of the cases shared the same chromosomal abnormalities with *BCL2*, *BCL6*, and *MYC* rearrangements by fluorescence *in situ* hybridization analysis. These findings are

similar to those of other studies evaluating the genomic landscape of FL and its transformed state,⁵ as there were no specific recurrent mutations identified to predict transformation to DLBCL. Not surprisingly, the most frequent mutations that were shared by the FL3B and DLBCL components were *CREBBP* and *KMT2D* (Figure 1).

The next question is how do patients with FL3B respond to intense chemotherapy? In a subset of the patients with FL3B and FL3B plus DLBCL who were enrolled in the prospective randomized PETAL trial,⁶ analysis of overall and progression-free survival showed that, in this limited cohort of patients, the survival outcomes of these patients were similar to those of patients with *de novo* DLBCL.

FL3B continues to be a difficult disease to analyze from genomic and clinical standpoints. The difficulties are due in part to the absence of these cases in large, prospective clinical trials, the heterogeneity of composite disease with low-grade FL or DLBCL, and issues with poor reproducibility of grading. Koch and colleagues³ show that the genomic abnormalities in cases of concurrent FL3B and DLBCL are shared by the two components, further supporting the concept that FL3B may represent DLBCL and can be managed with aggressive immunochemotherapy in a manner similar to *de novo* DLBCL. The retained follicular

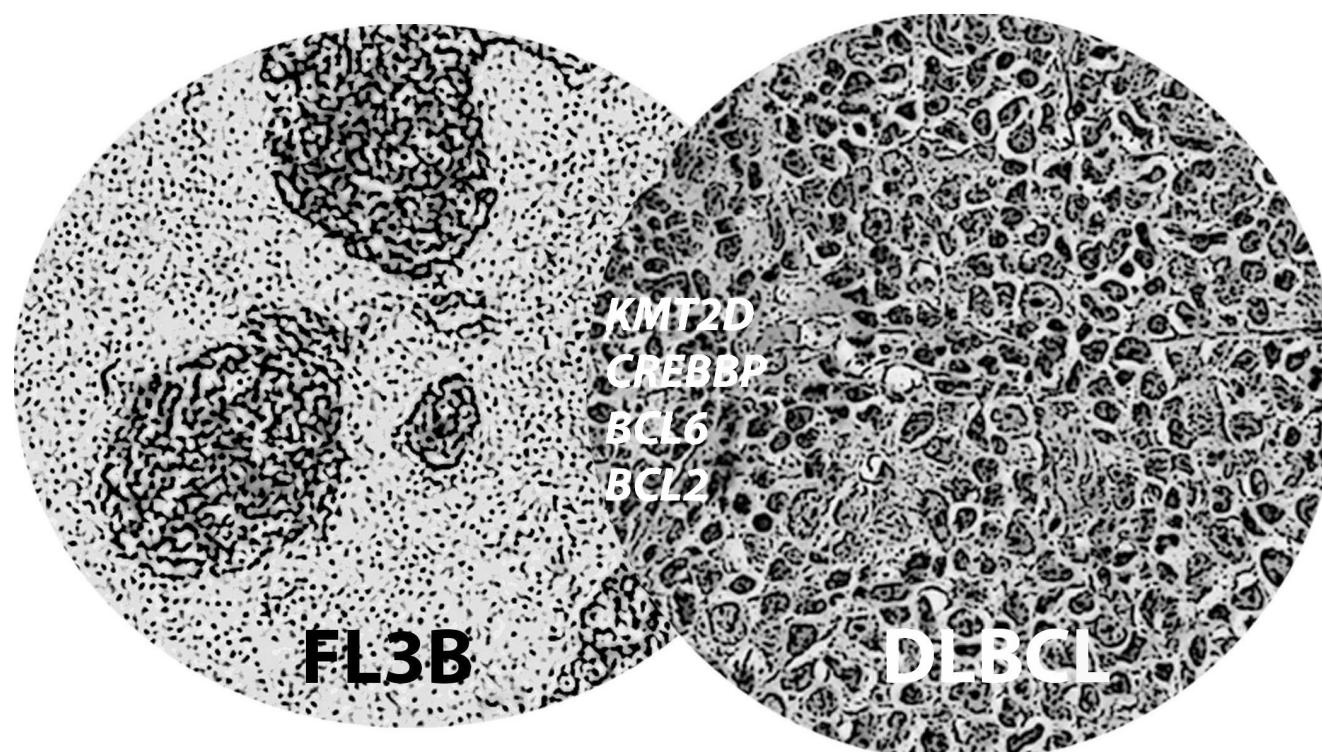


Figure 1. Follicular lymphoma grade 3B and diffuse large B-cell lymphoma. Left: follicular lymphoma grade 3B (FL3B) with an expanded follicular dendritic cell meshwork highlighted with CD21. Right: diffuse large B-cell lymphoma (DLBCL) with sheets of large and atypical cells. Concurrent FL3B and DLBCL show shared mutations and translocations with *KMT2D*, *CREBBP*, *BCL6*, and *BCL2*.

structure in FL3B may be related to the tumor micro-environment or an early snapshot of FL progressing to DLBCL. It is unclear whether cases of FL with development of DLBCL at a later time-point would also have many shared mutations like these composite cases. Clinical trials have recently started to include FL3B, as seen with the TRANSCEND NHL 001 trial, investigating anti-CD19 chimeric antigen receptor T cells. Another study, using selinexor plus chemotherapy for refractory aggressive B-cell lymphomas (NCT02471911), provides some promise for inclusion of this rare disease in future studies. The study by Koch and colleagues³ further underscores that FL3B may be a continuum of DLBCL with current evidence pointing towards grouping as an aggressive lym-

phoma. Cases with only FL3B may be a result of limited sampling with DLBCL being present in less surgically accessible sites. Mutational profiling has yet to provide a mechanism of disease progression and more cases of paired FL and DLBCL are required to address these issues. Although there are challenges in studying FL3B due to the rarity of the disease, inclusion of FL3B in prospective trials, with steps to study the combination with genomic correlates, will help to clarify how to define the disease better. This, in turn, will help to aid the process towards selecting appropriate treatment.

Disclosures

No conflicts of interest to disclose.

References

1. Barraclough A, Bishton M, Cheah CY, Villa D, Hawkes EA. The diagnostic and therapeutic challenges of grade 3B follicular lymphoma. *Br J Haematol.* 2021;195(1):15-24.
2. Ott G, Katzenberger T, Lohr A, et al. Cytomorphologic, immunohistochemical, and cytogenetic profiles of follicular lymphoma: 2 types of follicular lymphoma grade 3. *Blood.* 2002;99(10):3806-3812.
3. Koch C, Richter J, Hänel C, Hüttmann A, Dührsen U, Klapper W. Follicular lymphoma grade 3B and diffuse large B-cell lymphoma present a histopathological and molecular continuum lacking features of progression/transformation. *Haematologica.* 2022;107(9):2144-2153.
4. Swerdlow S, Campo E, Harris NL, et al. WHO Classification of Tumours of Haematopoietic and Lymphoid Tissues. Lyon, France: International Agency for Research on Cancer, 2017.
5. Bouska A, Zhang W, Gong Q, et al. Combined copy number and mutation analysis identifies oncogenic pathways associated with transformation of follicular lymphoma. *Leukemia.* 2017;31(1):83-91.
6. Dührsen U, Müller S, Hertenstein B, et al. Positron emission tomography-guided therapy of aggressive non-Hodgkin lymphomas (PETAL): a multicenter, randomized phase III trial. *J Clin Oncol.* 2018;36(20):2024-2034.

Novel-agent combination therapies in chronic lymphocytic leukemia: the law of relative contributions

Anthony R. Mato and Lindsey E. Roeker

Memorial Sloan Kettering Cancer Center, New York, NY, USA

E-mail: Matoa@mskcc.org

doi:10.3324/haematol.2021.280217

In this issue of *Haematologica*, Moreno *et al.*¹ present the final analysis of the randomized, phase III iLLUMINATE trial. In this study, the combination of the Bruton tyrosine kinase (BTK) inhibitor ibrutinib (administered in a treat-to-progression, continuous fashion) plus the anti-CD20 monoclonal antibody obinutuzumab was compared to time-limited chlorambucil plus obinutuzumab in the front-line setting. Now with a median of 45 months of follow-up, the data confirm an impressive progression-free survival (PFS) advantage of ibrutinib plus obinutuzumab over chlorambucil plus obinutuzumab (median PFS not reached for ibrutinib plus obinutuzumab vs. 22 months for chlorambucil plus obinutuzumab, hazard ratio=0.25, 95% confidence interval: 0.16-0.39, $P<0.0001$) without a clear advantage in overall survival (hazard ratio=1.08, $P=0.793$), although it should be noted that treatment crossover was allowed. For ibrutinib plus obinutuzumab, the overall response rate, complete response rate and rate of undetectable minimal residual disease were also impressive at 91%, 42% and 38%, respectively. The iLLUMINATE trial also allowed enrollment of patients with chromosome 17p deletion [(del17p)] providing efficacy data for ibrutinib-based therapy in this high-risk population of patients.

Taken in the context of the current treatment landscape, these data from iLLUMINATE should trigger important considerations regarding the relative contributions of drugs. While the ibrutinib plus obinutuzumab combination is unequivocally superior to the chlorambucil-based control arm in terms of PFS, we do not gain insight into how obinutuzumab adds to the already herculean activity of ibrutinib in the front-line setting as this trial did not include an ibrutinib monotherapy arm. In the current pandemic, assessing the contribution of obinutuzumab is particularly relevant given that the addition of an anti-CD20 monoclonal antibody will blunt or eliminate humoral responses to SARS-Cov-2 mRNA vaccines (all risk without a proven reward). Additionally, lessons learned from recent randomized trials in chronic lymphocytic leukemia (CLL) remind us that only with proper assessment of relative contributions can one determine the true risk *versus* benefit of a combination. For example, two prior randomized clinical trials compared ibrutinib to ibrutinib with the anti-CD20 monoclonal antibody rituximab and did not demonstrate a PFS or overall survival advantage for ibrutinib plus rituximab over ibrutinib alone.^{2,3} Based on these

trials which provided clarity on the relative contribution of rituximab to ibrutinib, nearly all clinicians favor ibrutinib monotherapy over ibrutinib plus rituximab combination therapy. In the ELEVATE-TN study the second generation BTK inhibitor acalabrutinib was compared alone and in combination with obinutuzumab to chlorambucil plus obinutuzumab in the front-line setting.⁴ In this three-arm, randomized, phase III, clinical trial, Sharman *et al.* demonstrated a PFS advantage for the combination of acalabrutinib plus obinutuzumab over acalabrutinib monotherapy. The ELEVATE-TN study design should be celebrated, as it allowed clinicians to examine the benefit of adding obinutuzumab to acalabrutinib and supports the use of the novel agent-based combination acalabrutinib plus obinutuzumab. Given differences in patient populations, clinical trial designs, and biases inherent to cross-trial comparisons of different agents, data from ELEVATE TN should not be freely extrapolated to other BTK inhibitors plus obinutuzumab combinations. This body of literature catalyzes careful consideration of how to design future novel agent combination studies in CLL to adequately assess the relative safety and efficacy contributions of individual components of a multi-agent combination regimen.

As future efforts to optimize treatment of CLL focus on novel agent-based doublet and triplet therapy, we must consider the relative contributions of each component. Phase I/II studies examining combination therapies have demonstrated safety and efficacy, leading to the development of phase III studies exploring the combinations. Rational phase III study design requires consideration of whether the combination is absolutely required to achieve the desired clinical outcome. For example, in the recently reported GLOW trial, the combination of ibrutinib and venetoclax demonstrated superior PFS to the chlorambucil plus obinutuzumab regimen.⁵ While the GLOW study is undoubtedly positive with regard to its primary PFS endpoint, the trial does not allow us to determine the relative contributions of the components of the ibrutinib plus venetoclax combination to safety or efficacy. With the current data, we cannot determine whether the combination is better than monotherapy or a single novel agent in combination with obinutuzumab. Novel agent monotherapy control arms are noticeably absent in many of the currently accruing trials examining novel agent-based doublet and triplet therapies, so assessment of the

relative contribution of each component will not be possible. A major unanswered question in the treatment of CLL is which patients require monotherapy, which require doublet therapy and which require triplet therapy.⁶ Active phase III studies, with the notable exception of CLL17 (NCT04608318), are not designed to answer this question. The issue of relative contribution is ubiquitous in oncology, as recently highlighted in an excellent review by Brewer *et al.*, which focused on regulatory considerations for the contribution of effects of drugs used in combination regimens.⁷ The authors concluded that for the approval of combination regimens, “it is necessary to demonstrate the contribution of effect of each monotherapy to the overall combination.” These authors further assessed the strengths and weaknesses of various methods we can use to assess relative contribution of effect. Perhaps the most applicable solution to the issue at hand in CLL is a multi-arm adaptive trial design in which patients can be randomized to trial arms performing at a “pre-specified level of efficacy.” Such an approach can yield data on the contribution of novel agent monotherapy control arms with the ability to drop such controls if they are underperforming. This adaptive approach was employed in UNITY-CLL, a front-line clinical trial in CLL which successfully assessed the relative contributions of umbralisib and ublituximab monotherapies to the combination of umbralisib and ublituximab.⁸

In their article, Moreno *et al.*¹ eloquently discuss the issue of relative contribution. Most notably, the authors com-

pare the 48-month PFS of ibrutinib monotherapy from the RESONATE-2 trial to the 48-month PFS of the ibrutinib plus obinutuzumab iLLUMINATE regimen demonstrating nearly identical PFS (~75%) at that time point. As we aim to understand the role of novel agent doublet and triplet therapy in CLL, iLLUMINATE shines a light on an ever-important issue to be considered in the next generation of clinical trials: the law of relative contributions.

Disclosures

ARM has received research support from TG Therapeutics, Pharmacyclics, Abbvie, Adaptive Biotechnologies, Johnson and Johnson, Acerta / AstraZeneca, DTRM BioPharma, Sunesis, BeiGene, Genentech, Genmab, Janssen and Loxo Oncology, Nurix; and has provided advisory, consultancy or data safety and monitoring board services for TG Therapeutics, Pharmacyclics, Adaptive Biotechnologies, Abbvie, Johnson and Johnson, Acerta / AstraZeneca, DTRM BioPharma, Sunesis, AstraZeneca, BeiGene, Genentech, Janssen and Loxo Oncology. LER has received research support from Pfizer, Loxo Oncology, and Aptose Biosciences; has served as a consultant for AbbVie, AstraZeneca, Beigene, Janssen, Loxo Oncology, Pharmacyclics, Pfizer, TG Therapeutics, and Viam group; and holds minority ownership interest in Abbott Laboratories.

Contributions

Both authors contributed equally.

References

1. Moreno C, Greil R, Demirkan F, et al. First-line treatment of chronic lymphocytic leukemia with ibrutinib plus obinutuzumab versus chlorambucil plus obinutuzumab: final analysis of the randomized, phase III iLLUMINATE trial. *Haematologica*. 2022;107(9):2108-2120.
2. Woyach JA, Ruppert AS, Heerema NA, et al. Ibrutinib regimens versus chemoimmunotherapy in older patients with untreated CLL. *N Engl J Med*. 2018;379(26):2517-2528.
3. Burger JA, Sivina M, Jain N, et al. Randomized trial of ibrutinib vs ibrutinib plus rituximab in patients with chronic lymphocytic leukemia. *Blood*. 2019;133(10):1011-1019.
4. Sharman JP, Egyed M, Jurczak W, et al. Acalabrutinib with or without obinutuzumab versus chlorambucil and obinutuzumab for treatment-naïve chronic lymphocytic leukaemia (ELEVATE TN): a randomised, controlled, phase 3 trial. *Lancet*. 2020;395(10232):1278-1291.
5. Kater A, Owen C, Moreno C, et al. Fixed duration ibrutinib and venetoclax (I+V) versus chlorambucil plus obinutuzumab (CLB+O) for first-line (1L) chronic lymphocytic leukemia (CLL): primary analysis of the phase 3 GLOW study. *HemaSphere*. 2021;5(S2):LB1902.
6. Sarraf Yazdy M, Mato AR, Cheson BD. Combinations or sequences of targeted agents in CLL: is the whole greater than the sum of its parts (Aristotle, 360 BC)? *Blood*. 2019;133(2):121-129.
7. Brewer JR, Chang E, Agrawal S, et al. Regulatory considerations for contribution of effect of drugs used in combination regimens: renal cell cancer case studies. *Clin Cancer Res*. 2020;26(24):6406-6411.
8. Gribben JG, Jurczak W, Jacobs RW, et al. Umbralisib plus ublituximab (U2) is superior to obinutuzumab plus chlorambucil (O+Chl) in patients with treatment naïve (TN) and relapsed/refractory (R/R) chronic lymphocytic leukemia (CLL): results from the phase 3 Unity-CLL study. *Blood*. 2020;136:37-39.

Diagnosis of immune thrombocytopenia, including secondary forms, and selection of second-line treatment

James B. Bussel¹ and Christine A. Garcia²

¹Weill Cornell Medicine, Division of Hematology-Oncology, Department of Pediatrics, New York, NY and ²Weill Cornell Medicine, Division of Hematology and Medical Oncology, New York, NY, USA

Correspondence: J.B. Bussel
jbussel@med.cornell.edu

Received: February 23, 2022.

Accepted: June 7, 2022.

Prepublished: June 16, 2022.

<https://doi.org/10.3324/haematol.2021.279513>

©2022 Ferrata Storti Foundation

Published under a CC-BY-NC license



Abstract

This article summarizes our approach to the diagnosis of immune thrombocytopenia (ITP), its secondary forms, and choice of second-line treatment options. We very briefly summarize first-line treatment and then utilize a case-based approach. We first explore persistent, chronic ITP in a younger female. We consider many possibilities beyond primary ITP e.g., hypogammaglobulinemia, chronic infection, and anemia, and how to approach their diagnosis and management. The journey continues throughout pregnancy and the post-partum period and eventually includes fourth-line treatment after a late relapse. We then consider an older male, emphasizing differences in diagnostic considerations and management. The focus is on initiation and continuation of second-line treatment, the pros and cons of each option, and briefly the impact of treatment choices related to the endemic presence of severe acute respiratory syndrome coronavirus 2. During the review of potential second-line treatment options, we also briefly touch upon novel treatments. Finally, there is a short section on refractory disease drawn from our previous extensive review published in February 2020.¹ The clinical nature of the discussions, replete with figures and tables and with the interspersed pearls regarding efficacy and toxicity at different ages and genders, will serve the reader in the management of “typical” adult patients who develop persistent and chronic ITP.

Introduction

Immune thrombocytopenia (ITP) is a complicated disease because of its heterogeneity and lack of diagnostic markers making selection of treatment difficult. Perhaps the most straightforward part of management is at presentation of ITP. If the platelet count is very low and no other findings are present, the worldwide consensus treatment is steroids. Whether dexamethasone, prednisone/prednisolone (prednis[ol]one), or intravenous (IV) methylprednisolone is used, the response rate and side effects are relatively predictable. IV methylprednisolone or dexamethasone increases the platelet counts faster and may have fewer side effects than have weeks of prednis(ol)one treatment.² Questions revolve around whether to add IV immunoglobulin (IVIG), and/or platelet transfusion. While the latter is rarely appropriate if there is serious bleeding and/or the diagnosis is unclear, an analysis based on medical records in the USA identified that as many as 25% of ITP patients receive platelet transfusion,³ which is far too many.

The management of ITP becomes more complicated if

other findings arise, if patients do not respond to steroids, or if patients continue to require treatment. Both the American Society of Hematology guidelines and an international consensus report emphasize that continued steroid use beyond 6 weeks is to be avoided.^{4,5} Compliance with this strong recommendation entails earlier use of “second-line” therapy in patients with ITP, a practice already gaining traction. However, the definition of “early” remains fluid; “early” can be at 1 month of steroid treatment to allow discontinuation of steroids. “Early” can also be in the first 3 months when ITP is “newly diagnosed.”⁶ These ill-defined distinctions are one reason for substantial variation in the management of ITP. Another is the uncertainty of diagnosis. A third, the focus of this discussion, is how to select second-line treatment.

This review focuses on the initiation of second-line treatment reviewing the pros and cons of different agents utilizing a case-based approach by first exploring ITP in a young female and continuing throughout her pregnancy. The review then outlines diagnostic considerations and management in an older male with particular attention to secondary ITP in both patients.

Section I. A young female patient with immune thrombocytopenia: second-line treatment options

The patient's history

A 20-year-old female returns home from college. She notes heavier periods and easy bruising. Her internist sees that she is pale and has visible petechiae on her arms. Complete blood counts show mild anemia (hemoglobin 10.2 g/dL) and thrombocytopenia with a platelet count of $5 \times 10^9/L$. The internist sends her urgently to the emergency room concerned that she might possibly have leukemia. There is no hepatosplenomegaly or lymphadenopathy or other abnormal findings on physical examination.

Review of a peripheral blood smear reveals no blasts or abnormalities of other cell lines although her mean corpuscular volume is low (72 fL) and several of her very few platelets are large. She is diagnosed with ITP and given prednisone 1 mg/kg. Over the next few days, she has typical steroid-related side effects: feeling "a little crazy", insomnia and abdominal pain. Her bruises and petechiae disappear, and her period ends. Her hematologist prescribes oral iron supplements and changes her prednisone to dexamethasone 40 mg daily for 4 days. Her steroid-related side effects worsen during the 4 days on dexamethasone 40 mg; however, she soon feels better with no further petechiae, bruising, or menstrual bleeding noted. Her platelet count normalizes to $147 \times 10^9/L$ and her hemoglobin improves to 11.2 g/dL. She begins checking her blood counts monthly. The improved complete blood count with a nearly normal mean corpuscular volume excludes bone marrow failure, and also thalassemia trait or microangiopathic hemolytic anemia. Similarly, the normal hemoglobin and neutrophil count do not suggest Evans syndrome. Her platelet counts remain in the normal range and her hemoglobin improves to the normal range. At her next visit, her platelet count has decreased to $80 \times 10^9/L$. One month later, her platelet count is $28 \times 10^9/L$ with continued normal hemoglobin and infrequent small bruises. With her platelets trending downward, second-line treatment for her ITP is considered.

There is less urgency to consider secondary ITP or a missed diagnosis since she is doing well but at any change of management, it is good practice to re-evaluate. Below we consider some of the "what if" clinical scenarios for this young female.

What if the patient is persistently anemic despite iron supplementation?

If the mean corpuscular volume is low, consider workup for underlying thalassemia trait or iron deficiency with the latter being common in the setting of heavy menses. Iron replacement is not always straightforward; using oral re-

placement every other day may be equally effective as daily administration.⁷ Resorting to IV iron may be important especially if oral replacement does not correct iron status and/or there are signs of a chronic inflammatory disease. If the mean corpuscular volume is high, bone marrow failure must be considered. There could also be pernicious anemia secondary to vitamin B12 deficiency or an autoimmune hemolytic anemia, such as Evans syndrome. Another possibility is microangiopathic anemia with thrombocytopenia, whether in the form of thrombotic thrombocytopenic purpura or hemolytic uremic syndrome. In these cases, there would likely be increased reticulocytosis. While individually each of these conditions is rare, having one of many rare conditions would not be as surprising.

If heavy menstrual bleeding persists, a progesterone-based approach is superior to an estrogen-based approach in women with ITP as the former raises the platelet count.⁸ While estrogen-based therapies are more commonly used in general practice for heavy menstrual bleeding, they might worsen ITP.⁹ In contrast, progestational agents have previously been tried as treatment in ITP with good effect. Progesterone may be administered orally at a dose of 5-10 mg daily or medroxyprogesterone acetate (Depo-Provera) can be given intramuscularly once every 3 months but the latter may result in intermittent vaginal bleeding.

What if the immune thrombocytopenia is part of a larger spectrum of autoimmune disease?

Our patient's immunoglobulins were normal, so she does not have common variable immunodeficiency (CVID) or IgA deficiency. Neither the diagnosis of CVID nor that of IgA deficiency requires a history of infections; in fact, there may be a history of autoimmunity, especially in a patient presenting with ITP, or allergy. Furthermore, the diagnosis of CVID is often not made until after the age of 30.¹⁰ The IgG level does not have to be very low in cases of CVID presenting as ITP, which may account for the lack of infectious history in many of these patients. In cases of CVID, and possibly systemic lupus erythematosus with ITP, there may have been an episode of ITP years before treated with steroids, with the patient having gone into remission for years without any medication (Charlotte Cunningham-Rundles, *personal communication*). Other immunodeficiency states are also associated with ITP, not all of which will include hypogammaglobulinemia.¹¹

Given our patient's age and gender, it would not be surprising if she was positive for antinuclear antibodies and was developing systemic lupus erythematosus. A study from France suggests that hydroxychloroquine may be considered in an ITP patient positive for antinuclear antibodies.¹² Nor would it be surprising if her thyroid tests were abnormal, as thyroid disorders in young women with ITP are usually autoimmune.¹³⁻¹⁶ In a young woman, there is a relatively high rate (as high as 5-10%) of abnormalities

of thyroid function and this finding may be more frequent in women with ITP. The question remains of whether these conditions should be tested for in all patients or only if there are suggestive findings. If the patient is fatigued that would necessarily instigate an evaluation of underlying causes that would include hypothyroidism. Fatigue and depression are relatively common but poorly understood in ITP,¹⁷ thus requiring comprehensive evaluation.

What if the immune thrombocytopenia is secondary to a subclinical viral infection?

Multiple viruses have been associated with ITP. In children, ITP is often thought to be a post-infectious sequela. There may also be an underlying viral disease which is asymptomatic and thus eludes detection. It remains unclear whether all patients with ITP should be screened for hepatitis C and human immunodeficiency virus; with the coronavirus pandemic, it might be appropriate to screen for severe acute respiratory syndrome coronavirus-2 (SARS-CoV-2).¹⁸ Treatment of these three viral infections would alter ITP management. The primary treatment for both hepatitis C and human immunodeficiency virus would likely increase the platelet count. However, if hepatitis C has progressed to cirrhosis, the platelet effects of antiviral treatment may be limited. Another viral infection that could be subclinical is cytomegalovirus which might be revealed only by atypical lymphocytes and/or mildly elevated liver tests. Cytomegalovirus can worsen ITP in patients receiving immunosuppressive treatments because these agents will activate the cytomegalovirus and thus worsen the ITP making it more resistant to treatment.^{19,20} *Helicobacter pylori* may “cause” ITP, but only in certain places, e.g., Japan and Italy, is searching for it at diagnosis of ITP routine and is its eradication a uniformly effective approach to ITP.²¹

What if the patient has an inherited thrombocytopenia?

Our patient’s bleeding resolved in parallel with the improvement of her platelet count, which suggests that she does not have platelet dysfunction, as seen in Bernard-Soulier or Wiskott-Aldrich syndrome. Furthermore, she does not have any syndromic features consistent with an inherited thrombocytopenia. Review of her prior records revealed that she has had at least one prior normal platelet count.

The stability of her blood counts after initial treatment excludes cyclic thrombocytopenia which is an often-forgotten form of inherited thrombocytopenia.²² There are very many forms of inherited thrombocytopenia and new ones seem to be discovered regularly. Certain features should suggest an inherited thrombocytopenia:^{23,24} (i) other family members with thrombocytopenia; (ii) no past normal platelet count; (iii) too many too large platelets on a blood smear (not all inherited thrombocytopenias have

macrothrombocytes but most do); (iv) features of a syndrome such as thrombocytopenia-absent radius syndrome; (v) failure to respond to treatment for ITP, such as IVIG and steroids; (vi) bleeding out of proportion to the platelet count e.g., Bernard-Soulier syndrome, Wiskott-Aldrich syndrome, RUNX-1 mutations; and (vii) a relatively stable platelet count. In the absence of an apparent specific syndrome, whole exome screening may be helpful, although this approach is effective in less than half of such cases.²⁵ Ideally this possibility would be explored in conjunction with an experienced geneticist. The importance of making a precise diagnosis is not limited to the management of the platelet count *per se*, but extends to the associated medical problems including a possible propensity to autoimmune conditions, malignancy, or bone marrow aplasia.

What if the immune thrombocytopenia is secondary to other blood disorders?

While chronic lymphocytic leukemia and myelodysplastic syndrome would be very unlikely in our patient given her young age, other clinical conditions could be present, such as autoimmune lymphoproliferative syndrome and systemic lupus erythematosus. It has not yet been decided which tests should be performed to search for specific conditions, particularly if there are not specific symptoms or conditions suggesting a particular entity. We assay immunoglobulin levels and do thyroid tests in our patients, as we certainly did in this young woman. Ideally in the future there would be an established panel of tests for patients with putative ITP which would explore inherited thrombocytopenias, bone marrow failure, secondary ITP, other diagnoses that could resemble ITP such as myelodysplastic syndrome, markers of the future course of the ITP, the degree of bleeding, and to which treatments the patient would respond best.

What is the optimal second-line treatment for a young female with immune thrombocytopenia?

There are numerous options that can be considered in this non-pregnant premenopausal female (Table 1)

Rituximab

Rituximab and other (generic) anti-CD20 monoclonal antibodies exert immunosuppressive effects by depleting B lymphocytes. This occurs uniformly in the blood and bone marrow but what happens to B cells in lymph nodes is not well-defined. Women under the age of 40 years with a less than 2-year history of ITP usually respond to rituximab, with the response rate and especially the “cure” rate being high.²⁶ If our patient and her hematologist opt for rituximab, she would receive four infusions of 375 mg/m² weekly for 4 weeks. If she has a good response, close monitoring may not be needed. While studies have not de-

Table 1. Comparing second-line treatment options in non-pregnant premenopausal females.

Treatment options	Pros	Cons
Rituximab	High likelihood of good response in both short and especially long term (>50%)	Risk of first-infusion reaction which can be mitigated by steroids COVID vaccination not possible for 6-12 months Very rare risk of PML ⁴⁵ Risk of hypogammaglobulinemia with rituximab + dexamethasone 10-20% with possible need for short-term IgG-replacement IVIG
TPO-RA: Eltrombopag Romiplostim Avatrombopag	Very high response rate (70-80%)	Risk of thrombosis (increased with OCP, underlying APLA, other prothrombotic causes) which usually occurs in 1 st year of use Pain from headache-myalgia may occur Abnormal liver function, especially for eltrombopag which also needs very strict ingestion on empty stomach
Splenectomy	High long-term response rate (60-70%)	Risk of perioperative bleeding, VTE, intracellular infection, sepsis Need to vaccinate at least 15 days prior to surgery ⁸⁸ Revaccination schedule unknown
Fostamatinib	Overall response 43% in first 12 weeks on treatment, time to response 15 days ⁴⁷	Side effects: hypertension, nausea-diarrhea, dizziness, ALT increases Clinically meaningful responses in patients with failure of splenectomy, TPO-RA and/or rituximab ⁴⁵
Immunomodulatory agents: azathioprine, mycophenolate mofetil, cyclosporine, dapsone, cytoxan	Many years of usage in some cases e.g., azathioprine, Attacks pathophysiology of autoimmune disease	Usually slow responses, which can take 1-3 months to develop without predictability Various individual toxicities: Cyclosporine - neurological and renal Azathioprine and danazol – liver abnormalities Danazol - facial hair and acne MMF-headache, gastrointestinal Dapsone - hemolysis

COVID: coronavirus disease 2019; PML: progressive multifocal leukoencephalopathy; IVIG: intravenous immunoglobulin; TPO-RA: thrombopoietin receptor agonist; OCP: oral contraceptive pills; APLA: anti-phospholipid antibody; VTE: venous thromboembolism; ALT: alanine aminotransferase; MMF: mycophenolate mofetil.

terminated the optimal dose, 375 mg/m² once a week for 4 weeks is the most commonly used dosing regimen. The addition of dexamethasone to the rituximab may provide an extra “curative” effect via the former’s anti-plasma cell effect, although it also increases the risk of hypogammaglobulinemia. Administration of dexamethasone would reduce the first-infusion side effects of rituximab, and our patient could stop the steroid after one or two cycles if she does not tolerate it well instead of completing three cycles.

It is prudent to check immunoglobulin levels to rule out COVID and a hepatitis B panel prior to starting rituximab. The risk of coronavirus disease 2019 (COVID) and delayed vaccination are in addition to other potential side effects such as first-infusion reactions, serum sickness, and even the very rare possibility of progressive multifocal leukoencephalopathy. If dexamethasone and rituximab are combined, there is a 10-20% possibility of developing hypogammaglobulinemia which may necessitate IVIG for a few months even in patients who start out with normal immunoglobulin levels. Combining this problem with the

issue of the patient being unable to undergo vaccination for COVID reduces the benefit/risk ratio of rituximab treatment substantially, despite its curative potential. If the coronavirus pandemic wanes, this may be less of a consideration.

If treatment with rituximab is delayed too long in this woman, the chance of “cure” may be reduced. Her immunoglobulin levels are normal and she does not have hepatitis B surface antigen, so the risks of aggravated hepatitis B and hypogammaglobulinemia are less substantial. Lucchini *et al.* provide more information on the place of rituximab treatment in ITP.²⁷

Whether because of vaccination and/or infection, the current COVID pandemic is affecting ITP management and may have an impact on patients who are on second-line ITP treatment options. Guidelines on post-infection or vaccination ITP treatment are summarized in Table 2. Our patient should be vaccinated against SARS-CoV-2 at least 5-8 weeks before initiating rituximab in order to have time to receive and fully respond to both doses of Moderna and Pfizer vaccines. It might be optimal to wait a little longer

Table 2. Considerations regarding severe acute respiratory syndrome coronavirus-2 and second-line treatments for immune thrombocytopenia.

Second-line option	COVID Infection	SARS-CoV-2 vaccination prior to initiation of ITP second-line treatment	SARS-CoV-2 vaccination after ITP second-line treatment
Rituximab	Limited information on effects of rituximab during active COVID infection ⁸⁹ Patients may be good candidates for administration of anti-SARS-CoV-2 antibodies via convalescent plasma or engineered monoclonal antibodies ⁴⁴	Vaccinations should be given prior to starting rituximab e.g. Moderna a minimum of 5 weeks prior, Pfizer a minimum of 6 weeks prior	If not vaccinated prior to starting rituximab, need to wait to be vaccinated until 6-12 months after completion of last rituximab dose ²⁸
TPO Agents	Risk of thrombosis ²⁹		
Fostamatinib	Potentially useful in COVID infections independent of platelet function ⁴⁷		
Immunomodulatory agents	Patients may be good candidates for administration of anti-SARS-CoV-2 antibodies via convalescent plasma or engineered monoclonal antibodies ⁴⁴	Vaccination is recommended at least 2-4 weeks prior to starting immunosuppressive agents ⁴⁴	If the patient is receiving or has received immunosuppressive therapy, consider vaccination 6 months after the patient has been taken off therapy to increase the likelihood of developing immunity ⁴⁴
Splenectomy *Recommend screening for COVID infection prior	Urgent administration of IV antibiotics is mandatory until bacterial cultures are documented as negative, even if the fever is attributed to proven or suspected SARS-CoV-2 infection ⁴⁴	Vaccination is recommended at least 2-4 weeks prior to the planned splenectomy ⁴⁴	Splenectomized persons and those who had received five or more prior lines of therapy were at highest risk of ITP exacerbation ²⁹

COVID: coronavirus disease 2019; SARS-CoV-2: severe acute respiratory syndrome coronavirus-2; ITP: immune thrombocytopenia; TPO: thrombopoietin; IV: intravenous.

afterwards to sustain the vaccine effect. If the patient is not vaccinated prior to rituximab treatment, she will not be able to be vaccinated against SARS-CoV-2 for at least 6 if not 12 months;²⁸ this would also apply to a booster vaccination (Table 2). The vaccination might affect her platelet count although she is not in a high-risk group which includes those who have had a prior splenectomy and/or five or more lines of previous ITP treatment.²⁹ There is limited information on the risk of developing severe COVID in ITP patients undergoing rituximab therapy. In COVID and especially agammaglobulinemia patients, the ability to clear the SARS-CoV-2 virus may be limited, and a patient may remain polymerase chain reaction-positive for weeks or even months.

On the one hand, rituximab with dexamethasone seems a good treatment option because, if she responds well to the four weekly infusions, she can be checked relatively infrequently afterward. On the other hand, the effects on response to SARS-CoV-2 vaccination are clinically signifi-

cant. There appears to have been a marked decrease in rituximab use in ITP since the onset of the COVID pandemic.

Other immunomodulators

Previously, immunomodulatory agents were widely used second-line treatments, but drawbacks include the need to wait 1-3 months for the platelet count to increase, side effects (depending on the agent) such as hepatic toxicity, and the need to take these medications consistently long-term.⁵ If a single agent is used, the risk of infection despite the immunosuppression seems very small, but for these agents, efficacy is less than 50%. This group is lumped together as if all agents are the same; it potentially includes mycophenolate mofetil, danazol, dapsone, azathioprine, cyclosporine, and cyclophosphamide.

Recently, a randomized controlled trial of steroids given with or without mycophenolate mofetil within 1 week of the diagnosis of ITP showed that the “cure” rate was

higher in the combination arm.³⁰ One surprise was that quality of life was significantly lower among patients treated with the combination despite them having a better platelet response. Another surprise was that more than 50% of patients on the steroid-alone arm were cured despite a low rate of dexamethasone usage and that 27% of the patients were over 65 years of age. The study nonetheless highlighted the potential advantage of earlier use of second-line treatment.

There are at least 20 studies of danazol, almost all of which demonstrated a positive effect on platelet counts; this drug induces facial hair and acne and may be toxic to the liver. Dapsone, beyond an immunosuppressive effect, induces hemolysis which mimics IV anti-D; in patients with glucose-6-phosphate dehydrogenase deficiency, the hemolysis can be severe. Azathioprine has a long-standing history of use in ITP and a contributing safety base in pregnancy in patients taking it following kidney transplantation; it may cause hepatic toxicity in 1%. We reported on its combination with danazol, with good results in 13 of 17 difficult-to-treat patients.³¹ Cyclosporine repolarizes cell membranes, which shuts down cell membrane pumps that extrude therapeutic agents from the cell. This may reinstate the effect of certain treatments e.g., steroids. Finally, cyclophosphamide can be given IV or orally. The best results appear to occur when using it IV in two or three infusions.³² Mechanistic information supporting the use of cyclophosphamide is that it has anti-plasma cell effects and that it spares megakaryocytes and platelets. Cyclophosphamide does, however, have well-known substantial side effects: hematuria, bladder fibrosis, immunosuppression, and nausea and vomiting.

Thrombopoietin receptor agonists

Another option for second-line therapy would be a thrombopoietin receptor agonist (TPO-RA). The primary advantages of these drugs are the high response rate and low likelihood of induction of malignancy or other irreversible toxicity. The primary toxicity is development of venous and arterial thrombosis. If our young female patient were on birth control, there may be an added risk of thrombosis.

There are three TPO-RA currently available in the USA and Western Europe: romiplostim,³³ eltrombopag³⁴ and avatrombopag;³⁵ their efficacy and toxicity have been outlined in a recent review, including discussion of class effects such as headache, myalgia, and thrombosis.³⁶ The mechanisms of effect of these agents differ by where they bind to the thrombopoietin receptor, in RNA upregulation of transcription factors by romiplostim and eltrombopag,³⁷ and by the essential role of intracellular iron chelation by eltrombopag.³⁸ The clinical importance of these mechanistic differences is “confirmed” by “switch studies” in

which one of romiplostim or eltrombopag was effective when the other was not.^{39,40} Recent studies demonstrated that switching from one of these two TPO-RA to avatrombopag was also often effective.^{29,41} Toxicity and efficacy do not differentiate the three agents substantially, although one article suggests that romiplostim maintains efficacy at higher endogenous thrombopoietin levels than does eltrombopag²⁹ and eltrombopag is thought to be associated with higher rates of transaminitis.^{34,36}

Eltrombopag. Eltrombopag is an oral TPO-RA which requires a very empty stomach ideally 2 hours before and after taking it, which is intimately related to its requirement to chelate intracellular iron as an integral part of its mechanism of effect.³⁸ If eltrombopag has chelated calcium or iron during ingestion, it cannot chelate intracellular iron and will, therefore, be ineffective. Liver function tests must be monitored in patients taking eltrombopag, as hepatotoxicity is considered common (1-10%) and 3% of adults and children cannot tolerate eltrombopag for this reason.³⁶

Romiplostim. Because romiplostim is injected subcutaneously weekly, there are no issues of absorption or doubts about compliance. There may be more cycling of the platelet count as compared to that with the oral TPO-RA, likely because of romiplostim’s weekly instead of daily administration. As with all the TPO-RA, making small changes in dosing will limit the likelihood of cycling. Development of antibodies, neutralizing and non-neutralizing, to romiplostim is more common in children than in adults;⁴⁴ however, these antibodies have surprisingly little effect on clinical efficacy for reasons that are not clear. Myalgia may be more common with romiplostim. As of writing, romiplostim can be self-injected by patients in Europe but not in the USA.

Avatrombopag. Avatrombopag, a second oral TPO-RA, has the least data describing its use. It is taken once daily using only tablets of 20 mg with dose ranges from 20 mg by mouth once a week to 40 mg (2 tablets) daily. There are very limited data on long-term usage. In one study, avatrombopag was associated with a 16.5% incidence of thrombosis but this was likely an artifact resulting from the small numbers of patient.⁴² Two recent studies testified to the effect of avatrombopag in patients not responding to romiplostim and/or eltrombopag.^{29,41} It is recommended that this TPO-RA is taken with food so that its absorption is more consistent.

There is much to recommend the use of a TPO-RA in our young woman.^{43,44} There is no reason to suspect that such an agent would have an adverse impact on the clinical course of COVID if an infection were to occur although there may be an additive risk of thrombosis.²⁹ In the COVID pandemic, the oral agents would be preferred over romiplostim to lessen exposure to SARS-CoV-2 secondary to weekly attendance at an outpatient department. Local

laboratory counts and virtual visits lessen this risk for patients; home nursing visits for injections would do the same.

Fostamatinib

Fostamatinib is a first-in-class, orally active spleen tyrosine kinase (Syk) inhibitor indicated for the treatment of ITP. The primary studies underestimated its efficacy, probably because the median duration of ITP in the trial population was more than 8 years and in 47% of patients a TPO-RA had failed.^{45,46} While the starting dose is 100 mg twice daily, 89% of responders increased to 150 mg twice daily. Long-term use and *in vitro* experiments have suggested that fostamatinib is anti-thrombotic but not pro-hemorrhagic because blocking Syk reduces signaling via the C-type lectin-like type II transmembrane receptor (CLEC2) and glycoprotein VI (GPVI) pathways. These two pathways have less redundancy in thrombosis than in control of bleeding. Fostamatinib is also thought to be anti-inflammatory and potentially useful in COVID, independently of any platelet effects.⁴⁷ On the other hand, of all approved second-line agents for ITP, it may be the least tolerable. It increases blood pressure in most recipients and there are relatively frequent gastrointestinal effects, including nausea with very occasional vomiting and the development of diarrhea; 5% of patients may develop transaminitis. There has not been evidence of increased frequency or severity of infections in association with fostamatinib use even though Syk is present in macrophages as well as in B cells and in other cells.

Splenectomy

The American Society of Hematology guidelines and international consensus report recommend that splenectomy be delayed to at least 1 year after the diagnosis of ITP, since the rate of resolution of ITP within the first 1-3 years of disease appears substantial even in adults.^{4,5} Laparoscopic splenectomy is infrequently complicated by perioperative problems; response rates are initially 80% which relapse reduces to 60%. Late relapse beyond 2 years after splenectomy is very uncommon. Whether delaying splenectomy reduces its efficacy is a concern; a recent study from France⁴⁸ suggests that efficacy is maintained, and some patients responded better to TPO-RA after splenectomy.

There are long-term risks of adverse effects of splenectomy which are clinically significant, including not only overwhelming sepsis but also thrombosis, especially stroke. The risk of sepsis is based on less efficient blood stream phagocytosis and is exacerbated by low antibacterial antibody levels. Pneumococci are a more frequent cause of post-splenectomy sepsis than all other infections

combined.⁴⁹ Following splenectomy, individuals also have an elevated risk of infections by encapsulated Gram-negative pathogens, e.g., *Capnocytophaga canimorsus* and *Bordetella holmesii*, as well as intraerythrocytic parasites, such as malaria and *Babesia*, as noted in a recent review of post-splenectomy infections.⁵⁰

Providing patients appropriate and timely immunization for pneumococci, *Hemophilus influenzae B*, and meningococcus, antibiotic prophylaxis, education, and prompt treatment of infection mitigates this risk;⁵¹ when to repeat pneumococcal and other vaccinations remains unclear. While vaccination appears more effective if given at least 2 weeks prior to splenectomy, vaccination can be administered after splenectomy if there is not time before the splenectomy or if vaccination would likely be ineffective because the patient is receiving high-dose immunosuppression or has recently received rituximab.

The risk of post-splenectomy thrombosis was not initially appreciated. Population studies using a Danish registry identified this risk, particularly with regard to stroke, with confirmation in other populations, e.g., the Nurses' Health Study.⁵² Splenectomy for hemolytic anemias has been complicated by pulmonary hypertension, with mitigation by partial splenectomy and reduction in the use of splenectomy. Partial splenectomy may "hit the sweet spot" by reducing red blood cell phagocytosis but maintaining enough phagocytosis to prevent pulmonary hypertension and sepsis. The apparent absence of pulmonary hypertension after splenectomy for ITP suggests that partial splenectomy, like splenic embolization and radiation, is very rarely if ever used.

How we treated the young woman with immune thrombocytopenia

As this woman could not taper her prednisone successfully, still had bleeding, and had a platelet count $<20 \times 10^9/L$, she met the criteria to receive a second-line treatment. After the considerations provided above and with her primary ITP, she opted for a TPO-RA which was based on her fear of COVID and need for vaccination and being in the first year of her disease. She chose to reserve rituximab, fostamatinib and immunosuppressives. She took a TPO-RA for a year and then was gradually able to discontinue it. She maintained a platelet count of $60-90 \times 10^9/L$ on no treatment for several years without manifestations of bleeding. She was not troubled by fatigue or heavy menstrual bleeding.

Section II. Immune thrombocytopenia in pregnancy

Years later, our patient becomes pregnant.

What are the treatment considerations for our patient during pregnancy?

As ITP is common in women of reproductive age, it is not surprising that it may complicate the course of pregnancy. For pregnant women with known ITP, management changes throughout the course of pregnancy.⁵³ Figure 1 reviews treatment options available during each trimester, leading up to delivery and the post-partum period. In the first trimester of pregnancy, platelet counts may spontaneously increase, apparently because of the increased progesterational hormones in the first trimester.⁵⁴ For this reason, relatively few women with ITP require treatment in the first trimester, which is fortunate

from a teratogenic point of view. Risk of cleft palate from steroid use in the first trimester appears to be small. In the second and especially third trimesters, platelet counts decrease even in healthy women without ITP, resulting in “gestational” thrombocytopenia.⁵⁵ Three large series suggest that the prevalence of gestational thrombocytopenia at the end of pregnancy is between 6.6% and 11.6%.⁵⁶⁻⁶⁰ This has been attributed to increased volume of distribution in the later stages of pregnancy as well as “consumption”. Recently, work from China presented at the 2021 European Hematology Association Congress hypothesized that very high estradiol levels towards the end of pregnancy inhibit platelet

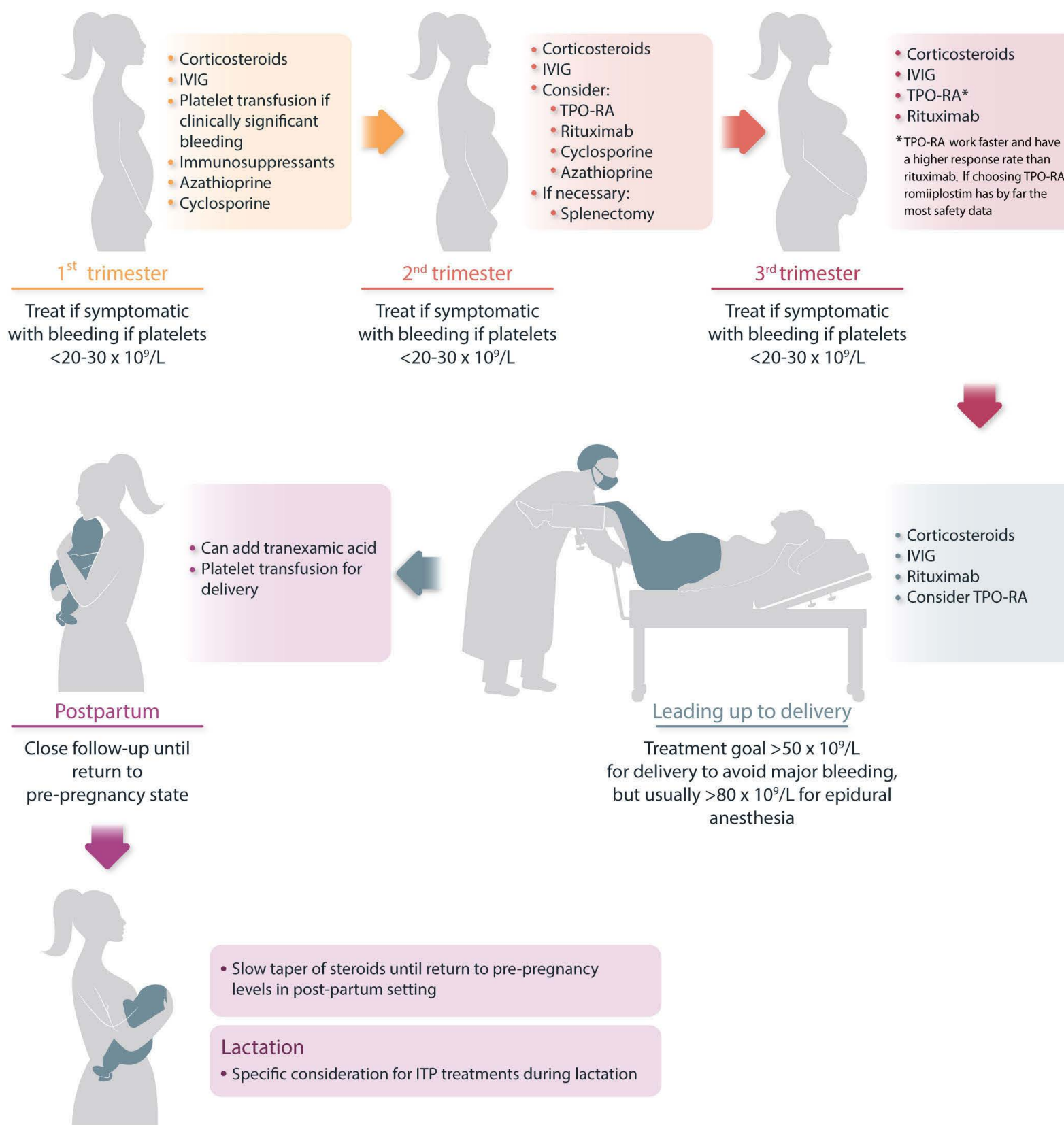


Figure 1. Treatment options for immune thrombocytopenia during pregnancy, leading up to delivery, and in the post-partum period. IVIG: intravenous immunoglobulin; TPO-RA: thrombopoietin receptor agonist; ITP: immune thrombocytopenia.

Table 3. Considerations regarding treatment options for immune thrombocytopenia during pregnancy.

Treatments (Drug category) Dosing regimen [FDA category]	Considerations for mother	Risks to fetus	Evidence for use in pregnancy/ effect on lactation
Prednisone (Steroid) 10-20 mg daily. Increase if necessary to 1 mg/kg [C]	Usually the first agent to use Risk of diabetes, weight gain, acne, hypertension, osteoporosis,	Very low risk of cleft palate from steroid use in first trimester(53).	Very low concentrations in maternal milk and without biological effect ⁹⁰
Dexamethasone (Steroid) High dose, 40 mg per day x 4 days [C]	Low cost, ease of administration	Dexamethasone can cross the placenta. Slight increased risk of premature rupture of fetal membranes and abruptio placentae.	50% response ⁶⁴
IVIg (Intravenous immunoglobulin) Standard dose 400-1000 mg/ kg/day for 1-5 days	Can be given first line, Initially good response but often decreases with repeated use Aggravates fluid retention and hypertension Can be used to increase platelet counts initially while awaiting low dose prednis(ol)one Can be used for delivery but needs to be scheduled (timed rupture of membranes) Can worsen pregnancy-associated heada- che, malaise, infusion reactions, aseptic me- ningitis, fluid overload		Very low concentrations in maternal milk and without biological effect ⁹⁰
Rituximab (Monoclonal antibody) 375 mg IV/ weekly x 4 [C]	Use only for very severe cases ⁵	Can cross placenta like any IgG Risk of B-cell depletion in neonates, perinatal and neonatal immunosuppression and sub- sequent infection	40-60% response rate within 1-8 weeks ⁶⁶
Anti-RhD (Blood group Rhod anti- body) IV 50-75 µg/kg [C]	Can be used in refractory cases Risk of hemolysis and anemia Less expensive, shorter infusion time than that for IVIG	Risk of neonatal jaundice, anemia, and direct antiglobulin test positivity Given routinely for HDFN prophylaxis but at 1/10 th the ITP dose	>70% of cases in a small series (n=8) ⁶⁷
Azathioprine (Immunomodulator) Variable dosing [D]	Increased risk of preterm birth	Can cross placenta, noted to have increased prematurity rate, lower birth weight, IUGR. No malformation risks across several studies Immune impairment reported in some expo- sed infants ⁶⁹	Several studies and large case series follow- ing renal transplantation, for autoimmune conditions ⁶⁸ Compatible with lactation

continued on following page.

Cyclosporine (<i>Immunomodulator</i>) Variable dosing [C]	For refractory cases No significant toxicity to mother or fetus when used in pregnancy for inflammatory bowel disease, possible increased risk of preterm birth	Increased risk of IUGR ⁷⁰	No published experience in ITP in pregnancy, but used for inflammatory bowel disease ⁹¹ Present in breast milk
Romiplostim (<i>TPO-RA</i>) [FDA category not assigned]	Risk of maternal thrombocytosis Increased risk of VTE		Case reports with safety data from women with ITP in pregnancy ⁷³
Eltrombopag (<i>TPO-RA</i>) Start at 25-50 mg PO daily and increase as needed [C]	Very limited data requires a very empty stomach (ideally 2 hours before and after taking it), elevated liver enzymes		Case reports in pregnancy If in breast milk, potentially may be neutralized by calcium
rhTPO [FDA category not assigned, available in China]	No overt maternal toxicity	Infants followed until 1 year did not have any side effects	70% response rate with increase in maternal platelet count in 33 pregnancies ⁷²
Splenectomy (na) For refractory ITP or if significant toxicity with other therapies	Risk of perioperative bleeding, VTE, opportunistic infection, miscarriage, preterm labor and preterm premature rupture of membranes Need to be vaccinated at least 15 days prior to surgery ⁵³	Risks to fetus least in second trimester. Minimal data Transplacental passage of circulating maternal antiplatelet antibodies and the risk of neonatal thrombocytopenia are not affected by splenectomy	88% response rate Few complications in second trimester when least risky to fetus and uterine size may not complicate procedure ⁹²
Tranexamic acid [B, post-partum setting only]		Can reduce the amount of blood loss after delivery, reduces blood transfusion requirements. Low risk of post-partum thrombosis, PE reported in two cases ⁶² .	Used only post-partum. Avoid antepartum due to potential risk of clotting of the placenta

Note on FDA pregnancy categories: (prior to 2015). Category B: animal reproduction studies have failed to demonstrate a risk to the fetus and there are no adequate and well-controlled studies in pregnant women. Category C: animal reproduction studies have shown an adverse effect on the fetus and there are no adequate and well-controlled studies in humans, but potential benefits may warrant use of the drug in pregnant women despite potential risks. Category D: there is positive evidence of human fetal risk based on adverse reaction data from investigational or marketing experience or studies in humans, but potential benefits may warrant use of the drug in pregnant women despite potential risks. FDA: Food and Drug Administration; IV: intravenous; IVIG: intravenous immunoglobulin; HDFN: hemolytic disease of the fetus and newborn; ITP: immune thrombocytopenia; IUGR: intrauterine growth restriction; TPO-RA: thrombopoietin receptor agonist; VTE: venous thromboembolism; PO: per os; rhTPO; recombinant human thrombopoietin; na: not applicable; PE: pulmonary embolism

production.⁶¹ While requiring confirmation, this hypothesis fits with both platelet counts falling and cases of ITP in pregnancy becoming progressively more difficult to treat with steroids and IVIG. Fortunately, there is rarely clinically significant bleeding in pregnant women with ITP unless the platelet counts become very low; one exception may be subchorionic hematomas.

Tranexamic acid can be used after delivery to reduce blood loss in this period and thus reduce blood transfusion requirements. The risk of postpartum thrombosis seems very low, although pulmonary emboli have been reported in two cases.⁶²

Steroids in pregnancy

The standard treatments for ITP during pregnancy are steroids and IVIG (Table 3) which are the most widely used and felt to be the safest. The prednis(ol)one recommendation for ITP in pregnancy, because of the limited duration of anticipated treatment, is relatively low-dose prednisone (e.g., 10-20 mg daily) based on targeting a platelet threshold of 20-30x10⁹/L. Prednis(ol)one often exacerbates physiological changes of pregnancy e.g., hyperglycemia, hypertension, and fluid retention; dexamethasone is to be avoided because of its fetal effects. If this lower dose of prednisone is successful, it avoids the risks of long-term high-dose steroids for the mother. Little to no prednisone enters the fetus because of placental β -11-hydroxylase.⁶³

Intravenous immunoglobulin in pregnancy

IVIG is effective; however, it must be given often e.g., bi-weekly so steroids are the recommended treatment. One study suggests that both steroids and IVIG are slightly less effective in pregnant women.⁶⁴ Overall, whether the efficacy of IVIG and prednis(ol)one in pregnancy is maintained becomes more important later in pregnancy. Patients who are difficult to treat require higher and higher doses of prednisone and more and more frequent IVIG dosing as pregnancy progresses.

The treatment of fetal and neonatal alloimmune thrombocytopenia has provided safety information that may be extrapolated to ITP. 'Aggressive intrapartum treatment' exceeds that of the treatment of ITP by including IVIG 1-2 g/kg/week and prednisone 0.5 mg/kg/day for many weeks. The apparent safety of these very high doses helps to assuage concerns regarding their use in ITP.⁶⁵

Even with less severe ITP, preparing for safe delivery often involves intervention to undergo epidural anesthesia, for which the platelet count is often "required" to be greater than 80x10⁹/L. The requirements for spinal anesthesia may not be as strict and are more variable than they are for epidural anesthesia. Even in a patient who responds well to IVIG and prednis(ol)one combination treatment, a platelet count of 80x10⁹/L or higher is

often achieved for only 2-5 days. If these treatments are relied upon, scheduling elective delivery is crucial so that administration of IVIG can be timed to achieve its optimal effect. The patient could either undergo a Caesarian section or have her membranes ruptured so she enters labor at the desired time. An amniocentesis may be required to assess fetal lung maturity.

Rituximab in pregnancy

In one study of 231 pregnancies with maternal exposure to rituximab for treatment of autoimmune cytopenias and other autoimmune disease, few neonatal infections were seen among the exposed neonates.⁶⁶ Hypogammaglobulinemia will not be present at birth if the mother does not herself have low IgG levels; however, it may manifest at 2 to 4 months of age if there is a persistent absence of infant B cells. Women are encouraged to avoid pregnancy for more than 4-6 months after rituximab exposure to prevent transmission of the rituximab to the fetus.⁶⁶ As shown in Figure 1, we believe that rituximab can be used in patients who do not respond well to steroids and IVIG.

Intravenous anti-D, azathioprine, cyclosporine, and splenectomy in pregnancy

Eight patients were treated with IV anti-D (WinRho) with reasonable efficacy and fetal safety;⁶⁷ no cases of neonatal anemia or hyperbilirubinemia were seen. Azathioprine has been extensively used in women who have undergone renal transplantation and become pregnant.⁶⁸ The registry of these patients suggested that azathioprine is relatively safe during pregnancy, but azathioprine takes 1-3 months to increase the platelet count. Infants of mothers taking azathioprine are noted to have an increased prematurity rate, lower birth weight, and intrauterine growth restriction; no malformations were seen. Immune impairment was reported in some exposed infants.⁶⁹ The effects of cyclosporine in pregnant women with ITP appear to be like those of azathioprine: reasonably effective, slow in onset, and with limited fetal risk. Experience of cyclosporine use in pregnant women has also been gained in the post-transplantation setting.⁷⁰ Mycophenolate is contraindicated in pregnancy.⁷¹ If splenectomy is required, it is recommended that it be performed in the second trimester because the risk to the fetus is less than in the first trimester and the size of the uterus will be less obstructive than in the third trimester. Experience consists of isolated case reports.

Thrombopoietin receptor agonists in pregnancy

A major recent development affecting ITP in pregnancy is the use of thrombopoietin agents. Three sets of evidence for the use of thrombopoietin agents in pregnancy exist beyond scattered case reports. One study used re-

combinant human thrombopoietin (rhTPO, available in China) and evaluated 33 pregnancies in 31 women with ITP in pregnancy who did not respond to or relapsed after an initial response to prednisone.⁷² Seventy percent of the women responded to rhTPO with an increase in the maternal platelet count and no overt maternal toxicity. Importantly, the babies, followed until 1 year of age, did not have any identified side effects of rhTPO treatment. A follow-up compilation of ITP cases explored 13 pregnancies in 12 women, including one who delivered a pair of twins, in whom a TPO-RA was used.⁷³ Usage of TPO-RA was divided equally between eltrombopag and romiplostim and both agents appeared effective and safe. Third, a safety surveillance program report of use of romiplostim in 186 women with ITP who received romiplostim during pregnancy indicated that in over 50 pregnancies with known pregnancy outcomes and in over 50 pregnancies with known birth outcomes, romiplostim appeared safe.⁷⁴ There were 12 births with thrombocytopenia requiring treatment, consistent with the maternal ITP; all were discharged home with eight having their thrombocytopenia resolved pre-discharge. Although limited by incomplete information, 75 women were exposed to romiplostim in the first trimester because of having been treated with romiplostim at the time they became pregnant. From the over 150 pregnancies for which any data were available, five infants had some kind of adverse finding: one had cytomegalovirus infection, one had unilateral inguinal hernia, one had a single umbilical artery with no other findings reported, one child was normal at birth but at the age of 2 was identified as autistic and one infant, whose mother received only one dose of romiplostim in the third trimester, had trisomy 8.

In summary, according to three reports of the use of three different thrombopoietin agents in pregnancy, these drugs appear to be safe as a class with no information available for avatrombopag, very limited information for eltrombopag, and considerable safety but little efficacy information for romiplostim. While efficacy is likely to be preserved in the mother, it is not known whether transplacental passage of these agents increases the neonatal platelet count. Our conclusion is that a thrombopoietin agent should only be used when the benefit outweighs the risk. However, if a thrombopoietin agent is considered in the third trimester, the available data strongly suggest that romiplostim is safe for the fetus (Figure 1, Table 2).

After scheduled vaginal delivery, our patient does well as does her baby. She breastfeeds but her newborn has persistent thrombocytopenia with platelet counts down to $30 \times 10^9/L$. She is prompted to stop breast feeding and, upon doing so, the infant's platelet count rapidly increases to normal. The mother's platelet count also re-

turn to its pre-pregnancy level and all treatment can be stopped.

Section III: Second-line treatment of immune thrombocytopenia in an older male patient

What if instead of a young woman in her early 20s, our patient is a 63-year-old male?

This patient is generally healthy but slightly overweight and had his gall bladder removed without incident 6 years ago. He has taken daily losartan, atorvastatin, and a baby aspirin for several years. Upon presentation with bruises, petechiae and profuse bleeding from his gums when he brushes his teeth, he is told to stop his aspirin. He is given dexamethasone 40 mg/day for 4 days and a single dose of IVIG 1 g/m²/kg because of the aspirin. His platelet count increases dramatically within 2 days.

What diagnostic considerations are important here? First, as with the young woman, ITP must be distinguished from other thrombocytopenias; these are common in the elderly but different from those in a young woman. Autoimmune diseases such as systemic lupus erythematosus are much less likely, as are inherited thrombocytopenias. CVID is possible at any age but in addition to assaying serum immunoglobulins, serum protein electrophoresis to look for monoclonal proteins is appropriate. Other congenital immunodeficiency diseases are less likely, but lymphoproliferative diseases are more common. Chronic lymphocytic leukemia and non-Hodgkin lymphoma are both B-cell diseases associated with ITP. A blood smear may show too many small mature-looking lymphocytes; if T- and B-cell studies are performed, they would reveal too many B cells. Clonal hematopoiesis of indeterminate potential might occur but it is not clear what this condition would portend assuming the clonal cells do not reflect an overt malignancy. Preliminary information suggests that clonal T-cell populations may mediate refractoriness.⁷⁵ Ultrasound and/or computed tomography scans to look for malignancy may be indicated.

An important cause of thrombocytopenia in elderly patients is myelodysplastic syndrome. A bone marrow examination is necessary to diagnose this condition. Typically, marrow will be hyperplastic, but marrow cells will be undergoing apoptosis and not producing mature blood cells and reveal dyspoiesis. Diagnostics have improved remarkably as has clinical discrimination of different subtypes of myelodysplastic syndrome. Nonetheless, cases of myelodysplastic syndrome early in their evolution may be difficult to distinguish from "difficult" ITP.⁷⁶

Drug-induced thrombocytopenia is a possibility since older patients may be taking more medications. Limited laboratory testing is available to demonstrate that thrombo-

cytopenia is drug-induced. Diagnosis generally relies on recognizing medications likely to cause thrombocytopenia; one approach is to change medications if any are newly initiated. Viral infections could also occur in this population e.g., hepatitis C, cytomegalovirus.

Patients over the age of 60 are thought to have a higher likelihood of fatal and non-fatal serious bleeding compared to younger patients;⁷⁷⁻⁷⁹ recent studies of intracranial hemorrhage have supported earlier findings demonstrating a higher risk in those above 60 years of age. Thus, it may be appropriate to pursue an aggressive approach in this patient, such as the addition of IVIG to steroids.

Which second-line treatment is optimal for a 63-year-old male?

Rituximab in an older male

In this case of ITP, the older man has a reasonable likelihood of a response but, even if he responds well, his response will very likely last only 6-12 months. The chance of a long-term (>1 year) response is low. Furthermore, as discussed previously, after rituximab it would not be possible to vaccinate the patient against SARS-CoV-2, which is important since this 63-year-old is in a high-risk group and would benefit from boosters. As indicated, there is a 10-20% possibility of developing significant hypogammaglobulinemia when the combination of dexamethasone with rituximab is used.²⁶ A good initial response followed by the expected relapse would allow rituximab to be reused, but it remains unlikely to lead to a cure⁸⁰ and the probability of hypogammaglobulinemia occurring is thought to increase with repeated use.

Splenectomy in an older male

Splenectomy is used even less in this age group, since efficacy is lower, and the risk of side effects is higher. The results of splenectomy are less successful in older patients with ITP, but there is no clear age at which this effect occurs.⁸¹ In addition, there may be a higher risk of peri-operative complications and post-splenectomy thrombosis in this older patient. One could take a risk-based approach to splenectomy for this 63-year-old by considering the comorbidities and proceeding if he has few to no comorbidities.

Thrombopoietin receptor agonists in an older male

Another second-line therapy is a TPO-RA. The primary advantages remain the high response rate and the low likelihood that there will be major side effects although venous and arterial thrombosis would be the primary concerns in this older man. It is important to fully assess the risk of thrombosis looking at risk factors such as obesity, family history, and personal history.⁵³ The use of thrombopoietin agents would be similar in both patients and is described in the package inserts and a recent review.³⁶

If romiplostim is chosen, we would initiate treatment with 3 µg/kg/week and increase by 2 µg/kg/week until the platelet count rises above 30-50x10⁹/L. In more practical terms, this could mean whole vials of 250 and 500 micrograms which are almost universally available; if smaller and larger vial sizes are/become available this would allow more precise weight-based dosing. If a sufficient platelet count is achieved, it is important not to change romiplostim doses too quickly, i.e., not more than 1 µg/kg/week. This minimizes cycling of platelet counts and prevents them from going too high or falling too low. If the platelet count goes very high (with any of the 3 TPO-RA), do not withhold the dose, but decrease it by 1 µg/kg (or equivalent); several days of aspirin can be given if there is concern of thrombosis.

If eltrombopag is chosen, the starting dose is 50 mg by mouth daily; lower doses might be required in East Asian patients. If the count does not increase sufficiently within 1-2 weeks, increase the dose to 75 mg daily. If the count increases too much, decrease the dose to 25 mg daily. The maximum change would be 25 mg/daily once a week. If none of the doses allows for a stable count of 50-100x10⁹/L, then alternating doses might be preferred e.g., 50 mg on odd days and 75 mg on even days. As discussed, eltrombopag must be taken on an empty stomach. In our experience, the best approach is to eat dinner, not eat after the end of dinner and then take the eltrombopag with water at bedtime, at least 2 hours after dinner. If this gentleman urinates every night, this could be a time to take eltrombopag. If avatrombopag is chosen, the starting dose is 20 mg daily. The dose could be adjusted to as high as 40 mg daily or as low as 20 mg on one day per week. There is only one size of avatrombopag tablet, i.e. 20 mg. The tablet is taken once daily and there are no dietary restrictions. As with the other agents, dose changes should be limited in magnitude and not performed more often than weekly.

With all three agents, it is not clear how/when to taper and attempt to discontinue treatment. A recent study demonstrated a greater than 50% successful discontinuation rate when at least 2-3 months of stable TPO-RA dosing, no bleeding, and a platelet count >100x10⁹/L were required for the discontinuation attempt.⁸² Patients were on romiplostim a median of 12 months before tapering; the doses administered were higher than normal to obtain stable counts >100x10⁹/L. The tapering protocol was at 2-weekly intervals for a total of not more than 2 months of tapering. It remains unclear how often a patient who has required a thrombopoietin agent for 2 or more years will be able to discontinue treatment. Other studies have suggested an approximately 20-25% rate of successful discontinuation in the first year.

Fostamatinib in an older male

If this patient were at particular risk of thrombosis, fostamatinib might be a particularly good option. Otherwise, in

general practice, it is usually reserved for patients who have failed to respond to thrombopoietin agents. With many second-line agents, there are various treat-

ment options and courses depending on individual responses, relapses and potential complications with each agent, as demonstrated in Figure 2.

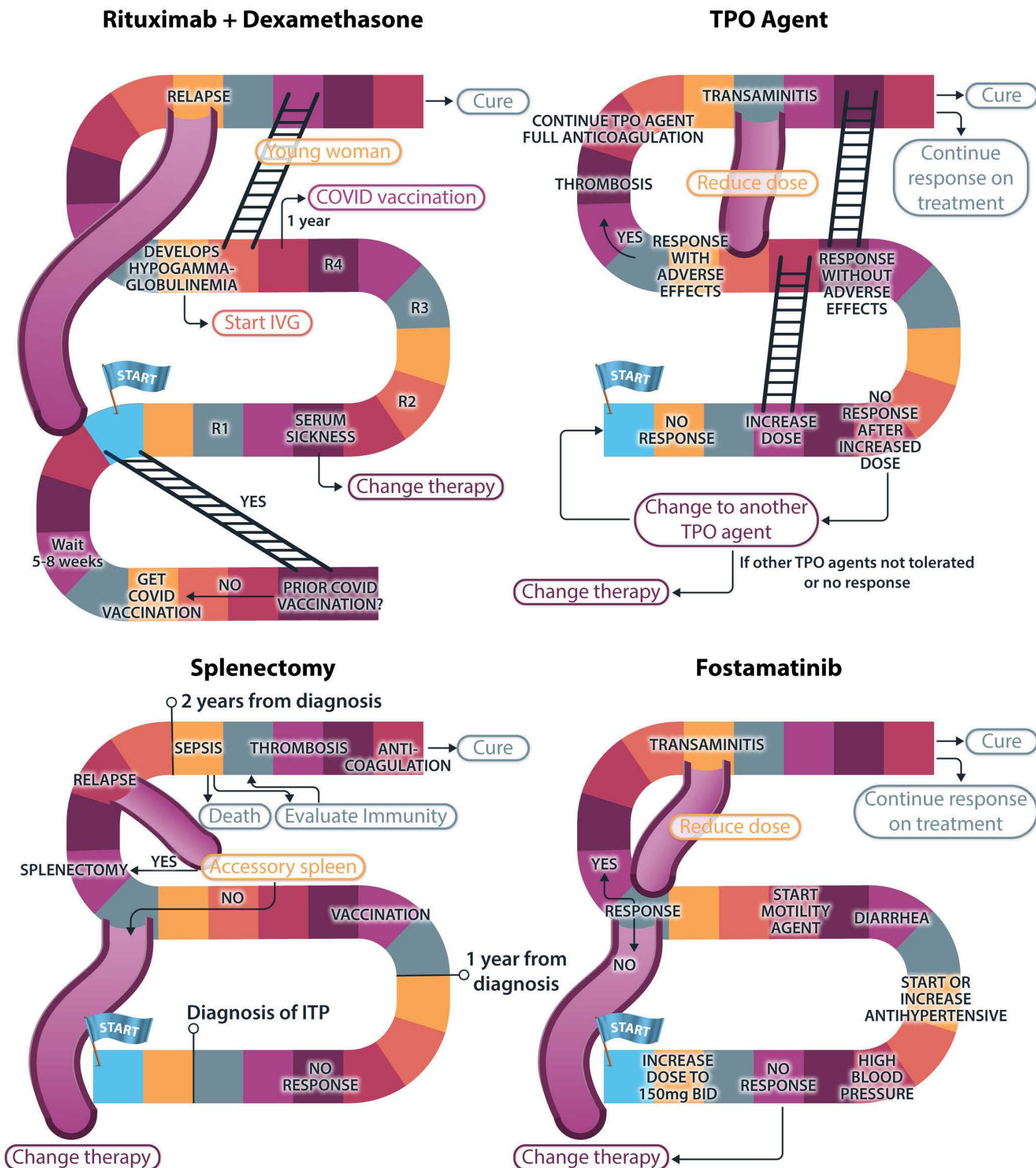


Figure 2. Second-line treatment options for immune thrombocytopenia and possible treatment courses. TPO: thrombopoietin; R1, R2, R3, R4: first, second, third and fourth weekly dose of rituximab; COVID: coronavirus disease 2019; ITP: immune thrombocytopenia; BID: *bis in die*.

Section IV: Third-line therapy for immune thrombocytopenia and beyond

What happens if the thrombopoietin agent used in the two patients does not work or at least cannot be tapered?

In the case of the young woman, the platelet count remained less than $20 \times 10^9/L$ and the young woman had heavy menses, bruising and nosebleeds. The now 26-year-old woman opted for rituximab. She had a long-term response but unfortunately relapsed after 4 years. She considered repeating the rituximab and undergoing splenectomy but opted to try a different thrombopoietin agent since she was not planning another pregnancy in the immediate future. Previously she used eltrombopag so she now tried avatrombopag. On a dose of 20 mg/day she was able to maintain an adequate platelet count and is very slowly tapering her dose. This choice was consistent with evidence that not responding well to one TPO-RA does not preclude good response to another.

Our older, male patient, given his continued bruising and minor nosebleeds, was afraid of major bleeding; he also felt very tired even though he was not anemic. The now 64-year-old man opted to try rituximab since avatrombopag did not work well for him. He received the standard dose of rituximab with dexamethasone. He responded with a platelet count of $60 \times 10^9/L$ by 6 weeks after initiating treatment; however, his count started to fall monthly down to $30 \times 10^9/L$. He and his doctor decided to initiate mycophenolate mofetil and he began with a dose of 500 mg twice daily and then increased to 1000 mg twice a day. He tolerates this treatment well and his platelet counts remain around $40\text{--}50 \times 10^9/L$.

Thus, both patients needed treatment. Some patients with low (not very low) platelet counts who have no bleeding or other issues e.g., need for anticoagulants or fatigue, may not require treatment. Avoiding treatment is always optimal if this does not jeopardize quality of life.

What if none of the obvious options (thrombopoietin agents, rituximab, splenectomy) helps and no single treatment, including fostamatinib and mycophenolate mofetil is effective?

It is difficult to predict what approach will be effective in these “refractory” patients. If a patient has been on too low a dose or for too short a period, it may not be clear that a given medication will not be helpful.

The approach to difficult-to-treat patients, such as these examples, is discussed at great length in our review of refractory ITP and in another recent review.^{1,83} The major principles are: (i) spend time reconfirming the diagnosis; reconsider all options if response to treatments of ITP is absent or very limited: (ii) do a complete bone marrow exam-

ination, unless one was performed recently, with aspirate, biopsy, flow cytometry, and cytogenetics; (iii) if a treatment is ineffective, continue the treatment and add another treatment initiating combination therapy. In our opinion, this is preferable to discontinuing the ineffective treatment and starting another one; (iv) if indeed the case is refractory ITP, combination approaches are often better than single treatments. Including treatments with different mechanisms of effect is useful; however, there are situations in which two agents targeting the same mechanism are effective such as combining IVIG and IV anti-D;³¹ and (v) when using combination treatments, it would be ideal to not give maximum doses and to select agents with differing toxicities. If an adverse event requiring a change in treatment occurs, it is then easier to choose the agent to stop and/or replace. In our review of published reports,¹ a TPO agent was often a crucial component of combination treatments.

In difficult patients, the inability to define the pathogenesis in most cases makes the treatment selection blind. Fortunately, multiply refractory patients for whom no treatment seems to bring their platelet count up at all are very rare. More commonly at least one treatment will transiently increase the platelet count. This minimizes the chance of serious bleeding and creates an approach for ongoing management, although continued steroid overuse must be avoided.

Section V. Agents currently under study

What are the experimental agents which are likely to be available in the future?

Various experimental agents for ITP are being studied and other drugs, currently used for other conditions, are now undergoing trials in ITP. It is uncertain whether, and if so in what context, any or all these agents will ultimately have a major role in the management of ITP. On the one hand, they could be more effective and less toxic than currently used agents and have specific areas of efficacy based on their unique mechanisms of effect. On the other hand, they might be redundant, have toxicities, and not provide substantial additional value.

FcRn inhibitors

The putative mechanism of effect of FcRn inhibitors is reduction of antiplatelet IgG levels by inhibition of “normal” IgG recycling. IgG levels fall dramatically with FcRn inhibition, and it is thought that the IgG anti-platelet antibody levels fall at least as much, resulting in less platelet destruction and greater platelet production. Efgartigimod and rozanolixizumab have gone through phase II studies; the results were published in 2020 and both studies demon-

strated more than 50% acute platelet responses.^{84,85} Both agents are in ongoing phase III trials which, like many studies, were slowed by the COVID pandemic. Since FcRn inhibition does not lower IgA and IgM levels nor does it affect T-cell or macrophage function, trials have not been complicated by the development of infections despite very low IgG levels being reached. Nonetheless, there is concern that IgG levels below 200 mg/dL (lower limit of normal: 639 mg/dL) may be dangerous. With one FcRn inhibitor, albumin levels were lowered, and cholesterol increased; FcRn also recycles albumin.

Active studies of FcRn inhibitors include treatment of myasthenia gravis, pemphigus vulgaris, hemolytic disease of the fetus and newborn, and antibody-mediated neurological diseases. In the phase III studies, the FcRn inhibitors are being administered weekly by subcutaneous administration with the goal of eventual home administration.

Bruton tyrosine kinase inhibitors

The most widely used Bruton tyrosine kinase (BTK) inhibitor is ibrutinib for chronic lymphocytic leukemia and non-Hodgkin lymphoma with excellent results in treating these entities; anecdotally, several thrombocytopenic patients with chronic lymphocytic leukemia had substantial platelet improvements. Thus, it was natural to think of BTK inhibition for B-cell diseases like ITP. However, ibrutinib was found to lead to serious bleeding in about 1% of cases, an effect that was subsequently suggested to be caused by inhibition of collagen-platelet interactions. Newer BTK inhibitors, e.g., rilzabrutinib, designed to allow normal platelet function for patients with ITP, have been effective in ITP in phase II trials, with a 50% response rate seen at the top dose, 400 mg twice a day.⁸⁶ As was seen in trials with fostamatinib and FcRn inhibitors, the patients enrolled have been heavily pre-treated with long-term histories. It is highly likely that BTK inhibitors will inhibit response to SARS-CoV-2 vaccination.

Complement inhibitors

Studies of complement pathway inhibitors in ITP would have begun years ago if the cost of the Alexion anti-C5 monoclonal antibody (eculizumab) had not been so enormous. Early results of C₁S inhibition are impressive but still preliminary. This strategy has yielded good results in cold agglutinin disease, demonstrating its biological effect on the complement system which is translated into clinical hematologic efficacy.

Conclusions

What would we have liked to have been able to offer our two patients with immune thrombocytopenia?

First, it would have been nice to have been able to predict

their course including many factors: risk of bleeding, likelihood of chronicity, which treatments would be most effective, and which most toxic.

Second, it would have been nice to have a curative but non-toxic treatment to offer. We discussed the use of rituximab in a younger woman as there is good likelihood of cure in a patient of this age and gender. But in other patients, there is very little likelihood of cure and in her case, vaccination for SARS-CoV-2 was a problem. This leaves splenectomy which is remarkably effective; recent work suggests that it remains effective even in patients who have been treated with thrombopoietin agents.⁴⁸ Why are patients so unwilling to undergo splenectomy? Perhaps the primary reasons are the inability to know whether a patient will get better on their own, whether the splenectomy will be successful, and the irreversibility of it. Furthermore, post-splenectomy risks of sepsis and thrombosis continue lifelong. In the future, use of combinations of agents (dexamethasone and rituximab, steroids and mycophenolate mofetil, dexamethasone and eltrombopag, or others) within 1 week of diagnosis may provide a higher level of cure and justify the extra expense and higher risks of these interventions.

Finally, treatment selection could be more rational if data were provided by randomized, controlled trials comparing agents and regimens. To date, all the randomized controlled double-blind trials of second-line agents have involved comparison of a treatment to placebo. We are not aware of any trials comparing one second-line agent to another, although Chinese hematologists have recently compared a given agent to the same agent plus a second agent. Examples include rituximab with and without thrombopoietin, and dexamethasone with and without eltrombopag. More of these studies are urgently needed.

In summary, it is not possible to have a “one size fits all” approach to ITP. Rather we have tried to emphasize that individualizing treatment is important and should include shared decision-making. The optimal choices vary with gender and age and the COVID pandemic has an impact as well. As additional information is accrued, management in certain situations may be clarified but there is a long way to go to achieve for ITP what we all take for granted in the evidence-based management of leukemia.⁸⁷

Disclosures

JBB is a consultant or on an advisory board for Amgen, Novartis, Sobi, Rigol, UCB, Argenx, Sanofi, Astra-Zeneca, Pfizer, and CSL-Behring; and is a member of a Data and Safety Monitoring Board for UCB, CSL-Behring. CAG has no conflicts of interest to disclose.

Contributions

JBB and CAG wrote and edited the manuscript and both agreed to its submission for publication.

References

- Miltiados O, Hou M, Bussel JB. Identifying and treating refractory ITP: difficulty in diagnosis and role of combination treatment. *Blood*. 2020;135(7):472-490.
- Mithoowani S, Gregory-Miller K, Goy J, et al. High-dose dexamethasone compared with prednisone for previously untreated primary immune thrombocytopenia: a systematic review and meta-analysis. *Lancet Haematol*. 2016;3(10):e489-e496.
- Goel R, Chopra S, Tobian AAR, et al. Platelet transfusion practices in immune thrombocytopenia related hospitalizations. *Transfusion*. 2019;59(1):169-176.
- Neunert C, Terrell DR, Arnold DM. American Society of Hematology 2019 guidelines for immune thrombocytopenia. *Blood Adv*. 2019;3(23):3829-3866.
- Provan D, Arnold DM, Bussel JB, et al. Updated international consensus report on the investigation and management of primary immune thrombocytopenia. *Blood Adv*. 2019;3(22):3780-3817.
- Rodeghiero F, Stasi R, Gernsheimer T, et al. Standardization of terminology, definitions and outcome criteria in immune thrombocytopenic purpura of adults and children: report from an international working group. *Blood*. 2009;113(11):2386-2393.
- VanderMeulen H, Sholzberg M. Iron deficiency and anemia in patients with inherited bleeding disorders. *Transfus Apher Sci*. 2018;57(6):735-738.
- Maric D. Effect of the successive application of estradiol and progesterone on the number of blood platelets of the rabbit. *C R Seances Soc Biol Fil*. 1960;154:1865-1866.
- Onel K, Bussel JB. Adverse effects of estrogen therapy in a subset of women with ITP. *J Thromb Haemost*. 2004;2(4):670-671.
- Ho HE, Cunningham-Rundles C. Non-infectious complications of common variable immunodeficiency: updated clinical spectrum, sequelae, and insights to pathogenesis. *Front Immunol*. 2020;11:149.
- Grace RF, Lambert MP. An update on pediatric immune thrombocytopenia (ITP): differentiating primary ITP, IPD, and PID. *Blood*. 2021 Sep 3. [Epub ahead of print].
- Khellaf M, Chabrol A, Mahevas M, et al. Hydroxychloroquine is a good second-line treatment for adults with immune thrombocytopenia and positive antinuclear antibodies. *Am J Hematol*. 2014;89(2):194-198.
- Aggarwal M, Mahapatra M, Seth T, Tyagi S, Tandon N, Saxena R. Thyroid dysfunction in patients with immune thrombocytopenia: prevalence and its impact on outcome. *Indian J Hematol Blood Transfus*. 2022;38(1):173-177.
- Velayutham K, Selvan SS, Unnikrishnan AG. Prevalence of thyroid dysfunction among young females in a South Indian population. *Indian J Endocrinol Metab*. 2015;19(6):781-784.
- Unnikrishnan AG, Kalra S, Sahay RK, Bantwal G, John M, Tewari N. Prevalence of hypothyroidism in adults: an epidemiological study in eight cities of India. *Indian J Endocrinol Metab*. 2013;17(4):647-652.
- Cordiano I, Betterle C, Spadaccino CA, Soini B, Girolami A, Fabris F. Autoimmune thrombocytopenia (AITP) and thyroid autoimmune disease (TAD): overlapping syndromes? *Clin Exp Immunol*. 1998;113(3):373-378.
- McMillan R, Bussel JB, George JN, Lalla D, Nichol JL. Self-reported health-related quality of life in adults with chronic immune thrombocytopenic purpura. *Am J Hematol*. 2008;83(2):150-154.
- Mahevas M, Moulis G, Andres E, et al. Clinical characteristics, management and outcome of COVID-19-associated immune thrombocytopenia: a French multicentre series. *Br J Haematol*. 2020;190(4):e224-e229.
- DiMaggio D, Anderson A, Bussel JB. Cytomegalovirus can make immune thrombocytopenic purpura refractory. *Br J Haematol*. 2009;146(1):104-112.
- Shragai T, Lebel E, Deshet D, et al. Characteristics and outcomes of adults with cytomegalovirus-associated thrombocytopenia: a case series and literature review. *Br J Haematol*. 2020;191(5):863-867.
- Stasi R, Sarpatwari A, Segal JB, et al. Effects of eradication of *Helicobacter pylori* infection in patients with immune thrombocytopenic purpura: a systematic review. *Blood*. 2009;113(6):1231-1240.
- Zhang H, Chien M, Hou Y, et al. Longitudinal study of 2 patients with cyclic thrombocytopenia, STAT3, and MPL mutations. *Blood Adv*. 2022 Apr 5. [Epub ahead of print].
- Pecci A, Balduini CL. Inherited thrombocytopenias: an updated guide for clinicians. *Blood Rev*. 2021;48:100784.
- Balduini C, Freson K, Greinacher A, et al. The EHA research roadmap: platelet disorders. *Hemasphere*. 2021;5(7):e601.
- Balduini CL, Melazzini F, Pecci A. Inherited thrombocytopenias—recent advances in clinical and molecular aspects. *Platelets*. 2017;28(1):3-13.
- Chapin J, Lee CS, Zhang H, Zehnder JL, Bussel JB. Gender and duration of disease differentiate responses to rituximab-dexamethasone therapy in adults with immune thrombocytopenia. *Am J Hematol*. 2016;91(9):907-911.
- Lucchini E, Zaja F, Bussel J. Rituximab in the treatment of immune thrombocytopenia: what is the role of this agent in 2019? *Haematologica*. 2019;104(6):1124-1135.
- Nazi I, Kelton JG, Larche M, et al. The effect of rituximab on vaccine responses in patients with immune thrombocytopenia. *Blood*. 2013;122(11):1946-1953.
- Lee EJ, Beltrami-Moreira M, Al-Samkari H, et al. SARS-CoV-2 vaccination and ITP in patients with de novo or preexisting ITP. *Blood*. 2022;139(10):1564-1574.
- Bradbury CA, Pell J, Hill Q, et al. Mycophenolate mofetil for first-line treatment of immune thrombocytopenia. *N Engl J Med*. 2021;385(10):885-895.
- Boruchov DM, Gururangan S, Driscoll MC, Bussel JB. Multiagent induction and maintenance therapy for patients with refractory immune thrombocytopenic purpura (ITP). *Blood*. 2007;110(10):3526-3531.
- Reiner A, Gernsheimer T, Slichter SJ. Pulse cyclophosphamide therapy for refractory autoimmune thrombocytopenic purpura. *Blood*. 1995;85(2):351-358.
- Bussel JB, Kuter DJ, George JN, et al. AMG 531, a thrombopoiesis-stimulating protein, for chronic ITP. *N Engl J Med*. 2006;355(16):1672-1681.
- Bussel JB, Cheng G, Saleh MN, et al. Eltrombopag for the treatment of chronic idiopathic thrombocytopenic purpura. *N Engl J Med*. 2007;357(22):2237-2247.
- Bussel JB, Kuter DJ, Aledort LM, et al. A randomized trial of avatrombopag, an investigational thrombopoietin-receptor agonist, in persistent and chronic immune thrombocytopenia. *Blood*. 2014;123(25):3887-3894.
- Ghanima W, Cooper N, Rodeghiero F, Godeau B, Bussel JB. Thrombopoietin receptor agonists: ten years later. *Haematologica*. 2019;104(6):1112-1123.

37. Bussel J, Kulasekararaj A, Cooper N, et al. Mechanisms and therapeutic prospects of thrombopoietin receptor agonists. *Semin Hematol.* 2019;56(4):262-278.
38. Liu ZJ, Deschmann E, Ramsey HE, et al. Iron status influences the response of cord blood megakaryocyte progenitors to eltrombopag in vitro. *Blood Adv.* 2022;6(1):13-27.
39. Cantoni S, Carpenedo M, Mazzucconi MG, et al. Alternate use of thrombopoietin receptor agonists in adult primary immune thrombocytopenia patients: a retrospective collaborative survey from Italian hematology centers. *Am J Hematol.* 2018;93(1):58-64.
40. Lakhwani S, Perera M, Fernandez-Fuertes F, et al. Thrombopoietin receptor agonist switch in adult primary immune thrombocytopenia patients: a retrospective collaborative survey involving 4 Spanish centres. *Eur J Haematol.* 2017;99(4):372-377.
41. Lee EJ, Seshadri M, Bussel JB. Clinical outcomes in eight patients with immune thrombocytopenia each treated with the three approved thrombopoietin receptor agonists. *Am J Hematol.* 2021;96(10):E373-E376.
42. Piatek CI, Jamieson B, Vredenburg M. Characterization of thromboembolic events occurring during the avatrombopag immune thrombocytopenia (ITP) clinical development program. *Blood.* 2020;136(Suppl 1):39.
43. Pavord S, Thachil J, Hunt BJ, et al. Practical guidance for the management of adults with immune thrombocytopenia during the COVID-19 pandemic. *Br J Haematol.* 2020;189(6):1038-1043.
44. American Hematology Society. COVID-19 and ITP. 2022 5/31/2022. Available from: <https://www.hematology.org/covid-19/covid-19-and-itp>. (last accessed March 2022)
45. Bussel J, Arnold DM, Grossbard E, et al. Fostamatinib for the treatment of adult persistent and chronic immune thrombocytopenia: results of two phase 3, randomized, placebo-controlled trials. *Am J Hematol.* 2018;93(7):921-930.
46. Connell NT, Berliner N. Fostamatinib for the treatment of chronic immune thrombocytopenia. *Blood.* 2019;133(19):2027-2030.
47. Strich JR, Tian X, Samour M, et al. Fostamatinib for the treatment of hospitalized adults with COVID-19 A [sic] randomized trial. *Clin Infect Dis.* 2021 Sep 1. [Epub ahead of print]
48. Mageau A, Terriou L, Ebbo M, et al. Splenectomy for primary immune thrombocytopenia revisited in the era of thrombopoietin receptor agonists: new insights for an old treatment. *Am J Hematol.* 2022;97(1):10-17.
49. Theilacker C, Ludewig K, Serr A, et al. Overwhelming postsplenectomy infection: a prospective multicenter cohort study. *Clin Infect Dis.* 2016;62(7):871-878.
50. Tahir F, Ahmed J, Malik F. Post-splenectomy sepsis: a review of the literature. *Cureus.* 2020;12(2):e6898.
51. Newland A, Provan D, Myint S. Preventing severe infection after splenectomy. *BMJ.* 2005;331(7514):417-418.
52. Feng Q, Tamimi R, Mu Y, Pen J, Bussel JB. Splenectomy results in venous thromboembolic events in women: a Nurses Health Study. *Blood.* 2021;138(Suppl 1):3163.
53. Rodeghiero F, Marranconi E. Management of immune thrombocytopenia in women: current standards and special considerations. *Expert Rev Hematol.* 2020;13(2):175-185.
54. Upson K, Harmon QE, Heffron R, et al. Depot medroxyprogesterone acetate use and blood lead levels in a cohort of young women. *Environ Health Perspect.* 2020;128(11):117004.
55. Bussel JB, Druzin ML, Cines DB, Samuels P. Thrombocytopenia in pregnancy. *Lancet.* 1991;337(8735):251.
56. Burrows RF, Kelton JG. Fetal thrombocytopenia and its relation to maternal thrombocytopenia. *N Engl J Med.* 1993;329(20):1463-1466.
57. Boehlen F, Hohlfeld P, Extermann P, Perneger TV, de Moerloose P. Platelet count at term pregnancy: a reappraisal of the threshold. *Obstet Gynecol.* 2000;95(1):29-33.
58. Sainio S, Kekomaki R, Riikonen S, Teramo K. Maternal thrombocytopenia at term: a population-based study. *Acta Obstet Gynecol Scand.* 2000;79(9):744-749.
59. Khanuja K, Levy AT, McLaren RA Jr, Berghella V. Pre- and postpregnancy platelet counts: evaluating accuracy of gestational thrombocytopenia and immune thrombocytopenia purpura diagnoses. *Am J Obstet Gynecol MFM.* 2022;4(3):100606.
60. Dockree S, Shine B, Impey L, Mackillop L, Randeve H, Vatish M. Improving diagnostic accuracy in pregnancy with individualised, gestational age-specific reference intervals. *Clin Chim Acta.* 2022;527:56-60.
61. Chen Q, Liu F, Sun X, Wang C, et al. High level of estradiol induces megakaryocyte apoptosis and impairs proplatelet formation via MST1-FOXO1 axis during pregnancy in patients with immune thrombocytopenia. *European Hematology Association; 2021 06/09/2021. EHA Library; (no. 324706).* Available from: <https://library.ehaweb.org/eha/2021/eha2021-virtual-congress/324706/qi.chen.high.level.of.estradiol.induces.megakaryocyte.apoptosis.and.impairs.html?f=listing%3D3%2Abrowseby%3D8%2Asortby%3D1%2Amedia%3D1>. (last accessed August 2021)
62. Peitsidis P, Kadir RA. Antifibrinolytic therapy with tranexamic acid in pregnancy and postpartum. *Expert Opin Pharmacother.* 2011;12(4):503-516.
63. Mantero F, Opocher G, Armanini D, Filipponi S. 11 Beta-hydroxylase deficiency. *J Endocrinol Invest.* 1995;18(7):545-549.
64. Sun D, Shehata N, Ye XY, et al. Corticosteroids compared with intravenous immunoglobulin for the treatment of immune thrombocytopenia in pregnancy. *Blood.* 2016;128(10):1329-1335.
65. Lakkaraja M, Berkowitz RL, Vinograd CA, et al. Omission of fetal sampling in treatment of subsequent pregnancies in fetal-neonatal alloimmune thrombocytopenia. *Am J Obstet Gynecol.* 2016;215(4):471.e1-9.
66. Chakravarty EF, Murray ER, Kelman A, Farmer P. Pregnancy outcomes after maternal exposure to rituximab. *Blood.* 2011;117(5):1499-1506.
67. Michel M, Novoa MV, Bussel JB. Intravenous anti-D as a treatment for immune thrombocytopenic purpura (ITP) during pregnancy. *Br J Haematol.* 2003;123(1):142-146.
68. Natekar A, Pupco A, Bozzo P, Koren G. Safety of azathioprine use during pregnancy. *Can Fam Physician.* 2011;57(12):1401-1402.
69. Sukenik-Halevy R, Ellis MH, Fejgin MD. Management of immune thrombocytopenic purpura in pregnancy. *Obstet Gynecol Surv.* 2008;63(3):182-188.
70. Bar Oz B, Hackman R, Einarson T, Koren G. Pregnancy outcome after cyclosporine therapy during pregnancy: a meta-analysis. *Transplantation.* 2001;71(8):1051-1055.
71. Pisoni CN, D'Cruz DP. The safety of mycophenolate mofetil in pregnancy. *Expert Opin Drug Saf.* 2008;7(3):219-222.
72. Kong Z, Qin P, Xiao S, et al. A novel recombinant human thrombopoietin therapy for the management of immune thrombocytopenia in pregnancy. *Blood.* 2017;130(9):1097-1103.
73. Michel M, Ruggeri M, Gonzalez-Lopez TJ, et al. Use of thrombopoietin receptor agonists for immune thrombocytopenia in pregnancy: results from a multicenter study. *Blood.* 2020;136(26):3056-3061.
74. Bussel JB, Cooper N, Lawrence T, et al. Surveillance program of

- romiplostim use connected to pregnancy. *Blood*. 2021;138(Suppl 1):585.
75. Zhang H, Zhang BM, Guo X, et al. Blood transcriptome and clonal T-cell correlates of response and non-response to eltrombopag therapy in a cohort of patients with chronic immune thrombocytopenia. *Haematologica*. 2020;105(3):e129-e132.
76. Ogawa S. Genetics of MDS. *Blood*. 2019;133(10):1049-1059.
77. Cohen YC, Djulbegovic B, Shamai-Lubovitz O, Mozes B. The bleeding risk and natural history of idiopathic thrombocytopenic purpura in patients with persistent low platelet counts. *Arch Intern Med*. 2000;160(11):1630-1638.
78. Tsuda H, Tsuji T, Tsuji M, Yamasaki H. Life-threatening bleeding episodes in primary immune thrombocytopenia: a single-center retrospective study of 169 inpatients. *Ann Hematol*. 2017;96(11):1915-1920.
79. Sokal A, de Nadai T, Maquet J, et al. Primary immune thrombocytopenia in very elderly patients: particularities in presentation and management: results from the prospective CARMEN-France Registry. *Br J Haematol*. 2022;196(5):1262-1270.
80. Hasan A, Michel M, Patel V, et al. Repeated courses of rituximab in chronic ITP: three different regimens. *Am J Hematol*. 2009;84(10):661-665.
81. Kojouri K, Vesely SK, Terrell DR, George JN. Splenectomy for adult patients with idiopathic thrombocytopenic purpura: a systematic review to assess long-term platelet count responses, prediction of response, and surgical complications. *Blood*. 2004;104(9):2623-2634.
82. Mahevas M, Guillet S, Viillard J-F, et al. Rate of prolonged response after stopping thrombopoietin-receptor agonists treatment in primary immune thrombocytopenia (ITP): results from a nationwide prospective multicenter interventional study (STOPAGO). *Blood*. 2021;138(Suppl 1):583.
83. Vianelli N, Auteri G, Buccisano F, et al. Refractory primary immune thrombocytopenia (ITP): current clinical challenges and therapeutic perspectives. *Ann Hematol*. 2022;101(5):963-978.
84. Newland AC, Sanchez-Gonzalez B, Rejto L, et al. Phase 2 study of efgartigimod, a novel FcRn antagonist, in adult patients with primary immune thrombocytopenia. *Am J Hematol*. 2020;95(2):178-187.
85. Robak T, Kazmierczak M, Jarque I, et al. Phase 2 multiple-dose study of an FcRn inhibitor, rozanolixizumab, in patients with primary immune thrombocytopenia. *Blood Adv*. 2020;4(17):4136-4146.
86. Kuter DJ, Efraim M, Mayer J, et al. Rilzabrutinib, an oral BTK inhibitor, in immune thrombocytopenia. *N Engl J Med*. 2022;386(15):1421-1431.
87. Varley CD, Winthrop KL. Long-term safety of rituximab (risks of viral and opportunistic infections). *Curr Rheumatol Rep*. 2021;23(9):74.
88. Rodeghiero F, Cantoni S, Carli G, et al. Practical recommendations for the management of patients with ITP during the COVID-19 pandemic. *Mediterr J Hematol Infect Dis*. 2021;13(1):e2021032.
89. Lee EJ, Liu X, Hou M, Bussel JB. Immune thrombocytopenia during the COVID-19 pandemic. *Br J Haematol*. 2021;193(6):1093-1095.
90. Berlin CM, Briggs GG. Drugs and chemicals in human milk. *Semin Fetal Neonatal Med*. 2005;10(2):149-159.
91. Reddy D, Murphy SJ, Kane SV, Present DH, Kornbluth AA. Relapses of inflammatory bowel disease during pregnancy: in-hospital management and birth outcomes. *Am J Gastroenterol*. 2008;103(5):1203-1209.
92. Anglin BV, Rutherford C, Ramus R, Lieser M, Jones DB. Immune thrombocytopenic purpura during pregnancy: laparoscopic treatment. *JLS*. 2001;5(1):63-67.

IgM monoclonal gammopathies of clinical significance: diagnosis and management

Jahanzaib Khwaja,¹ Shirley D'Sa,¹ Monique C. Minnema,² Marie José Kersten,³ Ashutosh Wechalekar¹ and Josephine M.I. Vos³

¹University College London Hospital, London, UK; ²Department of Hematology, University Medical Center Utrecht, University Utrecht, Utrecht, the Netherlands and ³Department of Hematology, Amsterdam University Medical Centers, University of Amsterdam, Cancer Center Amsterdam and Lymphoma and Myeloma Center Amsterdam, Amsterdam, the Netherlands

Correspondence: J.M. Vos
j.m.i.vos@amsterdamumc.nl

Received: March 9, 2022.

Accepted: June 16, 2022.

Prepublished: June 30, 2022.

<https://doi.org/10.3324/haematol.2022.280953>

©2022 Ferrata Storti Foundation

Published under a CC-BY-NC license



Abstract

IgM monoclonal gammopathy of undetermined significance is a pre-malignant condition for Waldenström macroglobulinemia and other B-cell malignancies, defined by asymptomatic circulating IgM monoclonal protein below 30 g/L with a lymphoplasmacytic bone marrow infiltration of less than 10%. A significant proportion, however, develop unique immunological and biochemical manifestations related to the monoclonal protein itself in the absence of overt malignancy and are termed IgM-related disorders or, more recently, monoclonal gammopathy of clinical significance. The indication for treatment in affected patients is dictated by the pathological characteristics of the circulating IgM rather than the tumor itself. The clinical workup and treatment options vary widely and differ from those for Waldenström macroglobulinemia. The aim of this review is to alert clinicians to IgM monoclonal gammopathy of clinical significance and to provide practical guidance on when to screen for these phenotypes. We discuss clinical characteristics, the underlying clonal profile, diagnostic workup and treatment considerations for five important subtypes: cold agglutinin disease, type I and II cryoglobulinemia, IgM-associated peripheral neuropathy, Schnitzler syndrome and IgM-associated AL amyloidosis. The inhibition of the pathogenic effects of the IgM has led to great success in cold agglutinin disease and Schnitzler syndrome, whereas the other treatments are centered on eradicating the underlying clone. Treatment approaches in cryoglobulinemia and IgM-associated peripheral neuropathy are the least well developed. A multidisciplinary approach is required, particularly for IgM-related neuropathies and Schnitzler syndrome. Future work exploring novel, clone-directed agents and pathogenic IgM-directed therapies is welcomed.

Introduction

IgM monoclonal gammopathy of undetermined significance (MGUS) is defined by asymptomatic circulating IgM monoclonal (M) protein below 30 g/L with a lymphoplasmacytic bone marrow infiltration of less than 10%.¹ IgM MGUS is a pre-malignant condition for non-Hodgkin lymphomas, mostly Waldenström macroglobulinemia (WM), chronic lymphocytic lymphoma, and plasma cell neoplasms. Most patients are candidates for observation. However, some develop diverse immunological and biochemical manifestations related to the monoclonal protein itself.² This may lead to organ damage, even in the absence of overt malignancy. These so-called IgM-related disorders are a distinct clinical entity termed monoclonal gammopathy of clinical significance (MGCS).³ The clinical workup and treatment options vary widely and differ from

those for WM, which have been outlined in recent consensus guidelines.⁴

The aim of this review is to alert clinicians to IgM MGCS and to provide practical guidance on when to screen for these phenotypes. We discuss the clinical characteristics, diagnostic workup and treatment considerations for five important subtypes: cold agglutinin disease (CAD), cryoglobulinemia, IgM-associated AL amyloidosis, IgM-related neuropathies and Schnitzler syndrome. A comprehensive list of IgM MGCS is listed below (Table 1).

Clonal characterization

It is important to identify the underlying clone as IgM MGUS may progress to a number of lymphoproliferative disorders or very rarely to myeloma.⁵ IgM MGUS most

Table 1. List of IgM monoclonal gammopathies of clinical significance.

IgM monoclonal gammopathies of clinical significance
Cold agglutinin disease*
Type 1 and 2 cryoglobulinemia*
IgM-related neuropathies (including anti-MAG peripheral neuropathy*, non-MAG peripheral neuropathy, antiganglioside neuropathies, chronic ataxic neuropathies with disialosyl antibodies)
IgM-associated AL amyloidosis*
Schnitzler syndrome*
Monoclonal gammopathy of renal significance (including immunoglobulin deposition disease, light chain proximal tubulopathy, proliferative glomerulonephritis with monoclonal immunoglobulin deposits)
Acquired von Willebrand syndrome and other coagulation factor deficiencies
Acquired C1 inhibitor deficiency
Pure red cell aplasia
IgM POEMS

*These entities are discussed in further detail in this review. MGUS: monoclonal gammopathies of clinical significance; MAG: myelin-associated glycoprotein; POEMS: polyneuropathy, organomegaly, endocrinopathy, monoclonal gammopathy and skin abnormalities.

commonly arises from a CD20⁺ lymphoplasmacytic cell without class-switching.¹ The risk of progression to lymphoma, chronic lymphocytic leukemia, AL amyloidosis or multiple myeloma is 1.1 event per 100 person-years.⁵ In the largest series of 210 patients with IgM MGUS with a median follow-up of 29.3 months, no patients progressed to IgM myeloma.⁵ The incidence and prevalence of IgM MGCS are unknown. Clonal B cells in MGUS have the same genetic and molecular signature as the WM clone. However, MGUS cases have a significantly lower number of mutations than in WM, indicating multiple genetic hits are required for progression. The somatic *MYD88*^{L265P} mutation constitutively activates nuclear factor κ B and triggers B-cell proliferation. It is considered an early acquired mutation and is present in the majority of patients with WM or IgM MGUS.^{6,7} The gene encoding the chemokine receptor CXCR4, involved in homing of B cells in the bone marrow, is mutated (*CXCR4*^{MUT}) in a smaller proportion. This is usually a subclonal mutation and likely a late event. IgM myeloma has a distinct cell of origin, a pro-B cell, with frequent t(11;14), an absence of *MYD88*^{L265P} mutation and high BCL2/BCL2L1 ratio.⁸ These clonal characteristics may have therapeutic implications. Table 2 summarizes the data on the underlying histology and clonal characteristics of IgM MGCS compared with those seen in WM and IgM MGUS in general.

Primary cold agglutinin disease

In primary CAD, autoimmune hemolytic anemia is caused by a cold agglutinin that is a monoclonal IgM κ in more than 90% of cases and is produced by clonal lymphocytes in the bone marrow. The antibody binds erythrocyte

antigens (typically type I) optimally at 4°C resulting in agglutination and classical complement pathway activation.⁹ The thermal amplitude describes the temperature range at which the antibodies are active, and only those with a thermal amplitude reaching higher than 28°C are considered pathogenic. In most cases, complement activation is incomplete and extravascular hemolysis of C3b-opsonized erythrocytes occurs in the liver. Less frequently there is initiation of the terminal pathway, assembly of the membrane attack complex (C5b-C9) and intravascular hemolysis, which can lead to acute life-threatening anemia. Cold agglutinins in the context of infection, autoimmune disease and overt lymphoma⁹ (including chronic lymphocytic lymphoma, diffuse large B-cell lymphoma and WM) are referred to as cold agglutinin syndrome. The management of cold agglutinin syndrome is directed at treating the underlying cause and is not further discussed here.

Clinical characteristics

Patients with CAD present with chronic anemia and/or cold-induced circulatory symptoms. Of 232 patients in an international retrospective case series, the median IgM was 3.2 g/L and over 90% had hemolytic anemia and circulatory symptoms. Thirty-eight percent required transfusions at or before diagnosis and 47% during follow-up. Around half had acrocyanosis or Raynaud syndrome affecting daily living. Ulcers or gangrene were rare (<2%).¹⁰ In a third of cases, hemoglobin concentration is below 80g/L.¹¹ Circulatory symptoms do not correlate with either the degree of anemia or the bone marrow histology.^{10,11} There is an increased risk of thrombosis in CAD, likely related to intravascular hemolysis,^{12,13} which is not correlated with the severity of the anemia.¹⁰ CAD is a chronic disease

Table 2. Clonal characteristics of IgM monoclonal gammopathies of clinical significance, monoclonal gammopathies of undetermined significance and Waldenström macroglobinemia.

	IgM MGUS	WM	Cold agglutinin disease	Cryoglobulinemia	IgM AL amyloidosis	Anti-MAG neuropathy	Schnitzler syndrome
Histology, %				Type I:			
MGUS (<10% infiltration)	100	0	70 ⁷¹	30-40 ^{27,30}	27 ⁴⁰	60 ^{72,73}	73 ⁶³
WM (>10% infiltration)	0	100	7 ⁷¹	30-40 ^{27,30}	54 ⁴⁰	35 ^{72,73}	13 ⁶³
Other			24 ⁷¹	20-30 ^{27,30}	19 ⁴⁰	8 ^{72,73}	15 ⁶³
				Type 2: not reported			
IgM light chain restriction, %	IgMκ 70 ⁷⁴	IgMκ 75 ⁷⁵	IgMν 100 ¹¹	IgMκ 85 type I IgMκ 77 type II ²⁶	IgMλ 60 ⁴⁰	IgMκ 81% ⁷²	IgMκ 91 ⁶³
Molecular studies in bone marrow, %							
<i>MYD88</i> ^{L265P}	Up to 80	>90	0	Not reported*	58	73	Not reported***
<i>CXCR4</i> ^{MUT}	5 ⁷	40 ⁷	22 ¹⁵	Not reported	17 ^{38**}	12 ⁷²	Not reported
IGHV/IGLV gene usage	VH3	VH3	VH4-34	Not reported	LV2	VH4-34	VH3

MYD88*^{L265P} reported in 92% of WM associated type I cryoglobulinemia.⁷⁶ **These mutations are not seen in the pure plasma cell neoplasm subtype. *30% in peripheral blood.⁶⁶ MGUS: monoclonal gammopathies of undetermined significance; WM: Waldenström macroglobinemia; MAG: myelin-associated glycoprotein.

and affected patients have an estimated 16-year survival.¹⁰ Clonality has been demonstrated in approximately 80% of cases^{10,14} and the remainder likely require more sensitive methods to detect the pathogenic clone. The CAD clone has a distinct phenotype that differs from that of WM. *MYD88*^{L265P} is rarely seen. Recurrent somatic mutations in *CXCR4* (20%),^{10,14,15} *KMT2D* (69%) and *CARD11* (31%) have been described.¹⁶ Recurrent chromosomal abnormalities have been identified.¹⁷ Based on bone marrow biopsies of 54 cases of CAD, the entity "CAD-associated lymphoproliferative disorder" has been defined, with typical morphology including absent plasmacytoid cells, universally restricted IGHV4-34 gene usage and lack of *MYD88*^{L265P}.¹⁴ Most patients meet the criteria for MGUS and extramedullary disease is rare.¹⁰

Diagnostic workup

Laboratory findings are consistent with hemolysis (and may, therefore, include reticulocytosis, elevated lactate dehydrogenase, unconjugated hyperbilirubinemia and decreased haptoglobin), the monospecific direct antiglobulin test is strongly positive for C3d and there is a cold agglutinin titer of $\geq 1:64$ at 4°C. Blood samples should be handled warm until separation to prevent agglutination.

Treatment

Treatment goals are to alleviate cold-induced symptoms and hemolytic anemia. Response assessment should evaluate hemolytic activity and symptoms as well as

clonal response. There are no standard criteria to assess response of cold-induced peripheral symptoms and instead clinicians depend on patient-reported outcomes. A treatment algorithm is provided in Figure 1 and *Online Supplementary Table S1*. All patients should avoid exposure to cold and be observed, particularly during periods of febrile illness and surgery.¹⁰ Red blood cells should be transfused via a blood warmer. Symptomatic patients should commence use of folic acid and be considered for thromboprophylaxis. It is important to note that steroids and splenectomy are not effective in CAD.^{9,12} We recommend a frontline clone-directed approach (Figure 1), although achieving complete eradication is rare. The most established treatment is rituximab-based therapy. Prospective trials of rituximab monotherapy show a modest response rate of 50% with rare complete responses.¹⁸ Real-world data show a 15-month median response duration and repeated responses in over a third of patients.¹⁰ Efficacy is greatly improved by the addition of bendamustine. In a prospective study of the bendamustine-rituximab combination with a reduced dose of 70 mg/m² bendamustine delivered for four cycles to 45 patients, the response rate was 71%, with 40% complete responses and a median increase of hemoglobin of 44 g/L. Grade 4 neutropenia was observed in 20% of the patients and 29% required a dose reduction.¹⁹ According to updated data, both the overall and complete response rates improved due to deeper responses over time.¹⁰ Rituximab-fludara-

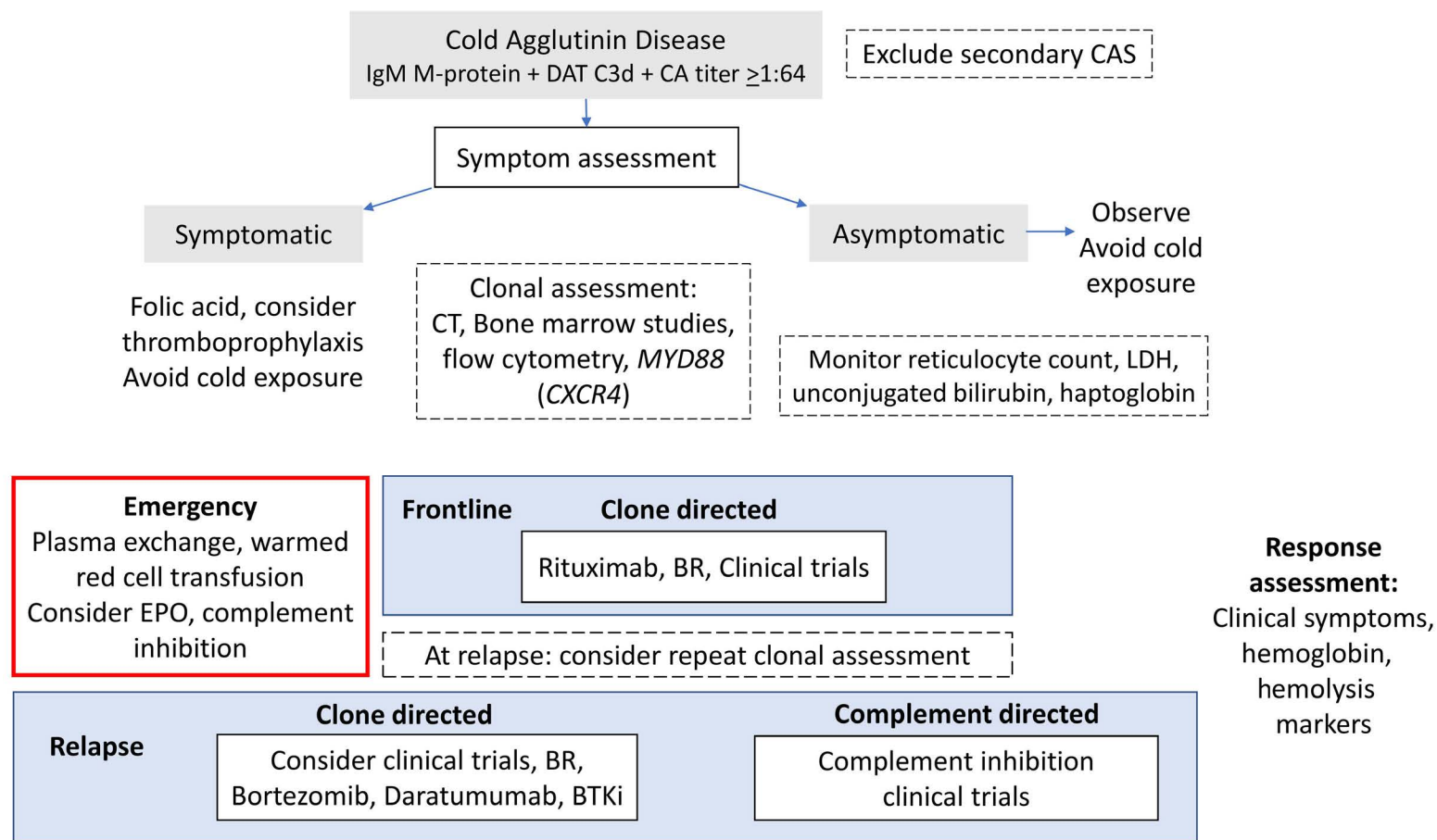


Figure 1. Management of cold agglutinin disease. DAT: direct antiglobulin test; CA: cold agglutinin; CAS: cold agglutinin syndrome; computed tomography; LDH: lactate dehydrogenase; EPO: erythropoietin; BR: bendamustine and rituximab; BTKi: Bruton tyrosine kinase inhibitor.

bine is efficacious (response rate: 62%; complete responses: 38%) but associated with an increased risk of secondary malignancy and is therefore not a preferred option.^{10,20} Based on a prospective study of 19 patients,²¹ the response rate to bortezomib-based treatment was 32%, although this was after only a single course of bortezomib. Bruton tyrosine kinase (BTK) inhibitors were effective in all four treated patients with relapsed CAD in a retrospective report.²² There is a case report of the use of daratumumab in CAD.²³

Clinical trials should be considered in relapsed disease. Promising studies have examined proximal complement inhibition to inhibit extravascular hemolysis. Complement inhibition necessitates indefinite treatment and fails to reduce vascular symptoms. In a phase III study of anti-C1s, sutimlimab, *versus* best supportive care, it was seen that the complement inhibitor rapidly halted hemolysis, produced transfusion independence in 73% of patients, increased hemoglobin concentration by more than 15 g/L and improved fatigue;²⁴ this drug has now been approved by the Food and Drug Administration.²⁴ The effect of complement inhibition on thrombosis has not been established; however, D-dimer and thrombin-antithrombin complex levels decreased on treatment.^{13,24} Use of the C5 inhibitor eculizumab rapidly abrogates the terminal complement pathway with a short time to response. However, in a phase II trial there was a marginal hemoglobin rise of 8 g/L.¹³ Proximal complement inhibition presumably has

greater effectiveness because it targets C3-mediated hemolysis via the liver, which is often predominant in CAD. Ongoing clinical trials of complement inhibition in CAD include those studying the C3b inhibitor, pegcetacoplan (phase III, NCT05096403), the complement factor B inhibitor, iptacopan (phase II, NCT05086744), the C1 esterase inhibitor, cinryze (phase II, 2012-003710-13/NL) and the C1s inhibitor BIVV020 (phase Ib, NCT04269551). Acute life-threatening intravascular hemolysis may necessitate transfusion. Plasma exchange may be employed provided that all priming fluids and the circuit apparatus are pre-warmed and that the replacement products are run through a warmer. Erythropoietin support can be considered as erythropoietin can be inappropriately low in autoimmune hemolytic anemia.²⁵ Complement-directed therapy may act as a bridge for rituximab combinations to target the underlying clone, which can take weeks to have an effect.

Cryoglobulinemia

Cryoglobulinemia is characterized by immunoglobulins that precipitate at temperatures below 37°C and redissolve on warming. Monoclonal IgM can be associated with type I and type II cryoglobulinemia. Type I cryoglobulinemia consists of monoclonal immunoglobulins only. In type II “mixed” cryoglobulinemia there is a monoclonal com-

ponent possessing avidity for the polyclonal component of a different isotype (most frequently IgM with rheumatoid factor activity, the ability to bind to the Fc portion of IgG). The rheumatoid factor detected in type II cryoglobulinemia is a monoclonal IgM κ in over 85% of cases.²⁶ While most cases of type II cryoglobulinemia are related to hepatitis C, here we focus on those related to monoclonal IgM.

Clinical characteristics

Data characterizing patients with monoclonal IgM and cryoglobulinemia are scant. The clinical characteristics have been gleaned from retrospective cohorts grouping together IgG and IgM cases. The largest series reported over 1,600 unselected patients with cryoglobulinemia. Nine percent had type I cryoglobulinemia and 47% had type II.²⁶ The only series characterizing the symptoms of IgM type I cryoglobulinemia included 26 patients; 35% had underlying MGUS, 35% had WM and 31% had non-Hodgkin lymphoma.²⁷ The incidence is likely underestimated as most literature reports are derived from centers that do not routinely screen for cryoglobulinemia upon recognition of an IgM clone.³

A wide spectrum of symptoms may be present (Figure 2). The symptoms of type I cryoglobulinemia are caused by vascular occlusion whereas those of type II are due to small and medium vessel vasculitis. Cutaneous involvement is most frequent in type I cryoglobulinemia. Cutaneous manifestations range from purpura, livedo reticularis, acrocyanosis to cold urticaria, digital ischemia, ulcers and necrosis. Among 26 patients, 46% had skin involvement and less than 10% had peripheral neuropathy (8%), arthralgia (8%) or renal involvement (4%).²⁷ Other studies found peripheral neuropathy in a higher proportion of IgM cases, mainly sensory neuropathy (70%), but sensorimotor polyneuropathy and mononeuritis multiplex were also seen.²⁸ Central nervous system involvement is rare unless due to hyperviscosity.²⁹ No studies have reported specific presenting features of type II cryoglobulinemia in patients with circulating monoclonal IgM. In a mixed cohort of 203 type II patients with an underlying hematologic disorder in 23%, skin manifestations predominated (85%). Compared to type I cryoglobulinemia there was a greater proportion of peripheral neuropathy (56%), joint (41%), renal (38%), gastrointestinal (6%) and pulmonary (2%) involvement. Hyperviscosity is almost never seen.

Diagnostic workup

Laboratory testing is critical as a minimal amount of measurable cryoglobulin may cause symptoms. In one study in which two-thirds of patients were symptomatic, 58% of the IgM type I cryoglobulinemia cases had a cryocrit of <1%, which was a significantly greater proportion

than in IgG cryoglobulinemia.²⁷ Symptoms do not correlate with the cryocrit and depend instead on the temperature at which precipitation occurs.²⁹ Accurate detection of cryoglobulins requires samples to be taken into pre-warmed tubes which must not be allowed to cool below 37°C until the serum is separated, as the cryoglobulin may precipitate and not be detected. Similarly, a false-negative M-protein result may result from the same process. In a French study, 9% of cases with negative results were positive on a follow-up test.²⁶ Care must be taken with pre-analytical variables; repeat testing of M-protein and cryoglobulins is indicated if the clinical suspicion is high. Increased plasma viscosity in the absence of a high IgM should trigger clinicians to consider cryoglobulinemia. A tissue biopsy may be indicated to identify renal or nerve involvement and distinguish it from other causes. Intra-vascular precipitation of IgM triggered by exposure to cold results in thrombotic obstruction and ischemia in small vessels as evidenced on biopsy in type I cryoglobulinemia. Leukocytoclastic vasculitis may be evident in type II cryoglobulinemia.

Treatment

A treatment approach is outlined in Figure 2. There is a paucity of data to guide optimal management. Mild symptoms may abate with cold prevention. Rapidly progressive nephropathy and neuropathy have been reported at various stages of the disease course, so careful monitoring is recommended.²⁸ When cryoglobulinemia is tested for exclusively in symptomatic patients, treatment is commenced for cryoglobulinemia-related symptoms in the majority (80%).³⁰ Response assessment is not standardized and mostly focuses on symptomatic improvement.²⁷ The cryocrit at treatment initiation, change in cryocrit and time to nadir were predictive of symptom improvement in a mixed cohort of patients with IgG and IgM type I cryoglobulinemia. The underlying diagnosis of MGUS or lymphoma did not affect symptom improvement.³⁰ Treatment regimens are heterogeneous and have been used in small series of patients. Plasma exchange may temporize critical symptoms and is used in up to a third of all cases of cryoglobulinemia in mixed cohorts; a warming procedure should be in place.³⁰⁻³² In the absence of robust evidence, definitive treatment should be directed at the underlying clone. Steroids (1 mg/kg) are used in up to 90% of all cases of cryoglobulinemia, often together with immunosuppression.^{31,32} Rituximab combinations or bortezomib-based treatment are typically employed²⁷ with symptomatic responses in approximately 80% of cases.^{27,29,31} Disappearance of cryoglobulin may be seen in half of patients.³⁰ Transient disease exacerbation (an 'IgM flare') has been described following the use of rituximab in type I cryoglobulinemia with a low disease burden (<10% infiltrate)³³ and in type II cryoglobulinemia.³⁴ Some

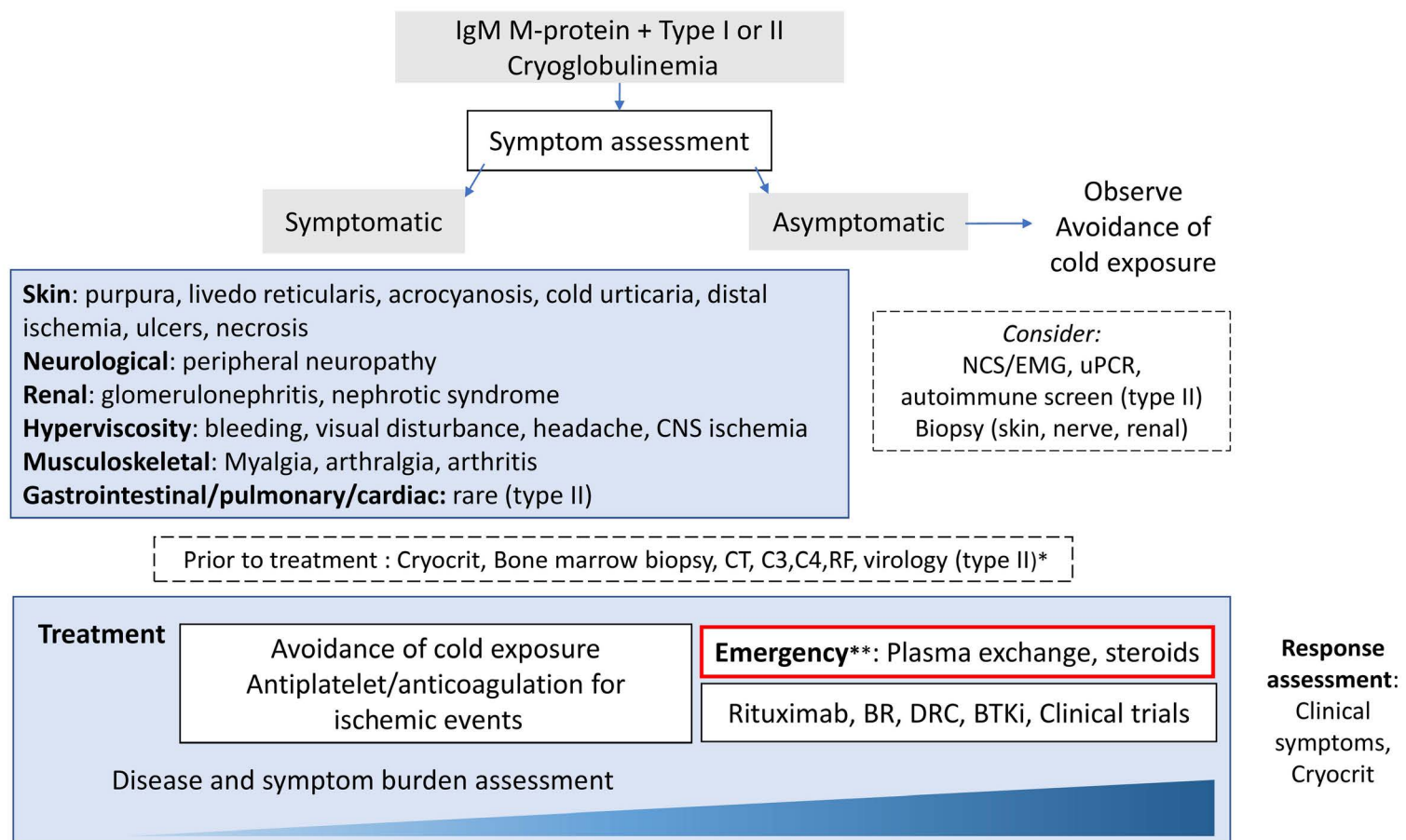


Figure 2. Management of cryoglobulinemia. *Virology testing includes a full hepatitis B profile, hepatitis C, and human immunodeficiency virus. **Emergency indications include symptomatic hyperviscosity, critical ischemia, severe neuropathy, and progressive renal impairment. CNS: central nervous system; NCS/EMG: nerve conduction studies, electromyography; uPCR, urine protein creatinine ratio; CT: computed tomography; BR: bendamustine and rituximab; DRC: dexamethasone, rituximab, cyclophosphamide; BTKi: Bruton tyrosine kinase inhibitor.

authors have suggested that a post-rituximab flare in type II cryoglobulinemia may be due to the exogenous IgG from the rituximab infusion which may also be a target of the monoclonal IgM. A study examining plasma exchange prior to rituximab to prevent IgM flares is ongoing (NCT04692363). Currently there are no data on the use of autologous stem cell transplantation or BTK inhibitors in IgM-associated cryoglobulinemia.

IgM-associated AL amyloidosis

AL amyloidosis is a rare disorder caused by extracellular deposition of insoluble misfolded monoclonal light chain fragments, produced by an underlying plasma cell dyscrasia or lymphoma, as amyloid fibrils in tissues. IgM-associated amyloidosis accounts for 5 to 7% of all systemic amyloidoses.³⁵⁻³⁹ In non-IgM AL amyloidosis, advances in treatment have resulted in marked improvement in survival, although patients with advanced disease have a poor outcome. Data on IgM-associated AL amyloidosis show no improvement over time.⁴⁰

Clinical characteristics

Due to its rarity, IgM-associated amyloidosis is less well characterized but increasingly recognized as a distinctive entity.⁴⁰ When compared to non-IgM amyloidosis, patients

are older^{36,37} with a history of MGUS or WM up to 65 months prior to diagnosis.³⁸

Multiple series^{36,38,41} indicate a smaller proportion of λ light chain involvement compared to that in non-IgM cases. Presenting free light chain levels are lower than in non-IgM AL amyloidosis and in the largest study so far of IgM-associated amyloidosis only two-thirds of the 250 patients had a greater than 50 mg/L difference between involved and uninvolved free light chains.⁴⁰ The pattern of organ involvement is also different, with a greater propensity for lymph node and soft tissue deposition (35%). Cardiac involvement is less common (45%) and neuropathy more frequent (28%).^{36,38,40}

Diagnostic workup

The exact nature of the clonal dyscrasia in IgM-associated AL amyloidosis remains unclear. The Mayo group has suggested two types, based on morphology; lymphoid predominant (lymphoplasmacytic lymphoma) or plasma cell predominant (pure plasma cell neoplasm).³⁸ Of 75 cases, the lymphoid predominant type (63%) showed a higher tumor infiltrate, *MYD88*^{L265P} in 84%, *CXCR4*^{MUT} in 29% but absent t(11;14), similar to WM. By contrast, the cases of pure plasma cell neoplasm (23%) had similar rates of t(11;14) compared to non-IgM-associated amyloidosis and no *MYD88*^{L265P}/*CXCR4*^{MUT}, similar to IgM myeloma.³⁸ Patients with the pure plasma cell neoplasm type appear to have

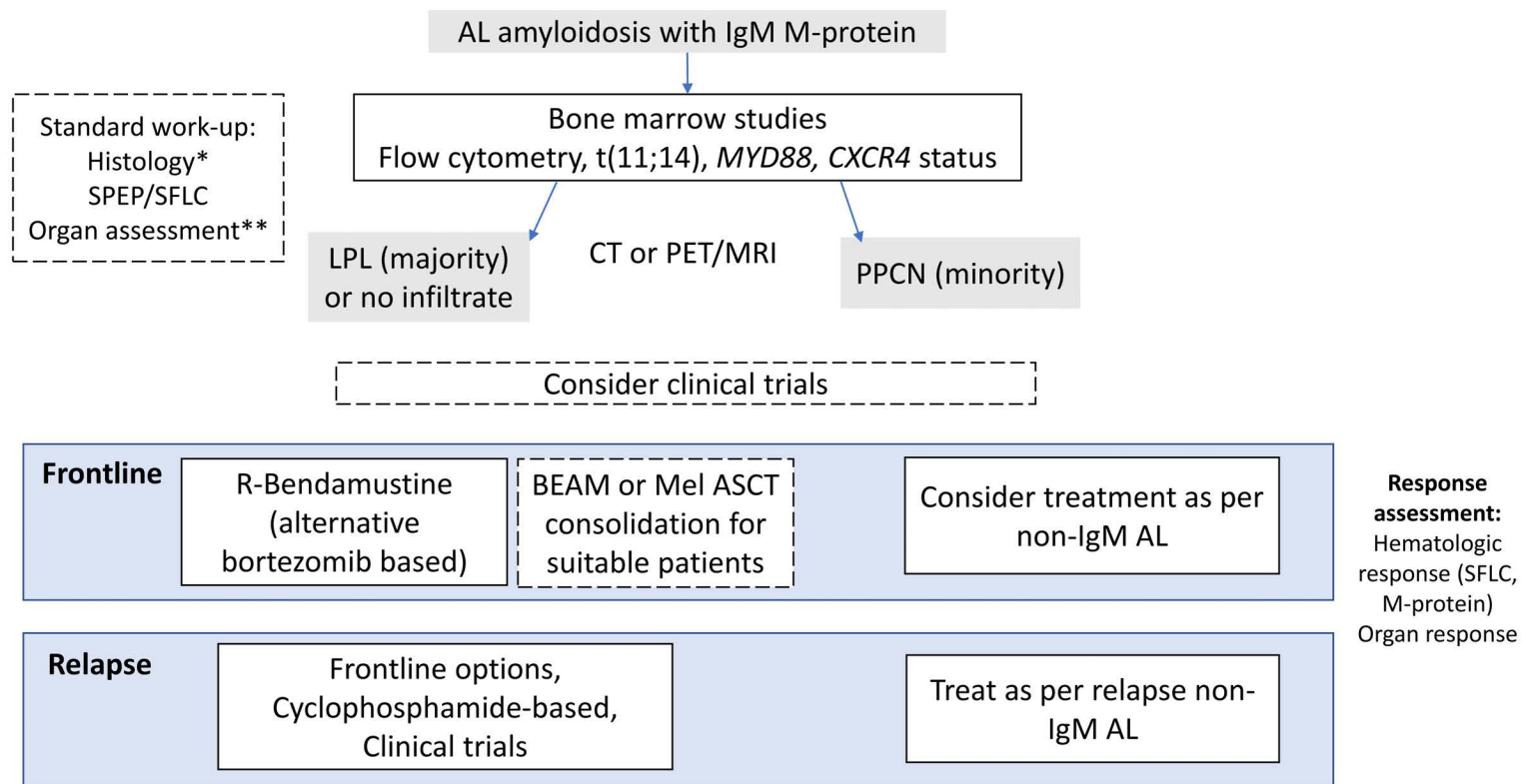


Figure 3. Management of IgM-associated amyloidosis. *Histological assessment includes targeting affecting organ, consider abdominal fat biopsy. Exclude other acquired and hereditary amyloidoses. **Organ assessment includes comprehensive evaluation of organs including cardiac, renal, neurological, gastrointestinal and soft tissue involvement. M-protein: monoclonal protein; SPEP: serum protein electrophoresis; SFLC: serum free light chains; LPL: lymphoplasmacytic lymphoma; CT: computed tomography; PET: positron emission tomography; MRI: magnetic resonance imaging; PPCN: pure plasma cell neoplasm; R-Bendamustine: rituximab plus bendamustine; BEAM: carmustine, etoposide, cytarabine, melphalan; Mel, melphalan; ASCT: autologous stem cell transplantation; AL: AL amyloidosis.

poorer outcomes. These findings need independent confirmation to hone treatment approaches.

Treatment

There are no consensus guidelines, approved treatments or prospective clinical trials for IgM amyloidosis. The aims of treatment are to reduce the clonal burden and improve performance status with a view to extending survival. A treatment algorithm is summarized in Figure 3. Evidence is largely limited to retrospective series with heterogeneous regimens. Criteria developed for response assessment in non-IgM AL amyloidosis are applicable to IgM-associated AL amyloidosis with assessment of hematologic response and organ response. Response assessment by both free light chains and M-protein had prognostic significance in retrospective series^{35,36} alongside age, Mayo stage, cardiac involvement, liver involvement⁴⁰ and prior WM treatment.³⁸ β_2 -microglobulin and lactate dehydrogenase levels do not independently affect survival,⁴¹ unlike in WM,⁴² which may be related to the low tumor burden. Despite less cardiac involvement, patients with IgM-associated amyloidosis do not have superior survival compared to those with non-IgM-associated amyloidosis,³⁸ attributable to the inability to achieve deep clonal responses.

Induction of hematologic response is more challenging with a reported 6-month overall response rate of 39% versus 59% ($P=0.008$), deep responses are seen in only 24%.³⁸

Organ response rates are consequently poor (5% cardiac, 18% renal) and lower than those in a non-IgM-associated cohort.⁴³

Strategies to target the lymphoplasmacytic and plasma cell clones have been employed. The best outcomes have been achieved by autologous stem cell transplantation, with more than 90% achieving a hematologic response.^{40,41,44} However, up to just 25% of all-comers were eligible for this intense therapy. The largest series of autologous stem cell transplantation in 38 patients⁴⁴ included 58% who had received prior therapy and the 100-day mortality was 5%. There was, however, a relatively low rate of cardiac involvement (26%), demonstrating the importance of the selection of patients. Induction chemotherapy prior to autologous stem cell transplantation is not universally utilized. Conditioning most commonly involves melphalan, however the BEAM (carmustine, etoposide, cytarabine, melphalan) regimen has also been used.⁴⁴

As the majority of cases have an underlying lymphoplasmacytic clone, induction therapy with rituximab-based combination chemotherapy is strongly preferred. In 27 cases, the bendamustine-rituximab combination resulted in an intention-to-treat hematologic response rate of 59%, with complete responses in 11%, and a median progression-free survival of 34 months. Sixty percent of patients treated with this combination in second line achieved a very good partial response.⁴⁵ Bendamustine is neither neurotoxic nor cardiotoxic. Bortezomib in combination with

rituximab and dexamethasone may provide rapid disease control. The only prospective trial of this strategy recruited ten patients over 1 year.⁴⁶ A hematologic response was achieved by 78% with sustained responses at a median of 11 months, after only two cycles. However, there were no complete responses. Treatment had to be interrupted in 30% of patients because of toxicity. Patients with grade 3 sensory and/or grade 1 painful neuropathy were excluded and treatment-related neuropathy is a particular concern in these patients. Responses to frontline alkylating agents have been disappointing. In a series of 46 patients treated after 2003, the hematologic response rate was 37% and there were no complete responses.⁴¹ Immunomodulatory drugs alone result in variable response rates, but mostly less than 50%. BTK inhibitors, although promising in WM, have been associated with low response rates in IgM-associated amyloidosis. Of eight patients treated with ibrutinib, only two achieved a hematologic response and the median overall survival was 9 months.⁴⁷ No studies have examined anti-CD38-bortezomib combinations, which is the standard of care in non-IgM AL amyloidosis.⁴⁸

We consider upfront bendamustine-rituximab the treatment of choice in IgM-associated amyloidosis, consolidated with autologous stem cell transplantation when the patient's performance status allows. There is no consensus regarding less fit patients; treatment choices need to be individualized depending on affected organs and tolerance of treatments. Overall in this condition, deep responses remain poor. Future studies are required to address whether regimens based on novel agents (including venetoclax, daratumumab and the newer BTK inhibitors) may lead to improvements in the outcomes of patients with non-IgM AL amyloidosis.

IgM-related neuropathies

IgM-related peripheral neuropathies encompass an array of entities including immune-mediated neuronal damage, such as that caused by antibodies to myelin-associated glycoprotein (MAG), or direct neurotoxicity with infiltration by lymphoma (neurolymphomatosis), light chains (amyloidosis) or cryoglobulins. Peripheral neuropathy has been found to occur in 15-30% of MGUS and WM cases,^{49,50} but the prevalence is likely affected by selection bias and variable neurological evaluation in patients as part of a work-up of IgM M-protein. The UK registry documented 153 patients with IgM-related neuropathy, comprising anti-MAG neuropathy (55%), non-MAG IgM neuropathy (35%) and less frequently (<4% each) AL amyloidosis, cryoglobulinemia, anti-ganglioside neuropathy and CANOMAD syndrome (chronic ataxic neuropathy, ophthalmoplegia, IgM M-protein, cold agglutinins and disialosyl ganglioside antibodies).⁵⁰

Clinical characteristics

Anti-MAG neuropathy is the most common and best-defined IgM-related neuropathy. Patients typically present with chronic-onset, distal, symmetric neuropathy, sensory ataxia and tremor. Patients may be misdiagnosed as having chronic inflammatory demyelinating polyneuropathy. It is important to correctly classify the neuropathy (Table 3) as this has significant management implications. Atypical "red flag" symptoms *not* consistent with anti-MAG peripheral neuropathies include acute onset, rapid tempo of symptoms, pain, dysautonomia, weight loss, and cutaneous or central nervous system signs. These should alert the clinician to consider alternate diagnoses (Figure 4). CANOMAD syndrome is a very rare chronic progressive condition associated with anti-ganglioside antibodies. This syndrome should be considered if there is sensory loss with ophthalmoplegia or ataxia. Bing-Neel syndrome is the term for central nervous system infiltration by lymphoplasmacytic lymphoma; consensus guidelines on its diagnosis, treatment and response criteria have been published.⁵¹ Cryoglobulinemia and amyloidosis are discussed in their respective sections.

Diagnostic workup

The majority of patients with IgM-related neuropathy (>90%) have symptoms of the underlying neurological disorder at diagnosis.⁵⁰ This supports the strong need for careful early evaluation of patients jointly with an expert neurologist. The presence of a peripheral neuropathy alongside a serum monoclonal IgM or anti-MAG antibody does not equal a causal relationship, since gammopathies as well as peripheral neuropathies are both increasingly prevalent with age. Patients should be tested for anti-MAG antibodies, but only high-titer antibodies are clinically relevant in the presence of a characteristic clinical picture in anti-MAG neuropathy.⁵² A reduction in anti-MAG titers and levels of IgM M-protein with therapy appeared to correlate with improvement in neuropathy in a retrospective analysis of 50 studies.⁵³ Responders also had a younger age of onset.⁵³

Nerve conduction tests and electromyography are warranted and characteristically show demyelination with reduced conduction velocity, disproportionately prolonged distal motor latency and absent sural potentials. Partial motor conduction block is rare. Progressive demyelination may result in secondary axonal loss which affects the likelihood of neural recovery.⁵² Magnetic resonance imaging of the neuraxis and evaluation of large volumes of cerebrospinal fluid may be required if central nervous system involvement is suspected. A nerve biopsy may be needed if the diagnosis remains elusive despite systematic investigation. Comprehensive consensus guidelines provide further details.⁵²

Table 3. Features of IgM and non-IgM-related neuropathies.

	Non-IgM-related			IgM-related					
	CIDP	Therapy related	Anti MAG	Non-MAG PN	Cryoglobulinaemia	POEMS	Amyloidosis	CANOMAD	Bing-Neel syndrome
Onset	Gradually progressive, relapsing remitting	Treatment-emergent	Gradually progressive	Gradually progressive	*Rapidly progressive <6 months	Gradually progressive	*Rapidly progressive <6 months	Gradually progressive	Gradually progressive
Peripheral nervous system features	Symmetrical, proximal, sensory and motor	Symmetrical, distal, progressive	Symmetrical, distal, sensory predominant, mild-moderate distal muscle weakness	Symmetrical, distal, sensory predominant, mild-moderate distal muscle weakness	Symmetrical, sensory, may be painful*	Symmetrical, ascending sensorimotor neuropathy	*Symmetrical, painful, length dependent, sensorimotor neuropathy. Autonomic dysfunction	Paraesthesia, hypoesthesia, ataxia, ophthalmoplegia	Rare involvement of peripheral nervous system
Demyelinating/axonal	Demyelinating	Axonal	Demyelinating	Demyelinating	Axonal	Mixed	Axonal	Mixed	Neither
Supportive tests	Conduction block and abnormal temporal dispersion	Timing is key. Most commonly bortezomib	High anti-MAG titer typical	Anti-MAG negative	Clinical features are key (see CG section)	VEGF, clinical features (skin, edema, endocrinopathy, thrombocytosis)	Organ involvement	Anti-ganglioside antibodies	CNS signs* CSF studies, MRI head
Light chain predominance	Not IgM associated	Not IgM associated	IgMκ 70%-80% ⁷⁷	Not reported	IgMκ 85% type I	Not reported in IgM. Overall λ LC restriction in POEMS	IgMλ predominance	No κ/λ predominance	IgMκ 84% ⁶¹

*Red flag features. CIDP: chronic inflammatory demyelinating polyneuropathy; MAG: myelin-associated glycoprotein; PN: polyneuropathies; POEMS: polyneuropathy, organomegaly, endocrinopathy, monoclonal gammopathy and skin abnormalities; CANOMAD: chronic ataxic neuropathy, ophthalmoplegia, IgM M-protein, cold agglutinins and disialosyl ganglioside antibodies; CG: cryoglobulinemia; LC: light chain; CNS: central nervous system; CSF: cerebrospinal fluid; MRI: magnetic resonance imaging.

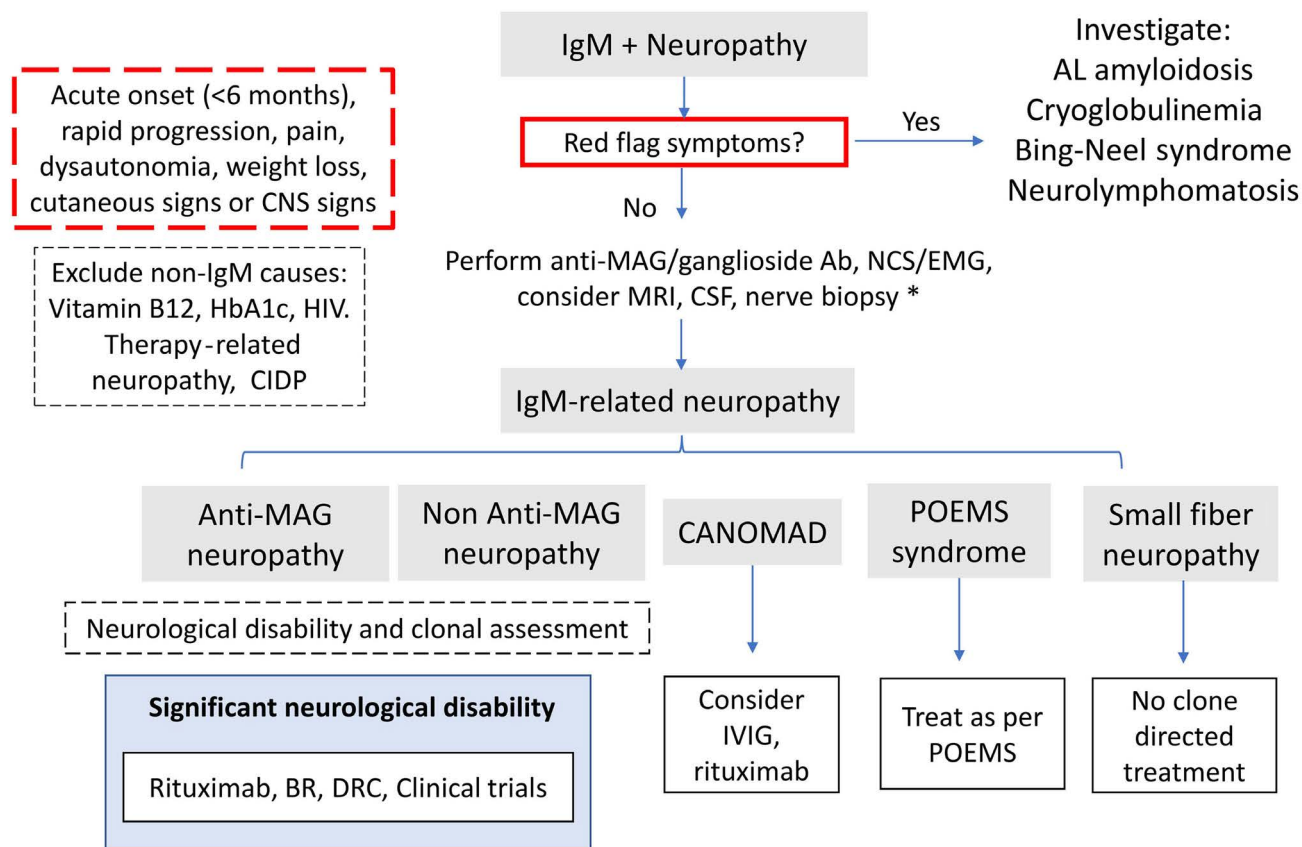


Figure 4. Management of IgM-related neuropathies. *Nerve biopsy after consultation with an expert neurologist, in selected cases only. CNS: central nervous system; HIV: human immunodeficiency virus; CIDP: chronic inflammatory demyelinating polyneuropathy; MAG: myelin-associated glycoprotein; Ab: antibody; NCS/EMG: nerve conduction studies/electromyography; MRI: magnetic resonance imaging; CSF: cerebrospinal fluid; CANOMAD: chronic ataxic neuropathy, ophthalmoplegia, IgM M-protein, cold agglutinins and disialosyl ganglioside antibodies; POEMS: polyneuropathy, organomegaly, endocrinopathy, monoclonal gammopathy and skin abnormalities; BR: bendamustine plus rituximab; DRC: dexamethasone, rituximab, cyclophosphamide.

Treatment

In general, in anti-MAG and non-anti-MAG neuropathy, treatment should be initiated only in those with significant or progressive disability.⁵² The aim of treatment is to halt progression and improve neurological function, although this may potentially take months to years, even after IgM responses. Although many neurological disability scales exist, they are not available outside of specialist neurology clinics and there is no standardized method of response assessment. The use of serial validated patient-reported outcome scores (e.g., the Inflammatory Rasch-Built Overall Disability Scale) is advocated, as this can be easily undertaken in non-specialist clinics.⁵² An observational trial is currently recruiting with an aim to develop an IgM-specific disability scale (NCT03918421). Patients should be managed in a multidisciplinary fashion with input from neurology, hematology, physiotherapy and occupational therapy.

Rituximab is widely, but inconsistently used in the setting of IgM-related neuropathies. A meta-analysis of rituximab demonstrated improvement in disability scales at 8 to 12 months and long-term efficacy was demonstrated in a third of patients.⁵⁴ A transient flare of symptoms following the administration of rituximab was observed in 12% in a large series of patients with anti-MAG antibodies.⁵⁵ Steroids, intravenous immunoglobulins and plasma exchange alone do not provide long-term clinical benefit in anti-MAG neuropathy^{56,57} and are resource-intensive, respectively. In contrast, intravenous immunoglobulins and

rituximab-based regimens are effective in CANOMAD syndrome (producing partial clinical responses or better in 53% and 52% of patients, respectively),⁵⁸ while chronic inflammatory demyelinating polyneuropathy is responsive to intravenous immunoglobulins,⁵² highlighting the relevance of correct diagnostic classification.

Although data are largely limited to retrospective series, targeting the underlying clone is feasible in IgM-related neuropathy; the optimum depth of response is unknown. Clinical improvement or stabilization is significantly more likely with rituximab-containing therapy (dexamethasone, rituximab, cyclophosphamide; bendamustine plus rituximab; cyclophosphamide, prednisolone, rituximab, vincristine), non-amyloid-related neuropathy and attainment of at least partial haematologic response.^{49,50}

There is an unmet need for reliable biomarkers for diagnosis, appropriate selection of patients for treatment and criteria for monitoring response.⁵⁹ There is a lack of prospective clinical trials to optimize treatment options. A phase II clinical trial, MAGNAZ, of the oral BTK inhibitor zanubrutinib in anti-MAG peripheral neuropathies is underway.⁶⁰

Schnitzler syndrome

Schnitzler syndrome is a rare auto-inflammatory disorder characterized by an IgM monoclonal gammopathy and

chronic recurrent urticarial rash. The Strasbourg criteria outline additional minor criteria of recurrent fever, abnormal bone remodeling with or without bone pain, neutrophilic dermal infiltrate, leukocytosis and elevated C-reactive protein.⁶¹ Around 300 cases have been reported to date. It is underdiagnosed and, despite its rarity, is important to identify as specific treatment can significantly improve quality of life.⁶²

Clinical characteristics

Of 281 cases in the largest case series, fever was present in 72%, anemia in 63%, arthralgia in 68%, bone pain in 55%, lymphadenopathy in 26%, and liver or spleen enlargement and neuropathy in less than 10%.⁶³ In smaller series fatigue and weight loss were documented in up to around 50% of cases.^{62,64} The urticarial rash can cover any part of the body, but face, palm and sole involvement is infrequent, as is intense pruritis. Skin lesions typically resolve within hours.⁶⁵ The time from onset of symptoms to diagnosis is long, at a median of 5 years and may be as long as 20 years.⁶²

The monoclonal gammopathy is almost always IgMκ. Bone marrow involvement is minimal, being around 4% in one series, and a median M-protein concentration of 6 g/L has been documented.⁶² In the largest case series, 63% of the 281 bone marrow samples were reported as normal.⁶³ The *MYD88*^{L265P} mutation was detected in the peripheral blood of 30% of 30 patients.⁶⁶ The authors suggested that the presence of this mutation may correlate with the risk of WM, although the mutation detection rate may have been underestimated as the sensitivity of detecting peripheral blood B-cell clones may be hampered when the level of disease burden is low. The frequency of the *MYD88*^{L265P} mutation in bone marrow has not been studied. Chronic inflammation may lead to AA amyloidosis in 2% of cases of Schnitzler syndrome. At a median of 8 years, the rate of evolution to lymphoma is 20%, which is in line with progression in unselected cohorts of patients with IgM MGUS.^{61,63}

Schnitzler syndrome is associated with cytokine dysregulation. It bears close phenotypic resemblance to an inherited disorder, cryopyrin-associated periodic syndrome, caused by gain-of-function mutations in the *NLRP3* gene. This results in upregulation of interleukin (IL)-1β production and has informed therapeutic options in Schnitzler syndrome, by targeting IL-1β.

Diagnostic workup

There is no single diagnostic test and the diagnosis is made based on clinical characteristics. Differential diagnoses for the rash and fever include adult-onset Still disease, systemic lupus erythematosus, acquired C1 esterase deficiency, cryopyrinopathies and cryoglobulinemia (cold-induced urticaria). Skin biopsy reveals a neutrophilic urticarial dermatosis without features of vasculitis.

Treatment

Treatment is aimed at reducing the considerable associated morbidity related to rash, fever and joint and bone pain. Symptoms respond poorly to historic first-line agents including antihistamines, nonsteroidal anti-inflammatory drugs, dapsone and colchicine.⁶⁵ The use of high-dose steroids, although moderately effective, is limited by long-term toxicities.

Without anti-IL treatment, morbidity is high. In a series of 21 patients, all had almost daily symptoms with a profound effect on their quality of life.⁶⁴ Anti-IL-1 agents, such as anakinra, canakinumab, and rilonacept, have all been used but not directly compared. Anakinra is the agent with which experience is greatest and is the treatment of choice. It is a recombinant IL-1-receptor antagonist and has the greatest efficacy (94% efficacy in 86 cases),⁶³ with durable responses (83% complete responses after a median of 36 months).⁶⁷ Anakinra has a half-life ($t_{1/2}$) of 4-6 hours and provides impressive control of all signs within hours, normalization of C-reactive protein levels and abrogation of the risk of AA amyloidosis.⁶⁴ Nonetheless, patients require continuous daily injections and relapse occurs after treatment discontinuation. Canakinumab, an IL-1β monoclonal antibody, is long-acting ($t_{1/2}$ 21-28 days) and is, therefore, administered less frequently. Data from phase II, placebo-controlled, randomized trials have demonstrated its efficacy. For 17 patients in a long-term study, clinical efficacy was greatest when patients injected canakinumab as needed. A systematic review of 34 patients showed that 59% achieved complete responses.⁶⁸ Rilonacept, an IL-1 binding and neutralizing fusion protein, achieved near complete responses in 50% of cases.⁶⁹ Tocilizumab, an IL-6 receptor antagonist, has been beneficial in three patients who were refractory to anakinra.⁷⁰ Cyclophosphamide, rituximab and ibrutinib have achieved responses when treatment was given for overt lymphoma but have been largely ineffective or untested in the absence of lymphoma.⁶⁵ There is little to support the notion that anti-IL therapy affects the underlying B-cell clone.

Conclusion

We have discussed a range of distinctive entities of IgM MGCS, including their specific clinical characteristics, underlying clonal profile, and diagnostic workup as well as treatment considerations. Careful evaluation of the presenting features and thorough interrogation of the underlying clone are critical. Determining the nature of either a mature B-cell derived clone or plasma cell clone will have management implications. There is an IgMκ predominance in all cases except IgM-associated AL amyloidosis. The indication for treatment is dictated by the

pathological characteristics of the circulating IgM rather than by the tumor itself. While deep suppression of the pathogenic IgM is typically required for response, achieving long-term clonal eradication is challenging, as demonstrated by low complete response rates. Treatment inhibiting the pathogenic effects of IgM while not directed at the underlying clone has led to great success in CAD (complement inhibitors) and Schnitzler syndrome (cytokine inhibition), whereas the other treatments are centered on eradicating the underlying clone. Treatment approaches in cryoglobulinemia and IgM-related peripheral neuropathies are the least well developed. A multidisciplinary approach is required particularly for IgM-related neuropathies and Schnitzler syndrome.

Due to the rarity of IgM MGCS, data are scant and collaborative research is imperative to aid defining optimal treatment strategies. International registries may better define characteristics and assess treatment outcomes. Future work exploring clone-directed treatment options and pathogenic IgM-directed therapies is welcomed.

Disclosures

JK has no conflicts of interest to disclose. SD'S has received research funding, honoraria for advisory board work and conference support from Janssen and BeiGene, and

honoraria for advisory board work from Sanofi. MCM has provided speakers bureau services for Medscape and BMS, consultancy for Janssen-Cilag and Gilead Sciences Netherlands B.V., sat on advisory boards for Janssen Pharmaceutica and Alnylam, and received hospitality support from Celgene. MJK has acted as a consultant for and received honoraria and travel support from Novartis and Miltenyi Biotec, has received research funding from Takeda and Celgene, has acted as a consultant for and received honoraria, travel support and research funding from Kite, a Gilead Company, and Roche, and has acted as a consultant for and received honoraria from BMS/Celgene. AW has provided consultancy services for Alexion, AstraZeneca Rare Diseases and Janssen, and has received honoraria from Celgene and Takeda, clinical trial funding from Caelum Biosciences, and research funding from Amgen. JMIV has received reimbursement of travel costs from Celgene, receives research funding from Beigene (institutional) and has participated in an advisory board as well as acted as a consultant for Sanofi (institutional honoraria)

Contributions

JK and JMIV wrote the first draft of the manuscript, SD'S, MCM, MJK, and AW equally reviewed and added critical discussions throughout the writing of the review.

References

1. Swerdlow SH, Campo E, Pileri SA, et al. The 2016 revision of the World Health Organization classification of lymphoid neoplasms. *Blood*. 2016;127(20):2375-2390.
2. Fermand JP, Bridoux F, Dispenzieri A, et al. Monoclonal gammopathy of clinical significance: a novel concept with therapeutic implications. *Blood*. 2018;132(14):1478-1485.
3. Owen RG, Treon SP, Al-Katib A, et al. Clinicopathological definition of Waldenstrom's macroglobulinemia: consensus panel recommendations from the Second International Workshop on Waldenstrom's Macroglobulinemia. *Semin Oncol*. 2003;30(2):110-115.
4. Castillo JJ, Advani RH, Branagan AR, et al. Consensus treatment recommendations from the tenth International Workshop for Waldenström Macroglobulinaemia. *Lancet Haematol*. 2020;7(11):e827-e837.
5. Kyle RA, Larson DR, Therneau TM, et al. Long-term follow-up of monoclonal gammopathy of undetermined significance. *N Engl J Med*. 2018;378(3):241-249.
6. Treon SP, Xu L, Yang G, et al. MYD88 L265P somatic mutation in Waldenström's macroglobulinemia. *N Engl J Med*. 2012;367(9):826-833.
7. Varettoni M, Zibellini S, Defrancesco I, et al. Pattern of somatic mutations in patients with Waldenström macroglobulinemia or IgM monoclonal gammopathy of undetermined significance. *Haematologica*. 2017;102(12):2077-2085.
8. Bazarbachi AH, Avet-Loiseau H, Szalat R, et al. IgM-MM is predominantly a pre-germinal center disorder and has a distinct genomic and transcriptomic signature from WM. *Blood*. 2021;138(20):1980-1985.
9. Jäger U, Barcellini W, Broome CM, et al. Diagnosis and treatment of autoimmune hemolytic anemia in adults: recommendations from the First International Consensus Meeting. *Blood Rev*. 2020;41:100648.
10. Berentsen S, Barcellini W, D'Sa S, et al. Cold agglutinin disease revisited: a multinational, observational study of 232 patients. *Blood*. 2020;136(4):480-488.
11. Berentsen S, Ulvestad E, Langholm R, et al. Primary chronic cold agglutinin disease: a population based clinical study of 86 patients. *Haematologica*. 2006;91(4):460-466.
12. Barcellini W, Fattizzo B, Zaninoni A, et al. Clinical heterogeneity and predictors of outcome in primary autoimmune hemolytic anemia: a GIMEMA study of 308 patients. *Blood*. 2014;124(19):2930-2936.
13. Röth A, Bommer M, Hüttmann A, et al. Eculizumab in cold agglutinin disease (DECADE): an open-label, prospective, bicentric, nonrandomized phase 2 trial. *Blood Adv*. 2018;2(19):2543-2549.
14. Randen U, Trøen G, Tierens A, et al. Primary cold agglutinin-associated lymphoproliferative disease: a B-cell lymphoma of the bone marrow distinct from lymphoplasmacytic lymphoma. *Haematologica*. 2014;99(3):497-504.
15. Małecką A, Trøen G, Delabie J, et al. The mutational landscape of cold agglutinin disease: CARD11 and CXCR4 mutations are correlated with lower hemoglobin levels. *Am J Hematol*. 2021;96(8):E279-E283.
16. Małecką A, Trøen G, Tierens A, et al. Frequent somatic mutations of KMT2D (MLL2) and CARD11 genes in primary cold agglutinin disease. *Br J Haematol*. 2018;183(5):838-842.

17. Malecka A, Delabie J, Ostlie I, et al. Cold agglutinin disease shows highly recurrent gains of chromosome 3, 12 and 18. *Blood*. 2019;134(Suppl 1):1488.
18. Berentsen S, Ulvestad E, Gjertsen BT, et al. Rituximab for primary chronic cold agglutinin disease: a prospective study of 37 courses of therapy in 27 patients. *Blood*. 2004;103(8):2925-2928.
19. Berentsen S, Randen U, Oksman M, et al. Bendamustine plus rituximab for chronic cold agglutinin disease: results of a Nordic prospective multicenter trial. *Blood*. 2017;130(4):537-541.
20. Berentsen S, Randen U, Vågan AM, et al. High response rate and durable remissions following fludarabine and rituximab combination therapy for chronic cold agglutinin disease. *Blood*. 2010;116(17):3180-3184.
21. Rossi G, Gramegna D, Paoloni F, et al. Short course of bortezomib in anemic patients with relapsed cold agglutinin disease: a phase 2 prospective GIMEMA study. *Blood*. 2018;132(5):547-550.
22. Jalink M, Berentsen S, Castillo JJ, et al. Effect of ibrutinib treatment on hemolytic anemia and acrocyanosis in cold agglutinin disease/cold agglutinin syndrome. *Blood*. 2021;138(20):2002-2005.
23. Tomkins O, Berentsen S, Arulogun S, Sekhar M, D'Sa S. Daratumumab for disabling cold agglutinin disease refractory to B-cell directed therapy. *Am J Hematol*. 2020 Jul 11. doi: 10.1002/ajh.25932. [Epub ahead of print]
24. Röth A, Barcellini W, D'Sa S, et al. Sutimlimab in cold agglutinin disease. *N Engl J Med*. 2021;384(14):1323-1334.
25. Fattizzo B, Michel M, Zaninoni A, et al. Efficacy of recombinant erythropoietin in autoimmune hemolytic anemia: a multicenter international study. *Haematologica*. 2021;132(5):622-625.
26. Kolopp-Sarda MN, Nombel A, Miossec P. Cryoglobulins today: detection and immunologic characteristics of 1,675 positive samples from 13,439 patients obtained over six years. *Arthritis Rheumatol*. 2019;71(11):1904-1912.
27. Zhang LL, Cao XX, Shen KN, et al. Clinical characteristics and treatment outcome of type I cryoglobulinemia in Chinese patients: a single-center study of 45 patients. *Ann Hematol*. 2020;99(8):1735-1740.
28. Néel A, Perrin F, Decaux O, et al. Long-term outcome of monoclonal (type 1) cryoglobulinemia. *Am J Hematol*. 2014;89(2):156-161.
29. Harel S, Mohr M, Jahn I, et al. Clinico-biological characteristics and treatment of type I monoclonal cryoglobulinaemia: a study of 64 cases. *Br J Haematol*. 2015;168(5):671-678.
30. Sidana S, Rajkumar SV, Dispenzieri A, et al. Clinical presentation and outcomes of patients with type 1 monoclonal cryoglobulinemia. *Am J Hematol*. 2017;92(7):668-673.
31. Terrier B, Karras A, Kahn JE, et al. The spectrum of type I cryoglobulinemia vasculitis: new insights based on 64 cases. *Medicine (Baltimore)*. 2013;92(2):61-68.
32. Terrier B, Krastinova E, Marie I, et al. Management of noninfectious mixed cryoglobulinemia vasculitis: data from 242 cases included in the CryoVas survey. *Blood*. 2012;119(25):5996-6004.
33. Nehme-Schuster H, Korganow AS, Pasquali JL, Martin T. Rituximab inefficiency during type I cryoglobulinaemia. *Rheumatology (Oxford)*. 2005;44(3):410-411.
34. Sène D, Ghillani-Dalbin P, Amoura Z, Musset L, Cacoub P. Rituximab may form a complex with IgM κ mixed cryoglobulin and induce severe systemic reactions in patients with hepatitis C virus-induced vasculitis. *Arthritis Rheum*. 2009;60(12):3848-3855.
35. Wechalekar AD, Lachmann HJ, Goodman HJ, Bradwell A, Hawkins PN, Gillmore JD. AL amyloidosis associated with IgM paraproteinemia: clinical profile and treatment outcome. *Blood*. 2008;112(10):4009-4016.
36. Palladini G, Russo P, Bosoni T, et al. AL amyloidosis associated with IgM monoclonal protein: a distinct clinical entity. *Clin Lymphoma Myeloma*. 2009;9(1):80-83.
37. Gertz MA, Buadi FK, Hayman SR. IgM amyloidosis: clinical features in therapeutic outcomes. *Clin Lymphoma Myeloma Leuk*. 2011;11(1):146-148.
38. Sidana S, Larson DP, Greipp PT, et al. IgM AL amyloidosis: delineating disease biology and outcomes with clinical, genomic and bone marrow morphological features. *Leukemia*. 2020;34(5):1373-1382.
39. la Torre A, Reece D, Crump M, et al. Light chain amyloidosis (AL) associated with B cell lymphoma a single center experience. *Clin Lymphoma Myeloma Leuk*. 2021;21(12):e946-e959.
40. Sachchithanatham S, Roussel M, Palladini G, et al. European collaborative study defining clinical profile outcomes and novel prognostic criteria in monoclonal immunoglobulin M-related light chain amyloidosis. *J Clin Oncol*. 2016;34(17):2037-2045.
41. Terrier B, Jaccard A, Harousseau JL, et al. The clinical spectrum of IgM-related amyloidosis: a French nationwide retrospective study of 72 patients. *Medicine (Baltimore)*. 2008;87(2):99-109.
42. Kastiris E, Morel P, Duhamel A, et al. A revised international prognostic score system for Waldenström's macroglobulinemia. *Leukemia*. 2019;33(11):2654-2661.
43. Venner CP, Lane T, Foard D, et al. Cyclophosphamide, bortezomib, and dexamethasone therapy in AL amyloidosis is associated with high clonal response rates and prolonged progression-free survival. *Blood*. 2012;119(19):4387-4390.
44. Sidiqi MH, Buadi FK, Dispenzieri A, et al. Autologous stem cell transplant for IgM-associated amyloid light-chain amyloidosis. *Biol Blood Marrow Transplant*. 2019;25(3):e108-e111.
45. Manwani R, Sachchithanatham S, Mahmood S, et al. Treatment of IgM-associated immunoglobulin light-chain amyloidosis with rituximab-bendamustine. *Blood*. 2018;132(7):761-764.
46. Palladini G, Foli A, Russo P, et al. Treatment of IgM-associated AL amyloidosis with the combination of rituximab, bortezomib, and dexamethasone. *Clin Lymphoma Myeloma Leuk*. 2011;11(1):143-145.
47. Pika T, Hegenbart U, Flodrova P, Maier B, Kimmich C, Schönland SO. First report of ibrutinib in IgM-related amyloidosis: few responses, poor tolerability, and short survival. *Blood*. 2018;131(3):368-371.
48. Kastiris E, Palladini G, Minnema MC, et al. Daratumumab-based treatment for immunoglobulin light-chain amyloidosis. *N Engl J Med*. 2021;385(1):46-58.
49. Treon SP, Hanzis CA, Ioakimidis LI, et al. Clinical characteristics and treatment outcome of disease-related peripheral neuropathy in Waldenström's macroglobulinemia (WM). *J Clin Oncol*. 2010;28(15_suppl):8114.
50. Tomkins O, Lindsay J, Keddie S, et al. Neuropathy with IgM gammopathy: incidence, characteristics and management, a Rory Morrison W.M.U.K Registry analysis. *Blood*. 2020;136(Suppl 1):1-2.
51. Minnema MC, Kimby E, D'Sa S, et al. Guideline for the diagnosis, treatment and response criteria for Bing-Neel syndrome. *Haematologica*. 2017;102(1):43-51.
52. D'Sa S, Kersten MJ, Castillo JJ, et al. Investigation and management of IgM and Waldenström-associated peripheral neuropathies: recommendations from the IWWM-8 consensus panel. *Br J Haematol*. 2017;176(5):728-742.
53. Hänggi P, Aliu B, Martin K, Herrendorff R, Steck AJ. Decrease in serum anti-MAG autoantibodies is associated with therapy

- response in patients with anti-MAG neuropathy: retrospective study. *Neurol Neuroimmunol Neuroinflamm*. 2022;9(1):e1109.
54. Lunn MP, Nobile-Orazio E. Immunotherapy for IgM anti-myelin-associated glycoprotein paraprotein-associated peripheral neuropathies. *Cochrane Database Syst Rev*. 2016;10(10):CD002827.
 55. Svahn J, Petiot P, Antoine JC, et al. Anti-MAG antibodies in 202 patients: clinicopathological and therapeutic features. *J Neurol Neurosurg Psychiatry*. 2018;89(5):499-505.
 56. Dalakas MC. Clinical benefits and immunopathological correlates of intravenous immune globulin in the treatment of inflammatory myopathies. *Clin Exp Immunol*. 1996;104 (Suppl 1):55-60.
 57. Nobile-Orazio E, Meucci N, Baldini L, Di Troia A, Scarlato G. Long-term prognosis of neuropathy associated with anti-MAG IgM M-proteins and its relationship to immune therapies. *Brain*. 2000;123(Pt 4):710-717.
 58. Le Cann M, Bouhour F, Viala K, et al. CANOMAD: a neurological monoclonal gammopathy of clinical significance that benefits from B-cell-targeted therapies. *Blood*. 2020;136(21):2428-2436.
 59. Amaador K, Wieske L, Koel-Simmelink MJA, et al. Serum neurofilament light chain, contactin-1 and complement activation in anti-MAG IgM paraprotein-related peripheral neuropathy. *J Neurol*. 2022;269(7):3700-3705.
 60. Minnema MC, Vos J, Eftimov F, Vrancken A. P-034: MAGNAZ trial - a prospective phase II study in patients with monoclonal gammopathy of unknown significance (MGUS) and anti-myelin associated glycoprotein (MAG) neuropathy and zanubrutinib treatment. *Clin Lymphoma Myeloma Leuk*. 2021;21(Suppl 2):S57.
 61. Simon A, Asli B, Braun-Falco M, et al. Schnitzler's syndrome: diagnosis, treatment, and follow-up. *Allergy*. 2013;68(5):562-568.
 62. Jain T, Offord CP, Kyle RA, Dingli D. Schnitzler syndrome: an under-diagnosed clinical entity. *Haematologica*. 2013;98(10):1581-1585.
 63. de Koning HD. Schnitzler's syndrome: lessons from 281 cases. *Clin Transl Allergy*. 2014;4:41.
 64. Rowczenio DM, Pathak S, Arostegui JI, et al. Molecular genetic investigation, clinical features, and response to treatment in 21 patients with Schnitzler syndrome. *Blood*. 2018;131(9):974-981.
 65. Lipsker D. The Schnitzler syndrome. *Orphanet J Rare Dis*. 2010;5:38.
 66. Pathak S, Rowczenio DM, Owen RG, et al. Exploratory study of MYD88 L265P, rare NLRP3 variants, and clonal hematopoiesis prevalence in patients with Schnitzler syndrome. *Arthritis Rheumatol*. 2019;71(12):2121-2125.
 67. Néel A, Henry B, Barbarot S, et al. Long-term effectiveness and safety of interleukin-1 receptor antagonist (anakinra) in Schnitzler's syndrome: a French multicenter study. *Autoimmun Rev*. 2014;13(10):1035-1041.
 68. Betrains A, Staels F, Vanderschueren S. Efficacy and safety of canakinumab treatment in Schnitzler syndrome: a systematic literature review. *Semin Arthritis Rheum*. 2020;50(4):636-642.
 69. Krause K, Weller K, Stefaniak R, et al. Efficacy and safety of the interleukin-1 antagonist rilonacept in Schnitzler syndrome: an open-label study. *Allergy*. 2012;67(7):943-950.
 70. Krause K, Feist E, Fiene M, Kallinich T, Maurer M. Complete remission in 3 of 3 anti-IL-6-treated patients with Schnitzler syndrome. *J Allergy Clin Immunol*. 2012;129(3):848-850.
 71. Swiecicki PL, Hegerova LT, Gertz MA. Cold agglutinin disease. *Blood*. 2013;122(7):1114-1121.
 72. Allain JS, Thonier F, Pihan M, et al. IGHV segment utilization in immunoglobulin gene rearrangement differentiates patients with anti-myelin-associated glycoprotein neuropathy from others immunoglobulin M-gammopathies. *Haematologica*. 2018;103(5):e207-e210.
 73. Vos JM, Notermans NC, D'Sa S, et al. High prevalence of the MYD88 L265P mutation in IgM anti-MAG paraprotein-associated peripheral neuropathy. *J Neurol Neurosurg Psychiatry*. 2018;89(9):1007-1009.
 74. Kyle RA, Benson J, Larson D, et al. IgM monoclonal gammopathy of undetermined significance and smoldering Waldenström's macroglobulinemia. *Clin Lymphoma Myeloma*. 2009;9(1):17-18.
 75. Kyle RA, Benson JT, Larson DR, et al. Progression in smoldering Waldenström macroglobulinemia: long-term results. *Blood*. 2012;119(19):4462-4466.
 76. Khwaja J, Patel AS, Arulogun SO, et al. IgM paraprotein-associated type 1 cryoglobulinaemia: clinical characteristics and outcomes. *Blood*. 2021;138(Suppl 1):4503-4503.
 77. Nobile-Orazio E, Barbieri S, Baldini L, et al. Peripheral neuropathy in monoclonal gammopathy of undetermined significance: prevalence and immunopathogenetic studies. *Acta Neurol Scand*. 1992;85(6):383-390.

Genetic and genomic analysis of acute lymphoblastic leukemia in older adults reveals a distinct profile of abnormalities: analysis of 210 patients from the UKALL14 and UKALL60+ clinical trials

Thomas Creasey,¹ Emilio Barretta,¹ Sarra L. Ryan,¹ Ellie Butler,¹ Amy A. Kirkwood,² Daniel Leongamornlert,³ Elli Papaemmanuil,⁴ Pip Patrick,² Laura Clifton-Hadley,² Bela Patel,⁵ Tobias Menne,⁶ Andrew K. McMillan,⁷ Christine J. Harrison,¹ Clare J. Rowntree,⁸ Nick Morley,⁹ David I. Marks,¹⁰ Adele K. Fielding¹¹ and Anthony V. Moorman¹

¹Leukaemia Research Cytogenetics Group, Translational and Clinical Research Institute, Newcastle University, Newcastle upon Tyne, UK; ²Cancer Research UK & UCL Cancer Trials Centre, UCL Cancer Institute University College London, London, UK; ³Sanger Institute, Cambridge, UK; ⁴Memorial Sloan Kettering Cancer Center, New York, NY, USA; ⁵Department of Haematology, Queen Mary University of London, London, UK; ⁶Northern Centre for Cancer Care, Newcastle-upon-Tyne Hospitals NHS Foundation Trust, Newcastle upon Tyne, UK; ⁷Department of Haematology, Nottingham University Hospitals NHS Trust, Nottingham, UK; ⁸Department of Haematology, Cardiff and Vale University Health Board, Cardiff, UK; ⁹Department of Haematology, Sheffield Teaching Hospitals NHS Foundation Trust, Sheffield, UK; ¹⁰Department of Haematology, University Hospitals Bristol and Weston NHS Foundation Trust, Bristol, UK and ¹¹UCL Cancer Institute, University College London, London, UK

Correspondence:

T. Creasey
tom.creasey@ncl.ac.uk

A.V. Moorman
anthony.moorman@ncl.ac.uk

Received: May 17, 2021.
Accepted: September 9, 2021.
Prepublished: November 18, 2021.

<https://doi.org/10.3324/haematol.2021.279177>

©2022 Ferrata Storti Foundation
Published under a CC-BY-NC license



Abstract

Despite being predominantly a childhood disease, the incidence of acute lymphoblastic leukemia (ALL) has a second peak in adults aged 60 years and over. These older adults fare extremely poorly with existing treatment strategies and very few studies have undertaken a comprehensive genetic and genomic characterization to improve prognosis in this age group. We performed cytogenetic, single nucleotide polymorphism (SNP) array and next-generation sequencing (NGS) analyses on samples from 210 patients aged ≥ 60 years from the UKALL14 and UKALL60+ clinical trials. *BCR-ABL1*-positive disease was present in 26% (55/210) of patients, followed by low hypodiploidy/near triploidy in 13% (28/210). Cytogenetically cryptic rearrangements in *CRLF2*, *ZNF384* and *MEF2D* were detected in 5%, 1% and $<1\%$ of patients, respectively. Copy number abnormalities were common and deletions in ALL driver genes were seen in 77% of cases. *IKZF1* deletion was present in 51% (40/78) of samples tested and the *IKZF1*^{plus} profile was identified in over a third (28/77) of cases of B-cell precursor ALL. The genetic good-risk abnormalities high hyperdiploidy (n=2), *ETV6-RUNX1* (no cases) and *ERG* deletion (no cases) were exceptionally rare in this cohort. RAS pathway mutations were seen in 17% (4/23) of screened samples. *KDM6A* abnormalities, including biallelic deletions, were discovered in 5% (4/78) of SNP arrays and 9% (2/23) of NGS samples, and represent novel, potentially therapeutically actionable lesions using EZH2 inhibitors. Outcome remained poor with 5-year event-free and overall survival rates of 17% and 24%, respectively, across the cohort, indicating a need for novel therapeutic strategies.

Introduction

Acute lymphoblastic leukemia (ALL) presents most commonly in early childhood.¹ However, the disease has a bimodal incidence with a second smaller peak in adults aged 60 years old and over.² Optimal care of these older adults (≥ 60 years) remains an area of unmet clinical need. Although they account for only 30–35% of diagnoses each year in adults, around 60% of disease-related deaths occur within this age group, and they are the only ALL patients not to have benefitted from the stepwise

improvements in prognosis driven through successive clinical trials in children and younger adults.^{2,3}

Primary chromosomal abnormalities are one of the hallmarks of ALL and greatly influence treatment decisions and prognosis.^{4,5} Although *BCR-ABL1* is well recognized as the most common genetic subgroup in adult ALL,⁵ to date, only limited biological characterization of older patients beyond the conventionally defined risk groups has been performed. One recent study provided a comprehensive genomic profile of 1,988 subjects with B-cell precursor (BCP)-ALL using a combination of transcrip-

tome, whole genome and exome sequencing and identified 23 genetic subtypes.⁶ Despite this impressive cohort, only 103 patients aged 60 years and over at diagnosis were included. Such efforts focused on older individuals are needed to improve prognostication and to identify novel therapeutic targets.^{7,8}

A proportion of patients do not harbor a cytogenetically visible disease-defining lesion, but have a gene expression profile similar to that of *BCR-ABL1*-positive disease (Ph-like/*BCR-ABL*-like ALL).^{9,10} Approximately 50% of children and young adults with this entity have cytogenetically-cryptic *IGH-CRLF2* or *P2RY8-CRLF2* rearrangements, which activate JAK-STAT signaling.^{11,12} Other recurrent gene rearrangements include *ABL*-class fusions (affecting *ABL1*, *ABL2*, *PDGFRB* or *CSF1R*) in 9-13% of Ph-like cases and the JAK-STAT pathway activating rearrangements of *JAK2* or *EPOR* in 7-10% and 3-6% of patients, respectively.^{11,12} To date, most studies have focused on pediatric and young adult (<60 years) cohorts,^{11,13} although one study found the Ph-like signature in 24% of older BCP-ALL patients in a restricted subgroup lacking large scale aneuploidy.¹² Separately, *ZNF384* and *MEF2D* rearrangements have been reported in 2-6% of pediatric BCP-ALL cases, and form distinct clinical entities.^{14,15}

Focal copy number abnormalities (CNA) frequently target genes that are involved in B-cell development or cell cycle regulation. These secondary abnormalities drive transformation of a pre-leukemic clone into overt disease and include deletions of *EBF1* on 5q33.3, *IKZF1* on 7p12.2, *CDKN2A* and *CDKN2B* on 9p21.3, *PAX5* on 9p13.2, *ETV6* on 12p13.2, *BTG1* on 12q21.33 and *RB1* on 13q14.2.¹⁶ Importantly, particular combinations of CNA have an impact on prognosis.¹⁷⁻¹⁹ The *IKZF1*^{plus} profile is based on the co-occurrence of *IKZF1* deletion with deletions of *CDKN2A*, *CDKN2B*, *PAX5* or the pseudoautosomal region 1 (PAR1) on Xp22.33/Yp11.31 (resulting in *P2RY8-CRLF2* fusion) in the absence of *ERG* deletion.¹⁷ This copy number profile is associated with a significantly poorer outcome in childhood ALL patients, highlighting the prognostic importance of large-scale copy number analyses.

To date, profiling the genetic and genomic landscape of ALL has been primarily restricted to younger patients with few analyses focused on older individuals. Here, we applied cytogenetic, copy number and next-generation sequencing (NGS) techniques to investigate whether the primary and secondary genetic abnormalities of ALL in older adults are distinct from those encountered in their younger counterparts. We additionally sought to identify novel druggable targets, a particular priority for such patients because of the high toxicity and low success rates of traditional chemotherapeutic approaches in this group.²⁰

Methods

Patients and samples

Patients aged 60 years and over were identified for genetic profiling studies from two large UK-wide multicenter clinical trials (UKALL14 and UKALL60+). The UKALL14 study is registered as NCT01085617 (<https://www.clinicaltrials.gov/ct2/show/NCT01085617>), and the UKALL60+ study is registered as NCT01616238 (<https://clinicaltrials.gov/ct2/show/NCT01616238>) (Online Supplementary Methods).

Baseline cytogenetic analyses, typically consisting of a diagnostic karyotype and fluorescence *in situ* hybridization (FISH) for *BCR-ABL1* fusion and *KMT2A* translocations, were performed in accredited diagnostic genetic laboratories throughout the UK and then centrally reviewed and entered into the Leukaemia Research Cytogenetics Group database.

The study was approved by the institutional review board of each treatment center and all patients gave written informed consent for data collection and genetic studies as specified by the trials' protocols.

Detection of primary genetic subgroups

Diagnostic karyotype and FISH results from the regional genetic centers were first examined and patients were coded into one of six subgroups: *BCR-ABL1*, *TCF3-PBX1*, *KMT2A* fusions, high hyperdiploidy (51-65 chromosomes), low hypodiploidy/near triploidy (HoTr) (30-39 or 60-78 chromosomes) or T-cell ALL (T-ALL). Reverse transcriptase polymerase chain reaction analysis was performed to identify the presence of Bcr-Abl p190, p210 and p230 oncoproteins in *BCR-ABL1*-positive cases. Next, all BCP-ALL cases lacking a primary chromosomal abnormality, hereafter termed B-other ALL, were identified. B-other cases with available fixed cell samples were further investigated by the Leukaemia Research Cytogenetics Group to determine the occurrence of cytogenetically cryptic abnormalities using dual color break-apart FISH probes for *CRLF2*, *PDGFRB/CSF1R*, *ABL2*, *IGH*, *ZNF384*, *MEF2D* (Cytocell, Cambridge, UK) and *JAK2* (Kreatech Diagnostics, Amsterdam, the Netherlands). Separately, multiplex ligation-dependent probe amplification (MLPA) using the *IKZF1*-P335 kit (MRC Holland, the Netherlands) was performed on cases with available DNA as previously described²¹ and permitted the detection of the *P2RY8-CRLF2* fusion that occurs through PAR1 deletion on Xp22.33/Yp11.31.

Copy number analysis

Single nucleotide polymorphism (SNP) arrays were performed on DNA extracted from diagnostic bone marrow samples obtained at trial enrolment. SNP arrays were performed at the Newcastle Genomics Centre, Newcastle-upon-Tyne Hospitals NHS Foundation Trust using the

Affymetrix Cytoscan HD (Affymetrix, Santa Clara, CA, USA) or Illumina CytoSNP 850k (Illumina, San Diego, CA, USA) arrays according to the manufacturers' protocols.

Deletions in *IKZF1*, *CDKN2A*, *CDKN2B*, *PAX5*, *RB1*, *ETV6*, *EBF1* and *BTG1* ('driver genes') were specifically identified from the SNP array results, with loss of any part of the gene considered significant. All arm-level and focal CNA were then examined to detect recurrent abnormalities.

Next-generation sequencing

Separately, targeted NGS analyses were performed on selected samples using a custom SureSelect XT2 target enrichment kit (Agilent, Santa Clara, CA, USA). Samples were selected based on availability of DNA and the presence of CNA by SNP array. The capture library was designed to target either the coding regions or full sequence of 44 genes that are well known to be implicated in ALL (*Online Supplementary Table S1*). Libraries were prepared in accordance with the manufacturer's protocol and sequenced on the NextSeq 550 (Illumina, San Diego, CA, USA) using 100 bp paired-end chemistry (*Online Supplementary Methods*).

Survival analysis

Survival analysis was restricted to patients enrolled in UKALL14 because all these patients received similar intensive treatment with curative intent.²² Patients were grouped according to primary chromosomal abnormalities as described previously.²³ Briefly, patients with complex karyotypes, HoTr or JAK-STAT activating rearrangements were classed as very high risk; patients with any *KMT2A* fusions were classed as high risk; patients with *BCR-ABL1* and other kinase-activating fusions were classed as having tyrosine kinase-activating (TKA) abnormalities; all other BCP-ALL patients were classed as standard risk; and T-ALL patients were analyzed separately. All *P*-values were two-sided and, because of multiple testing, values <0.01 were considered statistically significant. All analyses were performed using Intercooled Stata (StataCorp, College Station, TX, USA) and R version 3.4.3 (<http://www.R-project.org>).

Results

Patients' demographics and baseline cytogenetics

We identified a total of 210 patients aged ≥ 60 years from the UKALL14 (n=95) and UKALL60+ (n=115) clinical trials. The median age of the patients was 64 years (range, 60-83) and 24% (n=50) were over 70 years at diagnosis. The male:female ratio was 1:1. In total, 90% (n=189) had confirmed BCP-ALL and 5% (n=11) had T-cell disease. The remaining 5% (n=10) did not have a diagnostic immunophenotype centrally recorded. Numbers of patients decreased with advancing age but no significant dif-

ference was seen in the genetic subgroups represented in different age groups ($P=0.47$) (Figure 1A, B). The most prevalent abnormality was *BCR-ABL1*, present in 28% (55/200) of evaluable patients. Of these, the p210, p190 and p230 isoforms were present in 40% (22/55), 33% (18/55) and <1% (1/55) of patients, respectively. Two patients had both p190 and p210 isoforms identified and the Bcr-Abl isoform was unknown in the remaining 22% (12/55) patients. Low hypodiploidy/near triploidy (HoTr) was the second most prevalent primary chromosomal abnormality and was identified in 14% (28/200) of patients (*Online Supplementary Table S2*) and *KMT2A-v* rearrangements were discovered in a further 6% (12/200) of patients. Of the patients with BCP-ALL, 47% (88/189) did not have a primary chromosomal abnormality identified by routine cytogenetic and FISH analyses performed in regional cytogenetic centers (B-other ALL).

Among the 11 patients with T-ALL, *TLX1* (n=1) and *TLX3* (n=1) rearrangements were identified. The other nine patients either had no rearrangements identified (n=5) or were not tested (n=4).

Individual patients' demographic, clinical and genetic data are shown in *Online Supplementary Table S3*.

Gene rearrangements in patients with B-other acute lymphoblastic leukemia

Patients with B-other ALL included those with normal (n=21), failed (n=25) or complex karyotypes (n=5). Patients with dic(9;12) (n=2), *IGH* translocation (n=5) or other non-subgroup-defining chromosomal abnormalities (n=30) were also included in the B-other category. Fixed cell samples were available for 74% (65/88) of B-other patients and gene rearrangements were identified in 21% (19/65) (Table 2). Not all samples could be screened for all abnormalities due to lack of availability of material for multiple FISH experiments.

CRLF2 rearrangements were identified in 17% (8/48) of successfully screened cases. The *CRLF2* rearrangement partners were *IGH* (n=5), *P2RY8* (n=2) and unknown (n=1). Two additional patients had *P2RY8-CRLF2* fusion identified by MLPA, through the presence of PAR1 deletion (Table 1). *IGH* translocations were present in 26% (14/53) of B-other samples tested. Of these, five cases accounted for patients with *IGH-CRLF2* translocations detailed above, and three cases had separate primary genetic abnormalities identified (one *ZNF384* translocation and two *P2RY8-CRLF2* fusions). In the remaining six samples, the *IGH* partners were *CEBPA* (n=1), *CEBPD* (n=1), *CEBPE* (n=1), *BCL2* (n=1) and unknown (n=2). *ZNF384* and *MEF2D* rearrangements were each identified in 8% (3/40) and 3% (1/39) of screened B-other cases, respectively.

In total, *CRLF2*, *IGH*, and *ZNF384* rearrangements were present in 5%, 3% and 1% of the complete patient cohort, respectively (Figure 1C). No variant *ABL1* (0/83), *PDGFRB*

(0/56), *JAK2* (0/53) or *ABL2* (0/52) rearrangements were detected.

Copy number alterations

SNP arrays were performed on diagnostic bone marrow samples from 78 of the 210 patients (49 from UKALL14 and 29 from UKALL60+) using the Illumina CytoSNP 850k (n=51) and Affymetrix Cytoscan HD (n=27) arrays. The SNP array cohort was reasonably representative of the whole cohort of patients, although *BCR-ABL1*-positive patients were slightly over-represented (*Online Supplementary Table S4*).

Deletions were more frequent than gains in all cytogenetic subgroups apart from high hyperdiploidy. Following the exclusion of probable constitutional copy number variations, as described in the *Online Supplementary Methods*, a median of seven deletions (range, 0-52) and one gain (range, 0-29) were seen per patient sample.

In the 68/78 patients without a primary ploidy shift (defined as HoTr and high hyperdiploidy), large deletions on 9p were the most prevalent arm-level CNA, seen in 22%

(15/68) of cases (*Figure 2, Online Supplementary Table S5*). An additional copy of the Philadelphia chromosome was present in 12% (8/68) of patients (26% of *BCR-ABL1*-positive cases) and 1q gains and monosomy 7 were each present in 10% (7/68) of samples.

Of the CNA in known driver genes, *IKZF1* deletions were the most frequent abnormality, present in 51% (40/78) of cases. These were focal intragenic deletions in 19 cases, most commonly involving exons 4-7 (n=11) or exons 2-7 (n=4). Rarer *IKZF1* deletions involved exons 4-8 (n=2), exons 2-8 (n=1) and one patient had biallelic *IKZF1* loss involving exons 2-7 and 2-8. Focal *IKZF1* deletions were almost exclusively seen in patients with *BCR-ABL1* (n=13) or *CRLF2* rearrangements (n=5) (*Online Supplementary Table S6*). In the remaining cases, *IKZF1* loss resulted from monosomy 7 (n=16) or del(7p) (n=5) (*Figure 2, Online Supplementary Table S6*).

The pattern of gene deletions varied by *BCR-ABL1* status with a higher frequency of *IKZF1* deletion in *BCR-ABL1*-positive ALL, as previously described,²⁴ and a higher frequency of *ETV6* and *RB1* deletions in *BCR-ABL1*-negative

Table 1. Clinical and outcome data for all B-other patients with gene rearrangements detected by fluorescence *in situ* hybridization or multiplex ligation-dependent probe amplification.

Patient ID	Trial	Abnormality	WCC (x10 ⁹ /L)	Outcome
25130	UKALL14	<i>IGH-CRLF2</i>	33.6	Died after 1 month
25371	UKALL14	<i>IGH-CRLF2</i>	47.7	Alive >5 years
28235	UKALL60	<i>IGH-CRLF2</i>	5.3	Relapsed and died after 2 years
30102	UKALL60	<i>IGH-CRLF2</i>	Not known	Relapsed and died after 5 months
30299	UKALL60	<i>IGH-CRLF2</i>	Not known	Died after 4 months
25246	UKALL14	<i>P2RY8-CRLF2</i>	6.3	Died within 1 month
28039	UKALL60	<i>P2RY8-CRLF2</i>	Not known	Died after 9 months
25552	UKALL14	<i>P2RY8-CRLF2</i>	2.9	Died after 4 months
28011	UKALL14	<i>P2RY8-CRLF2</i>	3.5	Died after 16 months
30297	UKALL60	<i>CRLF2-r</i>	Not known	Alive >2 years
30487	UKALL14	<i>IGH-CEBPA</i>	11.7	Alive after 1 year
25894	UKALL60	<i>IGH-CEBPD</i>	0.8	Alive >5 years
27181	UKALL14	<i>IGH-CEBPE</i>	1.2	Died after 3 months
27833	UKALL60	<i>IGH-BCL2</i>	14.5	Died after 2 years
25907	UKALL60	<i>IGH-r</i>	2	Died after 1 year
29808	UKALL60	<i>IGH-r</i>	Not known	Relapsed and died after 1 year
25451	UKALL14	<i>EP300-ZNF384</i>	34.2	Relapsed and died >5 years
25235	UKALL14	<i>ZNF384-r</i>	3.5	Alive >5 years
30085	UKALL60	<i>ZNF384-r</i>	Not known	Alive >2 years
25267	UKALL14	<i>MEF2D-r</i>	1.4	Alive >5 years

Outcome of patients with *CRLF2* rearrangement was very poor with only 2/10 alive 2 years after diagnosis. In comparison, 2/3 patients with *ZNF384* rearrangements were still alive after 5 years with only one relapse that occurred nearly 7 years after diagnosis. ID: identifier; WCC: white blood cell count.

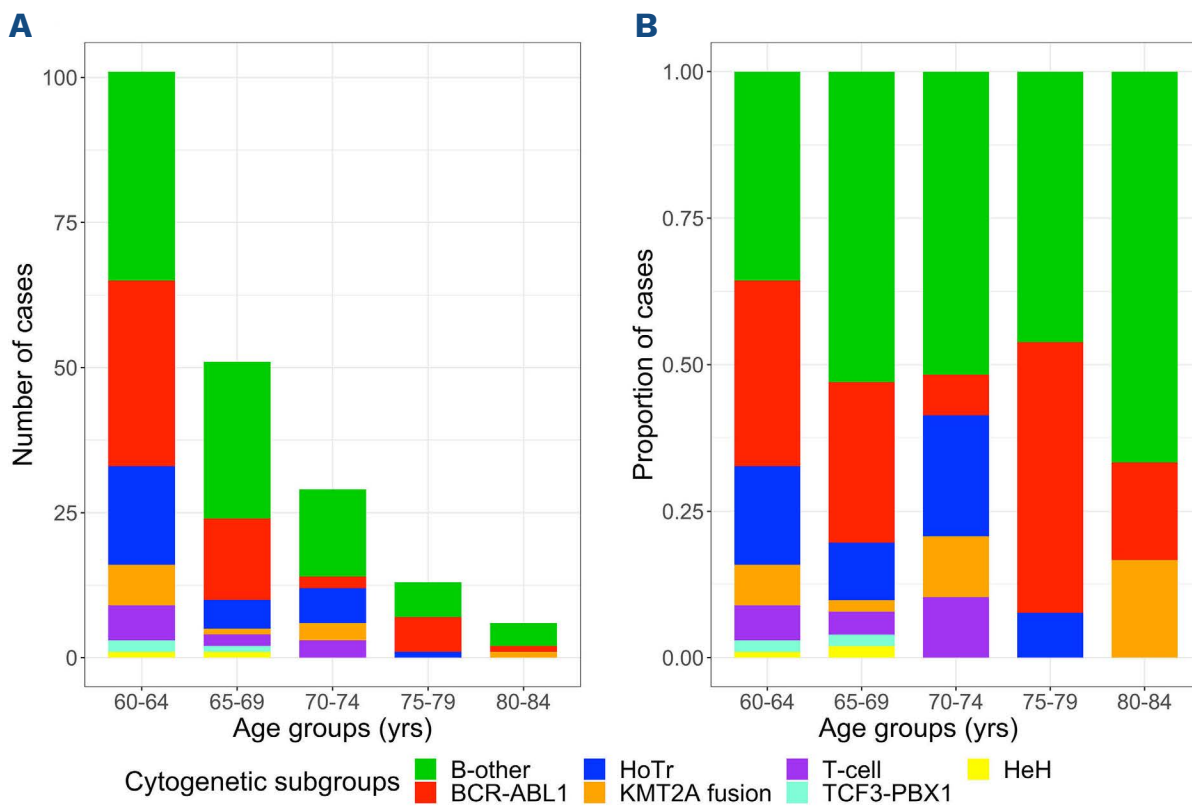
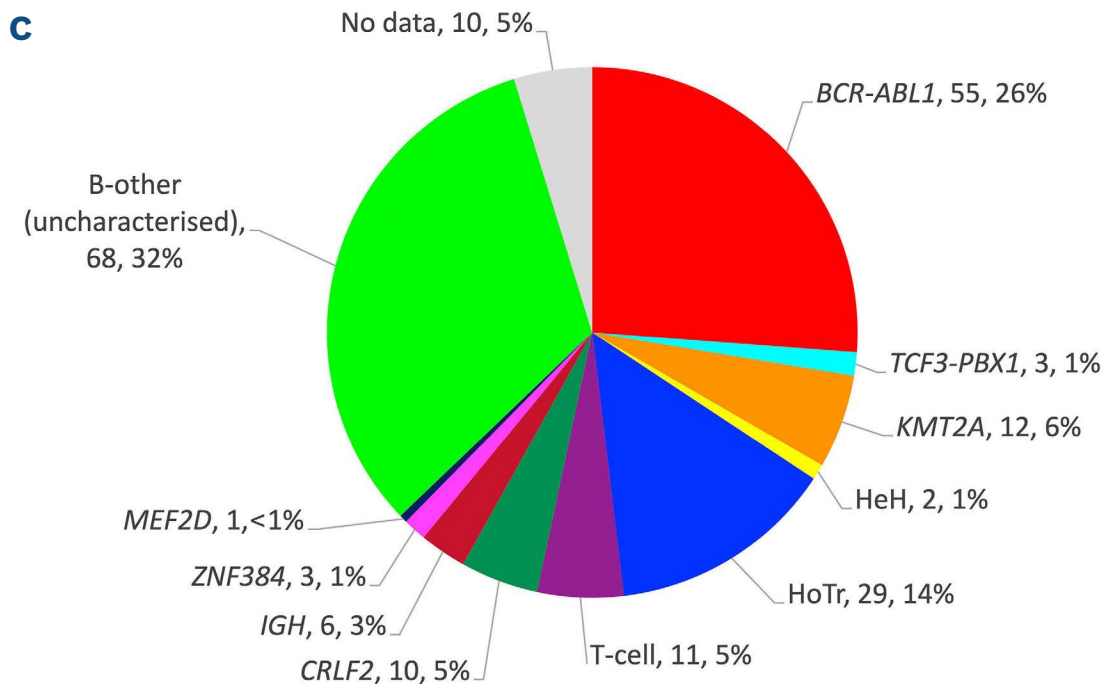


Figure 1. Distribution of primary chromosomal abnormalities by age groups across 210 adults aged ≥60 years. Primary genetic abnormalities shown by 5-year age groups, displayed by number (A) and proportion of cases (B) in each age group. Frequency of final genetic subgroups is shown following screening of B-other acute lymphoblastic leukemia cases for gene rearrangements (C). HoTr: low hypodiploidy/near triploidy; HeH: high hyperdiploidy; T-cell: T-cell acute lymphoblastic leukemia; B-other: B-cell precursor acute lymphoblastic leukemia in which no primary chromosomal abnormality was identified.



ALL (Table 2). Most deletions were heterozygous with the exception of *CDKN2A/B* which were homozygous in 50% of cases.

In total, 23% (18/78) of patients had no deletions in driver genes, 18% (14/78) had one deletion, 18% (14/78) had two deletions, 23% (18/78) had three deletions and 18% (14/78) had four or more gene deletions (*Online Supplementary Figure S1*). *IKZF1* deletions in particular co-occurred with other gene deletions much more commonly than in isolation (46% vs. 5%). The *IKZF1*^{plus} profile¹⁷ was present in 36% (28/77) of the BCP-ALL samples, specifically in *BCR-ABL1*-positive (n=13), B-other (n=8) and HoTr (n=7) patients.

We detected recurrent focal CNA in several other genes, which to date have not been defined in the pathogenesis of ALL. Focal deletions in *LEMD3* on 12q14.3 and *KDM6A* on Xp11.3 were seen in 6% (5/78) and 5% (4/78) of cases,

respectively. Demographic, genetic and outcome features of affected cases are shown in Table 3. *LEMD3* deletions ranged from 11-32kb in size (*Online Supplementary Table S7* and *Online Supplementary Figure S2*), although they were confined to intron 2 of the gene in three of these. *KDM6A* deletions ranged from 56-316 kb in size and were homozygous or hemizygous in three of the four cases (*Online Supplementary Table S7*). Deletion breakpoints for all *LEMD3* and *KDM6A* deletions were visually confirmed in IGV in the cases analyzed by NGS.

Mutational landscape

Twenty-three patients' samples covering all major genetic subgroups (*Online Supplementary Table S3*) were successfully sequenced using the 44-gene targeted panel. Across these samples, 25 single nucleotide variants and eight in-

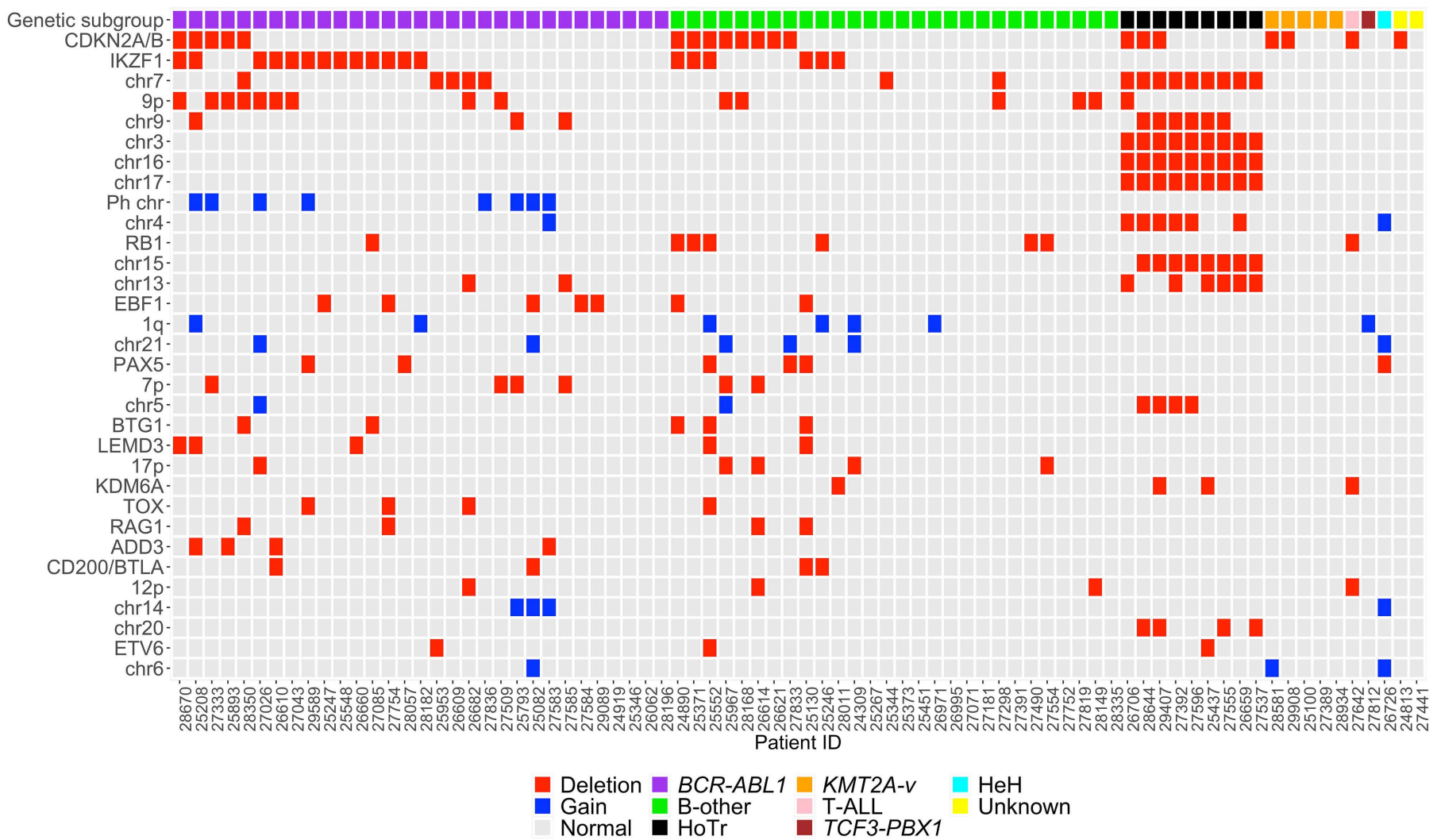


Figure 2. Complete copy number profile based on single nucleotide polymorphism array results from all 78 patients included in the single nucleotide polymorphism array cohort. Only copy number alterations present in at least three patients' samples are displayed. HoTr: low hypodiploidy/near triploidy; HeH: high hyperdiploidy; T-ALL: T-cell acute lymphoblastic leukemia; B-other: B-cell precursor acute lymphoblastic leukemia in which no primary chromosomal abnormality was identified.

Table 2. Frequency of individual deletions in known driver genes split by *BCR-ABL1* status. Significant differences identified in rate of *IKZF1*, *ETV6* and *RB1* deletions between *BCR-ABL1*-positive (*BCR-ABL1*⁺) and *BCR-ABL1* negative (*BCR-ABL1*⁻) cases.

Gene	Cases with deletion (n)	Deletion frequency by <i>BCR-ABL1</i> status			Heterozygous deletions	Homozygous deletions
		<i>BCR-ABL1</i> ⁺ cases (n=31)	<i>BCR-ABL1</i> ⁻ cases (n=47)	P-value		
<i>IKZF1</i>	51% (40)	68% (21)	40% (19)	0.02	41	2
<i>CDKN2A</i>	46% (36)	39% (12)	51% (24)	0.36	18	18
<i>CDKN2B</i>	46% (36)	39% (12)	51% (24)	0.36	21	15
<i>PAX5</i>	41% (32)	48% (15)	36% (17)	0.35	32	0
<i>RB1</i>	23% (18)	10% (3)	32% (15)	0.03	17	1
<i>ETV6</i>	21% (16)	6% (2)	30% (14)	0.02	16	0
<i>EBF1</i>	21% (16)	19% (6)	21% (10)	1	15	1
<i>BTG1</i>	13% (10)	6% (2)	17% (8)	0.3	9	1

deletions were identified (Figure 3). At least one gene in the NGS panel was mutated in 74% (17/23) of patients. Pathogenic mutations in the RAS signaling pathway were identified in 17% (4/23) of cases. *KRAS* p.G12D and *KRAS* p.R68W variants were seen in patients with *KMT2A* and *EP300-ZNF384* rearrangements, respectively. *NRAS* p.G12S and p.G12D were present in one B-other case and one patient with unidentified genetic subgroup, respectively. With the exception of the *KRAS* p.R68W variant, all RAS pathway mutations are reported in the COSMIC database.²⁵

Two patients' samples with HoTr were included. Consistent with the underlying chromosomal abnormality, a pathogenic *TP53* variant (*TP53* p.R282W) was detected in one of these.^{26,27} Two indels in *NF1* and an *FLT3* missense variant (*FLT3* p.V194M) were also seen, the latter being reported as a tolerated passenger mutation in acute myeloid leukemia.²⁸

Known pathogenic variants were also seen in *JAK2* (*JAK2* p.R683T in a patient with *IGH-CRLF2*), *CREBBP* (*CREBBP* p.L1499Q in a patient with *IGH-BCL2*), and *CSF1R* (*CSF1R*

p.V32G in a patient with *P2RY8-CRLF2*). Additionally, previously unreported *KDM6A* mutations were discovered in two *BCR-ABL1*-positive patients (*KDM6A* p.Y215H and p.K987Q).

We also investigated whether mutations associated with clonal hematopoiesis of indeterminate potential (CHIP)

(most commonly affecting *DNMT3A*, *TET2* and *ASXL1*) were present in older adults with ALL.^{29,30} These are found in 10% of adults over the age of 65 years without hematologic diseases, but are associated with an increased risk of subsequently developing myelodysplastic syndrome or acute myeloid leukemia.³⁰ Overall, these were discovered

Table 3. Demographic, clinical and outcome data of all cases with focal *LEMD3* or *KDM6A* deletions.

Gene	Patient ID	Sex (M/F)	Age (years)	Genetic subgroup	WCC (x10 ⁹ /L)	Outcome
<i>LEMD3</i>	25208	M	62	<i>BCR-ABL1</i>	205.4	Alive after 9 years
<i>LEMD3</i>	25130	F	62	<i>IGH-CRLF2</i>	33.6	Died after 1 month
<i>LEMD3</i>	28670	F	61	<i>BCR-ABL1</i>	1.6	Died after 2 months
<i>LEMD3</i>	26660	F	62	<i>BCR-ABL1</i>	18.2	Alive after 7 years
<i>LEMD3</i>	25552	M	61	<i>P2RY8-CRLF2</i>	2.9	Died after 4 months
<i>KDM6A</i>	28011	M	61	<i>B-other</i>	3.5	Died after 16 months
<i>KDM6A</i>	29407	F	60	<i>HoTr</i>	2.9	Died after 5 months
<i>KDM6A</i>	25437	F	64	<i>HoTr</i>	1.4	Died after 14 months
<i>KDM6A</i>	27642	F	72	<i>T-ALL</i>	Not known	Died after 18 months

All patients with *KDM6A* deletions died within 18 months of diagnosis. ID: identifier; M: male; F: female; WCC: white blood cell count; HoTr: low hypodiploidy/near triploidy; T-ALL: T-cell acute lymphoblastic leukemia

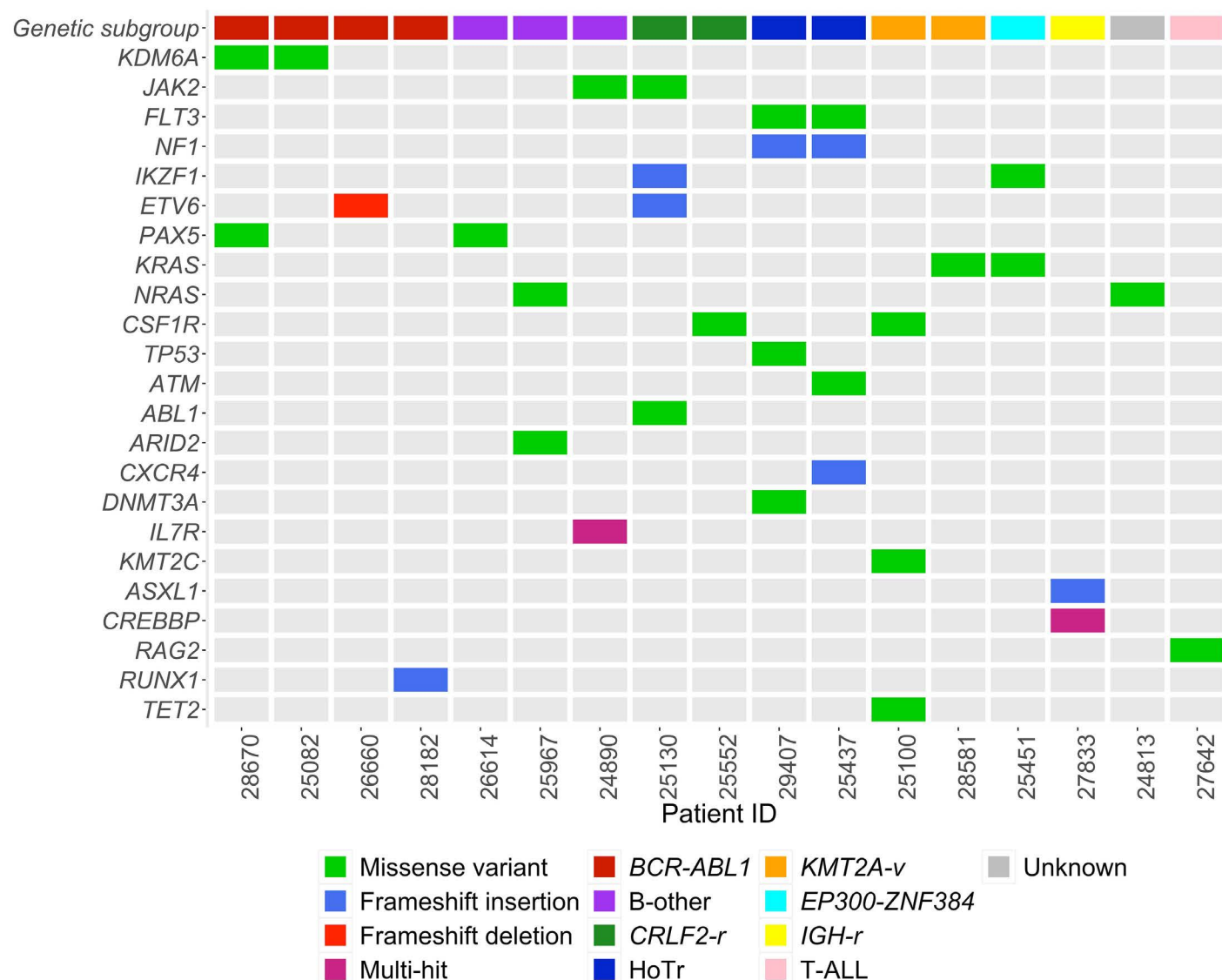


Figure 3. Mutations detected by the 44-gene next-generation sequencing panel in 23 patients. Only patients' samples with at least one mutation are displayed (n=17). In total, 24 single nucleotide variants, seven frameshift insertions and one frameshift deletion were identified. Two genes had both single nucleotide variants and indels within the same case ("multi-hit"). HoTr: low hypodiploidy/near triploidy; T-ALL: T-cell acute lymphoblastic leukemia; B-other: B-cell precursor acute lymphoblastic leukemia in which no primary chromosomal abnormality was identified.

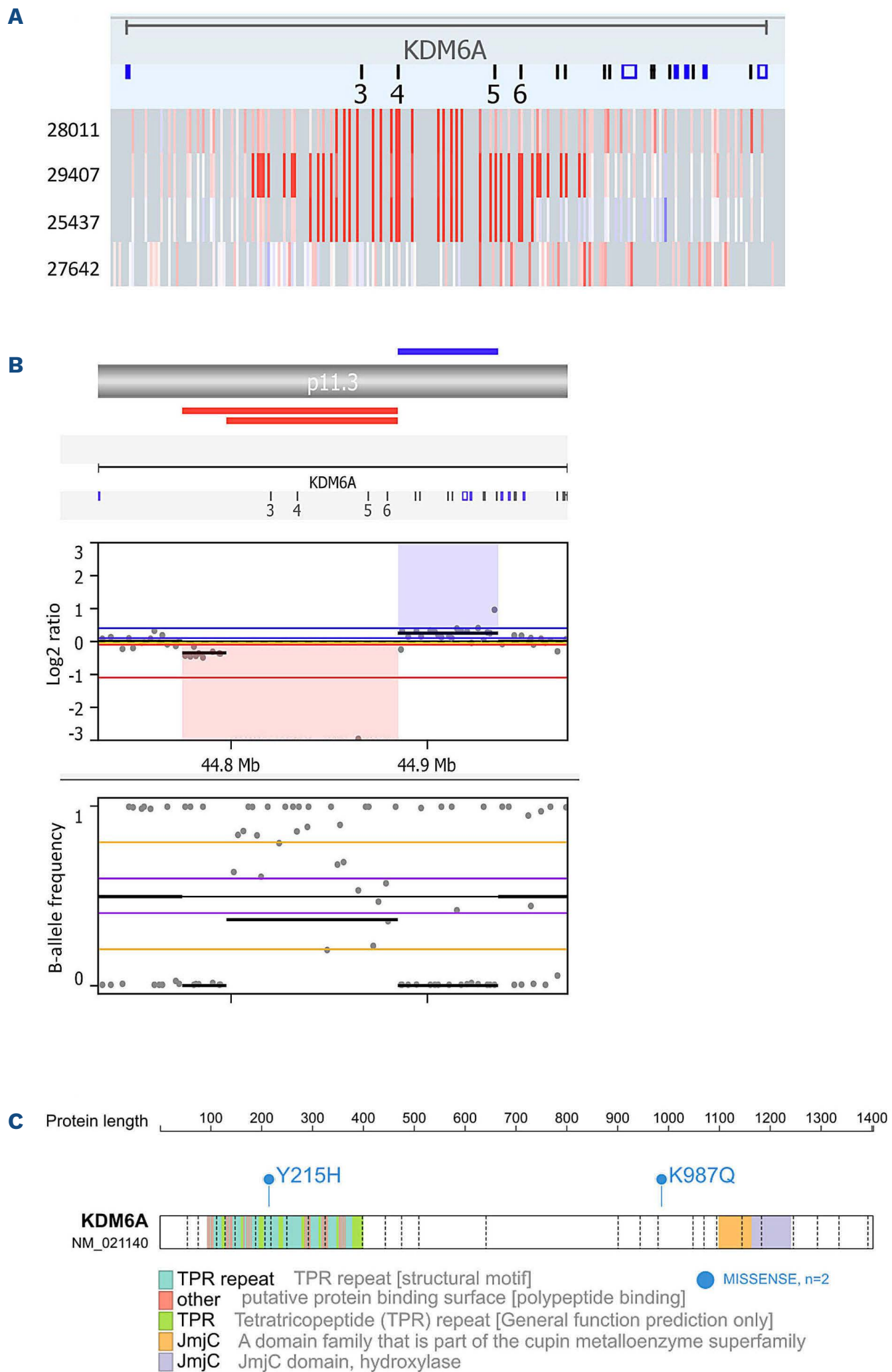


Figure 4. *KDM6A* aberrations detected by single nucleotide polymorphism array and next-generation sequencing. *KDM6A* deletions identified by single nucleotide polymorphism (SNP) array in four patients' samples (A). Each bar represents a probe on the SNP array. Red colors indicate negative log₂ ratio (copy number loss), blue colors represent positive log₂ ratio (copy number gain), and white represents no copy number change. Homozygous *KDM6A* deletion in patient 25437, demonstrating two slightly distinct *KDM6A* deletions measuring 110 kb and 87 kb, and resulting in biallelic loss of exons 3-6 (B). Small gain also noted following segment of homozygous deletion. *KDM6A* protein plot displaying two mutations detected by next-generation sequencing (C).

in only 13% (3/23) of cases with single variants in each of *DNMT3A*, *TET2* and *ASXL1*.

KDM6A alterations

Overall *KDM6A* was disrupted in six cases, with focal deletions in 5% (4/78) of SNP array samples (Table 3) and mutations in 9% (2/23) of NGS samples (Figure 3). Interestingly, the deletions resulted in homozygous or hemizygous *KDM6A* loss in three of the four cases (Figure 4A, *Online Supplementary Table S7*). Biallelic *KDM6A* deletions were seen in the two female patients with HoTr ALL, albeit by two different mechanisms. By cytogenetics and SNP array, patient #29407 had lost one copy of chromosome X and had a focal *KDM6A* deletion in the remaining homologue. In comparison, patient #25437 had two focal but subtly distinct intragenic *KDM6A* microdeletions on each X chromosome (Figure 4B). As *KDM6A* is not in a

pseudoautosomal region, the male patient (#28011) had a deletion affecting the only *KDM6A* allele, resulting in hemizygous loss. The *KDM6A* mutations detected by NGS were present in exons 8 (*KDM6A* p.Y215H) and 20 (*KDM6A* p.K987Q) (Figure 5C) and are not reported in the literature although the SIFT³¹ and Polyphen³² *in silico* prediction tools describe deleterious and probably damaging consequences, respectively, consistent with loss of function. Patients with *KDM6A* deletions had a poor outcome and all four affected patients died 5-18 months after diagnosis (Table 2). Similarly, the two patients with *KDM6A* mutations both died within 2 months of diagnosis.

Patients' outcome by genetic subtype

Outcome data were available for analysis for all 95 UKALL14 patients. Five-year event-free survival and overall survival rates were 17% and 24%, respectively (Figure 5,

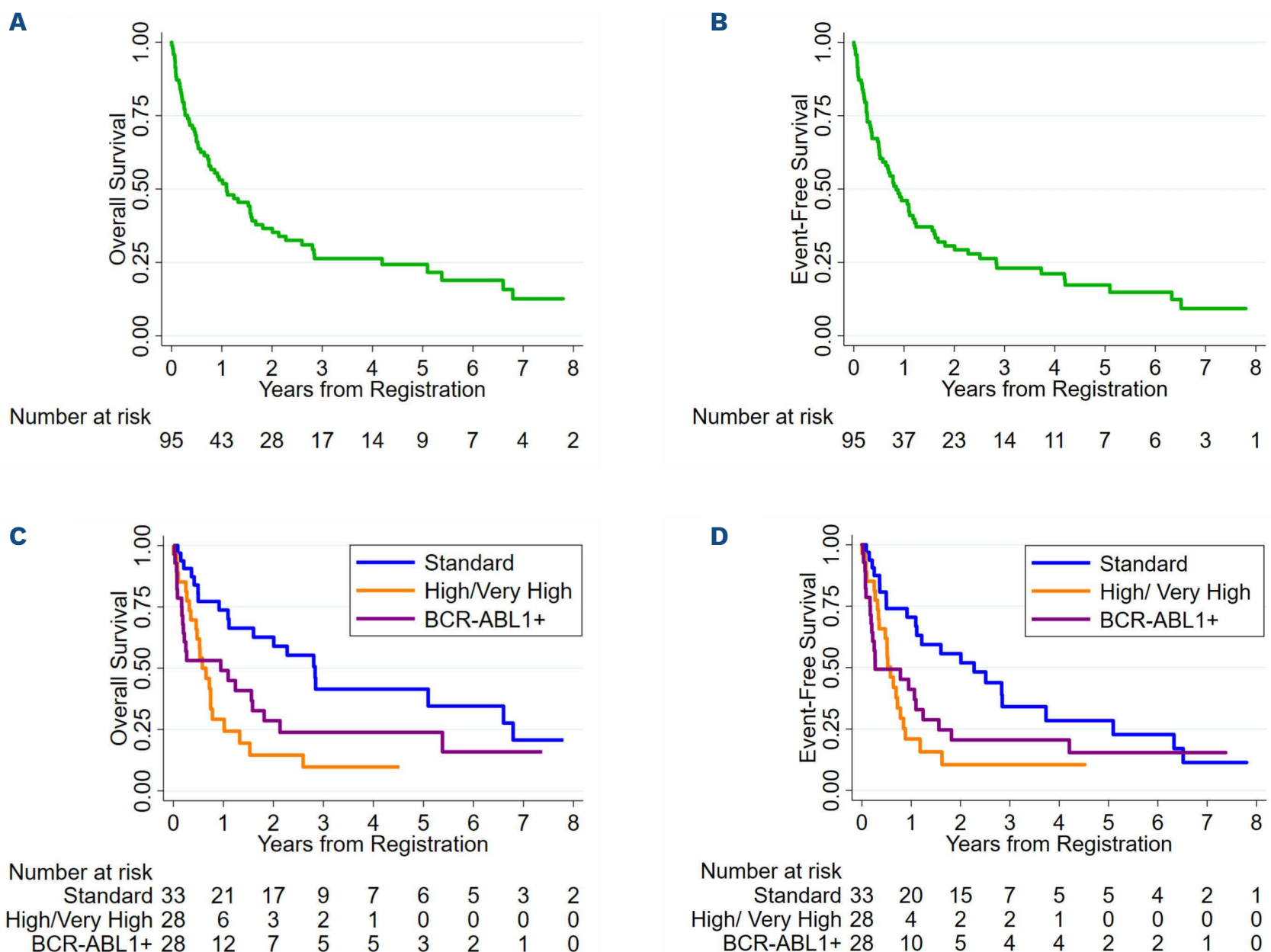


Figure 5. Overall survival and event-free survival for 95 adults aged ≥60 years recruited into the UKALL14 study. Overall survival (A) and event-free survival (B) for all patients combined; overall survival (C) and event-free survival (D) split by genetic risk group with very high risk and high risk combined into a single group. Patients with complex karyotypes, low hypodiploidy/near triploidy or *CRLF2* rearrangements were classed as very high risk; patients with any *KMT2A* fusions were classed as high risk; patients with *BCR-ABL1* and other kinase-activating fusions were classed as tyrosine kinase-activating abnormalities (all *BCR-ABL1*-positive in this study); all other patients with B-cell precursor acute lymphoblastic leukemia were classed as standard risk (SR). Patients with SR or *BCR-ABL1* had improved overall survival ($P=0.001$) and event-free survival ($P=0.002$) compared to patients with high or very high risk disease.

Online Supplementary Table S8). Even though the outcome of these older patients was poor there was evidence that tumor genetics remained a strong risk factor (Figure 5), as we have previously demonstrated for younger adults.²³ Patients with standard-risk genetics had the best outcome with 84% entering remission and 5-year event-free and overall survival rates of 28% and 41%, respectively. In comparison, over a third of patients with very high-risk genetics did not go into remission and all 28 patients with genetic high-risk or very high-risk disease died within 5 years of diagnosis.

Regarding patients with B-other ALL with gene rearrangements identified, all three patients with *ZNF384*-rearranged ALL survived more than 2 years from diagnosis whereas six out of eight of those with *CRLF2* rearrangements and four out of six with *IGH* translocations (excluding *CRLF2* partners) died within 2 years (Table 1).

Of the 40 patients with *IKZF1* deletions, no significant difference in outcome was identified between those with focal deletions of exons 4-7 (generating the dominant negative IK6 isoform)³³ compared with patients with other *IKZF1* deletions (*Online Supplementary Table S9*).

Discussion

To our knowledge, our study provides the largest genetic and genomic characterization to date of older adults with ALL.

The landscape of primary chromosomal abnormalities and CNA is distinct from that observed in children and younger adults. T-ALL was only seen in 5% of cases, which is less than half the rate seen in younger adults.³⁴

Overall, a quarter of patients had *BCR-ABL1*-positive ALL, although the frequency of this did not increase further over the age of 60 years. This corroborates the findings from a large analysis of three German Multicenter study group for adult ALL (GMALL) trials in which the proportion of *BCR-ABL1*-positive cases reached a plateau after 45 years of age.³⁵ In comparison, our study highlights that HoTr becomes more common with advancing age, such that it is encountered in <2% of childhood patients,³⁶ 4-9% of adults aged 25-60,²³ rising to around 15% of adults aged 60 years and over in our cohort. Other high-risk cytogenetic subgroups, specifically *KMT2A* fusions and complex karyotypes were present in 6% and 3% of patients, respectively, which are similar rates to those seen in younger adults.^{5,23} We found a lower frequency of *CRLF2* rearrangements than found in two USA studies that included older adults.^{12,37} This could be related to the higher prevalence of Hispanic ancestry in the USA, and the associated inheritance of *GATA3* risk alleles, which confer an elevated risk of *CRLF2*-rearranged ALL.³⁸ In comparison to younger patients, ABL-class fusions were notably ab-

sent in our cohort. Other studies have similarly identified very low frequencies of ABL-class fusions in older individuals. Indeed, only two cases were identified in 103 adults aged 60 years or over in a recent large USA study.⁶ Data from the GMALL group similarly demonstrated a rapid decrease in the frequency of Ph-like ALL in older age groups.³⁹

Although we limited our survival analysis to UKALL14 patients, we highlight that prognosis remains very poor in older adults with ALL (Figure 5). However, consistent with recent studies, patients with *ZNF384* rearrangements seemed to have a favorable outcome.²³

CNA in key genes recurrently disrupted in ALL were discovered in the majority of patients. *IKZF1* loss was present in over half of all cases tested by SNP array, occurring in 68% of *BCR-ABL1*-positive and 40% of *BCR-ABL1*-negative ALL. The high rate of *IKZF1* loss in *BCR-ABL1*-positive ALL is consistent with much of the published literature.^{24,40} However, the frequency of *IKZF1* deletion in the older patients with *BCR-ABL1*-negative ALL was double that reported in younger adults (40% vs. 19%).⁴¹ This discrepancy is at least in part driven by the increased frequency of low hypodiploid cases, as these usually only retain one copy of chromosome 7. However, *IKZF1* deletions were still encountered in 36% (10/28) of B-other cases. Deletions in other key driver genes in BCP-ALL (*CDKN2A/B*, *PAX5*, *RB1*, *ETV6* and *EBF1*) were also encountered more frequently than in younger patients.²³

The high-risk *IKZF1*^{plus} copy number profile was identified in over a third of patients, although its prognostic impact in older adults still needs to be elucidated. Interestingly, no focal *ERG* deletions, which are associated with a favorable outcome, were detected.⁴² Overall, these data confirm that all genetic biomarkers typically associated with a good prognosis, namely *ETV6-RUNX1* fusion, high hyperdiploidy and *ERG* deletions are exceedingly rare in older adults with ALL, contributing to the adverse outcomes of this population of patients. By virtue of the techniques used, we recognize that we were not able to identify certain novel subgroups, such as the recently described *PAX5*-driven subtypes⁶ or *DUX4* rearrangements, although the latter are associated with *ERG* deletions in the majority of cases.⁴³

Importantly, our study highlighted therapeutically actionable targets that would merit further investigation in older adults. We identified *KDM6A* deletions and mutations in 5% (4/78) and 9% (2/23) of screened patients, respectively. *KDM6A* (also known as *UTX*) on Xp11.3 is an H3K27me3 demethylase, involved in epigenetic regulation through repression of PRC2/EZH2 activity. Recurrent *KDM6A* mutations have been identified in T-ALL, and have been shown to have gender-specific tumor suppressor effects.⁴⁴ *KDM6A* escapes X-inactivation in females and therefore retains biallelic expression. Hence, loss of tumor sup-

pressor function through *KDM6A* abnormalities disproportionately affects males and has been postulated to explain the skewed gender distribution of T-ALL. To our knowledge, our study is the first to demonstrate *KDM6A* disruption in a significant proportion of older adults with ALL, most of whom had B-cell disease. Most interestingly, we have highlighted homozygous *KDM6A* deletions in female patients, and no evidence of skewed gender distribution. Loss of *KDM6A* function, resulting in EZH2 overactivity, has been shown to play an important pathogenic role in urothelial bladder cancer⁴⁵ and functional analyses have demonstrated susceptibility of *KDM6A*-null cell lines to the Food and Drug Administration-approved EZH2 inhibitor tazemetostat.⁴⁵ Our findings therefore identify a proportion of patients who may respond to EZH2 inhibition, a treatment as yet untested in ALL.

We also discovered recurrent small focal intragenic deletions in *LEMD3* in 6% (5/78) of cases. *LEMD3* regulates bone morphogenic protein and transforming growth factor β signaling and to date has not been implicated in cancer.⁴⁶ The significance of these deletions remains speculative, particularly as some were confined to introns. Recurrent RAS pathway mutations were identified in almost one fifth of patients (4/23), all of whom had *BCR-ABL1*-negative ALL. These activate RAS signaling and are potentially therapeutically actionable through MEK inhibition (e.g., with selumetinib).

Older adults with ALL fare extremely poorly with current chemotherapeutic approaches. Various studies have demonstrated the disproportionate treatment toxicities experienced by this group of patients, leading to treatment omissions or delays.²⁰ Our analysis confirms the additional challenges posed by the high proportion of poor-risk genetic subgroups. Moving forward, the comprehensive identification of druggable targets such as *KDM6A* abnormalities, JAK-STAT-activating rearrangements or RAS pathway mutations presents an opportunity to expand therapeutic options, likely to most benefit this patient population. As a paradigm, significant progress has been made in the management of *BCR-ABL1*-positive disease through these approaches, culminating in a promising chemotherapy-free protocol.⁴⁷ Further dedicated clinical trials that include comprehensive genomic profiling of

older adults, combined with targeted treatments and/or immunotherapy and a reduction in the traditional chemotherapy backbone will be key to improving the dismal outcome of these patients.

Disclosures

TC was supported by grants from the NIHR Newcastle Biomedical Research Centre and Bright Red. The UKALL14 and UKALL60+ trials were coordinated by the Cancer Research UK (CRUK) & UCL Cancer Trials Centre and funded by CRUK (C27995/A9609 and C27995/A13920, respectively). The UKALL60+ trial was also supported by an educational grant from Jazz Pharmaceuticals UK Ltd. This study was supported by research grants from Cancer Research UK (AVM and AKF) and Blood Cancer UK (AVM and CJH).

Contributions

TC and AVM designed the study. TC, AVM, EB and EB collected and assembled the data. TC, AVM, EB, EB and SLR performed data analysis and interpretation. CJH and AVM were responsible for administrative support. AKF was chief investigator of the UKALL14 and UKALL60+ clinical trials. AAK, DL, EP, PP, LCH, BP, TM, AKM, CJR, NM, DIM, and AKF participated in recruitment of patients and provided study materials. TC and AVM developed the first drafts of the manuscript. All authors contributed to the review and amendments of the manuscript and approved the final version for submission.

Acknowledgments

The authors thank all the participating sites, local investigators and research teams for their ongoing participation in the study, together with patients who took part in these trials as well as their families. We acknowledge the input of all the scientists and technicians working in the adult ALL MRD laboratory based at UCL. We thank the member laboratories of the UK Cancer Cytogenetic Group for cytogenetic data and material.

Data-sharing statement

The datasets generated or analyzed during the current study are available in the Online Supplementary Material or from the corresponding author on reasonable request.

References

- Inaba H, Greaves M, Mullighan CG. Acute lymphoblastic leukaemia. *Lancet*. 2013;381(9881):1943-1955.
- Moorman AV, Chilton L, Wilkinson J, et al. A population-based cytogenetic study of adults with acute lymphoblastic leukemia. *Blood*. 2010;115(2):206-214.
- Dinmohamed AG, Szabó A, van der Mark M, et al. Improved survival in adult patients with acute lymphoblastic leukemia in the Netherlands: a population-based study on treatment, trial participation and survival. *Leukemia*. 2016;30(2):310-317.
- Moorman AV, Ensor HM, Richards SM, et al. Prognostic effect of chromosomal abnormalities in childhood B-cell precursor acute lymphoblastic leukaemia: results from the UK Medical Research Council ALL97/99 randomised trial. *Lancet Oncol*. 2010;11(5):429-438.
- Moorman AV, Harrison CJ, Buck GAN, et al. Karyotype is an independent prognostic factor in adult acute lymphoblastic

- leukemia (ALL): analysis of cytogenetic data from patients treated on the Medical Research Council (MRC) UKALLXII/Eastern Cooperative Oncology Group (ECOG) 2993 trial. *Blood*. 2007;109(8):3189-3197.
6. Gu Z, Churchman ML, Roberts KG, et al. PAX5-driven subtypes of B-progenitor acute lymphoblastic leukemia. *Nat Genet*. 2019;51(2):296-307.
 7. Schultz KR, Pullen DJ, Sather HN, et al. Risk- and response-based classification of childhood B-precursor acute lymphoblastic leukemia: a combined analysis of prognostic markers from the Pediatric Oncology Group (POG) and Children's Cancer Group (CCG). *Blood*. 2007;109(3):926-935.
 8. Gökbüget N. How I treat older patients with ALL. *Blood*. 2013;122(8):1366-1375.
 9. Mullighan CG, Su X, Zhang J, et al. Deletion of IKZF1 and prognosis in acute lymphoblastic leukemia. *N Engl J Med*. 2009;360(5):470-480.
 10. Den Boer ML, van Slegtenhorst M, De Menezes RX, et al. A subtype of childhood acute lymphoblastic leukaemia with poor treatment outcome: a genome-wide classification study. *Lancet Oncol*. 2009;10(2):125-134.
 11. Roberts KG, Li Y, Payne-Turner D, et al. Targetable kinase-activating lesions in Ph-like acute lymphoblastic leukemia. *N Engl J Med*. 2014;371(11):1005-1015.
 12. Roberts KG, Zhaohui G, Debbie P-T, et al. High frequency and poor outcome of Philadelphia chromosome-like acute lymphoblastic leukemia in adults. *J Clin Oncol*. 2017;35(4):394-401.
 13. Roberts KG, Morin RD, Zhang J, et al. Genetic alterations activating kinase and cytokine receptor signaling in high-risk acute lymphoblastic leukemia. *Cancer Cell*. 2012;22(2):153-166.
 14. Hirabayashi S, Ohki K, Nakabayashi K, et al. ZNF384-related fusion genes define a subgroup of childhood B-cell precursor acute lymphoblastic leukemia with a characteristic immunotype. *Haematologica*. 2017;102(1):118-129.
 15. Gu Z, Churchman M, Roberts K, et al. Genomic analyses identify recurrent MEF2D fusions in acute lymphoblastic leukaemia. *Nat Commun*. 2016;7:13331.
 16. Mullighan CG, Goorha S, Radtke I, et al. Genome-wide analysis of genetic alterations in acute lymphoblastic leukaemia. *Nature*. 2007;446(7137):758-764.
 17. Stanulla M, Dagdan E, Zaliova M, et al. IKZF1plus defines a new minimal residual disease-dependent very-poor prognostic profile in pediatric B-cell precursor acute lymphoblastic leukemia. *J Clin Oncol*. 2018;36(12):1240-1249.
 18. Moorman AV, Enshaei A, Schwab C, et al. A novel integrated cytogenetic and genomic classification refines risk stratification in pediatric acute lymphoblastic leukemia. *Blood*. 2014;124(9):1434-1444.
 19. Hamadeh L, Enshaei A, Schwab C, et al. Validation of the United Kingdom copy-number alteration classifier in 3239 children with B-cell precursor ALL. *Blood Adv*. 2019;3(2):148-157.
 20. Sive JI, Buck G, Fielding A, et al. Outcomes in older adults with acute lymphoblastic leukaemia (ALL): results from the international MRC UKALL XII/ECOG2993 trial. *Br J Haematol*. 2012;157(4):463-471.
 21. Schwab CJ, Jones LR, Morrison H, et al. Evaluation of multiplex ligation-dependent probe amplification as a method for the detection of copy number abnormalities in B-cell precursor acute lymphoblastic leukemia. *Genes Chromosomes Cancer*. 2010;49(12):1104-1113.
 22. Marks DI, Kirkwood AA, Rowntree CJ, et al. First analysis of the UKALL14 phase 3 randomised trial to determine if the addition of rituximab to standard induction chemotherapy improves EFS in adults with precursor B-ALL (CRUK/09/006). *Blood*. 2019;134(Suppl_1):739.
 23. Moorman AV, Butler E, Barretta E, et al. Prognostic impact of chromosomal abnormalities and copy number alterations among adults with B-cell precursor acute lymphoblastic leukaemia treated on UKALL14. *Blood*. 2019;134(Suppl_1):288.
 24. Mullighan CG, Miller CB, Radtke I, et al. BCR-ABL1 lymphoblastic leukaemia is characterized by the deletion of Ikaros. *Nature*. 2008;453(7191):110-114.
 25. Tate JG, Bamford S, Jubb HC, et al. COSMIC: the catalogue of somatic mutations in cancer. *Nucleic Acids Res*. 2019;47(D1):D941-D947.
 26. Holmfeldt L, Wei L, Diaz-Flores E, et al. The genomic landscape of hypodiploid acute lymphoblastic leukemia. *Nat Genet*. 2013;45(3):242-252.
 27. Mühlbacher V, Zenger M, Schnittger S, et al. Acute lymphoblastic leukemia with low hypodiploid/near triploid karyotype is a specific clinical entity and exhibits a very high TP53 mutation frequency of 93%. *Genes Chromosomes Cancer*. 2014;53(6):524-536.
 28. Fröhling S, Scholl C, Levine RL, et al. Identification of driver and passenger mutations of FLT3 by high-throughput DNA sequence analysis and functional assessment of candidate alleles. *Cancer Cell*. 2007;12(6):501-513.
 29. Jaiswal S, Fontanillas P, Flannick J, et al. Age-related clonal hematopoiesis associated with adverse outcomes. *N Engl J Med*. 2014;371(26):2488-2498.
 30. Genovese G, Kähler AK, Handsaker RE, et al. Clonal hematopoiesis and blood-cancer risk inferred from blood DNA sequence. *N Engl J Med*. 2014;371(26):2477-2487.
 31. Sim N-L, Kumar P, Hu J, et al. SIFT web server: predicting effects of amino acid substitutions on proteins. *Nucleic Acids Res*. 2012;40(W1):W452-W457.
 32. Adzhubei IA, Schmidt S, Peshkin L, et al. A method and server for predicting damaging missense mutations. *Nat Methods*. 2010;7(4):248-249.
 33. Benjamin K, Nicola G, Stefan S, et al. Loss-of-function but not dominant-negative intragenic IKZF1 deletions are associated with an adverse prognosis in adult BCR-ABL-negative acute lymphoblastic leukemia. *Haematologica*. 2017;102(10):1739-1747.
 34. Marks DI, Paietta EM, Moorman AV, et al. T-cell acute lymphoblastic leukemia in adults: clinical features, immunophenotype, cytogenetics, and outcome from the large randomized prospective trial (UKALL XII/ECOG 2993). *Blood*. 2009;114(25):5136-5145.
 35. Burmeister T, Schwartz S, Bartram CR, et al. Patients' age and BCR-ABL frequency in adult B-precursor ALL: a retrospective analysis from the GMALL study group. *Blood*. 2008;112(3):918-919.
 36. Safavi S, Paulsson K. Near-haploid and low-hypodiploid acute lymphoblastic leukemia: two distinct subtypes with consistently poor prognosis. *Blood*. 2017;129(4):420-423.
 37. Tasian SK, Hurtz C, Wertheim GB, et al. High incidence of Philadelphia chromosome-like acute lymphoblastic leukemia in older adults with B-ALL. *Leukemia*. 2017;31(4):981-984.
 38. Perez-Andreu V, Roberts KG, Harvey RC, et al. Inherited GATA3 variants are associated with Ph-like childhood acute lymphoblastic leukemia and risk of relapse. *Nat Genet*. 2013;45(12):1494-1498.
 39. Herold T, Baldus CD, Gökbüget N. Ph-like acute lymphoblastic leukemia in older adults. *N Engl J Med*. 2014;371(23):2235.
 40. Fedullo AL, Messina M, Elia L, et al. Prognostic implications of additional genomic lesions in adult Philadelphia chromosome-

- positive acute lymphoblastic leukemia. *Haematologica*. 2019;104(2):312-318.
41. Moorman AV, Schwab C, Ensor HM, et al. IGH@ translocations, CRLF2 deregulation, and microdeletions in adolescents and adults with acute lymphoblastic leukemia. *J Clin Oncol*. 2012;30(25):3100-3108.
42. Clappier E, Auclerc MF, Rapon J, et al. An intragenic ERG deletion is a marker of an oncogenic subtype of B-cell precursor acute lymphoblastic leukemia with a favorable outcome despite frequent IKZF1 deletions. *Leukemia*. 2014;28(1):70-77.
43. Zhang J, McCastlain K, Yoshihara H, et al. Deregulation of DUX4 and ERG in acute lymphoblastic leukemia. *Nat Genet*. 2016;48(12):1481-1489.
44. Van der Meulen J, Sanghvi V, Mavrakis K, et al. The H3K27me3 demethylase UTX is a gender-specific tumor suppressor in T-cell acute lymphoblastic leukemia. *Blood*. 2015;125(1):13-21.
45. Ler LD, Ghosh S, Chai X, et al. Loss of tumor suppressor KDM6A amplifies PRC2-regulated transcriptional repression in bladder cancer and can be targeted through inhibition of EZH2. *Sci Transl Med*. 2017;9(378):eaai8312.
46. Hellemans J, Preobrazhenska O, Willaert A, et al. Loss-of-function mutations in LEMD3 result in osteopoikilosis, Buschke-Ollendorff syndrome and melorheostosis. *Nat Genet*. 2004;36(11):1213-1218.
47. Foà R, Bassan R, Vitale A, et al. Dasatinib–blinatumomab for Ph-positive acute lymphoblastic leukemia in adults. *N Engl J Med*. 2020;383(17):1613-1623.

Outcome of relapsed or refractory acute B-lymphoblastic leukemia patients and *BCR-ABL*-positive blast cell crisis of B-lymphoid lineage with extramedullary disease receiving inotuzumab ozogamicin

Sabine Kayser,^{1,2} Chiara Sartor,³ Marlise R. Luskin,⁴ Jonathan Webster,⁵ Fabio Giglio,⁶ Nydia Panitz,¹ Andrew M. Brunner,⁷ Matthias Fante,⁸ Christoph Lutz,^{9,10} Daniel Wolff,⁸ Anthony D. Ho,⁹ Mark J. Levis,⁵ Richard F. Schlenk^{2,9#} and Cristina Papayannidis^{11#}

¹Medical Clinic and Policlinic I, Hematology and Cellular Therapy, University Hospital Leipzig, Leipzig, Germany; ²NCT Trial Center, National Center of Tumor Diseases, German Cancer Research Center (DKFZ), Heidelberg, Germany; ³Istituto di Ematologia "Seràgnoli", Dipartimento di Medicina Specialistica, Diagnostica e Sperimentale, Università degli Studi, Bologna, Italy; ⁴Department of Medical Oncology, Dana-Farber Cancer Institute, Boston, MA, USA; ⁵Sidney Kimmel Comprehensive Cancer Center, Johns Hopkins University, Baltimore, MD, USA; ⁶Hematology and Bone Marrow Transplantation Unit, San Raffaele Scientific Institute, Milan, Italy; ⁷Massachusetts General Hospital, Boston, MA, USA; ⁸Department of Hematology and Oncology, Internal Medicine III, University Hospital Regensburg, Regensburg, Germany; ⁹Department of Internal Medicine V, Heidelberg University Hospital, Heidelberg, Germany; ¹⁰Praxis for Hematology and Oncology Koblenz, Koblenz, Germany and ¹¹IRCCS Azienda Ospedaliero-Universitaria di Bologna, Istituto di Ematologia "Seràgnoli" Bologna, Italy.

[#]RFS and CP contributed equally as co-senior authors.

Correspondence: S. Kayser
s.kayser@dkfz-heidelberg.de

Received: November 29, 2021.

Accepted: February 1, 2022.

Prepublished: February 10, 2022

<https://doi.org/10.3324/haematol.2021.280433>

©2022 Ferrata Storti Foundation

Published under a CC BY-NC license



Abstract

Acute lymphoblastic leukemia (ALL) can relapse in the extramedullary compartment, with or without medullary involvement. Response to treatment may be individual. We evaluated response to inotuzumab ozogamicin in 31 patients with relapsed/refractory B-ALL with extramedullary disease. Median age was 31 years (range, 19–81). All patients were heavily pretreated, including allogeneic hematopoietic stem cell transplantation (HSCT; n=18). Overall response rate after two cycles of inotuzumab ozogamicin was 84% (complete remission, 55%; partial remission, 29%; resistant disease, 13%; early death, 3%). The median follow-up was 29 months and median overall survival was 12.8 months. One-year and 2-year overall survival rates were 53% (95% CI: 37–76%) and 18% (95% CI: 8–43%), respectively. Age had no impact on overall survival when assessed as a continuous variable or dichotomized at 60 years. Twelve patients proceeded to allogeneic HSCT (complete remission, n=6; partial remission, n=3; resistant disease, n=3). Prior to allogeneic HSCT, eight patients received two or fewer cycles and four patients received three or four cycles of inotuzumab ozogamicin. Sinusoidal obstruction syndrome was reported in three patients, including one after transplantation. Allogeneic HSCT, evaluated as a time-dependent variable, had no impact on overall survival. Inotuzumab ozogamicin seems to be effective as a debulking strategy in relapsed/refractory ALL with extramedullary disease. However, inotuzumab ozogamicin followed by allogeneic HSCT seems not to be effective in maintaining long-term disease control.

Introduction

Historically, refractory/relapsed (r/r) B-cell acute lymphoblastic leukemia (B-ALL) in adults has a dismal prognosis, with less than 10% of patients being long-term survivors.¹ At present, allogeneic hematopoietic stem cell transplantation (HSCT) is considered the only curative option for

patients with r/r B-ALL with best outcomes achieved after effective salvage re-induction therapy and transplantation in complete remission (CR) without measurable residual disease.^{2,3}

The role of novel immune-based chimeric antigen receptor T-cell infusions in this setting has remained undefined.^{4–6} Although conventional salvage chemotherapy

is capable of inducing CR rates of 18% to 44% in patients with r/r B-ALL,⁷⁻¹³ antibody-based strategies using blinatumomab or inotuzumab ozogamicin (INO) have been proven to be more effective.^{14,15} INO is a humanized anti-CD22 monoclonal antibody conjugated to the potent cytotoxic agent calicheamicin, which was developed as a targeted therapy for B-cell malignancies.^{16,17} Upon binding to CD22 and internalization, calicheamicin is off-set and binds to DNA, thereby leading to double-strand breaks and apoptosis.^{16,17}

The phase III INO-VATE trial demonstrated that INO had superior efficacy compared to standard-of-care treatment for r/r B-ALL, inducing CR/CRi in 80.7% and 29.4% of the patients, respectively ($P < 0.001$).¹⁵ Additionally, the rate of negativity for measurable residual disease (0.01% marrow blasts assessed at a central laboratory by multicolor, multiparameter flow cytometry) in patients with CR/CRi was significantly higher after treatment with INO than after standard-of-care (78.4% vs. 28.1%; $P < 0.001$). After INO treatment, 41% of patients proceeded directly to allogeneic HSCT as compared to 11% after standard-of-care ($P < 0.001$). The median progression-free survival was significantly longer after INO than after standard-of-care (5.0 months vs. 1.8 months; $P < 0.001$). The median overall survival (OS) was 7.7 months after INO as compared to 6.2 months after standard-of-care, and the 2-year OS rates were 23% versus 10%, respectively.¹⁵ The most frequent grade 3 or higher non-hematologic adverse events after INO were liver-related. Veno-occlusive liver disease (VOD)/sinusoidal obstruction syndrome (SOS) of any grade occurred in 15 patients (11%), who received INO and in one patient (1%) after standard-of-care therapy. In addition, ten of 48 (21%) patients, who underwent allogeneic HSCT after INO treatment, developed VOD after transplantation; three of these ten patients had received a second transplant.¹⁵ Deep remissions with negativity for measurable residual disease can be achieved with INO treatment in patients with r/r ALL. However, the safety and efficacy of INO treatment in patients with r/r ALL and extramedullary disease (EMD) is currently unclear. Patients with central nervous system infiltration and/or isolated EMD were excluded from the phase III randomized INO-VATE trial.¹⁵ Of note, extramedullary relapses are common in r/r ALL patients following exposure to blinatumomab, occurring in up to 40%.^{18,19}

EMD in r/r B-ALL is characterized by a dismal outcome with no accepted standard therapeutic approaches.¹ The objectives of our study were to characterize a series of adult r/r B-ALL patients with EMD and evaluate their outcome after treatment with INO.

Methods

Patients

Information on 31 adult patients (median age, 31 years; range,

19–81 years) with histologically confirmed r/r B-ALL and EMD, who were treated with INO between 2015 and 2021 within a compassionate use program ($n=7$) or in-label after approval by the Food & Drug Administration or the European Medical Agency ($n=24$) was collected from six institutions in the USA and Europe. All 31 patients were CD22-positive at relapse/progressive disease. Three (10%) of the 31 patients had been previously treated with tyrosine kinase inhibitors for chronic myeloid leukemia and progressed to *BCR-ABL*-positive blast cell crisis of B-lymphoid lineage. Bone marrow evaluation and immunophenotyping by flow cytometry revealed B-ALL in all three patients. The 31 patients were heavily pretreated having received intensive chemotherapy with or without a tyrosine kinase inhibitor, as well as blinatumomab in 14, and local irradiation in five patients. In addition, allogeneic HSCT had been performed in 18 patients (first-line or at relapse, $n=9$, each).

Participating centers were chosen upon network relationships of the first and last authors. Detailed case report forms (including information on baseline characteristics, chemotherapy, allogeneic HSCT, response, and survival) were collected from all participating centers. Inclusion criteria were adult patients with r/r ALL and EMD. All patients who fulfilled these criteria were included by the participating institutions.

Chromosome banding was performed using standard techniques, and karyotypes were described according to the International System for Human Cytogenetic Nomenclature.²⁰ Data collection and analyses were approved by the Institutional Review Boards of the participating centers.

Treatment

INO was administered at a dose of 0.8 mg/m² body surface area as a continuous intravenous infusion over 1 h on day 1 and at 0.5 mg/m² body surface area on days 8 and 15. Once the patients had achieved CR, the dose on day 1 of each consecutive cycle was reduced to 0.5 mg/m² body surface area. Up to six INO cycles (≤ 2 cycles, $n=19$; 3–4 cycles, $n=7$; 5–6 cycles, $n=5$) were administered according to the previously approved regimen. The three patients with *BCR-ABL*-positive blast cell crisis of B-lymphoid lineage received a tyrosine kinase inhibitor in addition to INO. EMD response was assessed by computed tomography (CT) or positron emission tomography-computed tomography (PET-CT). VOD/SOS was assessed according to previously defined clinical criteria and diagnosed by the treating investigator.¹⁵

Statistical analyses

Patients' characteristics were compared with the Kruskal-Wallis rank sum test for continuous variables and the Fisher exact test for categorical variables. The median follow-up time was computed using the reverse Kaplan-Meier estimate.²¹ The Kaplan-Meier method was used to estimate the

distribution of relapse-free survival and OS.²² OS was calculated from the start of INO treatment until last follow-up or death. Relapse-free survival was calculated from achievement of CR after the start of INO treatment until last follow-up or relapse. The confidence interval (CI) estimation for survival curves was based on the cumulative hazard function using the Greenwood formula for variance estimation. Log-rank tests were employed to compare survival curves between groups. The effect of allogeneic HSCT on OS as a time-dependent intervening event was tested using the Mantel-Byar method²³ for univariable and Andersen-Gill model for multivariable analyses.²⁴ The method of Simon and Makuch was used to estimate survival distributions with respect to time-dependent interventions.²⁵ The individuals at risk were initially all represented in the INO therapy group. If patients underwent allogeneic HSCT, they were removed at this time point from the INO therapy group and further followed up within the allogeneic HSCT group. All statistical analyses were performed with the statistical software environment R, version 3.3.1, using the R packages *prodlm*, version 1.5.7, and *survival*, version 2.39-5.²⁶

Results

Patients' characteristics

At the time of r/r ALL with EMD, median white blood cell and platelet counts were $5.9 \times 10^9/L$ (range, $0.04-36 \times 10^9/L$) and $110.5 \times 10^9/L$ (range, $6-337 \times 10^9/L$), respectively. Fifteen patients (48%) were female; Eastern Cooperative Oncology Group score was ≤ 2 in 29 patients and 3 in two patients (Table 1). Overall, patients had a median of two EMD manifestations (range, 1-9). Localization of EMD is shown in Table

Table 1. Patients' characteristics at the time-point of relapsed/refractory acute lymphoblastic leukemia and extramedullary disease.

	Number (31)	%
Female gender	15	48
ECOG status		
≤ 2	29	94
3	2	6
	Value	Range
Median age, years	31	19-81
Median WBC $\times 10^9/L$	5.9	0.04-36
missing	3	
Platelets $\times 10^9/L$	110.5	6-337
missing	3	
Hemoglobin, g/dL	11.5	6.6-15.2
missing	3	
Median BM blast cells, %	10	0-100
missing	2	

ECOG: Eastern Cooperative Oncology Group; WBC: white blood cell count; BM: bone marrow.

2. In addition to EMD, 16 (52%) patients had a relapse in bone marrow.

Genetics

Cytogenetic analysis at the time of r/r ALL with EMD was available for 13 (42%) patients, of whom six had a bone marrow relapse as well. Of the 13 patients with cytogenetic information, six had a normal karyotype, four had a complex karyotype (≥ 3 abnormalities), two had a $t(9;22)(q34;q11)$ and one had an additional X-chromosome. In one patient clonal evolution to a complex karyotype was detected.

Response

Response was not assessed after the first induction cycle in seven (23%) of the 31 patients, including one who died at day 11 of the first INO cycle due to cerebral hemorrhage. Figures 1 and 2 are representative PET-CT images of patients with partial remission (PR) and CR, respectively. CR assessed by PET-CT (CR; including EMD and hematologic/bone marrow CR) after the first INO cycle was achieved in ten of the 24 assessed patients (42%) (Figure 2A, B), nine patients (37.5%) had a PR (Figure 1A, B), two (8%) had stable disease and three (12.5%) showed resistant/progressive disease. After two cycles of INO, 17 of 31 patients (55%) achieved CR, nine (29%) achieved PR, one patient (3%) experienced early death and four patients with stable, resistant or progressive disease did not receive further INO treatment (13%). Interestingly, only two patients with PR after the first cycle achieved a CR after the second INO cycle, whereas the other seven patients

Table 2. Localization of extramedullary disease.

Localization of extramedullary disease*	Number
Lymph nodes	15
Gastrointestinal organs	15
Osteolytic lesions	12
Skin lesions	7
Soft tissue	5
Genitals	4
Mediastinal mass	2
Lung/pleural effusion	2
Epidural mass	2
Nasopharyngeal mass	2
Central nervous system with epidural mass	1
Peripheral nerves	1
Vertebral mass	1
Pelvic mass	1
Cardiac involvement	1

*Overall, patients had in median two extramedullary disease manifestations (range, 1-9). Each localization of extramedullary disease was counted separately; thus, the total number does not add up to the total number of patients.

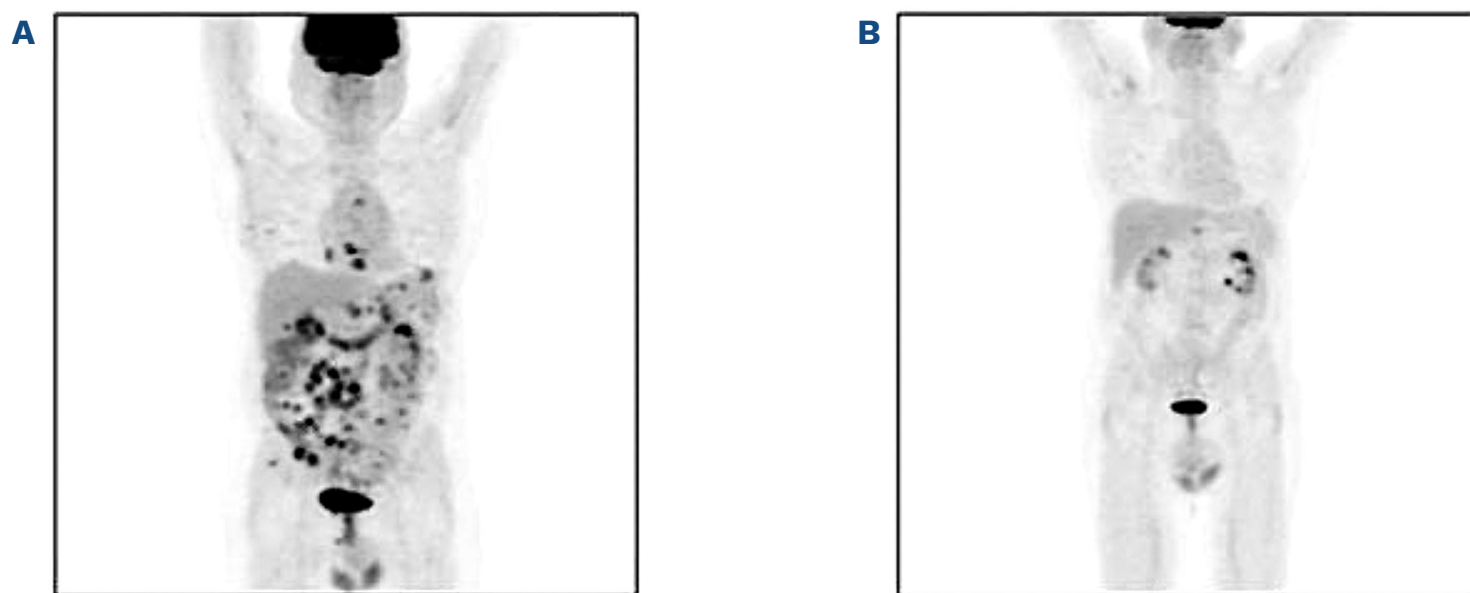


Figure 1. Whole body 18-fluorodeoxyglucose positron emission tomography-computed tomography. (A) Before the start of treatment with inotuzumab ozogamicin (B) After one cycle of inotuzumab ozogamicin, showing partial remission.

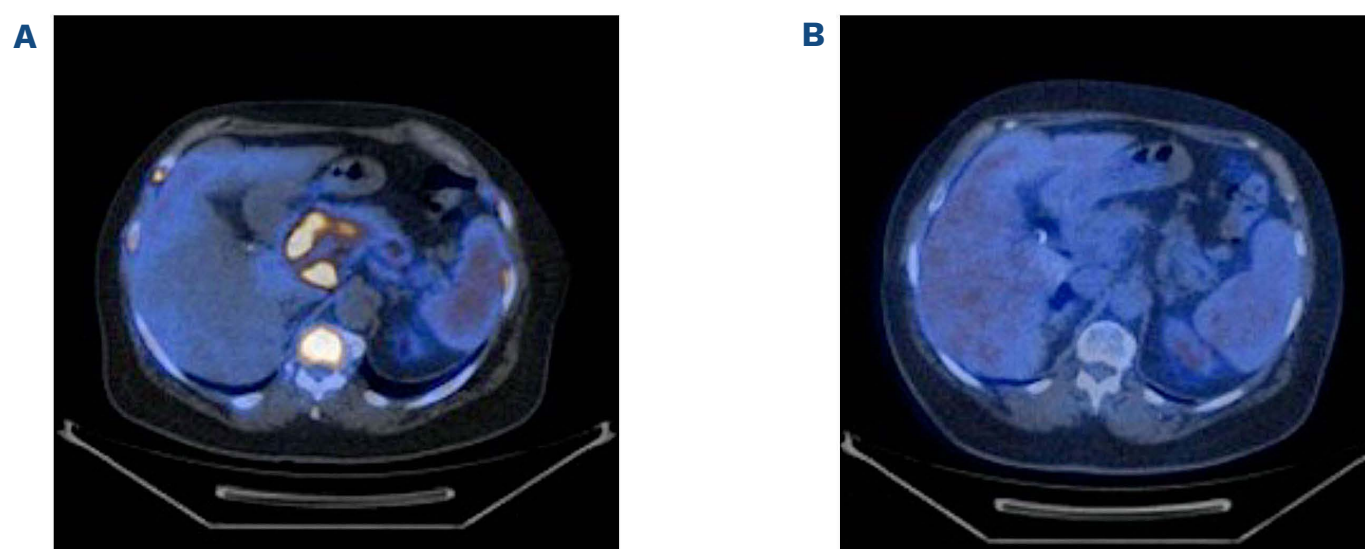


Figure 2. Contrast-enhanced imaging by positron emission tomography-computed tomography (axial slice). (A) Before the start of treatment with inotuzumab ozogamicin. (B) After one cycle of inotuzumab ozogamicin, showing complete remission.

with PR after the first cycle maintained the PR.

Patients, who achieved at least a PR after two INO cycles and did not proceed to allogeneic HSCT, could continue with INO for up to six cycles.

Survival

The median follow-up was 29 months (95% CI: 21 months - not reached) and the median OS was 12.8 months (95% CI: 9.9-16.2 months) (Figure 3). One-year and 2-years OS and relapse-free survival rates were 53% (95% CI: 37-76%) and 47% (95% CI: 25-88%) and 18% (95% CI: 8-43%) and 23% (95% CI: 7-75%), respectively (Figure 4). In Cox regression analysis age as a continuous variable had no impact on OS ($P=0.83$). This was also true when using 60 years as cut-off ($P=0.2$). Twelve patients went on to allogeneic HSCT (CR, $n=6$; PR, $n=3$; progressive disease, $n=3$). Prior to allogeneic HSCT, eight patients received two or fewer cycles of INO and four patients received three or four INO cycles. The influence of allogeneic HSCT assessed as a

time-dependent co-variable as post-remission therapy on OS is illustrated by a Simon Makuch plot (Figure 5). The Mantel-Byar test revealed no impact on OS ($P=0.19$) for patients proceeding to allogeneic HSCT as compared to consolidation with INO. A multivariable Andersen-Gill model including prior allogeneic HSCT before INO treatment, age at initial diagnosis and allogeneic HSCT after INO as a time-dependent variable did not show any significant impact of any of these variables on OS.

In patients achieving a CR after INO treatment ($n=17$), the median OS was 16.2 months. There was no difference in OS ($P=0.08$) or relapse-free survival ($P=0.2$) according to whether patients had EMD manifestations only as compared to EMD and bone marrow involvement.

Of the 26 patients in CR/PR after INO treatment, ten relapsed (38%; after allogeneic HSCT, $n=3$); of those, all except one succumbed to their disease. Two patients died in remission (sepsis, VOD/SOS/multi-organ failure, $n=1$; each); both had undergone allogeneic HSCT before INO

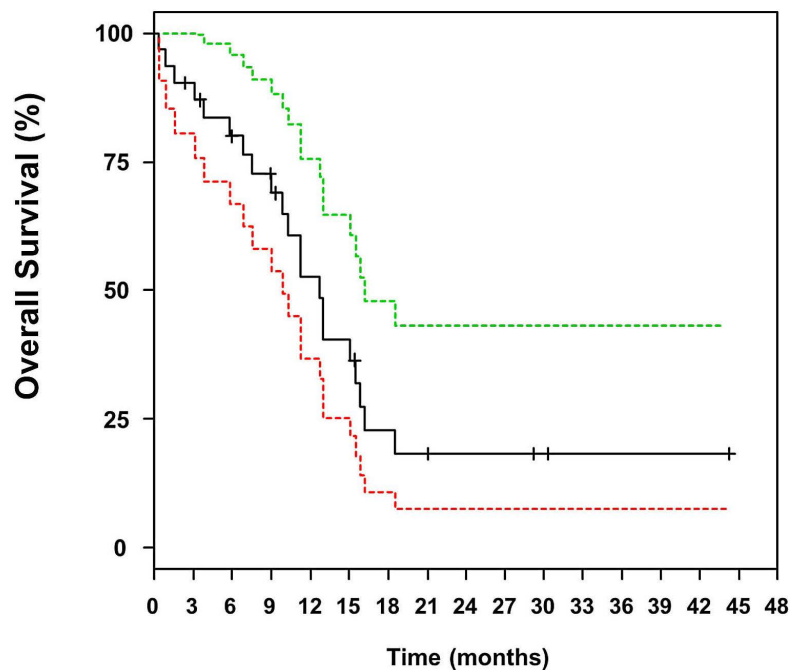


Figure 3. Overall survival of relapsed/refractory patients with B-acute lymphoblastic leukemia and extramedullary disease after treatment with Inotuzumab ozogamicin. Green and red dotted lines indicate upper and lower bounds of the 95% confidence interval.

Numbers at risk: 31 27 22 19 13 10 5 4 3 3 2 1 1 1 1 0 0

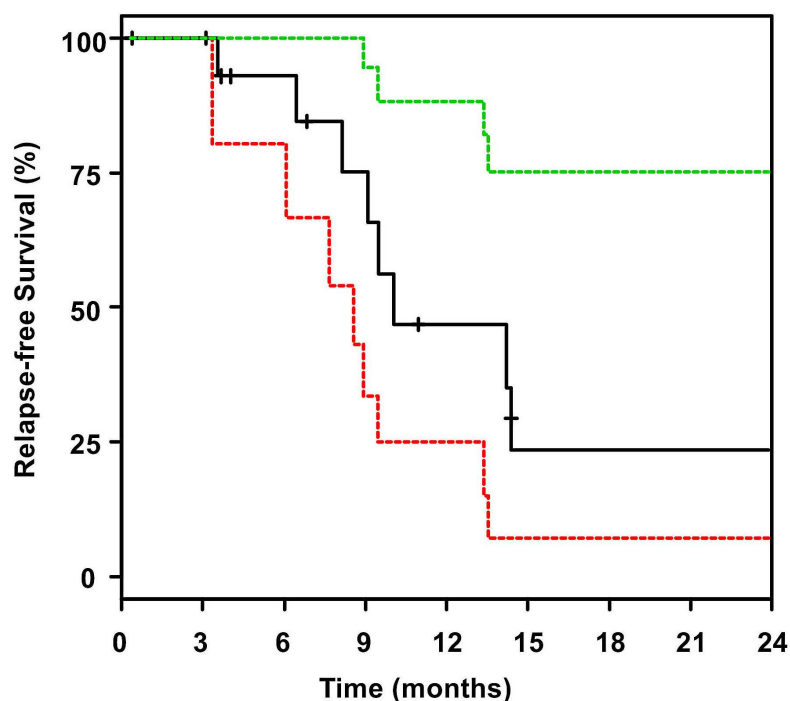


Figure 4. Relapse-free survival of patients attaining complete remission. Green and red dotted lines indicate upper and lower bounds of the 95% confidence interval.

Numbers at risk: 31 27 22 19 13 10 5 4 3

treatment. One patient experienced a molecular relapse, which was successfully treated with INO again. Ten patients are still in CR (n=9) or PR (n=1), including the patient with prior molecular relapse and re-exposure to INO. Our cohort also included three patients with central nervous system involvement. The first patient initially developed central nervous system relapse with positive cytology, but eventually progressed with an epidural mass treated with INO and ponatinib. This patient developed VOD after three INO cycles. Thus, all treatment was withheld. The cerebrospinal fluid remained intermittently positive for ALL (treated with intrathecal chemotherapy), but the peripheral blood remained negative and the epidural mass has not recurred. The second patient was treated with six cycles of intrathecal methotrexate/cytarabine/dexamethasone. The cerebrospinal fluid was negative after the second cycle and remained negative thereafter. The patient

also received four INO cycles and achieved CR without measurable residual disease after the second INO cycle. The patient went on to allogeneic HSCT, but relapsed 3.5 months later and died 8.2 months after relapse. Finally, in the last patient, central nervous system relapse was not confirmed (both cerebrospinal fluid evaluation and magnetic resonance imaging were equivocal), but suspected due to diplopia, which improved after high-dose methotrexate (given before INO). The patient was then switched to six INO cycles and achieved CR according to PET-CT after three INO cycles. Unfortunately, the patient developed systemic (blood/marrow/extramedullary) relapse 1.5 months later. Cerebrospinal fluid at that time was negative and there were additionally no suggestive central nervous systems symptoms (no recurrence of diplopia or other neurological deficits). The patient died 13 days after relapse due to rapidly progressive disease.

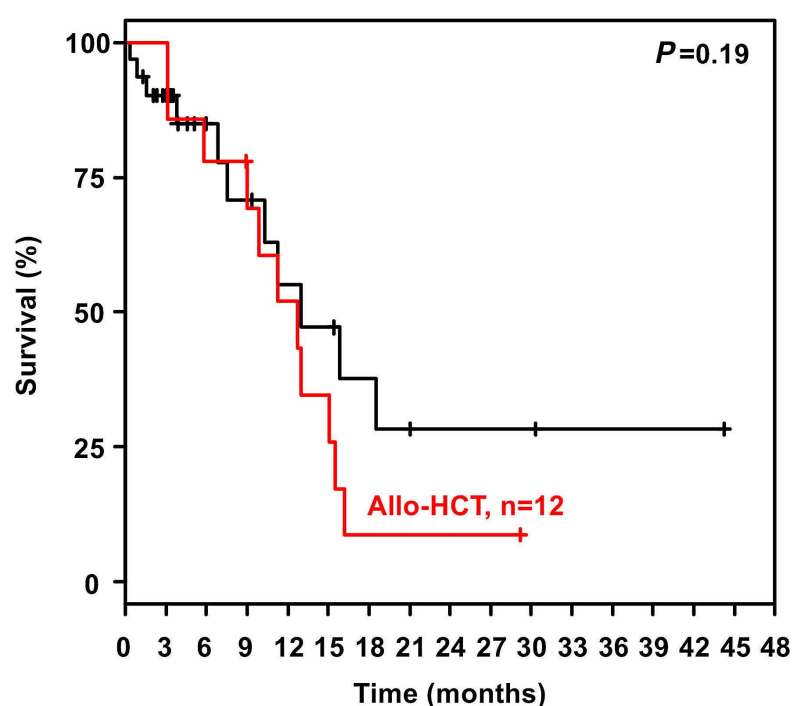
Veno-occlusive disease and sinusoidal obstruction syndrome

Up to four INO cycles were administered in patients as a bridge to transplantation (≤ 2 cycles, $n=9$; 3-4 cycles, $n=3$). Overall, VOD/SOS occurred in three (10%) patients, including one (8%) of 12 patients after transplantation. The first patient experienced VOD on the first day of the third INO cycle prior to allogeneic HSCT, but continued to transplantation after resolution and is in ongoing CR 24 months after transplant. The second patient developed VOD after three INO cycles and therefore stopped INO treatment. This patient did not proceed to allogeneic HSCT and is in CR 30.7 months after the start of INO treatment. The third patient received two cycles of INO prior to haplo-identical allogeneic HSCT with a conditioning regimen consisting of treosulfan/fludarabine/thiotepa. This patient developed VOD after transplantation and died 13.1 months after the transplant due to multi-organ failure and VOD.

Discussion

EMD is reported to occur in 20% of patients with ALL, being more common in patients with a T-cell phenotype, as well as in patients presenting with lymphoblastic lymphoma, without bone marrow involvement.²⁷ EMD may involve different sites, as observed in our series.^{28,29} The role of INO as treatment for patients with r/r ALL and EMD has largely not been studied. The randomized phase III INO-VATE trial included only seven r/r ALL patients with EMD given INO treatment as well as five patients treated with standard-of-care chemotherapy.³⁰ Among patients with baseline EMD, five of seven (71%) in the INO arm and two of five (40%) in the standard care arm achieved CR/CRi,

which included resolution of EMD.³⁰ Consistent with previous reports on the effectiveness of INO in patients with EMD, we observed a high CR rate of 55% after INO treatment in patients with r/r ALL and EMD.³⁰⁻³² There was no difference based on the presence or absence of concurrent bone marrow disease. Additionally, the median OS of 12.8 months in our cohort of heavily pretreated patients compares favorably to that of the less heavily pre-treated patients enrolled in the INO-VATE trial (7.7 months), although the number of patients with EMD in the aforementioned trial was very low limiting the comparison.³¹ The high response rate of ALL with EMD treated with INO may be an advantage of INO treatment since the presence or history of EMD may predict poor responses to other therapies, specifically blinatumomab.¹⁹ In a retrospective cohort study of 65 patients with r/r ALL, a high leukemia burden, defined as bone marrow blast cells $>50\%$ (odds ratio =0.24; $P=0.02$) as well as presence of EMD (odds ratio =0.19; $P=0.05$) or history of EMD (odds ratio =0.23; $P=0.005$) were associated with lower response to blinatumomab.¹⁹ It remains unknown whether increasing the dose of blinatumomab for ALL would be able to overcome this resistance (and be tolerable), since a higher dose has been studied for non-Hodgkin lymphomas and produced reasonable results.³³ In contrast to blinatumomab,³⁴ only a few cases of CD22 antigen loss have been described so far.^{35,36} In our cohort, we did not observe any CD22 antigen loss. In the INO-VATE trial, the inclusion of a small group of patients who were CD22-negative or had low CD22 expression was reported. Interestingly, three of five of these patients showed a response to INO treatment.¹⁵ Furthermore, response in a CD22-negative patient was also described in a case report.³⁷ Thus, INO might be active in CD22-negative patients and/or those with very dim CD22



Numbers at risk: 31 27 22 19 13 10 5 4 3 3 2 1 1 1 1 0 0
12 12 10 9 6 4 1 1 1 1 0 0 0 0 0 0 0

Figure 5. Simon Makuch plot illustrating the influence of allogeneic hematopoietic stem cell transplantation on overall survival. Allo-HCT: allogeneic hematopoietic stem cell transplantation.

expression, but this remains to be elucidated in larger studies. Recent data from the INO-VATE trial suggest that patients with high ($\geq 90\%$) CD22 expression levels had a higher CR rate compared to those with $< 90\%$ expression (42.1% [n=45/107] vs. 20% [n=7/35]).³⁸ According to the European Medicine Agency label, CD22 expression needs to be above 0%, thus also including patients with very dim CD22 expression levels. In the USA, the Food & Drug Administration did not specify any particular CD22 expression.

Lineage switch (myeloid conversion), described mostly in patients receiving chimeric antigen receptor T-cell therapy, does not seem to involve CD22 expression: the antigen is maintained in intermediate phenotype relapses, suggesting that simultaneous pressure on CD19 and CD22 might avoid this mechanism of resistance.³⁹

Increased exposure to INO has been associated with an increased risk of VOD/SOS following allogeneic HSCT, leading to the recommendation that patients being treated with INO as a bridge to allogeneic HSCT should be treated with two or fewer cycles of the drug (3 cycles if necessary to achieve a measurable residual disease-negative CR/CRi).⁴⁰⁻⁴² In our cohort, VOD/SOS occurred in only three patients, including one after allogeneic HSCT, although up to four INO cycles were administered prior to transplantation. These data compare favorably to previously reported data.¹⁵

Our analysis has several limitations. Since this is a retrospective, non-randomized cohort analysis no direct comparison to outcome of r/r ALL with EMD after standard-of-care chemotherapy treatment was feasible. However, since all patients were heavily pretreated with intensive chemotherapy including prior allogeneic HSCT in 58% of the patients, we believe that standard-of-care chemotherapy would have failed to induce a remission. The overall prognosis remains poor even if patients could be successfully bridged to allogeneic HSCT, strongly arguing for alternative consolidation approaches, such as chimeric antigen receptor T cells or advanced bi-specific

antibodies.⁴³ Nevertheless, the ability of INO to be given in an outpatient setting with few toxicities may continue to make it a valuable possibility in the treatment of B-ALL. In conclusion, this outcome analysis demonstrates that treatment with INO is an effective and promising approach in r/r ALL patients with EMD. The CD22 status should be routinely assessed at diagnosis and r/r B-ALL patients, in order to evaluate the indication for INO treatment better. However, allogeneic HSCT alone seems not to be effective in maintaining disease control. Thus, chimeric antigen receptor T cells or advanced bi-specific antibodies as consolidation therapy should be evaluated in the future.

Disclosures

No conflicts of interest to disclose.

Contributions

SK and RFS were responsible for the concept of this study, contributed to the literature search, collection, analysis and interpretation of the data, and wrote the manuscript. CP was responsible for the concept of the study, contributed to the literature search and data collection, contributed patients, analyzed and interpreted data, and critically revised the manuscript. NP analyzed and interpreted data. CS, MRL JW, FG, AMB, MF, CL, DW, ADH and MJL contributed patients and critically revised the manuscript. All authors reviewed and approved the final version of the manuscript.

Funding

SK was supported by the Olympia-Morata fellowship program from the Medical Faculty of Heidelberg University. We acknowledge publication support from Leipzig University.

Data-sharing statement

Questions regarding data sharing should be addressed to the corresponding author.

References

1. Hoelzer D, Bassan R, Dombret H, et al. Acute lymphoblastic leukaemia in adult patients: ESMO clinical practice guidelines for diagnosis, treatment and follow-up. *Ann Oncol*. 2016;27(Suppl 5):v69-82.
2. Spinelli O, Peruta B, Tosi M, et al. Clearance of minimal residual disease after allogeneic stem cell transplantation and the prediction of the clinical outcome of adult patients with high-risk acute lymphoblastic leukemia. *Haematologica*. 2007;92(5):612-618.
3. Schrappe M. Detection and management of minimal residual disease in acute lymphoblastic leukemia. *Hematology Am Soc Hematol Educ Program*. 2014;2014(1):244-249.
4. Davila ML, Riviere I, Wang X, et al. Efficacy and toxicity management of 19-28z CAR T cell therapy in B cell acute lymphoblastic leukemia. *Sci Transl Med*. 2014;6(224):224ra225.
5. Cruz CR, Micklethwaite KP, Savoldo B, et al. Infusion of donor-derived CD19-redirected virus-specific T cells for B-cell malignancies relapsed after allogeneic stem cell transplant: a phase 1 study. *Blood*. 2013;122(17):2965-2973.
6. Jacoby E. The role of allogeneic HSCT after CAR T cells for acute lymphoblastic leukemia. *Bone Marrow Transplant*. 2019;54(Suppl 2):810-814.
7. Kantarjian HM, Thomas D, Ravandi F, et al. Defining the course and prognosis of adults with acute lymphocytic leukemia in first salvage after induction failure or short first remission duration. *Cancer*. 2010;116(24):5568-5574.

8. Thomas DA, Kantarjian H, Smith TL, et al. Primary refractory and relapsed adult acute lymphoblastic leukemia: characteristics, treatment results, and prognosis with salvage therapy. *Cancer*. 1999;86(7):1216-1230.
9. Oriol A, Vives S, Hernández-Rivas JM, et al. Outcome after relapse of acute lymphoblastic leukemia in adult patients included in four consecutive risk-adapted trials by the PETHEMA Study Group. *Haematologica*. 2010;95(4):589-596.
10. Tavernier E, Boiron JM, Huguet F, et al. Outcome of treatment after first relapse in adults with acute lymphoblastic leukemia initially treated by the LALA-94 trial. *Leukemia*. 2007;21(9):1907-1914.
11. Gökbuğet N, Stanze D, Beck J, et al. Outcome of relapsed adult lymphoblastic leukemia depends on response to salvage chemotherapy, prognostic factors, and performance of stem cell transplantation. *Blood*. 2012;120(10):2032-2041.
12. Specchia G, Pastore D, Carluccio P, et al. FLAG-IDA in the treatment of refractory/relapsed adult acute lymphoblastic leukemia. *Ann Hematol*. 2005;84(12):792-795.
13. O'Brien S, Schiller G, Lister J, et al. High-dose vincristine sulfate liposome injection for advanced, relapsed, and refractory adult Philadelphia chromosome negative acute lymphoblastic leukemia. *J Clin Oncol*. 2013;31(6):676-683.
14. Kantarjian H, Stein A, Gokbuğet N, et al. Blinatumomab versus chemotherapy for advanced acute lymphoblastic leukemia. *N Engl J Med*. 2017;376(9):836-847.
15. Kantarjian HM, DeAngelo DJ, Stelljes M, et al. Inotuzumab ozogamicin versus standard therapy for acute lymphoblastic leukemia. *N Engl J Med*. 2016;375(9):740-753.
16. DiJoseph JF, Armellino DC, Boghaert ER, et al. Antibody-targeted chemotherapy with CMC-544: a CD22-targeted immunoconjugate of calicheamicin for the treatment of B-lymphoid malignancies. *Blood*. 2004;103(5):1807-1814.
17. Shor B, Gerber HP, Sapra P. Preclinical and clinical development of Inotuzumab-ozogamicin in hematological malignancies. *Mol Immunol*. 2015;67(2 Pt A):107-116.
18. Lau KM, Saunders IM, Goodman AM. Characterization of relapse patterns in patients with acute lymphoblastic leukemia treated with blinatumomab. *J Oncol Pharm Pract*. 2021;27(4):821-826.
19. Aldoss I, Song J, Stiller T, et al. Correlates of resistance and relapse during blinatumomab therapy for relapsed/refractory acute lymphoblastic leukemia. *Am J Hematol*. 2017;92(9):858-865.
20. Mitelman F. *ISCN: An International System for Human Cytogenetic Nomenclature*. S. Karger: Basel, Switzerland;1995.
21. Schemper M, Smith TL. A note on quantifying follow-up in studies of failure time. *Control Clin Trials*. 1996;17(4):343-346.
22. Kaplan E, Meier P. Nonparametric estimation from incomplete observations. *J Am Stat Assoc*. 1958;53(282):457-481.
23. Mantel N, Byar D. Evaluation of response-time data involving transient states: an illustration using heart transplant data. *J Am Stat Assoc*. 1974;69(345):81-86.
24. Simon R, Makuch RW. A non-parametric graphical representation of the relationship between survival and the occurrence of an event: application to responder versus non-responder bias. *Stat Med*. 1984;3(1):35-44.
25. Andersen P, Gill RD. Cox's regression model for counting processes: a large sample study. *Ann Stat*. 1982;10(4):1100-1120.
26. R Development Core Team. *R: A language and environment for statistical computing*. R Foundation for Statistical Computing: Vienna, Austria, 2014.
27. Geethakumari PR, Hoffmann MS, Pemmaraju N, et al. Extramedullary B lymphoblastic leukemia/lymphoma (B-ALL/B-LBL): a diagnostic challenge. *Clin Lymphoma Myeloma Leuk*. 2014;14(4):e115-e118.
28. Silva WFD, Marquez GL, Salim RC, Rocha V. Primary refractory B-cell lymphoblastic leukemia with extramedullary disease - a distinctive response to blinatumomab and inotuzumab ozogamicin. *Hematol Transfus Cell Ther*. 2019;41(4):356-359.
29. Lucas DR, Bentley G, Dan ME, Tabaczka P, Poulik JM, Mott MP. Ewing sarcoma vs lymphoblastic lymphoma. *Am J Clin Pathol*. 2001;115(1):11-17.
30. DeAngelo DJ, Advani AS, Marks DI, et al. Inotuzumab ozogamicin for relapsed/refractory acute lymphoblastic leukemia: outcomes by disease burden. *Blood Cancer J*. 2020;10(8):81.
31. Bertamini L, Nanni J, Marconi G, et al. Inotuzumab ozogamicin is effective in relapsed/refractory extramedullary B acute lymphoblastic leukemia. *BMC Cancer*. 2018;18(1):1117.
32. Lee SH, Yoon JH, Min GJ, et al. Response to blinatumomab or inotuzumab ozogamicin for isolated extramedullary relapse of adult acute lymphoblastic leukemia after allogeneic hematopoietic cell transplantation: a case study. *Int J Hematol*. 2022;115(1):135-139.
33. Sanders S, Stewart DA. Targeting non-Hodgkin lymphoma with blinatumomab. *Expert Opin Biol Ther*. 2017;17(8):1013-1017.
34. Ruella M, Maus MV. Catch me if you can: leukemia escape after CD19-directed T cell immunotherapies. *Comput Struct Biotechnol J*. 2016;14:357-362.
35. Jacoby E, Nguyen SM, Fountaine TJ, et al. CD19 CAR immune pressure induces B-precursor acute lymphoblastic leukaemia lineage switch exposing inherent leukaemic plasticity. *Nat Commun*. 2016;7:12320.
36. Paul MR, Wong V, Aristizabal P, Kuo DJ. Treatment of recurrent refractory pediatric pre-B acute lymphoblastic leukemia using inotuzumab ozogamicin monotherapy resulting in CD22 antigen expression loss as a mechanism of therapy resistance. *J Pediatr Hematol Oncol*. 2019;41(8):e546-e549.
37. Reinert J, Beitzel-Heineke A, Wethmar K, Stelljes M, Fiedler W, Schwartz S. Loss of CD22 expression and expansion of a CD22 dim subpopulation in adults with relapsed/refractory B-lymphoblastic leukaemia after treatment with Inotuzumab-Ozogamicin. *Ann Hematol*. 2021;100(11):2727-2732.
38. Kantarjian HM, Stock W, Cassaday RD, et al. Inotuzumab ozogamicin for relapsed/refractory acute lymphoblastic leukemia in the INO-VATE trial: CD22 pharmacodynamics, efficacy, and safety by baseline CD22. *Clin Cancer Res*. 2021;27(10):2742-2754.
39. Fingrut W, Davis W, Dallas K, et al. Inotuzumab ozogamicin as salvage therapy for relapsed B-cell acute lymphoblastic leukemia with only very dim expression of Cd22 on circulating blasts. A case report. *Clin Lymphoma Myeloma Leuk*. 2019;19:S184.
40. Kantarjian HM, DeAngelo DJ, Advani AS, et al. Hepatic adverse event profile of Inotuzumab ozogamicin in adult patients with relapsed or refractory acute lymphoblastic leukaemia: results from the open-label, randomised, phase 3 INO-VATE study. *Lancet Haematol*. 2017;4(8):e387-e398.
41. Marks DI, Kebriaei P, Stelljes M, et al. Outcomes of allogeneic stem cell transplantation after inotuzumab ozogamicin treatment for relapsed or refractory acute lymphoblastic leukemia. *Biol Blood Marrow Transplant*. 2019;25(9):1720-1729.
42. Kebriaei P, Cutler C, de Lima M, et al. Management of important adverse events associated with inotuzumab ozogamicin: expert panel review. *Bone Marrow Transplant*. 2018;53(4):449-456.
43. Wan X, Yang X, Yang F, et al. Outcomes of anti-CD19 CAR-T treatment of pediatric B-ALL with bone marrow and extramedullary relapse. *Cancer Res Treat*. 2022;54(3):917-925.

High tumor burden before blinatumomab has a negative impact on the outcome of adult patients with B-cell precursor acute lymphoblastic leukemia. A real-world study by the GRAALL

Aurélie Cabannes-Hamy,¹ Eolia Brissot,² Thibaut Leguay,³ Françoise Hugué,⁴ Patrice Chevallier,⁵ Mathilde Hunault,⁶ Martine Escoffre-Barbe,⁷ Thomas Cluzeau,⁸ Marie Balsat,⁹ Stéphanie Nguyen,¹⁰ Florence Pasquier,¹¹ Magda Alexis,¹² Véronique Lhéritier,¹³ Cédric Pastoret,¹⁴ Eric Delabesse,¹⁵ Emmanuelle Clappier,¹⁶ Hervé Dombret¹⁷ and Nicolas Boissel¹⁸

¹Hematology Department, Versailles Hospital, Le Chesnay; ²Sorbonne Université, AP-HP, Saint-Antoine Hospital, Hematology Department, UMRS 938, INSERM, Paris; ³Hematology Department, CHU de Bordeaux, Bordeaux; ⁴Hematology Department, CHU de Toulouse, Toulouse; ⁵Hematology Department, CHU de Nantes, Nantes; ⁶Hematology Department, CHU d'Angers, Angers; ⁷Hematology Department, CHU de Rennes, Rennes; ⁸Hematology Department, CHU de Nice, Nice; ⁹Hematology Department, Lyon Sud Hospital, Pierre Benite; ¹⁰Hematology Department, Pitié Salpêtrière Hospital, APHP, Paris; ¹¹Hematology Department, Gustave Roussy, Villejuif; ¹²Hematology Department, Orléans Hospital, Orléans; ¹³GRAALL, CHU de Lyon, Lyon; ¹⁴Hematology Lab, CHU de Rennes, Rennes; ¹⁵Hematology Lab, CHU de Toulouse, Toulouse; ¹⁶Hematology Lab, Saint-Louis Hospital, APHP, Paris; ¹⁷Adult Hematology Department, Saint-Louis Hospital, APHP, URP3518, Institut de Recherche Saint-Louis, Université de Paris, Paris and ¹⁸Hematology Adolescent and Young Adult Unit, Saint-Louis Hospital, APHP, URP3518, Institut de Recherche Saint-Louis, Université de Paris, Paris, France

Correspondence: N. Boissel
nicolas.boissel@aphp.fr

Received: September 27, 2021.

Accepted: February 28, 2022.

Prepublished: March 10, 2022.

<https://doi.org/10.3324/haematol.2021.280078>

©2022 Ferrata Storti Foundation

Published under a CC BY-NC license



Abstract

Blinatumomab is a bispecific T-cell engager approved for B-cell precursor acute lymphoblastic leukemia (B-ALL) with persistent minimal residual disease (MRD) or in relapse. The prognostic impact of tumor load has been suggested before other immunotherapies but remains poorly explored before blinatumomab. We retrospectively analyzed the outcome of 73 patients who received blinatumomab either in first complete remission (CR) with MRD (n=35) or at relapse (n=38). Among MRD patients, 91% had MRD >0.01% before blinatumomab, and 89% achieved complete MRD response after blinatumomab. High pre-blinatumomab MRD levels were associated with shorter relapse-free survival ($P=0.049$) and overall survival (OS) ($P=0.011$). At 3 years, OS was 33%, 58% and 86% for pre-blinatumomab MRD >1%, between MRD 0.1-1% and <0.1% respectively. Among relapsed patients, 23 received blinatumomab with overt relapse and 15 were in complete response (CR) after bridging chemotherapy. At 3 years, overall CR rate was 68% and complete MRD response rate was 84%. Patients who directly received blinatumomab had shorter relapse-free survival ($P=0.033$) and OS ($P=0.003$) than patients bridged to blinatumomab. Three-year OS was 66% in the latter group compared to 16% in the former group. Our observations suggest that pre-blinatumomab tumor burden should help to design more tailored strategies including tumor load reduction in relapsed patients.

Introduction

The outcome of adult patients with B-cell precursor acute lymphoblastic leukemia (BCP-ALL) has been dramatically improved in the last decades by the use of pediatric-inspired chemotherapy regimen,¹⁻³ the risk stratification based on minimal residual disease (MRD),^{4,5} and the introduction of tyrosine kinase inhibitor (ITK) in Philadelphia positive (Ph+) BCP-ALL.^{6,7} More than 90% of patients

below the age of 60 years achieve complete remission (CR) after induction with 5-year overall survival (OS) of about 60%. Early evaluation of MRD has been shown to be the most powerful prognostic factor associated with the risk of relapse.⁴ A high MRD level after induction or during consolidation reflects a poor response to chemotherapy, and identifies patients that benefit from allogeneic hematopoietic stem cell transplantation (HSCT) in first CR.⁵ Despite a global improvement in survival, about

30% of patients with Ph-negative BCP-ALL relapse, regardless of their age, with only 50% of second CR, and a poor long-term survival of around 10-20% at 5 years after relapse.⁸

Blinatumomab is a bispecific T-cell engager that recruits T cells on CD19-positive blast cells and induces anti-leukemic cytotoxicity. In a phase III study in patients with relapsed/refractory (R/R) BCP-ALL, blinatumomab showed a benefit over standard of care in terms of overall response rate and OS.⁹ In a phase II study including MRD-positive (MRD+) patients, blinatumomab resulted in complete MRD response in 78% of patients after one cycle, and was associated with significantly longer relapse-free survival (RFS) and OS than MRD non-responders.¹⁰ Among relapsed/TKI-refractory Ph+ BCP-ALL, blinatumomab showed anti-leukemia activity, with 36% of CR/CRh during the first two cycles, and 88% of complete MRD response among CR/CRh responders.¹¹

Predictors of the response to blinatumomab were poorly investigated.¹² Recent studies suggested some BCP-ALL subgroups including *CRLF2*-rearranged ALL may be more sensitive to blinatumomab.¹³ Whereas the absolute lymphocyte count is not correlated to the response, a high rate of regulator T cells may inhibit the cytotoxicity redirected by blinatumomab.¹⁴ Finally, the expression of specific CD19 isoforms lacking the epitope recognized by blinatumomab may also lead to primary resistance to this bispecific antibody.¹³ As for other immunotherapies, the effector/target ratio is supposed to play a critical role in the efficacy of blinatumomab. However, the prognostic impact of leukemic tumor burden on the response to blinatumomab remains a matter of debate and confounding results emerged from comparisons treated at different disease stages.

The present study aimed to explore the role of pre-blinatumomab tumor load on patient outcome in a real-life cohort of patients treated between 2012 and 2016 for R/R or MRD+ adult BCP-ALL. The prognostic impact of pretherapeutic leukemic burden was investigated.

Methods

Study design

The present study is a retrospective, multicenter, case series study evaluating the efficacy and the tolerance of blinatumomab in adult patients treated for a BCP-ALL in the French compassionate use program. The study focuses on the impact of pre-blinatumomab tumor burden on patient outcome.

Inclusion criteria were: i) patients aged 15 years or more, ii) patients treated in the GRAALL network, iii) patients with Ph-negative or Ph+ BCP-ALL, in R/R to salvage therapy (R/R cohort) or in first or second remission with MRD+

(MRD+ cohort), iv) patients treated with blinatumomab in the French compassionate use (ATU: Autorisation Temporaire d'Utilisation) program. The study was registered as clinicaltrials.gov. Identifier: NCT03751072 and was approved by an independent Ethic Committee, in accordance with the Declaration of Helsinki.

Response and safety assessment

Hematological CR was defined as <5% blasts in the bone marrow (BM) aspirates, with full hematologic recovery in the peripheral blood (neutrophil count $>1 \times 10^9/L$ and platelet count $>100 \times 10^9/L$). Complete remission with incomplete hematologic recovery (CRi) was defined as <5% BM blasts with neutrophil count $<1 \times 10^9/L$ or platelet count $<100 \times 10^9/L$. Complete MRD response was defined by the absence of detectable MRD, either by molecular immunoglobulin/T-cell receptor quantification, by flow cytometry (with sensitivity of 0.01%), or by BCR-ABL1 quantification in Ph+ ALL patients.

Statistical analysis

OS was defined as the time between blinatumomab first infusion and death, censoring patients alive at last follow-up. RFS was defined as the time between first blinatumomab infusion for MRD+ patients or the time of post-blinatumomab CR/CRi for relapsed patients and either death or relapse, censoring patients at last follow-up. In some analysis, OS and RFS were also censored at the time of HSCT. Univariate and multivariate analyses assessing the impact of pre-blinatumomab tumor burden were performed with a Cox model. Proportional hazards assumptions were graphically checked. MRD+ and relapse cohorts were analyzed separately. Statistical analysis was performed with the statistical software STATA/SE (Version 16.1, StataCorp LLC, College Station, Texas, USA).

Results

Patient's characteristics

Among the 80 patients who received blinatumomab in the French compassionate ATU program, 73 were included in this study from 11 GRAALL network centers (Figure 1). Thirty-five patients were in first complete remission (CR1) with persistent MRD (MRD+ cohort), and 38 were in first or subsequent relapse (relapse cohort). Patient in first CR1 were mostly treated according to GRAALL frontline protocols for Ph+ and Ph- BCP-ALL.^{3,15} The choice of salvage therapy was left to the discretion of the treating clinician and many different schedules were used including weekly dosing of alkaloids and steroids, second-line ITK, hyper-CVAD, or pediatric-inspired regimen.

Patient's characteristics are summarized in Table 1.

The median age of the MRD+ cohort was 32 years (range,

17-74). At diagnosis, the median white blood cell count (WBC) was $8.1 \times 10^9/L$ (range, 1.0-731.0). The karyotype showed a Philadelphia chromosome in three patients (9%), a *KMT2A* (formerly *MLL*) rearrangement in three patients (9%) and a low hypodiploidy/near triploidy in three patients (9%). An intragenic deletion of *IKZF1* gene was found in five of 19 screened patients (26%). Two patients had previously received an HSCT. Interim chemotherapy was given while waiting for treatment approval and delivery according to local investigator choice. Before blinatumomab infusion, only three of 32 (9%) patients had MRD $<0.01\%$, and the majority (18/32, 56%) had MRD $>0.1\%$.

The median age of the relapse cohort was 49 years (range, 16-74). Among these 38 patients, 11 had a Ph+ ALL (29%), two had a *KMT2A* rearrangement (6%), and three had a t(1;19) translocation. An *IKZF1* intragenic deletion was found in five of 21 evaluated patients (24%). Around two thirds of these patients received blinatumomab in first relapse (63%), and 15 of 38 (39%) had previously received an allogeneic HSCT. Due to local investigator decisions, patients could have received chemotherapy before blinatumomab. Among these 38 patients, 15 (39%) were in second or greater remission (CR2+) at the time of blinatumomab. Among these patients in CR2+, three of 11 (27%) had MRD of $<0.01\%$, while the majority (7/11, 64%) had MRD of $>0.1\%$.

Efficacy of blinatumomab in the minimal residual disease-positive cohort

Patients from the MRD+ cohort received a median of one cycle of blinatumomab (range, 1-2). Blinatumomab was started at the dose of 9 $\mu\text{g/day}$ in ten of 24 patients (29%)

and 28 $\mu\text{g/day}$ in the remainders (71%, 1 missing data). Among the 33 patients with available data, 23 received a premedication with dexamethasone (range, 20-40 mg total dose). Upon blinatumomab, a complete MRD response was observed in 31 of 35 patients (89%). Among the 35 patients, 23 (66%) proceeded to allogeneic HSCT in continuous CR. The median follow-up of this cohort was 3.6 years. A relapse was observed in six patients. Both the median RFS and OS were not reached (Table 2; Figure 2A and B). In this cohort, the 3-year RFS was 65% and the 3-year OS was 68%. When patients were censored at the time of HSCT performed in continuous CR after blinatumomab, the 3-year RFS was 71% and the 3-year OS was 77% (Online Supplementary Figure S1A and B).

Efficacy of blinatumomab in the relapse cohort

Patients from the relapse cohort received a median of one blinatumomab cycle (range, 1-5). CR was reached in 26 of 38 patients (68%, Table 2). Eleven of the 23 patients not in CR at the time of blinatumomab achieved CR (48%). Among the 26 patients in CR after blinatumomab, a complete MRD response was observed in 21 of 25 patients (84%) with no difference between patients in previous CR (12/14, 86%) or not (9/11, 82%, $P=0.99$). Twelve of 26 CR patients (46%) were bridged to allogeneic HSCT in continuous CR (Table 2). The median follow-up of this cohort was 3.3 years. The median RFS and OS were respectively 14.6 and 10.3 months (Table 2; Figure 3A and B). At 3 years, the RFS was 37% and OS was 35%. When follow-up was censored at transplant time, 3-year RFS was 38% and 3-year OS was 32% (Online Supplementary Figure 2A and B).

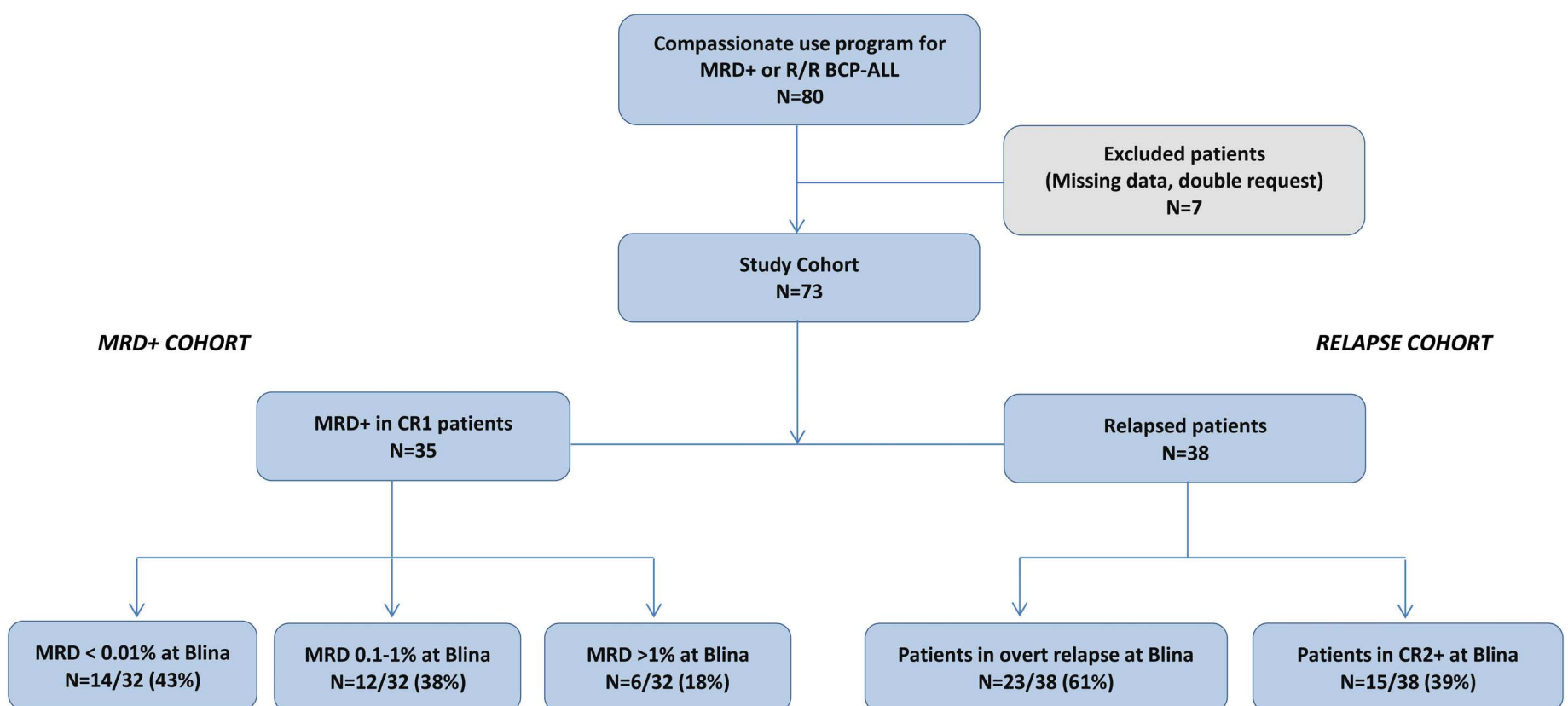


Figure 1. Flow-chart of the study population. CR1: first complete remission; CR2+: patients in second or greater complete remission; MRD: minimal residual disease; R/R: relapsed/ refractory; ALL: acute lymphoblastic leukemia.

Impact of pre-blinatumomab tumor burden on outcome

In order to address the impact of pre-blinatumomab tumor load on subsequent outcome, we first investigated the role of pre-blinatumomab MRD in the MRD+ cohort. Among the four patients who did not reach a complete MRD response after blinatumomab, two had a pre-blinatumomab MRD >1% (2/6, 33%) and two had MRD ≤1% (2/26, 8%; $P=0.15$). A high level of pre-blinatumomab MRD was significantly associated with a lower RFS and OS (Figure 4A and B). The 3-year RFS was respectively 33%, 58% and 78% respectively

for pre-blinatumomab MRD >1%, between MRD 0.1-1%, and <0.1% ($P=0.049$). The 3-year OS was 33%, 58% and 86% respectively for MRD >1%, between MRD 0.1-1%, and <0.1% ($P=0.011$). Of note, no difference in patient characteristics was observed between these three MRD subgroups (*Online Supplementary Table S1*). A multivariate analysis considering age, WBC at diagnosis, high-risk cytogenetics, and pre-blinatumomab MRD showed significantly shorter OS and RFS associated with higher MRD levels and a trend with high-risk cytogenetics (Table 3).

Table 1. Patient characteristics.

	All N=73	MRD+ cohort N=35	Relapse cohort N=38
Age in years, median (range)	42 (16-74)	32 (17-74)	49 (16-74)
Sex, male/female	43/30	21/14	22/16
WBC x10 ⁹ /L, median (range)	8.1 (0.4-731.0)	8.1 (1.0-731.0)	8.2 (0.4-207.0)
Cytogenetics			
- t(1;19)/E2A-PBX1	3 (4)	0	3 (8)
- t(9;22)/BCR-ABL1	14 (19)	3 (9)	11 (29)
- <i>KMT2A</i> -r (<i>MLL</i> -r)	5 (7)	3 (9)	2 (6)
- low hypodiploidy / near triploidy	4 (6)	3 (9)	1 (3)
<i>IKZF1</i> intragenic deletion, N (%)	10/40 (25)	5/19 (26)	5/21 (24)
Disease status			
CR1, n (%)	35/73 (48)	35 (100)	-
1 st relapse, n (%)	24 (33)	-	24 (63)
≥ 2 nd relapse, n (%)	14 (19)	-	14 (37)
Allo-HSCT before blinatumomab	17 (23)	2 (6)	15 (39)
CR at blinatumomab	50 (68)	35 (100)	15 (39)
% BM blasts, median (range)	0 (1-92)	1 (0-4)	2 (0-92)
MRD at blinatumomab (in CR patients), N (%)			
>1%	12/43 (28)	6/32 (18)	6/11 (55)
0.1%-1%	13/43 (30)	12/32 (38)	1/11 (9)
0.01-0.1%	12/43 (28)	11/32 (34)	1/11 (9)
<0.01%	6/43 (14)	3/32 (9)	3/11 (27)

WBC: white blood cell count; allo-HSCT: allogeneic hematopoietic stem cell transplantation; CR: complete remission; BM: bone marrow; MRD: minimal residual disease.

Table 2. Patient early response and late outcome.

	All N=73	MRD+ cohort N=35	Relapse cohort N=38
Complete Remission, N (%)	61 (85)	35 (100)	26 (68)
MRD Complete response, N (%)	52/60 (87)	31/35 (89)	21/25 (84)
Allo-HSCT in CCR, N (%)	35/61 (58)	23/35 (66)	12/26 (46)
Follow-up, median years (95% CI)	3.5 (3.1-3.7)	3.6 (3.1-3.8]	3.3 (2.5- 4.1)
RFS, median months (95% CI)	NR (14.9-NR)	NR (33.2-NR)	14.6 (5.7-41.6)
3y-RFS, % (95% CI)	45% (33-56)	65% (47-78)	37% (19-55)
OS, median months [95% CI)	40.7 (13.8-NR)	NR (NR-NR)	10.3 (7.1-40.7)
3y-OS, % (95% CI)	52% (39-62)	68% (50-81)	35% (21-51)

Allo-HSCT: allogeneic hematopoietic stem cell transplantation; CCR: continuous complete remission; MRD: minimal residual disease; PFS: progression-free survival (MRD+); RFS: relapse-free survival (REL); OS: overall survival; 95% CI: 95% confidence interval.

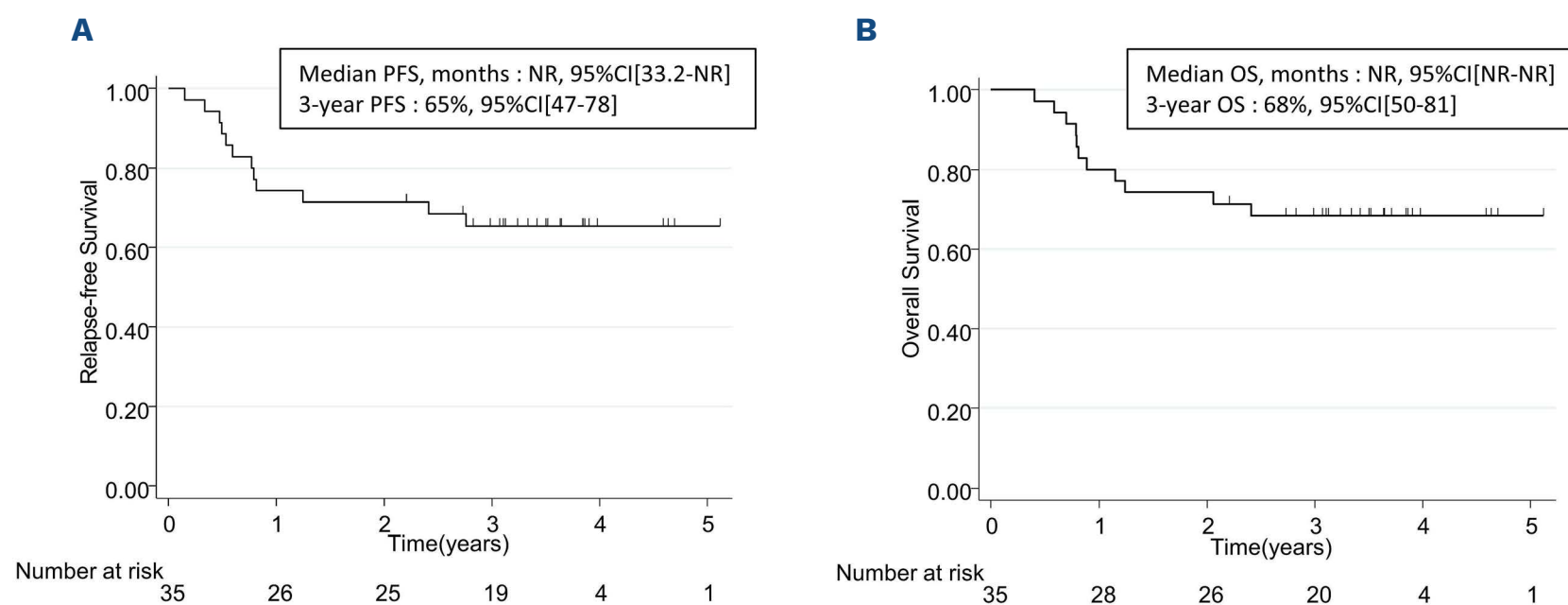


Figure 2. Outcome of MRD+ patients. A) Relapse-free survival and (B) overall survival (OS) without censoring patients at allogeneic hematopoietic stem cell transplantation time. PFS: progression-free survival; CI: confidence interval; NR: not reached.

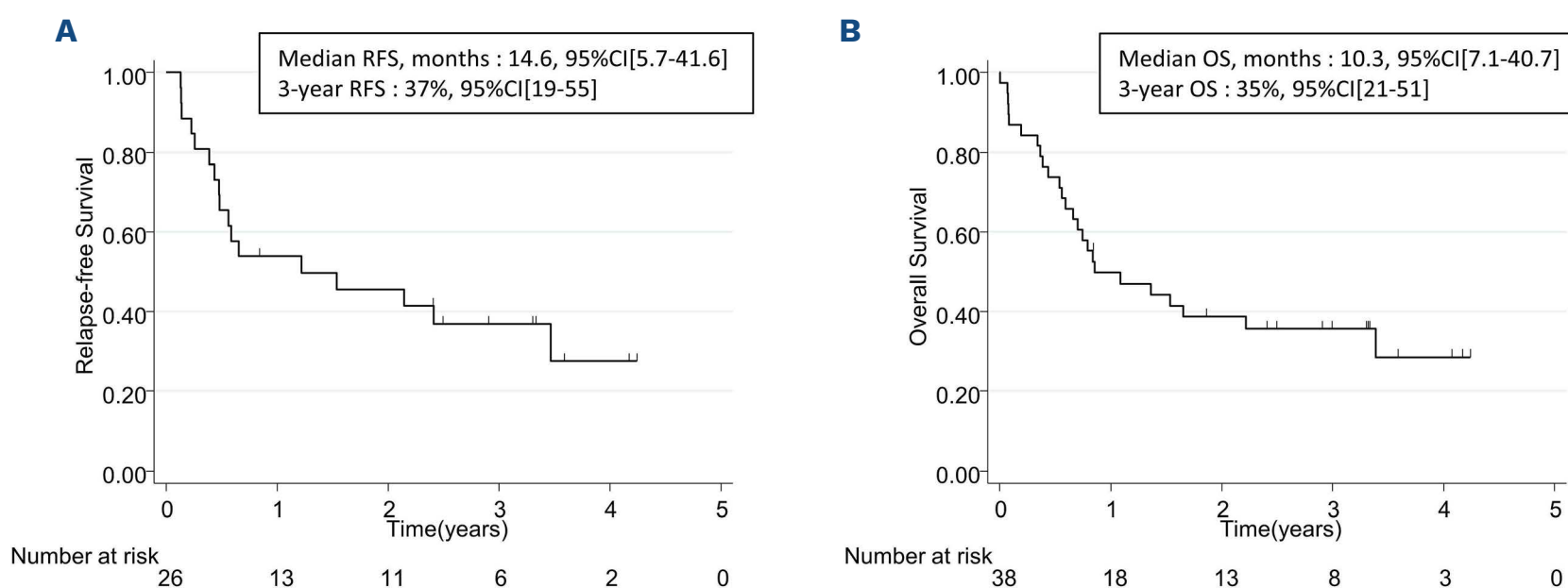


Figure 3. Outcome of relapsed patients. (A) Relapse-free survival and (B) overall survival (OS) without censoring patients at allogeneic hematopoietic stem cell transplantation time. CI: confidence interval.

We further investigated the prognostic impact of pre-blinatumomab tumor load in the relapse cohort. In the whole cohort, regardless of the treatment line, patients who received blinatumomab in CR2+ had similar characteristics (*Online Supplementary Table S2*) and a better outcome as compared to patients treated in overt relapse. Indeed, 3-year RFS and OS for patients in CR2+ at the time of blinatumomab were 59% and 66% respectively *versus* $\leq 9\%$ (not evaluable, $P=0.033$) and 16% ($P=0.003$) respectively for patients in overt relapse (Figure 3C and D). Median RFS and OS were respectively 41.6 months and not reached in CR2+ patients, *versus* 6.7 months and 8.9 months respectively in patients with overt relapse at time of blinatumomab initiation. A multivariate analysis considering age, high-risk cytogenetics, number of prior relapses, allogeneic HSCT, and CR status at blinatumomab showed significantly shorter OS and RFS associated with CR status at blinatumomab and more advanced disease (Table 3).

A similar analysis performed in patients in first relapse showed the same advantage for patients exposed to blinatumomab in second CR after chemotherapy compared to patients who received blinatumomab in overt first hematological relapse. The 3-year RFS and OS for patients in second CR were 70% (median OS not reached) and 80% ($n=10$) respectively *versus* $\leq 11\%$ (not evaluable, $P=0.067$) and 27% ($P=0.025$) in first hematological relapse (*Online Supplementary Figure S3*).

Discussion

This retrospective, multicenter study reports the outcome of 73 adult patients treated with blinatumomab for MRD+ or relapsed BCP-ALL within the French compassionate use program. Patient outcomes, CR and MRD response rates after blinatumomab were similar to those observed in

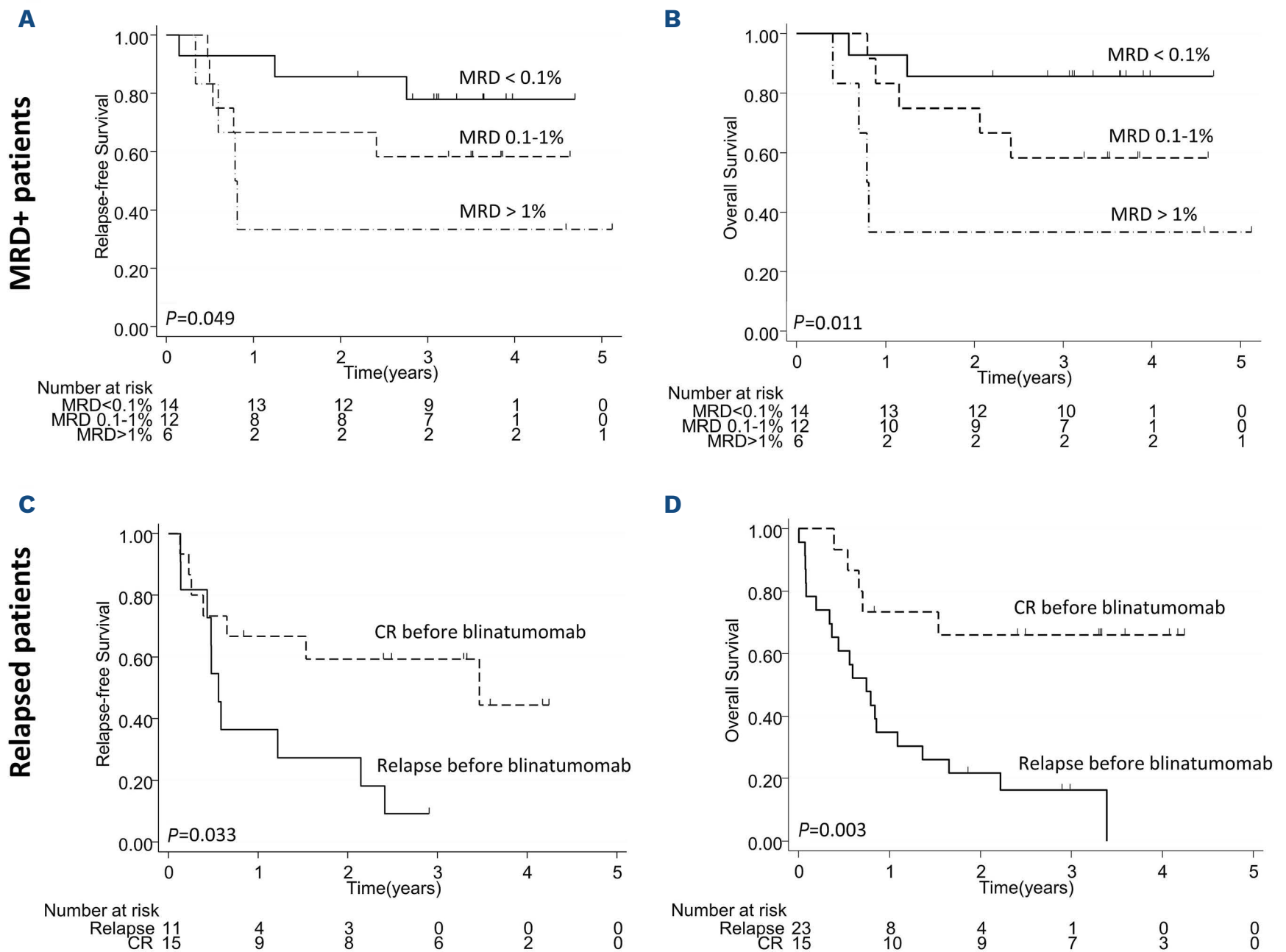


Figure 4. Impact of pre-blinatumomab tumor burden on outcome. (A) Relapse-free survival (RFS) and (B) overall survival (OS) in minimal residual disease-positive (MRD+) patients according to pre-blinatumomab MRD. (C) RFS and (D) OS in relapsed patients according to pre-blinatumomab complete response (CR).

larger prospective trials.^{9,10} In addition, we report here that the tumor load before blinatumomab initiation has a strong impact on patient outcome whatever the disease status. This parameter should thus be considered to design future salvage strategies.

Among the patients exposed to blinatumomab in first CR and with persistent MRD, 89% achieved a complete MRD response. The median RFS and OS were not reached with a 3-year RFS and OS of 65% and 68% respectively. This observation is in line with the BLAST trial for adults with MRD+ ALL that reported a 80% complete MRD response rate after one course of blinatumomab.¹⁰ In the BLAST subgroup analysis, patients in CR1 achieved a complete MRD response in 83% of cases after the first course of blinatumomab and the median RFS was not reached for patients who achieved complete MRD response. In the present cohort, censoring outcome analyses at the time of HSCT did not modify estimates, which should encourage to further investigate the role of transplantation in MRD+ patients after

blinatumomab therapy. Of note, heterogeneity in the techniques used to assess MRD response may be considered as a limitation of the present study.

Whereas the prognostic impact of MRD response after blinatumomab is well described,¹⁰ the role of pre-blinatumomab MRD remains poorly explored. In the BLAST study, which included patients with MRD ≥0.1%, a complete MRD response was achieved in only six of nine (67%) patients with an MRD level ≥10%.¹⁰ In the present MRD+ cohort, pre-blinatumomab MRD levels had a strong impact on patient outcome and inversely correlated with RFS and OS. In previous pediatric and adult ALL studies, the same impact was observed for pre-transplant MRD identified as a post-transplant relapse predictor.^{16,17} In both pre-blinatumomab or pre-transplant settings, it remains unclear whether a high MRD level is just a marker of higher intrinsic resistance of the disease, or also contributes to unfavorable target-to-effector ratios that disable effector cells. In MRD+ patients, there are limited options in terms of

Table 3. Multivariate analysis for relapse-free survival and overall survival in minimal residual disease-positive and relapse cohorts.

	MRD+ cohort						Relapse cohort					
	RFS			OS			RFS			OS		
	HR	95% CI	P	HR	95% CI	P	HR	95% CI	P	HR	95% CI	P
Age*	0.99	(0.96-1.04)	0.99	1.00	(0.96-1.05)	0.97	0.98	(0.95-1.01)	0.17	0.98	(0.95-1.01)	0.24
White blood cell count*	1.00	(0.99-1.00)	0.40	1.00	(0.99-1.00)	0.28	NA	NA	NA	NA	NA	NA
High-risk cytogenetics**	3.09	(0.56-17.0)	0.19	6.83	(0.86-53.99)	0.07	1.08	(0.48-2.39)	0.86	1.70	(0.69-4.19)	0.25
Number of prior relapses*	NA	NA	NA	NA	NA	NA	1.85	(1.10-3.12)	0.02	5.23	(2.56-10.72)	<0.001
Prior allo-HSCT	NA	NA	NA	NA	NA	NA	0.84	(0.37-1.95)	0.69	0.55	(0.19-1.63)	0.28
MRD at blinatumomab***	3.00	(1.15-7.84)	0.03	5.41	(1.67-17.44)	0.005	NA	NA	NA	NA	NA	NA
CR at blin vs. overt relapse	NA	NA	NA	NA	NA	NA	0.13	(0.04-0.37)	<0.001	0.07	(0.02-0.25)	<0.001

NA: not applicable; HR: hazard ratio; CI: confidence interval; blin: blinatumomab; RFS: relapse-free survival; MRD: minimal residual disease. *continuous variables **defined by either $t(9;22)/BCR-ABL1$, $KMT2A-r$, $t(1;19)/TCF3-PBX1$, or low hyploidy/near triploidy. *** 3-class MRD levels (<0.1%, 0.1-1%, >1%). allo-HSCT: allogeneic hematopoietic stem cell transplantation.

pre-blinatumomab intervention to reduce MRD levels. Pre-blinatumomab MRD level should thus remain a warning to guide further intervention.

In R/R patients, blinatumomab is approved as a single agent based on the results of two studies including the phase III TOWER study which demonstrated a superiority of blinatumomab on standard of care in terms of overall response rate and OS.⁹ Whether blinatumomab should be used in fully relapsed patients or after a tumor burden reduction remains a matter of debate with a lack of controlled study addressing this question. In the TOWER study, 44% of R/R patients achieved a CR at 12 weeks, with 76% of MRD negativity among responders and a median OS of 7.7 months.¹⁸ In patients with full relapse at the time of blinatumomab, we report very similar results with a CR rate of 48%, 82% of responders achieving a complete MRD response, and a median OS of 8.9 months. Interestingly, the outcome of the 15 relapsed patients who were exposed to blinatumomab in CR2+ was significantly better than those of relapsed patients exposed to blinatumomab in overt relapse (Figure 4C and D). There are obvious limitations to this non-controlled comparison including the fact that relapsed patients who achieved CR prior to blinatumomab exposure were by definition good responders at relapse, achieving a new CR having been described as one of the most important prognostic factor after relapse.^{19,20} However, the difference in RFS between patients in CR before blinatumomab exposure (n=15) and patients achieving CR after blinatumomab (n=11) also suggests that,

despite similar MRD responses, the advantage of having reached a CR after chemotherapy *versus* blinatumomab still persists after CR (Figure 4C; Table 3). Thus, the prognostic value of a negative MRD after blinatumomab differs depending on disease status before blinatumomab. Combined with CR status at blinatumomab, it could have many implications in terms of relapse prevention strategies post blinatumomab. Of note, the prognostic impact of pre-therapeutic tumor burden was also pointed out with CAR-T cell therapy.²¹ After tisagenlecleucel, it was suggested that a high tumor burden was associated with a higher risk of CD19-negative relapse and escape to CAR-T surveillance. In the present study, we were not able to collect the CD19 status of leukemic cells at relapse. Given that CD19-negative relapse after blinatumomab was reported in up to one third of patients, further studies should investigate whether the risk of CD19 antigen loss does correlate with tumor burden at the time of treatment.²² Recently, the use of blinatumomab in second CR was strongly supported by two different randomized studies conducted in children and young adults with first intermediate- or high-risk disease. In the study by Locatelli *et al.*,²³ the 36-month OS was 81.1% after blinatumomab consolidation *versus* 55.8% after chemotherapy-based consolidation. In the study by Brown *et al.*,²⁴ the 24-month OS was 71.3% after blinatumomab consolidation and 58.4% after chemotherapy. Interestingly, in the present study, the 3-year OS of the few patients (n=10) who received blinatumomab in second CR was 80%. In adult Ph-negative

BCP-ALL aged up to 60 years old, a second CR is expected in about 50% of cases.^{19,20} The most important factor associated with the chance to reach a second CR is CR1 duration. In late relapses with CR1 duration >18 months, reported CR2 rates ranged from 58% to 68%.^{19,20} In the TOWER study for adult R/R B-ALL, patients in first relapse could be included if CR1 duration was shorter than 12 months or after HSCT. Patients who received blinatumomab as first salvage, most of them being in first relapse, had an overall response rate of 51%, a CR rate of 44%, and a median survival of 11.1 months.²⁵ Altogether, these observations encourage to try to reach a second CR with chemotherapy-based regimen before exposing patients to blinatumomab consolidation, particularly in younger patients with late relapse.

The place of blinatumomab combined to chemotherapy in frontline or R/R B-ALL is being intensively explored. The MD Anderson Cancer Center reported on the combination of Hyper-CVAD-derived regimen, inotuzumab ozogamicin, and blinatumomab in elderly patients with frontline B-ALL or in younger adult patients with R/R diseases.^{26,27} More recently, phase II assessing the role of frontline consolidation with blinatumomab in adult B-ALL were reported by the GIMEMA group and by our group.^{28,29}

In conclusion, this real-world study confirms the benefit of blinatumomab in adult patients with either primary resistant BCP-ALL or at relapse and suggests an impact of pre-blinatumomab tumor burden on patient outcome. Many limitations have been highlighted throughout the discussion, mostly related to the retrospective nature of the study, to the non-controlled nature of the comparisons, and more specifically to the selection of patients in second CR after chemotherapy compared to patients exposed to blinatumomab in overt relapse. It is however unlikely that

a randomized study will address this important question. In early resistant disease with MRD+, our observation supports the design of post-blinatumomab strategies including transplantation. In relapsed patients, especially in first salvage, our results along with recent published observations support to discuss the best timing schedule of blinatumomab, after salvage chemotherapy rather than in overt relapse. The underlying mechanisms that contribute to an increased risk of failure in patients with high tumor burden remain to be explored.

Disclosures

ACH declare no conflicts of interest. NB was employed on advisory boards and received research subsidies from AMGEN.

Contributions

ACH, NB and VL designed, performed and coordinated the research. ACH and VL collected data. NB performed statistical analyses and produced the figures. ACH and NB analyzed, interpreted the data and wrote the manuscript. EB, TL, FH, PC, MH, MEB, TC, MB, SN, SB, MA, CP, ED, EC, HD included patients, contributed data and commented on the manuscript

Acknowledgements

We thank all data managers for their help in collecting and updating data.

Funding

This study was supported by Amgen.

Data-sharing statement

For original data, please contact nicolas.boissel@aphp.fr

References

- Dombret H, Cluzeau T, Huguet F, Boissel N. Pediatric-like therapy for adults with ALL. *Curr Hematol Malig Rep.* 2014;9(2):158-164.
- Huguet F, Leguay T, Raffoux E, et al. Pediatric-inspired therapy in adults with Philadelphia chromosome-negative acute lymphoblastic leukemia: the GRAALL-2003 study. *J Clin Oncol.* 2009;27(6):911-918.
- Huguet F, Chevret S, Leguay T, et al. Intensified therapy of acute lymphoblastic leukemia in adults: report of the randomized GRAALL-2005 clinical trial. *J Clin Oncol.* 2018;36(24):2514-2523.
- Beldjord K, Chevret S, Asnafi V, et al. Oncogenetics and minimal residual disease are independent outcome predictors in adult patients with acute lymphoblastic leukemia. *Blood.* 2014;123(24):3739-3749.
- Dhédin N, Huynh A, Maury S, et al. Role of allogeneic stem cell transplantation in adult patients with Ph-negative acute lymphoblastic leukemia. *Blood.* 2015;125(16):2486-2496; quiz 2586.
- Tanguy-Schmidt A, Rousselot P, Chalandon Y, et al. Long-term follow-up of the imatinib GRAAPH-2003 study in newly diagnosed patients with de novo Philadelphia chromosome-positive acute lymphoblastic leukemia: a GRAALL study. *Biol Blood Marrow Transplant.* 2013;19(1):150-155.
- Chalandon Y, Thomas X, Hayette S, et al. Randomized study of reduced-intensity chemotherapy combined with imatinib in adults with Ph-positive acute lymphoblastic leukemia. *Blood.* 2015;125(24):3711-3719.
- Desjonquères A, Chevallier P, Thomas X, et al. Acute lymphoblastic leukemia relapsing after first-line pediatric-inspired therapy: a retrospective GRAALL study. *Blood Cancer J.* 2016;6(12):e504.
- Kantarjian H, Stein A, Gökbuget N, et al. Blinatumomab versus chemotherapy for advanced acute lymphoblastic leukemia. *N Engl J Med.* 2017;376(9):836-847.
- Gökbuget N, Dombret H, Bonifacio M, et al. Blinatumomab for minimal residual disease in adults with B-cell precursor acute lymphoblastic leukemia. *Blood.* 2018;131(14):1522-1531.
- Martinelli G, Boissel N, Chevallier P, et al. Complete hematologic and molecular response in adult patients with

- relapsed/refractory Philadelphia chromosome–positive B-precursor acute lymphoblastic leukemia following treatment with blinatumomab: results from a phase II, single-arm, multicenter study. *J Clin Oncol.* 2017;35(16):1795-1802.
12. Boissel N. ALL in escape room. *Blood.* 2021;137(4):432-434.
 13. Zhao Y, Aldoss I, Qu C, et al. Tumor-intrinsic and -extrinsic determinants of response to blinatumomab in adults with B-ALL. *Blood.* 2021;137(4):471-484.
 14. Duell J, Dittrich M, Bedke T, et al. Frequency of regulatory T cells determines the outcome of the T-cell-engaging antibody blinatumomab in patients with B-precursor ALL. *Leukemia.* 2017;31(10):2181-2190.
 15. Chalandon Y, Thomas X, Hayette S, et al. Randomized study of reduced-intensity chemotherapy combined with imatinib in adults with Ph-positive acute lymphoblastic leukemia. *Blood.* 2015;125(24):3711-3719.
 16. Bader P, Kreyenberg H, Henze GHR, et al. Prognostic value of minimal residual disease quantification before allogeneic stem-cell transplantation in relapsed childhood acute lymphoblastic leukemia: the ALL-REZ BFM Study Group. *J Clin Oncol.* 2009;27(3):377-384.
 17. Logan AC, Vashi N, Faham M, et al. Immunoglobulin and T cell receptor gene high-throughput sequencing quantifies minimal residual disease in acute lymphoblastic leukemia and predicts post-transplantation relapse and survival. *Biol Blood Marrow Transplant.* 2014;20(9):1307-1313.
 18. Kantarjian H, Stein A, Gökbuget N, et al. Blinatumomab versus chemotherapy for advanced acute lymphoblastic leukemia. *N Engl J Med.* 2017;376(9):836-847.
 19. Gökbuget N, Stanze D, Beck J, et al. Outcome of relapsed adult lymphoblastic leukemia depends on response to salvage chemotherapy, prognostic factors, and performance of stem cell transplantation. *Blood.* 2012;120(10):2032-2041.
 20. Desjonquères A, Chevallier P, Thomas X, et al. Acute lymphoblastic leukemia relapsing after first-line pediatric-inspired therapy: a retrospective GRAALL study. *Blood Cancer J.* 2016;6(12):e504.
 21. Dourthe M-E, Rabian F, Yakouben K, et al. Determinants of CD19-positive vs CD19-negative relapse after tisagenlecleucel for B-cell acute lymphoblastic leukemia. *Leukemia.* 2021;35(12):3383-3393.
 22. Pillai V, Muralidharan K, Meng W, et al. CAR T-cell therapy is effective for CD19-dim B-lymphoblastic leukemia but is impacted by prior blinatumomab therapy. *Blood Adv.* 2019;3(22):3539-3549.
 23. Locatelli F, Zugmaier G, Rizzari C, et al. Effect of blinatumomab vs chemotherapy on event-free survival among children with high-risk first-relapse B-cell acute lymphoblastic leukemia: a randomized clinical trial. *JAMA.* 2021;325(9):843-854.
 24. Brown PA, Ji L, Xu X, et al. Effect of postreinduction therapy consolidation with blinatumomab vs chemotherapy on disease-free survival in children, adolescents, and young adults with first relapse of B-cell acute lymphoblastic leukemia: a randomized clinical trial. *JAMA.* 2021;325(9):833-842.
 25. Dombret H, Topp MS, Schuh AC, et al. Blinatumomab versus chemotherapy in first salvage or in later salvage for B-cell precursor acute lymphoblastic leukemia. *Leuk Lymphoma.* 2019;60(9):2214-2222.
 26. Jabbour EJ, Sasaki K, Ravandi F, et al. Inotuzumab ozogamicin in combination with low-intensity chemotherapy (mini-HCVD) with or without blinatumomab versus standard intensive chemotherapy (HCVD) as frontline therapy for older patients with Philadelphia chromosome-negative acute lymphoblastic leukemia: a propensity score analysis. *Cancer.* 2019;125(15):2579-2586.
 27. Jabbour E, Sasaki K, Short NJ, et al. Long-term follow-up of salvage therapy using a combination of inotuzumab ozogamicin and mini-hyper-CVD with or without blinatumomab in relapsed/refractory Philadelphia chromosome-negative acute lymphoblastic leukemia. *Cancer.* 2021;127(12):2025-2038.
 28. Bassan R, Chiaretti S, Della Starza I, et al. Preliminary results of the GIMEMA LAL2317 sequential chemotherapy-blinatumomab front-line trial for newly diagnosed adult Ph-negative B-lineage ALL patients. *Hemasphere.* 2021;5(S2):8.
 29. Boissel N, Huguet F, Graux C, et al. Frontline consolidation with blinatumomab for high-risk Philadelphia-negative acute lymphoblastic adult patients. Early results from the Graall-2014-QUEST phase 2. *Blood.* 2021;138(Suppl 1):S1232.

Syndromes predisposing to leukemia are a major cause of inherited cytopenias in children

Oded Gilad,^{1,2} Orly Dgany,³ Sharon Noy-Lotan,³ Tanya Krasnov,³ Joanne Yacobovich,^{1,2} Ron Rabinowicz,^{1,2} Tracie Goldberg,¹ Amir A. Kuperman,^{4,5} Abed Abu-Quider,⁶ Hagit Miskin,^{7,8} Noa Kapelushnik,^{2,9} Noa Mandel-Shorer,^{10,11} Shai Shimony,^{2,12,13} Dan Harlev,¹⁴ Tal Ben-Ami,^{8,15} Etai Adam,¹⁶ Carina Levin,^{11,17} Shraga Aviner,¹⁸ Ronit Elhasid,^{2,19} Sivan Berger-Achituv,^{2,19} Lilach Chaitman-Yerushalmi,²⁰ Yona Kodman,¹ Nino Oniashvili,¹ Michal Hameiri-Grosman,¹ Shai Izraeli,^{1,2} Hannah Tamary^{1,2,3} and Orna Steinberg-Shemer^{1,2,3}

¹Department of Hematology-Oncology, Schneider Children's Medical Center of Israel, Petach Tikva, Israel; ²Sackler Faculty of Medicine, Tel Aviv University, Tel Aviv, Israel; ³Pediatric Hematology Laboratory, Felsenstein Medical Research Center, Petach Tikva, Israel; ⁴Blood Coagulation Service and Pediatric Hematology Clinic, Galilee Medical Center, Nahariya, Israel; ⁵Azrieli Faculty of Medicine, Bar-Ilan University, Safed, Israel; ⁶Pediatric Hematology, Soroka University Medical Center, Ben-Gurion University, Beer Sheva, Israel; ⁷Pediatric Hematology Unit, Shaare Zedek Medical Center, Jerusalem, Israel; ⁸Faculty of Medicine, Hebrew University, Jerusalem, Israel; ⁹Goldschleger Eye Institute, Sheba Medical Center, Tel Hashomer, Israel; ¹⁰Department of Pediatric Hematology-Oncology, Ruth Rappaport Children's Hospital, Rambam Healthcare Campus, Haifa, Israel; ¹¹Rappaport Faculty of Medicine, Technion-Institute of Technology, Haifa, Israel; ¹²Rabin Medical Center, Institute of Hematology, Davidoff Cancer Center, Beilinson Hospital, Petach-Tikva, Israel; ¹³Department of Medical Oncology, Dana-Farber Cancer Institute, Boston, MA, USA; ¹⁴Pediatric Hematology-Oncology Department, Hadassah University Medical Center, Jerusalem, Israel; ¹⁵Pediatric Hematology Unit, Kaplan Medical Center, Rehovot, Israel; ¹⁶Pediatric Hematology-Oncology Department, Sheba Medical Center, Tel Hashomer, Israel; ¹⁷Pediatric Hematology Unit and Research Laboratory, Emek Medical Center, Afula, Israel; ¹⁸Department of Pediatrics, Barzilai University Medical Center, Ashkelon, affiliated to Ben Gurion University, Beer-Sheva, Israel; ¹⁹Department of Pediatric Hemato-Oncology, Tel Aviv Medical Center Tel Aviv, Israel and ²⁰Genoox, Health Care Technology, Tel Aviv, Israel.

Correspondence: H. Tamary
htamary@tauex.tau.ac.il

Received: September 30, 2021.

Accepted: March 10, 2022.

Prepublished: March 17, 2022.

<https://doi.org/10.3324/haematol.2021.280116>

©2022 Ferrata Storti Foundation

Published under a CC BY-NC license



Abstract

Prolonged cytopenias are a non-specific sign with a wide differential diagnosis. Among inherited disorders, cytopenias predisposing to leukemia require a timely and accurate diagnosis to ensure appropriate medical management, including adequate monitoring and stem cell transplantation prior to the development of leukemia. We aimed to define the types and prevalences of the genetic causes leading to persistent cytopenias in children. The study comprises children with persistent cytopenias, myelodysplastic syndrome, aplastic anemia, or suspected inherited bone marrow failure syndromes, who were referred for genetic evaluation from all pediatric hematology centers in Israel during 2016-2019. For variant detection, we used Sanger sequencing of commonly mutated genes and a custom-made targeted next-generation sequencing panel covering 226 genes known to be mutated in inherited cytopenias; the minority subsequently underwent whole exome sequencing. In total, 189 children with persistent cytopenias underwent a genetic evaluation. Pathogenic and likely pathogenic variants were identified in 59 patients (31.2%), including 47 with leukemia predisposing syndromes. Most of the latter (32, 68.1%) had inherited bone marrow failure syndromes, nine (19.1%) had inherited thrombocytopenia predisposing to leukemia, and three each (6.4%) had predisposition to myelodysplastic syndrome or congenital neutropenia. Twelve patients had cytopenias with no known leukemia predisposition, including nine children with inherited thrombocytopenia and three with congenital neutropenia. In summary, almost one third of 189 children referred with persistent cytopenias had an underlying inherited disorder; 79.7% of whom had a germline predisposition to leukemia. Precise diagnosis of children with cytopenias should direct follow-up and management programs and may positively impact disease outcome.

Introduction

Prolonged cytopenias are a non-specific sign with a wide

differential diagnosis, including acquired and inherited disorders.¹⁻² Among inherited disorders, predisposition to leukemia has recently emerged as an important clinical

entity with immediate implications for follow-up and management programs of patients and their family members.³ The clinical presentation of syndromes predisposing to leukemia is variable, and may include isolated thrombocytopenia, neutropenia, anemia or pancytopenia, with or without bone marrow failure. Diagnosing such syndromes before the emergence of leukemia is essential for proper treatment and cure.

Classical inherited bone marrow failure syndromes (IBMFS) are well recognized as predisposing to myeloid malignancies.^{4,5} Non-classical IBMFS with pathogenic variants in an increasing number of genes has been profusely described.⁶ IBMFS differ in their extra-hematopoietic congenital anomalies, the age of onset of BMF, and the risk and age of developing myelodysplastic syndrome (MDS) and acute myeloid leukemia (AML). Refractory cytopenia of childhood (RCC) is the most common form of MDS in children.⁷ In contrast to MDS in adults, pediatric MDS is more commonly associated with genetic predisposition.⁸ Genetic alterations in *GATA2* and *SAMD9L* have emerged as the most common cause of inherited pediatric MDS.⁹ Familial platelet disorder, associated with MDS and leukemia, was first described in 1999, with the identification of deleterious heterozygous *RUNX1* variants in families with inherited thrombocytopenia (IT) and AML.¹⁰ Later, additional genes causing thrombocytopenia and a predisposition to MDS/AML were described, for example, *ETV6* and *ANKRD26*.¹¹ *RUNX1* and *ETV6* variants also predispose to lymphocytic malignancies.¹² The presentation of IT in individuals with a predisposition to MDS may include isolated mild to moderate thrombocytopenia, and normal platelet size and morphology; and thus overlaps with classical IT.^{9,13}

An accurate diagnosis of inherited syndromes with a predisposition to leukemia has major therapeutic implications, including intensive follow-up of patients; this may entail an annual bone marrow examination.¹⁴ The diagnosis is also crucial for determining the management program, including decisions regarding hematopoietic stem cell transplantation (HSCT) prior to the development of acute leukemia, and for selecting the appropriate conditioning for transplant. In addition, accurate molecular diagnosis is essential for identifying asymptomatic family members who may be at risk for myeloid transformation, for providing genetic counseling to affected patients and family members, and for selecting unaffected related donors for transplantation.

Genetic workup may be initiated with Sanger sequencing, when a single gene is the major cause of a particular disorder. However, due to the non-specific clinical and laboratory presentation of syndromes causing cytopenias, an unbiased diagnosis, as offered by next-generation sequencing (NGS) technologies, is usually essential.^{11,15,16} Indeed, several studies have demonstrated advantages of

NGS technologies for improving diagnosis,^{11,13,15-18} and reported genetic diagnostic rates of 13-54%. However, differences were evident in the patient populations (IBMFS only, MDS only, IT only or all these conditions), age (children, adults or both), sequencing method (NGS panel or whole exome sequencing [WES]), the type of variants detected (germline variants or both somatic and germline variants) and the types of sequence variants reported (pathogenic and likely pathogenic [P/LP]) only or also variants of unknown significance [VOUS]). Therefore, comparing the results of those studies is challenging.

We hypothesized that a substantial fraction of children with persistent cytopenias may have inherited syndromes predisposing to MDS/AML and should be identified prior to the development of leukemia. We hereby present the results of a comprehensive Israeli nationwide study of germline variants detected in children with prolonged cytopenias, referred to our laboratory during a 4-year period. Only P/LP sequence changes were reported. Our study revealed that almost one third of the children had identifiable inherited disorders, of whom 79.7% predisposed to leukemia. Based on our findings, we suggest that children and young adults presenting with prolonged cytopenias should undergo genetic evaluation.

Methods

Patients

The study included children and adolescents (aged 0-20 years at presentation) with prolonged cytopenias, evaluated between January 2016 and December 2019. The patients were classified into five subgroups according to referral diagnoses: (i) suspected IBMFS, based on the presence of extra-hematopoietic manifestations and early onset cytopenias; (ii) MDS with BM dysplasia and less than 20% blasts or BM cytogenetic abnormality;^{7,8,19} (iii) severe aplastic anemia (SAA), based on an abrupt onset of severe pancytopenia and marrow aplasia;²⁰ (iv) a refractory single cytopenia including thrombocytopenia (platelet count $<150 \times 10^9/L$) or neutropenia (absolute neutrophil count $<1 \times 10^9/L$ up to 1 year of age or $<1.5 \times 10^9/L$ in older children and adults).²¹ Exclusion criteria were hemolytic and microcytic anemias, overt leukemia, and a known pathogenic variant in the family.

Data extracted from medical charts included age at presentation, current age, ethnic origin, family history, extra-hematopoietic manifestations, and therapy. The laboratory data recorded comprised complete blood counts, hemoglobin electrophoresis, fluorescent *in situ* hybridization (FISH) telomere length, chromosomal breakage tests and BM morphology, cellularity (based on trephine biopsies in the majority of patients), cytogenetics and FISH-MDS panels for detecting common chromosomal changes.²²

The study was approved by the Rabin Medical Center Institutional Review Board.

Sanger sequencing

We initiated the genetic workup by Sanger sequencing in patients with a clear clinical presentation and when variants in a single gene were a common cause of the specific suspected diagnosis. This approach included the genes *FANCA* for Fanconi anemia (FA), *ELANE* for severe congenital neutropenia (SCN), *RPS19* for Diamond Blackfan anemia (DBA), *SBDS* for Shwachman Bodian Diamond syndrome (SBDS) and *DKC1* for dyskeratosis congenita (DC). Sanger sequencing was also used to confirm NGS findings and family segregation.

Next-generation sequencing

Our custom-made NGS panel is continuously updated. The latest version included 226 known genes that cause inherited cytopenias (*Online Supplementary Table S1*). Importantly, the panel includes the *TERC* gene encoding for the RNA component of the telomerase, the non-coding 5'UTR regions of *DKC1* and *ANKRD26*, and intron 5 of *GATA2*, in which disease-causing variants have been described.²³ Panel design, library preparation and sequencing were performed as previously described.²⁴ The DNA used for genetic analysis was extracted from peripheral blood. Germline variants were identified by the variant allele frequency. In patients for whom it was uncertain whether the variant was of a germline origin, we performed Sanger sequencing on DNA extracted from fibroblasts.

Whole exome sequencing

WES was performed as described in Goldberg et al.²⁵

Sequencing results and bioinformatics pipeline

Sequencing reads were aligned against a reference genome (GRCh37/UCSC hg19) and variants were called and annotated using the SureCall software (v.3.5.1.46; Agilent Technologies). SNP filtering was established as previously described,²⁴ using both an in-house platform and the Emedgene AI-based genomic analysis platform (Emedgene Technologies, Tel-Aviv, Israel). Genetic variants were reported according to the American College of Medical Genetics guidelines.^{26,27} Only P/PL results were reported.

Copy number variant detection

Copy number variant (CNV) analysis was performed using "Rainbow"-Genoox CNV Caller. The Rainbow caller employs a machine-learning based anomaly detection algorithm, in which variants are determined based on exon-level coverage, using a cohort of samples (n>30). The model considers several factors including GC content, coverage variance over multiple samples and neighboring gene coverage (Genoox, Tel-Aviv, Israel). CNV findings were confirmed by multiplex ligation-dependent probe amplification (MLPA, MRC, Amsterdam, Holland) available for: *FANCA*, *RPS19*, *RPL5*, *RPS26*, *RPL11*, *RPS17*, *RPL35A*, *TERT* and *DKC1* and by cytoscan-high density SNP-array.²⁸

Statistical analysis

Fisher exact test was used to compare the clinical and demographic characteristics between patients who were and were not diagnosed with inherited disorders. A *P*-value of <0.05 was considered statistically significant.

Table 1. Referrals and genetic diagnoses in our cohort.

Referral diagnosis	N of pts	N of genetically diagnosed pts (%)	Diagnosis according to molecular findings (N of pts)
IBMFS	48	29 (60.4)	IBMFS (29)
MDS	26	6 (23.1)	MDS predisposition (3)
			IBMFS (2)
			IT with MDS predisposition (1)
SAA	31	1 (3.2)	IBMFS (1)
Isolated thrombocytopenia	33	17 (51.5)	Classical IT (9)
			IT with MDS predisposition (8)
Isolated neutropenia	51	6 (11.8)	Congenital neutropenia (6)
Total	189	59 (31.2)	

IBMFS: inherited bone marrow failure syndromes; IT: inherited thrombocytopenia; MDS: myelodysplastic syndrome; SAA: severe aplastic anemia; No: number; pts: patients.

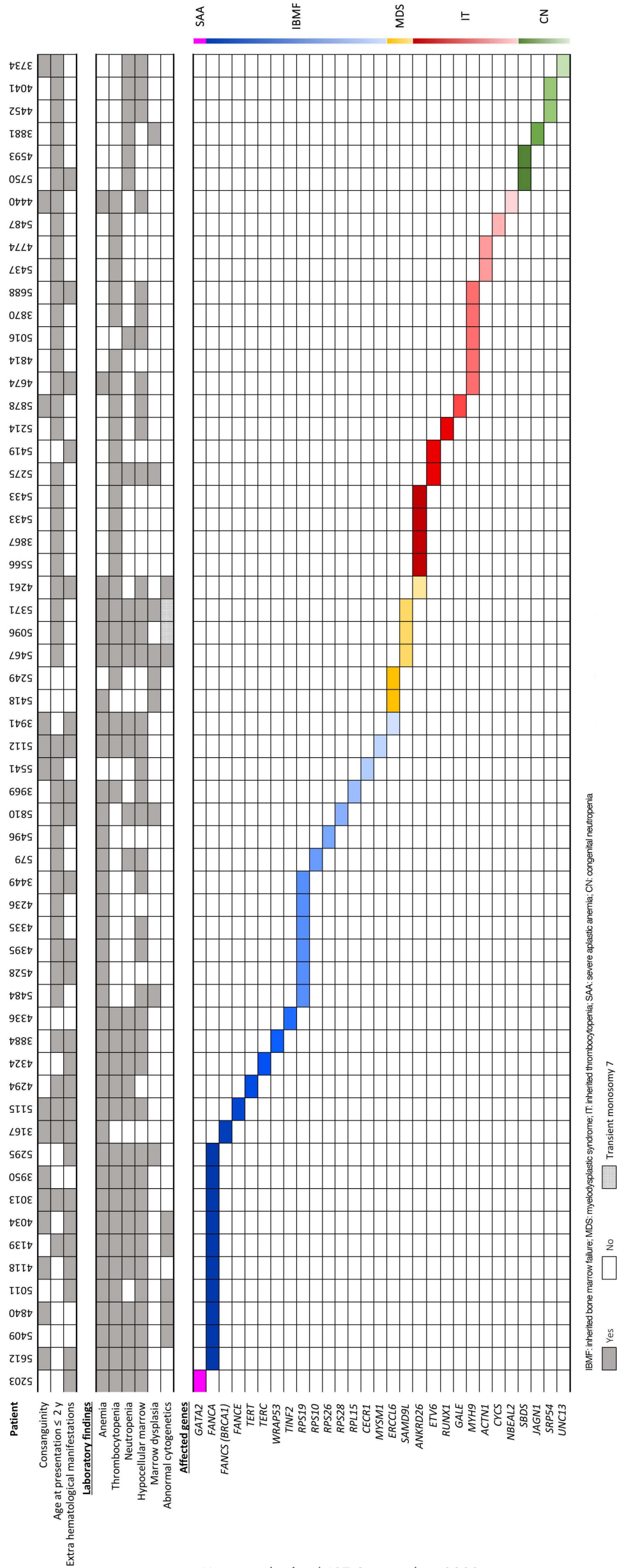


Figure 1. Integrated matrix of the 59 patients diagnosed with inherited cytopenias. The upper part of the panel shows demographic, clinical and laboratory details of our patients; the lower part shows the affected genes. Genes are ordered according to the diagnoses. The column on the right and the box colors relate to the referral diagnoses, and demonstrate the overlapping phenotypes caused by some affected genes. IBMFs: inherited bone marrow failure syndromes; MDS: myelodysplastic syndrome; SAA: severe aplastic anemia; CN: congenital neutropenia.

Results

Clinical diagnosis

During the study period, 189 DNA samples of children presenting with persistent cytopenias from twelve pediatric hematology centers in Israel were sent to the Molecular Hematology Laboratory in Schneider Children's Medical Center of Israel. The clinical referral diagnosis, defined by the treating hematologists, was IBMFS (48 patients), MDS (26 patients), SAA (31 patients), isolated neutropenia (51 patients) and isolated thrombocytopenia (33 patients) (Table 1).

Most patients were Israelis (96%). Eighty-seven (46%) of our patients were of non-Jewish origin, mainly Arabic, which is considerably higher than their proportion in the Israeli population (26.1%).²⁹ Almost one-third of the patients originated from consanguineous families (*Online Supplementary Table S2*). The median age at clinical presentation was 1 year (range, 0-20) and the median age at referral was 8 years (range, 0.5-41). Patients were referred at a median of 5.8 years following their first clinical presentation.

Genetic diagnosis

Of the 189 children referred for genetic evaluation, 49 had a clinical presentation suggestive of a specific diagnosis and, therefore, Sanger sequencing of commonly mutated genes was initially performed (*Online Supplementary Figure S1*). Diagnosis was reached for 13 (6 were homozygous for *FANCA* variants, 5 had heterozygous variants in *RPS19* and 2 were compound heterozygous for variants in the *SBDS* gene). Fourteen patients with a negative Sanger sequencing result were further evaluated using our NGS panel and 22 did not undergo further genetic workup (11 recovered, 6 are clinically stable and are being followed, 4 underwent successful HSCT and one was lost to follow-up). In total, 140 patients were initially directly referred for NGS panel diagnosis (*Online Supplementary Figure S1*).

Overall, P/LP variants were identified in 59 of 189 patients (31.2%). Of the diagnosed patients, 47 (24.9% of the whole cohort and 79.7% of the diagnosed patients) had an inherited predisposition to leukemia, while nine had IT affecting platelet production and function, and three had congenital neutropenia not currently known to cause leukemia predisposition (Figure 1; Tables 2 to 7; *Online Supplementary Table S3*). Eleven sequence variants, in ten patients, were defined as VOUS; these patients are not included in the analyses (*Online Supplementary Table S4*). In addition, 12 patients with a clinical and genetic diagnosis compatible with benign ethnic neutropenia were not included in the analyses.

Overall, 28.6% of the patients had congenital anomalies, with a statistically significant higher proportion among patients that were genetically diagnosed (39% and 23.8% in

diagnosed and undiagnosed patients, respectively; *P*-value =0.038, *Online Supplementary Table S2*).

Patients presenting with inherited bone marrow failure syndromes

Of 48 patients who were referred with IBMFS, five had increased chromosomal breakage and three had short telomeres (Table 2; Table 3). In 29 of 48 (60.4%) patients, genetic variants explaining the clinical phenotype were found; of those, 27 had classical and two had non-classical IBMFS. Twelve patients were diagnosed with FA: ten were homozygous for *FANCA* variants, one had a homozygous *FANCS* (*BRCA1*) variant and one had a *FANCE* variant. Ten patients were diagnosed with DBA: six had heterozygous variant in *RPS19*, and one each had a heterozygous variant in the genes *RPS10*, *RPS15*, *RPS26* and *RPS28*. One additional patient carried a homozygous variant in the *CECR1* gene, which caused a DBA-like phenotype. Four patients with DC had genetic alterations in the *TERT*, *TERC*, *WRAP53* and *TINF2* genes. Two patients had non-classical IBMFS, with homozygous variants in the *ERCC6L2* and *MYSM1* genes (Figure 1; Table 3; *Online Supplementary Table S3*). Both were of consanguineous Arab families. The patient with the biallelic *ERCC6L2* variant also had congenital anomalies and developmental delay. The patient with a *MYSM1* homozygous variant had early onset pancytopenia, with a hypocellular marrow and a paucity of red cell precursors and mild developmental delay and short stature. This phenotype was similar to that previously described for a few individuals.^{30,31}

Patients presenting with myelodysplastic syndrome

Twenty-six patients in this study had MDS, including 19 with RCC and seven with MDS and excess blasts (MDS-EB). Germline disease-causing variants were found in six of the 19 patients with RCC (31.6%). Three patients had variants in the *SAMD9L* gene, two in *ERCC6L2* and one in *ANKRD26* (Figure 1; Table 4; *Online Supplementary Table S3*). No germline pathogenic variants were detected in the seven patients presenting with MDS-EB. All three patients diagnosed with *SAMD9L* variants had monosomy 7, which was subsequently resolved in two (7 months and 4 years later) (Figure 1). The two patients with biallelic variants in *ERCC6L2* originated in consanguineous Arab families with no known relatives with MDS. Both were referred with pancytopenia and had BM dysplastic changes.

One child presented with a variant in the initiation codon of *ANKRD26*. He was born at term following a normal pregnancy, with a low birth weight (1.9 kg), a single umbilical artery and dysmorphic features. He had severe recurrent infections including *Pneumocystis Jiroveci* and *Cytomegalovirus* lung infections. Rechavi et al.³² extensively studied this patient, who is now 8 years old, and found a mosaic monosomy 21, as well as defects in immunoglobulin

Table 2. Clinical characteristics of patients referred with the diagnosis of inherited bone marrow failure syndrome (diagnosed by Sanger sequencing).

Patient	Ethnic origin/ Consanguinity (+/-)	Gene	Disease/ Inheritance	MHGVS Coding	Age at presentation/ diagnosis	Hematological presentation	BM, cytogenetics and functional tests	Extra hematological manifestations	Outcome
4118	Arab Muslim (+)	FANCA	FA/AR	NM_000135: c.3490C>T-Hm	6y/6y	Pancytopenia	Hypocellular marrow, re- duced megakaryocytes	Short stature, café au lait spots, pelvic kidneys	Post HSCT
4139	Arab Christian (-)	FANCA	FA/AR	NM_000135: c.4261-2A>C- Hm	1-7d/25y	Pancytopenia	Hypocellular marrow	Short stature, dysmorphic features	Post HSCT
4034	Arab Muslim (+)	FANCA	FA/AR	NM_000135.4): c.3382C>T-Hm	5y/5y	Pancytopenia	Hypocellular marrow, tri- somy 1q, increased chro- mosomal breakage	Short stature, dysmorphic features	Followup
3013	Jewish (+)	FANCA	FA/AR	NM_000135.4: c.3788_3790delTCT- Hm	2y/4.5y	Pancytopenia	Aplastic marrow	Short stature, dysmor- phic features, café au lait spots, skeletal anomalies	Died of SCC, post HSCT
3950	Arab Muslim (+)	FANCA	FA/AR	NM_000135.4: c.3788_3790delTCT- Hm	10y/10y	Pancytopenia	Hypocellular marrow, in- creased chromosomal breakage	None	Post HSCT
5295	Jewish (-)	FANCA	FA/AR	NM_000135.4: c.2172dupG- Hm	11y/15y	Pancytopenia	Hypocellular marrow, dyserythropoiesis, increased chromosomal breakage	Short stature, schizophrenia	Post HSCT
4528	Jewish (-)	RPS19	DBA/AD	NM_001022.3: c.98G>A-Ht	1-7d/0.9y	Anemia	Not done	Short stature	Followup
4337	Jewish (-)	RPS19	DBA/AD	NM_001022.4): c.184C>T-Ht	8-28d/0.5y	Anemia	Early erythroid matura- tion arrest	Short stature	Followup
4335	Other (-)	RPS19	DBA/AD	NM_001022.4): c.184C>T-Ht	1-7d/3y	Anemia	Hypocellular marrow, pure red cell aplasia	None	Followup
4236	Jewish (-)	RPS19	DBA/AD	NM_001022.3: c.98G>A-Ht	0.2y/16y	Anemia	Not done	None	Followup
3449	Jewish (-)	RPS19	DBA/AD	NM_001022.3: c.134T>C-Ht	8-28d/0.9y	Anemia	Hypocellular marrow, early erythroid maturation arrest	Short stature, hearing defect	Followup

BM: bone marrow; BMF: bone marrow failure; AR: autosomal recessive; AD: autosomal dominant; y: years; d: days; FA: Fanconi anemia; DBA: Diamond-Blackfan anemia; SCC: squamous cell carcinoma; Ht: heterozygous; Hm homozygous; HSCT: hematopoietic stem cell transplantation.

switching. Thrombocytopenia was noted at birth. When referred to a pediatric hematology center (at age 6 years) he had macrocytosis (MCV 98fL), thrombocytopenia ($48 \times 10^9/L$), substantially high fetal hemoglobin (30%) and a hypoplastic BM with dysplastic changes.

Patients presenting with thrombocytopenia

Thirty-three patients presented with thrombocytopenia and an inherited cause was found in 17 (51.5%). Of them, nine (52.9%) had IT that was known to affect platelet production and function and eight (47.1%) had variants in genes that were known to cause thrombocytopenia with a predisposition to leukemia (Figure 1; Table 5; *Online Supplementary Table S3*). Of the nine patients with IT due to platelet production or function defects, five had variants in the *MYH9* gene, two in *ACTN1* and one each in *NBEAL2* and *CYCS*. Their thrombocytopenia ranged from mild to severe ($7-125 \times 10^9/L$), with a normal to high MPV, 8-17.7 fL (normal values 5.6-12.1 fL³³). Of the eight patients with thrombocytopenia and an inherited predisposition to MDS/AML, four had variants in the 5'UTR of *ANKRD26*, 2 in *ETV6*, 1 in *RUNX1* and one in the *GALE* gene. Seven patients had mild to moderate thrombocytopenia ($45-117 \times 10^9/L$), with a normal MPV, 8.5-12 fL (normal values 5.6-12.1 fL³³). The patient diagnosed with a variant in *GALE* had giant and pale platelets (MPV 17 fL), as we previously described.³⁴ He was of Bedouin origin and not related to the original family we described.

Patients presenting with neutropenia

Of the 51 patients presenting with neutropenia 6 (11.8%) were molecularly diagnosed (Figure 1; Table 6; *Online Supplementary Table S3*). Two patients had compound heterozygous variants in the *SBDS* gene. One had a homozygous variant in a known neutropenia causing gene, *JAGN1*³⁵. One additional patient, presenting with familial neutropenia and recurrent infections, was subsequently diagnosed by WES with a novel SRP54 variant causing SCN and SBDS.^{25,36} This gene was not known to cause neutropenia at the time the NGS study was performed. We later incorporated this gene into the subsequent versions of our NGS panel and detected a variant in this gene in one more patient that had a re-do of the NGS panel. An additional patient who presented with isolated neutropenia was later diagnosed by WES with a homozygous variant in *UNC13D*.

Twelve patients in our neutropenia group (8 patients of Muslim Arab origin and 4 of Yemenite Jewish origin), were homozygous to the known polymorphism in the *DARK* promoter (rs2814778, -30 T>C)³⁷. They all had absolute neutrophil counts (ANC) $>0.5 \times 10^9/L$ ($0.6-0.76 \times 10^9/L$) and no recurrent infections, compatible with the diagnosis of benign ethnic neutropenia. This same polymorphism was also found in one additional patient of Arabic origin, who

presented with severe neutropenia (ANC levels $<0.2 \times 10^9/L$) and recurrent infections, and therefore underwent HSCT. His phenotype suggests the presence of a yet undiscovered gene causing congenital neutropenia; the patient underwent successful HSCT.

Patients referred with suspected severe acquired aplastic anemia

Thirty-one patients with suspected SAA were referred to rule out IBMFS or other MDS predisposing syndromes. A pathogenic variant in the *GATA2* gene was found in one patient (3.2%) and his diagnosis was amended to IBMFS (Figure 1; Table 7; *Online Supplementary Table S3*). This patient had mild to moderate neutropenia ($0.6-1.2 \times 10^9/L$) 2 years prior to the diagnosis of SAA. He had normal baseline monocyte counts, which were reduced to 0.02-0.2 K/micL, together with the development of neutropenia.

Discussion

In this paper, we presented the results of the genetic diagnosis of 189 children with prolonged cytopenias. P/LP germline variants were identified in 59 children (31.2%). Most of the diagnosed children (47/59, 79.7%) with persistent cytopenias had leukemia predisposition, while 12 children (20.3%) had either congenital thrombocytopenia with impairment of platelet production (9 children) or congenital neutropenia not currently known to predispose to malignant transformation (3 children).

In most children referred for genetic evaluation of cytopenias, NGS diagnosis was performed upfront. In the minority, when the clinical picture suggested a known disorder commonly caused by variants in a single gene, we initiated the genetic workup with Sanger sequencing. Of the various NGS methods, we used NGS panels as they offer a uniformly high depth of sequencing of the genes of interest. An advantage of our panel is that it was designed also to include non-protein coding regions such as the 5'UTR of *ANKRD26* and *DKC1*; the RNA component of the telomerase, encoded by the *TERC* gene; and intronic regions in *GATA2*. We report only P/LP sequence changes. The drawback of the NGS panel method is that the time lag between the identification of a new gene and its insertion into the panel requires frequent panel updating. We modified our panel seven times during the 4-year study period. All children referred for a molecular workup had a provisional diagnosis determined by their treating hematologist. For most patients, the genetic diagnosis supported the referral diagnosis. One patient with suspected SAA, who was evaluated to rule out an inherited disorder, was indeed diagnosed with a germline *GATA2* variant; this changed the diagnosis to IBMFS. Three patients had pathogenic variants in the *ERCC6L* gene; two of them were

Table 3. Clinical characteristics of patients referred with the diagnosis of inherited bone marrow failure syndrome (diagnosed with next generation sequencing panel).

Patient	Ethnic origin/ Consanguinity (+/-)	Gene	Disease/ Inheritance	MHGVS Coding	Age at presentation/ diagnosis	Hematological presentation	BM, cytogenetics and functional tests	Extra hematological manifestations	Outcome
5612	Arab Muslim (+)	FANCA	FA/AR	NM_000135.4: c.3749_3750insT-Hm	7y/8y	Pancytopenia	Hypoplastic marrow, increased chromosomal breakage	Short stature, café au lait spots	Followup
5409	Jewish (-)	FANCA	FA/AR	1. NM_000135.2: c.2172-2173 insG-Ht 2. NM_000135.4: c.891_893+1delCTGG-Ht	6y/6y	Pancytopenia	Hypoplastic marrow, monosomy 7, increased chromosomal breakage	None	Post HSCT
4840	Arab Muslim (+)	FANCA	FA/AR	NM_000135.2: c.4069_4070insT-Hm	6y/7y	Pancytopenia	Hypoplastic marrow, del7q	Short stature	Lost to followup
5011	Yazidi (+)	FANCA	FA/AR	NM_000135.2: c.1361_1374delinsGAG -Hm	4y/14y	Neutropenia, thrombocytopenia	Severe aplastic marrow, complex karyotype	Café au lait spots	Lost to followup
3167	Arab Muslim (+)	FANCS (BRCA1)	FA/AR	NM_007300.4: c.1115G>A - Hm	1-7d/4y	Anemia	Normal	Café au lait spots, short stature, dysmorphism, developmental delay	Followup
5115	Arab Muslim (+)	FANCE	FA/AR	NM_021922.2: c.1114-8G>A -Hm	1y/10y	Pancytopenia	Aplastic marrow	Café au lait spots, short stature	Post 2nd HSCT
4294	Jewish (-)	TERT	DC/AD	NM_198253.3: c.2834_2842delACTACTCCA insCACCT-Ht	1-7d/30y	Pancytopenia	Red cell hyperplasia	Short stature, splenomegaly	Followup
4324	Arab Muslim (-)	TERC	DC/AD	NR_001566: r.172A>G -Ht	4y/8y	Pancytopenia	Hypoplastic marrow, short telomeres	Café au lait spots, short stature	Post HSCT
3884	Jewish (-)	WRAP53	DC/AR	NM_001143990.1: c.936c>G-Hm	1-7d/4y	Pancytopenia	Hypocellular marrow, short telomeres	Short stature	Followup

Continued on following page.

Patient	Ethnic origin/ Consanguinity (+/-)	Gene	Disease/ Inheritance	MHGVS Coding	Age at presentation/ diagnosis	Hematological presentation	BM, cytogenetics and functional tests	Extra hematological manifestations	Outcome
4336	Arab Muslim (-)	<i>TINF2</i>	DC/AD	NM_001099274.3: c.813dupA-Ht	4y/5y	Pancytopenia	Hypoplastic marrow, short telomeres	None	Lost to followup
5484	Jewish (-)	<i>RPS19</i>	DBA/AD	NM_001022.4: c.384_385delAA -Ht	1-7d/2.5y	Anemia	Hypoplastic and mild red cell dysplasia	None	Followup
579	Jewish (-)	<i>RPS10</i>	DBA/AD	NM_001202470.2: c.71A>G-Ht	8-28d/30y	Anemia	Aplastic marrow	None	Post HSCT
5496	Arab Muslim (-)	<i>RPS26</i>	DBA/AD	NM_001029.5: c.23delA-Ht	8-28d/41y	Anemia	Not done	None	Followup
5810	Arab Muslim (-)	<i>RPS28</i>	DBA/AD	NM_001031.4: c.2T>C -Ht	1-7d/2y	Anemia, neutropenia	Mild dysplastic red cell precursors	None	Followup
3969	Jewish (-)	<i>RPL15</i>	DBA/AD	NM_001253379.2: c.29T>C - Ht	1-7d/0.4y	Anemia	Pure red aplasia	Preterm 27 weeks	Followup
5541	Arab Christian (+)	<i>CECR1</i>	DBA-like/ AR	NM_001282225.1: c.1397_1403del-Hm	8-28d/20y	Anemia	Pure red aplasia	None	Followup
5112	Arab Muslim (+)	<i>MYSM1</i>	BMF/AR	NM_001085487.2: c.2329-2A>G-Hm	1-7d/1.2y	Pancytopenia	Hypocellular marrow	Dysmorphic features	Followup
3941	Druze (+)	<i>ERCC6L</i> 2	BMF/AR	NM_020207.4: c.3525+2T>G - Hm	7y/9y	Pancytopenia	Hypocellular marrow	Short stature, dysmorphic facies, café au lait spots, hearing loss, developmental delay, schizo- affective disorder	Followup

NGS: next generation sequencing; BM: bone marrow; BMF: bone marrow failure; AR: autosomal recessive; AD: autosomal dominant; y: years; d: days; FA: Fanconi anemia; DC: Dyskeratosis Congenita; DBA: Diamond-Blackfan anemia; Ht: heterozygous; Hm: homozygous; HSC: hematopoietic stem cell transplantation.

referred with MDS and one with a suspected IBMF. Similarly, of the five patients with variants in *ANKRD26*, four had isolated thrombocytopenia and one had MDS (Table 1; Figure 1). This emphasizes the variable phenotypic presentation of children with inherited cytopenias and supports an unbiased diagnostic approach.

Inherited bone marrow failure syndromes

Of the 48 patients referred for an NGS workup with a diagnosis of IBMFS, 60.4% were genetically diagnosed. All but two had classical IBMFS, including FA, DBA and DC (Figure 1; Table 2; Table 3; *Online Supplementary Table S3*). These results are similar to those obtained in recent studies, in which the diagnosis rate of IBMFS was 48-59%.^{38,39} The relatively high accurate referral diagnosis of patients with IBMFS is probably related to the classical clinical presentation, including typical congenital anomalies (in 70.8% of the patients in this group; *Online Supplementary Table S2*), as well as to the availability of functional screening tests for FA (chromosomal breakage

test) and DC (telomere length) that support the diagnosis.

Myelodysplastic syndromes

Of 26 children referred with MDS, based on cytopenias and BM morphology, with or without cytogenetic abnormalities, six (23.1%) were found to have germline variants: three in *SAMD9L*, two in *ERCC6L2* and one in *ANKRD26* (Figure 1; Table 4; *Online Supplementary Table S3*). Interestingly, although germline variants in *GATA2* are commonly found in pediatric patients with MDS,⁹ none of our patients referred with MDS had genetic alterations in this gene. Feurstein et al. recently found that 19% (13/68) of young adults with MDS/AML had sequence variants in leukemia predisposition genes,¹⁷ including in *GATA2*, *ERCC6L2*, *RUNX1*, *ANKRD26*, *CSF3R*, DC genes, *FANCA* and *PARN*. None of them had *SAMD9/L* variants; the latter have been commonly described in children with MDS.⁹ In our study, all pathogenic variants were found in patients with RCC, while none of the seven patients with MDS-EB car-

Table 4. Clinical characteristics of patients referred with a diagnosis of myelodysplastic syndrome.

Patient	Ethnic origin/ Consanguinity (+/-)	Gene	Disease/ Inheritance	MHGVS Coding	Age at presentation/ diagnosis	Hematological presentation	BM, cytogenetics and functional tests	Extra hematological manifestations	Outcome
5467	Jewish (-)	<i>SAMD9L</i>	MDS/AD	NM_152703: c.4736A>G-Ht	0.4y/0.8y	Pancytopenia	Hypocellular with myelodysplasia, monosomy 7	None	Followup
5096	Jewish (-)	<i>SAMD9L</i>	MDS/AD	NM_152703.4: c.4045C>G-Ht	0.9y/5.5y	Pancytopenia	Hypocellular mar- row, monosomy 7 -re- solved	None	Followup
5371	Eritrean (-)	<i>SAMD9L</i>	MDS/AD	NM_152703.2: c.2957G>A -Ht	1.2y/2y	Pancytopenia	Hypocellular, dysplastic megakaryocytes, monosomy 7 -re- solved	None	Followup
5418	Arab Muslim (+)	<i>ERCC6L2</i>	BMF/AR	NM_001010895.2: c.535A>G- Hm	20y/27y	Anemia, followed by pancytopenia	Dysplastic red cell precursors	None	Died of sepsis
5249	Druze (+)	<i>ERCC6L2</i>	BMF/AR	NM_020207.7: c.3492+2T>G Hm	16y/16y	Anemia, thrombocyto- penia	Hypercellular dysplasia	None	Died of sepsis
4261	Jewish (-)	<i>ANKRD 26</i>	IT-MDS/AD	NM_001256053.1: c.3G>A -Ht	1-7d/6y	Thrombocytope- nia	Hypocellular mar- row, monosomy 7, monosomy 21 (germline)	Short stature, mildly dysmorphic features, combined immune deficiency, bicuspid aortic valve	Followup

BM: bone marrow; BMF: bone marrow failure; IT: inherited thrombocytopenia; MDS: myelodysplastic syndrome; AR: autosomal recessive; AD: autosomal dominant; y: years; d: days; Ht: heterozygous; Hm: homozygous.

ried variants in known relevant genes. Similarly, of 43 patients with germline variants in *SAMD9/L* enrolled in the European Working Group of MDS in childhood (EWOG-MDS), 39 (91%) had RCC and only four (9%) had MDS-EB.⁴⁰ The reason for this observation is currently unclear. We observed phenotypic variability among the three patients with biallelic variants in *ERCC6L2*: one is a 7-year-old boy who presented with IBMFS and two patients, aged 16 and 20 years, presented with MDS. The *ERCC6L2* gene encodes for a transcription-coupled nucleotide excision

repair protein and when mutated, causes genomic instability and affects mitochondrial function, leading to increased levels of reactive oxygen species.³¹ Most patients described so far were children presenting with IBMFS.⁴¹ Bluteau et al. found *ERCC6L2* variants in seven (8%) of 86 patients diagnosed with IBMFS. However, two of these seven patients, both aged 22 years, had marrow dysplastic changes; and one patient developed AML at the age of 43 years.⁶ Poor prognosis AML-M6 was recently identified in adult members (aged 39-59 years) of four Finnish families,

Table 5. Clinical characteristics of patients referred with isolated thrombocytopenia.

Patient	Ethnic origin/Consanguinity (+/-)	Gene	Disease/Inheritance	MHGVS Coding	Age at diagnosis/presentation	Hematological presentation	BM, cytogenetics and functional tests	Extra hematological manifestations	Outcome
4674	Jewish (-)	<i>MYH9</i>	IT/AD	NM_002473.6: c.287C>T -Ht	8-28d/18y	Thrombocytopenia	Mild myeloid hypoplasia	Mental retardation, renal failure	Followup
4814	Jewish (-)	<i>MYH9</i>	IT/AD	NM_002473.5: c.4270G>A -Ht	1-7d/0.3y	Thrombocytopenia	Not done	None	Followup
5016	Arab Muslim (-)	<i>MYH9</i>	IT/AD	NM_002473.4: c.5797C>T -Ht	1-7d/5y	Thrombocytopenia	Reduced megakaryocytes	None	Followup
3870	Jewish (-)	<i>MYH9</i>	IT/AD	NM_002473.6: c.287C>T-Ht	1y/5y	Thrombocytopenia ("ITP")	Reduced megakaryocytes	None	Followup
5688	Jewish (-)	<i>MYH9</i>	IT/AD	NM_002473.5: c.4641G>T-Ht	0.9y/15y	Thrombocytopenia	Normal	None	Followup
5437	Jewish (-)	<i>ACTN1</i>	IT/AD	NM_001130004.1: c.1019C>T -Ht	1-7d/10.5y	Thrombocytopenia	Not done	None	Followup
4774	Jewish (-)	<i>ACTN1</i>	IT/AD	NM_001130004.1: c.1019C>T-Ht	8-28d/17y	Thrombocytopenia	Not done	None	Followup
5487	Arab Muslim (-)	<i>CYCS</i>	IT/AD	NM_018947.5: c.274A>G-Ht	0.5y/5y	Thrombocytopenia ("ITP")	Not done	None	Followup
4440	Arab Muslim (+)	<i>NBEAL2</i>	IT/AR	NM_015175.3: c.7225-1G>C-Hm	8-28d/4y	Thrombocytopenia	Reduced megakaryocytes	None	Followup
5566	Jewish (-)	<i>ANKRD26</i>	IT-MDS/AD	NM_001256053: c.-134G>A -Ht	8-28d/4y	Thrombocytopenia ("ITP")	Not done	None	Followup
3867	Jewish (-)	<i>ANKRD26</i>	IT-MDS/AD	NM_014915.2: c.-127A>G -Ht	8-28d/20y	Thrombocytopenia	Not done	None	Followup
3610	Jewish (-)	<i>ANKRD26</i>	IT-MDS/AD	NM_014915.3: c.-128G>T-Ht	8-28d/1.5y	Thrombocytopenia ("ITP")	Normal	None	Followup
5433	Jewish (-)	<i>ANKRD26</i>	IT-MDS/AD	NM_001256053: c.-134G>A -Ht	1-7d/1y	Thrombocytopenia	Not done	None	Followup
5275	Jewish (-)	<i>ETV6</i>	IT-MDS/AD	NM_001987.4: c.1103T>G -Ht	0.7d/18y	Thrombocytopenia ("ITP")	Hypocellular marrow	None	Followup
5419	Arab Muslim (-)	<i>ETV6</i>	IT-MDS/AD	NM_001987.4 c.1104C>G-Ht	5.5d/6y	Thrombocytopenia	Not done	Developmental delay, short stature	Followup
5214	Jewish (-)	<i>RUNX1</i>	IT-MDS/AD	NM_001001890.2: c.532+1_532+10del GTAAGTGCAT-Ht	8-28d/2.5y	Thrombocytopenia	Reduced megakaryocytes	None	Followup
5878	Arab Muslim (+)	<i>GALE</i>	IT-MDS/AR	NM_000403.3: c.151C>T -Hm	8-28d/1.5y	Thrombocytopenia	Not done	None	Followup

BM: bone marrow; IT: inherited thrombocytopenia; MDS: myelodysplastic syndrome; AR: autosomal recessive; AD: autosomal dominant; y: years; d: days; Ht: heterozygous; Hm: homozygous; ITP: immune thrombocytopenia.

with variants in *ERCC6L2*.⁴² Future studies will help elucidate the full natural history of this disorder.

Monoallelic nucleotide substitutions at the 5'UTR of the *ANKRD26* gene were found in 18% of the patients with IT and are the most common cause of IT with a predisposition to MDS/AML.^{11,43} These variants cause gain of function and disrupt the downregulation of the expression of *ANKRD26* by *RUNX1* and *FLI1*. This causes suppression of megakaryopoiesis, which leads to thrombocytopenia and to MDS/AML later in life.⁴⁴ We describe here an initiation codon variant in *ANKRD26* (c.3G>A), in an 8-year-old boy with mosaic monosomy 21 who presented with MDS. This variant was previously described in two adult patients with AML and was shown to cause *ANKRD26* overexpression as well.⁴⁵

Inherited thrombocytopenia

Of the 33 patients referred with thrombocytopenia, 17 (51.5%) had IT (Figure 1; Table 5; *Online Supplementary Table S3*). Of them, nine (27.3% of 33) had variants affecting late megakaryopoiesis and platelet production, without a predisposition to leukemia (in *MYH9*, *ACTN1*, *NBEAL2* and *CYCS*); while eight patients (24.2% of 33) had variants in genes encoding for growth factors involved in early megakaryopoiesis and a predisposition to leukemia (4 had variants in the 5'UTR of *ANKRD26*, 2 in *ETV6* and 1 in *RUNX1*; and 1 had a biallelic genetic alteration in *GALE*). Molecular

diagnosis of IT is essential, not only for identifying patients with a predisposition to leukemia but also for offering accurate diagnosis and avoiding the false diagnosis of immune thrombocytopenia (ITP), with possible subsequent futile treatment including splenectomy.^{46,47} Indeed, five of our IT patients (29.4%), diagnosed with *ANKRD26*, *ACTN1*, *ETV6*, *CYCS* and *MYH9* variants, were considered to have chronic ITP and were treated as such (Table 5). These results emphasize that persistence of mild to moderate thrombocytopenia from birth, and a lack of response to ITP therapy should alert physicians to suspect IT.

Congenital neutropenia

In six of 51 (11.8%) pediatric patients with a clinical and laboratory diagnosis of congenital neutropenia we detected variants explaining the clinical phenotype (Figure 1; Table 6; *Online Supplementary Table S3*). Two patients were diagnosed with SBDS; one patient was diagnosed with a *JAGN1* homozygous variant. Two other patients who had negative panel results were later diagnosed by WES, with variants in *SRP54* and in *UNC13D*, a rare cause of neutropenia.⁴⁸ Another patient was diagnosed with *SRP54* following its incorporation into the NGS panel.

Since benign ethnic neutropenia is not rare in our population, we subsequently looked for the known homozygous polymorphism in the *DARK* promoter (rs2814778, -30 T>C), which was previously described in people of African and

Table 6. Clinical characteristics of patients referred with isolated neutropenia.

Patient	Ethnic origin/Consanguinity (+/-)	Gene	Disease/Inheritance	MHGVS Coding	Age at presentation /diagnosis	Hematological presentation	BM, cytogenetics and functional tests	Extra hematological manifestations	Outcome
3881	Jewish (-)	<i>JAGN1</i> (CN)	CN/AR	NM_032492.3: c.3G>A -Hm	2y/20y	Neutropenia	Early myeloid maturation arrest	Recurrent infections	Followup
4452**	Jewish (-)	<i>SRP54</i>	CN/AD	NM_003136.3: c.349_351delIACA	2y/30y	Neutropenia	Hypoplastic marrow, early myeloid arrest	Recurrent Aphthae	Followup
4041	Arab Christian (-)	<i>SRP54</i>	CN/AD	NM_003136.3: c.349_351delIACA	8-28d/11y	Neutropenia	Late myeloid arrest	Recurrent infections	Followup
5750*	Jewish (-)	<i>SBDS</i>	SBDS/AR	1. NM_016038: c.183_184 delTAinsCT - Ht 2. NM_016038: c.258+2 t>c: splice - Ht	0.3y/1y	Neutropenia	Normal marrow, abnormal exocrine pancreatic functions	Short stature, shortened long bones, small kidneys	Followup
4593*	Jewish (-)	<i>SBDS</i>	SBDS/AR	1. NM_016038: c.183_184 delTAinsCT - Ht 2. NM_016038: c.258+2 t>c: splice - Ht	0.2y/1.5y	Neutropenia	Normal	Short stature	Followup
3734**	Arab Muslim (+)	<i>UNC13</i>	CN/AD	NM_199242.2: c.679C>T- Hm	8-28d/2.4y	Neutropenia, later pancytopenia	Hypocellular marrow	None	Post HSCT

BM: bone marrow; CN: congenital neutropenia; AR: autosomal recessive; AD: autosomal dominant; y: years; d: days; SBDS: Shwachman-Bodian-Diamond syndrome; Ht: heterozygous; Hm: homozygous; HSCT: hematopoietic stem cell transplant. * Diagnosed by Sanger sequencing, **diagnosed by whole exome sequencing.

Table 7. Clinical characteristics of patients referred with a presumptive diagnosis of severe aplastic anemia.

Patient	Ethnic origin/ Consanguinity (+/-)	Gene	Disease/ Inheritance	MHGVS Coding	Age (years) at presentation/ diagnosis	Hematological presentation	BM, cytogenetics and functional tests	Extra hematological manifestations	Outcome
5203	Jewish (-)	GATA2	BMF/AD	NM_001145661.1: c.1186C>T -Ht	11/11	Pancytopenia	Severe hypoplastic marrow	Mild dysmorphic features	Post HSCT

BM: bone marrow; BMF: bone marrow failure; AD: autosomal dominant; Ht: heterozygous; HSCT: hematopoietic stem cell transplant.

Arab ancestry, and in Yemenite Jews.³⁷ Thirteen of our patients were indeed found to be homozygous for the described polymorphism. In twelve, the clinical phenotype was compatible with ethnic neutropenia, while one patient had a severe phenotype and underwent successful HSCT, suggesting the presence of a yet undiscovered gene causing congenital neutropenia.

Notably, most patients referred with prolonged neutropenia had no genetic diagnosis. Using both NGS panels and WES, Blombery *et al.* did not identify a molecular diagnosis in ten of 11 patients with IBMFS who were referred with suspected SCN.³⁸ Using an NGS panel, Galvez *et al.* successfully diagnosed only three of 25 patients with prolonged neutropenia.¹⁸ Overlap with primary immunodeficiencies,⁴⁹ new unrecognized genes (estimated to be the cause in about 25% of patients with SCN)⁵⁰ and acquired neutropenia probably contribute to the low yield of pathogenic variant detection among these patients. The overall poor results that we and others achieved calls for better selection of candidates for genetic diagnosis due to isolated neutropenia.

Severe acquired aplastic anemia

Only one patient of 31 (3.2%) referred with SAA was found to have IBMFS with a variant in GATA2 (Figure 1; Table 7; *Online Supplementary Table S3*). Most patients in this group underwent an NGS workup. However, three patients underwent only a partial workup by Sanger sequencing. Keel *et al.* found that among 98 pediatric and young adult patients who underwent HSCT due to what was considered SAA, five (5.1%) had germline genetic alterations in *DKC1*, *MPL* and *TP53*.¹⁵ In their study of germline variants in young adults with aplastic anemia, Feurstein *et al.* found that six of 39 (15.4%) patients had MDS germline predisposition.¹⁷ Our patient was already on immunosuppressive therapy when the genetic test results were received. Immunosuppressive therapy was discontinued, and he successfully underwent HSCT. Interestingly, asymptomatic neutropenia was documented 2 years prior his development of pancytopenia. The low number of patients with SAA diagnosed with an underlying inherited syndrome in our cohort may be related to our routine use of an extensive workup to exclude inherited disorders, including chromosomal breakage test and evaluation of telomere length.

A main limitation of this nationwide study is that it was conducted retrospectively and that patients were referred

at the discretion of the treating physicians. All the patients referred during the study period were included in our cohort, yielding a wide variety of clinical presentations. Therefore, we divided the patients to subgroups according to referral diagnoses and analyzed the results of each subgroup independently.

In summary, using NGS panels, we performed a nationwide study of 189 children who presented with prolonged cytopenias. To the best of our knowledge, this is the first comprehensive genetic study of children presenting with a wide range of clinical manifestations including IBMFS, MDS, SAA, thrombocytopenia, and neutropenia. We were able to identify P/LP variants in 31.2% of the children, the majority in genes predisposing to leukemia. Positive diagnostic results were most often achieved in children with suspected IBMFS and with isolated thrombocytopenia. We conclude that applying Sanger sequencing and NGS panels to children with persistent cytopenias is important for identifying inherited syndromes, especially those predisposing to leukemia. This may direct close monitoring and intervention prior to the development of overt leukemia.

Disclosures

No conflicts of interest to disclose.

Contributions

OG, HT and OSS designed the study, analyzed the data and wrote the paper; JY, RR, TG, AK, AAQ, HM, NK, NMS, SS, DH, TBA, EA, CL, SA, RE and SBA provided the clinical data of the patients enrolled; OD, SNY, TK, LCY, YK, NO and MHG performed the laboratory research and analyzed the data; SI contributed to data analysis and paper writing. All the authors approved the manuscript and submission.

Funding

This work was supported by grants from the Israeli Cancer Association to HT, OD and OSS; from the Israeli Center for Better Childhood to HT; and from grants of the Israeli Health Ministry (# 3-15001) and the Israeli Ministry of Science (#3-14354 and #14940-3) to SI.

Data-sharing statement

The authors will make their original data available to future researchers upon request directed to the corresponding author.

References

- Gnanaraj J, Parnes A, Francis CW, Go RS, Takemoto CM, Hashmi SK. Approach to pancytopenia: diagnostic algorithm for clinical hematologists. *Blood Rev.* 2018;32(5):361-367.
- Erlacher M, Strahm B. Missing cells: pathophysiology, diagnosis, and management of (Pan)cytopenia in childhood. *Front Pediatr.* 2015;3:64.
- Kraft IL, Godley LA. Identifying potential germline variants from sequencing hematopoietic malignancies. *Hematology Am Soc Hematol Educ Program.* 2020;136(22):2498-2506.
- Shimamura A, Alter BP. Pathophysiology and management of inherited bone marrow failure syndromes. *Blood Rev.* 2010;24(3):101-122.
- Wegman-Ostrosky T, Savage SA. The genomics of inherited bone marrow failure: from mechanism to the clinic. *Br J Haematol.* 2017;177(4):526-542.
- Bluteau O, Sebert M, Leblanc T, et al. A landscape of germ line mutations in a cohort of inherited bone marrow failure patients. *Blood.* 2018;131(7):717-732.
- Galaverna F, Ruggeri A, Locatelli F. Myelodysplastic syndromes in children. *Curr Opin Oncol.* 2018;30(6):402-408.
- Arber DA, Orazi A, Hasserjian R, et al. The 2016 revision to the World Health Organization classification of myeloid neoplasms and acute leukemia. *Blood.* 2016;127(20):2391-2405.
- Sahoo SS, Kozyra EJ, Wlodarski MW. Germline predisposition in myeloid neoplasms: unique genetic and clinical features of GATA2 deficiency and SAMD9/SAMD9L syndromes. *Best Pract Res Clin Haematol.* 2020;33(3):101197.
- Song WJ, Sullivan MG, Legare RD, et al. Haploinsufficiency of CBFA2 causes familial thrombocytopenia with propensity to develop acute myelogenous leukaemia. *Nat Genet.* 1999;23(2):166-175.
- Galera P, Dulau-Florea A, Calvo KR. Inherited thrombocytopenia and platelet disorders with germline predisposition to myeloid neoplasia. *Int J Lab Hematol.* 2019;41 Suppl 1:131-141.
- Hock H, Shimamura A. ETV6 in hematopoiesis and leukemia predisposition. *Semin Hematol.* 2017;54(2):98-104.
- Noris P, Pecci A. Hereditary thrombocytopenias: a growing list of disorders. *Hematology Am Soc Hematol Educ Program.* 2017;2017(1):385-399.
- Porter CC, Druley TE, Erez A, et al. Recommendations for surveillance for children with leukemia-predisposing conditions. *Clin Cancer Res.* 2017;23(11):e14-e22.
- Keel SB, Scott A, Sanchez-Bonilla M, et al. Genetic features of myelodysplastic syndrome and aplastic anemia in pediatric and young adult patients. *Haematologica.* 2016;101(11):1343-1350.
- Zhang MY, Keel SB, Walsh T, et al. Genomic analysis of bone marrow failure and myelodysplastic syndromes reveals phenotypic and diagnostic complexity. *Haematologica.* 2015;100(1):42-48.
- Feurstein S, Churpek JE, Walsh T, et al. Germline variants drive myelodysplastic syndrome in young adults. *Leukemia.* 2021;35(8):2439-2444.
- Galvez E, Vallespin E, Arias-Salgado EG, et al. Next-generation sequencing in bone marrow failure syndromes and isolated cytopenias: experience of the Spanish Network on Bone Marrow Failure Syndromes. *Hemasphere.* 2021;5(4):e539.
- Hasle H. Myelodysplastic and myeloproliferative disorders of childhood. *Hematology Am Soc Hematol Educ Program.* 2016;2016(1):598-604.
- Camitta BM, Thomas ED, Nathan DG, et al. Severe aplastic anemia: a prospective study of the effect of early marrow transplantation on acute mortality. *Blood.* 1976;48(1):63-70.
- Hsieh MM, Everhart JE, Byrd-Holt DD, Tisdale JF, Rodgers GP. Prevalence of neutropenia in the U.S. population: age, sex, smoking status, and ethnic differences. *Ann Intern Med.* 2007;146(7):486-492.
- Noy-Lotan S, Krasnov T, Dgany O, et al. Incorporation of somatic panels for the detection of haematopoietic transformation in children and young adults with leukaemia predisposition syndromes and with acquired cytopenias. *Br J Haematol.* 2021;193(3):570-580.
- Hsu AP, Johnson KD, Falcone EL, et al. GATA2 haploinsufficiency caused by mutations in a conserved intronic element leads to MonoMAC syndrome. *Blood.* 2013;121(19):3830-3837, S1-7.
- Shefer Averbuch N, Steinberg-Shemer O, Dgany O, et al. Targeted next generation sequencing for the diagnosis of patients with rare congenital anemias. *Eur J Haematol.* 2018;101(3):297-304.
- Goldberg L, Simon AJ, Rechavi G, et al. Congenital neutropenia with variable clinical presentation in novel mutation of the SRP54 gene. *Pediatr Blood Cancer.* 2020;67(6):e28237.
- Richards S, Aziz N, Bale S, et al. Standards and guidelines for the interpretation of sequence variants: a joint consensus recommendation of the American College of Medical Genetics and Genomics and the Association for Molecular Pathology. *Genet Med.* 2015;17(5):405-424.
- Rehm HL, Bale SJ, Bayrak-Toydemir P, et al. ACMG clinical laboratory standards for next-generation sequencing. *Genet Med.* 2013;15(9):733-747.
- Scionti F, Di Martino MT, Pensabene L, Bruni V, Concolino D. The cytoscan HD array in the diagnosis of neurodevelopmental disorders. *High Throughput.* 2018;7(3):28.
- <https://www.cbs.gov.il/en/mediarelease/Pages/2020/Population-of-Israel-on-the-Eve-of-2021.aspx>
- Li N, Xu Y, Yu T, et al. Further delineation of bone marrow failure syndrome caused by novel compound heterozygous variants of MYSM1. *Gene.* 2020;757:144938.
- Tummala H, Kirwan M, Walne AJ, et al. ERCC6L2 mutations link a distinct bone-marrow-failure syndrome to DNA repair and mitochondrial function. *Am J Hum Genet.* 2014;94(2):246-256.
- Rechavi E, Levy-Mendelovich S, Stauber T, et al. Combined immunodeficiency in a patient with mosaic monosomy 21. *Immunol Res.* 2016;64(4):841-847.
- Hoffmann JJ. Reference range of mean platelet volume. *Thromb Res.* 2012;129(4):534-535.
- Seo A, Gulsuner S, Pierce S, et al. Inherited thrombocytopenia associated with mutation of UDP-galactose-4-epimerase (GALE). *Hum Mol Genet.* 2019;28(1):133-142.
- Boztug K, Jarvinen PM, Salzer E, et al. JAGN1 deficiency causes aberrant myeloid cell homeostasis and congenital neutropenia. *Nat Genet.* 2014;46(9):1021-1027.
- Bellanne-Chantelot C, Schmaltz-Panneau B, Marty C, et al. Mutations in the SRP54 gene cause severe congenital neutropenia as well as Shwachman-Diamond-like syndrome. *Blood.* 2018;132(12):1318-1331.
- Palmblad J, Hoglund P. Ethnic benign neutropenia: a phenomenon finds an explanation. *Pediatr Blood Cancer.* 2018;65(12):e27361.
- Blombery P, Fox L, Ryland GL, et al. Utility of clinical comprehensive genomic characterization for diagnostic categorization in patients presenting with hypocellular bone marrow failure syndromes. *Haematologica.* 2021;106(1):64-73.

39. Ghemlas I, Li H, Zlateska B, et al. Improving diagnostic precision, care and syndrome definitions using comprehensive next-generation sequencing for the inherited bone marrow failure syndromes. *J Med Genet*. 2015;52(9):575-584.
40. Pastor VB, Sahoo SS, Boklan J, et al. Constitutional SAMD9L mutations cause familial myelodysplastic syndrome and transient monosomy 7. *Haematologica*. 2018;103(3):427-437.
41. Shabanova I, Cohen E, Cada M, Vincent A, Cohn RD, Dror Y. ERCC6L2-associated inherited bone marrow failure syndrome. *Mol Genet Genomic Med*. 2018;6(3):463-468.
42. Douglas SPM, Siipola P, Kovanen PE, et al. ERCC6L2 defines a novel entity within inherited acute myeloid leukemia. *Blood*. 2019;133(25):2724-2728.
43. Pippucci T, Savoia A, Perrotta S, et al. Mutations in the 5' UTR of ANKRD26, the ankirin repeat domain 26 gene, cause an autosomal-dominant form of inherited thrombocytopenia, THC2. *Am J Hum Genet*. 2011;88(1):115-120.
44. Bluteau D, Balduini A, Balayn N, et al. Thrombocytopenia-associated mutations in the ANKRD26 regulatory region induce MAPK hyperactivation. *J Clin Invest*. 2014;124(2):580-591.
45. Marconi C, Canobbio I, Bozzi V, et al. 5'UTR point substitutions and N-terminal truncating mutations of ANKRD26 in acute myeloid leukemia. *J Hematol Oncol*. 2017;10(1):18.
46. Balduini CL, Savoia A, Seri M. Inherited thrombocytopenias frequently diagnosed in adults. *J Thromb Haemost*. 2013;11(6):1006-1019.
47. Noris P, Perrotta S, Seri M, et al. Mutations in ANKRD26 are responsible for a frequent form of inherited thrombocytopenia: analysis of 78 patients from 21 families. *Blood*. 2011;117(24):6673-6680.
48. Donadieu J, Fenneteau O, Beaupain B, Mahlaoui N, Chantelot CB. Congenital neutropenia: diagnosis, molecular bases and patient management. *Orphanet J Rare Dis*. 2011;6:26.
49. Miano M, Grossi A, Dell'Orso G, et al. Genetic screening of children with marrow failure. The role of primary Immunodeficiencies. *Am J Hematol*. 2021;96(9):1077-1086.
50. Skokowa J, Dale DC, Touw IP, Zeidler C, Welte K. Severe congenital neutropenias. *Nat Rev Dis Primers*. 2017;3:17032.

Increased visceral fat distribution and body composition impact cytokine release syndrome onset and severity after CD19 chimeric antigen receptor T-cell therapy in advanced B-cell malignancies

David M. Cordas dos Santos,^{1-3*} Kai Rejeski,^{1,3-4*} Michael Winkelmann,⁵ Lian Liu,⁶ Paul Trinkner,^{1,2} Sophie Günther,^{1,2} Veit L. Bücklein,^{1,4} Viktoria Blumenberg,^{1,3-4} Christian Schmidt,¹ Wolfgang G. Kunz,⁵ Michael von Bergwelt-Baildon,^{1,3,6} Sebastian Theurich^{1-3#} and Marion Subklewe^{1,3-4#}

¹Department of Medicine III, University Hospital, LMU Munich, Munich; ²Cancer- and Immunometabolism Research Group, LMU Gene Center, Munich; ³German Cancer Consortium (DKTK), Munich Site, and German Cancer Research Center, Heidelberg; ⁴Laboratory for Translational Cancer Immunology, LMU Gene Center, Munich; ⁵Department of Radiology, University Hospital, LMU Munich and ⁶Comprehensive Cancer Center Munich, LMU Munich, Munich, Germany

*DMCDS and KR contributed equally as co-first authors.

#ST and MS contributed equally as co-senior authors.

Correspondence: M. Subklewe
marion.subklewe@med.uni-muenchen.de

S. Theurich
sebastian.theurich@med.uni-muenchen.de

Received: October 13, 2021.

Accepted: February 9, 2022.

Prepublished: February 17, 2022.

<https://doi.org/10.3324/haematol.2021.280189>

©2022 Ferrata Storti Foundation

Published under a CC BY-NC license



Abstract

Chimeric antigen receptor T-cell (CAR-T) therapy is associated with a distinct toxicity profile that includes cytokine release syndrome (CRS) and immune effector cell-associated neurotoxicity syndrome (ICANS). CRS is characterized by the release of pro-inflammatory cytokines such as interleukin 6 (IL-6) and is closely linked to CAR-T expansion and bystander cells like monocytes/macrophages. In other hyperinflammatory states, obesity contributes to inflammatory cascades and acts as a risk factor for disease severity. We aimed to study the influence of anthropometric and body composition (BC) measurements on CAR-T-related immunotoxicity in 64 patients receiving CD19-directed CAR-T for relapsed/refractory B-cell malignancies. Patients with grade ≥ 2 CRS presented with a significantly higher median body mass index (BMI), waist circumference, waist-to-height ratio (WtHR) and visceral adipose tissue (VAT). These parameters were also found to be associated with an earlier CRS onset. Other adipose deposits and muscle mass did not differ between patients with grade 0-1 CRS *versus* grade ≥ 2 CRS. Moreover, BC parameters did not influence ICANS severity or onset. In a multivariate binary logistic regression incorporating known risk factors of immunotoxicity, the factors BMI, waist circumference, WtHR and VAT increased the probability of grade ≥ 2 CRS. Receiver operating characteristic analyses were utilized to determine optimal discriminatory thresholds for these parameters. Patients above these thresholds displayed markedly increased peak IL-6 levels. Our data imply that increased body composition and VAT in particular represent an additional risk factor for severe and early CRS. These findings carry implications for risk-stratification prior to CD19 CAR-T and may be integrated into established risk models.

Introduction

The advent of chimeric antigen receptor T-cell (CAR-T) therapy as a powerful new class of immunotherapeutic agents has improved outcomes for multiple B-cell malignancies in the relapsed/refractory (R/R) setting.¹⁻⁴ As these therapies move to the clinical mainstream, understanding the mechanisms that drive the unique spectrum of CAR-T-related immunotoxicity becomes paramount.

Cytokine release syndrome (CRS) represents the most commonly observed adverse event and is characterized by an increase of pro-inflammatory cytokines such as interleukin-6 (IL-6), resulting in endothelial activation and diffuse capillary leakage.⁵ The clinical management of CRS follows a risk-adapted strategy for monitoring and therapy, and the anti-IL-6 receptor antagonist tocilizumab is commercially available to ameliorate symptoms.⁶ Several patient-associated risk factors have been identified that

facilitate CRS development. These include high tumor burden, concomitant and previous infections, increased C-reactive protein (CRP) or ferritin, and thrombocytopenia.⁷⁻¹¹ While CRS represents a prevalent CAR-T-associated toxicity, the wide-spread adoption of risk-adapted supportive measures has reduced the frequency of its high-grade presentation. Still, the systemic hyperinflammation found in CRS can predispose for the neurological side effects of CAR-T, which remain a major clinical challenge. Immune effector cell-associated neurotoxicity syndrome (ICANS) is found in approximately 20-60% of CAR-T-treated patients and presents with symptoms ranging from mild confusion to aphasia, seizures, cerebral edema, and potentially death.¹²⁻¹⁴ Patient-associated and dynamic risk factors that predispose for ICANS include prior neurologic diseases and structural impairments, organ dysfunction, older age and severe CRS.¹⁵⁻¹⁷ High-grade ICANS has also been linked to higher peak levels of systemic cytokines and inflammatory mediators (e.g., CRP, ferritin and IL-6),⁸ and a lower median peak absolute monocyte count.¹⁸ In other hyperinflammatory states including COVID-19 or influenza infections, as well as sepsis, obesity has been demonstrated to be a risk factor for disease severity.¹⁹⁻²¹ Amongst the underlying mechanisms, obesity-associated chronic systemic inflammation, termed metaflammation, has been proposed to enhance an hyperinflammatory immune response, which precedes organ dysfunction.²² Mechanistically, macrophages and CD8⁺ T cells can infiltrate fat deposits turning adipose tissue into an inflammatory endocrine organ secreting pro-inflammatory cytokines such as IL-6, TNF- α and IL-1 β .²³ Various adipose tissue sites differentially contribute to metaflammation: visceral adipose tissue (VAT) in particular plays an important role in metaflammation and obesity-associated pathologies such as type II diabetes and cardiovascular diseases.^{24,25} Epicardial adipose tissue (EAT) has been described as a surrogate marker of VAT and, in turn, as a marker for cardiovascular and metabolic morbidity.^{26,27} In contrast, subcutaneous adipose tissue (SAT) displays a more heterogeneous effect on systemic inflammatory processes.^{28,29} More recently, skeletal muscle has also been recognized as a regulator of immune responses.^{30,31} Skeletal muscle cells modulate immune function by signaling through muscle cell-derived cytokines, termed myokines, cell surface molecules and cell-to-cell interactions. Myokines such as IL-6, IL-7 and IL-15 can modulate CD8⁺ T-cell homeostasis and promote survival and proliferation of naïve T and B cells.³²⁻³⁵ Sarcopenia, which describes the loss of skeletal muscle as a consequence of old age and cancer, is often found in cancer patients and has been linked to immune senescence.³⁰ Despite rapidly growing evidence that adipose and muscle tissue play an important role in shaping immune re-

sponses, the influence of body composition in the context of CAR-T therapy remains poorly understood. Therefore, we aimed to investigate the impact of body composition on severity and dynamics of CRS and ICANS, as well as serum cytokine levels.

Methods

Patient cohort

We performed a retrospective chart review of R/R large B-cell lymphoma (LBCL), B-cell precursor acute lymphoblastic leukemia (BCP-ALL) and mantle cell lymphoma (MCL) patients who underwent CAR-T at the University Hospital of the LMU Munich between 01/2019 until 08/2021. Patients received the commercial CAR-T products Axicabtagene ciloleucel (Axi-cel), Tisagenlecleucel (Tisa-cel), or received KTE-X19 in the compassionate use program for MCL. Patients received lymphodepleting chemotherapy (LDC) with fludarabine and cyclophosphamide according to the manufacturers' instructions.^{2,3} CRS and ICANS were graded according to the American Society for Transplantation and Cellular Therapy (ASTCT) consensus criteria.⁶ All patients were closely monitored prospectively for CRS and ICANS from the day of CAR-T transfusion until at least day 21, or until symptoms resolved. Swimmers plots were generated via day-by-day recording of ASTCT grade according to the treating physicians' discretion (*Online Supplementary Figures S1 and S2*). Heat maps were generated by cross-sectional analysis of the mean CRS/ICANS grade between days 0-21. Toxicity management followed institutional guidelines. Patients with CRS grade ≥ 2 and persistent CRS grade 1 (> 24 hours) were treated with the anti-IL-6 receptor antagonist tocilizumab. In the absence of concurrent CRS or if ICANS was refractory to anti-cytokine therapy, corticosteroids were initiated for grade ≥ 2 ICANS. Clinical metadata was obtained with Institutional Review Board approval and included a waiver of informed consent.

Measurements of body composition

Body composition (BC) analyses were performed using clinical records (weight, height) and computerized tomography (CT) scans (waist, adipose/muscle tissue distribution) obtained prior to CAR-T transfusion. The majority of patients received CT imaging on the day before LDC initiation (median imaging to LDC time -1 day, interquartile range [IQR] -4 to 0 days). Three anthropometric measures were included: body mass index (BMI), waist circumference (waist) and waist-to-height ratio (WtHR). Waist was derived from single CT slices.³⁶ WtHR was calculated by dividing waist by height. For quantification of SAT, VAT and muscle tissue distribution (psoas muscle index [PMI] and skeletal muscle index [SMI]), segmentation analyses of

single CT slices at lumbar spine 3 (L3) were performed. Muscle indices (PMI, SMI) were calculated by dividing mean muscle area by height. EAT content was quantified by calculating the mean EAT amount at the bottom, middle (4-chamber view) and top (left main coronary artery view) of the heart. Adipose and muscle tissue discrimination was based on predefined Hounsfield units (HU) ranges (-190 to -30 HU for SAT, -150 to -50 HU for VAT, -190 to -30 HU for EAT, -29 to +150 HU for PM/SM).³⁶⁻³⁸ Cross-sectional areas of respective tissues were computed for each image. Segmentation analyses were performed with ImageJ and the Slice-O-Matic software package (v5.0, Tomovision, Magog, Quebec, Canada). Waist was measured with ImageJ software (v2.0).

Analysis of cytokine dynamics

Baseline cytokine levels were determined prior to LDC (e.g., day -5). Peak CRP (mg/dL), IL-6 (pg/mL), and ferritin (µg/L) levels were measured daily from CAR-T transfusion until discharge and on subsequent outpatient visits. The total study time frame was day 0-21. Laboratory measurements were performed according to clinical standard procedures in the clinical laboratory of the University Hospital of the LMU Munich. The temporal analysis of IL-6 (pg/mL) over time was performed by computing the aggregated median value for each day between days 0-21. In order to distinguish differences between curves, mixed-effects analysis considering both time and effect size using the restricted maximum likelihood method was performed (GraphPad Prism v9.0).

Statistical analysis

Patient characteristics, BC and serum parameters analyses were compared using the Mann Whitney test or Student's *t*-test according to data distribution for continuous variables, and the Fisher's exact test and chi-squared test for categorical variables. Continuous variables were reported as median and IQR if not stated otherwise. The area under the curve (AUC) and the 95% confidence interval (95% CI) of the receiver operating characteristic (ROC) analysis was computed using the predicted probability for the development of CRS grade ≥ 2 . Optimal discriminatory thresholds were determined by optimizing the respective Youden *J* statistic. Multivariate adjusted analysis was performed as binary logistic regression for the outcome of grade ≥ 2 CRS. The model included baseline clinical characteristics (e.g., age, costimulatory domain), laboratory parameters (e.g., albumin, platelet count), markers of inflammation (e.g., CRP, ferritin, IL-6), and markers of tumor burden (e.g., LDH, STLV) as candidate predictors. The individual BC parameters (BMI, Waist, WtHR, and VAT) were introduced to the model separately to account for multicollinearity (*Online Supplementary Table S6*). In order to measure the relationship between two

continuous variables, Spearman correlation analyses were used. Significance was defined as $P < 0.05$. Statistical analysis was performed using GraphPad Prism v9.0 (GraphPad Software, Inc.) and SPSS v26.0.

Results

Description of the cohort and the real-world toxicity profile

Between January 2019 and August 2021, the incidence and clinical severity of CRS and ICANS was assessed in 52 R/R LBCL, eight MCL and four BCP-ALL patients (Table 1; Figure 1A). These patients were treated with the commercial CD19-specific CAR-T products Axi-cel (n=22), Tisa-cel (n=

Table 1. Baseline patient characteristics.

Characteristic	All Patients (N=64)
Basic data	
Age in years, median (range)	61 (19-82)
Female patients, N (%)	23 (35.9)
Disease entities, N (%)	
DLBCL including THRBCL	33 (51.6)
Transformed aggressive non-Hodgkin lymphoma (from MCL, FL, CLL, HL)	16 (25)
PMBCL	2 (3.1)
MCL	8 (12.5)
B-ALL	5 (7.8)
Lines of prior therapy, median (IQR)	4 (3-5)
Prior autologous/allogeneic SCT, N (%)	24 (37.5)
Costimulatory domain, N (%)	
4-1BB	34 (53.1)
CD28z	30 (46.9)
CRS, any grade, N (%)	59 (92.2)
Grade 1	31 (48.4)
Grade 2	22 (34.4)
Grade 3	6 (9.4)
CRS onset, days (IQR)	2 (1-5)
CRS duration, days (IQR)	6 (4-9)
ICANS, any grade, N (%)	28 (43.8)
Grade 1	13 (20.3)
Grade 2	7 (11)
Grade 3	4 (6.3)
Grade 4	3 (6.4)
Grade 5	1 (2.1)
ICANS onset, days (IQR)	8 (3-9)
ICANS duration, days (IQR)	8 (4-14)
Toxicity management, N (%)	
Tocilizumab administration	54 (79)
Corticosteroid administration	24 (37.5)

B-ALL: B-cell acute lymphoblastic leukemia; CLL: chronic lymphocytic leukemia; CRS: cytokine release syndrome; DL/PM/THRBCL: diffuse large/T-cell/histocyte-rich/primary mediastinal B-cell lymphoma; FL: follicular lymphoma; HL: Hodgkin lymphoma; ICANS: immune effector cell-associated neurotoxicity syndrome; IQR: interquartile range; MCL: mantle cell lymphoma; SCT: stem cell transplantation.

34), or received KTE-X19 under compassionate use for MCL (n=8). All transfused patients were included in the analysis. The median BMI was 23.5 kg/m² (IQR 21.6-26.7 kg/m²), and the majority of patients displayed a normal BMI according to World Health Organization criteria (66%, Figure 1B). Pre-LDC CT imaging studies were utilized to calculate individual SAT, VAT, EAT values as well as skeletal muscle values with respective indices (PM/I, SM/I) (Figure 1C).

CRS of any grade was observed in 59 (92.2%) patients, nearly half of which developed grade ≥2 CRS (Figure 2A; Table 1). Median CRS onset was 2 days (IQR 1-5) and lasted a median of 6 days (IQR 4-9) (Figure 2B). ICANS was observed in 28 patients (43.8%), though only eight patients (14.8%) developed grade ≥2 ICANS (Figure 2A). Median ICANS onset was 8 days (IQR 3-9) and the median ICANS duration was 8 days (IQR 4-14) (Figure 2C). We found that patients that developed more severe immunotoxicity often

displayed an earlier onset of toxicity (*Online Supplementary Figure S1 and S2*). Life-threatening (grade 4) and fatal (grade 5, 1 patient) ICANS only occurred in patients with grade ≥2 CRS (*Online Supplementary Figure S3A*). In line with this finding, the median CRS grade was higher in patients with grade ≥2 neurotoxicity (median CRS grade 2 vs. 1, *P*=0.07, *Online Supplementary Figure S3B*). These data are consistent with the known role of CRS as a risk factor of neuroinflammation.^{16,17} Across all patients, 79% (54/64) received IL-6 receptor blockade with tocilizumab, while 37.5% (24/64) were treated with corticosteroids. When comparing the grade 0-1 *versus* grade ≥2 CRS and ICANS groups, baseline markers of tumor burden (e.g., LDH, mean tumor volume), inflammation (e.g., CRP, ferritin), and endothelial dysfunction (e.g., platelet count) were balanced between cohorts (*Online Supplementary Table S1*). Temporally, CRS predominantly occurred in week 1, while ICANS most commonly occurred in week 2 (Figure 2D). In-

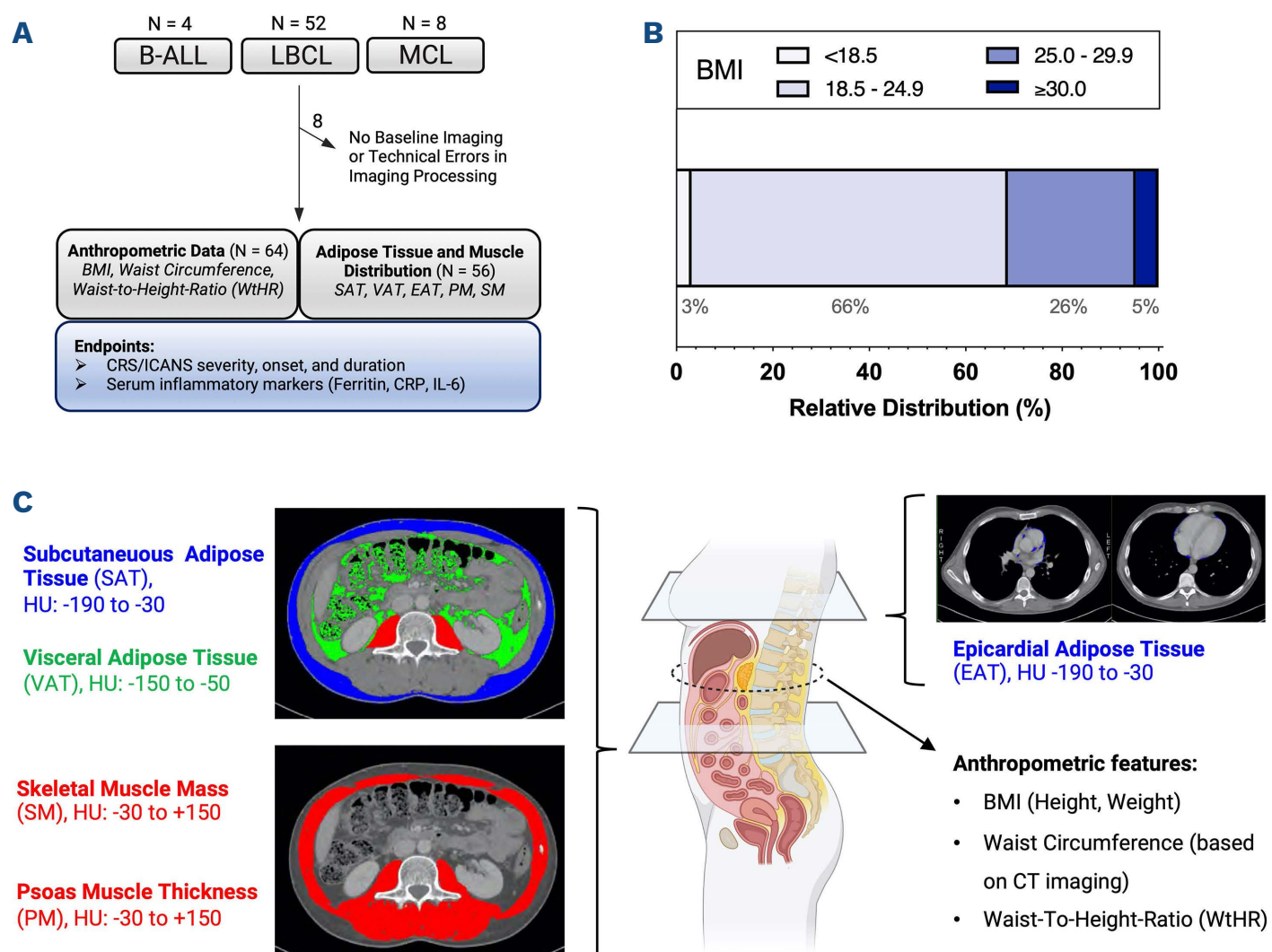


Figure. 1 Measurement of prechimeric antigen receptor T-cell body composition and fat deposition. (A) Cohort description; the primary endpoint was cytokine release syndrome (CRS)/immune effector cell-associated neurotoxicity syndrome (ICANS) severity, onset, and duration; peak cytokine levels represented the exploratory endpoint. Adipose tissue and muscle distribution at baseline (= prior to lymphodepleting chemotherapy [LDC]) could not be determined in 8 patients due to lack of appropriate imaging modalities. Anthropometric data was collected for the entire study cohort (n=64). (B) Relative distribution of body mass index (BMI) according to the 2019 World Health Organization criteria (underweight <18.5 kg/m², normal weight 18.5-24.9 kg/m², overweight 25-29.9 kg/m², obese >30 kg/m²). (C) Pretreatment computerized tomography (CT) images were utilized to measure subcutaneous (SAT), epicardial (EAT) and visceral (VAT) adipose tissue deposits, as well as the psoas muscle (PM) thickness and skeletal muscle (SM) mass. SAT, VAT, PM and SM segmentation analyses were performed at lumbar spine 3 level. EAT content was quantified by calculating the mean EAT amount at the bottom, middle (4-chamber view) and top (left main coronary artery view) of the heart. Hounsfield units (HU) describing radiodensity of the respective tissue types are indicated. Anthropometric data included BMI, waist circumference (Waist), and waist-to-height ratio (WtHR).

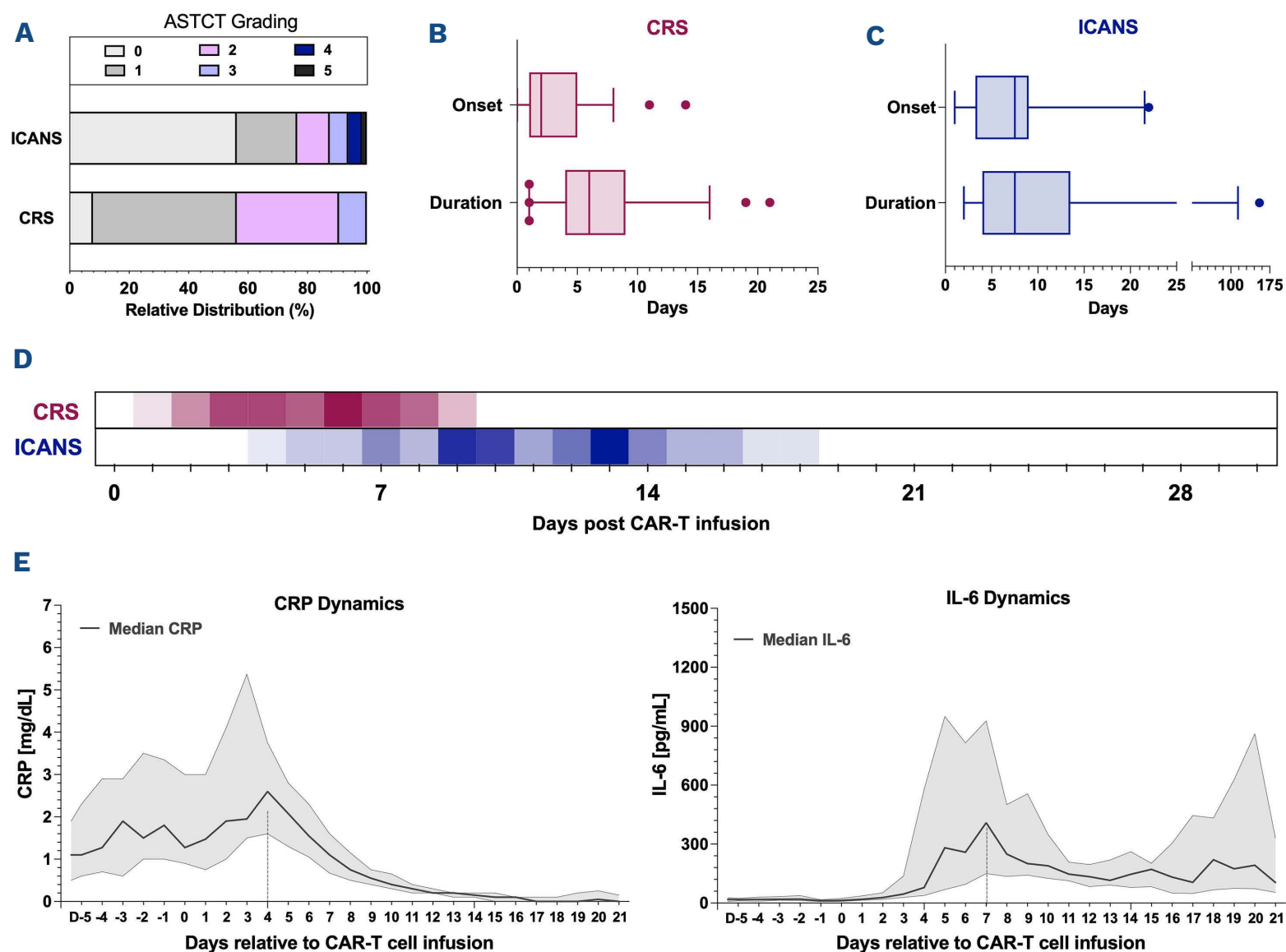


Figure 2. Incidence, onset, and duration of cytokine release syndrome and immune effector cell-associated neurotoxicity syndrome in the study cohort. (A) Relative distribution of cytokine release syndrome (CRS) and immune effector cell associated neurotoxicity syndrome (ICANS) in the studied patient cohort ($n=64$). Grading was performed according to American Society for Transplantation and Cellular Therapy criteria (Lee *et al.*, BBMT 2019) with color-coding based on severity. (B to C) Box plot displaying median onset and duration of CRS (B) and ICANS (C) in days. The median is reflected by a vertical line, the box displays the interquartile range, whiskers indicate the 95% confidence interval (CI) of the median. (D) Heatmap outlining the day-by-day time course of CRS (red) and ICANS (blue) after chimeric antigen receptor T-cell (CAR-T) infusion (day 0 [D0]). Darker color indicates higher mean CRS or ICANS grade. (E) Aggregated median C-reactive protein (CRP) (left) and interleukin 6 (IL-6) (right) values over time relative to CAR-T infusion (D0). Light shading depicts the 95% CI of the median for each time point.

inflammatory marker profiles revealed a two-phase pattern for IL-6 serum levels with an early peak on day 4 and a second peak observed between days 19-21 (Figure 2F). On the other hand, CRP levels were elevated at baseline, likely reflecting underlying tumor-mediated inflammation.³⁹ They reached a peak at day 4 and normalized by day 10 after CAR-T cell transfusion. Overall, these data indicate a representative toxicity profile in our patient cohort.

Body mass index, waist circumference, waist-to-height ratio and visceral adipose tissue are associated with severe cytokine release syndrome

Previous studies have revealed a link between BC and systemic inflammatory disorders.²² We therefore analyzed the distribution of BC parameters in patients with grade 0-1 CRS versus grade ≥ 2 CRS.

In terms of anthropometric features, we found that the median BMI, waist circumference, and WtHR were signifi-

cantly elevated in patients with grade ≥ 2 CRS (Figure 3; *Online Supplementary Table S2*). The median BMI was 24.3 kg/m² in patients with grade ≥ 2 CRS compared to 22.9 kg/m² in patients with grade 0-1 CRS ($P=0.01$, Figure 3A). Of the different adipose tissue types, visceral fat deposits in particular were significantly different between the CRS severity groups (127 cm² vs. 91 cm², $P=0.048$, Figure 3D). While a trend was observed for a higher SAT in grade ≥ 2 CRS, this did not reach statistical significance (169 cm² vs. 141 cm², $P=0.054$). EAT and muscle mass distribution did not differ between CRS severity cohorts (*Online Supplementary Table S2*).

Next, we performed ROC analyses to determine optimal discriminatory thresholds for each parameter that reached statistical significance (*Online Supplementary Figure S4*) and calculated the concomitant odds ratios (OR) for the outcome grade ≥ 2 CRS (Table 2). The observed odds for developing grade ≥ 2 CRS were signifi-

cantly higher for patients with a BMI ≥ 27.05 kg/m² ($P=0.007$), waist ≥ 99.23 cm ($P=0.04$), WtHR ≥ 0.594 cm/m² ($P=0.01$) and VAT ≥ 144.3 cm² ($P=0.02$). The AUC of the ROC curve ranged between 0.63 to 0.67. Importantly, previously identified CRS risk factors such as age, tumor burden and certain laboratory parameters⁷⁻¹¹ were distributed equally between patient cohorts based on the defined thresholds for BMI, waist, WtHR and VAT (*Online Supplementary Table S3*). On multivariate adjusted analysis, we confirmed that these four BC parameters represent independent risk factors of grade ≥ 2 CRS (Table 3). With adjusted odds ratios ranging from 1.15 to 1.37, they significantly increased the

probability of grade ≥ 2 CRS. Collectively, these findings suggest a contributing role of visceral adipose tissue for CRS severity.

Body mass index, waist, waist-to-height ratio and visceral adipose tissue correlate with cytokine release syndrome dynamics

In addition to CRS severity, we analyzed the impact of anthropometric and BC measurements on CRS dynamics. Linear regression analyses revealed significant negative correlations between CRS onset and BMI, waist, WtHR, and VAT (Figure 3B; *Online Supplementary Table S4*). Ac-

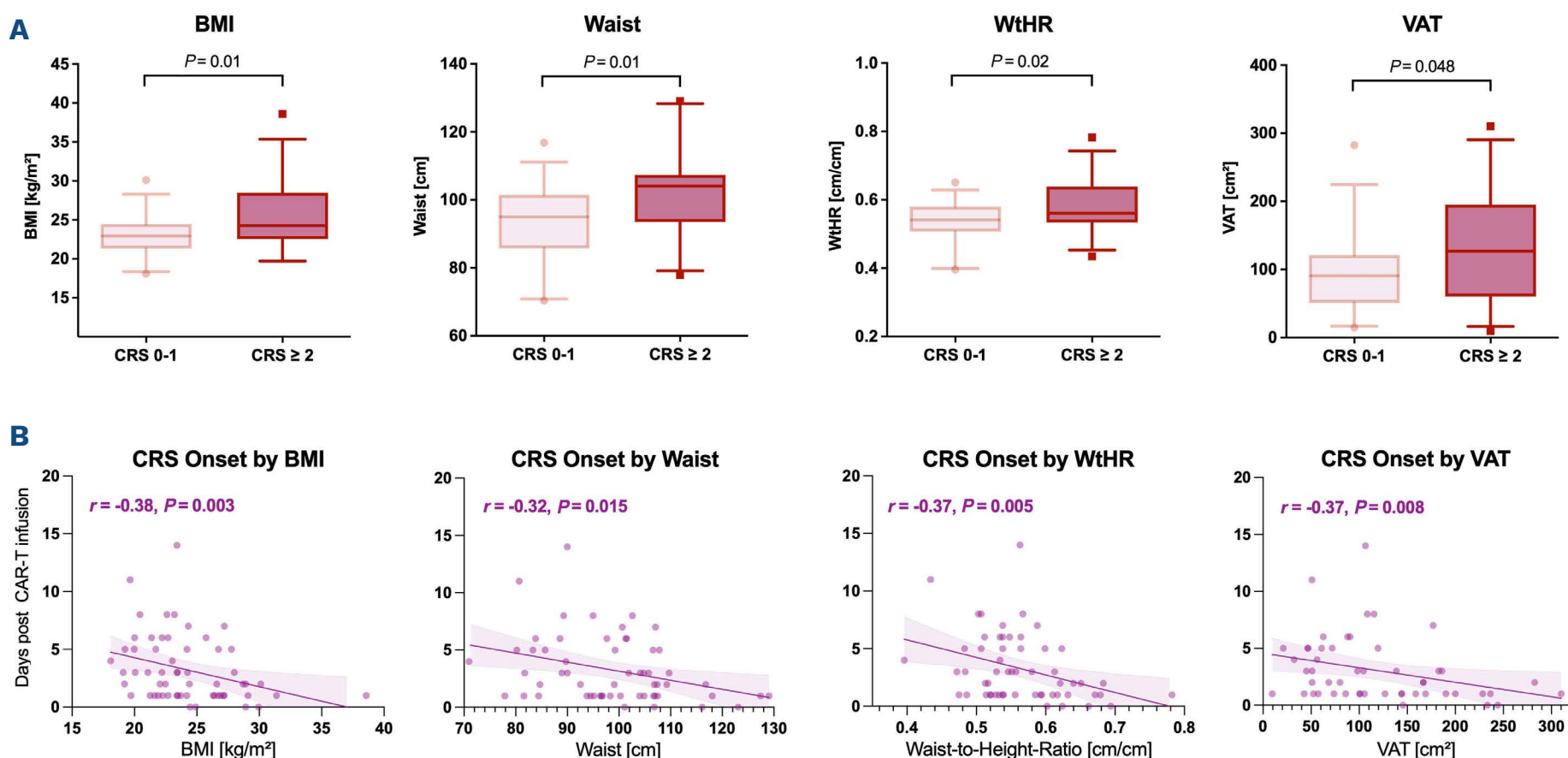


Figure 3. Body mass index and metabolic high-risk adipose tissue are associated with more severe cytokine release syndrome and early cytokine release syndrome onset. (A) Box plots comparing body mass index (BMI), waist circumference (Waist), waist-to-height ratio (WtHR), and visceral adipose tissue (VAT) by cytokine release syndrome (CRS) severity. Higher-grade CRS defined as American Society for Transplantation and Cellular Therapy grade ≥ 2 , non-severe CRS as grade 0-1. The box indicates the interquartile range with the horizontal line describing the median, and whiskers denoting the 95% confidence interval [CI] of the median. (B) Univariate linear regression analysis comparing BMI, Waist, WtHR, and VAT (from left to right) vs. CRS onset (purple) in days. The graphical inset depicts the Spearman correlation coefficient with a positive r-value indicating a positive correlation and a negative r-value indicating a negative correlation, as well as the respective P-value. The 95% CI bands of the best-fit line from the simple linear regression are shown in light shading.

Table 2. Determination of discriminatory thresholds and odds ratios based on receiver operating characteristic analysis computed for predicted probability of grade ≥ 2 cytokine release syndrome.

Body composition parameter	Discriminatory threshold	AUC	P-Value AUC	OR (95% CI)	P-Value OR
BMI, kg/m ²	27.05	0.66	0.03	6.11 (1.7-22.1)	0.007
Waist, cm	99.23	0.67	0.02	2.96 (1.03-8.29)	0.04
WtHR, cm/m ²	0.5935	0.65	0.04	4.06 (1.4-11.3)	0.01
VAT, cm ²	144.3	0.63	0.09	4.8 (1.4-15.2)	0.02

95% CI: 95% confidence interval; AUC: area under curve; BMI: body mass index; CRS: cytokine release syndrome; OR: odds ratio; VAT: visceral adipose tissue; WtHR: waist-to-height ratio

cordingly, BMI^{high} (≥ 27.05 kg/m²) patients exhibited an earlier median CRS onset compared to their BMI^{low} counterparts (day 1 vs. day 3, $P=0.05$, *Online Supplementary Figure S5*). Earlier CRS onset was also noted for WtHR and VAT (*Online Supplementary Figure S5*). On the other hand, anthropometric and BC parameters did not significantly correlate with CRS duration (*Online Supplementary Table S4*). These data may reflect the aggressive and early CRS management in this patient cohort, as 91.5% (54/59) of patients with CRS received tocilizumab after a median of 4 days. In summary, adipose tissue parameters were associated with an earlier CRS onset but not duration.

Sarcopenia and body composition are neither associated with immune effector cell-associated neurotoxicity syndrome severity nor dynamics

In addition to adipose tissue distribution analyses, whole skeletal muscle mass and psoas muscle mass with respective indices (SMI, PMI) were measured for all patients. Twenty-four patients were classified as sarcopenic corrected for sex and BMI. Distribution of sarcopenia and muscle masses (SMI, PMI) did not differ between grade ≥ 2 CRS and grade 0-1 CRS patients (*Online Supplementary Table S2*). Moreover, muscle parameters did not affect CRS onset or CRS duration. Since CRS represents a risk factor for ICANS,^{16,17} we also investigated the influence of BC parameters on severity and dynamics of ICANS. However, none of the measured BC parameters differed between patients with grade 0-1 ICANS versus grade ≥ 2 ICANS nor did they correlate with either ICANS onset or ICANS duration (*Online Supplementary Tables S2 and S5*).

Adipose tissue correlates with peak IL-6 levels and IL-6 dynamics

In order to better understand the potential pathomechan-

Table 3. Body mass index, waist, waist-to-height ratio and visceral adipose tissue represent independent risk factors for grade ≥ 2 cytokine release syndrome in a multivariate logistic regression analyses including previously described risk factors.

Body composition parameter	OR	95% CI	P-Value
BMI, kg/m ²	1.37	1.02-1.83	0.04
Waist, cm	1.16	1.04-1.29	0.009
WtHR, cm/m ²	1.24	1.05-1.46	0.01
VAT, cm ²	1.15	1.02-1.3	0.02

Odds ratios were calculated based on four separate multivariate logistic regressions for each of the body composition parameters. Complete model parameters and estimates are shown in the *Online Supplementary Table S6*. 95% CI: 95% confidence interval; AUC: area under curve; BMI: body mass index; CRS: cytokine release syndrome; OR: odds ratio; VAT: visceral adipose tissue; WtHR: waist-to-height ratio.

isms that may underlie earlier and more severe CRS in patients with increased adipose tissue, we analyzed serum levels of pro-inflammatory markers and their distribution according to the BC groups.

First, we correlated BC parameters with baseline and peak serum levels of ferritin, CRP and IL-6—revealing an effect for IL-6 in particular (*Online Supplementary Figure S6*). Interestingly, peak IL-6 levels were significantly increased in patients with elevated waist circumference (3.442 vs. 1.019 pg/mL, $P=0.008$), WtHR (3.768 pg/ml vs. 1.385 pg/mL, $P=0.03$), and VAT (6.530 pg/ml vs. 1.143 pg/ml, $P=0.01$) (*Figure 4A*). A comparison of aggregated median IL-6 courses over time (baseline until day 21) further demonstrated that the median time-to-peak IL-6 was earlier in patients with an increased amount of adipose tissue (*Figure 4B*). In a comparison of curves accounting for both time and effect size, BMI^{high} patients developed an earlier IL-6 peak (5 days vs. 7 days) and the peak was approximately 5-fold higher than in BMI^{low} patients (top left panel, *Figure 4B*). The observed differences in IL-6 dynamics were especially prominent in patients with excess visceral adipose tissue (peak 11-fold higher, day 4 vs. day 8, $P<0.0001$, lower right panel, *Figure 4B*). Notably, patients rich in adipose tissue developed a second IL-6 peak, which occurred between days 19-21 in the WtHR^{high} and VAT^{high} patients (*Figure 4B*). These results demonstrate that pro-inflammatory cytokines such as IL-6 are elevated in patients with abundant visceral fat.

Discussion

The CAR-T-related side effects CRS and ICANS represent a novel toxicity category in the 21st century armamentarium of cancer therapy. However, their underlying pathomechanisms remain incompletely understood. Here, we present the first comprehensive analysis of immunometabolically relevant tissues and their impact on CRS and ICANS in patients with advanced B-cell malignancies receiving CAR-T. Our data indicate that increased visceral adipose tissue is associated with CRS severity and early CRS onset. On the other hand, skeletal muscle mass measures did not impact CRS or ICANS occurrence.

The finding that visceral adipose tissue deposits drive differences in CRS severity is in line with previous reports demonstrating a strong association of VAT with obesity-associated metaflammation and the development of cardiovascular diseases and diabetes.^{24,25} The ‘obesity paradox’, meaning the unexpected inverse relationship between excess adipose tissue and immunotherapy efficacy, has been established for immune checkpoint blockade both in preclinical models and in cancer patients.⁴⁰⁻⁴¹ The observed therapeutic benefit in the excess weight population was further enhanced when immune-related ad-

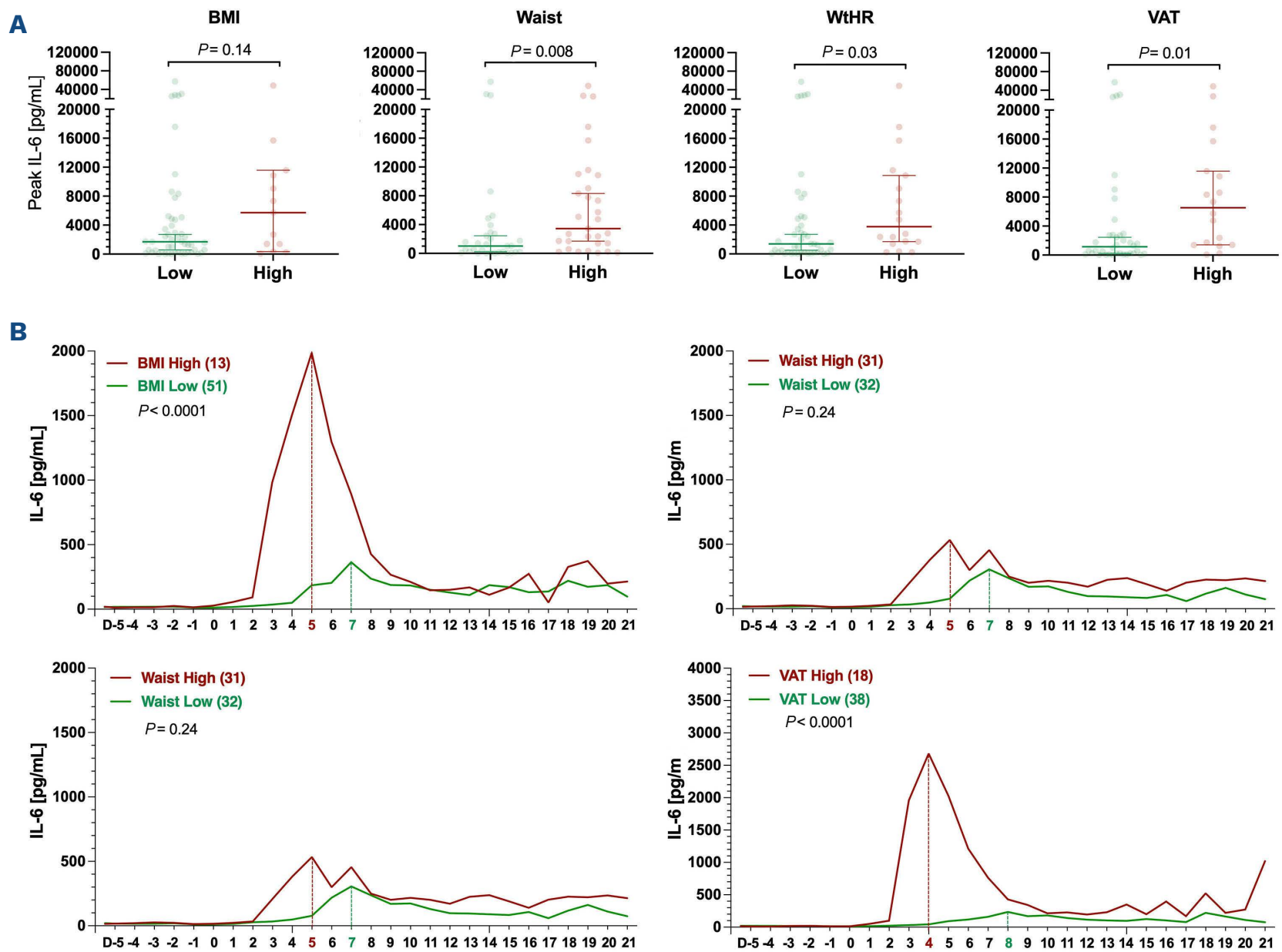


Figure 4. Adipose tissue correlates with peak interleukin 6 and interleukin 6 dynamics. (A) Peak interleukin 6 (IL-6) by body mass index (BMI), waist circumference (Waist), waist-to-height ratio (WtHR), and visceral adipose tissue (VAT) (from left to right). The previously established discriminatory values were used to distinguish high vs. low groups. (B) Aggregated median IL-6 values over time comparing BMI/Waist/WtHR/VAT^{high} vs. BMI/Waist/WtHR/VAT^{low} patients. The dotted vertical line indicates the median day of the peak for each group. Significance values were determined by two-way ANOVA considering both time and effect size.

verse events occurred.⁴² However, the impact of overweight and obesity on survival and toxicity has been more mixed in the context of BCL in the pre-CAR-T era. For example, improved outcomes were noted for overweight patients in first-line rituximab-containing chemotherapy regimens, though the opposite was observed in obese patients receiving autologous stem cell transplantation.^{43,44} One study analyzing the impact of body weight on clinical outcomes in R/R LBCL patients receiving CAR-T was negative, though detailed body composition analyses were not performed and only Axi-cel patients were included.⁴⁵ In our study, BC parameters negatively correlated with CRS onset, suggesting that overweight patients harbor a pro-inflammatory environment that predisposes them for earlier and more severe systemic inflammation. This would be consistent with prior studies establishing the role of adipose tissue as an endocrine organ with the potential of amplifying immune responses.²² Consistent with this hypothesis, the anthropometric body fat indices and VAT were all associated with elevated peak IL-6 serum

levels. VAT^{high} patients exhibited not only markedly increased peak IL-6 levels, but also a shorter time to peak IL-6, mirroring the clinical observation of an earlier CRS onset in VAT^{high} patients. While we did not observe a link between body composition and CRS duration, this may reflect early tocilizumab administration in this patient cohort, which may have blunted the natural CRS time course. Notably, IL-6 analyses revealed a second peak around day 19-21 for patients with excess body fat. Wei and colleagues propose a conceptual framework wherein a minimal IL-6 peak in week 3 coincides with the redistribution of CAR T-cells into the periphery in the absence of target cells.⁴⁶ Such redistribution results in the activation of tissue-resident immune cells such as macrophages or neutrophils, and may be potentiated by metaflammation-inherent feedback loops. The second peak also temporally coincides with the burgeoning hematopoietic recovery observed in the third week after CAR-T transfusion.⁴⁷ As diet can impact remodeling of the bone marrow niche and skew hematopoietic stem and

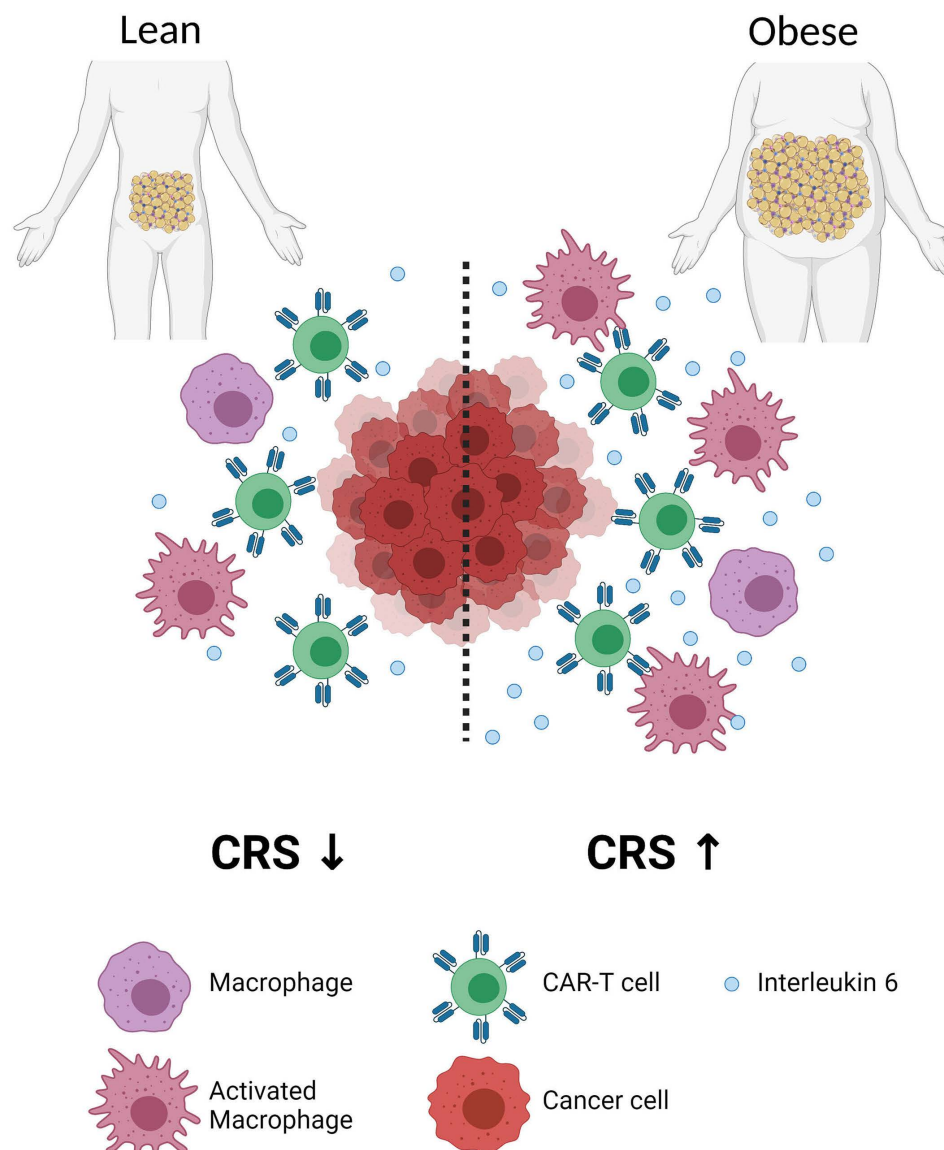


Figure 5. Proposed model of meta-inflammation as potentiating factor in cytokine release syndrome pathogenesis.

progenitor cell function,⁴⁸ this may indirectly affect inflammation cascades facilitated by mobilized immune cells – though this remains to be systematically studied in the context of CAR T-cell therapy.

Based on our results, we postulate that elevated visceral adipose tissue mass in overweight or obese CAR-T patients predisposes to more severe and earlier CRS. Furthermore, obesity-associated metaflammation with subsequent elevation of serum IL-6 levels may represent the potential link for the adipose tissue-induced effects (Figure 5). The relationship between obesity and IL-6 in the context of metaflammation has been extensively described, and is predominantly driven via IL-6 secretion by adipocytes and adipose-tissue macrophages.⁴⁹⁻⁵¹ Surprisingly, we found an association between adipose tissue and CRS in a patient cohort with very few obese patients as defined by World Health Organization criteria (BMI >30 kg/m², n=4). However, this may be explained by the long-lasting effect of metaflammation that can be preserved even after weight loss.⁵² Unfortunately, we did not have BMI data at the time of initial diagnosis for all patients to test this hypothesis. However, we expect that most patients were subject to weight loss due to their disease and treatment. Alternatively, even low amounts of adipose tis-

sue may be sufficient to facilitate a pro-immunogenic effect. Nevertheless, further prospective studies, preferably in patient cohorts with a higher percentage of obese patients, are needed to validate the role of overweight and obesity as a risk factor for severe CRS. If validated, anthropometric data like BMI and waist circumference may serve as an attractive auxiliary component in the risk-stratification tool box of the CAR-T treating physician due to the easy-to-measure nature of these parameters. For example, acquiring BC data requires only a tape measure and a scale, underlining clinical ease-of-use. This may be especially pertinent for patients who are fit enough to receive CAR-T in an outpatient setting.⁵³

In contrast to the interactions between adipose tissue and CRS, we did not find that skeletal muscle mass impacts CRS or ICANS. Although nearly half of our patients were defined as sarcopenic according to the published sarcopenia classifications,⁵⁴ CRS and ICANS severity was equally distributed between sarcopenic and non-sarcopenic patients. There are several potential explanations for this observation. First, patient numbers may have been too small to discern interactions between skeletal muscle and systemic inflammation. Second, previously described interactions between muscle mass and the immune sys-

tem were performed under stringent physiologic conditions or in the context of aging,⁵⁵ which may be negligible in the context of adoptive immunotherapies like CAR-T. Third, sarcopenia arises from a dysbalance in obesity-associated pro-inflammatory effects leading to muscle catabolism, as well as skeletal muscle-derived anti-inflammatory signaling resulting in muscle anabolism.³⁰ The pro-inflammatory effects of adipose tissue and concomitant metaflammation may outweigh the influence of skeletal muscle on immune reactions.

Limitations of this study include its retrospective and single-center design with a limited sample size. Additionally, only a small subset of the cohort was obese, making it difficult to generalize assumptions on obesity as a risk factor for CRS. Importantly, the results of the present study need to be validated in larger patient cohorts across multiple health care systems and institutions. This may lead to the development of a BC-based risk score for CRS in patients receiving CD19 CAR-T. Moreover, we have described optimal discriminatory thresholds for BC parameters, which may be integrated into existing risk models of CAR-T related immunotoxicity to improve diagnostic accuracy and predictive capacity.^{71,47,56} Such enhanced risk models can form the basis of interventional studies exploring how CAR-T toxicity and efficacy are impacted by early and/or prophylactic anti-cytokine therapies (e.g., tocilizumab, anakinra) or corticosteroids. Finally, further mechanistic exploration of (CAR) T-cell expansion and distribution of immune cell phenotypes in the context of elevated BMI or VAT appears warranted.

Still, these initial data provide evidence that BC and adipose tissue distribution matter in patients receiving T-cell based immune therapies. The finding that patients with an elevated BMI develop earlier and more severe CRS invites future translational research, and underlines how metaflammation may serve as a potentiating force in systemic inflammatory disorders.

Disclosures

KR has received research funding from Kite/Gilead. VB has received research funding from Kite/Gilead, BMS/Celgene and Janssen and consulted for Kite/Gilead and Novartis. VLB received research funding from BMS/Celgene, Miltenyi and Novartis; received honoraria and travel support from Amgen, Kite/Gilead, Novartis and Pfizer; consulted for Kite/Gilead, BMS/Celgene, Novartis and Pfizer; was part of speakers bureau for Novartis and Pfizer. CS work was funded by Bayer and Kite/Gilead; has received honoraria

and travel costs from BMS, Janssen, Kite/Gilead, Novartis and consulted for BMS, Kite/Gilead, Novartis and Takeda. MB received honoraria, was part of the speakers bureau of and consulted for MSD Sharpe & Dohme, Novartis, Roche, Kite/Gilead, BMS/Celgene, Astellas, Mologen and Miltenyi. ST received honoraria from and consulted for Amgen, BMS/Celgene, GSK, Janssen, Pfizer, Sanofi and Takeda. MS received honoraria, was part of speakers bureau and was funded by Amgen, BMS/Celgene, Gilead, Novartis; she further received funding from Miltenyi, MorphoSys, Roche; she received honoraria and research funding from Seattle Genetics, honoraria from Janssen and Pfizer and was part of speakers bureau for Pfizer and Takeda. All other authors have no conflicts of interest to disclose.

Contributions

DMCDS, KR, ST and MS designed the study and developed the concept; DMCDS, KR, MW, LL, PT, SG, VLB, VB, CS, WGK, MBB, ST, and MS carried out the research; DMCDS, KR, ST and MS performed the formal analysis and visualized the study; DMCDS, KR and LL developed the methodology; DMCDS, KR, ST and MS wrote the original draft; DMCDS, KR, MW, LL, VLB, VB, CS, WGK, MBB, ST and MS revised and edited the manuscript. All authors read and approved the final manuscript.

Acknowledgments

We are grateful for the support of all patients and the personnel of the LMU University Hospital who supported this work. Figure 1 and 5 were created with BioRender.com.

Funding

DMCDS, KR, VB received a fellowship from the School of Oncology of the German Cancer Consortium (DKTK). DMCDS received funding from Medical Faculty of Ludwig-Maximilians-University in Munich, Germany (FöFoLe Reg.-Nr. 1089). KR, VB and VLB were funded by the Else Kröner Forschungskolleg. LL received funding from the China Scholarship Council (grant no. 201908080031). PT and SG received a doctoral scholarship from Medical Faculty of Ludwig-Maximilians-University in Munich, Germany. This work was partly supported by the Deutsche Forschungsgemeinschaft (DFG, German Research Foundation, SFB-TRR 338/1 2021-452881907 to ST and MS).

Data-sharing statement

For original data and material, please contact the corresponding authors.

References

1. Maude SL, Laetsch TW, Buechner J, et al. Tisagenlecleucel in children and young adults with B-cell lymphoblastic leukemia. *N Engl J Med.* 2018;378(5):439-448.
2. Locke FL, Ghobadi A, Jacobson CA, et al. Long-term safety and

- activity of axicabtagene ciloleucel in refractory large B-cell lymphoma (ZUMA-1): a single-arm, multicentre, phase 1-2 trial. *Lancet Oncol.* 2019;20(1):31-42.
3. Schuster SJ, Bishop MR, Tam CS, et al. Tisagenlecleucel in adult relapsed or refractory diffuse large B-cell lymphoma. *N Engl J Med.* 2019;380(1):45-56.
 4. Wang M, Munoz J, Goy A, et al. KTE-X19 CAR T-cell therapy in relapsed or refractory mantle-cell lymphoma. *N Engl J Med.* 2020;382(14):1331-1342.
 5. Shimabukuro-Vornhagen A, Godel P, Subklewe M, et al. Cytokine release syndrome. *J Immunother Cancer.* 2018;6(1):56.
 6. Lee DW, Santomasso BD, Locke FL, et al. ASTCT consensus grading for cytokine release syndrome and neurologic toxicity associated with immune effector cells. *Biol Blood Marrow Transplant.* 2019;25(4):625-638.
 7. Greenbaum U, Strati P, Saliba RM, et al. CRP and ferritin in addition to the EASIX score predict CAR-T-related toxicity. *Blood Adv.* 2021;5(14):2799-2806.
 8. Morris EC, Neelapu SS, Giavridis T, Sadelain M. Cytokine release syndrome and associated neurotoxicity in cancer immunotherapy. *Nat Rev Immunol.* 2022;22(2):85-96.
 9. Brudno JN, Kochenderfer JN. Toxicities of chimeric antigen receptor T cells: recognition and management. *Blood.* 2016;127(26):3321-3330.
 10. Hay KA, Hanafi LA, Li D, et al. Kinetics and biomarkers of severe cytokine release syndrome after CD19 chimeric antigen receptor-modified T-cell therapy. *Blood.* 2017;130(21):2295-2306.
 11. Pennisi M, Sanchez-Escamilla M, Flynn JR, et al. Modified-EASIX predicts severe cytokine release syndrome and neurotoxicity after chimeric antigen receptor (CAR) T cells. *Blood Adv.* 2021;5(17):3397-3406.
 12. Nastoupil LJ, Jain MD, Feng L, et al. Standard-of-care axicabtagene ciloleucel for relapsed or refractory large B-cell lymphoma: results from the US lymphoma CAR T consortium. *J Clin Oncol.* 2020;38(27):3119-3128.
 13. Pasquini MC, Hu ZH, Curran K, et al. Real-world evidence of tisagenlecleucel for pediatric acute lymphoblastic leukemia and non-Hodgkin lymphoma. *Blood Adv.* 2020;4(21):5414-5424.
 14. Neelapu SS, Locke FL, Bartlett NL, et al. Axicabtagene ciloleucel CAR T-cell therapy in refractory large B-cell lymphoma. *N Engl J Med.* 2017;377(26):2531-2544.
 15. Karschnia P, Jordan JT, Forst DA, et al. Clinical presentation, management, and biomarkers of neurotoxicity after adoptive immunotherapy with CAR T cells. *Blood.* 2019;133(20):2212-2221.
 16. Gust J, Hay KA, Hanafi LA, et al. Endothelial activation and blood-brain barrier disruption in neurotoxicity after adoptive immunotherapy with CD19 CAR-T cells. *Cancer Discov.* 2017;7(12):1404-1419.
 17. Santomasso BD, Park JH, Salloum D, et al. Clinical and biological correlates of neurotoxicity associated with CAR T-cell therapy in patients with B-cell acute lymphoblastic leukemia. *Cancer Discov.* 2018;8(8):958-971.
 18. Strati P, Nastoupil LJ, Westin J, et al. Clinical and radiologic correlates of neurotoxicity after axicabtagene ciloleucel in large B-cell lymphoma. *Blood Adv.* 2020;4(16):3943-3951.
 19. Louie JK, Acosta M, Samuel MC, et al. A novel risk factor for a novel virus: obesity and 2009 pandemic influenza A (H1N1). *Clin Infect Dis.* 2011;52(3):301-312.
 20. Kolyva AS, Zolota V, Mpatsooulis D, et al. The role of obesity in the immune response during sepsis. *Nutr Diabetes.* 2014;4(9):e137.
 21. Petronilho F, Giustina AD, Nascimento DZ, et al. Obesity exacerbates sepsis-induced oxidative damage in organs. *Inflammation.* 2016;39(6):2062-2071.
 22. Hotamisligil GS. Inflammation, metaflammation and immunometabolic disorders. *Nature.* 2017;542(7640):177-185.
 23. Ferrante AW, Jr. The immune cells in adipose tissue. *Diabetes Obes Metab.* 2013;15(3):34-38.
 24. Ibrahim MM. Subcutaneous and visceral adipose tissue: structural and functional differences. *Obes Rev.* 2010;11(1):11-18.
 25. Misra A, Vikram NK. Clinical and pathophysiological consequences of abdominal adiposity and abdominal adipose tissue depots. *Nutrition.* 2003;19(5):457-466.
 26. Ansaldo AM, Montecucco F, Sahebkar A, Dallegri F, Carbone F. Epicardial adipose tissue and cardiovascular diseases. *Int J Cardiol.* 2019;278:254-260.
 27. Iacobellis G. Epicardial adipose tissue in endocrine and metabolic diseases. *Endocrine.* 2014;46(1):8-15.
 28. Smith SR, Lovejoy JC, Greenway F, et al. Contributions of total body fat, abdominal subcutaneous adipose tissue compartments, and visceral adipose tissue to the metabolic complications of obesity. *Metabolism.* 2001;50(4):425-435.
 29. Lundbom J, Hakkarainen A, Lundbom N, Taskinen MR. Deep subcutaneous adipose tissue is more saturated than superficial subcutaneous adipose tissue. *Int J Obes (Lond).* 2013;37(4):620-622.
 30. Nelke C, Dziewas R, Minnerup J, Meuth SG, Ruck T. Skeletal muscle as potential central link between sarcopenia and immune senescence. *EBioMedicine.* 2019;49:381-388.
 31. Rogeri PS, Gasparini SO, Martins GL, et al. Crosstalk between skeletal muscle and immune system: which roles do IL-6 and glutamine play? *Front Physiol.* 2020;11:582258.
 32. Giudice J, Taylor JM. Muscle as a paracrine and endocrine organ. *Curr Opin Pharmacol.* 2017;34:49-55.
 33. Conlon KC, Lugli E, Welles HC, et al. Redistribution, hyperproliferation, activation of natural killer cells and CD8 T cells, and cytokine production during first-in-human clinical trial of recombinant human interleukin-15 in patients with cancer. *J Clin Oncol.* 2015;33(1):74-82.
 34. Munoz-Canoves P, Scheele C, Pedersen BK, Serrano AL. Interleukin-6 myokine signaling in skeletal muscle: a double-edged sword? *FEBS J.* 2013;280(17):4131-4148.
 35. Duggal NA, Pollock RD, Lazarus NR, Harridge S, Lord JM. Major features of immunosenescence, including reduced thymic output, are ameliorated by high levels of physical activity in adulthood. *Aging Cell.* 2018;17(2):e12750.
 36. Gomez-Perez SL, Haus JM, Sheean P, et al. Measuring abdominal circumference and skeletal muscle from a single cross-sectional computed tomography image: a step-by-step guide for clinicians using National Institutes of Health ImageJ. *JPEN J Parenter Enteral Nutr.* 2016;40(3):308-318.
 37. Prado CM, Baracos VE, McCargar LJ, et al. Body composition as an independent determinant of 5-fluorouracil-based chemotherapy toxicity. *Clin Cancer Res.* 2007;13(11):3264-3268.
 38. Jayawardena E, Li D, Nakanishi R, et al. Non-contrast cardiac CT-based quantitative evaluation of epicardial and intra-thoracic fat in healthy, recently menopausal women: reproducibility data from the Kronos Early Estrogen Prevention Study. *J Cardiovasc Comput Tomogr.* 2020;14(1):55-59.
 39. Jain MD, Zhao H, Wang X, et al. Tumor interferon signaling and suppressive myeloid cells are associated with CAR T-cell failure in large B-cell lymphoma. *Blood.* 2021;137(19):2621-2633.
 40. Trestini I, Caldart A, Dodi A, et al. Body composition as a modulator of response to immunotherapy in lung cancer: time to deal with it. *ESMO Open.* 2021;6(2):100095.
 41. Cortellini A, Ricciuti B, Tiseo M, et al. Baseline BMI and BMI variation during first line pembrolizumab in NSCLC patients with a PD-L1 expression \geq 50%: a multicenter study with

- external validation. *J Immunother Cancer*. 2020;8(2):e001403.
42. Rogado J, Sanchez-Torres JM, Romero-Laorden N, et al. Immune-related adverse events predict the therapeutic efficacy of anti-PD-1 antibodies in cancer patients. *Eur J Cancer*. 2019;109:21-27.
43. Stevenson JKR, Qiao Y, Chan KKW, et al. Improved survival in overweight and obese patients with aggressive B-cell lymphoma treated with rituximab-containing chemotherapy for curative intent. *Leuk Lymphoma*. 2019;60(6):1399-1408.
44. Scheich S, Enssle JC, Mucke VT, et al. Obesity is associated with an impaired survival in lymphoma patients undergoing autologous stem cell transplantation. *PLoS One*. 2019;14(11):e0225035.
45. Wudhikarn K, Bansal R, Khurana A, et al. The impact of obesity and body weight on the outcome of patients with relapsed/refractory large B-cell lymphoma treated with axicabtagene ciloleucel. *Blood Cancer J*. 2021;11(7):124.
46. Wei J, Liu Y, Wang C, et al. The model of cytokine release syndrome in CAR T-cell treatment for B-cell non-Hodgkin lymphoma. *Signal Transduct Target Ther*. 2020;5(1):134.
47. Rejeski K, Perez A, Sesques P, et al. CAR-HEMATOTOX: a model for CAR T-cell-related hematologic toxicity in relapsed/refractory large B-cell lymphoma. *Blood*. 2021;138(24):2499-2513.
48. Emmons R, Niemi GM, De Lisio M. Hematopoiesis with obesity and exercise: role of the bone marrow niche. *Exerc Immunol Rev*. 2017;23:82-95.
49. Eder K, Baffy N, Falus A, Fulop AK. The major inflammatory mediator interleukin-6 and obesity. *Inflamm Res*. 2009;58(11):727-736.
50. Roytblat L, Rachinsky M, Fisher A, et al. Raised interleukin-6 levels in obese patients. *Obes Res*. 2000;8(9):673-675.
51. Fain JN, Madan AK, Hiler ML, Cheema P, Bahouth SW. Comparison of the release of adipokines by adipose tissue, adipose tissue matrix, and adipocytes from visceral and subcutaneous abdominal adipose tissues of obese humans. *Endocrinology*. 2004;145(5):2273-2282.
52. Christ A, Latz E. The Western lifestyle has lasting effects on metaflammation. *Nat Rev Immunol*. 2019;19(5):267-268.
53. Myers GD, Verneris MR, Goy A, Maziarz RT. Perspectives on outpatient administration of CAR-T cell therapy in aggressive B-cell lymphoma and acute lymphoblastic leukemia. *J Immunother Cancer*. 2021;9(4):e002056.
54. Martin L, Birdsell L, Macdonald N, et al. Cancer cachexia in the age of obesity: skeletal muscle depletion is a powerful prognostic factor, independent of body mass index. *J Clin Oncol*. 2013;31(12):1539-1547.
55. Cruz-Jentoft AJ, Bahat G, Bauer J, et al. Sarcopenia: revised European consensus on definition and diagnosis. *Age Ageing*. 2019;48(4):16-31.
56. Rubin DB, Al Jarrah A, Li K, et al. Clinical predictors of neurotoxicity after chimeric antigen receptor T-cell therapy. *JAMA Neurol*. 2020;77(12):1536-1542.

First-line treatment of chronic lymphocytic leukemia with ibrutinib plus obinutuzumab *versus* chlorambucil plus obinutuzumab: final analysis of the randomized, phase III iLLUMINATE trial

Carol Moreno,^{1,2} Richard Greil,³ Fatih Demirkan,⁴ Alessandra Tedeschi,⁵ Bertrand Anz,⁶ Loree Larratt,⁷ Martin Simkovic,⁸ Jan Novak,⁹ Vladimir Strugov,¹⁰ Devinder Gill,¹¹ John G. Gribben,¹² Kevin Kweij,¹³ Sandra Dai,¹³ Emily Hsu,¹³ James P. Dean¹³ and Ian W. Flinn¹⁴

¹Hospital de la Santa Creu i Sant Pau, Autonomous University of Barcelona, Barcelona, Spain; ²Josep Carreras Leukemia Research Institute, Barcelona, Spain; ³3rd Medical Department, Paracelsus Medical University, Salzburg Cancer Research Institute-CCCIT, Salzburg, Austria; ⁴Dokuz Eylul University, Division of Hematology, Izmir, Turkey; ⁵Niguarda Ca Granda Hospital, Milan, Italy; ⁶Tennessee Oncology, Chattanooga, TN, USA; ⁷University of Alberta Hospital, Edmonton, Alberta, Canada; ⁸Department of Internal Medicine, Haematology, University Hospital and Medical School Hradec, Králové, Czech Republic; ⁹University Hospital Kralovske Vinohrady and Third Faculty of Medicine, Charles University, Prague, Czech Republic; ¹⁰Almazov National Medical Research Centre, St. Petersburg, Russia; ¹¹Princess Alexandra Hospital, Brisbane, Queensland, Australia; ¹²Barts Cancer Institute, London, UK; ¹³Pharmacocyclics LLC, an AbbVie Company, Sunnyvale, CA, USA and ¹⁴Sarah Cannon Research Institute, Nashville, TN, USA

Correspondence: C. Moreno
cmoreno@santpau.cat

Received: May 5, 2021.
Accepted: November 4, 2021.
Prepublished: January 13, 2022.

<https://doi.org/10.3324/haematol.2021.279012>

©2022 Ferrata Storti Foundation

Published under a CC BY-NC license 

Abstract

iLLUMINATE is a randomized, open-label phase III study of ibrutinib plus obinutuzumab (n=113) *versus* chlorambucil plus obinutuzumab (n=116) as first-line therapy for patients with chronic lymphocytic leukemia or small lymphocytic lymphoma. Eligible patients were aged ≥ 65 years, or < 65 years with coexisting conditions. Patients received oral ibrutinib 420 mg once daily until disease progression or unacceptable toxicity or six cycles of oral chlorambucil, each in combination with six cycles of intravenous obinutuzumab. After a median follow-up of 45 months (range, 0.2-52), median progression-free survival continued to be significantly longer in the ibrutinib plus obinutuzumab arm than in the chlorambucil plus obinutuzumab arm (median not reached *versus* 22 months; hazard ratio=0.25; 95% confidence interval: 0.16-0.39; $P < 0.0001$). The best overall rate of undetectable minimal residual disease ($< 0.01\%$ by flow cytometry) remained higher with ibrutinib plus obinutuzumab (38%) than with chlorambucil plus obinutuzumab (25%). With a median treatment duration of 42 months, 13 months longer than the primary analysis, no new safety signals were identified for ibrutinib. As is typical for ibrutinib-based regimens, common grade ≥ 3 adverse events were most prevalent in the first 6 months of ibrutinib plus obinutuzumab treatment and generally decreased over time, except for hypertension. In this final analysis with up to 52 months of follow-up (median 45 months), ibrutinib plus obinutuzumab showed sustained clinical benefit, in terms of progression-free survival, in first-line treatment of chronic lymphocytic leukemia, including in patients with high-risk features. ClinicalTrials.gov identifier: NCT02264574.

Introduction

Over the past decade, the introduction of novel therapies targeting B-cell receptor signaling has shifted the treatment landscape for patients with chronic lymphocytic leukemia (CLL), including for patients with high-risk genomic features who previously had limited treatment options.¹ Ibrutinib is an oral, once-daily inhibitor of Bruton tyrosine kinase (BTK) approved for the treatment of pa-

tients with CLL, including in combination with the anti-CD20 monoclonal antibody obinutuzumab based on the primary results of the iLLUMINATE study.^{2,3} In two first-line studies ibrutinib or ibrutinib-based combination therapy was associated with superior progression-free survival (PFS) and overall survival (OS) compared with chlorambucil⁴ or fludarabine, cyclophosphamide, and rituximab (FCR)⁵ regimens in patients with CLL/small lymphocytic lymphoma (SLL). Ibrutinib (with or without rituximab) was also associated with superior PFS compared to benda-

mustine plus rituximab.⁶ With up to 7 years of follow-up (median: 74.9 months; range, 0.1–86.8) in the phase III RESONATE-2 study in patients with CLL aged ≥ 65 years, single-agent ibrutinib provided sustained PFS with extended follow-up, with a PFS of 61% at 6.5 years.^{4,7} Notably, in patients with high-risk genomic features such as del(17p)/TP53 mutation, del(11q), and unmutated immunoglobulin heavy-chain variable region gene (IGHV), which are known to be associated with inferior outcomes with chemoimmunotherapy,⁸ ibrutinib-based regimens have consistently achieved superior PFS *versus* established chemotherapy/chemoimmunotherapies and appear to confer comparable outcomes to those of ibrutinib-treated patients without these high-risk features.^{4,5,9,10}

The multicenter, randomized, phase III iLLUMINATE study was initiated to compare the efficacy of ibrutinib combined with obinutuzumab *versus* chlorambucil combined with obinutuzumab as first-line therapy for patients with CLL/SLL. Results from the primary analysis with a median follow-up of 31 months demonstrated that ibrutinib plus obinutuzumab significantly prolonged PFS compared with chlorambucil plus obinutuzumab as assessed by an independent review committee (median not reached vs. 19 months) as well as by the study investigators (median not reached vs. 22 months) in both the intention-to-treat population and in patients with high-risk genomic features.³

Here we report the final analysis of iLLUMINATE with a median follow-up of 45 months.

Methods

Study design

iLLUMINATE was a multicenter, randomized, open-label, phase III study that enrolled patients at 71 sites in Australia, New Zealand, Canada, Israel, Turkey, Russia, the European Union, and the USA (ClinicalTrials.gov identifier: NCT02264574). The study was conducted in accordance with the Declaration of Helsinki, the International Conference on Harmonisation Guidelines for Good Clinical Practice, and local regulations. The protocol was approved by the institutional review boards, research ethics boards, or independent ethics committees of participating institutions. All patients provided written informed consent. Full details of the study methodology have been published previously³ and are briefly described below.

Participants

Eligible patients had previously untreated CLL/SLL requiring treatment according to International Workshop on Chronic Lymphocytic Leukemia (iwCLL) criteria¹¹ and were aged ≥ 65 years or < 65 years with at least one of the following co-existing conditions: a cumulative illness rating

score > 6 , creatinine clearance < 70 mL/min, del(17p) confirmed by fluorescence *in situ* hybridization analysis, or TP53 mutation confirmed by next-generation sequencing. Additional eligibility criteria included an Eastern Cooperative Oncology Group (ECOG) performance status 0–2, measurable lymph node disease (longest diameter > 1.5 cm), adequate hematologic function (absolute neutrophil count $\geq 1 \times 10^9$ cells/L; platelet count $> 50 \times 10^9$ cells/L), and adequate hepatic and renal function.

Treatments

Patients were randomized 1:1 to receive ibrutinib plus obinutuzumab or chlorambucil plus obinutuzumab, as stratified by geographic region (North America vs. rest of world), ECOG performance status (0–1 vs. 2), and cytogenetic status (del[17p] vs. del[11q] without del[17p] vs. others [neither del11q nor del[17p]]). Patients received oral ibrutinib 420 mg once daily until disease progression or unacceptable toxicity or oral chlorambucil 0.5 mg/kg body weight on days 1 and 15 of each 28-day cycle for six cycles. Intravenous obinutuzumab (100 mg on day 1 and 900 mg on day 2, and 1,000 mg on days 8 and 15 of cycle 1, followed by 1,000 mg on day 1 of each subsequent 28-day cycle) was administered for up to six cycles.

Outcomes

The primary endpoint for the final analysis was PFS by investigator assessment based on iwCLL 2008 criteria with subsequent clarifications to account for treatment-related lymphocytosis.¹¹ Secondary endpoints included overall response rate (ORR; defined as complete response [CR], CR with incomplete bone marrow (BM) recovery [CRi], nodular partial response [nPR], or partial response [PR]), rate of undetectable minimal residual disease (MRD) (< 1 CLL cell per 10,000 leukocytes in peripheral blood (PB) and/or BM aspirate, as measured by central laboratory flow cytometry), OS, sustained hematologic improvement (continuous ≥ 2 g/dL increase in hemoglobin levels from baseline, or $\geq 50\%$ increase in platelet counts from baseline for ≥ 56 days without blood transfusion or growth factors), and safety. Responses were assessed by the investigator for the final analysis. Non-hematologic adverse events were graded using National Cancer Institute Common Terminology Criteria for Adverse Events, version 4.03; hematologic adverse events were assessed using iwCLL criteria.¹¹ Because the additional follow-up since the primary analysis extends beyond the adverse event reporting period for the chlorambucil plus obinutuzumab arm, safety findings are presented only for the ibrutinib plus obinutuzumab arm.

Results

Patient demographics and characteristics

Two hundred twenty-nine patients were randomized to receive ibrutinib plus obinutuzumab (n=113) or chlorambucil plus obinutuzumab (n=116). Patient baseline demographics and disease characteristics were generally comparable between treatment arms (*Online Supplementary Table S1*). The median age was 71 years (range, 40-87), with most patients (n=183; 80%) aged ≥ 65 years. Most patients (148 [65%]) had high-risk disease features of del(17p), TP53 mutation, del(11q), or unmutated IGHV.

Patient disposition and treatment

The final analysis was performed upon study completion. The median time on study was 45 months (range, 0.2-52 months) for the total study population, 45.5 months (range, 0.2-52 months) for the ibrutinib plus obinutuzumab arm, and 43 months (range, 1-52 months) for the chlorambucil plus obinutuzumab arm. With study completion, discontinuations across both arms were due to sponsor termination of the study (74%; n=170), death (18%; n=42), withdrawal of consent (6%; n=14), and other (1%; n=1 each: high dose of steroids, obinutuzumab allergy, and infusion reaction). Of patients treated with ibrutinib and obinutuzumab, 26 (23%) and 10 (9%) patients, respectively, discontinued these agents due to adverse events; notably, treatment duration in the ibrutinib plus obinutuzumab arm was longer than that in the chlorambucil plus obinutuzumab arm (median: 42 vs. 5 months). In the ibrutinib plus obinutuzumab arm, discontinuation of ibrutinib therapy due to disease progression was infrequent (n=5; 4%);

65 (58%) patients remained on ibrutinib until study completion (Table 1) and 100 (88%) patients completed six cycles of obinutuzumab (*Online Supplementary Figure S1*). In the chlorambucil plus obinutuzumab arm, 103 (89%) patients and 100 (86%) patients completed the planned six cycles of chlorambucil and obinutuzumab, respectively. Of the 116 patients randomized to chlorambucil plus obinutuzumab, 50 (43%) patients subsequently received ibrutinib with study crossover (n=45; 39%) or with commercial ibrutinib (n=6; 5%); one patient received both commercial and crossover ibrutinib. At study completion, 35 of the 45 crossover patients (78%) were still receiving single-agent ibrutinib.

All patients received concomitant medications during study treatment; in the ibrutinib plus obinutuzumab arm, 63/113 (56%) patients received any anticoagulant or antiplatelet agent; of these, 36/113 (32%) patients received anticoagulants and 48/113 (42%) received antiplatelet agents. Ninety-three of 113 patients (82%) received systemic antibacterial drugs. Of the 113 patients in the ibrutinib plus obinutuzumab arm, 78 (69%) received acid-reducing medications; 71/113 (63%) received proton pump inhibitors, 14/113 (12%) received H₂-receptor antagonists, and 8/113 (7%) received other acid-reducing agents.

Progression-free survival

At the final analysis, with a median follow-up of 45 months, PFS remained significantly longer in the ibrutinib plus obinutuzumab arm (median not reached; 95% confidence interval [95% CI], 49 months to not estimable [NE]) than in the chlorambucil plus obinutuzumab arm (22 months; 95% CI: 18-27 months), resulting in a 75%

Table 1. Summary of treatment disposition.

	Ibrutinib plus obinutuzumab (N=113)		Chlorambucil plus obinutuzumab (N=116)	
	Ibrutinib	Obinutuzumab	Chlorambucil	Obinutuzumab
Treatment status, N (%)				
Did not receive study drug	0	0	1 (1)	1 (1)
Completed/ongoing at study closure	65 (58)	100 (88)	103 (89)	100 (86)
Primary reason for discontinuation of study treatment, N (%)				
Disease progression	5 (4)	1 (1)	0	0
Adverse events	25 (22)	10 (9)	11 (9)	15 (13)
Death	5 (4)	0	0	0
Withdrawal of consent	6 (5)	1 (1)	0	0
Investigator decision	3 (3)	0	1 (1)	0
Other	4 (4)	1 (1)	0	0

reduction in the risk of disease progression or death with ibrutinib plus obinutuzumab (hazard ratio [HR]=0.25; 95% CI: 0.16-0.39; $P<0.0001$) (Figure 1). The estimated PFS at 42 months was 74% in the ibrutinib plus obinutuzumab arm and 33% in the chlorambucil plus obinutuzumab arm.

Similar to the overall population, there was a significant

PFS benefit for patients with high-risk features (del[17p], del[17p]/TP53 mutation, del[11q] and/or unmutated IGHV) treated with ibrutinib plus obinutuzumab versus chlorambucil plus obinutuzumab (HR=0.17; 95% CI: 0.10-0.28; $P<0.0001$). Within the high-risk population, PFS estimates at 42 months were significantly higher in the ibrutinib plus obinutuzumab arm than in the chlorambucil plus obinu-

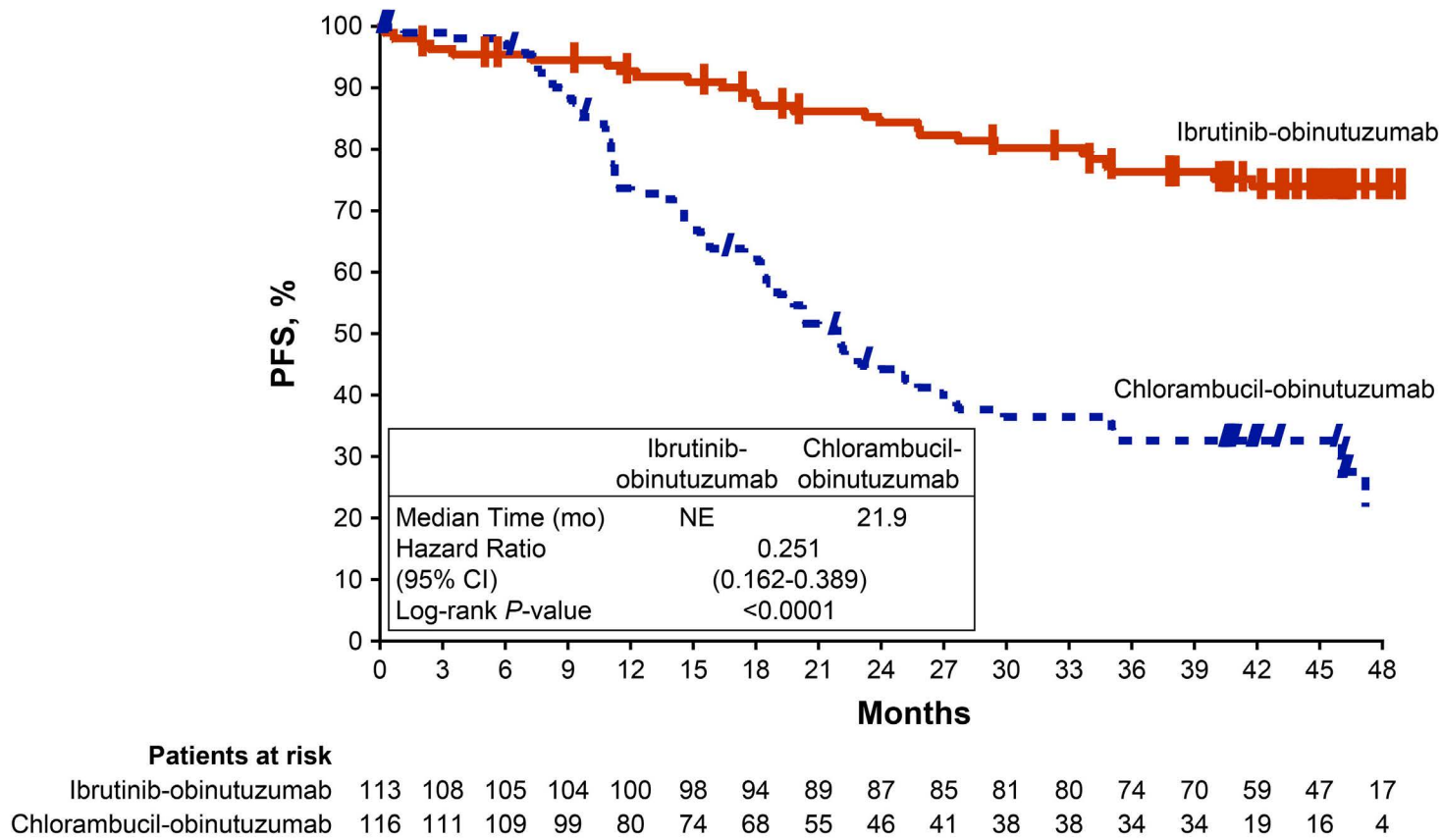


Figure 1. Progression-free survival per investigator assessment in the intention-to-treat population. CI: confidence interval; mo: months; NE, not estimable; PFS, progression-free survival.

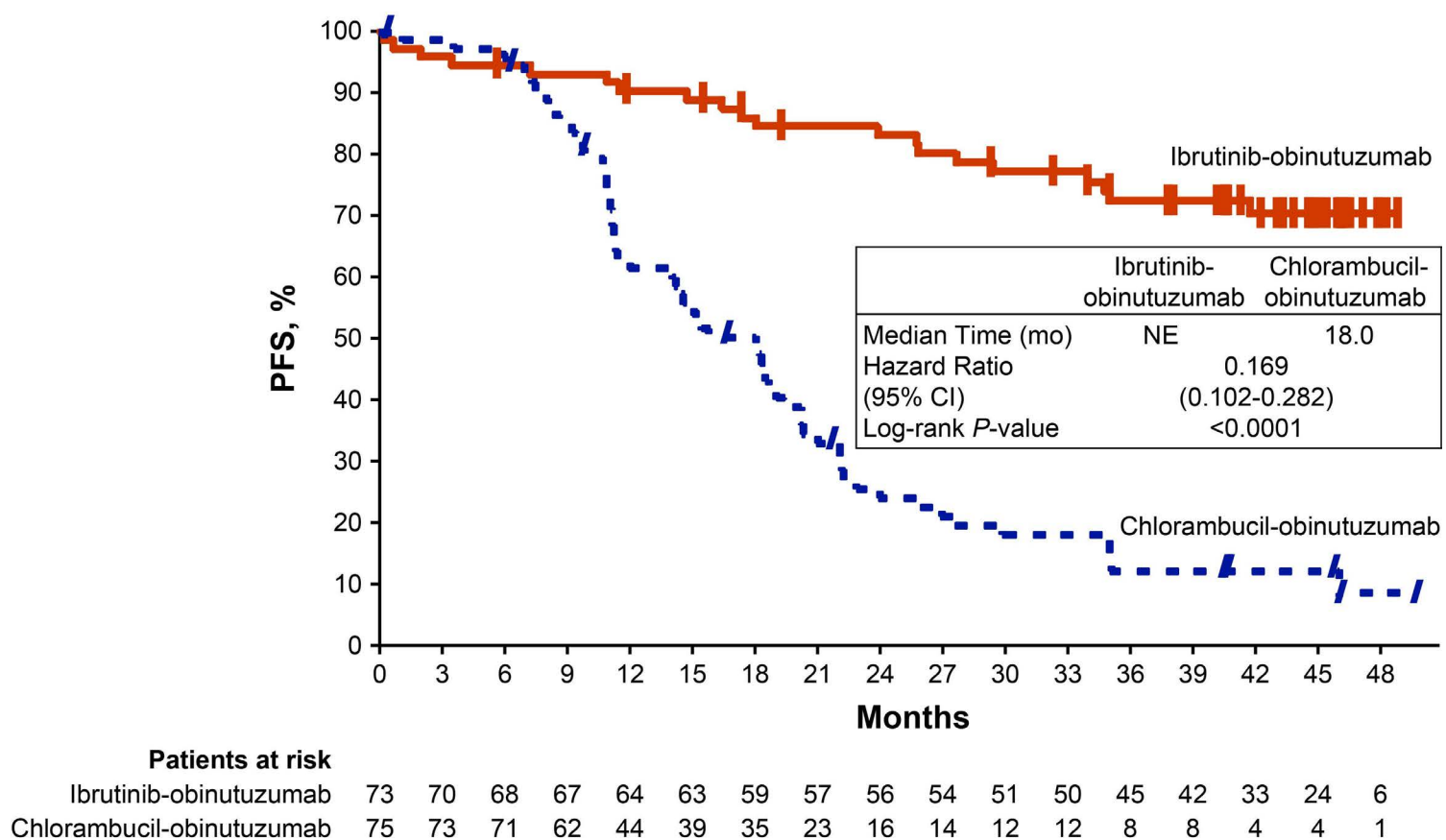


Figure 2. Progression-free survival per investigator assessment in the high-risk population of patients with del(17p), del(11q), TP53 mutations, and/or unmutated IGHV. CI: confidence interval; mo: months; NE: not estimable; PFS: progression-free survival.

tuzumab arm (70% vs. 12%). At 48 months, the PFS benefit was maintained since the time of the primary analysis at 30 months (70% vs. 77%, respectively) (Figure 2). The exclusion of patients with del(17p) did not affect 42-month PFS estimates for the rest of the high-risk population, which were 71% and 14%, respectively, for the two treatment arms (*Online Supplementary Figure S2*).

Likewise, a PFS benefit with ibrutinib plus obinutuzumab was observed irrespective of IGHV mutation status (Figure 3). Among patients with unmutated IGHV, up to 48 months median PFS was not reached with ibrutinib plus obinutuzumab versus 15 months with chlorambucil plus obinutuzumab (HR=0.17; 95% CI: 0.10-0.29). Whereas the median PFS was not reached in either treatment arm for patients with mutated IGHV, ibrutinib plus obinutuzumab significantly reduced the risk of progression or death in this subgroup (HR=0.20; 95% CI: 0.07-0.59). Within the ibrutinib plus obinutuzumab arm, the estimated PFS at 48 months was 67% and 89% for patients with unmutated and mutated IGHV, respectively. The PFS benefit

from ibrutinib plus obinutuzumab among both subgroups of unmutated and mutated IGHV patients persisted after excluding patients with del(17p) (unmutated: HR=0.17; 95% CI: 0.09-0.30; mutated: HR=0.25; 95% CI: 0.08-0.74) (*Online Supplementary Figure S3*). The hazard ratios of 0.20 and 0.17 observed in the mutated and unmutated IGHV subgroups of the ibrutinib plus obinutuzumab arm are consistent with the hazard ratio for the intention-to-treat population (HR=0.25) which includes other non-high-risk subgroups (Figure 1). *Online Supplementary Figure S4* depicts consistently superior PFS associated with ibrutinib plus obinutuzumab across various subgroups of patients defined by age, Rai stage, ECOG performance status, and bulky disease, in addition to specified genomic risk factors mentioned above.

In patients randomized to ibrutinib plus obinutuzumab, no significant difference in PFS was shown between patients with or without del(17p)/TP53 mutation (HR=0.93; 95% CI: 0.32-2.69; P=0.895) (Figure 4). The median PFS was not reached in either subgroup, with estimated 48-month PFS

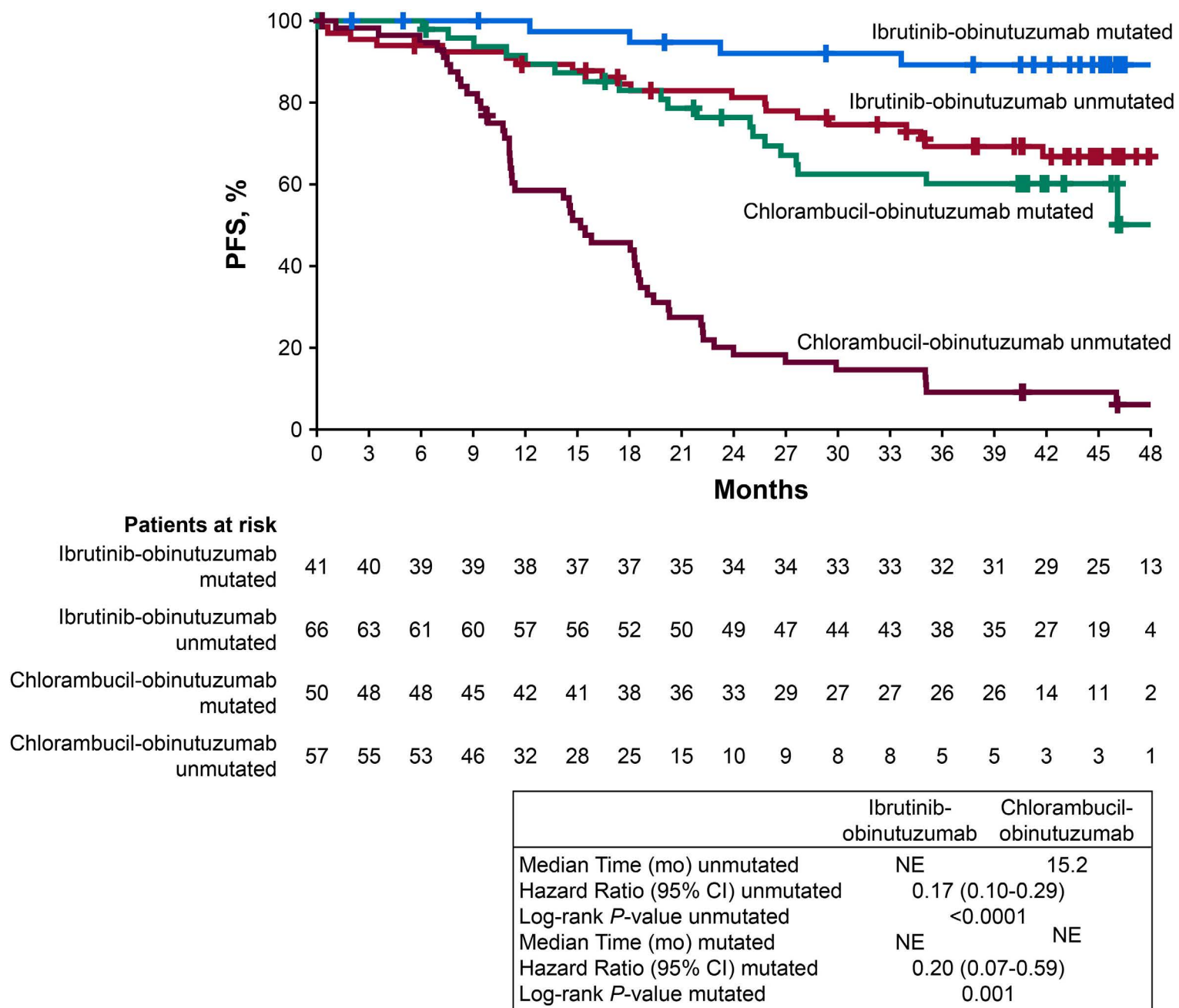


Figure 3. Progression-free survival per investigator assessment according to IGHV mutation status. CI: confidence interval; mo: months; NE, not estimable; PFS, progression-free survival.

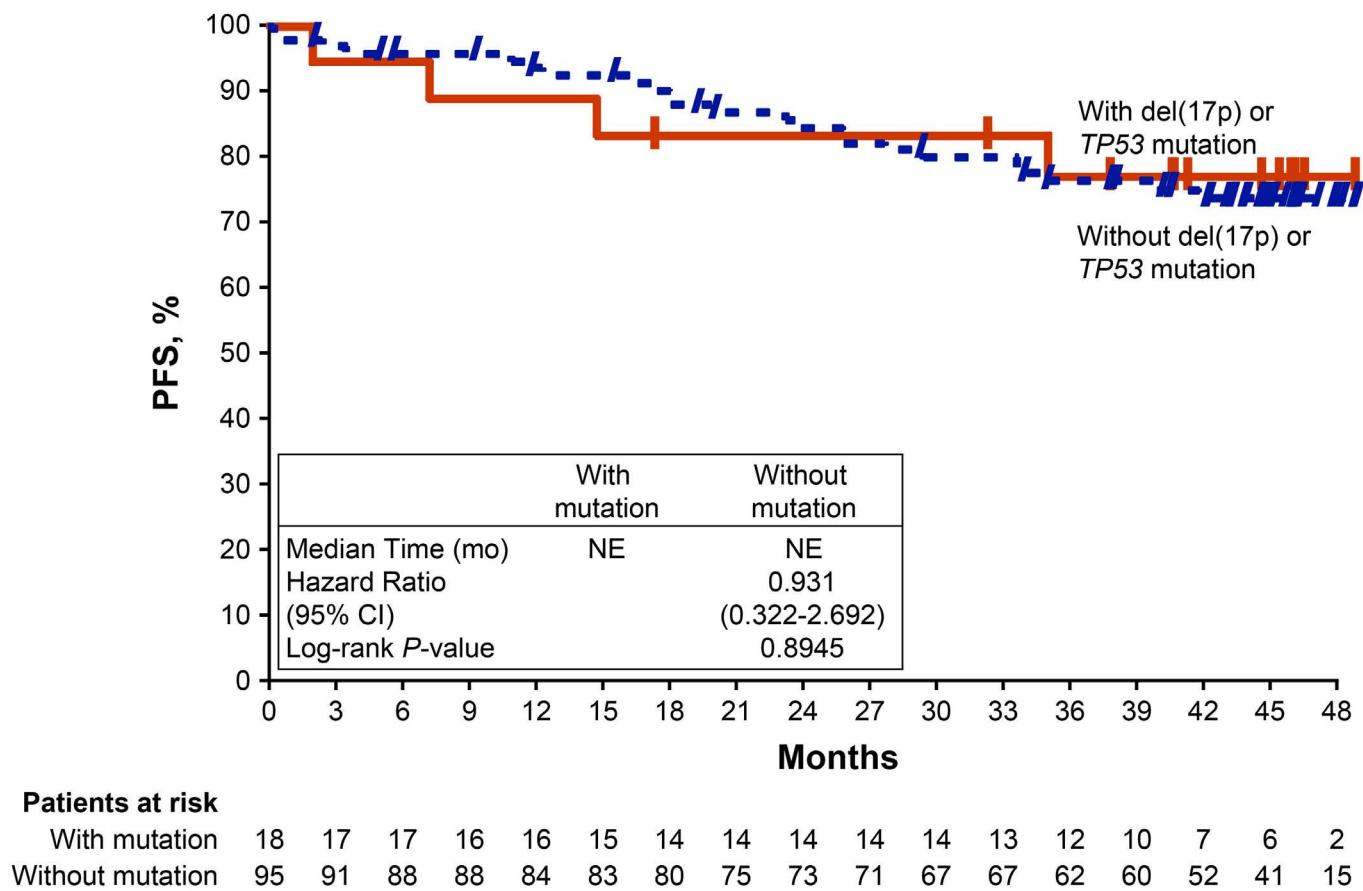


Figure 4. Progression-free survival per investigator assessment according to *TP53* aberration status (del[17p] or *TP53* mutation) in the ibrutinib plus obinutuzumab arm. CI: confidence interval; mo: months; NE, not estimable; PFS, progression-free survival.

rates of 77% and 74% in patients with and without del(17p)/*TP53* mutation, respectively.

Time to next treatment

Over a median follow-up of 45 months, fewer patients receiving ibrutinib plus obinutuzumab initiated subsequent treatment for CLL/SLL compared with those receiving chlorambucil plus obinutuzumab (3/113 [3%] vs. 55/116 [47%] patients, respectively). The median time to next treatment was not reached in the ibrutinib plus obinutuzumab arm compared with 33 months (95% CI: 24 months-NE) in the chlorambucil plus obinutuzumab arm, corresponding to a 96% reduction in the risk of needing next-line therapy (HR=0.04; 95% CI: 0.01-0.13; $P<0.0001$).

Response rates

Consistent with the primary analysis, the ORR by investigator assessment was higher in the ibrutinib plus obinutuzumab arm (n=103/113; 91%) than in the chlorambucil plus obinutuzumab arm (n=94/116; 81%) (Figure 5). CR rates, including CRi, in the ibrutinib plus obinutuzumab arm (47 [42%]) were slightly increased relative to rates reported at the primary analysis (46 [41%]); CR/CRi rates in the chlorambucil plus obinutuzumab arm were unchanged compared to those reported at the primary analysis (n=20 [17%]; $P<0.0001$ for the difference between arms). The median duration of response was not reached in the ibrutinib plus obinutuzumab arm (95% CI: NE-NE) and was 19 months (95% CI: 16-31) in the chlorambucil plus obinutuzumab arm.

Minimal residual disease

Initially MRD information was obtained from BM from all patients at cycle 9 and upon achieving CR, but subsequent protocol amendments enabled data collection from both BM and PB, and from all responders on a scheduled basis thereafter. Overall, MRD assessments were obtained from 101/113 patients on ibrutinib plus obinutuzumab (93 BM and 90 PB) and from 92/116 patients in the chlorambucil plus obinutuzumab arm (84 BM and 60 PB). Most patients with undetectable MRD (<0.01%) were subsequently followed with at least one repeat MRD assessment (91% for ibrutinib plus obinutuzumab; 86% for chlorambucil plus obinutuzumab), with a median follow-up of 23 and 30 months, respectively, following initial attainment of undetectable MRD. Overall, 38% (43/113) of patients in the ibrutinib plus obinutuzumab arm achieved undetectable MRD in BM or PB compared with 25% (29/116) in the chlorambucil plus obinutuzumab arm ($P=0.033$) (Online Supplementary Table S2). Rates of undetectable MRD for the ibrutinib plus obinutuzumab arm were 25% for BM (28/113) and 33% for PB (37/113); rates for the chlorambucil plus obinutuzumab arm were 17% (20/116) in BM and 20% (23/116) in PB. In these patients, the cumulative rate of undetectable MRD (<0.01%) increased over the first 3 years with continuous ibrutinib therapy and then remained stable through final analysis (Figure 6). As expected, given the differences in PFS for the two arms following initial attainment of undetectable MRD, 60% of patients receiving ibrutinib plus obinutuzumab maintained undetectable MRD status through last PB or BM testing compared to 31% of patients receiving

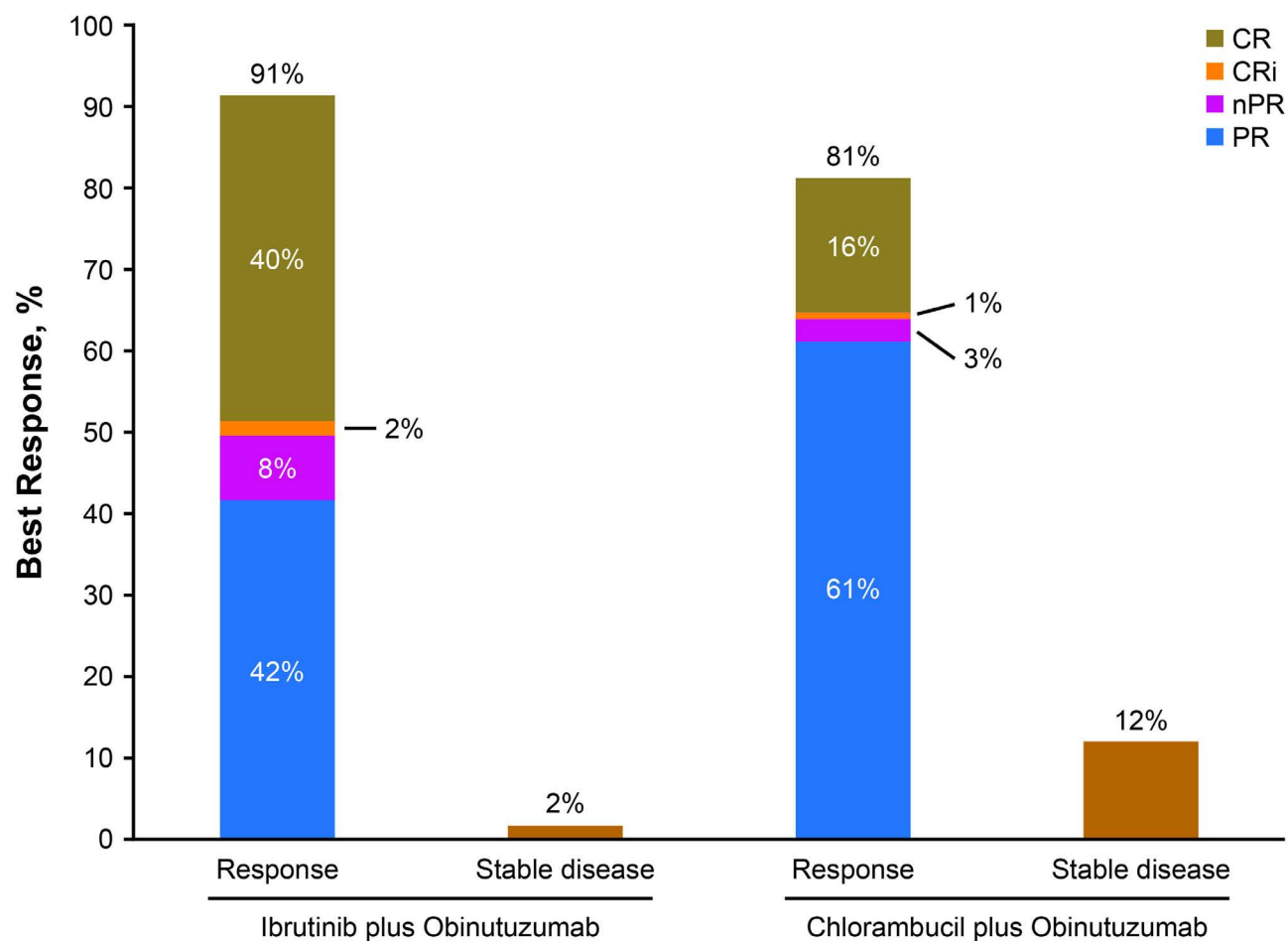


Figure 5. Best overall response per investigator assessment with ibrutinib plus obinutuzumab versus chlorambucil plus obinutuzumab. CR: complete response; CRi, complete response with incomplete bone marrow recovery; nPR, nodular partial response; PR, partial response.

ing chlorambucil plus obinutuzumab (*Online Supplementary Figure S5A*). The cumulative MRD relapse rate (defined as MRD $\geq 1\%$ after previously achieving undetectable MRD) was lower in the ibrutinib plus obinutuzumab group than in the chlorambucil plus obinutuzumab group (12% vs. 24%) and the median time to MRD relapse was not estimable (range, 0.03-44.2 months) in the ibrutinib plus obinutuzumab arm *versus* 37.5 months (range, 0.03-44.2 months) in the chlorambucil plus obinutuzumab arm.

Examined among patients who achieved a best response of CR/CRi with ibrutinib plus obinutuzumab, 28/47 patients (60%) had undetectable MRD while among those in the chlorambucil plus obinutuzumab arm achieving CR, 15/20 patients (75%) had undetectable MRD in PB or BM. By contrast, among patients who achieved a best response of PR/nPR, 14/56 patients had undetectable MRD levels in PB or BM in the ibrutinib plus obinutuzumab arm (25%) and 14/74 (19%) in the chlorambucil plus obinutuzumab arms. Although limited by the small number of evaluable patients, the median PFS was similar in patients with CR/CRi, regardless of MRD status (*Online Supplementary Figure S5B, C*); undetectable MRD trended to correlate positively with longer PFS in patients with PR/nPR, especially in the chlorambucil plus obinutuzumab arm.

Likewise, in the high-risk population, more than double the percentage of patients in the ibrutinib plus obinutuzumab arm maintained undetectable MRD than in the

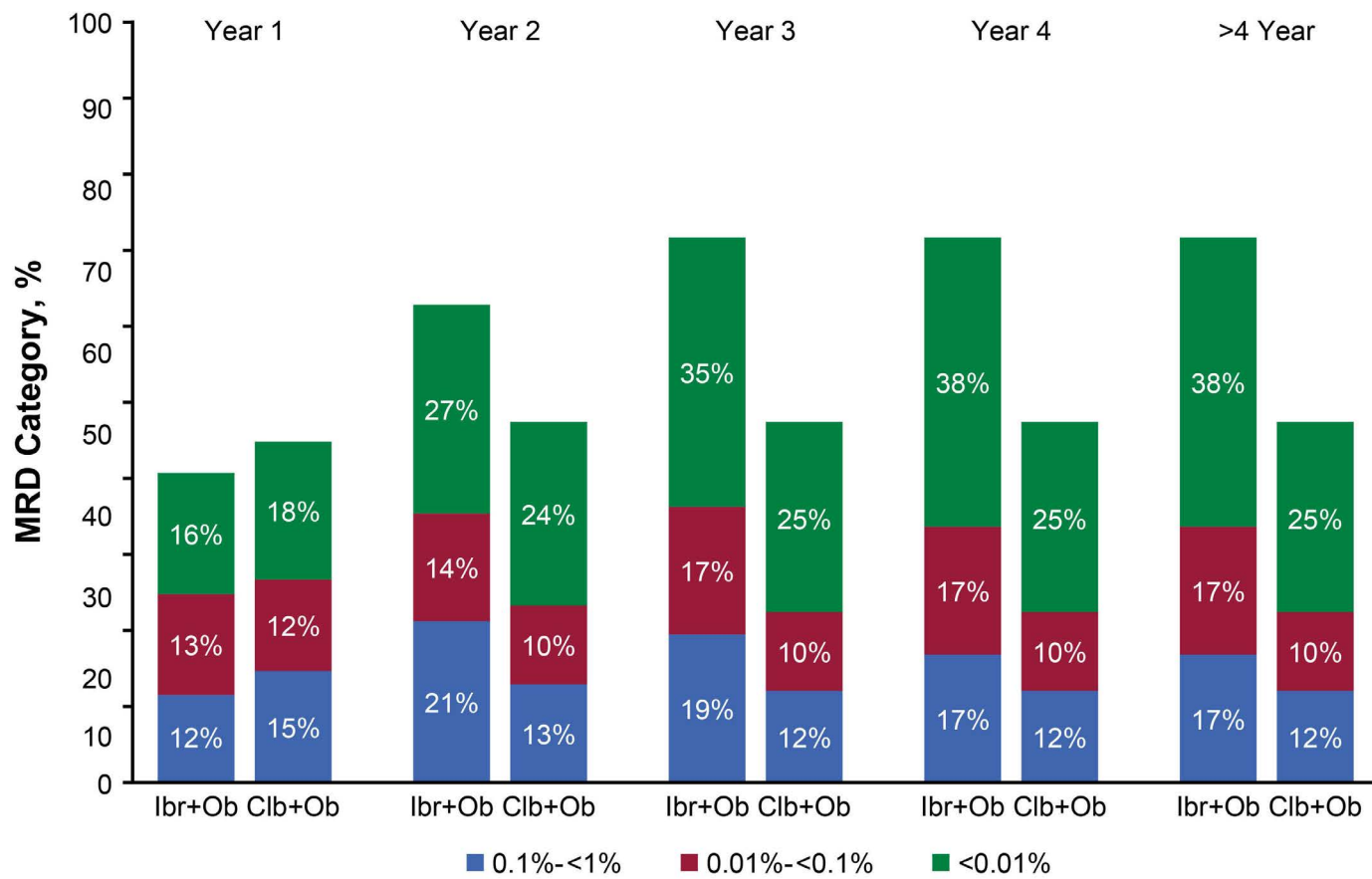
chlorambucil plus obinutuzumab group ([n=15/23]; 65% vs. [n=3/11]; 27%). In high-risk patients with >24 months of MRD follow-up, five of six patients (83%) in the ibrutinib plus obinutuzumab arm remain MRD negative compared with two of five patients (40%) in the chlorambucil plus obinutuzumab arm. As in the overall population, the cumulative MRD relapse rate in the high-risk population after achieving undetectable MRD was lower in the ibrutinib plus obinutuzumab group than in the chlorambucil plus obinutuzumab group (0%; [n=0/23] vs. 27%; [n=3/11]). The median time to MRD relapse was not estimable in either the ibrutinib plus obinutuzumab arm (range, 0.03-38.6 months) or the chlorambucil plus obinutuzumab arm (range, 0.03-33.4 months).

Overall survival

At the time of final analysis, the median OS was not reached in either treatment arm (HR=1.08; 95% CI: 0.60-1.97; $P=0.793$) (*Online Supplementary Figure S6*). Among the 45 patients who crossed-over to single-agent ibrutinib, the 24-month OS was 88% (95% CI: 74.0-94.9) and six deaths were reported (13%). Overall, 22 (19%) patients in the ibrutinib plus obinutuzumab arm and 21 (18%) patients in the chlorambucil plus obinutuzumab died during the study.

Adverse events in the ibrutinib plus obinutuzumab arm

At final analysis, the median duration of exposure to ibrutinib was 42 months (range, 0.1-52) in the ibrutinib



Time	Subjects with valid MRD by Year, n (%)		Cumulative Subjects with Valid MRD by Year, n (%)	
	Ibrutinib plus obinutuzumab (n=113)	Chlorambucil plus obinutuzumab (n=116)	Ibrutinib plus obinutuzumab (n=113)	Chlorambucil plus obinutuzumab (n=116)
Year 1	85 (75)	84 (72)	85 (75)	84 (72)
Year 2	72 (64)	46 (40)	98 (87)	89 (77)
Year 3	85 (75)	45 (39)	101 (89)	92 (79)
Year 4	67 (59)	31 (27)	101 (89)	92 (79)
Year >4	3 (3)	4 (3)	101 (89)	92 (79)

Figure 6. Cumulative rates of minimal residual disease over time (in bone marrow or peripheral blood). Clb: chlorambucil; Ibr: ibrutinib; MRD: minimal residual disease; Ob: obinutuzumab.

plus obinutuzumab group, which was 13 months longer than ibrutinib exposure at the primary analysis (median 29 months³); 73 patients (65%) received ≥ 3 years of ibrutinib and 18 (16%) received ≥ 4 years of ibrutinib therapy. All patients had completed or discontinued obinutuzumab (on both arms) and chlorambucil before the primary analysis, thus the median durations of treatment for obinutuzumab did not change since the primary analysis (4.6 months [range, 4.6-4.9] for the chlorambucil plus obinutuzumab group; 4.6 months [range, 4.6-4.7] for the ibrutinib plus obinutuzumab group).³ The median duration of treatment with chlorambucil was 5.1 months (range, 5.1-5.3) in the chlorambucil plus obinutuzumab group.³ With ongoing treatment in the ibrutinib plus obinutuzumab arm, no new safety signals were noted in this analysis relative to the primary analysis.³ With a median treatment exposure of 42 months in the ibrutinib plus obinutuzumab

arm, the most common adverse events (occurring in $\geq 10\%$ of patients in either arm) were neutropenia (44%), thrombocytopenia (35%), diarrhea (35%), cough (29%), infusion-related reaction (25%), and arthralgia (24%) (*Online Supplementary Table S3*). The most common grade ≥ 3 adverse events in the ibrutinib plus obinutuzumab arm were neutropenia (36%), thrombocytopenia (19%), pneumonia (9%), atrial fibrillation (6%), and febrile neutropenia (5%). The prevalence of these grade ≥ 3 adverse events was highest during the first 6 months of treatment with ibrutinib plus obinutuzumab and generally decreased over time, with the exception of hypertension (Figure 7). The prevalence of grade ≥ 3 hypertension was 2% (n=2/113), 3% (n=3/98), 4% (n=3/84), and 3% (n=2/74) in years 0-1, 1-2, 2-3, and 3-4, respectively. No patient discontinued ibrutinib therapy due to hypertension of any grade. The prevalence of any grade atrial fibrillation decreased, being 10%

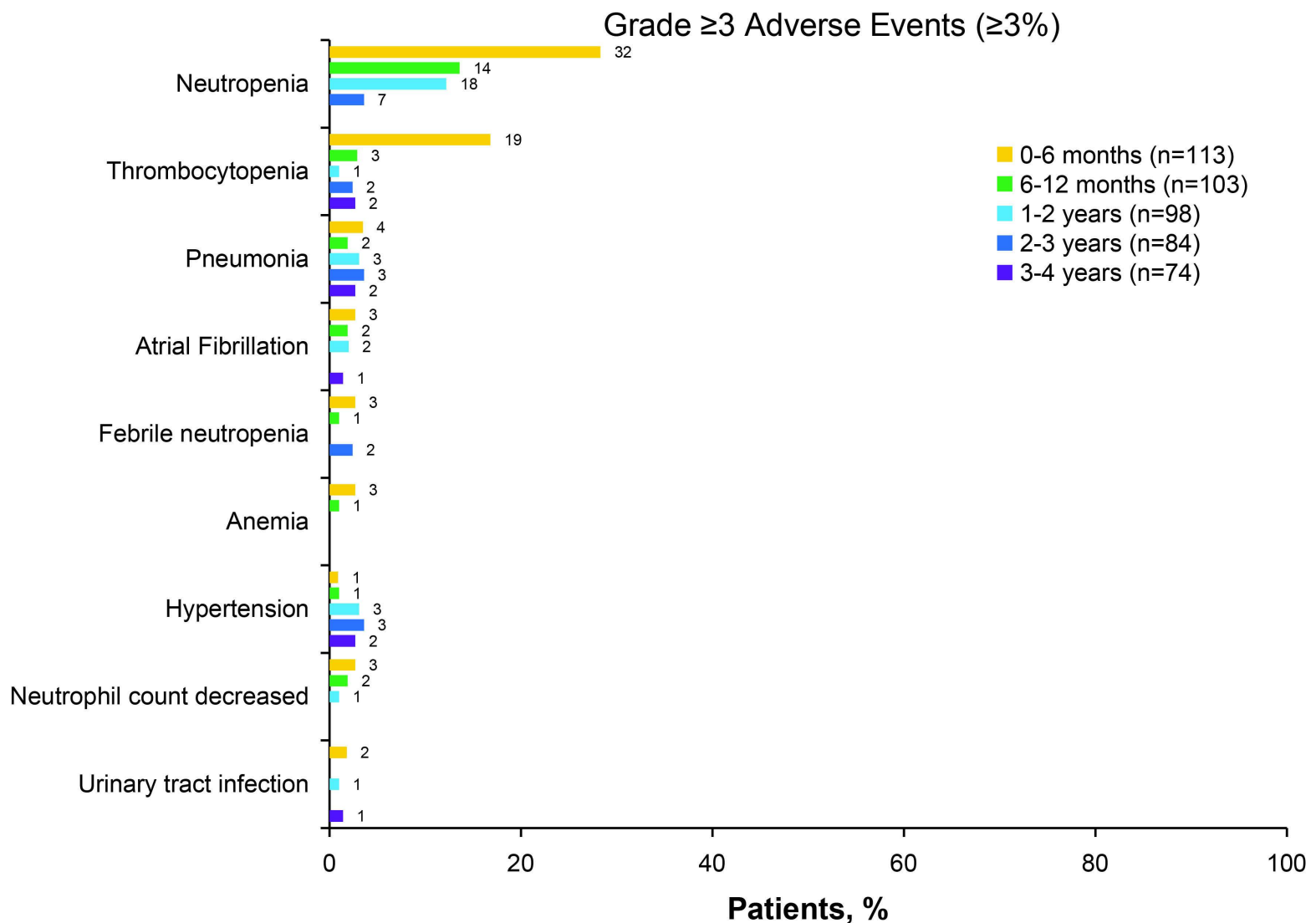
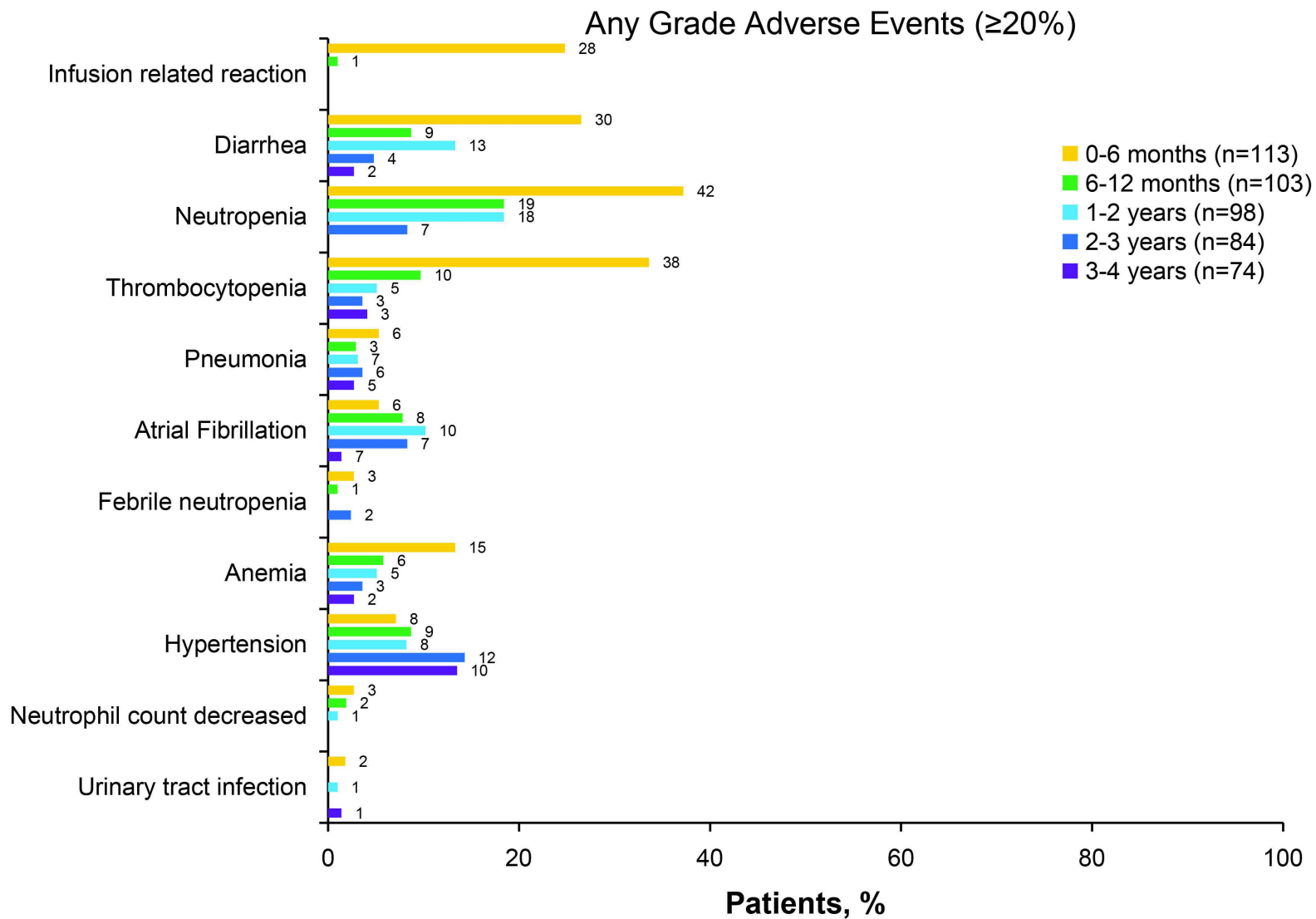


Figure 7. Prevalence of most common adverse events of any grade (≥20%) and grade ≥3 adverse events (≥3%) over time in patients treated with ibrutinib plus obinutuzumab.

(n=11/113), 10% (n=10/98), 8% (n=7/84), and 9% (n=7/74) in years 0-1, 1-2, 2-3, and 3-4, respectively; the prevalence of grade ≥ 3 atrial fibrillation was 4% (n=5/113), 2% (n=2/98), 0%, and 1% (n=1/74), in years 0-1, 1-2, 2-3, and 3-4, respectively. Among 17 patients with atrial fibrillation of any grade, atrial fibrillation led to discontinuation of ibrutinib in one patient (a grade 3 event).

Seven major hemorrhagic adverse events (grade 1/2 for 2 events, grade 3 for 5 events, and no grade 4/5 events) occurred in five (4%) patients in the ibrutinib plus obinutuzumab arm: catheter site hematoma, ecchymosis, hematemesis, hemoptysis, post-procedural hematoma, subdural hematoma, and traumatic hematoma. Major hemorrhage led to discontinuation of ibrutinib in one patient (grade 2 hemoptysis).

Over a median duration of 42 months of ibrutinib therapy, the only adverse event leading to discontinuation of ibrutinib in more than one patient was thrombocytopenia (n=2); all other adverse events leading to discontinuation of ibrutinib occurred in only one patient each. Of these, seven and six patients discontinued during the first 6 and 12 months of treatment, respectively. Four patients each discontinued at time intervals of >12– \leq 24 months, >24– \leq 36 months, and >36– \leq 48 months.

In the ibrutinib plus obinutuzumab arm, 17 (15%) patients experienced a total of 32 adverse events (including 18 grade ≥ 3 events) that led to ibrutinib dose reduction, most commonly due to neutropenia (6 [5%] patients) (*Online Supplementary Figure S7*). Most (28/32 [88%]) of these adverse events resolved or recovered with dose reduction, including 94% (17/18) of grade ≥ 3 events.

At the time of final analysis, 14 and three patients had died from treatment-emergent adverse events in the ibrutinib plus obinutuzumab and chlorambucil plus obinutuzumab arms, respectively (*Online Supplementary Table S4*). Of the five deaths that occurred in the ibrutinib plus obinutuzumab arm with the additional follow-up, four were due to adverse events (1 each due to respiratory tract infection, pneumonia, septic shock and one death was due to an unknown cause after the adverse event reporting period). In the chlorambucil plus obinutuzumab arm, an additional two deaths occurred since the primary analysis, after crossover to the ibrutinib plus obinutuzumab arm. One was due to sepsis, the other was due to progressive disease.

Outcomes after discontinuation of ibrutinib

Thirty-eight patients discontinued ibrutinib after a median of 15.5 months (range, 0.1–43.7) of treatment for reasons other than progression or death at any time on study, 25 patients discontinued due to adverse events (Table 1). Among patients who discontinued ibrutinib for reasons other than progressive disease or death, eight patients had achieved a CR or CRi, 22 patients had PR or nPR, and

one patient had stable disease; seven patients had no opportunity for response assessment. With a median follow-up of 17 months (range, 0.03–42) after ibrutinib discontinuation, 18-month PFS in these 38 patients who discontinued for reasons other than progression or death was 73.8% (95% CI: 55.4–85.5).

Discussion

Results from the final analysis of the iLLUMINATE study with up to 52 months of follow-up (median: 45 months) confirmed the durable efficacy of ibrutinib plus obinutuzumab in previously untreated patients with CLL. Ibrutinib plus obinutuzumab resulted in sustained PFS compared to chlorambucil plus obinutuzumab, with median PFS not reached after a median follow-up of 45 months and the risk of disease progression or death reduced by 75%. Notably, durable PFS was also seen in the high-risk patient population (i.e., with del[17p], TP53 mutation, del[11q], or unmutated IGHV) treated with ibrutinib plus obinutuzumab, confirming earlier observations from the primary analysis of iLLUMINATE.³ At 42 months, the PFS estimates among patients with del(17p), TP53, unmutated IGHV or del(11q) mutations were significantly higher in the ibrutinib plus obinutuzumab arm than in the chlorambucil plus obinutuzumab arm. Importantly, the benefit in PFS was observed regardless of high-risk features.³ A similar benefit was observed in the CLL14 trial for the venetoclax plus obinutuzumab regimen in patients with unmutated and mutated IGHV.¹² These results support current global consensus guidelines,^{13,14} noting ibrutinib as a preferred therapeutic regimen for older patients and/or those with comorbidities regardless of the presence of del(17p)/TP53 mutations and unmutated CLL. The follow-up for other, similarly recommended novel treatment options is more limited.

With this extended follow-up, as has been observed consistently across several large, randomized phase III studies of ibrutinib in previously untreated¹⁵ and relapsed/refractory patients with CLL/SLL,^{16,17} highly durable PFS and OS have been confirmed even in patients with high-risk disease characteristics.

In line with the results of the iLLUMINATE trial, other phase III studies have also reported the superiority of ibrutinib-based regimens over chemoimmunotherapy in the first-line treatment of CLL. Concurrently, in the phase III ALLIANCE 041202 study in patients with CLL aged ≥ 65 years (median follow-up: 38 months), first-line single-agent ibrutinib or ibrutinib plus rituximab significantly prolonged PFS compared with bendamustine plus rituximab; estimated 2-year PFS rates were 87% and 88% versus 74%, respectively.⁶ In patients aged ≤ 70 years, the phase III ECOG1912 study (median follow-up: 34 months)

demonstrated that first-line treatment with ibrutinib plus rituximab resulted in significantly longer PFS (3-year rate 89% vs. 73%) and OS (3-year rate 99% vs. 92%) compared with FCR.⁵ With additional follow-up (median: 45 months), PFS favored ibrutinib plus rituximab over FCR (HR=0.39; 95% CI: 0.26-0.57; $P<0.0001$).¹⁸

With additional follow-up since the primary analysis of iLLUMINATE, the percentage of patients treated with ibrutinib plus obinutuzumab achieving undetectable MRD increased (from 34.5% at primary analysis to 38.1% at final analysis), demonstrating deepening of remission with continued ibrutinib treatment. Furthermore, fewer patients in the ibrutinib arm experienced MRD relapse, with approximately 60% of patients maintaining undetectable MRD at a median follow-up of 2 years after first attaining undetectable MRD status. Due to the small numbers of patients in the subgroups, the association between MRD status and PFS was not further studied.

Few patients discontinued treatment during the additional 13 months of follow-up after the primary analysis ($n=14$), and no new safety signals were reported with ongoing ibrutinib treatment. This is consistent with prior reports that rates of most adverse events are highest during the first year of ibrutinib-based treatment and decrease in frequency thereafter.^{4,9,19,20} Most patients had improvement or resolution of adverse events following dose reduction, suggesting that many such events are managed effectively by dose modification, allowing patients to stay on therapy and continue to maintain disease control. The discontinuation rate due to adverse events (22%) is comparable to that for first-line, single-agent ibrutinib after 4 years of follow-up in the RESONATE-2 study (19%)⁴ and is supported by real-world studies showing that treatment discontinuation is similar in patients with CLL/SLL receiving single-agent ibrutinib or ibrutinib-based combination therapy.²¹

Overall, first-line ibrutinib plus obinutuzumab was well tolerated, which is important given that the median age at diagnosis of CLL is over 70 years,²² a demographic that often presents with comorbidities that preclude the use of chemotherapy-containing regimens. In patients receiving concomitant medications, ibrutinib was well tolerated. Notably, ibrutinib can be co-administered with acid-reducing medications, offering an advantage over other kinase inhibitors known to have drug-drug interactions with acid-reducing agents.²³ Overall, these results strengthen and build upon the broad experience with ibrutinib.

Several studies have assessed whether adding anti-CD20 therapy to ibrutinib results in a clinically relevant improvement in efficacy in CLL.^{5,6,24} Evidence suggests that addition of anti-CD20 therapy to ibrutinib may increase depth of response and decrease the time to absolute lymphocyte count normalization relative to single-agent ibrutinib therapy, although survival outcomes have not been sig-

nificantly improved over the impressive results with single-agent ibrutinib.^{6,24,25} The lack of data showing quality of life or survival outcome benefits notwithstanding, the addition of an anti-CD20 agent may nonetheless provide reassurance for patients concerned with increased absolute lymphocyte count. In a cross-trial comparison of RESONATE-2 and iLLUMINATE, patients treated with ibrutinib plus obinutuzumab combination therapy had higher CR/CRi rates (44% vs. 27%; $P=0.006$) and shorter time to absolute lymphocyte count normalization (8 vs. 55 weeks) than patients treated with single-agent ibrutinib.²⁵ Compared to single-agent ibrutinib, the combination of ibrutinib plus rituximab was demonstrated by Burger et al. to improve CR/CRi rates (particularly in the first-line setting: 50% vs. 20%) and shortened time to absolute lymphocyte count normalization (24 vs. 48 weeks) in a phase II study with a median follow-up of 36 months.²⁴ In the phase III ALLIANCE 041202 study, the CR rates (12% and 7%) and rates of undetectable MRD (4% and 1%) were slightly higher with ibrutinib plus rituximab than with single-agent ibrutinib.⁶ The difference in response rates tended to be greater in patients with high-risk disease, suggesting that combination therapy may be most useful for patients with high-risk or bulky disease.²⁴ In the relapsed/refractory high-risk setting, the GENUINE study demonstrated significantly higher ORR with ublituximab plus ibrutinib compared to single-agent ibrutinib after a median follow-up of 41.6 months (83% vs. 65%; $P=0.02$).²⁶ In the setting of other BTK inhibitors, the ELEVATE-TN study reported investigator-assessed CR/CRi rates of 24% with acalabrutinib plus obinutuzumab compared to 8% for acalabrutinib monotherapy and 13% for obinutuzumab plus chlorambucil.²⁷

In terms of PFS, 48-month estimates between RESONATE-2 and the current study were similar across ibrutinib-based treatment arms (76% vs. 74%), although it is worth noting that the current study included patients with high-risk genomic features whereas RESONATE-2 excluded those with del17p.^{4,10} Regardless, these broad clinical data clearly refute preclinical hypotheses of ibrutinib negating anti-CD20 efficacy, although anti-CD20 use may be important to optimize efficacy of other BTK inhibitors.²⁷

In conclusion, ibrutinib plus obinutuzumab remains an effective chemotherapy-free regimen for patients with CLL/SLL that provides sustained efficacy and significantly reduces the risk of disease progression or death compared with chlorambucil plus obinutuzumab, including in patients with high-risk genomic features. With ongoing once-daily dosing, long-term ibrutinib therapy was well tolerated with no new safety signals observed.

Disclosures

CM has provided consulting/advisory services for Janssen, AbbVie, AstraZeneca, and BeiGene; has received research

funding from AbbVie and Janssen; and participated in speakers bureaus for AbbVie and Janssen. RG has received honoraria from Celgene, Roche, Merck, AstraZeneca, Novartis, Amgen, Bristol Myers Squibb, Merck Sharp & Dohme, Sandoz, AbbVie, Gilead, and Daiichi Sankyo; has provided consulting/advisory services for Celgene, Novartis, Roche, Bristol Myers Squibb, Takeda, AbbVie, AstraZeneca, Janssen, Merck Sharp & Dohme, Merck, Gilead, and Daiichi Sankyo; has received research funding from Celgene, Merck, Takeda, AstraZeneca, Novartis, Amgen, Bristol Myers Squibb, Merck Sharp & Dohme, Sandoz, Gilead, and Roche; has received travel or accommodation funds from Roche, Amgen, Janssen, AstraZeneca, Novartis, Merck Sharp & Dohme, Celgene, Gilead, Bristol Myers Squibb, and AbbVie. FD has had a consulting/advisory role for AbbVie, AstraZeneca, Roche, and Amgen; has received research funding from AbbVie, Janssen, Pharmacyclics LLC, an AbbVie company, and AstraZeneca; has participated in speakers bureaus for Janssen, AbbVie, and Amgen; and has received travel or accommodation expenses from Amgen, Janssen, AbbVie, and Pfizer. AT has received honoraria from Janssen, AbbVie, AstraZeneca, and BeiGene; and has participated in speakers bureaus for Janssen, BeiGene, AstraZeneca, and AbbVie. BA has nothing to disclose. LL has provided consulting/advisory services for AbbVie and Janssen. MS has received honoraria from AbbVie, Roche, Janssen-Cilag, Gilead, and Acerta Pharma; has played a consulting/advisory role for AbbVie; has participated in speakers bureaus for AbbVie, Roche, Janssen-Cilag, and Gilead; and has received travel or accommodation expenses from AbbVie, Roche, Janssen-Cilag, and Gilead. JN has played a consulting/advisory role for Amgen, Takeda, Roche, Celgene, Pfizer, and Novartis; and has received travel or accommodation expenses from Amgen and Janssen. VS is employed by Eco-Safety Medical Center; has stock ownership in Portola Pharmaceuticals, Gilead, Moderna, and Clovis Oncology; has received research funding from Janssen; and has received travel or accommodation expenses from AbbVie and Janssen. DG has received honoraria from Janssen-Cilag; and has played a consulting/advisory role for Janssen-Cilag. JGG has received honoraria from AbbVie, Roche, Bristol Myers Squibb, Janssen, and AstraZeneca; has provided consulting/advisory services for AbbVie, Janssen, and Gilead; and received research funding from Janssen, AstraZeneca, and Celgene. KK is employed by Pharmacyclics LLC, an AbbVie Company; and owns stock in Pharmacyclics LLC, an AbbVie Company, and Gilead. SD has been employed by Pharmacyclics LLC, an AbbVie Company, and Horizon Therapeutics; and has stock ownership in AbbVie, Bristol Myers Squibb, Gilead, GlaxoSmithKline, Exelixis, Revance, Horizon Therapeutics,

and Myovant Science. EH and JPD are employed by Pharmacyclics LLC, an AbbVie Company; and own stock in AbbVie. IWF has provided consulting/advisory services for AbbVie, AstraZeneca, BeiGene, Genentech, Gilead, Great Point Partners, Iksuda Therapeutics, Janssen, Juno Therapeutics, Kite Pharma, MorphoSys, Nurix Therapeutics, Pharmacyclics LLC, an AbbVie Company, Roche, Seattle Genetics, Takeda, TG Therapeutics, Unum Therapeutics, Verastem, and Yingli Pharma; and has received research funding from AbbVie, Acerta Pharma, Agios, ArQule, AstraZeneca, BeiGene, Calithera Biosciences, Celgene, Constellation Pharmaceuticals, Curis, Forma Therapeutics, Forty Seven, Genentech, Gilead, IGM Biosciences, Incyte, Infinity Pharmaceuticals, Janssen, Juno Therapeutics, Karyopharm Therapeutics, Kite Pharma, Loxo, Merck, MorphoSys, Novartis, Pfizer, Pharmacyclics LLC, an AbbVie Company, Portola Pharmaceuticals, Rhizen Pharmaceuticals, Roche, Seattle Genetics, Takeda, Teva, TG Therapeutics, Trillium Therapeutics, Triphase Pharma, Unum Therapeutics, and Verastem.

Contributions

As members of the Steering Committee, CM, DG, JGG, and IWF collaborated with the study sponsors to design the study and protocol; CM, RG, RD, AT, BA, LL, MS, JN, VS, DG, JGG, and IWF collected the study data; SD analyzed the data; KK collected and tested the high-risk genomic factor data for the study; SD, EH, and JD confirmed the accuracy of the data and compiled it for analysis. All authors had access to the data and were involved in the interpretation of data, contributed to the manuscript review and revisions, and approved the final version for submission.

Acknowledgments

The authors thank the patients who participated in this trial and their families. The authors also thank Cindi A. Hoover, PhD, for medical writing, which was supported by Pharmacyclics LLC, an AbbVie Company.

Funding

Pharmacyclics LLC, an AbbVie Company, sponsored and designed the study. Study investigators and their research teams collected the data. The sponsor confirmed data accuracy and analyzed the data. Medical writing was funded by the sponsor.

Data-sharing statement

Requests for access to individual participant data from clinical studies conducted by Pharmacyclics LLC, an AbbVie Company, can be submitted through Yale Open Data Access (YODA) Project site at <http://yoda.yale.edu>.

References

- Burger JA, O'Brien S. Evolution of CLL treatment - from chemoimmunotherapy to targeted and individualized therapy. *Nat Rev Clin Oncol*. 2018;15(8):510-527.
- IMBRUVICA (ibrutinib) [prescribing information]. Sunnyvale, CA: Pharmacyclics LLC, an AbbVie Company; 2020.
- Moreno C, Greil R, Demirkan F, et al. Ibrutinib plus obinutuzumab versus chlorambucil plus obinutuzumab in first-line treatment of chronic lymphocytic leukaemia (iLLUMINATE): a multicentre, randomised, open-label, phase 3 trial. *Lancet Oncol*. 2019;20(1):43-56.
- Burger JA, Barr PM, Robak T, et al. Long-term efficacy and safety of first-line ibrutinib treatment for patients with CLL/SLL: 5 years of follow-up from the phase 3 RESONATE-2 study. *Leukemia*. 2020;34(3):787-798.
- Shanafelt TD, Wang XV, Kay NE, et al. Ibrutinib-rituximab or chemoimmunotherapy for chronic lymphocytic leukemia. *N Engl J Med*. 2019;381(5):432-443.
- Woyach JA, Ruppert AS, Heerema NA, et al. Ibrutinib regimens versus chemoimmunotherapy in older patients with untreated CLL. *N Engl J Med*. 2018;379(26):2517-2528.
- Barr PM, Owen C, Robak T, et al. Up to seven years of follow-up in the RESONATE-2 study of first-line ibrutinib treatment for patients with chronic lymphocytic leukemia. *J Clin Oncol*. 2021;39(15_suppl):7253.
- Byrd JC, Gribben JG, Peterson BL, et al. Select high-risk genetic features predict earlier progression following chemoimmunotherapy with fludarabine and rituximab in chronic lymphocytic leukemia: justification for risk-adapted therapy. *J Clin Oncol*. 2006;24(3):437-443.
- Munir T, Brown JR, O'Brien S, et al. Final analysis from RESONATE: up to 6 years of follow-up on ibrutinib in patients with previously treated chronic lymphocytic leukemia or small lymphocytic lymphoma. *Am J Hematol*. 2019;94(12):1353-1363.
- Burger JA, Robak T, Demirkan F, et al. Outcomes of first-line ibrutinib in patients with chronic lymphocytic leukemia/small lymphocytic lymphoma (CLL/SLL) and high-risk genomic features with up to 6.5 years follow-up: integrated analysis of two phase 3 studies (RESONATE-2 and iLLUMINATE). *Blood*. 2020;136(Suppl 1):25-26.
- Hallek M, Cheson BD, Catovsky D, et al. Guidelines for the diagnosis and treatment of chronic lymphocytic leukemia: a report from the International Workshop on Chronic Lymphocytic Leukemia updating the National Cancer Institute-Working Group 1996 guidelines. *Blood*. 2008;111(12):5446-5456.
- Al-Sawaf O, Zhang C, Tandon M, et al. Venetoclax plus obinutuzumab versus chlorambucil plus obinutuzumab for previously untreated chronic lymphocytic leukaemia (CLL14): follow-up results from a multicentre, open-label, randomised, phase 3 trial. *Lancet Oncol*. 2020;21(9):1188-1200.
- National Comprehensive Cancer Network. Chronic lymphocytic leukemia/small cell lymphocytic Lymphoma. Version 3.2021. Available from: <https://www.nccn.org/guidelines/guidelines-detail?category=1&id=1478>
- Eichhorst B, Robak T, Montserrat E, et al. Chronic lymphocytic leukaemia: ESMO Clinical Practice Guidelines for diagnosis, treatment and follow-up. *Ann Oncol*. 2021;32(1):23-33.
- Burger JA, Tedeschi A, Barr PM, et al. Ibrutinib as initial therapy for patients with chronic lymphocytic leukemia. *N Engl J Med*. 2015;373(25):2425-2437.
- Byrd JC, Brown JR, O'Brien S, et al. Ibrutinib versus ofatumumab in previously treated chronic lymphoid leukemia. *N Engl J Med*. 2014;371(3):213-223.
- Chanan-Khan A, Cramer P, Demirkan F, et al. Ibrutinib combined with bendamustine and rituximab compared with placebo, bendamustine, and rituximab for previously treated chronic lymphocytic leukaemia or small lymphocytic lymphoma (HELIOS): a randomised, double-blind, phase 3 study. *Lancet Oncol*. 2016;17(2):200-211.
- Shanafelt TD, Wang V, Kay NE, et al. Ibrutinib and rituximab provides superior clinical outcome compared to FCR in younger patients with chronic lymphocytic leukemia (CLL): extended follow-up from the E1912 trial. *Blood*. 2019;134(Suppl 1):33.
- Byrd JC, Furman RR, Coutre SE, et al. Ibrutinib treatment for first-line and relapsed/refractory chronic lymphocytic leukemia: final analysis of the pivotal phase Ib/II PCYC-1102 study. *Clin Cancer Res*. 2020;26(15):3918-3927.
- Uminski K, Brown K, Bucher O, et al. Descriptive analysis of dosing and outcomes for patients with ibrutinib-treated relapsed or refractory chronic lymphocytic leukemia in a Canadian centre. *Curr Oncol*. 2019;26(5):e610-e617.
- Mato AR, Nabhan C, Thompson MC, et al. Toxicities and outcomes of 616 ibrutinib-treated patients in the United States: a real-world analysis. *Haematologica*. 2018;103(5):874-879.
- Siegel R, DeSantis C, Virgo K, et al. Cancer treatment and survivorship statistics, 2012. *CA Cancer J Clin*. 2012;62(4):220-241.
- CALQUENCE (acalabrutinib) capsules, for oral use [package insert]. Wilmington, DE: AstraZeneca Pharmaceuticals LP; 2019.
- Burger JA, Sivina M, Jain N, et al. Randomized trial of ibrutinib vs ibrutinib plus rituximab in patients with chronic lymphocytic leukemia. *Blood*. 2019;133(10):1011-1019.
- Tedeschi A, Greil R, Demirkan F, et al. A cross-trial comparison of single-agent ibrutinib versus chlorambucil-obinutuzumab in previously untreated patients with chronic lymphocytic leukemia or small lymphocytic lymphoma. *Haematologica*. 2020;105(4):e164-e168.
- Sharman JP, Brander DM, Mato AR, et al. Ublituximab plus ibrutinib versus ibrutinib alone for patients with relapsed or refractory high-risk chronic lymphocytic leukaemia (GENUINE): a phase 3, multicentre, open-label, randomised trial. *Lancet Haematol*. 2021;8(4):e254-e266.
- Sharman JP, Egyed M, Jurczak W, et al. Acalabrutinib with or without obinutuzumab versus chlorambucil and obinutuzumab for treatment-naive chronic lymphocytic leukaemia (ELEVATE TN): a randomised, controlled, phase 3 trial. *Lancet*. 2020;395(10232):1278-1291.

The von Willebrand factor A-1 domain binding aptamer BT200 elevates plasma levels of von Willebrand factor and factor VIII: a first-in-human trial

Katarina D. Kovacevic,¹ Jürgen Grafeneder,¹ Christian Schörghofer,¹ Georg Gelbenegger, Gloria Gager,¹ Christa Firbas,¹ Peter Quehenberger,² Petra Jilma-Stohlawetz,² Andrea Bileck,³ Shuhao Zhu,⁴ James C. Gilbert,⁴ Martin Beliveau,⁵ Bernd Jilma¹ and Ulla Derhaschnig¹

¹Department of Clinical Pharmacology, Medical University of Vienna, Vienna, Austria; ²Clinical Institute of Laboratory Medicine, Medical University of Vienna, Vienna, Austria; ³Joint Metabolome Facility, University of Vienna & Medical University of Vienna, Vienna, Austria;

⁴Guardian Therapeutics Inc., Lexington, KY, USA and ⁵Certara, Montreal, Quebec, Canada

Correspondence: K. Kovacevic
katarina.kovacevic@meduniwien.ac.at

Received: September 6, 2021.

Accepted: October 21, 2021.

Prepublished: November 25, 2021.

<https://doi.org/10.3324/haematol.2021.279948>

©2022 Ferrata Storti Foundation

Published under a CC BY-NC license



Abstract

von Willebrand factor (VWF) and factor VIII (FVIII) circulate in a noncovalent complex in blood and promote primary hemostasis and clotting, respectively. A new VWF A1-domain binding aptamer, BT200, demonstrated good subcutaneous bioavailability and a long half-life in non-human primates. This first-in-human, randomized, placebo-controlled, double-blind trial tested the hypothesis that BT200 is well tolerated and has favorable pharmacokinetic and pharmacodynamic effects in 112 volunteers. Participants received one of the following: a single ascending dose of BT200 (0.18–48 mg) subcutaneously, an intravenous dose, BT200 with concomitant desmopressin or multiple doses. Pharmacokinetics were characterized, and the pharmacodynamic effects were measured by VWF levels, FVIII clotting activity, ristocetin-induced aggregation, platelet function under high shear rates, and thrombin generation. The mean half-lives ranged from 7–12 days and subcutaneous bioavailability increased dose-dependently exceeding 55% for doses of 6–48 mg. By blocking free A1 domains, BT200 dose-dependently decreased ristocetin-induced aggregation, and prolonged collagen-adenosine diphosphate and shear-induced platelet plug formation times. However, BT200 also increased VWF antigen and FVIII levels 4-fold ($P < 0.001$), without increasing VWF propeptide levels, indicating decreased VWF/FVIII clearance. This, in turn, increased thrombin generation and accelerated clotting. Desmopressin-induced VWF/FVIII release had additive effects on a background of BT200. Tolerability and safety were generally good, but exaggerated pharmacology was seen at saturating doses. This trial identified a novel mechanism of action for BT200: BT200 dose-dependently increases VWF/FVIII by prolonging half-life at doses well below those which inhibit VWF-mediated platelet function. This novel property can be exploited therapeutically to enhance hemostasis in congenital bleeding disorders.

Introduction

von Willebrand factor (VWF) and factor VIII (FVIII) circulate in a noncovalent complex in blood and promote primary hemostasis and clotting, respectively.¹ VWF plays a dual role in hemostasis: firstly, it is crucial for platelet adhesion as it bridges glycoprotein GpIb on platelets via the A1 domain to collagen localized in the subendothelial matrix of damaged vessels,² secondly it reduces the clearance of coagulation FVIII.³ Deficiency of VWF (Willebrand disease or syndrome) causes primarily mucocutaneous bleeding,^{4,5} and deficiency of FVIII (hemophilia A) leads to joint and muscle bleeding. Both of these disorders can result in disastrous bleeding during surgery or after trauma, and

necessitate substitution of VWF or FVIII, or non-factor replacement therapy in severe cases.⁶

Only recently, VWF has become a target for therapeutic interventions in prothrombotic diseases. As VWF mediates thrombus formation under high shear rates, therapeutic inhibition of VWF is a potential target for cardiovascular diseases.^{7–9} Proof of this concept was first established by demonstrating: (i) that inhibition of the VWF A1-domains reduced the number of microembolic signals during carotid endarterectomy;¹⁰ and (ii) that it improved thrombocytopenia in thrombotic thrombocytopenic purpura,¹¹ a condition caused by a congenital or acquired deficiency of the VWF cleaving enzyme (ADAMTS-13).¹² This led to small^{13,14} and larger clinical trials,^{15–17} which eventually led to the success-

ful testing of the anti-VWF nanobody caplacizumab in phase II/III trials and its subsequent marketing authorization for acquired thrombotic thrombocytopenic purpura. Aptamer-mediated blockade of VWF A1-domains was also demonstrated to be effective in patients with a gain-of-function VWF mutation (type 2B von Willebrand disease [VWD]), increasing both VWF and FVIII plasma levels, as well as platelet counts.^{18,19} These pro-hemostatic actions might also be exploited therapeutically. Previous generations of anti-VWF aptamers, for example aptamer ARC1779, had a suboptimal short half-life^{11, 20} or suboptimal stability at higher temperatures. For those reason we designed a next-generation VWF-A1-binding aptamer, BT200, which recently showed good subcutaneous bioavailability ($\geq 77\%$) and a long half-life in non-human primates (>100 h).²¹ This first-in-human, randomized, double-blind, placebo-controlled trial set out to test the hypothesis that BT200 is well tolerated, safe and has favorable pharmacokinetics and pharmacodynamic effects.

Methods

This trial was approved by the national competent authority (BASG) and the Ethics Committee of the Medical University of Vienna. The study protocol, subsequent amendments, and informed consent were written according to the Declaration of Helsinki and the trial was conducted according to the International Council on Harmonization guidelines for Good Clinical Practice, which was monitored by an external contract research organization. Patients provided written informed consent prior to their participation in the trial. This trial was registered under EUDRA-CT# 2019-001818-42 and NCT04103034 at www.clinicaltrials.gov. This was a single-center trial and all authors had open access to the primary clinical data. Upon a justified request, the principal investigator will grant access to the primary clinical trial data.

This trial used a 3:1 randomized, double-blind, placebo-controlled integrated protocol design with 14 dose cohorts. Each cohort comprised six subjects receiving active treatment and two receiving placebo. Placebo-treated volunteers were pooled within each part of the study and analyzed together. Randomization was done centrally using an electronic system provided by Assign Data Management and Biostatistics (Innsbruck, Austria). Part A of the study was a single ascending dose study, part B a multiple ascending dose study, part D an intravenous (IV) bioavailability study (IV infusion over 24 h) and part C was a drug-drug interaction study with the VWF secretagogue, desmopressin, given as a single dose (0.3 $\mu\text{g}/\text{kg}$ IV over 30 min) approximately 96 h after administration of 48 mg BT200 (i.e., at approximately the t_{max} of BT200). Healthy male or female subjects of non-

childbearing potential were invited to participate. Because reproductive toxicology studies do not exist at this point, the relevant regulatory agency recommended excluding women of childbearing potential at this early stage of development. After written informed consent and passing a screening examination subjects received single doses of BT200 ranging from 0.18 to 24 mg via subcutaneous (SC) injection (cohorts 1-7), SC infusion (drug diluted in 100 mL NaCl) of 24, 36 and 48 mg over 1 h (cohorts 8-10) or a 24-hour IV infusion of 24 mg (cohort 11) (Table 1). Subjects were confined to bed rest for the first hour; oxygen saturation and heart rate were monitored, and blood pressure was measured repeatedly. Subjects in the multiple-dose cohorts received a split loading dose (IV over 2 h/SC) of 12/12 mg or 24/24 mg. In cohort 13 this was followed by weekly SC injections of 12 mg until day 28.

BT200 is a fully 2'-O-methylated RNA aptamer²¹ conjugated to a 40 kD polyethylene glycol, and it was supplied at a concentration of 15 mg/mL in sterile saline for injection (all doses refer to the unconjugated aptamer). A sterile saline solution (0.9 NaCl) was used as placebo

Table 1. Enrolled study population and treatment.

Study Part	Cohort	Treatment	N
A	1	0.18 mg BT200/placebo – SC injection	8
A	2	0.6 mg BT200/placebo – SC injection	8
A	3	1.8 mg BT200/placebo – SC injection	8
A	4	6 mg BT200/placebo – SC injection	8
A	5	12 mg BT200/placebo – SC injection	8
A	6	18 mg BT200/placebo – SC injection	8
A	7	24 mg BT200/placebo – SC injection	8
A	8	24 mg BT200/placebo – SC infusion	8
A	9	36 mg BT200/placebo – SC infusion	8
A	10	48 mg BT200/placebo – SC infusion	8
D	11	24 mg BT200/placebo – IV infusion	8
C	12	48 mg BT200/placebo – SC injection with desmopressin challenge	8
B	13	24 mg BT200/placebo – IV infusion with 12 mg SC injection, followed by 4 weekly doses of 12 mg	8
B	14	24 mg BT200/placebo – IV infusion with 24 mg SC injection	8

In each cohort six volunteers were randomized to BT200 and two to placebo. N: number of subjects; SC: subcutaneous; IV: intravenous.

and desmopressin was supplied as a commercially available sterile solution for injection in 4.0 µg/mL ampoules (Octostim, Ferring, Austria).

A description of analytical methods and the statistical analysis is provided in the *Online Supplementary Data*.

Results

Randomization of 112 subjects was planned; due to slower recruitment during the COVID pandemic, 20 subjects from part A were re-exposed (once) in part B, C or D. Thus, a total of 92 individual subjects were enrolled in 14 cohorts.

Single subcutaneous doses and intravenous bioavailability study

In part A, 86 subjects were screened, 60 were randomized to BT200 and 20 to placebo. Cohort 9 included one early termination and cohort 10 two early terminations due to COVID-19. Two volunteers were Asian, one African, and the rest Caucasian. The male:female sex ratio of participants was 72:8, and their age ranged from 18 to 60 years. Complete demographic characteristics are given in *Online Supplementary Table S1*.

In part D, eight subjects from part A (including 1 woman and the 2 Asian volunteers) were re-exposed and they received intravenous doses of placebo or BT200; their mean age was 31.3 years (*Online Supplementary Table S2*).

Pharmacokinetics

The rate and extent of exposure to BT200 increased with increasing doses over the dose range of 0.18 mg to 24 mg after single SC injections (Figure 1). The increase over the dose range for areas under the concentration curve (AUC) and maximum concentration (C_{max}) appeared to be proportional to dose for dose levels ≥ 6 mg. For SC infusions, the rate and extent of exposure to BT200 also increased in a dose-proportional manner. Geometric mean half-lives ($t_{1/2}$) ranged from 121 to 279 h (Table 2). Clearance (CL/F) decreased as a function of body weight and age. The half-life was 204 h after a 24 h IV infusion and the C_{max} reached 4.8 µg/mL, the geometric mean clearance (CL) was 0.0264 L/h and the volume of distribution (V_{ss}) was 4.54 L. Therefore, as had been expected, clearance was much lower than glomerular filtration rate (7.5 L/h). The volume of distribution was consistent with the blood volume of human volunteers (5 L), and similar to that seen for other pegylated aptamers²² which are not primarily eliminated via passive renal filtration.

The bioavailability of BT200 was approximately 64% following SC injection and 75% following SC infusion. Bioavailability was lower for doses below 1.8 mg (33 to 50%), as expected from the dose proportionality analysis.

Multiple ascending dose cohorts (cohorts 13, 14)

In part B, 16 subjects (14 men and 2 women) were included (8 of whom were re-exposed from part A). One subject was Asian and the rest were Caucasian. The mean age was 43 years (standard deviation [SD] 13), mean height was 180 cm (SD 11), mean weight was 87 kg (SD 17) and the mean body mass index was 26.8 kg/m² (SD 4.5) (*Online Supplementary Table S3*).

Pharmacokinetics

As expected, the combination of IV infusions over 2 h and SC injections in a split SC/IV loading dose resulted in peak levels being observed much earlier than was seen after the same dose was administered via the SC route alone (Figure 1). The exposure (AUC and C_{max}) was only slightly higher than that of an equivalent injected or SC infused dose in part A. Mean trough concentrations of BT200 appeared to plateau by day 7 and remained consistent through to day 28 following weekly maintenance doses of 12 mg BT200 (*Online Supplementary Figure S1*). Subjects in cohort 14 received only the initial dose but not any of the subsequent maintenance doses, because the maximum tolerated dose had been reached and the aims of the trial fulfilled.

Pharmacodynamic effects in all cohorts

BT200 concentration-dependently inhibited VWF-dependent platelet function (*Online Supplementary Figures S2 and S3*): a 12 mg dose was necessary to fully prolong collagen-ADP closure times as measured by the Platelet Function Analyzer (PFA) (*Online Supplementary Figures S4 and S5*) to a median of 300 s (range: 148–300 s; $P < 0.001$) 48 h after SC injection, which coincided with the nadir of free VWF A1-domains in this cohort (Figure 2). Maximal PFA closure prolongation was short lived and did not persist even until the maximal plasma concentration of 1.2 µg/mL was observed at 72 h following the 12 mg dose. Likewise, ristocetin-induced platelet aggregation decreased from 92 U (range, 69–117 U) to a nadir of 34 U (range, 13–58 U; $P < 0.001$) after 96 h (*Online Supplementary Figures S5 and S6*).

All three lower SC doses of BT200 had a minimal effect on free VWF A1-domains which was comparable to that observed for placebo (Figure 2). The 6 mg dose moderately suppressed free VWF A1-domains by ~30% ($P < 0.001$). Doses of 12–48 mg invariably decreased free VWF A1-domains to <50% of normal values, although the extent of decrease appeared to be more pronounced in subjects with low baseline levels of VWF. The 48 mg dose reduced median free VWF A1-domains to 2% (range, 2–6%) at 48 h, and the 24-h IV infusion of 24 mg BT200 quickly reduced free VWF A1-domains to 1% (range, 0–7%). At equivalent exposure, the IV infusion yielded a greater extent of suppression compared to the SC injection, consistent with

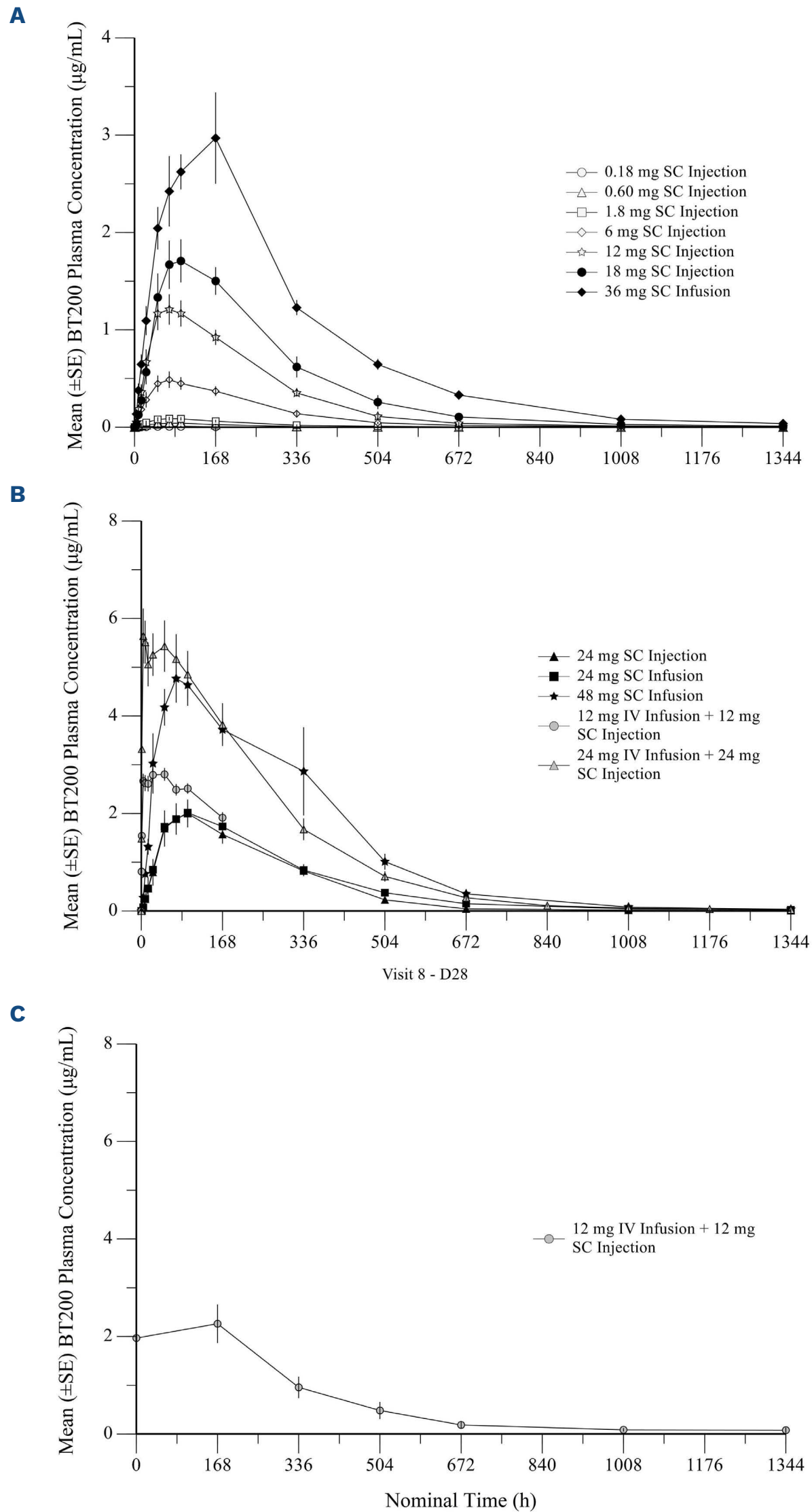


Figure 1. Plasma concentration versus time profiles of the anti-von Willebrand factor aptamer, BT200, in healthy volunteers. Mean (with standard error) plasma levels of BT200 over time after: (A) single subcutaneous injections or infusions in healthy volunteers (n=6); (B) single subcutaneous injections or infusions in healthy volunteers (n=6); (C) the last of five subcutaneous doses in healthy volunteers (part B of the study) (n=6). SE: standard error; SC: subcutaneous; IV: intravenous; D28: day 28.

the different kinetic profiles observed following IV or SC administration.

The effect of BT200 on VWF:RCo appeared to be less pronounced when compared to that on free VWF A1-domains. For example, the 36 mg dose reduced median VWF:RCo from 108% to 30% (*Online Supplementary Figure S7*), but median free VWF A1-domains from 84% to 6% after 48 h (both $P < 0.001$; Friedman ANOVA). This apparent discrepancy reflects the 2-fold increase in circulating VWF antigen levels after 48 h, and because VWF:RCo is sensitive to changes in VWF levels, the effects of BT200 were less pronounced in VWF:RCo when compared to the free VWF A1-domains. Circulating VWF antigen mass increased as early as 24 h after the start

of the IV infusion, and reached levels 4-fold higher than baseline between 7-14 days after SC doses of 24-48 mg ($P < 0.001$) (Figure 3). VWF antigen levels increased 4-fold following multiple SC maintenance doses of 12 mg BT200 ($P < 0.001$) (Figure 4).

As VWF is the carrier for FVIII, there was a corresponding 3- to 4-fold increase in FVIII activity levels 7 days after SC administration of 24-48 mg BT200 ($P < 0.001$) (Figure 5). Multivariate analysis showed that the FVIII levels not only correlated with the dose, but also with baseline VWF antigen levels (multiple r^2 values ranging from 0.66-0.78 from 48 h to 21 days; $P < 0.001$). Whereas a minimal increase of FVIII activity was observed following SC injection of BT200 at lower dose levels (0.18, 0.6, 1.8 mg),

Table 2. Plasma BT200 pharmacokinetic parameters following a single administration of BT200 to normal human volunteers (parts A and B).

Plasma pharmacokinetic parameters ^a							
Dose in mg (N)	AUC ₀₋₁₆₈ (h*µg/mL)	AUC _{0-∞} ^d (h*µg/mL)	C _{max} (µg/mL)	t _{max} ^b (h)	t _{1/2} (h)	CL ^f (L/h)	V _{ss} ^f (L)
Part A (SC injection)							
0.18 (6)	0.968 (75.4);6	3.42 (21.5);3 ^{c,d}	0.00903 (60.3);6	71.93 (46.83; 336.90);6	149 (11.8);3 ^{c,d}	0.0526 (21.5);3 ^{c,d}	12.4 (22.9);3 ^{c,d}
0.6 (6)	5.02 (45.8);6	8.06 (41.5);5 ^c	0.0431 (50.4);6	83.64 (47.58; 97.95);6	121 (55.8);5 ^c	0.0744 (41.5);5 ^c	14.1 (50.4);5 ^c
1.8 (6)	10.7 (43.4);6	22.3 (31.0);6	0.0890 (37.9);6	71.68 (47.90; 97.43);6	239 (55.2);6	0.0807 (31.0);6	21.9 (58.4);6
6 (6)	60.5 (42.6);6	127 (24.6);6	0.475 (45.0);6	72.86 (48.28; 168.98);6	279 (22.2);6	0.0471 (24.6);6	11.3 (41.8);6
12 (6)	157 (25.6);6	315 (21.9);6	1.22 (25.0);6	73.24 (48.20; 97.45);6	263 (26.5);6	0.0381 (21.9);6	8.71 (28.1);6
18 (5) ^e	213 (29.5);5	499 (29.7);5	1.69 (28.7);5	94.93 (72.07; 97.50);5	204 (25.5);5	0.0361 (29.7);5	9.32 (29.9);5
24 (6)	235 (59.9);6	550 (42.7);6	1.92 (54.0);6	95.72 (48.58; 168.62);6	184 (27.4);6	0.0436 (42.7);6	10.4 (60.0);6
Part A (SC infusion)							
24 (6)	260 (23.2);6	646 (19.8);6	2.03 (24.0);6	96.10 (48.22; 98.00);6	240 (41.8);6	0.0371 (19.8);6	10.6 (25.9);6
36 (6)	359 (22.0);6	1007 (12.1);6	3.09 (34.3);6	166.77 (72.83; 168.73);6	203 (6.53);6	0.0358 (12.1);6	10.9 (20.1);6
48 (6)	633 (14.8);6	1507 (14.5);4	5.46 (16.2);6	71.86 (24.50; 336.23);6	193 (17.0);4	0.0319 (14.5);4	8.44 (5.66);4
Part B							
24 (6)	408 (7.81);6	NC	3.00 (8.61);6	23.69 (4.00; 71.82);6	NC	NC	NC
48 (6)	787 (25.4);6	1527 (28.5);6	5.69 (24.7);6	5.77 (4.00; 49.33);6	243 (17.7);6	0.0314 (28.5);6	6.99 (24.4);6

^aData are presented as geometric means with geometric coefficients of variation (GeoCV%); n. of subjects. ^bMedian (minimum, maximum); n. of subjects. ^cAUC_{0-∞} and all λ_z -related pharmacokinetic parameters were not calculated for concentration-time profiles that did not have a well-characterized terminal phase. ^dThe AUC_{0-∞} values were extrapolated by more than 20% for one subject in cohort 1, the AUC_{0-∞} and all λ_z -related pharmacokinetic parameter results should be interpreted with caution. ^eDose information was missing for one subject in cohort 6: the pharmacokinetic results for this subject were excluded from the summary statistics. ^fFollowing extravascular administration (subcutaneous), this parameter is expressed over F (i.e., CL/F and V_{ss}/F). AUC: area under the concentration-time curve; C_{max}: maximum concentration; t_{max}: time at which peak concentration occurs; t_{1/2}: half-life; CL: clearance; V_{ss}: apparent volume of distribution at steady state; NC: not calculated; λ_z : terminal rate constant; F: absolute bioavailability.

doubling of FVIII was already seen in some individuals after a single 6 mg dose. Increased FVIII levels were reflected by a reciprocal shortening of the activated partial thromboplastin time ($P < 0.001$) (*Online Supplementary Figure S8*), and an up to 2-fold increase in peak thrombin generation ($P < 0.001$) (*Online Supplementary Figure S9*). To investigate the potential mechanism of action for the

increased VWF/FVIII levels, we considered that increased VWF secretion might contribute to the VWF elevation and therefore measured VWF propeptide levels. However, BT200 did not raise VWF propeptide levels (*Online Supplementary Figure S10*), resulting in a 4-fold lower VWF propeptide/antigen ratio and demonstrating that BT200 does not increase VWF secretion or release.

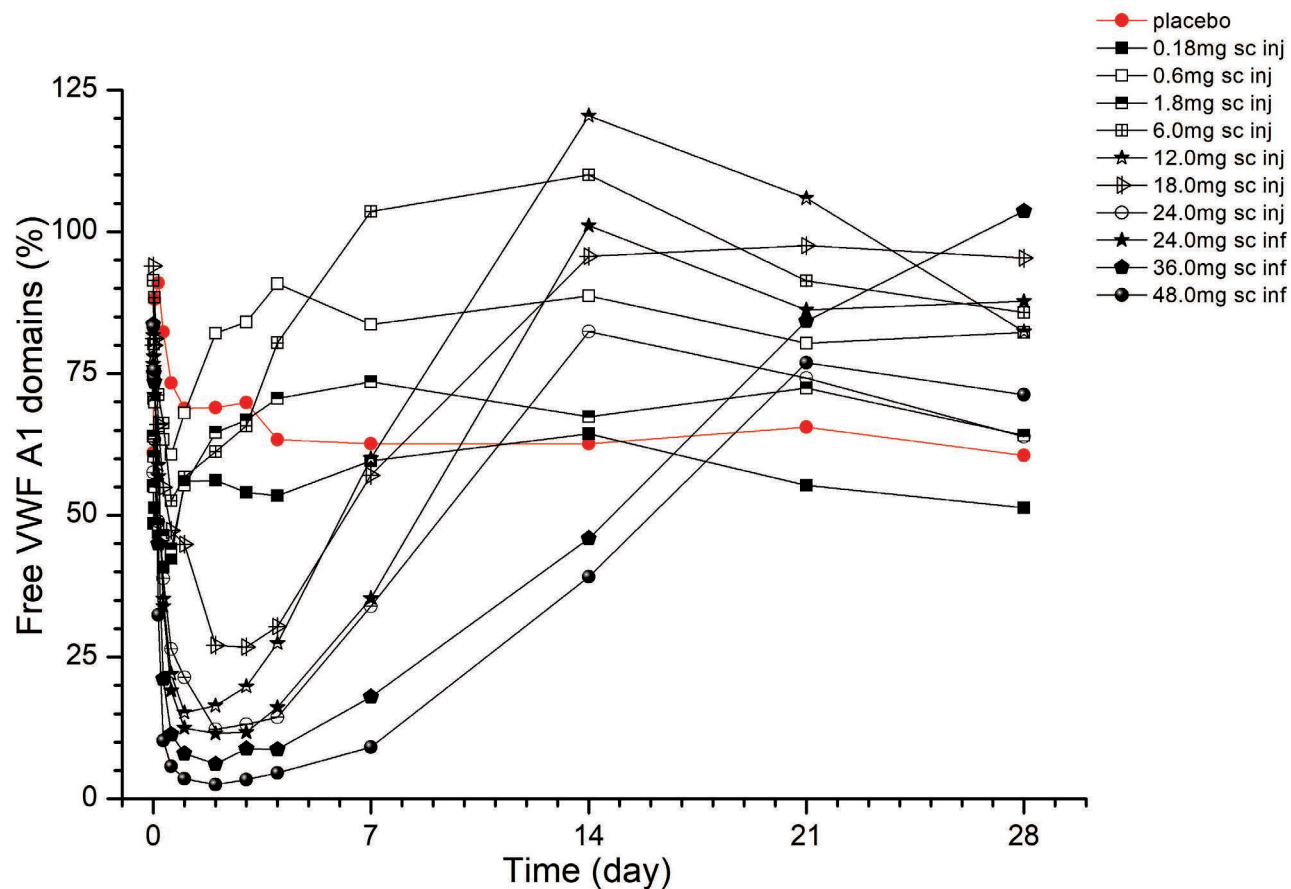


Figure 2. Free von Willebrand factor A1-domains (%) after single doses of BT200, measured by enzyme-linked immunosorbent assay. Data are mean values without error bars for better visibility ($n=6$ for BT200 groups, $n=20$ for placebo). VWF: von Willebrand factor; sc: subcutaneous; inj: injection; inf: infusion.

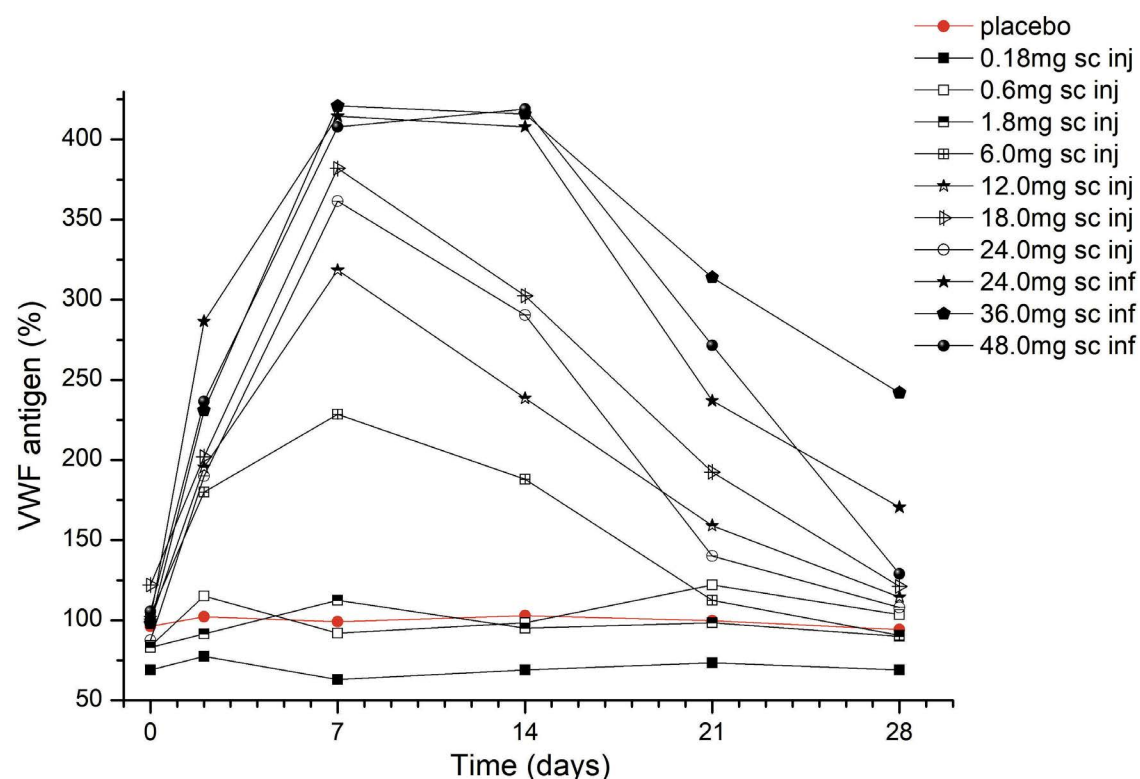


Figure 3. Plasma levels of von Willebrand factor antigen (%) after single doses of BT200. Data are mean values without error bars for better visibility ($n=6$ for BT200 groups, $n=20$ for placebo). VWF: von Willebrand factor; sc: subcutaneous; inj: injection; inf: infusion.

No apparent sex differences were noted in pharmacokinetic or pharmacodynamic values.

Desmopressin challenge

Eight subjects were included in part C, of whom four (including 1 woman) were re-exposed from part A. All were Caucasian and their mean age was 38 years (SD 13) (*Online Supplementary Table S4*). Desmopressin did not alter BT200 exposure in any meaningful manner (*data not shown*). In fact, the responses to BT200 and desmopressin appeared to be additive, with the higher FVIII activity observed following BT200 plus desmopressin infusion taking a proportionally longer time to return to baseline (Figure 6).

Half-life estimation

To estimate the increase in half-life of endogenous VWF/FVIII the following assumptions were made: (i) 4-fold higher levels of VWF/FVIII will increase the AUC 4-fold; (ii) BT200 does not alter endogenous VWF/FVIII release/production (as evidenced by unchanging VWF propeptide levels); (iii) endogenous VWF/FVIII release/production is constant (i.e., similar to a continuous infusion of VWF/FVIII at a constant dose); and (iv) the volume of distribution of VWF does not change (as BT200 is a large molecule with predominantly intravascular distribution).

From this it can be calculated that: (i) the clearance of VWF/FVIII decreased to 25% of the baseline value (clearance = dose [1x] / AUC [4x]); and (ii) the half-life of endogenous FVIII increases by ~ 2.77-fold ($t_{1/2} = 0.693/\text{clearance}$) (Figure 4).

Specificity of blocking von Willebrand factor clearance

One of the main clearance pathways of VWF/FVIII complex is macrophage low density lipoprotein receptor-related protein 1 (LRP1). BT200 has been demonstrated to affect VWF clearance and this is probably due to the inhibition of the VWF/FVIII-LRP1 clearance pathway²³ (explained in the Discussion). To exclude a non-specific effect on LRP1, we measured levels of two additional molecules: ADAMTS²⁴ and connective tissue growth factor²⁵ in a subgroup of patients. These molecules are specifically cleared by the LRP1 receptor. Their levels remained unchanged, indicating that the influence of BT200 on blocking VWF clearance is highly specific (*data not shown*).

Safety

A list of adverse events, presented according to affected system organ class, is provided in *Online Supplementary Table S5*. Overall, the tolerability and safety of BT200 were good and similar to those of placebo, with an exception attributable to exaggerated pharmacology: dose-related

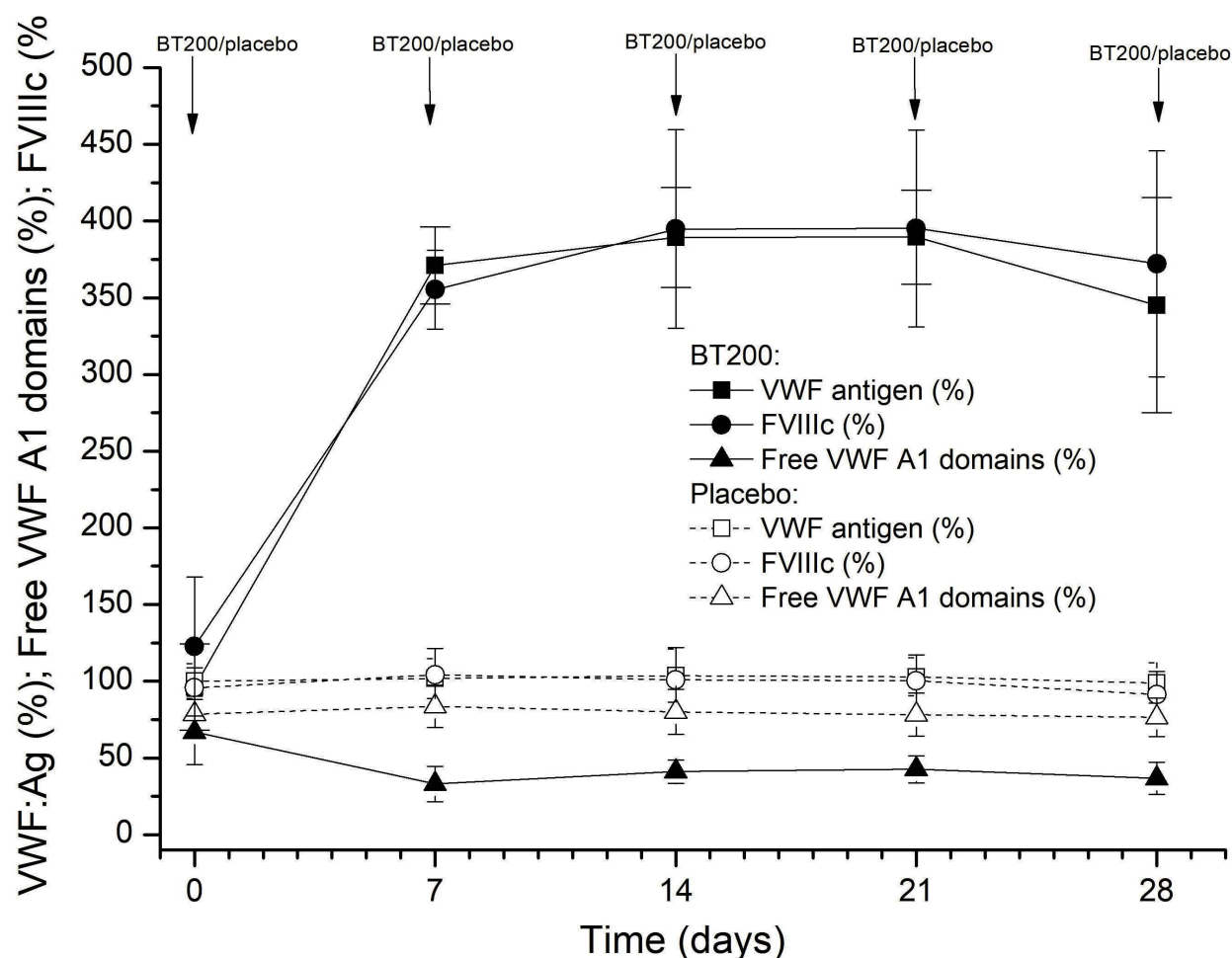


Figure 4. von Willebrand factor antigen levels, free A1-domains and factor VIII activity (%) after multiple doses of BT200. Subjects received 12 mg BT200 intravenously plus 12 mg subcutaneously on the first day and 12 mg subcutaneously weekly or placebo. Data are presented as mean values with 95% confidence intervals (n=6 for BT200 groups, n=20 for placebo). VWF: von Willebrand factor; Ag: antigen; FVIIIc: factor VIII activity.

episodes of minor spontaneous bleeding that occurred in the form of epistaxis and gingival bleeding, and minor provoked bleeding in the form of venepuncture-related hematomata. This occurred in one of 24 subjects given 24 mg BT200, and in 5/18 subjects given a 48 mg single-dose of BT200. There was only one healthy volunteer with thrombocytopenia (he received BT200 intravenously). He

had low platelet counts at the start of the trial ($142 \times 10^9/L$ decreasing to a minimum of $117 \times 10^9/L$), but these normalized towards the end of the trial. He also experienced a local hematoma. There was no fall in hemoglobin in any participant.

It is of note that one subject developed venous thrombosis and another subject thrombophlebitis at the insertion

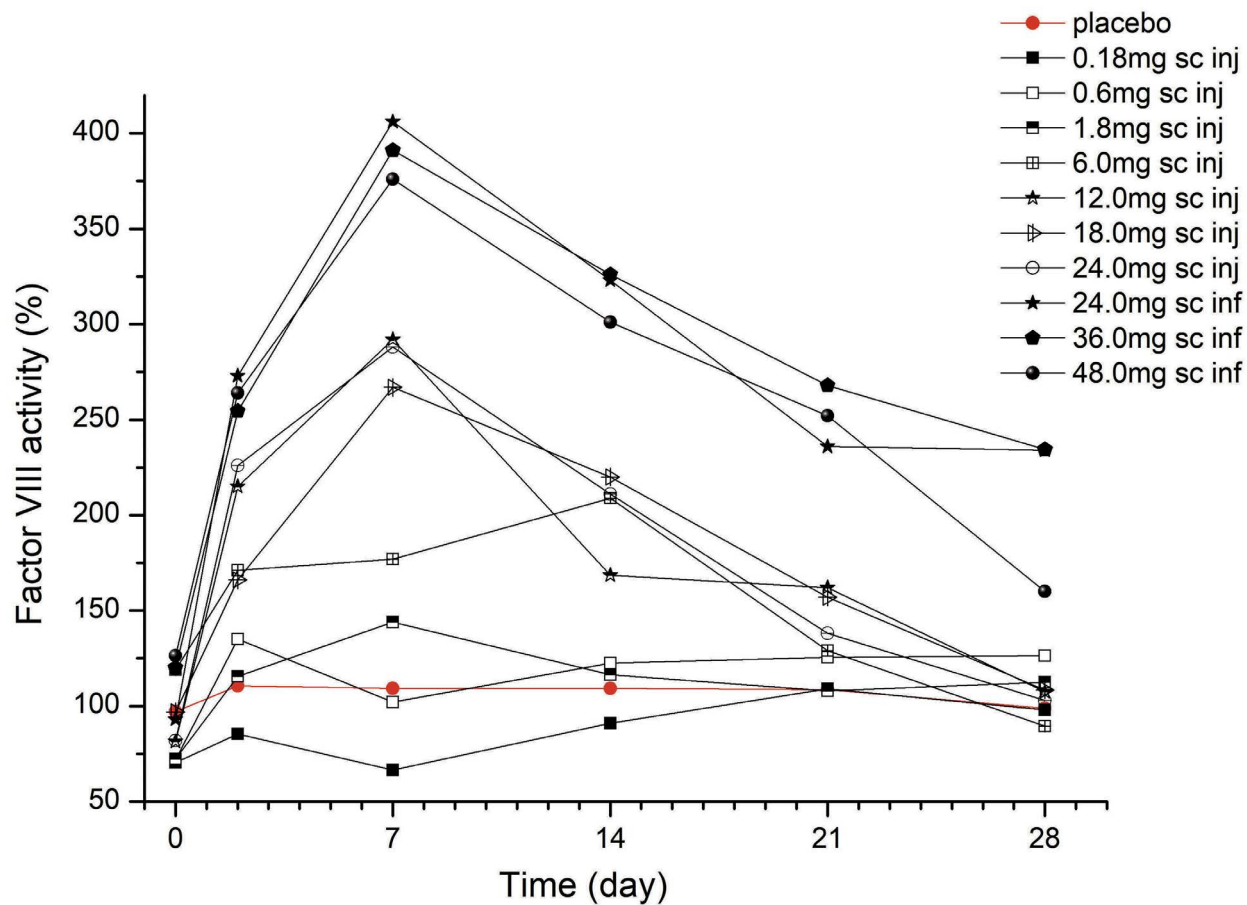


Figure 5. Factor VIII activity levels after single doses of BT200. Data are mean values without error bars for better visibility (n=6 for BT200 groups, n=20 for placebo). sc: subcutaneous; inj: injection; inf: infusion.

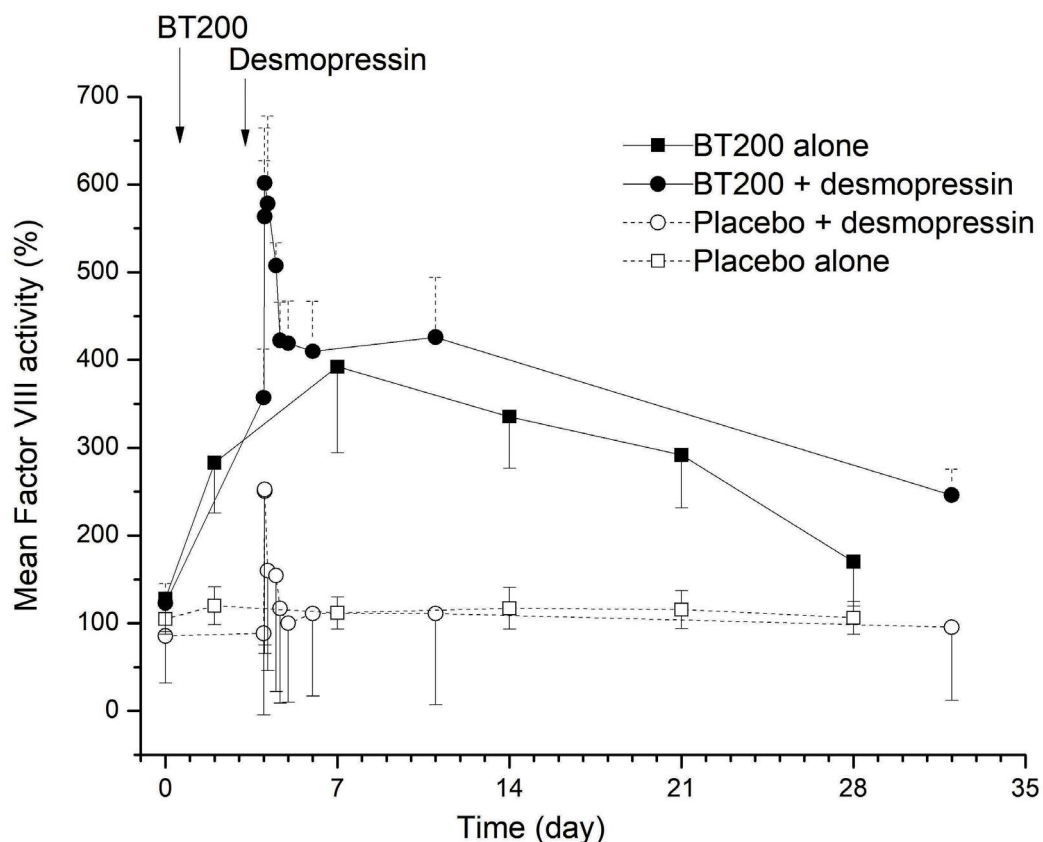


Figure 6. Factor VIII clotting activity (%) after combined administration of BT200/placebo with desmopressin or BT200/placebo alone. Data are represented as mean values with 95% confidence interval (n=6 for BT200 groups, n=20 for placebo, n=2 for placebo+desmopressin).

site of the venous catheter (median cubital vein). This was diagnosed with color-coded duplex sonography and both events were treated with enoxaparin. One subject received 8000 IE SC once daily, and the other 4000 IE SC once daily. Additionally, one volunteer developed venous thrombosis of the limb (lower left leg) and was treated with enoxaparin 6000 IE SC for 4 days, and then with edoxaban 60 mg once a day for 11 weeks. Furthermore he was prescribed compression stockings. Lastly, one subject developed thrombophlebitis of the cubital vein and a superficial thrombophlebitis which extended into the great saphenous vein. In this subject factor V Leiden, which would predispose him to thrombotic events, was diagnosed. He was treated with enoxaparin 8000 IE SC 2x1 for 5 days and then with edoxaban 60 mg orally 1x1. Subjects who experienced these events received a single dose of BT200 ≥ 36 mg (3 of 4 subjects and 1 of them also received desmopressin), or repeated weekly doses of 12 mg (in the remaining 1 subject).

D-dimer and prothrombin fragment levels were measured in 28 subjects. Although no significant difference between levels in the placebo and BT200 groups was seen, two out of seven subjects in the placebo arm had elevated D-dimer levels at baseline (0.95 and 1.61 $\mu\text{g/mL}$), and three more placebo-treated subjects showed elevated D-dimer levels in at least one blood sample (0.75, 1.07, 1.43 $0\mu\text{g/mL}$). Therefore, due to its low specificity, we decided not to continue measuring D-dimer levels. However, D-dimer levels do demonstrate a good negative predictive value for ruling out pulmonary embolism when in the normal range.²⁶

Three serious adverse events occurred, all of which were considered to be unrelated to the study drug. One subject on placebo had severe back pain which was treated in hospital, one subject receiving 24 mg suffered a bone fracture 24 days after dosing and underwent surgery, and one subject had an intervertebral disc protrusion 17 days after treatment with 48 mg BT200. She was managed with repeated desmopressin infusions to restore VWF-dependent platelet function before undergoing surgery.

Discussion

This first-in-human trial examined the tolerability, safety, pharmacokinetics and pharmacodynamic effects of the VWF A1-binding aptamer, BT200. In previous non-human primate studies the median half-life was found to be 3-4 days for BT200 doses ranging from 0.5-10 mg/kg.²¹ In our healthy volunteers, the estimated half-life ranged from 7-12 days for BT200 doses approximately ≥ 0.02 mg/kg, which is 2- to 3-fold longer than the dose in monkeys. Single SC doses of ≥ 12 mg BT200 yielded plasma concentrations of ~ 1 $\mu\text{g/mL}$ in humans which dose-dependently decreased

VWF activity and shear-dependent platelet function by $>50\%$. This indicates that the concentration-effect relationships seen in recent *in vitro* studies using human blood^{7,27,28} are directly applicable to the *in vivo* clinical pharmacology. Treatment with ≥ 1 mg/kg BT200 inhibited VWF-dependent platelet function and thrombus formation in non-human primates,²¹ suggesting a possible therapeutic role for BT200 in the secondary prevention of cardio- and cerebrovascular diseases.²⁷ Interestingly, as this was not seen in the preliminary monkey studies, BT200 increased VWF antigen levels and FVIII activity up to 4-fold above baseline. As BT200 did not increase VWF propeptide levels, this increase in VWF/FVIII can be explained by decreased clearance of VWF. The mechanism of VWF clearance is complex and involves different receptors,²⁹ and VWF clearance dominates FVIII clearance.³⁰ While this trial was still ongoing, it was published that pegylation of VWF A1-domains with 40 kDa polyethylene glycol decreases their clearance by the macrophage LRP1.²³ BT200 binding to the A1-domain of VWF indirectly “pegylates” the A1-domain, and decreased clearance is the likely underlying mechanism of action for the observed increase in VWF/FVIII levels. X-ray crystallography demonstrates that BT200 binds to the VWF A1-domain with multiple contacts in the region from R1395 to Q1402.²¹ This region includes a critical binding site on VWF-A1 for LRP1, the primary clearance receptor for the VWF/FVIII complex, i.e., K1408 on VWF A1.³¹ This same region from R1395 to Q1402 on VWF-A1 partially overlaps with that of the corresponding binding site for glycoprotein Ib, providing a biophysical basis for the observed pharmacological competition between BT200 and platelet glycoprotein Ib.²¹

The FVIII was hemostatically active, which was not only reflected by a shortening of the activated partial thromboplastin time, but also by an increase in the endogenous thrombin potential. While the overall safety and tolerability profiles of BT200 were good and similar to nonclinical safety experience in non-human primates, this heightened hemostatic activity resulted in the occurrence of venous thrombosis and thrombophlebitis at the insertion site of venous catheters in two subjects. Additionally, distal venous thrombosis/thrombophlebitis occurred in two further subjects, one of whom had a medical history of previous thrombosis associated with the factor V Leiden mutation. One may potentially be able to explain the otherwise rare events of thrombosis of the upper limbs as follows. After venous puncture, normal hemostasis induces a localized platelet plug to stop bleeding. Normally, thrombus growth is stopped by endogenous fibrinolysis. However, after the administration of BT200 there is an increase in endogenous thrombin potential due to supra-normal FVIII levels. This leads to the localized plug growing, and it then becomes clinically visible thrombosis.

The increased procoagulant properties are suboptimal for further development of BT200 for the secondary prevention of arterial diseases, because they would mandate simultaneous anticoagulation to prevent venous thrombosis in an elderly population. The only exception may be rare patients with low FVIII levels, who require secondary prevention of arterial thrombosis with a potent antiplatelet drug, which clearly represents a therapeutic dilemma.³²

This requires strategic rethinking and pivoting BT200 as a pro-hemostatic agent. From a safety perspective, BT200 caused only a minor mucocutaneous bleeding pattern, with epistaxis seen at high doses (≥ 24 mg). This is consistent with the clinical phenotype of deficiency in VWD and consistent with the exaggerated pharmacology of other VWF inhibitors.¹⁵ If needed, a rapidly acting, specific, reversal agent has been developed,³³ and will allow immediate restoration of VWF-dependent hemostasis, for example in the case of trauma or emergency surgery.

The dose- and concentration-response relationship between BT200 and the inhibition of VWF-mediated platelet function, and the increase of FVIII, can, however, be partially separated. The FVIII elevating effect begins at a lower dose (~ 6 mg) while the VWF inhibiting effect does not yet occur (≥ 12 mg). In addition, the plasma levels of free A1-domains of VWF appear to stabilize mostly around 40% of normal values under repeated maintenance doses of 12 mg due to an increase in circulating VWF mass. It can be anticipated that repeated doses of ≥ 6 mg can be used to elevate VWF/FVIII, without inhibiting primary hemostasis by a relevant degree, and heavier patients or those with high baseline VWF levels may even benefit from higher doses.

Which groups of patients might potentially benefit from BT200? From the estimated 2- to 3-fold increase in FVIII half-life, one would expect a similar increase in half-life of exogenous FVIII in patients with severe hemophilia or type 3 VWD practising prophylactic replacement therapy. Such a half-life prolongation could be seen with regular FVIII products and even extended half-life products, which would be welcome because of the ceiling effect of VWF on the FVIII half-life. This property can be used to prolong the dosing interval, thus permitting treatment once a week rather than every second day. Additionally, dosages could also be individually tailored to obtain higher trough FVIII levels.

Apart from patients with severe hemophilia, BT200 could for the first time provide an opportunity for patients with moderate or mild hemophilia or female carriers with low FVIII levels and associated severe menstrual bleeding to practise prophylaxis. It has previously been shown that even a modest pharmacologically induced increase in plasma VWF levels can favorably affect the pharmacokinetics of FVIII concentrates used in people with severe

hemophilia.³⁴ Although desmopressin is effective in a majority of such patients, its antidiuretic effects, adverse events, short duration of action and tachyphylaxis make it unsuitable for long-term prophylaxis.^{34,35} However, our data show that combined use of desmopressin with BT200 has an additive effect on VWF and FVIII levels, and together with previous data on ARC1779, it appears that the effect of desmopressin could be prolonged by BT200.¹⁸ This could also allow lower doses or intranasal desmopressin to be used at intervals, which would minimize antidiuretic effects. However, based on the estimated 2.8-fold prolongation in half-life, we would expect that a 2- to 3-fold increase in endogenous FVIII levels can be achieved by BT200 alone. Finally, certain patients with other subtypes of VWD including, but not necessarily limited to, high clearance variants of type 1C VWD, or type 2B VWD may benefit from the use of BT200. In type 2B VWD, there are gain-of-function mutations often in the A1 domain, which increase the affinity of VWF for Gplb leading to spontaneous VWF attachment to platelets. This often results in a loss of large multimers,³⁶ and low VWF plasma levels due to high clearance, as indicated by the increased VWFpp:VWF ratios in type 2B patients.³⁷ Similarly, murine variants carrying type 2B mutations result in a shortened VWF half-life, as well as increased clearance of platelets coated with such mutants.³⁸ We previously provided proof of the concept that blocking the A1-domain of VWF by infusion of ARC1779 was able to increase VWF/FVIII levels, to normalize multimer patterns and to improve the associated thrombocytopenia in patients suffering from type 2B VWD.^{18,19} As BT200 increases VWF/FVIII levels by decreasing the clearance of these proteins in healthy individuals, it could potentially increase their levels in all VWD patients, but particularly in those with high clearance variants (VWD type 1C). For example, patients with type Vicenza VWD may have a VWF half-life 10-fold shorter than normal, as well as FVIII deficiency.³⁹ It is conceivable that BT200 may be beneficial as it counteracts the increased clearance.

This study does have some limitations. We were only able to include women of non-childbearing potential due to a demand from the regulatory agency. Therefore, only 11 women participated in the trial. Similarly, ethnic diversity was limited. However, as BT200 is a large molecule, which predominantly distributes to the intravascular compartment without being metabolized, no relevant differences are expected between sexes or people of different ethnicity. As the bleeding burden in females with hemophilia A has long been neglected, which has only recently resulted in a new nomenclature,⁴⁰ future trials will have to include a larger proportion of women.

In summary, BT200 is a first-in-class molecule with a novel mechanism of action representing a new therapeutic strategy to break the ceiling effect that VWF imposes on

FVIII half-life. This prolongs the half-life of VWF/FVIII, which could allow regular prophylaxis in patients with non-severe hemophilia A, as well as allowing VWD patients to increase their VWF/FVIII levels.

Disclosures

JCG and SZ are founders of, and BJ and BM are consultants for Guardian Therapeutics. The other authors have no relevant conflicts of interest to declare.

Contributions

KDK and AB performed the pharmacokinetic and part of the pharmacodynamic analyses. JG, GGe, GGa, CS, CF and UD (the principal investigator) were responsible for conducting the trial. BJ and JCG designed the trial, wrote the protocol and SZ developed the analytical methods. PJ-S and PQ were

responsible for laboratory analyses and for quality checking methods. MB performed the pharmacokinetic/pharmacodynamic modeling and wrote the pharmacokinetic/pharmacodynamic report. All authors contributed to both writing and critically reviewing the manuscript.

Acknowledgments

This trial was sponsored by Guardian Therapeutics. We would like to thank the following staff members for their outstanding logistic support and help: Christa Drucker, Karin Petroczi, Sabine Schranz, RN and Sarah Ely, RN, BA, PgDip who also edited the manuscript.

Data-sharing statement

Upon a justified request, the principal investigator will grant access to the primary clinical trial data.

References

- Lollar P. The association of factor VIII with von Willebrand factor. *Mayo Clin Proc.* 1991;66(5):524-534.
- Ruggeri ZM, Mendolicchio GL. Interaction of von Willebrand factor with platelets and the vessel wall. *Hamostaseologie.* 2015;35(3):211-224.
- Kiouptsi K, Reinhardt C. Physiological roles of the von Willebrand factor-factor VIII interaction. *Subcell Biochem.* 2020;94:437-464.
- Lavin M, O'Donnell JS. How I treat low von Willebrand factor levels. *Blood.* 2019;133(8):795-804.
- Lillicrap D. von Willebrand disease: advances in pathogenetic understanding, diagnosis, and therapy. *Blood.* 2013;122(23):3735-3740.
- Tomeo F, Mariz S, Brunetta AL, Stoyanova-Beninska V, Penttila K, Magrelli A. Haemophilia, state of the art and new therapeutic opportunities, a regulatory perspective. *Br J Clin Pharmacol.* 2021;87(11):4183-4196.
- Kovacevic KD, Jilma B, Zhu S, et al. von Willebrand factor predicts mortality in ACS patients treated with potent P2Y12 antagonists and is inhibited by aptamer BT200 ex vivo. *Thromb Haemost.* 2020;120(9):1282-1290.
- Spiel AO, Mayr FB, Ladani N, et al. The aptamer ARC1779 is a potent and specific inhibitor of von Willebrand factor mediated ex vivo platelet function in acute myocardial infarction. *Platelets.* 2009;20(5):334-340.
- Buchtele N, Schwameis M, Gilbert JC, Schorghofer C, Jilma B. Targeting von Willebrand factor in ischaemic stroke: focus on clinical evidence. *Thromb Haemost.* 2018;118(6):959-978.
- Markus HS, McCollum C, Imray C, Goulder MA, Gilbert J, King A. The von Willebrand inhibitor ARC1779 reduces cerebral embolization after carotid endarterectomy: a randomized trial. *Stroke.* 2011;42(8):2149-2153.
- Jilma-Stohlawetz P, Gilbert JC, Gorczyca ME, Knobl P, Jilma B. A dose ranging phase I/II trial of the von Willebrand factor inhibiting aptamer ARC1779 in patients with congenital thrombotic thrombocytopenic purpura. *Thromb Haemost.* 2011;106(3):539-547.
- Lammler B, Kremer Hovinga JA, Alberio L. Thrombotic thrombocytopenic purpura. *J Thromb Haemost.* 2005;3(8):1663-1675.
- Cataland SR, Peyvandi F, Mannucci PM, et al. Initial experience from a double-blind, placebo-controlled, clinical outcome study of ARC1779 in patients with thrombotic thrombocytopenic purpura. *Am J Hematol.* 2012;87(4):430-432.
- Jilma-Stohlawetz P, Gorczyca ME, Jilma B, Siller-Matula J, Gilbert JC, Knobl P. Inhibition of von Willebrand factor by ARC1779 in patients with acute thrombotic thrombocytopenic purpura. *Thromb Haemost.* 2011;105(3):545-552.
- Knobl P, Cataland S, Peyvandi F, et al. Efficacy and safety of open-label caplacizumab in patients with exacerbations of acquired thrombotic thrombocytopenic purpura in the HERCULES study. *J Thromb Haemost.* 2020;18(2):479-484.
- Peyvandi F, Scully M, Kremer Hovinga JA, et al. Caplacizumab reduces the frequency of major thromboembolic events, exacerbations and death in patients with acquired thrombotic thrombocytopenic purpura. *J Thromb Haemost.* 2017;15(7):1448-1452.
- Scully M, Cataland SR, Peyvandi F, et al. Caplacizumab treatment for acquired thrombotic thrombocytopenic purpura. *N Engl J Med.* 2019;380(4):335-346.
- Jilma B, Paulinska P, Jilma-Stohlawetz P, Gilbert JC, Hutabarat R, Knobl P. A randomised pilot trial of the anti-von Willebrand factor aptamer ARC1779 in patients with type 2b von Willebrand disease. *Thromb Haemost.* 2010;104(3):563-570.
- Jilma-Stohlawetz P, Knobl P, Gilbert JC, Jilma B. The anti-von Willebrand factor aptamer ARC1779 increases von Willebrand factor levels and platelet counts in patients with type 2B von Willebrand disease. *Thromb Haemost.* 2012;108(2):284-290.
- Jilma-Stohlawetz P, Gorczyca ME, Jilma B, Siller-Matula J, Gilbert JC, Knobl P. Inhibition of von Willebrand factor by ARC1779 in patients with acute thrombotic thrombocytopenic purpura. *Thromb Haemost.* 2011;105(3):545-552.
- Zhu S, Gilbert JC, Hatala P, et al. The development and characterization of a long acting anti-thrombotic von Willebrand factor (VWF) aptamer. *J Thromb Haemost.* 2020;18(5):1113-1123.
- Kovacevic KD, Gilbert JC, Jilma B. Pharmacokinetics, pharmacodynamics and safety of aptamers. *Adv Drug Deliv Rev.* 2018;134:36-50.
- Fazavana J, Brophy TM, Chion A, et al. Investigating the clearance of VWF A-domains using site-directed PEGylation and

- novel N-linked glycosylation. *J Thromb Haemost.* 2020;18(6):1278-1290.
24. Yamamoto K, Troeberg L, Scilabra SD, et al. LRP-1-mediated endocytosis regulates extracellular activity of ADAMTS-5 in articular cartilage. *FASEB J.* 2013;27(2):511-521.
25. Gerritsen KG, Bovenschen N, Nguyen TQ, et al. Rapid hepatic clearance of full length CCN-2/CTGF: a putative role for LRP1-mediated endocytosis. *J Cell Commun Signal.* 2016;10(4):295-303.
26. Kearon C, de Wit K, Parpia S, et al. Diagnosis of pulmonary embolism with d-dimer adjusted to clinical probability. *N Engl J Med.* 2019;381(22):2125-2134.
27. Kovacevic KD, Greisenegger S, Langer A, et al. The aptamer BT200 blocks von Willebrand factor and platelet function in blood of stroke patients. *Sci Rep.* 2021;11(1):3092-3101.
28. Kovacevic KD, Buchtele N, Schoergenhofer C, et al. The aptamer BT200 effectively inhibits von Willebrand factor (VWF) dependent platelet function after stimulated VWF release by desmopressin or endotoxin. *Sci Rep.* 2020;10(1):11180.
29. O'Sullivan JM, Ward S, Lavin M, O'Donnell JS. von Willebrand factor clearance - biological mechanisms and clinical significance. *Br J Haematol* 2018;183(2):185-195.
30. Pipe SW, Montgomery RR, Pratt KP, Lenting PJ, Lillicrap D. Life in the shadow of a dominant partner: the FVIII-VWF association and its clinical implications for hemophilia A. *Blood.* 2016;128(16):2007-2016.
31. Chion A, Aguila S, Fazavana J, et al. VWFA1 interacts with scavenger receptor LRP1 via lysine 1408. *Res Pract Thromb Haemost.* 2019;3(S1):1-228.
32. Martin K, Key NS. How I treat patients with inherited bleeding disorders who need anticoagulant therapy. *Blood.* 2016;128(2):178-184.
33. Zhu S, Gilbert JC, Liang Z, et al. Potent and rapid reversal of the von Willebrand factor inhibitor aptamer BT200. *J Thromb Haemost.* 2020;18(7):1695-1704.
34. Deitcher SR, Tuller J, Johnson JA. Intranasal DDAVP induced increases in plasma von Willebrand factor alter the pharmacokinetics of high-purity factor VIII concentrates in severe haemophilia A patients. *Haemophilia.* 1999;5(2):88-95.
35. Lethagen S. Desmopressin in mild hemophilia A: indications, limitations, efficacy, and safety. *Semin Thromb Hemost.* 2003;29(1):101-106.
36. Casonato A, Daidone V, Galletta E, Bertomoro A. Type 2B von Willebrand disease with or without large multimers: a distinction of the two sides of the disorder is long overdue. *PLoS One.* 2017;12(6):e0179566.
37. Casonato A, Gallinaro L, Cattini MG, et al. Reduced survival of type 2B von Willebrand factor, irrespective of large multimer representation or thrombocytopenia. *Haematologica.* 2010;95(8):1366-1372.
38. Casari C, Lenting PJ, Wohner N, Christophe OD, Denis CV. Clearance of von Willebrand factor. *J Thromb Haemost.* 2013;11(Suppl 1):202-211.
39. Casonato A, Pontara E, Sartorello F, et al. Identifying type Vicenza von Willebrand disease. *J Lab Clin Med.* 2006;147(2):96-102.
40. van Galen KPM, d'Oiron R, James P, et al. A new hemophilia carrier nomenclature to define hemophilia in women and girls: communication from the SSC of the ISTH. *J Thromb Haemost.* 2021;19(8):1883-1887.

The impact of aberrant von Willebrand factor-GPIb α interaction on megakaryopoiesis and platelets in humanized type 2B von Willebrand disease model mouse

Sachiko Kanaji,^{1,2} Yosuke Morodomi,¹ Hartmut Weiler,² Alessandro Zarpellon,^{1,3} Robert R. Montgomery,^{2,4,5} Zaverio M. Ruggeri^{1,3} and Taisuke Kanaji^{1,2}

¹Department of Molecular Medicine, MERU-Roon Research Center on Vascular Biology, The Scripps Research Institute, La Jolla, CA; ²Blood Research Institute, Blood Center of Wisconsin, Versiti, Milwaukee, WI; ³MERU-VasImmune, Inc., San Diego, CA; ⁴Children's Research Institute, Children's Hospital of Wisconsin, Milwaukee, WI and ⁵Department of Pediatrics, Medical College of Wisconsin, Milwaukee, WI, USA

Correspondence: S. Kanaji
skana@scripps.edu

Received: December 22, 2021.

Accepted: February 2, 2022.

Prepublished: February 10, 2022.

<https://doi.org/10.3324/haematol.2021.280561>

©2022 Ferrata Storti Foundation

Published under a CC BY-NC license



Abstract

Type 2B von Willebrand disease (VWD) is caused by gain-of-function mutations in von Willebrand factor (VWF). Increased VWF affinity for GPIb α results in loss of high molecular weight multimers and enhanced platelet clearance, both contributing to the bleeding phenotype. Severity of the symptoms vary among type 2B VWD patients, with some developing thrombocytopenia only under stress conditions. Efforts have been made to study underlying pathophysiology for platelet abnormalities, but animal studies have been limited because of species specificity in the VWF-GPIb α interaction. Here, we generated a severe form of type 2B VWD (p.V1316M) knockin mice in the context of human VWF exon 28 (encoding A1 and A2 domains) and crossed them with human GPIb α transgenic strain. Heterozygous mutant mice recapitulated the phenotype of type 2B VWD in autosomal dominant manner and presented severe macrothrombocytopenia. Of note, platelets remaining in the circulation had extracytoplasmic GPIb α shed-off from the cell surface. Reciprocal bone marrow transplantation determined mutant VWF produced from endothelial cells as the major cause of the platelet phenotype in type 2B VWD mice. Moreover, altered megakaryocyte maturation in the bone marrow and enhanced extramedullary megakaryopoiesis in the spleen were observed. Interestingly, injection of anti-VWF A1 blocking antibody (NMC-4) not only ameliorated platelet count and GPIb α expression, but also reversed MK ploidy shift. In conclusion, we present a type 2B VWD mouse model with humanized VWF-GPIb α interaction which demonstrated direct influence of aberrant VWF-GPIb α binding on megakaryocytes.

Introduction

Von Willebrand disease (VWD) is a common inherited bleeding disorder caused by defects in the function or synthesis of von Willebrand factor (VWF).¹ VWD is classified into three primary categories: type 1, type 2, and type 3. Among them, type 2B VWD represents variants with increased affinity for platelet GPIb α , which is paradoxically associated with bleeding symptoms, not thrombosis.^{2,3} It has been known that enhanced binding of gain-of-function mutant VWF to platelets and accelerated clearance, in combination with higher susceptibility to ADAMTS13, result in loss of the largest VWF multimers and thrombocytopenia.²⁻⁴ Of note, clinical manifestations and results of laboratory tests are heterogeneous among type 2B VWD

patients, depending on the mutations involved.⁵ In addition, one unsolved issue in the pathophysiology of type 2B VWD is the regulatory mechanism of aberrant VWF A1-GPIb α on megakaryocytes (MK) and thrombopoiesis. In addition to accelerated platelet clearance, impaired megakaryopoiesis have also been implicated as the cause of thrombocytopenia.^{6,7}

To date, limited research of VWD using mouse models have been reported due to species-incompatibility of VWF A1-GPIb α interaction. Previous efforts have been made to overcome species-specificity in VWF A1-GPIb α interaction.⁸ However, later study found that single amino acid substitutions may not be sufficient to fully convert the species-specific binding property,⁹ suggesting that replacement of the entire VWF A1 is desired to mimic human

VWF A1-GPIb α interaction *in vivo*. In addition, mouse VWF A1-GPIb α interaction was found not to be identical to that of human.¹⁰⁻¹² In this study, we report the first mouse model of type 2B VWD having gain-of-function mutation in humanized VWF A1-GPIb α interaction. We have employed the strategy to target *Vwf* exon 28 to humanize VWF A1/A2 domains,¹³ and generated type 2B VWD model by mutagenizing the human VWF A1 with the p.V1316M substitution. This strain was bred with humanized GPIb α transgenic strain to humanize VWF A1-GPIb α interaction *in vivo*. As expected, this model closely recapitulated platelet phenotype of human type 2B VWD in autosomal dominant manner and was proven to be a valuable tool to study the biological effect of VWF A1-GPIb α interaction *in vivo*.

Methods

Animal experiments

All animal procedures were performed in accordance with the National Institute of Health Guideline for the Care and Use of Laboratory Animals. All protocols for animal studies were approved by the Institutional Animal Care and Use Committees (IACUC) of The Scripps Research Institute and Medical College of Wisconsin.

Generation of human von Willebrand factor exon 28 knockin mice with p.V1316M mutation and cross-breeding with human GPIb α transgenic mice

A new knockin strain having type 2B VWD mutation was generated at the Transgenic Core Facility, Blood Research Institute/Medical College of Wisconsin. The targeting vector previously used to generate a knockin mouse with *Vwf* exon28 replaced by human homolog (VWF^{hA1}) was used with additional mutagenesis of p.V1316M in the A1 domain.¹³ Correctly targeted embryonic stem cells were injected into blastocyst stage embryos to generate chimeric mice. In order to remove the loxP-flanked Neo cassette, these mice were bred with B6.FVB-Tg (Ella-Cre) C5379Lmgd/J mice (The Jackson Laboratory) and then crossed with the human GPIb α transgenic mouse strain in which platelets express only human GPIb α in the GPIb-IX-V complex. The knockin strain having human VWF exon 28 with p.V1316M substitution was bred into homozygous (VWF^{2Bhomo} hGPIb α). VWF^{2Bhomo} hGPIb α strain was bred with previously generated VWF^{hA1} hGPIb α strain to generate VWF^{2Bhet} hGPIb α mice having heterozygous p.V1316M mutation.

Platelet count analysis

For blood cell counting, blood obtained by retro-orbital bleeding were analyzed using the IDEXX ProCyte™ (IDEXX Laboratories Inc., Westbrook, ME).

NMC-4 injection study

Monovalent Fab fragment¹⁴ expressed in *D. melanogaster* S2 cells was purified from culture supernatant and administered (2 mg/kg) by retro-orbital vein injection for 4 consecutive days.

Bone marrow hematopoietic stem cell transplantation

Bone marrow (BM) cells were collected from femurs and tibia of donor mice, and BM mononuclear cells (BM MNC) were isolated using ficoll as described previously.^{15,16} Six- to 8-week-old recipient mice were conditioned with a lethal dose of 1,100 cGy total body irradiation using a Gammacell 40 Exactor cesium irradiator. Twenty-four hours after irradiation, a dose of 1 \times 10⁷ BM MNC was infused by retro-orbital vein injection. Recipients were analyzed beginning at 6 weeks after transplantation.

Plasma von Willebrand factor analysis

VWF antigen (VWF:Ag) was measured by enzyme-linked immunosorbent assay (ELISA) using a rabbit anti-human VWF polyclonal antibody (IgG) cross-reacting with mouse VWF (produced at the Scripps Research Institute).¹⁶ Normal pooled plasma from C57BL/6J wild-type (WT) mice was used as a reference and defined as 1 U/mL. VWF multimers were analyzed by electrophoresis through 1% HGT(P) agarose containing 0.1% sodium dodecyl sulfate followed by western blotting with the same antibodies used for ELISA.¹³

Flow cytometry analysis

Mouse blood samples were collected from the retro-orbital plexus using sodium citrate as anti-coagulant. Blood samples were diluted in phosphate-buffered saline (pH 7.4) containing 2 mM ethylenediaminetetraacetic acid. Samples were stained with anti-CD41 (integrin α IIb) (MWRReg30, Biolegend, San Diego, CA), anti-GPIb α (LJ-P3 for hGPIb α , 5A7 for mGPIb α ¹⁷, MERU-VasImmune, San Diego, CA), anti-VWF [polyclonal antibodies¹³]. Samples were analyzed using a NovoCyte flow cytometer (ACEA Biosciences). The results were analyzed with FlowJo v.10.7.1.

Results

Generation and characterization of type 2B von Willebrand disease model mice with humanized von Willebrand factor A1-GPIb α interaction

We have previously generated a mouse strain expressing human VWF A1/A2 in the context of mouse VWF and human GPIb α (VWF^{hA1} hGPIb α).¹³ In the current study, the same strategy was employed to generate a strain having type 2B VWD mutation (p.V1316M) in human VWF exon 28 (encoding A1/A2 domains). The substitution p.V1316M

was chosen as the mutation associated with the most severe bleeding and thrombocytopenia with morphological abnormalities in patients with type 2B VWD.⁵ A knockin strain having p.V1316M mutation in human VWF exon 28 was cross-bred with transgenic mice expressing human GPIb α on platelets.^{13,18} The mutant VWF allele (p.V1316M) was maintained either in heterozygous (VWF^{2Bhet} hGPIb α) or homozygous (VWF^{2Bhomo} hGPIb α) status, and a list of the mouse strains used in the cur-

rent study is shown in Figure 1A. One of our interests in generating type 2B VWD model mice was whether they present macrothrombocytopenia in autosomal dominant manner as observed with human patients. As expected, platelet counts were significantly decreased in both VWF^{2Bhet} hGPIb α and VWF^{2Bhomo} hGPIb α mice compared to VWF^{hA1} hGPIb α mice (Figure 1B). Mice having homozygous p.V1316M mutation with mouse GPIb α (VWF^{2Bhomo} mGPIb α) showed normal platelet count, confirming that

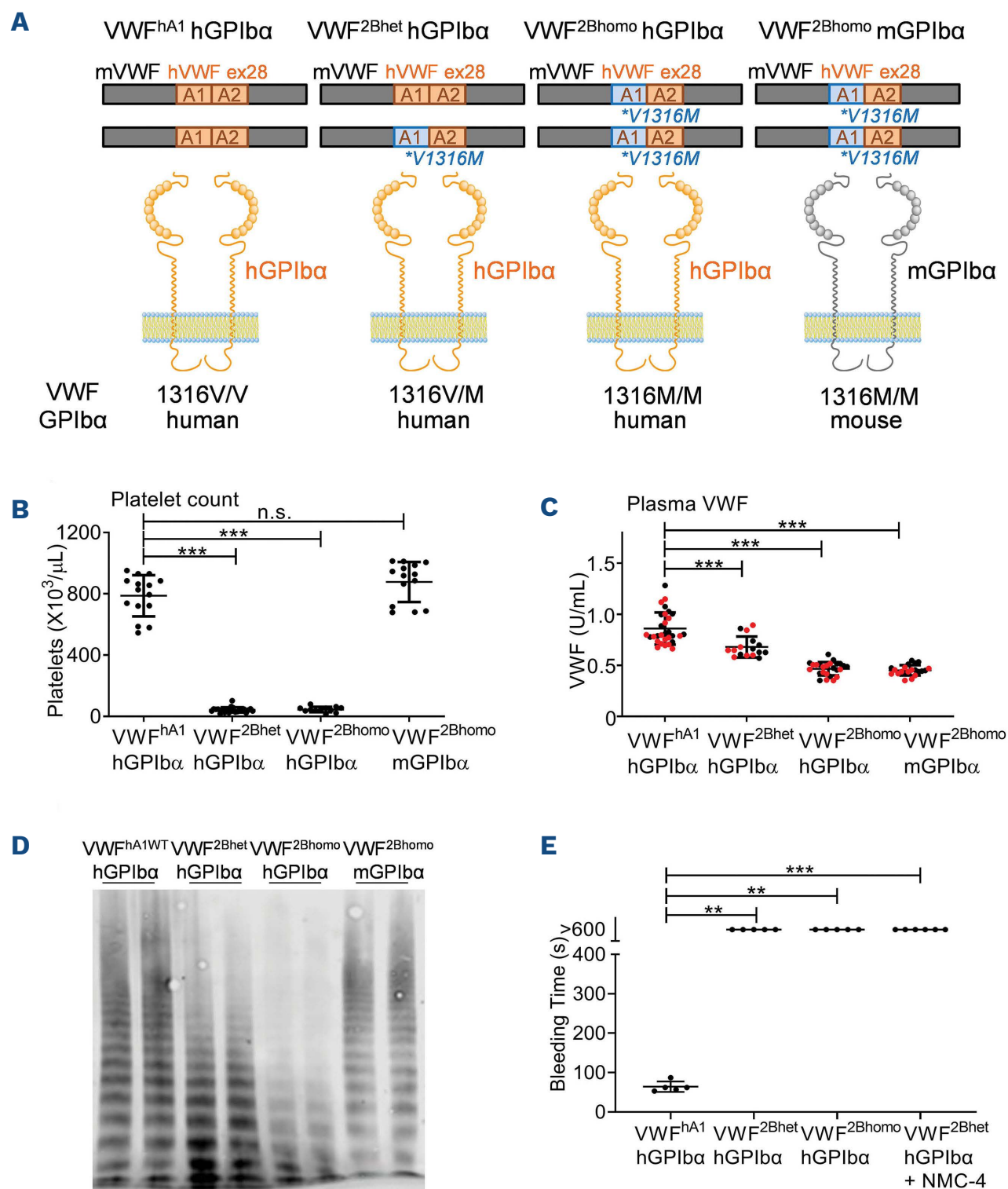


Figure 1. Generation of a mouse model of type 2B von Willebrand disease with humanized von Willebrand factor A1-GPIb α interaction. (A) A knockin strain having human von Willebrand factor (VWF) exon 28 (encoding A1 and A2) bred with human GPIb α transgenic strain (VWF^{hA1} hGPIb α) has been previously described.¹³ A new knockin strain of human VWF exon28 with p.V1316M mutation has been generated in the background of mouse GPIb α (VWF^{2Bhomo} mGPIb α) and crossed with human GPIb α transgenic strain, and maintained either heterozygote or homozygote (VWF^{2Bhet} hGPIb α or VWF^{2Bhomo} hGPIb α , respectively). These 4 mouse strains were analyzed for platelet count (B), plasma VWF (C), and VWF multimer distribution (D). In (C), males and females are depicted as black and red dots, respectively. (E) VWF^{hA1} hGPIb α , VWF^{2Bhet} hGPIb α , and VWF^{2Bhomo} hGPIb α mice (n=5 in each strain) were analyzed by tail bleeding time assay. VWF^{2Bhet} hGPIb α mice treated with intravenous NMC-4 administration (2 mg/kg daily for 4 consecutive days, n=6) were also tested by tail bleeding time assay on the fourth day. Statistical analysis was performed by Kruskal-Wallis non-parametric test followed by Dunn's multiple comparison test. ***P*<0.01, ****P*<0.001.

thrombocytopenia is caused by gain-of-function VWF mutation only when species compatible GPIIb α is expressed. Platelet size was increased in both VWF^{2Bhet} hGPIIb α and VWF^{2Bhomo} hGPIIb α mice (*Online Supplementary Figure S1A*). Decrease in the levels of VWF in plasma might be attributed to spontaneous binding to platelet GPIIb α and enhanced clearance of high molecular weight (HMW) VWF multimers. In support of this idea, VWF multimer analysis showed loss of HMW VWF multimers in the plasma of VWF^{2Bhet} hGPIIb α and VWF^{2Bhomo} hGPIIb α mice, the effect was more profound in the latter (Figure 1D). In addition, increased susceptibility of type 2B mutant VWF to ADAMTS13 has been previously reported^{4,10} and this mechanism may also contribute to loss of HMW VWF multimers in our mice. Interestingly, plasma VWF level was also decreased in VWF^{2Bhomo} mGPIIb α mice. In this strain, gain-of-function VWF has minimum spontaneous binding to mGPIIb α expressed on platelet surface, and therefore, loss of HMW VWF multimer was less obvious compared to the strains with hGPIIb α . Decreased plasma VWF in this strain may be, at least partly, caused by impaired VWF synthesis, secretion or accelerated degradation. Consistently, plasma VWF level of VWF^{2Bhomo} hGPIIb α mice was lower than that of VWF^{2Bhet} hGPIIb α mice despite similar severity of thrombocytopenia, indicating the presence of additional mechanism for reduced VWF beyond spontaneous binding and clear-

ance. As expected, both VWF^{2Bhet} hGPIIb α and VWF^{2Bhomo} hGPIIb α mice showed prolonged tail bleeding time which did not stop in 600 seconds (n=5 in each strain, Figure 1E).

Activation of circulating platelets in VWF^{2Bhet} hGPIIb α and VWF^{2Bhomo} hGPIIb α mice

In order to characterize circulating platelets of VWF^{2Bhet} hGPIIb α and VWF^{2Bhomo} hGPIIb α mice, blood samples were analyzed by flow cytometry. In both strains, the expression of hGPIIb α on platelet surface was markedly reduced, and VWF^{2Bhomo} hGPIIb α mouse was more severely affected than VWF^{2Bhet} hGPIIb α mice (Figure 2A). A small proportion of platelets with preserved hGPIIb α expression were found in circulation of VWF^{2Bhet} hGPIIb α and VWF^{2Bhomo} hGPIIb α mice with bound VWF on their surface (Figure 2A, upper right quadrant). There was not obvious GPIIb α cleavage or VWF binding observed with platelets from mice having homozygous p.V1316M mutation with mouse GPIIb α (VWF^{2Bhomo} mGPIIb α), confirming that GPIIb α cleavage is triggered by spontaneous binding of gain-of-function mutant VWF (Figure 2B). Western blotting of plasma samples confirmed cleavage of hGPIIb α , glycofascin, was abundantly present in VWF^{2Bhomo} hGPIIb α mice and VWF^{2Bhet} hGPIIb α mice (Figure 2C). GPVI is a collagen receptor expressed on platelets and is also known to be proteolytically cleaved in response to activation stimuli such as

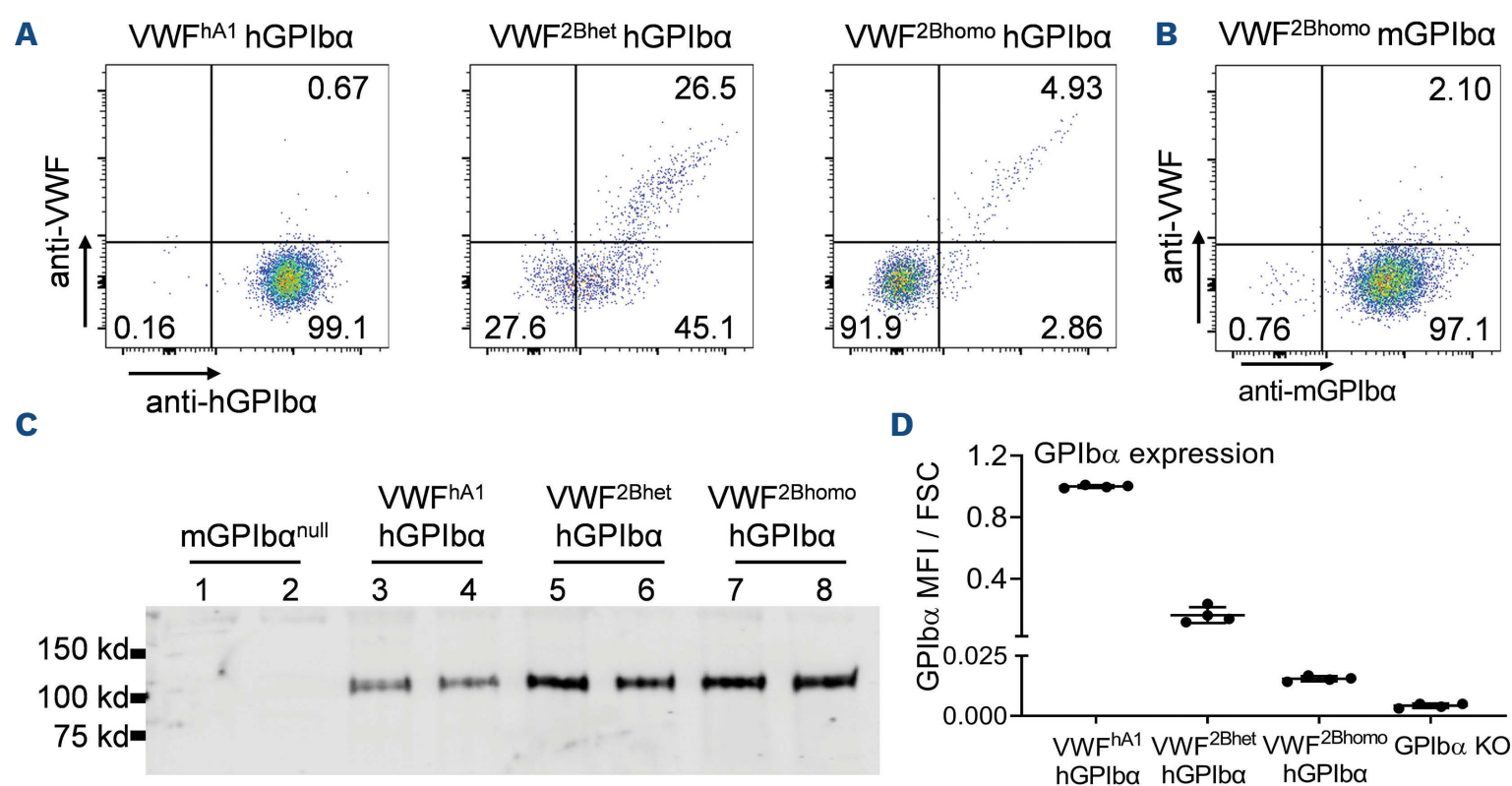


Figure 2. Platelet hGPIIb α is cleaved off from platelets in type 2B von Willebrand disease model mice. (A and B) Whole blood samples collected from each strain were stained with AlexaFluor 488 labeled anti-hGPIIb α antibody (LJ-P3) or anti-mGPIIb α antibody (5A7) and AlexaFluor 647 labeled von Willebrand factor polyclonal antibody (anti-VWF). After staining, blood cells were analyzed by flow cytometry. (C) Plasma samples collected from 2 mice of each strain were analyzed by sodium dodecyl sulfate gel electrophoresis followed by western blotting. PVDF membrane was probed with anti-glycofascin polyclonal antibody, and the signal was detected with IRDye 800 goat anti-rabbit IgG. The image was obtained using LI-COR Odyssey imaging system. (D) Mean fluorescence intensity (MFI) of hGPIIb α signal analyzed by flow cytometry (n=4 in each strain) was normalized by forward side scatter (FSC) MFI to correct platelet size varied among strains.

ligand engagement, elevated shear, and coagulation.¹⁹ The expression of GPIIb/IIIa on platelet surface was also decreased in VWF^{2Bhet} hGPIIb/IIIa and VWF^{2Bhomo} hGPIIb/IIIa mice compared to VWF^{hA1} hGPIIb/IIIa mice (*Online Supplementary Figure S1B*). Western blotting of VWF^{2Bhomo} hGPIIb/IIIa mouse platelet lysate confirmed loss of full-length hGPIIb/IIIa, leaving C-terminal fragment after shedding (*Online Supplementary Figure S1C*). Interestingly, the amount of intracellular filamin A (FlnA) was decreased in VWF^{2Bhomo} hGPIIb/IIIa mouse platelets compared to VWF^{hA1} hGPIIb/IIIa mouse platelets. The level of FlnA was also quantified by staining platelets intracellularly after fixation and permeabilization, followed by platelet size correction (*Online Supplementary Figure S1D*). Reduced FlnA content in VWF^{2Bhomo} hGPIIb/IIIa mouse platelets was confirmed by flow cytometry, indicating activation of μ -calpain and enhanced FlnA degradation in VWF^{2Bhomo} hGPIIb/IIIa mouse platelets.^{20,21} Functional defect of platelets in response to agonist stimulation has been reported in patients and mouse model of type 2B VWD.²²⁻²⁴ Thus, mouse platelets have been stimulated with PAR4 activating peptide (PAR4-AP) and fibrinogen binding was evaluated by flow cytometry. As expected, fibrinogen binding was impaired in VWF^{2Bhet} hGPIIb/IIIa and VWF^{2Bhomo} hGPIIb/IIIa mouse platelets compared to VWF^{hA1} hGPIIb/IIIa mouse platelets (*Online Supplementary Figure S2*). Defect in fibrinogen binding following agonist stimulation has also been previously reported in a mouse model of platelet-type VWD.²⁵

Contribution of megakaryocyte/platelet versus endothelial cells to the pathophysiology of type 2B von Willebrand disease

Plasma VWF is primarily derived from endothelial cells (EC), and platelets contain 10-15% of total blood VWF.¹ Thus, one could postulate that the pathology of type 2B VWD is caused by endothelial synthesis of mutant VWF. Previous study showed that VWF spontaneously bound to the surface and intracellular canals of cultured MK derived from patients with type 2B VWD.⁶ This result suggests a possibility that mutant VWF binds to GPIIb/IIIa during synthesis in MK, leading to impaired platelet generation. Thus, reciprocal BM transplantation between VWF^{hA1} hGPIIb/IIIa and VWF^{2Bhomo} hGPIIb/IIIa mice was performed. VWF^{hA1} hGPIIb/IIIa mice lethally irradiated and transplanted with VWF^{2Bhomo} hGPIIb/IIIa BM hematopoietic stem cells (HSC) expressed VWF with normal human A1 sequence in EC and gain-of-function mutant VWF (p.V1316M) in MK/platelets (2B^{MK}, Figure 3A). Conversely, VWF^{2Bhomo} hGPIIb/IIIa mice irradiated and transplanted with VWF^{hA1} hGPIIb/IIIa BM HSC expressed mutant VWF in EC and normal VWF in MK/platelets (2B^{EC}). VWF^{hA1} hGPIIb/IIIa mice irradiated and transplanted with allogenic VWF^{hA1} hGPIIb/IIIa mouse BM HSC were prepared as controls. Platelet count analyzed after BM reconstitution showed marked thrombocytopenia in 2B^{EC} (Figure 3B). Platelet count in 2B^{MK} mice was lower than control VWF^{hA1} hGPIIb/IIIa mice but the difference did not reach statistical significance. Flow cytometry

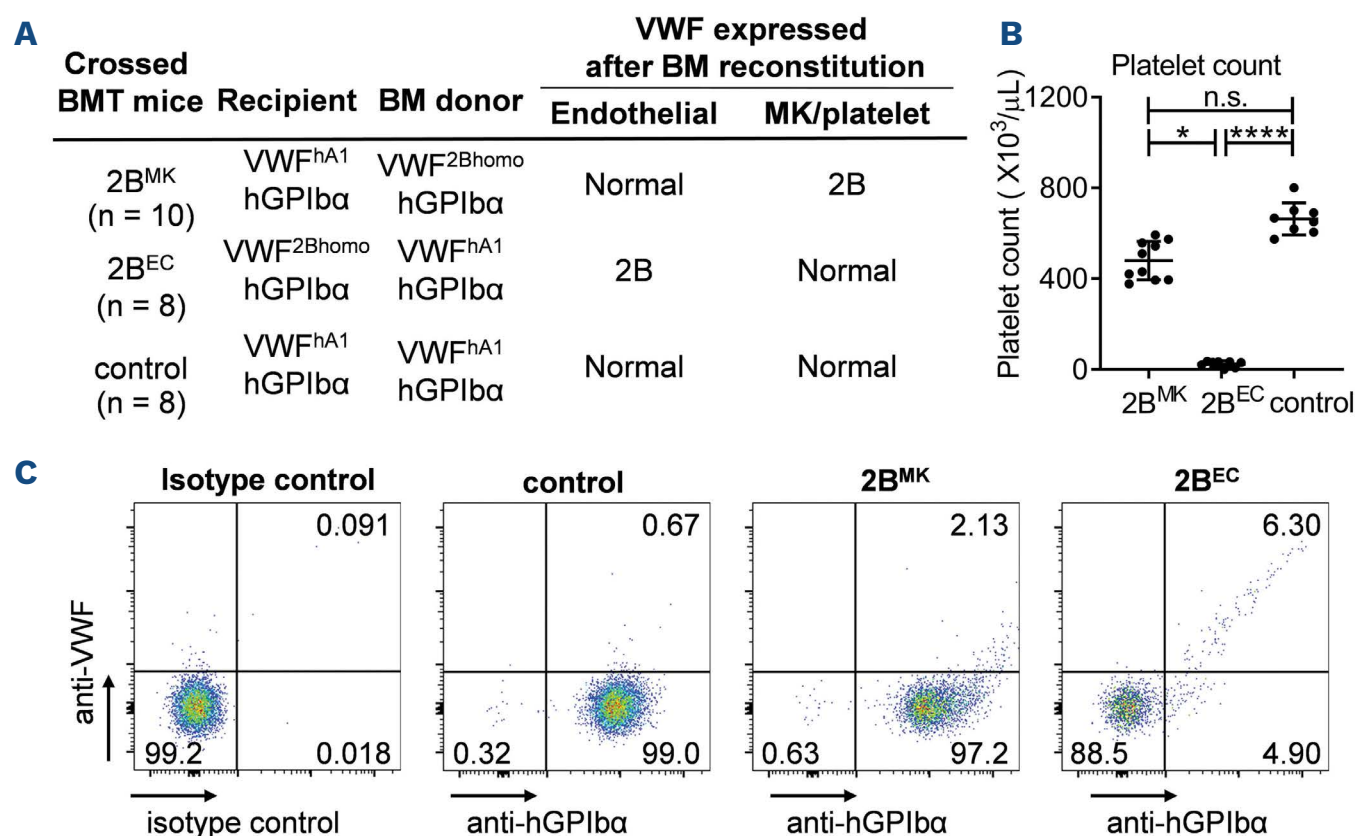


Figure 3. Crossed bone marrow transplantation between VWF^{hA1} hGPIIb/IIIa and VWF^{2Bhomo} hGPIIb/IIIa mice. (A) In order to express type 2B von Willebrand factor (VWF) selectively in endothelial cells (EC) or megakaryocytes[MK]/platelets, VWF^{hA1} hGPIIb/IIIa and VWF^{2Bhomo} hGPIIb/IIIa mice were lethally irradiated (1,100 cGy) and transplanted with hematopoietic stem cells (HSC) derived from the other strain. (B and C) Platelet count and platelet flow cytometry analyses. Surface expression of GPIIb/IIIa and VWF binding were analyzed using the method described in Figure 2A after bone marrow (BM) reconstitution. Data are shown as mean \pm standard deviation. Statistical analysis performed with the Kruskal-Wallis non-parametric test followed by Dunn's multiple comparison test. * $P < 0.05$, **** $P < 0.0001$.

analysis showed that hGPIb α was shed off from the surface of the 2B^{EC} mouse platelets (Figure 3C). The expression of hGPIb α was preserved and platelets with spontaneously bound VWF was not abundantly present in 2B^{MK} mice (Figure 3C, upper right quadrant). These results demonstrate that severe thrombocytopenia and hGPIb α cleavage observed with type 2B VWD model mice are primarily caused by mutant VWF synthesized in EC.

Enhanced megakaryocyte maturation in the bone marrow and extramedullary megakaryopoiesis in spleen

Previous studies have indicated abnormal megakaryopoiesis and thrombopoiesis in type 2B VWD. The challenging aspect of MK study using patients' samples is the difficulty in obtaining BM cells for analysis because BM aspirate or biopsy is an invasive procedure especially for patients with a bleeding tendency. Therefore, earlier studies have been performed with MK differentiated *in vitro* from CD34⁺ cells isolated from patients' peripheral

blood.^{6,7} In the current study, we have studied newly generated type 2B VWD mouse model to evaluate MK in the BM and extramedullary megakaryopoiesis in other organs. Interestingly, total number of MK in the BM was significantly higher in VWF^{2Bhet} hGPIb α mice compared to VWF^{hA1} hGPIb α mice (Figure 4A). MK ploidy analysis showed increased percentage of high ploidy MK (32N) in VWF^{2Bhet} hGPIb α mice compared to VWF^{hA1} hGPIb α mice (Figure 4B). In order to examine whether increased ploidy observed with VWF^{2Bhet} hGPIb α mouse BM MK is caused by increased thrombopoietin (TPO) level, plasma TPO was measured by ELISA. Plasma TPO levels in VWF^{2Bhet} hGPIb α mice were slightly higher than VWF^{hA1} hGPIb α mice but the difference was not significant (Figure 4C). Dissection of VWF^{2Bhet} hGPIb α mice showed splenomegaly, indicating the presence of extramedullary hematopoiesis (Figure 4D). As expected, immunofluorescence microscopy showed increased number of MK present in the spleen of VWF^{2Bhet} hGPIb α mice (Figure 4E and F).

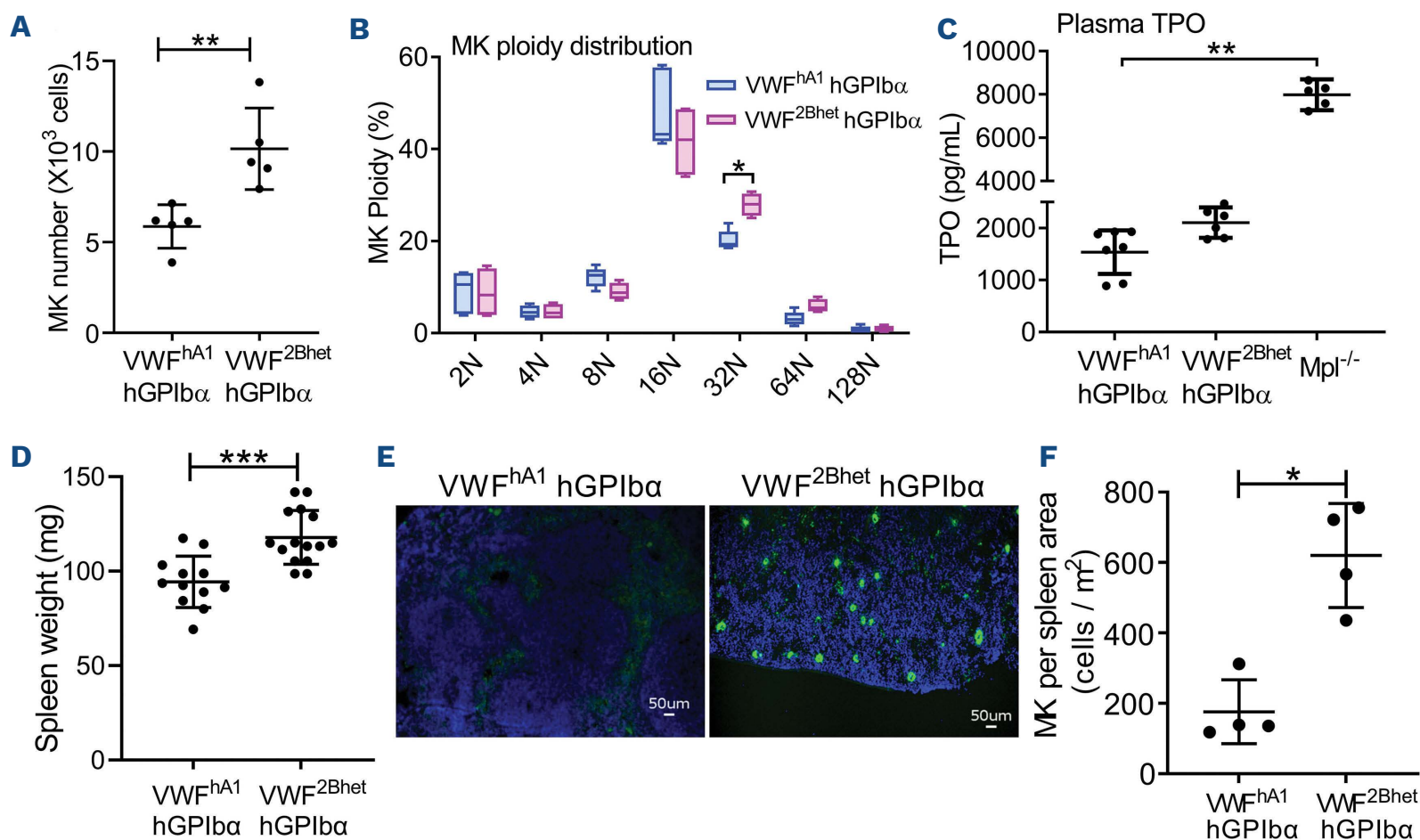


Figure 4. Analysis of megakaryocytes in bone marrow and spleen. (A and B) Bone marrow (BM) cells of VWF^{hA1} hGPIb α and VWF^{2Bhet} hGPIb α mice (n=5 in each group) were flushed from right femurs, stained with Brilliant Violet 421 labeled anti-mouse CD41 antibody and propidium iodide in the presence of RNase A, and analyzed by flow cytometry. Total megakaryocyte (MK) number per femur and MK ploidy distribution are shown. (C) Thyroid peroxidase antibody (TPO) levels in the plasma of VWF^{hA1} hGPIb α (n=7), VWF^{2Bhet} hGPIb α (n=6), and c-Mpl^{-/-} (as controls, n=5) were measured by enzyme-linked immunosorbant assay. (D) Weight of the spleens dissected from VWF^{hA1} hGPIb α (n=12) and VWF^{2Bhet} hGPIb α (n=15) are shown. Females of 9-11 weeks old mice were used to minimize the effect of body size difference. (E and F) Spleens isolated from VWF^{hA1} hGPIb α and VWF^{2Bhet} hGPIb α mice were cryosectioned and immunostained for MK/platelets using rat anti-mouse CD41 antibody and AlexaFluor488-labeled goat anti-rat IgG. Nuclei were counterstained with DAPI. Scale bars =50 μ m. The number of MK per spleen area were counted using BZ-X700 Fluorescence microscope (Keyence). Data were shown as scatter plots with mean \pm standard deviation or 25th-75th percentile boxes with min-to-max-whiskers. Data were analyzed by Mann-Whitney non-parametric test in (A) and (F), two-way ANOVA with Šidák's multiple comparisons test in (B), Kruskal-Wallis test with Dunn's multiple comparisons test in (C), and unpaired *t*-test in (D). **P*<0.05, ***P*<0.01, ****P*<0.001; only significant differences are shown.

Megakaryocytes bind to and internalize gain-of-function mutant von Willebrand factor of endothelial synthesis

One unsolved question was whether MK have a chance to encounter plasma VWF and are influenced by gain-of-function mutant VWF during thrombopoiesis. In order to distinguish VWF of endothelial and MK origin, BM HSC prepared from VWF^{-/-} hGPIb α mice were transplanted into VWF^{hA1} hGPIb α (hA1 MK^{null}) and VWF^{2Bhomo} hGPIb α (2B MK^{null}) to eliminate VWF synthesis in MK (Figure 5A). hA1 MK^{null} and 2B MK^{null} mice express VWF with normal human A1 or p.V1316M mutant A1 sequence only in EC. As expected, 2B MK^{null} presented marked thrombocytopenia and circulating platelets had hGPIb α shed-off from surface (Figure 5B). Immunofluorescent analyses confirmed absence of VWF in the MK of BM and spleen in the hA1 MK^{null} mice (Figure 5C). Interestingly, 2B MK^{null} mice showed weak staining of VWF in the BM MK and strong signal in the splenic MK (Figure 5D). Splenic red pulp harbors an open circulatory system where MK may potentially bind to plasma VWF.²⁶ Thus, higher VWF staining observed with splenic MK is in agreement with exposure to an open circulatory system. These results show that in the absence of VWF synthesis in MK, MK of 2B MK^{null} mice contain substantial amount of VWF derived from EC synthesis. In order to further characterize

platelets generated from these MK, blood samples were fixed, permeabilized, stained with anti-VWF antibody and analyzed by flow cytometry (Online Supplementary Figure S3). hA1 MK^{null} platelets had no VWF signal inside because of defective VWF synthesis in MK, and the result was similar to VWF^{-/-} hGPIb α mouse platelets. On the other hand, about half of platelets derived from 2B MK^{null} mice had VWF inside of cells and partially co-localized with hGPIb α signal. These results confirm that MK of type 2B VWD model mice are exposed to and bind to mutant VWF of EC origin. MK with internalized mutant VWF have potential to produce platelets with intracellular VWF and reduced surface GPIb α expression into circulation.

Blocking von Willebrand factor A1-GPIb α interaction inhibits hGPIb α cleavage and ameliorates thrombocytopenia

In order to test if platelet abnormalities and MK ploidy shift observed with VWF^{2Bhet} hGPIb α mice can be reversed by inhibiting VWF A1-GPIb α interaction, anti-VWF A1 blocking antibody (NMC-4) was injected *in vivo*.^{27,28} Daily administration of NMC-4 (2 mg/kg, n=6) led to platelet count increase to the levels comparable to VWF^{hA1} hGPIb α mice (Figure 6A). Blocking VWF A1-GPIb α interaction also ameli-

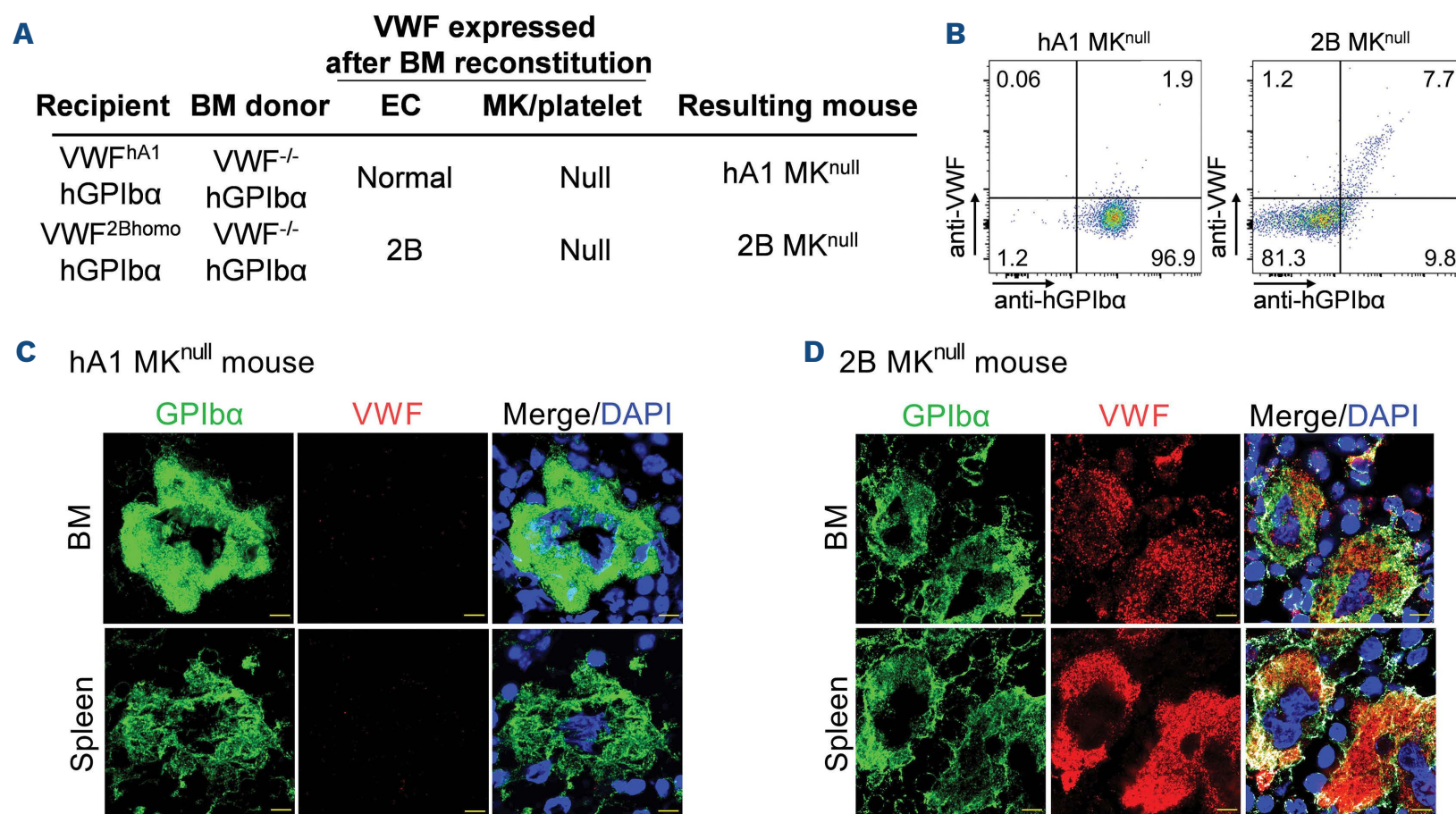


Figure 5. Binding and internalization of gain-of-function mutant von Willebrand factor in megakaryocytes. (A) In order to generate mouse models expressing von Willebrand factor (VWF) only in the endothelial cells (EC), bone marrow hematopoietic stem cells (BM HSCs) prepared from VWF^{-/-} hGPIb α mice were transplanted into lethally irradiated VWF^{hA1} hGPIb α or VWF^{2Bhomo} hGPIb α mice. Upon BM reconstitution, resulting mice produce normal or gain-of-function mutant VWF only in the EC. (B) Blood samples were collected from hA1 MK^{null} and 2B MK^{null} mice 6 weeks after transplantation. Representative results of platelet flow cytometry analysis are shown. Blood samples were stained with the method described in Figure 2A. (C and D) Femurs and spleen were snap frozen, cryosectioned, and stained for GPIb α (LJ-Ib1, green, MERU-VasImmune), VWF (anti-VWF polyclonal antibody, red), counterstained (DAPI, blue), and analyzed by LSM880 laser scanning confocal microscope (Zeiss). Merged signal of GPIb α (green) and VWF (red) is shown in white. Scale bars = 5 μ m.

orated hGPIb α shedding and the hGPIb α expression was recovered on VWF^{2Bhet} hGPIb α mouse platelets (Figure 6B). It has been known that NMC-4 blocks VWF binding to GPIb α , and we have previously reported that administration of NMC-4 (0.8 mg/kg) prolongs bleeding time even in mice having normal sequence of humanized VWF exon 28 (VWF^{hA1} hGPIb α).¹³ Thus, as predicted, despite correction of thrombocytopenia and hGPIb α expression, tail bleeding time was still prolonged in VWF^{2Bhet} hGPIb α administered with NMC-4 (see Figure 1E). Interestingly, BM MK analysis performed after 4 doses of NMC-4 injection showed that MK ploidy shift observed with VWF^{2Bhet} hGPIb α mice was reversed by anti-VWF A1 blocking antibody (Figure 6C, compare with Figure 4B).

Discussion

Mouse models of type 2B VWD have been described using hydrodynamic injection of mutated mouse VWF expression plasmids into VWF^{-/-} mice.^{10,11} In these models, mutations were introduced into mouse VWF cDNA, and expressed ectopically in the liver, not in EC or MK. Subsequently, a knockin mouse harboring a type 2B VWD mutation (p.V1316M) in mouse *Vwf* gene has been described.^{12,23} This model enabled physiologic expression in EC and MK and provided valuable information. However,

introduction of a single point mutation in the context of mouse *VWF* did not reproduce platelet phenotype in autosomal dominant manner and had to be bred into homozygous, suggesting that mutagenesis in mouse VWF A1 in association with mouse GPIb α may not be identical to that of human. Here, we generated a type 2B VWD model with humanized VWF A1-GPIb α interaction. Using the knockin strategy to replace *Vwf* exon 28 - encoding domains A1 and A2 - with that of the human homologue, we have generated a strain with a mutation (p.V1316M) in the sequence of human VWF A1. Subsequent cross-breeding with hGPIb α transgenic mice successfully established a mouse model of type 2B VWD that present macrothrombocytopenia in autosomal dominant manner. Reciprocal HSC transplantation determined VWF of endothelial synthesis as the cause of platelet abnormalities. An open question is whether ADAMTS13 sensitivity is altered by *Vwf* exon28 replacement encoding A1 and A2 (ADAMTS13 cleavage) domains. Enhanced susceptibility of type 2B VWF by ADAMTS13 has been previously reported and the roles of ADAMTS13-mediated proteolysis in the loss of HMW VWF multimers, regulation of platelet aggregates, and impaired hemostasis have been well established.^{4,10} Further study is warranted to explore the alteration of ADAMTS13 sensitivity by humanizing VWF A1/A2 domains in VWF^{hA1} hGPIb α mice and potential contribution to the phenotype of type 2B VWD model mice.

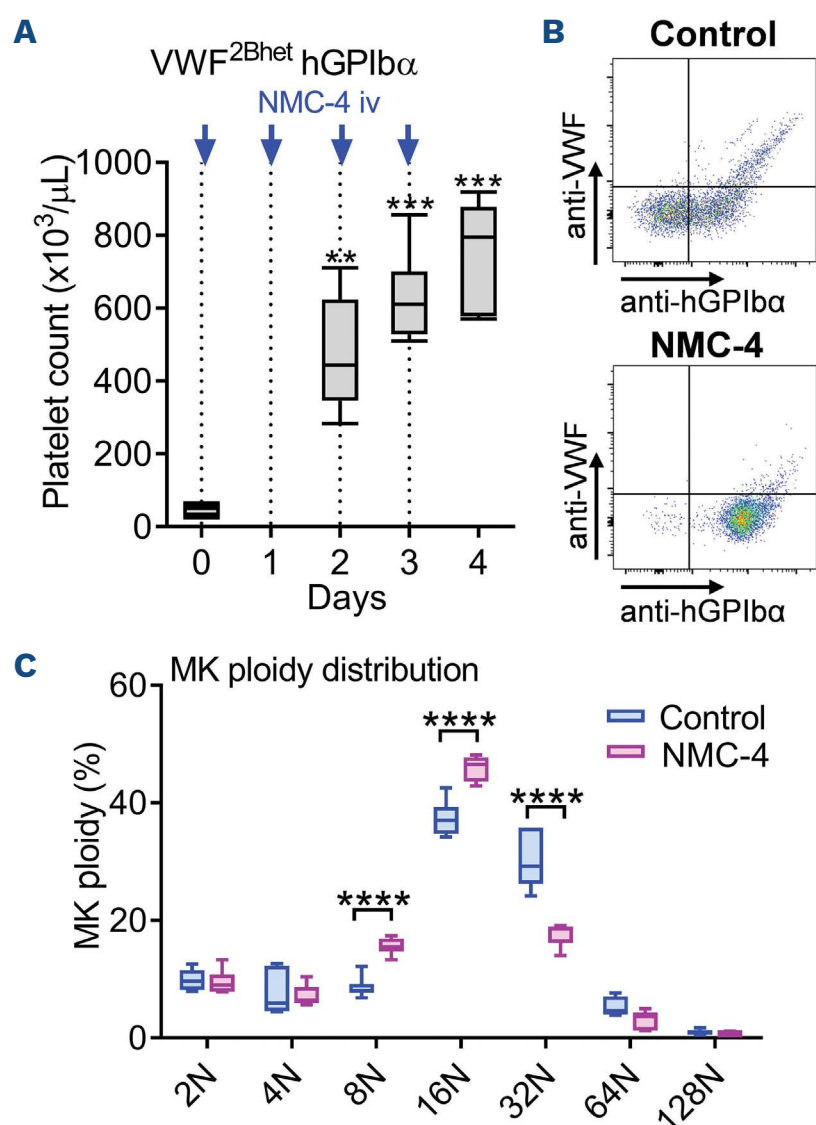


Figure 6. Inhibition of VWF A1-GPIb α reverses the effect of gain-of-function mutant von Willebrand factor on platelets and megakaryocytes. (A) A recombinant monoclonal antibody against von Willebrand factor (VWF) A1 which blocks binding to GPIb α (NMC-4) was intravenously administered into VWF^{2Bhet} hGPIb α mice (2 mg/kg, n=6) daily, and platelet counts were monitored. Data were analyzed by RM one-way ANOVA without assuming sphericity and with Holm-Sidak's post-test for comparing pretreatment values with those at each day post injection. (B) Representative profiles of blood flow cytometry analysis showing recovery of hGPIb α expression on VWF^{2Bhet} hGPIb α mouse platelets after 4 doses of NMC-4 administration. (C) Bone marrow (BM) cells of VWF^{2Bhet} hGPIb α mice treated with daily NMC-4 administration were harvested on day 4 and analyzed by flow cytometry as in the Figure 4B. Data are shown as 25th-75th percentile boxes with min-to-max-whisker and analyzed by two-way ANOVA with Šidák's multiple comparisons test. ***P*<0.01, ****P*<0.001, *****P*<0.0001; only significant differences are shown.

Our type 2B VWD mouse model exhibited exaggerated platelet phenotype compared to human patients. In fact, platelet count in VWF^{2Bhet} hGPIb α mice was about 5% of the control mice with normal VWF A1 sequence (VWF^{hA1} hGPIb α), which was more severe than human patients having the same mutation.⁵ In addition, hGPIb α was cleaved from platelet surface, and VWF^{2Bhomo} hGPIb α mice were more severely affected than VWF^{2Bhet} hGPIb α mice. Shedding of mouse GPIb α has also been reported in a study expressing mutant VWF by hydrodynamic gene transfer.²⁴ In their study, mouse GPIb α cleavage was not reduced when mutant VWF was expressed in mice deficient in ADAM17, indicating ADAM17-independent cleavage.²⁴ Mechanical cleavage by shear stress caused by engagement of hGPIb α binding to VWF A1 may contribute to the shedding of hGPIb α . Shedding of hGPIb α from the platelet surface has not been previously documented in human type 2B VWD patients.²² Thus, cleavage of hGPIb α observed in type 2B VWD model might be caused by mouse-specific factors. Of note, both VWF^{2Bhet} hGPIb α and VWF^{2Bhomo} hGPIb α mice presented marked splenomegaly (see Figure 4). In the developing embryo, hematopoiesis occurs in the liver and spleen. In mouse but not in human, the spleen remains as hematopoietic organ throughout the life.²⁹ In our study, histological analysis revealed abundant presence of MK in the spleen of VWF^{2Bhet} hGPIb α and VWF^{2Bhomo} hGPIb α mice, suggesting extramedullary megakaryopoiesis and potential exposure of MK and platelets to plasma VWF in the open circulatory system of spleen. In support of this idea, transplantation of VWF^{-/-} hGPIb α mouse BM into VWF^{2Bhomo} hGPIb α (2B MK^{null}) showed splenic MK bound to and internalized plasma-derived mutant VWF, and presence of VWF-containing platelets in the circulation of 2B MK^{null} mice. Thus, we speculate that the extramedullary megakaryopoiesis in the spleen contributes to exaggerated platelet phenotype observed with our type 2B VWD model mice. Another interesting finding is that the expression of gain-of-function mutant VWF protein leads to MK ploidy shift to mature population (see Figure 4). Plasma TPO level was not significantly changed in VWF^{2Bhet} hGPIb α compared to VWF^{hA1} hGPIb α , indicating that the ploidy shift was not caused by elevated TPO levels but by direct influence of aberrant VWF binding to MK. In support of this idea, MK ploidy shift observed in VWF^{2Bhet} hGPIb α mouse was reversed by administration of NMC-4 which blocks VWF A1-GPIb α interaction. Taken together, these results demonstrate that aberrant VWF-hGPIb α occurs not only in platelets but also in MK, the latter leads to altered megakaryopoiesis and possibly platelet generation. We have previously reported signaling effects of GPIb α cytoplasmic tail on MK proliferation and maturation.³⁰ Crosstalk of GPIb α signaling with TPO-Mpl pathway, mediated by 14-3-3 ξ and phosphoinositol-3-kinase/Akt (PI3K/Akt) pathways, might be involved in the effect of gain-of-function mutant VWF

on MK proliferation and maturation.³⁰ Further study is required to elucidate the mechanism of gain-of-function VWF A1 on GPIb α signaling.

As to the functional defect of platelets, impaired activation of the small GTPase Rap1 has been previously reported as a cause of thrombocytopathy and bleeding tendency in type 2B VWD model mice.²² Subsequent study determined preactivation and exhaustion of the PKC pathway as the cause of impaired Rap1 signaling and thrombopathy in type 2B VWD.²⁴ In addition, the same group identified the effect of dysregulated RhoA/ROCK/LIMK/cofilin pathway on Mk and macrothrombocytopenia.²³ In the current study, we found enhanced degradation of intracellular FlnA, a major substrate for μ -calpain in VWF^{2Bhet} hGPIb α and VWF^{2Bhomo} hGPIb α mouse platelets (*Online Supplementary Figure S7*).^{21,31} FlnA is a scaffold protein which links cytoskeletal proteins to GPIb-IX in platelets and plays an important role in the regulation of contractile force and production of normal size platelets.^{32,33} We have previously reported in a mouse model of sitosterolemia that activation of μ -calpain and enhanced degradation of FlnA led to cytosolic redistribution of FlnA, thereby contributing to generation of large platelets.²¹ In the current study, there was a significant population of VWF^{2Bhet} hGPIb α and VWF^{2Bhomo} hGPIb α mouse platelets refractory to agonist stimulation and failed to bind fibrinogen, which was similar to what was previously observed with sitosterolemia mice. Thus, μ -calpain activation and FlnA degradation may partly explain the mechanism for platelet abnormalities observed in type 2B VWD.²¹ Further studies are warranted to elucidate the involvement of FlnA in generation of large platelets in type 2B VWD.

Currently, type 2B VWD is treated mostly with VWF replacement therapy with adjunct therapies used for other types of VWD.³⁴ 1-Desamino-8-D-arginine vasopressin (DDAVP) needs to be carefully considered because of the concern for the exacerbation of thrombocytopenia. VWF A1-GPIb α has been focused as a target for the development of therapeutics against type 2B VWD.³⁵⁻³⁷ Interestingly, MK ploidy shift, thrombocytopenia, and GPIb α cleavage were found to be corrected by administration of an antibody against VWF A1 which blocks binding to GPIb α (NMC-4). However, in agreement with our previous report on VWF^{hA1} hGPIb α mice,¹³ tail bleeding time of our type 2B VWD mice was not corrected after normalization of platelet counts by high-dose NMC-4 administration. Due to the primary role in hemostasis, targeting VWF A1-GPIb α needs to be carefully studied and our animal models serve as useful tools for *in vivo* evaluation. Dysregulated VWF-GPIb α interaction can be seen not only in type 2B VWD but also in platelet-type VWD (PT-VWD), which is caused by mutations in *GP1BA*.³⁸ PT-VWD mouse models have been previously generated and platelet phenotypes similar to type 2B VWD have been reported.^{25,39-42} Thus, results obtained from this study will

help understand other forms of hematologic disorders which involve dysregulated VWF-GPIIb interaction, and our mouse model with humanized VWF-GPIIb interaction may serve as a useful tool to explore therapeutic strategy.

Disclosures

ZMR is founder, President, and CEO, AZ is Chief Innovation Officer of MERU-VasImmune, Inc. SK and TK have equity interest in MERU-VasImmune, Inc. The remaining authors declare no competing financial interests.

Contributions

SK designed and performed experiments, analyzed data, and wrote the manuscript; YM performed histologic analysis and flow cytometry analysis; HW is a director of Transgenic Core Facility, Blood Research Institute/Medical College of Wisconsin and helped to design and generate

p.V1316M knockin mouse; AZ provided key reagents; RRM and ZMR supervised the study and reviewed the manuscript; TK designed, directed the study, analyzed data, and co-wrote the manuscript.

Funding

This work was supported by National Institutes of Health grants HL-56027 and HL-44612 (RRM), HL-135290 (ZMR), and HL-129011 (TK); by fellowships and additional financial support from MERU Foundation (Italy) to YM, SK, and TK; and by the National Foundation for Cancer Research (SK and TK).

Data-sharing statement

Further details of the data generated or analyzed in the current study are available from the corresponding author upon request.

References

- Nichols WL, Hultin MB, James AH, et al. von Willebrand disease (VWD): evidence-based diagnosis and management guidelines, the National Heart, Lung, and Blood Institute (NHLBI) Expert Panel report (USA). *Haemophilia*. 2008;14(2):171-232.
- Ruggeri ZM, Pareti FI, Mannucci PM, Ciavarella N, Zimmerman TS. Heightened interaction between platelets and factor VIII/von Willebrand factor in a new subtype of von Willebrand's disease. *N Engl J Med*. 1980;302(19):1047-1051.
- Ruggeri ZM, Lombardi R, Gatti L, Bader R, Valsecchi C, Zimmerman TS. Type IIB von Willebrand's disease: differential clearance of endogenous versus transfused large multimer von Willebrand factor. *Blood*. 1982;60(6):1453-1456.
- Rayes J, Hommais A, Legendre P, et al. Effect of von Willebrand disease type 2B and type 2M mutations on the susceptibility of von Willebrand factor to ADAMTS-13. *J Thromb Haemost*. 2007;5(2):321-328.
- Federici AB, Mannucci PM, Castaman G, et al. Clinical and molecular predictors of thrombocytopenia and risk of bleeding in patients with von Willebrand disease type 2B: a cohort study of 67 patients. *Blood*. 2009;113(3):526-534.
- Nurden P, Debili N, Vainchenker W, et al. Impaired megakaryocytopoiesis in type 2B von Willebrand disease with severe thrombocytopenia. *Blood*. 2006;108(8):2587-2595.
- Nurden P, Gobbi G, Nurden A, et al. Abnormal VWF modifies megakaryocytopoiesis: studies of platelets and megakaryocyte cultures from patients with von Willebrand disease type 2B. *Blood*. 2010;115(13):2649-2656.
- Chen J, Tan K, Zhou H, et al. Modifying murine von Willebrand factor A1 domain for in vivo assessment of human platelet therapies. *Nat Biotechnol* 2008;26(1):114-119.
- Navarrete AM, Casari C, Legendre P, et al. A murine model to characterize the antithrombotic effect of molecules targeting human von Willebrand factor. *Blood*. 2012;120(13):2723-2732.
- Rayes J, Hollestelle MJ, Legendre P, et al. Mutation and ADAMTS13-dependent modulation of disease severity in a mouse model for von Willebrand disease type 2B. *Blood*. 2010;115(23):4870-4877.
- Golder M, Pruss CM, Hegadorn C, et al. Mutation-specific hemostatic variability in mice expressing common type 2B von Willebrand disease substitutions. *Blood*. 2010;115(23):4862-4869.
- Adam F, Casari C, Prevost N, et al. A genetically-engineered von Willebrand disease type 2B mouse model displays defects in hemostasis and inflammation. *Sci Rep*. 2016;6:26306.
- Kanaji S, Orje JN, Kanaji T, et al. Humanized GPIIb-von Willebrand factor interaction in the mouse. *Blood Adv*. 2018;2(19):2522-2532.
- Celikel R, Varughese KI, Madhusudan, Yoshioka A, Ware J, Ruggeri ZM. Crystal structure of the von Willebrand factor A1 domain in complex with the function blocking NMC-4 Fab. *Nat Struct Biol*. 1998;5(3):189-194.
- Kanaji S, Kuether EL, Fahs SA, et al. Correction of murine Bernard-Soulier syndrome by lentivirus-mediated gene therapy. *Mol Ther*. 2012;20(3):625-632.
- Kanaji S, Fahs SA, Shi Q, Haberichter SL, Montgomery RR. Contribution of platelet versus endothelial VWF to platelet adhesion and hemostasis. *J Thromb Haemost*. 2012;10(8):1646-1652.
- Yokota N, Zarpellon A, Chakrabarty S, et al. Contributions of thrombin targets to tissue factor-dependent metastasis in hyperthrombotic mice. *J Thromb Haemost*. 2014;12(1):71-81.
- Ware J, Russell S, Ruggeri ZM. Generation and rescue of a murine model of platelet dysfunction: the Bernard-Soulier syndrome. *Proc Natl Acad Sci U S A*. 2000;97(6):2803-2808.
- Gardiner EE. Proteolytic processing of platelet receptors. *Res Pract Thromb Haemost*. 2018;2(2):240-250.
- Artemenko EO, Yakimenko AO, Pichugin AV, Ataulkhanov FI, Panteleev MA. Calpain-controlled detachment of major glycoproteins from the cytoskeleton regulates adhesive properties of activated phosphatidylserine-positive platelets. *Biochem J*. 2016;473(4):435-448.
- Kanaji T, Kanaji S, Montgomery RR, Patel SB, Newman PJ. Platelet hyperreactivity explains the bleeding abnormality and macrothrombocytopenia in a murine model of sitosterolemia. *Blood*. 2013;122(15):2732-2742.
- Casari C, Berrou E, Leuret M, et al. von Willebrand factor mutation promotes thrombocytopenia by inhibiting integrin alphaIIb beta3. *J Clin Invest*. 2013;123(12):5071-5081.

23. Kauskot A, Poirault-Chassac S, Adam F, et al. LIM kinase/cofilin dysregulation promotes macrothrombocytopenia in severe von Willebrand disease-type 2B. *JCI Insight*. 2016;1(16):e88643.
24. Casari C, Paul DS, Susen S, et al. Protein kinase C signaling dysfunction in von Willebrand disease (p.V1316M) type 2B platelets. *Blood Adv*. 2018;2(12):1417-1428.
25. Guerrero JA, Kyei M, Russell S, et al. Visualizing the von Willebrand factor/glycoprotein Ib-IX axis with a platelet-type von Willebrand disease mutation. *Blood*. 2009;114(27):5541-5546.
26. Steiniger B, Bette M, Schwarzbach H. The open microcirculation in human spleens: a three-dimensional approach. *J Histochem Cytochem*. 2011;59(6):639-648.
27. Fujimura Y, Usami Y, Titani K, et al. Studies on anti-von Willebrand factor (vWF) monoclonal antibody NMC-4, which inhibits both ristocetin- and botrocetin-induced vWF binding to platelet glycoprotein Ib. *Blood*. 1991;77(1):113-120.
28. Celikel R, Madhusudan, Varughese KI, et al. Crystal structure of NMC-4 fab anti-von Willebrand factor A1 domain. *Blood Cells Mol Dis*. 1997;23(1):123-134.
29. Wolber FM, Leonard E, Michael S, Orschell-Traycoff CM, Yoder MC, Srour EF. Roles of spleen and liver in development of the murine hematopoietic system. *Exp Hematol*. 2002;30(9):1010-1019.
30. Kanaji T, Russell S, Cunningham J, Izuhara K, Fox JE, Ware J. Megakaryocyte proliferation and ploidy regulated by the cytoplasmic tail of glycoprotein Ibalpha. *Blood*. 2004;104(10):3161-3168.
31. Gardiner EE, Karunakaran D, Shen Y, Arthur JF, Andrews RK, Berndt MC. Controlled shedding of platelet glycoprotein (GP)VI and GPIb-IX-V by ADAM family metalloproteinases. *J Thromb Haemost*. 2007;5(7):1530-1537.
32. Falet H, Pollitt AY, Begonja AJ, et al. A novel interaction between FlnA and Syk regulates platelet ITAM-mediated receptor signaling and function. *J Exp Med*. 2010;207(9):1967-1979.
33. Kanaji T, Ware J, Okamura T, Newman PJ. GPIbalpha regulates platelet size by controlling the subcellular localization of filamin. *Blood*. 2012;119(12):2906-2913.
34. Kruse-Jarres R, Johnsen JM. How I treat type 2B von Willebrand disease. *Blood*. 2018;131(12):1292-1300.
35. Jilma-Stohlawetz P, Knöbl P, Gilbert JC, Jilma B. The anti-von Willebrand factor aptamer ARC1779 increases von Willebrand factor levels and platelet counts in patients with type 2B von Willebrand disease. *Thromb Haemost*. 2012;108(2):284-290.
36. Hulstein JJ, de Groot PG, Silence K, Veyradier A, Fijnheer R, Lenting PJ. A novel nanobody that detects the gain-of-function phenotype of von Willebrand factor in ADAMTS13 deficiency and von Willebrand disease type 2B. *Blood*. 2005;106(9):3035-3042.
37. Jilma B, Paulinska P, Jilma-Stohlawetz P, Gilbert JC, Hutabarat R, Knöbl P. A randomised pilot trial of the anti-von Willebrand factor aptamer ARC1779 in patients with type 2b von Willebrand disease. *Thromb Haemost*. 2010;104(3):563-570.
38. Scott JP, Montgomery RR. The rapid differentiation of type IIb von Willebrand's disease from platelet-type (pseudo-) von Willebrand's disease by the "neutral" monoclonal antibody binding assay. *Am J Clin Pathol*. 1991;96(6):723-728.
39. Suva LJ, Hartman E, Dilley JD, et al. Platelet dysfunction and a high bone mass phenotype in a murine model of platelet-type von Willebrand disease. *Am J Pathol*. 2008;172(2):430-439.
40. Kaur H, Corscadden K, Ware J, Othman M. Thrombocytopenia leading to impaired in vivo haemostasis and thrombosis in platelet type von Willebrand disease. *Thromb Haemost*. 2017;117(3):543-555.
41. Bury L, Falcinelli E, Mezzasoma AM, Guglielmini G, Momi S, Gresele P. Platelet dysfunction in platelet-type von Willebrand disease due to the constitutive triggering of the Lyn-PECAM1 inhibitory pathway. *Haematologica*. 2022;107(7):1643-1654.
42. Bury L, Malara A, Momi S, Petito E, Balduini A, Gresele P. Mechanisms of thrombocytopenia in platelet-type von Willebrand disease. *Haematologica*. 2019;104(7):1473-1481.

Follicular lymphoma grade 3B and diffuse large B-cell lymphoma present a histopathological and molecular continuum lacking features of progression/transformation

Karoline Koch,¹ Julia Richter,¹ Christoph Hänel,¹ Andreas Hüttmann,² Ulrich Dührsen² and Wolfram Klapper¹

¹Department of Pathology, Hematopathology Section, University Hospital Schleswig-Holstein, Kiel and ²Department of Hematology, University Hospital Essen, University of Duisburg-Essen, Essen, Germany

Correspondence: K. Koch
karoline.koch@uksh.de

Received: June 1, 2021.

Accepted: November 11, 2021.

Prepublished: January 13, 2022.

<https://doi.org/10.3324/haematol.2021.279351>

©2022 Ferrata Storti Foundation

Published under a CC BY-NC license



Abstract

The sole distinguishing feature of follicular lymphoma grade 3B and diffuse large B-cell lymphoma is the growth pattern assessed by histopathology. Diffuse growth defines diffuse large B-cell lymphoma but the clinical relevance of this finding when occurring in follicular lymphoma grade 3B is uncertain. To address this issue, individual and coexisting follicular lymphoma grade 3B and diffuse large B-cell lymphoma were separated and analyzed for immunophenotype and molecular genetic features by fluorescence *in situ* hybridization, targeted sequencing and gene expression profiling. Clinical features of follicular lymphoma grade 3B with and without coexisting diffuse large B-cell lymphoma were studied in homogeneously treated patients from a prospective randomized trial. Follicular lymphoma grade 3B and diffuse large B-cell lymphoma frequently show an intermediate growth pattern and/or occur simultaneously in the same tissue at the time of initial diagnosis. When occurring simultaneously follicular lymphoma grade 3B and diffuse large B-cell lymphoma do not differ significantly for genetic aberrations or phenotype but have distinct gene expression features reflecting a divergent micro-environment. Follicular lymphoma grade 3B with and without coexisting diffuse large B-cell lymphoma do not differ for major clinical parameters such as International Prognostic Index, response to immuno-chemotherapy, progression or overall survival. Follicular lymphoma grade 3B and simultaneous diffuse large B-cell lymphoma are molecularly homogenous. Histological detection of diffuse large B-cell lymphoma is not associated with features of a more aggressive disease and does not reflect transformation or progression of follicular lymphoma grade 3B.

Introduction

Follicular lymphoma (FL) is one of the most frequent lymphoma entities in central Europe and Northern America and is subdivided into “grades” by morphology.¹ Follicular lymphoma grades 1, 2 and 3A are composed of centrocytes and centroblasts and distinguished by centroblast content whereas FL grade 3B (FL3B) consists exclusively of centroblasts.¹ Since the cytomorphology of FL3B is identical to that of diffuse large B-cell lymphoma (DLBCL), the sole distinguishing feature of FL3B and DLBCL is the growth pattern assessed by histopathology which is follicular in FL3B and diffuse in DLBCL. Once the neoplastic cells in FL3B display areas of diffuse growth the lymphoma fulfills the diagnostic

criteria of DLBCL according to the World Health Organization (WHO) classification.¹ Thus, diffuse areas of FL3B are considered “transformation” and this feature has been suggested to be of clinical significance.^{2,3} Unlike FL grades 1, 2 and 3A, FL3B is considered an aggressive lymphoma by most clinical research groups and treated in the same way as DLBCL⁴ despite the fact that under rituximab-containing poly-chemotherapy (e.g., rituximab, cyclophosphamide, doxorubicin, vincristine, prednisone [R-CHOP]) outcomes might not be very different between FL3A and FL3B.^{5,6} Transformation of FL grades 1, 2 and 3A to DLBCL has been shown to be associated with major changes in molecular pathogenic pathways and is well established to reflect a true “transformation” with change in clinical behavior and

necessity of treatment strategies that may differ from those for FL 1, 2 and 3A.⁷ In a large retrospective study FL3B seemed to be associated with a favorable outcome.⁸ However, following the current definition of the WHO classification FL3B harboring areas of diffuse growth fulfilling the criteria of DLBCL are rather rare and probably underrepresented^{5,9} or even excluded from analysis in more recent studies on the clinical features of FL3B.^{6,8} It is, therefore, unclear whether histological transition of follicular to diffuse growth reflects a clinically relevant transformation at all. Lack of knowledge regarding the biological and clinical significance of transformation of FL3B may however create a considerable clinical problem since FL3B occurs in patients who are often young - a subgroup of patients who warrant careful consideration of therapy intensity with respect to long-term toxicity.¹⁰

As FL3B is one of the rarest grades of FL very few molecular studies have been conducted and most of them focused on the distinction of FL3B from other grades and DLBCL.¹¹⁻¹⁴ In the current study we aimed to understand the molecular and clinical features of FL3B showing transition into DLBCL in order to provide a definition of “transformation” in FL3B guiding clinical decision-making.

Methods

Case selection, histological evaluation and immunohistochemistry

Cases with a diagnosis of FL3B with or without a DLBCL component diagnosed between 2012 and 2016 at the Hematopathology Section and Lymph Node Registry of the University Hospital Schleswig-Holstein, (Kiel, Germany) were identified in the files and re-evaluated with regard to diagnosis and growth patterns as well as suitability for molecular analysis. In total, 51 specimens with a histological picture of FL3B were identified, two of which were excluded later as they turned out to have an *IRF4* break and these are considered a separate entity by the WHO classification.¹ Staining for CD20 (clone L26, DAKO), CD10 (clone 56C6, Novocastra), Mum1 (clone MUM1P, Dako), Bcl6 (clone BL6.02, DCS) and Bcl2 (clone 100/D5, DBS) was evaluated semiquantitatively (negative, <25% of lymphoma cells positive, <50% positive, <75% positive, >75% positive) and proliferative rate was determined according to Ki67 (clone SP6, Neomarkers) in steps of 10% by visual inspection. Immunohistochemical classification of the cell of origin of DLBCL components was performed applying the Hans classifier.¹⁵ Areas of defined growth patterns were selected for tissue microarray construction in 47 cases with sufficient material. Meshworks of follicular dendritic cells were evaluated in tissue microarrays for each growth pattern semiquantitatively by CD21 staining (0 = absence of meshworks, 1 = markedly reduced covering <50% of fol-

licles, 2 = slightly reduced covering >50% of follicles and 3 = intact covering whole area of follicle; clone 2G9, Novocastra). Punches with a tissue microarray needle (1 mm diameter) from each area were also used for nucleic acid extraction. To prevent cross-contamination of DNA/RNA analytes the tissue microarray needle was punched three to five times in an empty paraffin block between each punching of a patient's specimen.

The study was conducted in accordance with the recommendations of the ethics board of the Medical Faculty, University of Kiel (D447/10) for the use of archival tissue specimens. Informed consent was obtained from patients treated in the PETAL trial (see below).

Fluorescence *in situ* hybridization

Fluorescence *in situ* hybridization (FISH) was performed on 5 µm slides from the tissue microarrays, allowing separate analysis of different growth patterns. Probes for *IRF4*, *BCL2*, *BCL6* and *MYC* were obtained from ZytoVision (Bremerhaven, Germany) and applied as previously described.¹⁶

DNA and RNA extraction

Cases for molecular genetic analyses were chosen when the tissue quality was assumed to be sufficient for nucleic acid extraction. Simultaneous DNA and RNA extraction was done using the AllPrep DNA/RNA FFPE Kit (Qiagen) according to the manufacturer's instructions. For each patient different growth patterns were extracted separately from tissue microarray needle biopsies taken from the respective areas (2-3 biopsies per specimen).

Mutation analyses

Mutation analyses were done on DNA isolated from the formalin-fixed paraffin-embedded material of the diagnostic biopsy using an AmpliSeq Custom DNA Panel covering genes or mutational hotspots known to be recurrently mutated in aggressive B-cell lymphomas (*Online Supplementary Table S1*). Libraries were prepared according to the manufacturer's instructions and sequencing was performed on a MiSeq instrument using V3 sequencing chemistry. FASTQ data were analyzed using JSI SeqNext software (JSI Medical Systems GmbH, Ettenheim, Germany). Formalin-fixed paraffin-embedded tissue from reactive lymph nodes from eight healthy individuals (a cancer infiltration was excluded by expert hematopathologists) was used as control tissue, and sequence alterations identified in those samples were subtracted from those of the lymphoma patients. Furthermore, common single nucleotide polymorphisms with ≥1% variant allele frequency were excluded. Potential protein changing alterations with at least 15% variant allele fraction were analyzed in more detail using the ENSEMBL variant effect predictor (http://www.ensembl.org/Homo_sapiens/Tools/VEP). However, as the library preparation process contains polymerase chain reaction amplification

steps to enrich the target regions no interpretation of the variant allele fractions was possible. Furthermore, no germline material was available from those samples in order to be able to differentiate between somatic and germline variants. To overcome this limitation, variants were categorized based on the variant effect prediction by SIFT, PolyPhen, FATHMM and Condel into six different groups: (i) high impact; (ii) moderate impact and deleterious or damaging effect; (iii) moderate impact but mixed effect prediction (deleterious/damaging or tolerated based on the different tools used); (iv) moderate impact and tolerated or benign; (v) moderate impact but no additional information; and (vi) low impact. Variants with high impact, moderate/deleterious effect prediction and moderate/mixed effect prediction were considered to affect protein function negatively.

Gene expression analysis

Gene expression was analyzed as previously described applying NanoString technology and the PanCancer Immune Profiling Panel.¹⁷ Background thresholding and normalization were performed by the NSolver software (version 4.0; NanoString Technologies). Twenty housekeeping genes were chosen for normalization in a two-step process: (i) housekeeping genes with average counts <100 were excluded; and (ii) 20 housekeeping genes with the lowest count variability were chosen for normalization. Endogenous genes with normalized expression levels below the calculated background threshold in >20% of the analyzed specimens were excluded from further analysis. Fold changes between follicular and diffuse growth patterns were calculated for each individual case. Genes with a fold change of >1.2 or <-1.2 in at least 50% of cases were chosen and mean fold changes of these genes were calculated as fold change of the geometric means of the respective single case gene expression levels. Genes with a mean fold change of >1.5 or <-1.5 were considered to be differentially expressed.

Clinical analysis

The features of patients with FL3B (n=17) and FL3B+DLBCL (n=16) were analyzed in patients treated in the prospective randomized 'Positron Emission Tomography-Guided Therapy of Aggressive Non-Hodgkin Lymphomas' trial (PETAL: clinicaltrials.gov NCT00554164 and EudraCT 2006-001641-33).¹⁸ Patients received two cycles of standard R-CHOP followed by interim [¹⁸F]fluorodeoxy-glucose-positron emission tomography (PET). Interim PET-negative patients continued R-CHOP whereas interim PET-positive patients were randomized between continued R-CHOP and an intensive methotrexate- and cytarabine-based Burkitt lymphoma protocol. According to current treatment guidelines¹⁹ all patients were treated at the timepoint of first diagnosis.

Statistical analysis

Statistical analysis was performed using GraphPadPrism (version 7.00 for Windows, GraphPad software, La Jolla, CA, USA) applying the χ^2 test, Fisher exact test and unpaired *t*-test as indicated in the Results section. Kaplan-Meier curves were generated using SPSS statistics (version 26.0, IBM, Armonk, NY, USA).

Results

Growth pattern of follicular lymphoma grade 3B with a continuum to diffuse large B-cell lymphoma

Forty-nine lymphomas with a diagnosis FL3B were reanalyzed for growth pattern. All cases fulfilled the criteria of FL3B and 27/49 (55%) additionally harbored areas with diffuse growth representing DLBCL by definition (FL3B+DLBCL). None of the cases included any low-grade FL component. None of the cases showed the typical constellation of pediatric type FL according to the current WHO classification.¹ Relapse biopsies were available for two patients both of whom had FL3B+DLBCL at primary diagnosis and DLBCL at relapse. The proportion of DLBCL ranged between 10% and 95% in individual cases (mean: 49%). The cytomorphology of the DLBCL component was centroblastic in 25/27 cases and immunoblastic in 2/27 cases. In all cases, the morphology of the DLBCL component matched the morphology of the FL3B component. Within the areas of follicular growth two different growth patterns were noticed: (i) clearly demarcated, roundish follicles that were separated from each other (follicular pattern) (Figure 1) and (ii) follicles localized close to each other appearing to merge (confluent pattern) (Figure 1). The confluent pattern was clearly distinguishable from a diffuse pattern/DLBCL in hematoxylin and eosin staining and could be further highlighted by staining for T cells and follicular dendritic cells (Figure 1). Of the 22 pure FL3B lacking an additional DLBCL component, only four cases showed a pure follicular pattern (4/22, 18%), whereas 11/22 (50%) cases solely displayed the confluent pattern. A combination of both patterns was detectable in 7/22 (32%) of pure FL3B. The distribution of these growth patterns within the FL3B component was different in FL3B+DLBCL cases (confluent pattern 14/27 [52%], follicular pattern 7/27 [26%] and a combination of both patterns 6/27 [22%], *P*=0.0421, χ^2 test) although the differences must be interpreted with caution because of the small number of cases. All growth patterns and their combinations are indicated in Table 1.

Homogeneous immunophenotype in follicular lymphoma grade 3B and diffuse large B-cell lymphoma

CD20 was homogeneously expressed in all 49 cases. CD10 expression was more variable with 22/49 cases (45%) being completely negative, 4/49 cases (8%) with ex-

pression in <50% of cells and 23/49 cases (47%) with expression in >75% of cells. Bcl2 staining was available for 48 cases. Bcl2 was completely negative in 5/48 cases (10%), positive in <50% of cells in 7/48 cases (15%) and positive in >50% of cells in 36/48 cases (75%). Staining for Mum1 was done in 36 cases. Mum1 was completely negative in 3/36 cases (8%), positive in <25% of cells in 9/36 cases (25%), positive in 25% to <50% of cells in 4/36 cases (11%), positive in 50% to <75% of cells in 11/36 cases (31%) and positive in \geq 75% of cells in 9/36 cases (25%). Bcl6 staining was available for 29 cases. Of these, seven cases (24%) were positive in 50% to <75% of cells and 22 cases (76%) were positive in \geq 75% of cells. The proliferative rate by Ki67 ranged between 30% and 90% with a mean proliferative rate of 63% in the whole cohort. Classification of the cell of origin was available for 26 cases with a DLBCL component. Of these, 19 cases (73%) displayed a germinal center B-cell-phenotype and seven cases (27%) displayed a non-germinal center B-cell-phenotype according to the Hans classifier.¹⁵ Despite inter-tumoral variability, expression of the above-mentioned antigens did not differ between different growth patterns within an individual patient/lymphoma. Of note, FL3B and

DLBCL areas in the same specimen showed the same proliferative rate according to Ki67 (Figure 2). Comparing FL3B and FL3B+DLBCL, no significant differences between mean proliferative rates were detectable (59% and 65%, respectively, $P=0.1349$, unpaired t -test). CD21 staining was evaluable in 12 follicular FL3B components, 26 confluent FL3B components and 16 DLBCL components of 34 cases. Meshworks of follicular dendritic cells showed considerable intercase variability. The highest scores were reached in follicular FL3B (8/12, 67% slightly reduced/intact and 4/12, 33% markedly reduced); DLBCL components mostly showed markedly reduced or absent meshworks (1/16, 6% slightly reduced and 15/16, 94% markedly reduced/absent). Confluent FL3B presented intermediate stages of follicular dendritic cell preservation (14/26, 54% slightly reduced/intact and 12/26, 46% markedly reduced/absent meshworks), supporting the idea that confluent FL3B represents an intermediate stage between follicular FL3B and DLBCL. Within individual cases with evaluable FL3B and DLBCL components ($n=14$), a reduction of meshworks could be observed between the FL3B and DLBCL components in 9/14 cases (64%) and the same stage of preservation in 5/14 cases (36%).

Chromosomal aberrations are mostly stable between follicular lymphoma grade 3B and diffuse large B-cell lymphoma

Lymphomas with breaks in *IRF4* were excluded since these are considered a distinct entity in the WHO classification. FISH to detect breaks in *BCL2*, *BCL6* and *MYC* was performed for 40 cases, 21 of which contained a DLBCL component. In any lymphoma containing multiple growth patterns these were analyzed separately. Overall, 27 chromosomal breaks were detectable in 25 cases and 15 cases did not show breaks in the above-mentioned genes. One case presented a double-hit constellation with *MYC* and *BCL6* rearrangements (FL3B with confluent pattern). Chromosomal breaks occurred at a similar frequency in FL3B and

Table 1. Coexistence of growth patterns in follicular lymphoma grade 3B.

	Follicular	Confluent	Diffuse	Total
FL3B (N=22)	+	-	-	4/22 (18%)
	-	+	-	11/22 (50%)
	+	+	-	7/22 (32%)
FL3B/DLBCL (N=27)	+	-	+	7/27 (26%)
	-	+	+	14/27 (52%)
	+	+	+	6/27 (22%)

Numbers and percentages correspond to the respective subgroup. FL3B: follicular lymphoma grade 3B; DLBCL: diffuse large B-cell lymphoma.

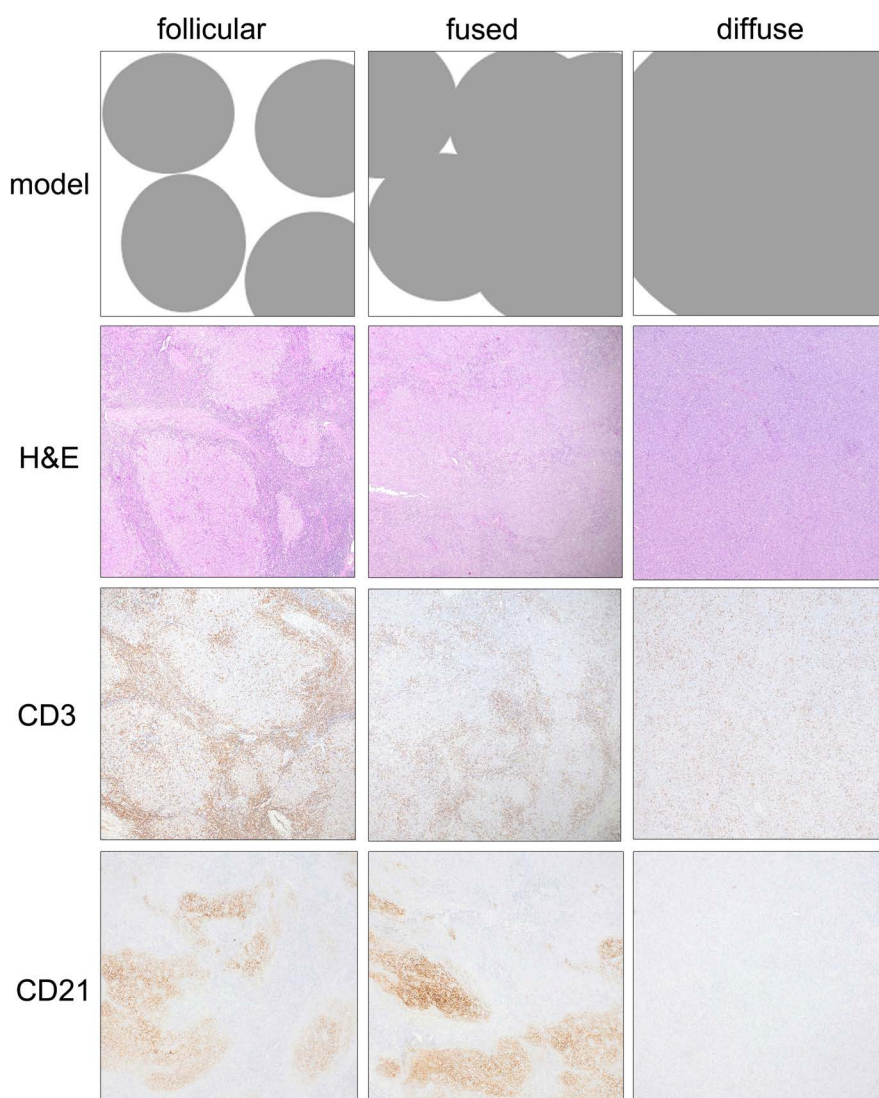


Figure 1. Growth pattern of follicular lymphoma grade 3B and diffuse large B-cell lymphoma. The three patterns observed are shown for exemplary cases in the three columns as a scheme/model, hematoxylin and eosin staining (H&E) and staining for CD3 and CD21. Original magnification 40x.

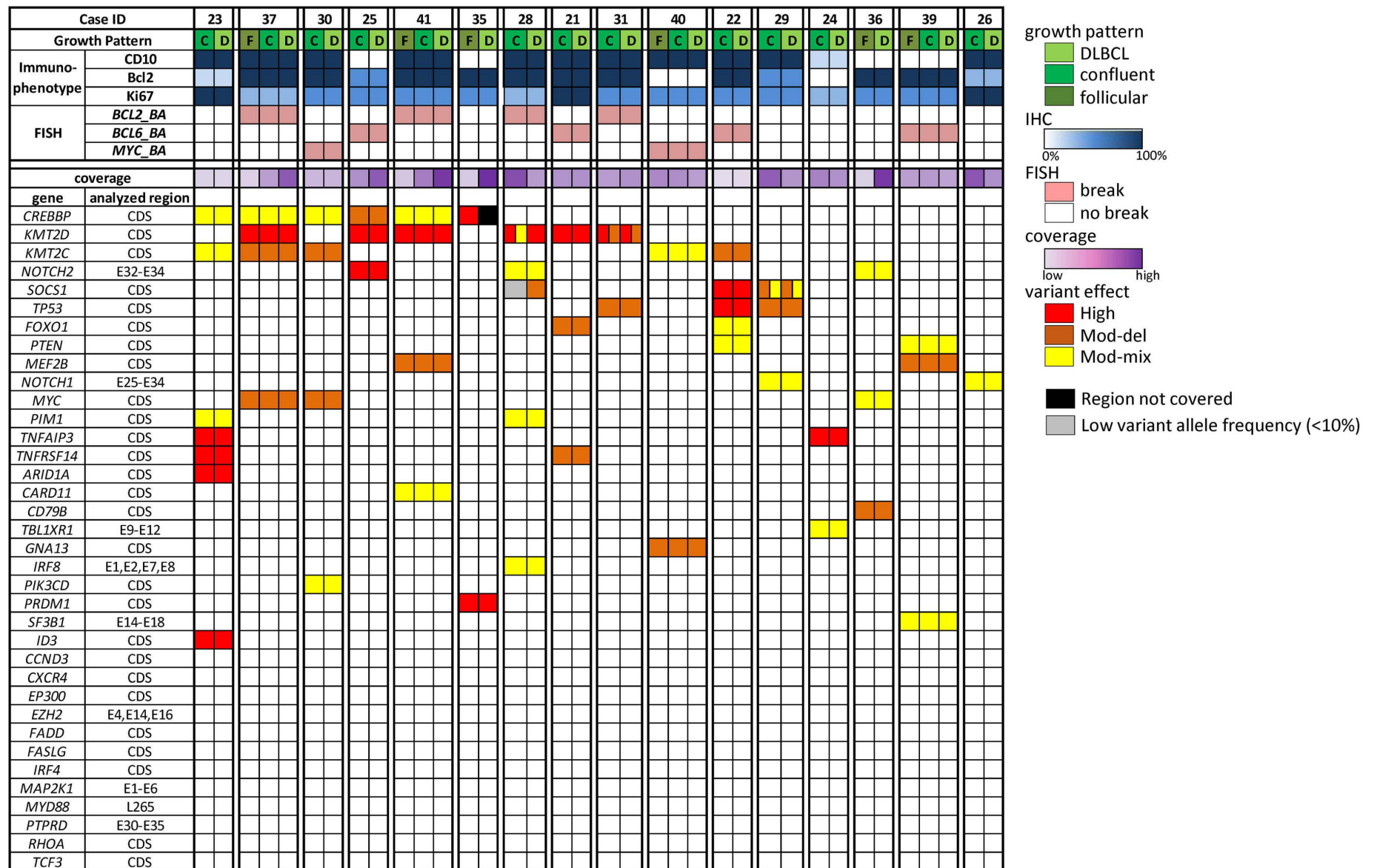


Figure 2. Mutational pattern of the different growth patterns of follicular lymphoma grade 3B + diffuse large B-cell lymphoma.

Within each lymphoma the patterns were analyzed separately. Individual cases are indicated by the case identifier (ID) and growth pattern as D: diffuse large B-cell lymphoma (DLBCL) component; F: follicular component; C: confluent component. The immunophenotype was scored in a five-tiered way 0%; 1-25%; 26-50%; 51-75%; >75% positive tumor cells and is displayed as a color code as shown in the scale bar. Fluorescence *in situ* hybridization (FISH) was done using break apart probes (BA). Potential protein-changing variants identified in the different components were colored according to the variant effect prediction (red: high; dark orange: moderate, deleterious; yellow: moderate, deleterious and tolerated effect based on different algorithms used, black: region was not covered in the DLBCL sample, gray: variant was identified with low variant allele frequency (<10%) in the confluent component. If more than one variant with different effects targeting one gene was identified in one component both variant effects are shown separately. E: exon; CDS: coding region; #: region was not covered in the DLBCL component of that sample. \$: variant was identified with low (<10%) variant allele frequency in the confluent component. IHC: immunohistochemistry.

FL3B+DLBCL (FL3B: *BCL2* in 2/19 [11%], *BCL6* in 8/19 [42%], *MYC* in 1/19 [5%]; FL3B+DLBCL: *BCL2* in 6/21 [29%], *BCL6* in 7/21 [33%], *MYC* in 3/21 [14%], $P=0.2409$ for *BCL2*, $P>0.9999$ for *BCL6*, $P=0.6094$ for *MYC*, Fisher exact test). FISH results for at least two growth patterns of the same lymphoma were available for 21 cases. In most cases the chromosomal aberrations were shared between the different growth patterns (20/21 cases, 95%). However, in 1/21 (5%) cases a divergent result was observed concerning *BCL6*. This case harbored a *BCL6* break in the confluent area but not in the follicular areas of a FL3B (*data not shown*).

The microenvironmental composition of follicular lymphoma grade 3B and diffuse large B-cell lymphoma differs

In order to understand whether the growth patterns rep-

resent molecular progression/evolution of the disease, gene expression was analyzed in FL3B+DLBCL cases. Assuming that the follicular pattern and DLBCL represent the two ends of a spectrum of growth patterns in each individual lymphoma, these areas were analyzed separately in cases with both components available (n=6). Since DLBCL are known to be a heterogeneous disease with their molecular features differing from patient to patient, we analyzed differential expression within each patient comparing the follicular FL3B with the DLBCL component in cases with both components available. Using the criteria described in the Methods section we identified a low number of genes (n=45) differentially expressed in multiple patients (*Online Supplementary Figure S1*). Of these, 33/45 (73%) genes were more highly expressed in the follicular FL3B area and reflected the expression pat-

tern of the germinal center microenvironment, such as follicular dendritic cells (*CD21*), follicular T helper cells (*ICOS*, *STAT4*), T cells (*CD3*, *TCF7*, *TXK*) and *CXCL12*, which has previously been described to be upregulated in FL stromal cells.²⁰ Furthermore, genes more highly expressed in follicular areas reflected a greater abundance of cells of innate immunity (*C1QB*, *SIGLEC1*, *TPSAB1*) including natural killer cells (*KLRB1*, *KLRG1*) compared to the DLBCL component. In line with a higher content of immune cells, genes involved in trafficking e.g. by adhesion and motility, were more highly expressed in follicular areas (*CCR7* and its ligand *CCL21*, *CDH1*, *ITGA6*, *ITGB6*). Alterations of the extracellular matrix between follicular and diffuse areas are reflected by differential expression of collagen III α and fibronectin which were more highly expressed in the DLBCL component. Of note, two of 12 genes more highly expressed in the diffuse part are known to be involved in T-cell activation (*CD70* and *TNFSF4/OXL40*). Only a few of the differentially expressed genes could be assigned to B-cell differentiation (e.g. *CD27*) suggesting that the gene expression pattern of the neoplastic B cells does not differ substantially between follicular (FL3B) and diffuse (DLBCL) areas. No differences were observed in genes described to be associated with transformation or an aggressive phenotype of FL (*MYC*, *NOTCH*, NF κ B signaling pathway genes, data not shown).

Molecular genetic features are stable between follicular lymphoma grade 3B and diffuse large B-cell lymphoma

Genes recurrently mutated in mature B-cell lymphoma were analyzed by targeted sequencing in pure FL3B (n=11) and FL3B+DLBCL (n=16). The FL3B+DLBCL group consisted of two cases containing follicular and diffuse components, ten cases with a confluent and a diffuse component and four cases with all growth patterns in the same specimen. Areas representing growth patterns were separated by macrodissection and analyzed individually (yielding 36 sequencing results). Sequencing retrieved a mean read depth of 4,258 (min 276, max 10,131). Overall, 81 genetic variants were detected (*Online Supplementary Table S2*). The genetic variants were mostly missense variants (n=56), followed by nonsense (n=9), and splice site or splice region variants (n=8), frameshift (n=4) and inframe variants (n=4). The pure FL3B group consisted of nine cases with a confluent growth pattern, one case with a follicular growth pattern and one case with a follicular and confluent growth pattern of which only the confluent component was analyzed. Sequencing retrieved a mean read depth of 5,146 (min 967, max 9,769). Overall, 22 genetic variants were detected (*Online Supplementary Table S2*). The genetic variants were missense in most cases (n=14), followed by nonsense (n=7) and splice site or splice region variants (n=1). Since germline DNA was not available, variant effect prediction using ENSEMBLE was performed to estimate the functional rel-

evance of the genetic alterations. In the FL3B+DLBCL group, variant effect prediction identified 16/81 (20%) variants with high impact, 17/81 (21%) with moderate/deleterious effects, 29/81 (36%) with moderate/mixed effects, 13/81 (16%) with moderate/tolerated or unclear effects and 6/81 (7%) with low impact. In the pure FL3B group, 9/22 (41%) variants were predicted to have high impact, 6/22 (27%) with moderate/deleterious effects, 4/22 (18%) with moderate/mixed effects and 3/22 (14%) with moderate/tolerated effects. The number of variants detected per case was significantly different between pure FL3B (0 to 6; mean 2) and FL3B+DLBCL (1 to 11; mean 5.1; $P=0.0037$, unpaired *t*-test). Overall, 62/81 (77%) variants in FL3B+DLBCL and 19/22 (86%) variants in pure FL3B were predicted to affect protein function negatively. Considering only variants with potentially negative effects on protein function, significant differences between FL3B and FL3B+DLBCL could still be observed (FL3B: 0 to 6 variants per case, mean 1.7 and FL3B+DLBCL: 1 to 8 variants per case, mean 3.9; $P=0.0091$, unpaired *t*-test). However, as a targeted sequencing approach was applied, this does not allow conclusions on the whole load of genetic variants in individual tumors. The most frequently altered genes with potentially negative effects on protein function were *KMT2D* (6/16 cases, 38%), *CREBBP* (6/16 cases, 38%) and *KMT2C* (5/16 cases, 31%) in FL3B+DLBCL and *TP53* (3/11 cases, 27%), *MYD88* (2/11 cases, 18%) and *KMT2D* (2/11 cases, 18%) in pure FL3B. No significant differences were found between FL3B and FL3B+DLBCL considering variants in specific genes (*Online Supplementary Table S4*).

In 14/16 (88%) cases of FL3B+DLBCL all variants were shared between the different specimens/areas of the corresponding sample. Thus, overall 77/81 (95%) variants did not differ between FL3B and DLBCL occurring in the same patient (Figure 2). In only two cases, four variants were detected that differed between FL and DLBCL within the same patient. In one sample (case 35) a variant in the *CREBBP* gene was detected in the follicular component but no sequencing result was obtained for the DLBCL component due to low coverage. In the other sample (case 28), three variants were discrepant between the FL3B (confluent pattern) and the DLBCL component. Two variants affecting *NOTCH1* and *SOCS1* were identified in the confluent and the DLBCL component, respectively; both had a very low frequency (<10% of reads) in the other component and were therefore initially not considered. In contrast, a *KMT2D* mutation was present in the FL3B and completely absent in the DLBCL component (Figure 2). This variant was predicted to have a moderate/mixed effect.

The clinical features of follicular lymphoma grade 3B alone and with diffuse large B-cell lymphoma do not differ

To understand whether the co-occurrence of DLBCL with

FL3B is associated with clinical progression, we analyzed the subgroup of FL3B in the prospective randomized PETAL trial.¹⁸ In this clinical cohort 17 patients were classified as having FL3B and 16 as having FL3B+DLBCL. All the patients with FL3B and 15/16 of those with FL3B+DLBCL had a favorable interim PET scan and were treated with six cycles of R-CHOP, while one FL3B+DLBCL patient had an unfavorable interim PET scan and received two cycles of R-CHOP followed by the Burkitt lymphoma protocol. The presence of the confluent pattern described in the current manuscript was not assessed by central pathology review in PETAL and is thus not available for further analysis. The baseline characteristics of the FL3B and FL3B+DLBCL cohorts did not differ for parameters known to be associated with aggressive disease such as advanced stage, increased lactate dehydrogenase level or International Prognostic Index (Table 2, comparison with DLBCL treated in PETAL in *Online Supplementary Table S3*). Moreover, we did not find any significant difference in overall treatment response and overall survival (Table 2).

As a consequence, progression-free survival and overall survival did not differ between FL3B and FL3B+DLBCL (Figure 3).

Discussion

FL3B is a rare subtype of FL, underrepresented in clinical and translational research studies.²¹ The definition of FL3B is exclusively based on histological features: (i) differentiation arrest of neoplastic germinal center cells as centroblasts leading to absence of centrocytes and (ii) follicular growth. The latter is the sole feature distinguishing FL3B from DLBCL. Follicular growth describes an arrangement of lymphoma cells in roundish accumulations of cells which contain microenvironmental structures of physiological germinal centers such as follicular dendritic cells, follicular T-helper cells and occasionally follicle mantle cells.²² These organoid arrangements resemble physiological germinal centers more closely in low-grade FL such as

Table 2. Clinical characteristics and treatment response of follicular lymphoma grade 3B with or without diffuse large B-cell lymphoma in patients treated in the prospective randomized ‘Positron Emission Tomography-Guided Therapy of Aggressive Non-Hodgkin Lymphomas’ (PETAL) trial.¹⁸

	FL3B alone		FL3B with DLBCL		
Number of patients	17		16		
Median age (range)	51 years (29-72)		57 years (29-76)		
Baseline characteristics	Number	Percent	Number	Percent	P
Male sex	13	76.5	7	43.8	0.0799
Age ≥60 years	5	29.4	6	37.5	0.7207
ECOG performance status >1	1	5.9	0	0.0	>0.9999
Lactate dehydrogenase >ULN	10	58.8	7	43.8	0.4935
Ann Arbor stage III or IV	11	64.7	10	62.5	>0.9999
Extranodal manifestations >1	2	11.8	3	18.8	0.6562
Bone marrow infiltration	1	5.9	0	0.0	>0.9999
B symptoms	5	29.4	1	6.3	0.1748
International Prognostic Index			0.7673		
Low	9	53.0	8	50.0	
Low-intermediate	3	17.6	3	18.8	
High-intermediate	4	23.5	5	31.2	
High	1	5.9	0	0.0	
Treatment response					
Overall response	16	94.1	15	93.8	>0.9999
Complete remission	12	70.6	10	62.5	>0.9999

P-values according to the Fisher exact test and for the International Prognostic Index by the χ^2 test. FL3B: follicular lymphoma grade 3B; DLBCL: diffuse large B-cell lymphoma; ECOG: Eastern Cooperative Oncology Group; ULN, upper limit of normal.

FL grades 1 and 2 compared to FL grade 3A and FL3B. Initially, the grades of FL were thought to reflect a multistep process of tumor progression in analogy to grades of differentiation in solid tumors.²³ However, there are several findings suggesting that at least a large fraction of FL3B cases are not a progressive form of FL grades 1, 2 and 3A. First, unlike FL grades 1, 2 and 3A, FL3B is diagnosed more frequently in younger patients, suggesting a unique pathogenesis.^{10,21} Second, molecular studies, e.g. on chromosomal translocations show, a much lower frequency of aberrations involving *BCL2* and a higher frequency of *BCL6* translocations in FL3B than in FL grades 1, 2, and 3A.^{9,11,13,24}

Third, FL3B often co-exists with a DLBCL at initial diagnosis whereas transformation of indolent FL grades 1, 2 and 3A mostly occurs at a later stage of the disease.^{5,9} Fourth, FL3B rarely follows or co-exists with FL grades 1, 2 and 3A, again suggesting differences in pathogenic pathways.⁹

In the current study we analyzed an aspect of FL3B biology not addressed by previous studies. We aimed to understand whether the loss of follicular growth indicates molecular and clinical progression/transformation. To the best of our knowledge, this is the first study specifically analyzing the intratumoral heterogeneity of FL3B and

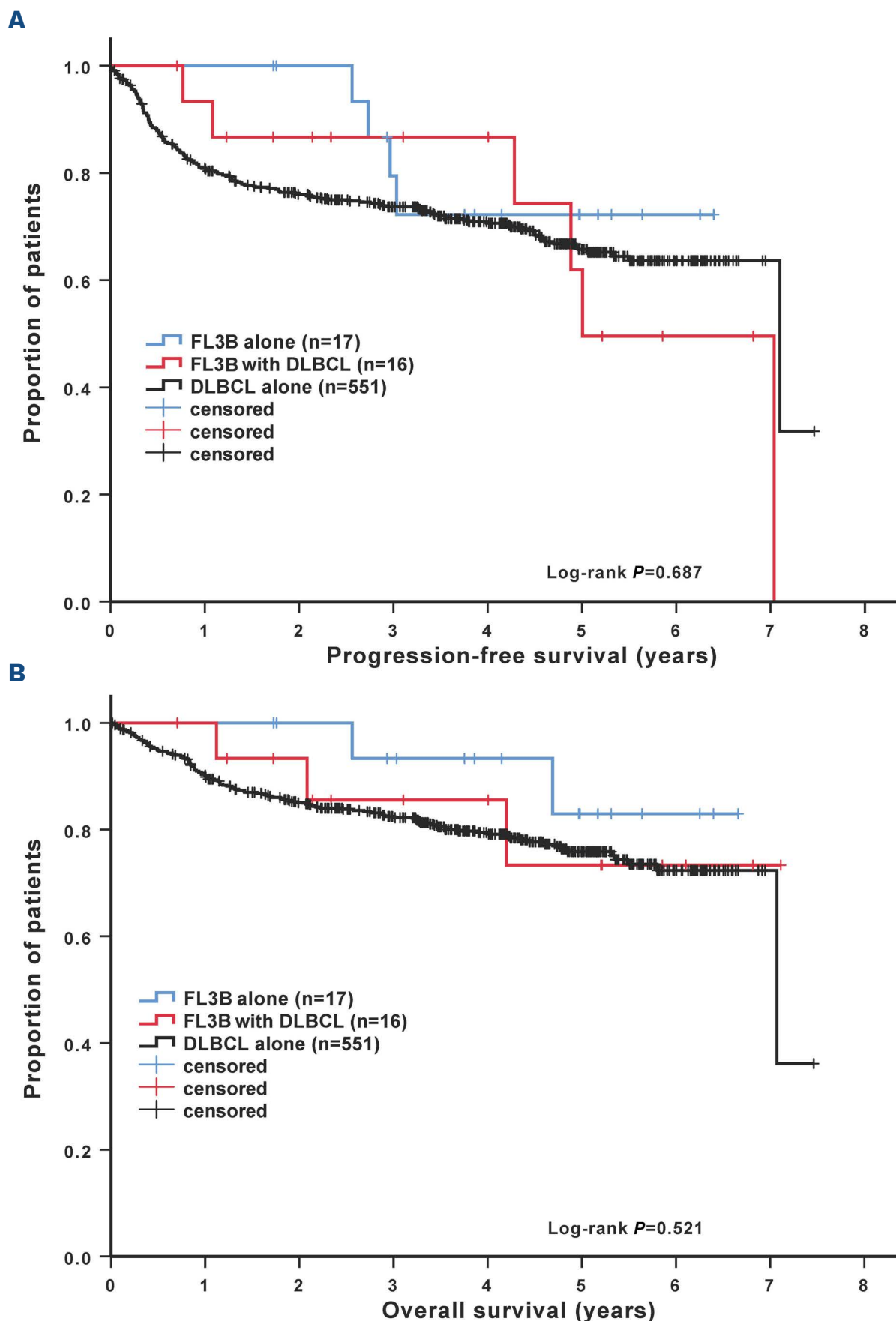


Figure 3. Kaplan-Meier survival estimates for progression free (A) and overall survival (B) of patients with follicular lymphoma grade 3B with or without diffuse large B-cell lymphoma. Patients with diffuse large B-cell lymphoma (DLBCL) treated in the same trial are shown as a control (see *Online Supplementary Table S3*). As patients with activated B-cell or germinal center B-cell DLBCL did not differ significantly regarding progression-free survival and overall survival these subgroups were not differentiated.

DLBCL within individual patients/lymphomas. Similarly to previous studies,^{5,9} we found that a large number of cases of FL3B were associated with DLBCL at first diagnosis. Moreover, we found a pattern intermediate between follicular and diffuse growth endorsing the impression of a pathological continuum between FL3B and DLBCL. Furthermore, we showed that the molecular features of co-existing FL3B and DLBCL were homogeneous and that there was no molecular evidence of progression/transformation. In fact, the differences between follicular and diffuse growth - representing FL3B and DLBCL, respectively - were subtle and restricted to the features of the non-neoplastic microenvironment. Considering these findings it was not surprising to see that clinical features did not differ between patients with FL3B and those with FL3B+DLBCL. It seems reasonable to assume that FL3B represents a molecular and clinical continuum with DLBCL. Thus, FL3B+DLBCL does not reflect progression or transformation of the disease, suggesting that treatment should follow the same guidelines for FL3B and DLBCL. Of note, the subtype of *IRF4* translocation-positive lymphomas now recognized by the WHO classification was excluded from our analysis. However, large B-cell lymphoma with *IRF4* translocations shares features with FL3B such as histology (mostly presenting as FL3B and/or DLBCL),²⁵ patients' age (younger adults)^{10,26} and outcome (favorable).²⁷ To what extent FL3B lacking *IRF4* aberrations and large B-cell lymphoma with *IRF4* translocations may in fact share pathogenic features needs to be addressed in future studies that might help to specify diagnostic criteria. Another interesting group of patients to analyze in the future might be those with FL3B at primary diagnosis and DLBCL at relapse. However, this is hindered by the fact that only a small proportion of patients with FL3B relapse and of those who do only few undergo a second biopsy. This also holds true for our cohort, in which a second biopsy was only available for two patients. Moreover, a more detailed molecular analysis of FL3B and

FL3B+DLBCL, such as that applied in our current study, may provide a molecular genetic definition of FL3B independent of the histological detection of follicular growth. One could speculate that a molecular definition of FL3B might identify a molecular counterpart among DLBCL lacking a histopathologically detectable FL3B component but sharing clinical features.

Disclosures

AH has received travel expenses from Celgene and Roche. UD has received research funding from Amgen; has received honoraria and research funding from Celgen and Roche; has acted as a consultant for and received honoraria from AbbVie and Gilead; and has received honoraria from Janssen. WK has received honoraria and research funding from Amgen, Regeneron, Hoffman-La Roche and Takeda.

Contributions

KK and WK designed the research project, KK, CH and JR generated and analyzed pathological and molecular data, AH and UD analyzed clinical data. KK, JR and WK wrote the manuscript. All authors read and agreed on the final version of the manuscript.

Acknowledgments

The authors would like to thank Dana Germer, Charlotte Botz von Drathen, Reina Zühlke-Jenisch and Lorena Vallés Uriarte for excellent technical support.

Funding

This work was supported by an intramural grant of the Medical Faculty of the University of Kiel to KK (F359991). The PETAL trial is funded by Deutsche Krebshilfe (grants n. 107592 and 110515), Amgen Germany, and Roche Pharma.

Data-sharing statement

Data will be shared according to ethical and administrative guidelines upon request for collaboration.

References

1. WHO Classification of Tumors of Haematopoietic and Lymphoid Tissues. Revised 4th ed: International Agency for Research on Cancer, 2018.
2. Hans CP, Weisenburger DD, Vose JM, et al. A significant diffuse component predicts for inferior survival in grade 3 follicular lymphoma, but cytologic subtypes do not predict survival. *Blood*. 2003;101(6):2363-2367.
3. Ganti AK, Weisenburger DD, Smith LM, et al. Patients with grade 3 follicular lymphoma have prolonged relapse-free survival following anthracycline-based chemotherapy: the Nebraska Lymphoma Study Group experience. *Ann Oncol*. 2006;17(6):920-927.
4. Dreyling M, Ghielmini M, Rule S, et al. Newly diagnosed and relapsed follicular lymphoma: ESMO clinical practice guidelines for diagnosis, treatment and follow-up. *Ann Oncol*. 2021;32(3):298-308.
5. Mustafa Ali M, Rybicki L, Nomani L, et al. Grade 3 follicular lymphoma: outcomes in the rituximab era. *Clin Lymphoma Myeloma Leuk*. 2017;17(12):797-803.
6. Shustik J, Quinn M, Connors JM, Gascoyne RD, Skinnider B, Sehn LH. Follicular non-Hodgkin lymphoma grades 3A and 3B have a similar outcome and appear incurable with anthracycline-based therapy. *Ann Oncol*. 2010;22(5):1164-1169.
7. Kumar E, Pickard L, Okosun J. Pathogenesis of follicular lymphoma: genetics to the microenvironment to clinical translation. *Br J Haematol*. 2021;194(5):810-821.
8. Wahlin BE, Yri OE, Kimby E, et al. Clinical significance of the WHO grades of follicular lymphoma in a population-based

- cohort of 505 patients with long follow-up times. *Br J Haematol.* 2012;156(2):225-233.
9. Koch K, Hoster E, Ziepert M, et al. Clinical, pathological and genetic features of follicular lymphoma grade 3A: a joint analysis of the German Low-Grade and High-Grade Lymphoma Study Groups GLSG and DSHNHL. *Ann Oncol.* 2016;27(7):1323-1329.
 10. Paul U, Richter J, Stuhlmann-Laiasz C, et al. Advanced patient age at diagnosis of diffuse large B-cell lymphoma is associated with molecular characteristics including ABC-subtype and high expression of MYC. *Leuk Lymphoma.* 2018;59(5):1213-1221.
 11. Horn H, Schmelter C, Leich E, et al. Follicular lymphoma grade 3B is a distinct neoplasm according to cytogenetic and immunohistochemical profiles. *Haematologica.* 2011;96(9):1327-1334.
 12. Piccaluga PP, Califano A, Klein U, et al. Gene expression analysis provides a potential rationale for revising the histological grading of follicular lymphomas. *Haematologica.* 2008;93(7):1033-1038.
 13. Bosga-Bouwer AG, van Imhoff GW, Boonstra R, et al. Follicular lymphoma grade 3B includes 3 cytogenetically defined subgroups with primary t(14;18), 3q27, or other translocations: t(14;18) and 3q27 are mutually exclusive. *Blood.* 2003;101(3):1149-1154.
 14. Horn H, Kohler C, Witzig R, et al. Gene expression profiling reveals a close relationship between follicular lymphoma grade 3A and 3B, but distinct profiles of follicular lymphoma grade 1 and 2. *Haematologica.* 2018;103(7):1182-1190.
 15. Hans CP, Weisenburger DD, Greiner TC, et al. Confirmation of the molecular classification of diffuse large B-cell lymphoma by immunohistochemistry using a tissue microarray. *Blood.* 2004;103(1):275-282.
 16. Au-Yeung KHR, Padilla LA, Burkhardt B, Woessmann W, Klapper W. Features of pediatric B-lymphoblastic lymphoma with KMT2A rearrangements in the German NHL-BFM group. The 108th Annual Meeting of the Japanese Society of Pathology. Tokyo: Proceedings of the Japanese Society of Pathology, 2019:420.
 17. Reinke S, Bröckelmann PJ, Iaccarino I, et al. Tumor and microenvironment response but no cytotoxic T-cell activation in classic Hodgkin lymphoma treated with anti-PD1. *Blood.* 2020;136(25):2851-2863.
 18. Duhrsen U, Muller S, Hertenstein B, et al. Positron Emission Tomography-Guided Therapy of Aggressive Non-Hodgkin Lymphomas (PETAL): a multicenter, randomized phase III trial. *J Clin Oncol.* 2018;36(20):2024-2034.
 19. Tilly H, Gomes da Silva M, Vitolo U, et al. Diffuse large B-cell lymphoma (DLBCL): ESMO clinical practice guidelines for diagnosis, treatment and follow-up. *Ann Oncol.* 2015;26(Suppl 5):v116-125.
 20. Pandey S, Mourcin F, Marchand T, et al. IL-4/CXCL12 loop is a key regulator of lymphoid stroma function in follicular lymphoma. *Blood.* 2017;129(18):2507-2518.
 21. Barraclough A, Bishton M, Cheah CY, Villa D, Hawkes EA. The diagnostic and therapeutic challenges of grade 3B follicular lymphoma. *Br J Haematol.* 2021;195(1):15-24.
 22. Klapper W. Pathobiology and diagnosis of follicular lymphoma. *Semin Diagn Pathol.* 2011;28(2):146-160.
 23. Mann RB, Berard CW. Criteria for the cytologic subclassification of follicular lymphomas: a proposed alternative method. *Hematol Oncol.* 1983;1(2):187-192.
 24. Ott G, Katzenberger T, Lohr A, et al. Cytomorphologic, immunohistochemical, and cytogenetic profiles of follicular lymphoma: 2 types of follicular lymphoma grade 3. *Blood.* 2002;99(10):3806-3812.
 25. Salaverria I, Philipp C, Oschlies I, et al. Translocations activating IRF4 identify a subtype of germinal center-derived B-cell lymphoma affecting predominantly children and young adults. *Blood.* 2011;118(1):139-147.
 26. Klapper W, Kreuz M, Kohler CW, et al. Patient age at diagnosis is associated with the molecular characteristics of diffuse large B-cell lymphoma. *Blood.* 2012;119(8):1882-1887.
 27. Au-Yeung RKH, Arias Padilla L, Zimmermann M, et al. Experience with provisional WHO-entities large B-cell lymphoma with IRF4-rearrangement and Burkitt-like lymphoma with 11q aberration in paediatric patients of the NHL-BFM group. *Br J Haematol.* 2020;190(5):753-763.

A pilot study of the use of dynamic analysis of cell-free DNA from aqueous humor and vitreous fluid for the diagnosis and treatment monitoring of vitreoretinal lymphomas

Xiaoxiao Wang,^{1,2*} Wenru Su,^{3*} Yan Gao,^{1,2*} Yanfen Feng,^{1,4} Xiaoxia Wang,⁵ Xiaoqing Chen,³ Yunwei Hu,³ Yutong Ma,⁵ Qiuxiang Ou,⁵ Dan Liang³ and Huiqiang Huang^{1,2}

¹State Key Laboratory of Oncology in South China, Collaborative Innovation Center for Cancer Medicine, Guangzhou; ²Department of Medical Oncology, Sun Yat-sen University Cancer Center, Guangzhou; ³State Key Laboratory of Ophthalmology, Zhongshan Ophthalmic Center, Sun Yat-sen University, Guangzhou; ⁴Department of Pathology, Sun Yat-sen University Cancer Center, Guangzhou and ⁵Geneseeq Research Institute, Nanjing Geneseeq Technology Inc., Nanjing, Jiangsu, China

*XW, WS and YG contributed equally as co-first authors.

Correspondence: H. Huang
huanghq@sysucc.org.cn

D. Liang
liangdan@gzzoc.com

Received: September 7, 2021.

Accepted: February 2, 2022.

Prepublished: February 10, 2022.

<https://doi.org/10.3324/haematol.2021.279908>

©2022 Ferrata Storti Foundation

Published under a CC BY-NC license



Abstract

The diagnosis of vitreoretinal lymphoma (VRL), a rare subtype of primary central nervous system lymphoma, is challenging. We aimed to investigate the mutational landscape of VRL by sequencing circulating tumor DNA (ctDNA) from aqueous humor (AH) and/or vitreous fluid (VF), as well as applying ctDNA sequencing to diagnosis and treatment monitoring. Baseline AH and/or VF specimens from 15 VRL patients underwent comprehensive genomic profiling using targeted next-generation sequencing. The molecular profiles of paired baseline AH and VF specimens were highly concordant, with comparable allele frequencies. However, the genetic alterations detected in cerebrospinal fluid ctDNA only partially overlapped with those from simultaneously collected AH/VF samples, with much lower allele frequencies. Serial post-treatment AH or VF samples were available for five patients and their changes in ctDNA allele frequency displayed a similar trend as the changes in interleukin-10 levels; an indicator of response to treatment. A cohort of 23 patients with primary central nervous system lymphoma was included as a comparison group for the genetic landscape and evaluations of the efficacy of ibrutinib. More *MYD88* mutations, but fewer *IRF4* mutations and *CDKN2A/B* copy number losses were observed in the baseline samples of primary central nervous system lymphoma than VRL patients. The objective response rate to ibrutinib treatment was much higher for patients with primary central nervous system lymphoma (64.7%, 11/17) than for those with VRL (14.3%, 1/7). In summary, we provide valuable clinical evidence that AH is a good source of tumor genomic information and can substitute VF. Moreover, molecular profiling of AH has clinical utility for the diagnosis of VRL and treatment monitoring.

Introduction

Vitreoretinal lymphoma (VRL) is a rare type of primary central nervous system lymphoma (PCNSL) which primarily involves the retina and vitreous.¹⁻³ Based on the origins of the lymphoma, it can be classified as primary VRL, synchronous VRL with central nervous system or systemic involvement, or secondary VRL, which occurs as a site of relapsed lymphoma.^{4,5} Approximately 95% of primary VRL are histologically identified as diffuse large B-cell lymphomas, while at the molecular level, both PCNSL and pri-

mary VRL are classified into MCD/C5 subgroups of diffuse large B-cell lymphoma based on concurrent *MYD88* (L265P) and *CD79B* mutations.⁶⁻⁸ Primary VRL is highly aggressive with an elevated mortality rate, and 65% to 90% of patients eventually develop brain parenchymal involvement. In contrast, 15% to 25% of patients with PCNSL have vitreoretinal involvement, either as synchronous VRL and PCNSL or secondary VRL.¹ The diagnosis of VRL remains a challenge for clinicians as the symptoms of VRL can mimic those of posterior uveitis. Thus, patients are typically diagnosed with intermediate and/or posterior uveitis,

with vitritis and/or subretinal infiltrates.^{1,9,10} The diagnosis of VRL is made on the basis of histological and molecular tests. First, cytology and flow cytometry of ocular samples are used to identify a monoclonal neoplastic B lymphocyte population. Second, elevated levels of interleukin (IL)-10 in aqueous humor (AH) and/or vitreoretinal fluid (VF), and the detection of *MYD88* mutations in tumor cells can also be used as ancillary tests.¹¹ However, cytomorphological evaluations often fail to detect lymphoma cells because of the limited sample volume, low cellularity of VF samples, and cell lysis during biopsies.¹²⁻¹⁴

Recently, several studies reported the genetic profiles of VRL using VF ctDNA sequencing.¹⁵⁻¹⁷ Vitreous biopsy is a common surgical procedure, but it is an invasive process and may cause severe complications. It has been reported that AH can serve as a source of liquid biopsy for molecular profiling in retinoblastomas, which is enriched in eye-specific tumor-derived cell-free DNA (cfDNA) and can be collected for repeated sampling.¹⁸ Thus, AH is an emerging tool for the diagnosis, prognosis, and treatment monitoring of tumors with ocular invasion.

The *MYD88* L265P mutation is a primary oncogenic driver in PCNSL and was recently identified as a disease biomarker in VRL as well.^{17,19} *MYD88* L265P continuously activates the nuclear factor kappa light-chain enhancer of activated B cells (NF- κ B) by Bruton tyrosine kinase (BTK), promoting tumor proliferation. As ibrutinib, a BTK inhibitor, can cross the blood-brain barrier, ibrutinib-based combination therapy is widely used in PCNSL patients, with promising responses.²⁰ However, the efficacy of ibrutinib in patients with VRL remains to be evaluated.

In this study, we sought to investigate the mutational landscape of VRL and the application of serial molecular profiling of AH/VF ctDNA for treatment monitoring. We also explored the differences in genomic profiles between VRL and PCNSL patients, and their responses to ibrutinib treatment.

Methods

Patients and the diagnosis of vitreoretinal lymphoma

A total of 15 patients who presented with severe vitreous opacity and/or diffuse yellow subretinal lesions were admitted to the Department of Medical Oncology at Sun Yat-sen University Cancer Center (SYSUCC) between December 2018 and December 2020. VRL was diagnosed by two experienced specialists (DL and WS) at the Zhongshan Ophthalmic Center of the Sun Yat-Sen University (Guangzhou, China). The VRL diagnoses of three patients were confirmed by pathology studies using standard cytology and immunocytochemistry of B-cell markers, and clonality analyses for the presence of immunoglobulin heavy chain (*IGH*) rearrangements. The other 12 patients

were diagnosed based on typical clinical manifestations, including elevation of the IL-10/IL-6 ratio and/or *IGH* rearrangements in AH/VF. All patients underwent further examinations, including positron emission tomography and computed tomography (PET/CT) or magnetic resonance imaging and seven also underwent lumbar puncture for cytology and cerebrospinal fluid (CSF) ctDNA sequencing.

This study was approved by the ethics committee of SYSUCC (approval n.: B2020-315-01) and was conducted in accordance with the Declaration of Helsinki. All participants provided written informed consent prior to sample collection.

Sample collection and DNA extraction

The median volume of AH/VF samples used for cfDNA extraction was 0.1 mL (range, 0.02–3.5 mL). Samples were transported to the laboratory at 4°C. cfDNA was extracted from the supernatants of AH/VF samples (1,800 g \times 10 min) within 48 h of collection. DNA was extracted using a Circulating Nucleic Acid Kit (Qiagen, Hilden, Germany) following the manufacturer's protocol and stored at -80°C until further analysis. Fragment distribution was determined on a Bioanalyzer 2100 using a High Sensitivity DNA Kit (Agilent Technologies, Santa Clara, CA, USA).

The tumor cell content of formalin-fixed, paraffin-embedded (FFPE) sections from 23 PCNSL patients was determined by a pathologist. Genomic DNA of the 23 PCNSL patients was purified from the FFPE slides using a QIAamp DNA FFPE Tissue Kit (Qiagen) and from oral swabs using a DNeasy Blood & Tissue Kit (Qiagen). This DNA was then quantified using a Nanodrop2000 (Thermo Fisher Scientific, Waltham, MA, USA). All DNA was quantified using the dsDNA HS Assay Kit on a Qubit 3.0 Fluorometer (Life Technologies, Carlsbad, CA, USA).

DNA sequencing and genomic mutational analyses

Targeted next-generation sequencing (NGS) was performed using a panel (Hemasalus™) of exons and splice sites of more than 400 genes that are recurrently mutated in B-cell lymphomas. The full list of genes included in the panel is provided in *Online Supplementary Table S1*. NGS was performed in a testing laboratory (Nanjing Geneseeq Technology, Inc., Nanjing, China) accredited by the Clinical Laboratory Improvement Amendments (CLIA) and the College of American Pathologists (CAP). The depth of coverage of the NGS panel was 500 \times for liquid biopsies. Sequencing libraries were prepared using the KAPA Hyper Prep Kit (KAPA Biosystems) and sequenced on a HiSeq 4000 NGS platform (Illumina).²¹ Sequencing data were processed as previously described.²² In brief, the data were first demultiplexed and the FASTQ file was subjected to quality control to remove low-quality data or N bases. Qualified reads were mapped to the reference human ge-

genome, hg19, using the Burrows-Wheeler Aligner. The Genome Analysis Toolkit (GATK 3.4.0) was used to perform local realignment around indels and base quality score recalibration. Picard was used to remove polymerase chain reaction duplicates. VarScan2 was used to detect single-nucleotide variants and insertion/deletion mutations. A mutant allele frequency cutoff of 1% was used for tissue samples and 0.3% for cfDNA samples. ADTEX was used to identify copy number variations with a normal human DNA sample, NA18535. A cutoff \log_2 ratio was set at ± 0.6 for copy number changes (corresponding to a 1.5-fold copy number gain and 0.65-fold copy number loss).

Results

Overview of the patients with vitreoretinal lymphoma

As shown in Table 1, a total of 15 VRL patients were enrolled in this study with a median age of 56 years (range, 38-68 years). Almost all patients (14/15) had binocular disease. Vitreous involvement was more frequent than

Table 1. Patients' characteristics.

Characteristics	VRL	PCNSL
Total number	15	23
Age in years, median (range)	56 (38-68)	58 (28-83)
Sex, N (%)		
Male	8 (53.3)	11 (47.8)
Female	7 (46.7)	12 (52.2)
Location, N (%)		
Vitreous	11* (73.3)	-
Subretinal	8* (53.3)	-
Subtype, N (%)		
Primary VRL (%)	13 (86.7)	-
No brain involvement	11 (84.6)	
Subsequent brain involvement	2 (15.4)	
Synchronous VRL and PCNSL	2 (13.3)	-
Treatment, N (%)		
Systemic treatment with ibrutinib	7 (46.7)	17 (73.9)
Local ocular treatment	8 (53.3)	6 (26.1)

*Four patients had both vitreous and subretinal involvement. VRL: vitreoretinal lymphoma; PCNSL: primary central nervous system lymphoma.

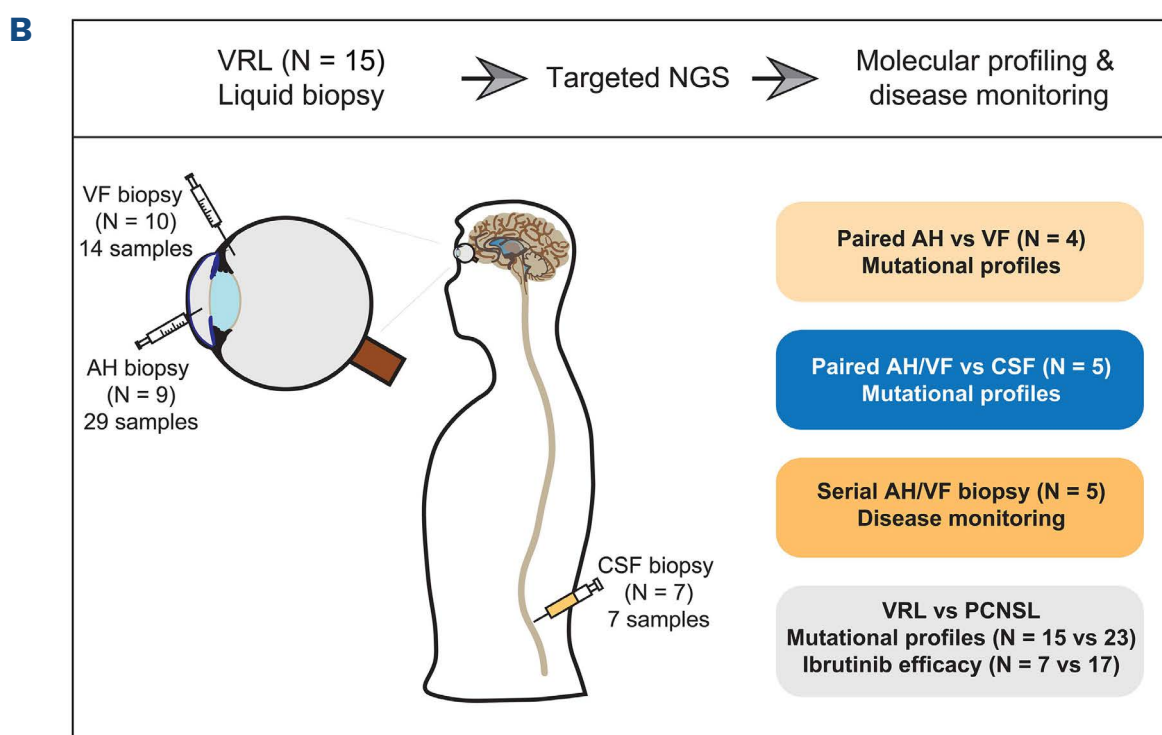
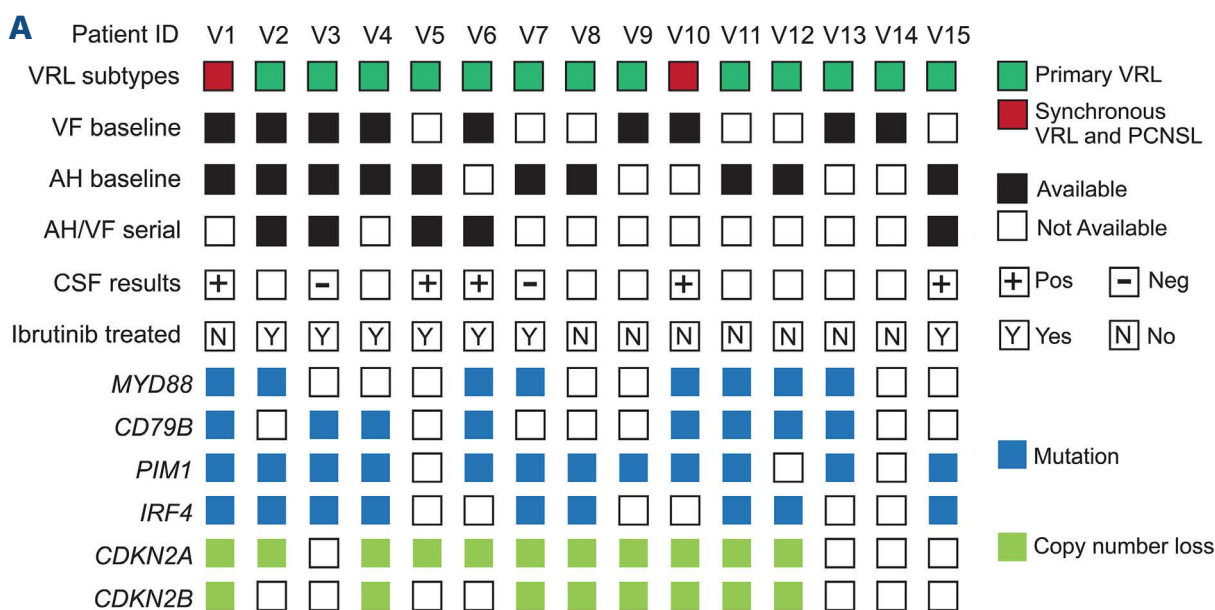


Figure 1. Overview of the patients' characteristics and study design.

(A) The availability of samples from all enrolled patients, as well as ibrutinib treatment information are shown as indicated in the legend. The molecular features of the most prevalent gene alterations detected in baseline samples are also provided. (B) An illustration of sampling aqueous humor, vitreous fluid, and cerebrospinal fluid is shown on the left. The four aims of this study are listed on the right. ID: identity; VRL: vitreoretinal lymphoma; PCNSL: primary central nervous system lymphoma; AH: aqueous humor; VF: vitreous fluid; CSF: cerebrospinal fluid; NGS: next-generation sequencing.

subretinal infiltrates (11/15 vs. 8/15, respectively) and lymphoma was found at both locations in four patients. Thirteen individuals had primary VRL without brain involvement or histories of other systemic lymphomas at diagnosis, and the remaining two patients (V1 and V10) were diagnosed with synchronous VRL and PCNSL. Representative cytological and immunohistochemistry images of a VRL patient (V4) are shown in *Online Supplementary Figure S1*, with large, atypical cells positive for Ki67, CD20, and CD79A. Baseline AH and/or VF samples were collected from all patients, of whom five also underwent sequential sampling during their treatment for disease monitoring. The median concentration of cfDNA extracted from AH/VF samples was 0.5 ng/ μ L. A full list of liquid biopsy volumes and cfDNA concentrations is provided in *Online Supplementary Table S2*. Seven VRL patients received ibrutinib therapy, mainly for first- and second-line treatments (Figure 1A), while the remaining eight VRL patients were administered local

ocular treatments (Table 1).

High concordance of mutations detected in paired aqueous humor and vitreous fluid cell-free DNA samples

Baseline AH and/or VF samples were collected from all 15 VRL patients and underwent targeted NGS. Two-thirds of samples carried *MYD88* L265P and/or *CD79B* mutations (Figure 1A). Other frequently mutated genes included *PIM1* (80%), *IRF4* (60%), and *CDKN2A/B* copy number losses (73.3% and 53.3%). A complete list of mutations in all samples is provided in *Online Supplementary Table S3*. Four patients (V1-V4) had matched baseline AH and VF samples that were subjected to sequencing. Two patients (V1 and V2) shared an identical mutational spectrum in the matched AH and VF samples; their allele frequencies were also comparable (Figure 2A). The concordance rates of mutations between AH and paired VF samples in the other two patients (V3 and

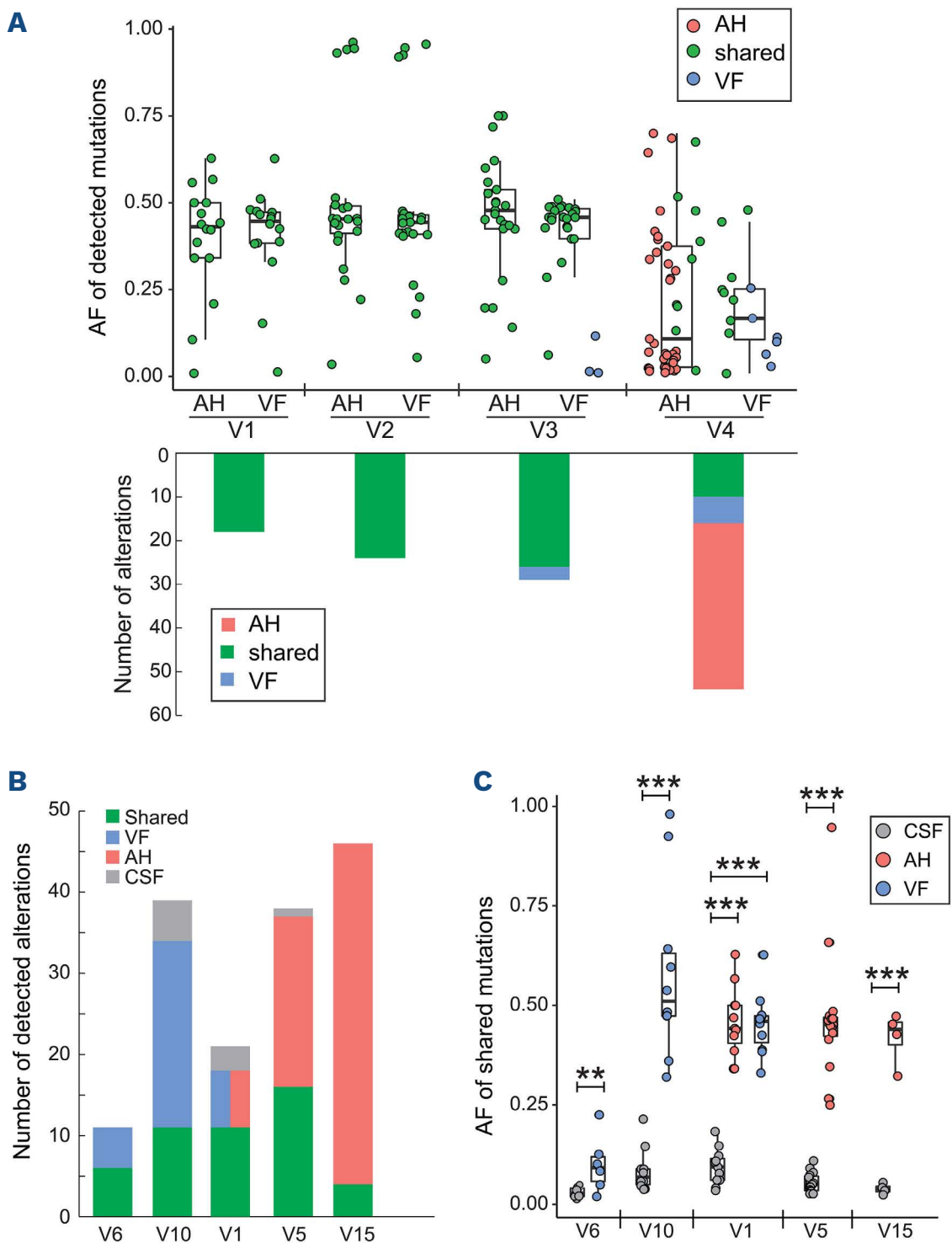


Figure 2. Mutational comparisons between matched aqueous humor, vitreous fluid and cerebrospinal fluid samples. (A) Four pairs of baseline aqueous humor (AH) and vitreous fluid (VF) samples underwent targeted next-generation sequencing. The allele frequencies of shared and unique mutations detected in matched AH and VF samples are shown in the top panel. The number of alterations detected in each patient is shown at the bottom of the panel. Shared, AH-only, and VF-only alterations are colored green, red, and blue, respectively. (B) The number of alterations detected in cerebrospinal fluid (CSF) and AH/VF samples from five patients is as labeled in the legend. The brain involvement in patients V1 and V10 was confirmed by positron emission tomography/computed tomography examinations. (C) Allele frequencies of mutations present in both CSF and AH/VF samples. $**P < 0.05$, $***P < 0.01$. AF: allele frequency.

V4) were 90% (26/29) and 60% (10/16), respectively. Thus, those results suggest that AH can serve as a surrogate for mutational analysis of VRL and is more easily accessible than VF biopsies.

In addition, to avoid unnecessary clinical injury to patients with binocular disease, AH/VF sampling is usually

performed in a single eye. However, patient V5 underwent AH extraction from both eyes for sequencing. Overall, 32 mutations were identified in AH samples from either the left or right eye, over 80% (26/32) of which were detected in both samples, with similar allele frequencies ($R^2=0.899$) (Online Supplementary Figure S2).

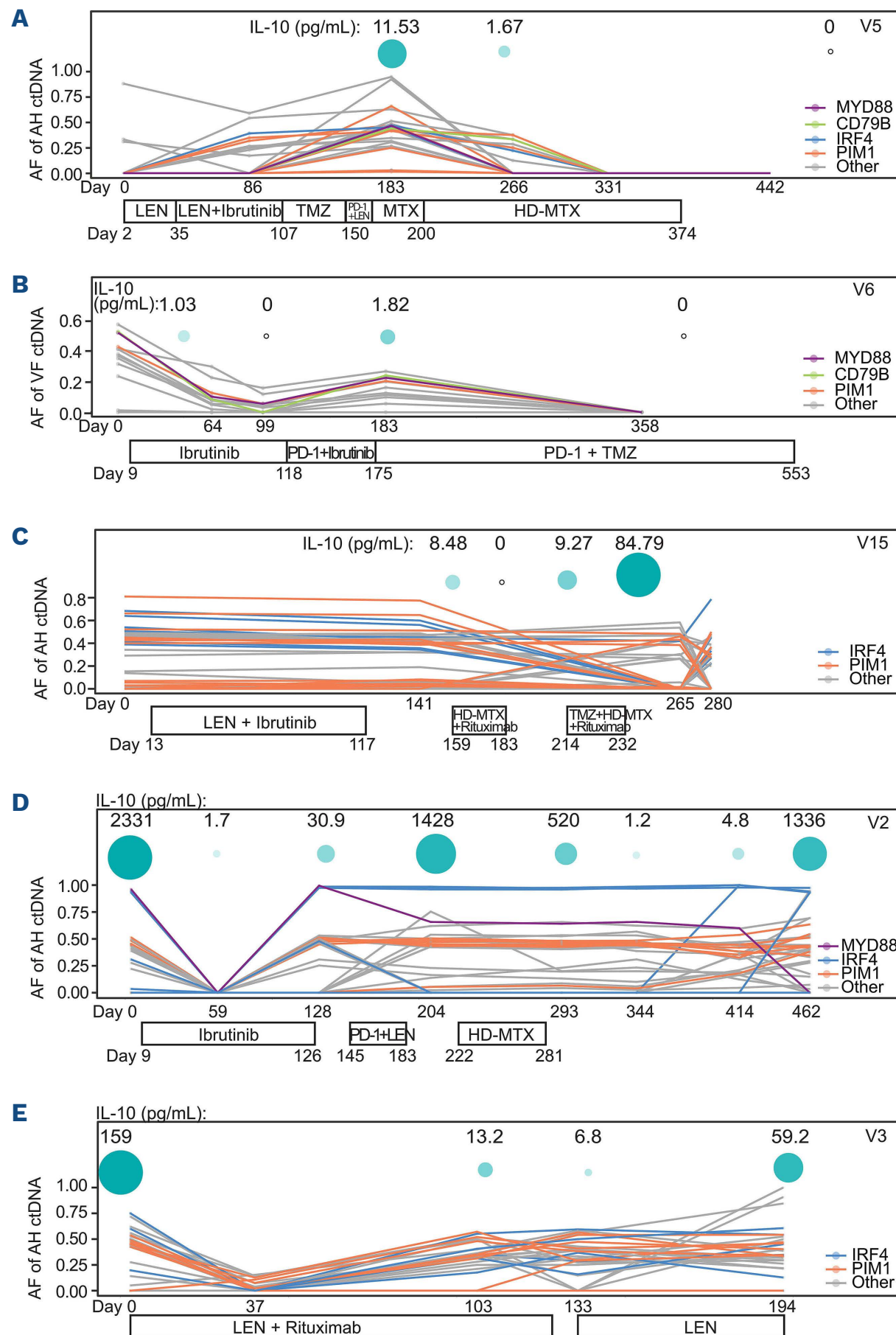


Figure 3. Dynamic profiling of circulating tumor DNA and interleukin-10 levels in aqueous humor or vitreous fluid samples. The treatment histories of five patients (identity numbers in the top right corner of each panel) with dynamic and sequential sampling of aqueous humor (AH) or vitreous fluid (VF) are shown at the bottom of each panel. The allele frequency changes to driver mutations and other alterations are shown in the line chart. Interleukin-10 levels (pg/mL) at each time point are indicated by the green circles at the top of each panel. AF: allele frequency; ctDNA: circulating tumor DNA; IL-10: interleukin.10; LEN: lenalidomide; TMZ: temozolomide; HD-MTX: high-dose methotrexate.

Early detection of circulating tumor DNA in cerebrospinal fluid in patients with primary vitreoretinal lymphoma may predict parenchymal invasion of the brain

CSF samples were collected from seven patients for whom CSF cytology examinations were negative. Five of the patients were positive for CSF ctDNA and the median concentration of the extracted cfDNA from CSF samples was 1.1 ng/ μ L (*Online Supplementary Table S2*). The numbers of alterations in VF/AH and CSF samples are shown in Figure 2B, while the allele frequencies of the shared mutations are shown in Figure 2C. All five patients had significantly higher allele frequencies for the shared mutations in AH and/or VF samples than in CSF ctDNA. It is also of note that patients V1 and V10, who had synchronous PCNSL confirmed by PET/CT examinations, harbored a higher number of mutations detected only in CSF samples with significantly higher allele frequencies ($P < 0.01$) than those of the other three patients (V5, V6, and V15). Notably, brain involvement developed in patients V5 and V6 after 9 and 19 months, respectively. Thus, positive CSF ctDNA detection might be an early indicator of brain involvement with a subset of alterations in patients with primary VRL.

Dynamic profiling of circulating tumor DNA in aqueous humor or vitreous fluid samples to monitor response to treatment

Of the seven VRL patients who received systemic treatment, five underwent a series of dynamic AH/VF sampling (4 underwent serial AH sampling and 1 underwent serial VF sampling) (Figure 3, *Online Supplementary Table S4*). AH or VF samples were collected for ctDNA detection throughout treatment to dynamically monitor the therapeutic re-

sponses. In addition, the IL-10 levels in AH/VF samples were also analyzed to assist with the response evaluation of VRL patients. For patients V5 and V6, the changes of IL-10 levels were highly concordant with the allele frequencies of AH/VF ctDNA (Figure 3A, B). For patient V15, all four IL-10 tests were performed within the interval of two rounds of AH ctDNA sequencing, which provided limited information about the correlation between the IL-10 levels and ctDNA allele frequencies (Figure 3C). The remaining two patients (V2 and V3) with extremely high levels of IL-10 at baseline showed dramatic decreases in post-treatment IL-10 levels and AH ctDNA allele frequencies (Figure 3D, E). These findings imply that AH/VF ctDNA profiling could assist in the evaluation of treatment efficacy, in addition to the use of IL-10 tests and eye examinations.

Comparisons of mutational landscape between patients with vitreoretinal lymphoma and primary central nervous system lymphoma

To further compare the mutational landscapes of VRL and PCNSL, we included another cohort of 23 PCNSL patients. When comparing the mutations detected in the baseline VRL AH/VF samples and PCNSL tumor biopsy specimens, we found that *PIM1* mutations (80%) and *CDKN2A* copy number loss (73.3%) were the two most frequently observed alterations in VRL patients, but were underrepresented in the PCNSL cohort with frequencies of 56.5% and 39.1%, respectively (*Online Supplementary Figure S3*). Furthermore, the canonical oncogenic driver mutation, *MYD88* L265P, was less frequently detected in VRL patients than in the PCNSL cohort (53.3% vs. 82.6%, respectively, $P = 0.07$) (Figure 4A). In contrast, the frequencies of *IRF4* mutations and *CDKN2B* copy number loss were significantly higher in the VRL cohort (Figure 4A).

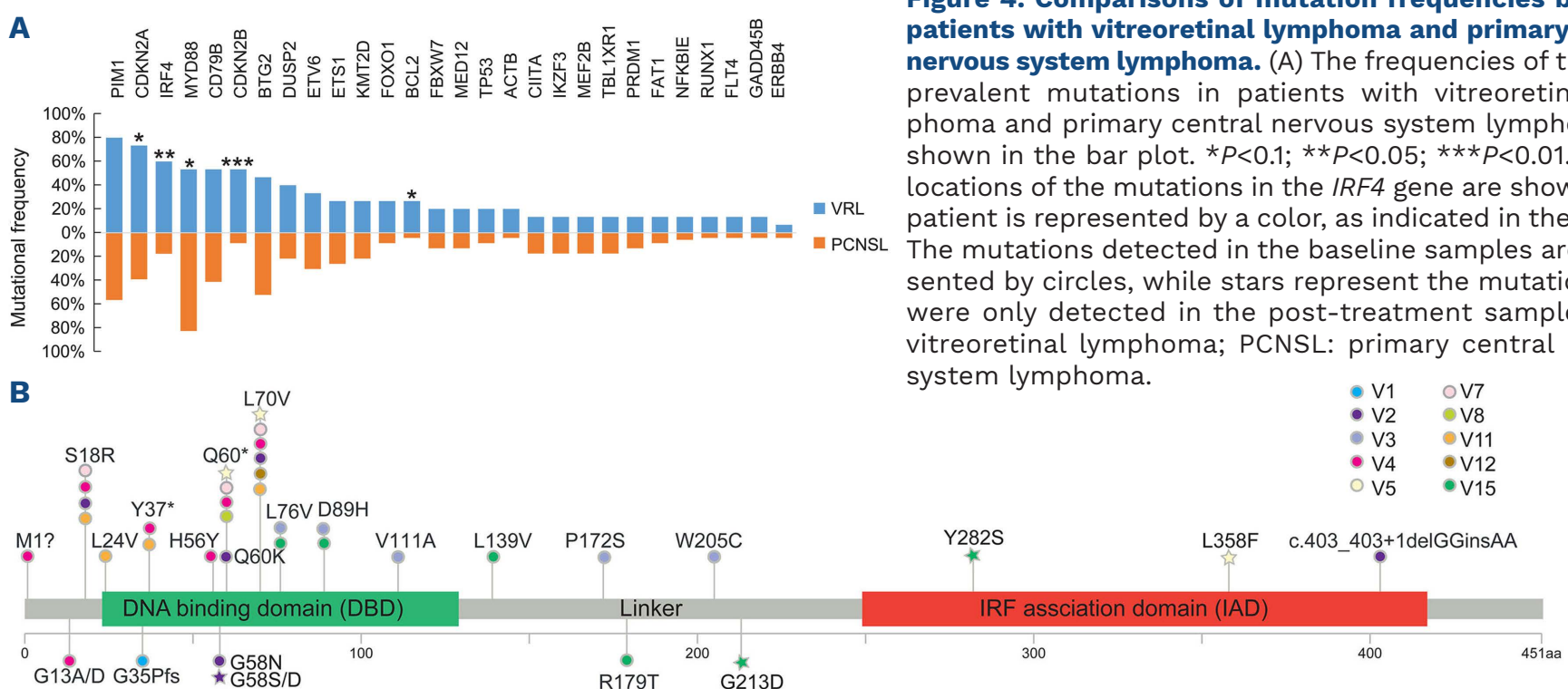


Figure 4. Comparisons of mutation frequencies between patients with vitreoretinal lymphoma and primary central nervous system lymphoma. (A) The frequencies of the most prevalent mutations in patients with vitreoretinal lymphoma and primary central nervous system lymphoma are shown in the bar plot. * $P < 0.1$; ** $P < 0.05$; *** $P < 0.01$. (B) The locations of the mutations in the *IRF4* gene are shown. Each patient is represented by a color, as indicated in the legend. The mutations detected in the baseline samples are represented by circles, while stars represent the mutations that were only detected in the post-treatment samples. VRL: vitreoretinal lymphoma; PCNSL: primary central nervous system lymphoma.

In addition, we further investigated the mutational sites of *IRF4* in VRL patients. Recurrent *IRF4* mutations mainly occurred in the DNA binding domain with L70V, Q60* and S18R being the most frequent mutations (Figure 4B). Most *IRF4* mutation sites were detected in primary and post-treatment AH/VF samples (e.g., V1-V3 and V15), while G58S/D, G213D, Y282S, and L358F were acquired after multiple lines of treatment (e.g., V2, V5, and V15).

In the VRL cohort, seven patients received ibrutinib, only one of whom (V2) achieved a partial response and had a significant improvement in visual acuity, leading to an overall response rate of 14% to ibrutinib (*Online Supplementary Table S5*). In contrast, 17 PCNSL patients received systemic treatment containing ibrutinib and the overall response rate was 65%, with nine complete responses and two partial responses. It should be noted that these patients received either ibrutinib monotherapy (PCNSL, 41%; VRL, 29%) or combined therapies (PCNSL, 59%; VRL, 71%); 29% (5/17) of the PCNSL patients and 57% (4/7) of the VRL patients received ibrutinib as first-line treatment. The diverse treatment regimens prevented a direct comparison of the efficacy of ibrutinib between VRL and PCNSL patients; however, there was a trend to the efficacy of ibrutinib being poorer in VRL patients.

Discussion

To our knowledge, this study was the first to investigate the molecular profiles of AH/VF ctDNA using a large NGS panel covering over 400 lymphoma-related genes in the Chinese population. The findings revealed the potential utility of analyzing AH ctDNA for the diagnosis of VRL, as well as for disease monitoring with serial sampling. The high concordance between AH and VF profiles indicated that AH could serve as a surrogate for VF liquid biopsies, as AH is more easily accessible. We also revealed differences in the molecular landscapes between VRL and PCNSL, and the suboptimal responses to ibrutinib in the VRL cohort.

Due to the low incidence of VRL, our study cohort was relatively small; however, this was a common limitation of other published studies as well.⁴ For instance, Lee *et al.* investigated the mutational signatures of primary VRL using whole-exon sequencing in an Asian cohort (n=9), finding that all patients carried *MYD88* mutations. The frequencies of *IRF4* and *PIM1* mutations in that cohort were 44.4% and 88.9%, respectively, which were comparable to the frequencies observed in the current study (60% and 80%, respectively).¹⁶ However, in another study of 16 primary VRL patients analyzed using targeted NGS, only 18.8% harbored *IRF4* mutations, and the frequencies of *MYD88* and *PIM1* mutations were both 68.8%.¹⁵ Notably, that study¹⁵ was conducted in a Western population,

which might explain the different mutational frequencies. Bonzheim *et al.*¹⁵ also reported a similar frequency of *CD79B* mutations (43.8%) as that in our study (53.3%) and in a study by Yonese *et al.* (35%).²³ Another small cohort study (n=8) detected *MYD88* L265P in 75% of patients' AH samples, with a consistency of 87.5% when compared to VF samples using polymerase chain reaction and pyrosequencing assays.¹⁹ Overall, the mutational frequencies reported in those studies were comparable to those observed in the current study, although factors including the small cohort sizes and different ethnic populations being studied should be taken into consideration.

IRF4 encodes a transcription factor that controls the differentiation of B, T, dendritic, and myeloid cells, and regulates various aspects of their respective immune responses.²⁴ *IRF4* is also an oncogene in some subtypes of diffuse large B-cell lymphoma and a tumor-suppressor in c-Myc-induced malignancies.²⁵⁻²⁹ *IRF4* rearrangement and aberrant hypermutation were commonly characterized in lymphoproliferative malignancies, especially pediatric large B-cell lymphomas.³⁰ In our study, the detected *IRF4* mutation sites spanned the complete coding region, and especially affected the DNA-binding domain (DBD) and the IRF association domain (IAD).

CDKN2B (cyclin dependent kinase inhibitor 2B) is a tumor suppressor gene located adjacent to *CDKN2A*, both of which are frequently deleted in multiple tumors.^{31,32} In our VRL cohort, 73.3% and 53.3% of patients carried *CDKN2A* and *CDKN2B* deletions, respectively. In contrast, PCNSL patients showed much lower frequencies of deletions (*CDKN2A*: 39% and *CDKN2B*: 8.7%). These findings revealed the genetic differences between VRL and PCNSL, suggesting that more precise clinical management is needed for this rare and unique type of cancer.

There is a limited evidence-base to guide the treatment of VRL. There have been no randomized clinical trials directed at the treatment of VRL specifically, although some trials of treatments for PCNSL have included patients with VRL, facilitating limited subset analyses.³³ Recently, a phase II clinical trial showed promising efficacy of ibrutinib monotherapy in relapsed or refractory PCNSL and VRL patients, independently of B-cell antigen receptor pathway alterations, including *CD79A/B*.³⁴ Conversely, another study suggested that diffuse large B-cell lymphomas with mutated *CD79B* and *MYD88* were more responsive to ibrutinib, while *MYD88*-only mutant tumors were likely to be ibrutinib-resistant.³⁵ In our study, four PCNSL patients harboring concurrent *CD79B* and *MYD88* mutations all achieved a complete response to ibrutinib treatment (*Online Supplementary Table S5*). The efficacy of ibrutinib treatment in our VRL cohort was suboptimal compared to that in PCNSL patients. There are a few possible explanations for this observation, including the fact that both ibrutinib monotherapy and combined therapies were in-

cluded in this study; the line of treatment varied from first-line to third-line; and subset analyses were not performed because of the restricted cohort size. These limitations prevented a direct comparison of the efficacy of ibrutinib treatment between VRL and PCNSL patients; however, the findings should promote additional well-designed and comprehensive studies of the efficacy of ibrutinib in VRL patients in the future.

The evaluation of disease progression in VRL patients, unlike that of patients with solid tumors, relies mainly on eye examinations and patients' visual acuities, which are subjective rather than quantitative. Our results suggest that the changes in AH/VF ctDNA allele frequencies were relatively concordant with IL-10 levels in AH/VF. It is known that IL-10 is a clinical marker of VRL,^{36,37} so AH ctDNA monitoring might be an efficient and quantitative tool to evaluate treatment responses in patients with VRL. In addition, we found that the early detection of CSF ctDNA might be an indication of brain involvement, suggesting that patients with positive CSF ctDNA require close monitoring. Of note, although CSF has been accepted as a better surrogate than plasma for the molecular profiling of brain tumors,^{38,39} the allele frequencies of CSF ctDNA-derived mutations were significantly lower than those of AH/VF-derived aberrations. Furthermore, mutations detected in CSF samples represented only a subset of AH/VF-borne mutations. That observation suggested that lymphoma was likely to be of an ocular origin in those patients, but considering that CSF has a much higher dilution volume than AH/VF, caution in the interpretation of disease origin is warranted.

Several limitations of this study should be noted. First, the cohort size was restricted due to the rarity of VRL, and thus, further validation in larger cohorts is warranted. Second, the volume of AH/VF samples available for cfDNA extraction varied between patients, but sample volumes were usually small, leading to a limited amount of cfDNA for NGS. Therefore, ctDNA sequencing with AH/VF biopsies was technically demanding. Lastly, the efficacy profile of ibrutinib in VRL and PCNSL requires further investigation because of the heterogeneity and diverse

treatment conditions between cohorts in this study. However, our collective findings revealed the molecular heterogeneity of VRL and PCNSL, and highlighted the clinical utility of serial AH/VF ctDNA profiling for the diagnosis and monitoring of VRL.

Disclosures

Xiaoxia W, YM, and QO are employees of Nanjing Geneseeq Technology Inc. The remaining authors have no conflicts of interest to declare.

Contributions

Xiaoxiao W and HH designed the study; Xiaoxiao W established the methodology; WS, YG, XC, and YH curated data; WS and Xiaoxiao W performed the investigation; Xiaoxiao W, WS, YH, and YM performed the formal analysis; YG, YF, XC, QO, and DL validated the data; YF, Xiaoxiao W and YM visualized the data; Xiaoxiao W and YM wrote the draft of the article; WS, YG, and QO edited the manuscript; DL administrated the project; HH acquired the funding. All authors read and agreed to the final version of the manuscript.

Acknowledgments

The authors would like to thank the patients and family members who gave their consent to presenting the data in this study, as well as the investigators and research staff involved in the study.

Funding

This study was supported by the National Science & Technology Major Project (grant number: 2017ZX09304021).

Data-sharing statement

The human sequence data generated in this study are not publicly available due to patient privacy requirements but are available from the corresponding author upon reasonable request. Other data generated in this study are available within the article and its Online Supplementary Data Files.

References

1. Chan CC, Rubenstein JL, Coupland SE, et al. Primary vitreoretinal lymphoma: a report from an International Primary Central Nervous System Lymphoma Collaborative Group symposium. *Oncologist*. 2011;16(11):1589-1599.
2. Buggage RR, Chan CC, Nussenblatt RB. Ocular manifestations of central nervous system lymphoma. *Curr Opin Oncol*. 2001;13(3):137-142.
3. Chan CC, Buggage RR, Nussenblatt RB. Intraocular lymphoma. *Curr Opin Ophthalmol*. 2002;13(6):411-418.
4. Soussain C, Malaise D, Cassoux N. Primary vitreoretinal lymphoma: a diagnostic and management challenge. *Blood*. 2021;138(17):1519-1534.
5. Salomao DR, Pulido JS, Johnston PB, Canal-Fontcuberta I, Feldman AL. Vitreoretinal presentation of secondary large B-cell lymphoma in patients with systemic lymphoma. *JAMA Ophthalmol*. 2013;131(9):1151-1158.
6. Coupland SE, Hummel M, Stein H, Willerding G, Jahnke K, Stoltenburg-Didinger G. Demonstration of identical clonal derivation in a case of "oculocerebral" lymphoma. *Br J Ophthalmol*. 2005;89(2):238-239.

7. Chapuy B, Stewart C, Dunford AJ, et al. Molecular subtypes of diffuse large B cell lymphoma are associated with distinct pathogenic mechanisms and outcomes. *Nat Med*. 2018;24(5):679-690.
8. Schmitz R, Wright GW, Huang DW, et al. Genetics and pathogenesis of diffuse large B-cell lymphoma. *N Engl J Med*. 2018;378(15):1396-1407.
9. Chan CC, Wallace DJ. Intraocular lymphoma: update on diagnosis and management. *Cancer Control*. 2004;11(5):285-295.
10. Reichstein D. Primary vitreoretinal lymphoma: an update on pathogenesis, diagnosis and treatment. *Curr Opin Ophthalmol*. 2016;27(3):177-184.
11. Dawson AC, Williams KA, Appukuttan B, Smith JR. Emerging diagnostic tests for vitreoretinal lymphoma: a review. *Clin Exp Ophthalmol*. 2018;46(8):945-954.
12. Caraballo JN, Snyder MR, Johnston PB, et al. Vitreoretinal lymphoma versus uveitis: cytokine profile and correlations. *Ocul Immunol Inflamm*. 2014;22(1):34-41.
13. Kimura K, Usui Y, Goto H, Japanese Intraocular Lymphoma Study Group. Clinical features and diagnostic significance of the intraocular fluid of 217 patients with intraocular lymphoma. *Jpn J Ophthalmol*. 2012;56(4):383-389.
14. Davis JL, Miller DM, Ruiz P. Diagnostic testing of vitrectomy specimens. *Am J Ophthalmol*. 2005;140(5):822-829.
15. Bonzheim I, Sander P, Salmeron-Villalobos J, et al. The molecular hallmarks of primary and secondary vitreoretinal lymphoma. *Blood Adv*. 2022 6(3):1598-1607.
16. Lee J, Kim B, Lee H, et al. Whole exome sequencing identifies mutational signatures of vitreoretinal lymphoma. *Haematologica*. 2020;105(9):e458-460.
17. Bonzheim I, Giese S, Deuter C, et al. High frequency of MYD88 mutations in vitreoretinal B-cell lymphoma: a valuable tool to improve diagnostic yield of vitreous aspirates. *Blood*. 2015;126(1):76-79.
18. Xu L, Kim ME, Polski A, et al. Establishing the clinical utility of ctDNA analysis for diagnosis, prognosis, and treatment monitoring of retinoblastoma: the aqueous humor liquid biopsy. *Cancers (Basel)*. 2021;13(6):1282.
19. Miserocchi E, Ferreri AJM, Giuffrè C, et al. MYD88 L265P mutation detection in the aqueous humor of patients with vitreoretinal lymphoma. *Retina*. 2019;39(4):679-684.
20. Lionakis MS, Dunleavy K, Roschewski M, et al. Inhibition of B cell receptor signaling by ibrutinib in primary CNS lymphoma. *Cancer Cell*. 2017;31(6):833-843.
21. Shu Y, Wu X, Tong X, et al. Circulating tumor DNA mutation profiling by targeted next generation sequencing provides guidance for personalized treatments in multiple cancer types. *Sci Rep*. 2017;7(1):583.
22. Yang Z, Yang N, Ou Q, et al. Investigating novel resistance mechanisms to third-generation EGFR tyrosine kinase inhibitor osimertinib in non-small cell lung cancer patients. *Clin Cancer Res*. 2018;24(13):3097-3107.
23. Yonese I, Takase H, Yoshimori M, et al. CD79B mutations in primary vitreoretinal lymphoma: diagnostic and prognostic potential. *Eur J Haematol*. 2019;102(2):191-196.
24. Nam S, Lim JS. Essential role of interferon regulatory factor 4 (IRF4) in immune cell development. *Arch Pharm Res*. 2016;39(11):1548-1555.
25. Klein U, Casola S, Cattoretti G, et al. Transcription factor IRF4 controls plasma cell differentiation and class-switch recombination. *Nat Immunol*. 2006;7(7):773-782.
26. De Silva NS, Simonetti G, Heise N, Klein U. The diverse roles of IRF4 in late germinal center B-cell differentiation. *Immunol Rev*. 2012;247(1):73-92.
27. Mittrucker HW, Matsuyama T, Grossman A, et al. Pillars article: requirement for the transcription factor LSIRF/IRF4 for mature B and T lymphocyte function. *Science*. 1997. 275: 540-543. *J Immunol*. 2017;199(11):3717-3720.
28. Yang Y, Shaffer AL, 3rd, Emre NC, et al. Exploiting synthetic lethality for the therapy of ABC diffuse large B cell lymphoma. *Cancer Cell*. 2012;21(6):723-737.
29. Acquaviva J, Chen X, Ren R. IRF-4 functions as a tumor suppressor in early B-cell development. *Blood*. 2008;112(9):3798-3806.
30. Blunt MD, Koehrer S, Dobson RC, et al. The dual Syk/JAK inhibitor cerdulatinib antagonizes B-cell receptor and microenvironmental signaling in chronic lymphocytic leukemia. *Clin Cancer Res*. 2017;23(9):2313-2324.
31. Laharanne E, Chevret E, Idrissi Y, et al. CDKN2A-CDKN2B deletion defines an aggressive subset of cutaneous T-cell lymphoma. *Mod Pathol*. 2010;23(4):547-558.
32. Tu Q, Hao J, Zhou X, et al. CDKN2B deletion is essential for pancreatic cancer development instead of unmeaningful co-deletion due to juxtaposition to CDKN2A. *Oncogene*. 2018;37(1):128-138.
33. Nguyen DT, Houillier C, Choquet S, et al. Primary oculocerebral lymphoma: MTX polychemotherapy alone on intraocular disease control. *Ophthalmology*. 2016;123(9):2047-2050.
34. Soussain C, Choquet S, Blonski M, et al. Ibrutinib monotherapy for relapse or refractory primary CNS lymphoma and primary vitreoretinal lymphoma: final analysis of the phase II 'proof-of-concept' iLOC study by the Lymphoma Study Association (LYSA) and the French Oculo-cerebral Lymphoma (LOC) network. *Eur J Cancer*. 2019;117:121-130.
35. Wilson WH, Young RM, Schmitz R, et al. Targeting B cell receptor signaling with ibrutinib in diffuse large B cell lymphoma. *Nat Med*. 2015;21(8):922-926.
36. Cassoux N, Giron A, Bodaghi B, et al. IL-10 measurement in aqueous humor for screening patients with suspicion of primary intraocular lymphoma. *Invest Ophthalmol Vis Sci*. 2007;48(7):3253-3259.
37. Costopoulos M, Touitou V, Golmard JL, et al. ISOLD: a new highly sensitive interleukin score for intraocular lymphoma diagnosis. *Ophthalmology*. 2016;123(7):1626-1628.
38. Zhao Y, He JY, Cui JZ, et al. Detection of genes mutations in cerebrospinal fluid circulating tumor DNA from neoplastic meningitis patients using next generation sequencing. *BMC Cancer*. 2020;20(1):690.
39. McEwen AE, Leary SES, Lockwood CM. Beyond the blood: CSF-derived cfDNA for diagnosis and characterization of CNS tumors. *Front Cell Dev Biol*. 2020;8:45.

Humoral immune depression following autologous stem cell transplantation is a marker of prolonged response duration in patients with mantle cell lymphoma

Louise Bouard,¹ Benoit Tessoulin,² Catherine Thieblemont,³ Kamal Bouabdallah,⁴ Thomas Gastinne,¹ Lucie Oberic,⁵ Sylvain Carras,⁶ Caroline Delette,⁷ Olivier Casasnovas,⁸ Caroline Dartigeas,⁹ Victoria Cacheux,¹⁰ Sibylle Masse,¹¹ Olivier Hermine¹² and Steven Le Gouill^{2,13}

¹Department of Hematology, CHU Nantes, Nantes; ²Department of Hematology CHU Nantes, INSERM CRCINA Nantes-Angers, and NeXT, Nantes University, Nantes; ³Department of Hematology, Saint-Louis Hospital, AP-HP, Paris 7 University, Paris; ⁴Department of Hematology, CHU Bordeaux, Bordeaux; ⁵Department of Hematology, IUC Toulouse Oncopole, Toulouse; ⁶Department of Hematology, CHU Grenoble, Grenoble; ⁷Department of Hematology, CHU Amiens, Amiens; ⁸Department of Hematology, CHU Dijon Bourgogne, INSERM 1231, Dijon; ⁹Department of Hematology, CHU Tours, Tours; ¹⁰Department of Hematology, CHU Clermont-Ferrand, Clermont-Ferrand; ¹¹Lysarc Institut Carnot CALYM, Lyon-Sud Hospital, Lyon; ¹²Necker University Hospital, Paris and ¹³Institut Curie, Paris France.

Correspondence: S. Le Gouill

steven.legouill@curie.fr

Received: July 8, 2021.

Accepted: February 10, 2022.

Prepublished: February 17, 2022.

<https://doi.org/10.3324/haematol.2021.279561>

©2022 Ferrata Storti Foundation

Published under a CC BY-NC license



Abstract

Rituximab maintenance (RM) after autologous stem cell transplantation (ASCT) is standard-of-care for young patients with mantle cell lymphoma (MCL). RM may enhance post-transplantation immune depression and risk of infections. We compared infection incidence and immune consequences of RM *versus* observation in transplanted MCL patients. All randomized patients included in the LyMa trial were eligible. The following parameters were collected prospectively: occurrence of fever, infection, hospitalization, neutropenia, hypogammaglobulinemia, CD4 lymphopenia and γ globulin (Ig) substitution. The post-ASCT period was divided into four periods in order to assess the possible effects of RM or ASCT on immune status. Each arm included 120 patients. Concerning infection incidence and all biological parameters, there was no difference between the two arms during the first year post ASCT. After this period, RM patients were more exposed to fever ($P=0.03$), infections ($P=0.001$), hypogammaglobulinemia ($P=0.0001$) and Ig substitution ($P<0.0001$). Incidences of hospitalization, neutropenia and CD4 lymphopenia were not different between the two arms. The number of rituximab injections was correlated with infections and hypogammaglobulinemia, $P<0.0001$ and $P=0.001$; but was not correlated with neutropenia and CD4 lymphopenia. Ig substitution did not modify infection incidence. Patients who presented hypogammaglobulinemia <6 g/L or <4 g/L had longer 3-years progression-free survival (PFS), this applies to RM patients ($P=0.012$ and $P=0.03$) and to the global cohort ($P=0.008$ and $P=0.003$). Hypogammaglobulinemia did not influence overall survival. Occurrence of infectious event, neutropenia and CD4 lymphopenia did neither influence PFS nor overall survival. Post-ASCT RM in MCL patients causes sustained hypogammaglobulinemia, which is independently correlated with improved PFS.

Introduction

Mantle cell lymphoma (MCL) is a B-cell non-Hodgkin lymphoma (NHL) which accounts for approximately 6% of NHL among adults.¹ Standard-of-care for young and fit patients consists in induction with high-dose cytarabine plus rituximab containing chemotherapy, followed by autologous stem cell transplantation (ASCT).² It has been demonstrated that a 3-year rituximab maintenance (RM) with one injection every 2 months following ASCT im-

proved event-free, progression-free and overall survivals (EFS, PFS and OS respectively).³

Rituximab is a chimeric IgG1 monoclonal antibody targeting CD20, with high efficiency in patients with B-cell lymphomas.⁴ Data on infectious toxicity caused by RM in MCL are sparse, and sometimes collected from heterogeneous or retrospective cohorts which contain different types of B-cell disorders, chemotherapy associations and treatment schedules.⁵ For patients with follicular lymphoma receiving RM, prospective studies reported an increased

infection incidence,^{6,7,8} but no additional infection-related deaths.⁹ It has been shown that prolonged rituximab administration induces hypogammaglobulinemia,¹⁰ while some authors have also reported rituximab-induced neutropenia episodes.^{11,12,13} Rituximab, when combined with chemotherapy, was also associated with increased incidence of opportunistic infections such as *Pneumocystis jiroveci* pneumonia¹⁴ and progressive multifocal leukoencephalopathy due to JC virus.¹⁵ The common condition for these infections might be T CD4 lymphopenia and absence of prophylaxis for *Pneumocystis* infections.

RM is the cornerstone of MCL treatment, but there is limited reporting on its infectious and immune consequences on a homogeneous population undergoing a myeloablative procedure. Therefore, we conducted a pre-planned ancillary study including patients from the LyMa trial, a phase III prospective trial in which patients were randomized between RM and observation. The primary objective was to investigate infectious and immune consequences of RM after ASCT. Secondary objectives were to describe infection sites reported, use of γ globulin substitution as well as to analyze the impact of RM-induced immunodeficiency on patients' outcome.

Methods

Patient selection

All patients included, transplanted and randomized in the LyMa trial (clinicaltrials.gov. Identifier: NCT 00921414) were considered eligible (n=240). All patients provided informed consent in writing. The trial's final results have been published. In brief, 299 patients were included in LyMa trial. Two hundred and seventy-nine patients completed all four courses of R-DHAP (rituximab, dexamethasone, cytarabine and platinum derivative) induction, among whom 20 received four additional courses of RCHOP (rituximab, cyclophosphamide, doxorubicin, vincristine and prednisolone) because of an insufficient response to R-DHAP. Only those patients considered as in response, i.e., complete response (certain or uncertain) or partial response with a minimum of 75% decrease in tumor burden, were eligible for ASCT. Two hundred and fifty-seven patients received intensification with R-BEAM (rituximab, carmustine, etoposide, cytarabine and melphalan). A total of 240 were randomized between observation arm (Obs arm) and rituximab arm (RM arm). Each treatment arm included 120 patients. There was no difference in patients' characteristics, and EFS, PFS and OS were statistically better in the RM arm.³ Patients in the RM arm were planned to receive an injection of rituximab every 2 months for 3 years, for a total of 18 injections.

This study is a preplanned ancillary study of the randomized phase III trial LyMa (clinicaltrials.gov. Identifier: NCT

00921414), which was approved by a formally constituted Ethics Review Board.

Monitoring and end points

Clinical examination was performed by local investigators every 2 months, before rituximab injection or during medical consultation. The following data collected prospectively were analyzed: occurrence of febrile event (defined as body temperature above 38°C), occurrence of clinically documented infection (possibly non-exclusive with febrile event), hospitalization for infectious reason and Ig substitution. Occurrences of neutropenia $<0.5 \times 10^9/L$, T CD4 lymphopenia $<0.2 \times 10^9/L$ and hypogammaglobulinemia <6 g/L and <4 g/L were measured at points in time as defined by the protocol: neutrophils counts and Ig rates were collected every 2 months from month (M) 2 to M36. CD4 lymphocytes rates were measured at M2, M4, M8, M12, M24 and M36. In order to evaluate the respective impacts of ASCT and RM on infectious risk and/or impaired immune restoration, follow-up periods were prospectively divided into four: from randomization to 6 months (period 1), from 6 to 12 months (period 2), from 12 to 24 months (period 3) and from 24 months to 36 months (period 4). The division was pre-planned before analysis.

Statistical analysis

The number of patients with clinical or biological events in the two arms were compared with a chi-square test or Fischer test if numbers were inferior to five. These tests are bilateral with a significance threshold of 5%. For each period, the number of patients affected was compared to the number of patients not excluded from the trial (*Online Supplementary Table S2*). Survival data were analyzed according to the occurrence of the five following events: infectious episode, neutropenia $<0.5 \times 10^9/L$, hypogammaglobulinemia <6 g/L and <4 g/L and CD4 lymphopenia $<0.2 \times 10^9/L$. A Kaplan Meier survival analysis and log-rank test were conducted. Patients were set as « yes » for the occurrence of an event if it had occurred at least once at the time of analysis. Treatment-effect was estimated by hazard ratio and the confidence interval were obtained by Cox regression model. Correlation analysis and substitution by γ globulins were compared by using the Wilcoxon test for paired data. In order to identify patients with an increased infectious risk and/or delayed immune restoration, we conducted univariate and multivariate analysis of the following variables (defined as occurrence of biological event: PNN $<0.5 \times 10^9/L$; Ig levels <6 g/L or 4 g/L and T CD4 lymphopenia $<0.2 \times 10^9/L$). We selected epidemiologic and disease diagnostic characteristics such as sex, age, performance status, Ann Arbor stage, mantle cell lymphoma international prognostic index (MIPI) score, morphologic variant or bone marrow involvement. Morphologic, meta-

bolic and bone marrow responses, as well as the use of salvage therapy, were also taken into account to analyze patients' response to induction. Delay between ASCT and first rituximab injection was selected to report post-ASCT hematopoietic restoration. We also analyzed the impact of the number of CD34 stem cells injected. We analyzed the number of rituximab injections in order to determine its dose effect involvement in infectious risk.

For univariate analysis, variables were compared with a Fischer test. Multivariate analysis is based on logistic regression, and includes data from the univariate analysis with a P -value <0.20 .

Results

Patient characteristics, occurrence of clinical events and infections sites

The Obs and RM arms included 120 patients each. Patient characteristics and distribution are reported in the *Online Supplementary Appendix*. No significant difference was observed between the two arms as previously published. Concerning febrile events, the difference between the two arms was only statistically significant after 1 year post ASCT (periods 3 and 4, Table 1), with 1 of 107 patients (0,9%) in the Obs arm *versus* seven of 99 patients (7,1%) in the RM arm; and two of 89 patients (2,3%) in the Obs arm *versus* ten of 97 patients (10,3%) in the RM arm, $P=0.03$ and $P=0.02$; respectively. Median duration of fever episode was not different between the two arms: 1 day (range, 1-3) in the Obs arm *versus* 2 days (range, 1-15) in the RM arm, $P=0.20$. Concerning infectious events, there were significantly more infections reported in the RM

arm during period 3: 28 of 99 patients (28.3%) experienced an infection *versus* 11 of 107 patients (10.3%) in the Obs arm, $P=0.001$ (Table 1). More than 50% of infectious episodes were located in the upper or lower respiratory tracts, regardless of the arm treatment or period. In the RM arm, infections sites revealing a significantly increased incidence were: upper and lower respiratory tracts; respectively $P=0.0025$ and $P=0.008$, digestive infections; $P=0.0003$ and bacteriemia; $P=0.04$; Figure 1. It should be noted that there were four and five acute pneumonia in the Obs and RM arms, respectively. In the RM arm, 13 episodes of bacterial diarrheas were reported: six *Clostridium difficile* colitis, five *Campylobacter jejuni* documentations, one *Salmonella enterica* documentation and one *Escherichia coli* documentation. The digestive tract was the only infection site with a larger proportion of total infectious episodes in the RM arm, compared to the Obs arm, 14.2% *versus* 3.8% respectively, $P=0.05$. Other infection sites showing similar incidences and proportions in both arms, are reported in Figure 1. Of note, there was no infections due to *Pneumocystis jiroveci* or LEMP due to *JC virus* in any arm.

In total 55 hospitalizations due to infections were reported, involving 45 of 239 patients (18.8%, Table 1). There were no differences between the two arms in any period, $P=0.61$, $P=1.0$, $P=0.09$ and $P=0.10$ for periods 1, 2, 3 and 4, respectively. Median hospitalization duration was not different: 6 days (range, 1-25) in the Obs arm *versus* 6 days (range, 1-27) in RM arm, $P=0.78$.

There was no death related to infectious complications.

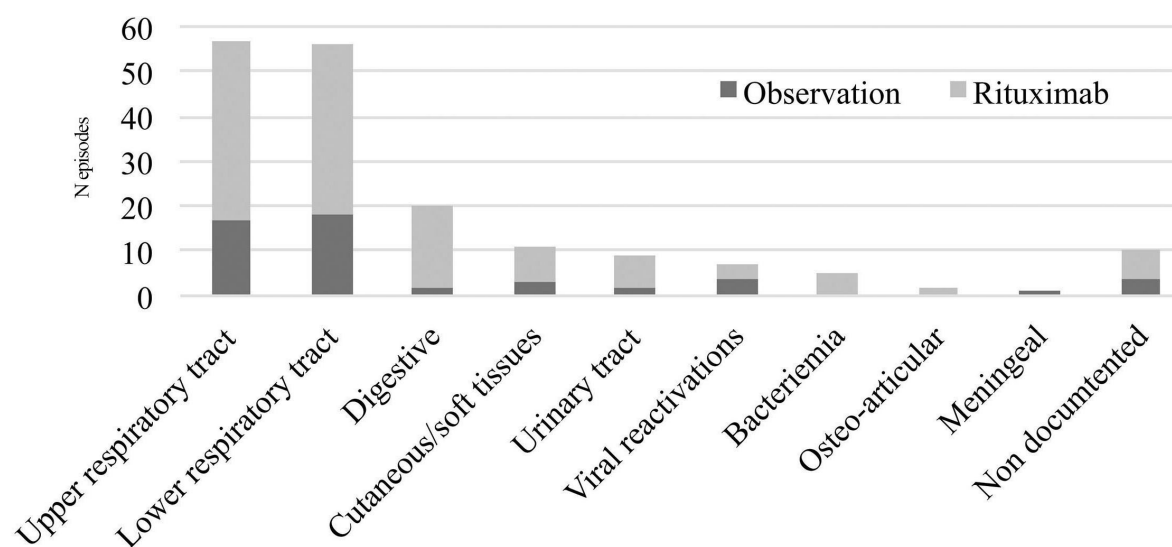
Immune restoration and biologic parameters

The data available for each parameter is reported in the *Online Supplementary Table S2*.

Table 1. Number of patients concerned by febrile events, infectious events hospitalizations due to infections and γ globulin substitution in the two arms according to post autograft.

	< 6 months			6-12 months			12-24 months			24-36 months		
	Obs N=120	RM N=119	P	Obs N=116	RM N=104	P	Obs N=107	RM N=99	P	Obs N=89	RM N=97	P
Fever episodes N patients (%) N events	7 (5,8) 7	10 (8,4) 11	0,440	1 (0,9) 1	5 (4,8) 5	0,103	1 (0,9) 1	7 (7,1) 8	0,030	2 (2,2) 3	10 (10,3) 14	0,025
Infectious episodes N patients (%) N events	11 (9,2) 12	16 (13,4) 19	0,296	9 (7,8) 11	16 (15,4) 22	0,075	11 (10,3) 15	28 (28,3) 45	0,001	13 (14,6) 13	22 (22,7) 41	0,159
Hospitalizations N patients (%) N events	8 (6,7) 8	10 (8,4) 11	0,611	5 (4,3) 5	4 (3,8) 5	1,000	3 (2,8) 3	8 (8,1) 9	0,092	3 (3,4) 4	9 (9,3) 10	0,101
γ globulin substitution N patients (%) N events	2 (2) 9	6 (6,2) 19	0,171	2 (2) 10	5 (5,2) 41	0,259	5 (5) 23	11 (11,3) 48	0,0075	1 (1) 3	19 (19,6) 165	<.0001

Obs: observation arm; RM: rituximab maintenance arm.



Infection sites	Total		Observation		Rituximab		P
	N episodes	Median occurrence (months)	N episodes	Median occurrence (months)	N episodes	Median occurrence (months)	
Upper respiratory tract	57	20 (4-36)	17	16 (4-32)	40	22 (4-36)	0.0025
Lower respiratory tract	56	18 (4-36)	18	13 (4-34)	38	19 (4-36)	0.008
Digestive	20	16 (4-36)	2	19 (10-28)	18	16 (4-36)	0.0003
Cutaneous/soft tissues	12	14 (4-36)	4	10 (6-28)	8	14 (4-36)	0.25
Urinary tract	9	14 (4-30)	2	14 (4-24)	7	14 (4-30)	0.11
Viral reactivations	7	8 (4-36)	4	17 (4-36)	3	4 (4-18)	0.62
Bacteriemia	5	6 (4-14)	0	NA	5	6 (4-14)	0.04
Osteo-articular	2	34 (32-36)	0	NA	2	34 (32-36)	0.16
Meningeal	1	22,0	1	22,0	0	NA	0.32
Not documented	10	23 (8-36)	4	21 (10-36)	6	23 (8-36)	0.53

Figure 1. Infection sites. (A) Graphical repartition of infections sites. (B) Number of infections per infection sites presented with median time of occurrence.

Neutropenia

Concerning neutropenia $<0,5 \times 10^9/L$, there was no difference between the two arms for any period, $P=0.26$, $P=0.10$, $P=0.61$ and $P=NA$, respectively, in chronological order (Table 2). For all patients, the median time of occurrence of neutropenia was located in period 1: 2.40 months (range, 0-30.8 months). However, the median time of occurrence was significantly delayed in the RM arm: 4.35 months (range, 0.6-19.8 months) versus 1.86 months (range, 0.0-16.1 months) in the Obs arm, $P=0.048$.

γ globulin levels

Using a 6 g/L cutoff, the difference between the two groups with regards to hypogammaglobulinemia was statistically significant only after 1 year post ASCT, $P<0.0001$ (Table 2). During period 3, 56 of 107 patients (52.3%) in the Obs arm versus 77 of 99 patients (77.8%) in

RM arm presented at least one event of hypogammaglobulinemia, $P<0.0001$. During period 4, 38 of 89 patients (42.7%) in the Obs arm versus 82 of 97 patients (84.5%) in the RM arm presented at least one event of hypogammaglobulinemia, $P<0.0001$. Using a 4 g/L cutoff, the difference was statistically significant as from 6 months post ASCT. During period 2, 20 of 116 patients (17.2%) presented hypogammaglobulinemia in the Obs arm versus 34 of 104 patients (32.7%) in the RM arm, $P=0.0078$. During period 3, 16 of 107 patients (15.0%) presented events of hypogammaglobulinemia in the Obs arm versus 38 of 99 patients (38.4%) in the RM arm, $P=0.0001$. During period 4, 15 of 89 patients (16.9%) presented events of hypogammaglobulinemia in the Obs arm versus 46 of 97 patients (47.4%) and 114 events in the RM arm, $P<0.0001$. In the Obs and RM arms, Ig median rate changed from 5.11 g/L (range, 2.1-11.1) to 6.41 g/L (range, 0.6-11.7) and from 4.68 g/L (range,

Table 2. Number of patients concerned by neutropenia, hypogammaglobulinemia and T CD4 lymphopenia in the two arms according to post autograft periods.

	< 6 months			6-12 months			12-24 months			24-36 month		
	Obs N=120	RM N=119	P	Obs N=116	RM N=104	P	Obs N=107	RM N=99	P	Obs N=89	RM N=97	P
Neutropenia <0,5x10 ⁹ /L N patients (%) N events	13 (10,8) 15	8 (6,7) 8	0,26	0 (0) 0	3 (2,9) 4	0,10	1 (0,9) 1	2 (2,0) 2	0,61	0 (0) 0	0 (0) 0	NA
Hypogamma globulinemia <6 g/L N patients (%) N events	80 (66,7) 163	85 (71,4) 154	0,43	67 (57,8) 131	63 (60,6) 127	0,67	56 (52,3) 169	77 (77,8) 243	0,0001	38 (42,7) 126	82 (84,5) 266	0,001
Hypogamma globulinemia <4 g/L N patients (%) N events	30 (25,0) 57	38 (31,9) 56	0,24	20 (17,2) 39	34 (32,7) 53	0,008	16 (15,0) 35	38 (38,4) 104	0,0001	15 (16,9) 38	46 (47,4) 114	<0,001
T CD4 lymphopenia <0,2x10 ⁹ /L N patients (%) N events	17 (14,2) 18	19 (16,0) 20	0,70	14 (12,1) 17	11 (10,6) 14	0,73	0 (0) 0	2 (2) 2	0,23	1 (1,1) 1	1 (1,0) 1	1,00

Obs: observation arm; RM: rituximab maintenance arm.

1.6-10.3) to 4.68 g/L (range, 1.0-9.5), from period 1 to period 4, respectively. Median rates of Ig significantly differed between the two arms in periods 3 and 4: 6.11 g/L (range, 1.2-12.9) versus 4.70 g/L (range, 1.2-9.1), $P<0.0001$ and 6.41 g/L (range, 0.6-11.7) versus 4.68 (range, 1.0-9.5), $P<0.0001$, for the Obs and RM arms, respectively.

T CD4 lymphopenia

Concerning T CD4 lymphopenia, there was no difference between the two arms for any of the periods, $P=0.70$, $P=0.73$, $P=0.23$ and $P=1.0$, in chronological order respectively (Table 2). In the Obs arm, median rates of T CD4 lymphocytes increased from 0.320x10⁹/L (range, 0.0-0.980) to 0.670x10⁹/L (range, 0.100-1.312) in periods 1 to 4. These values were respectively 0.300x10⁹/L (range, 0.0-1.021) and 0.630x10⁹/L (range, 0.200-0.885) the in RM arm. Median rate did not differ between the two arms during any of the periods: $P=0.83$, $P=0.44$, $P=0.08$ and $P=0.45$, in chronological order respectively.

Biological events are reported in Figure 2.

γ globulin substitution

In the Obs arm, five of 120 patients (4.2%) received 45 substitutions, while in the RM arm, 23 of 119 patients (19.3%) received 273 substitutions, $P=0.0002$. In period 4, one patient of 89 (1.1%) received three substitutions in the Obs arm while 19 of 97 (19.6%) received 165 substitutions in the RM arm, $P<0.0001$, Table 1. For those patients substituted, median number of substitutions was 8 (range, 1-19) in the Obs arm versus 6 (range, 1-82) in the RM arm, which was not different, $P=0.93$. Correlation analysis showed that Ig substitution was correlated with hypogammaglobulinemia <6 g/L and <4 g/L ($P=0.035$ and

$P<0.001$, respectively) and occurrence of infectious episodes ($P=0.002$). As of the first substitutive injection, the number of hypogammaglobulinemia <6 g/L and <4 g/L events was significantly reduced, the median difference (before-after) being 3.5 events, $P=0.037$. However, the median number of infectious episodes within patient (before-after) was not reduced with Ig substitution, even after a dozen of injections, $P=0.09$.

Impact of immune restoration and occurrence of infectious events on progression-free survival and overall survival

Occurrence of infectious events did not impact PFS or OS in either arm (Obs arm, PFS $P=0.31$ and OS $P=0.55$; RM arm PFS $P=0.13$ and OS $P=0.09$) nor did it impact PFS or OS in the whole cohort (PFS $P=0.08$ and OS $P=0.16$). This was also noted for the occurrence of neutropenia (Obs arm, PFS $P=0.16$ and OS $P=0.26$; RM arm PFS $P=0.96$ and OS $P=0.21$; whole cohort PFS, $P=0.28$ and OS $P=0.10$). In contrast, occurrence of hypogammaglobulinemia <6 g/L ($n=86/120$; 71.6% in the Obs arm and $n=103/119$, 86.3% in the RM arm, $n=189/239$; 79.1% in the whole cohort) was correlated with an improved 36 months PFS in the whole cohort (85.6% vs. 63.6%, $P=0.0005$; Figure 3A), with a treatment arm adjusted hazard ratio (HR)=0.488 (95% CI: 0.287-0.830; $P=0.008$). In the RM arm, 36 months PFS was also improved in patients with hypogammaglobulinemia (93.2% vs. 63.5%, $P=0.008$; Figure 3B, HR=0.294; 95%CI: 0.113-0.767). In the Obs arm, this was not significant, $P=0.09$. For a hypogammaglobulinemia cutoff at 4 g/L ($n=40/120$, 33.3% in the Obs arm; $n=71/119$, 59.7% in RM arm and $n=111/239$, 46.4% in the whole cohort), PFS also correlated with occurrence of hypogammaglobulinemia,

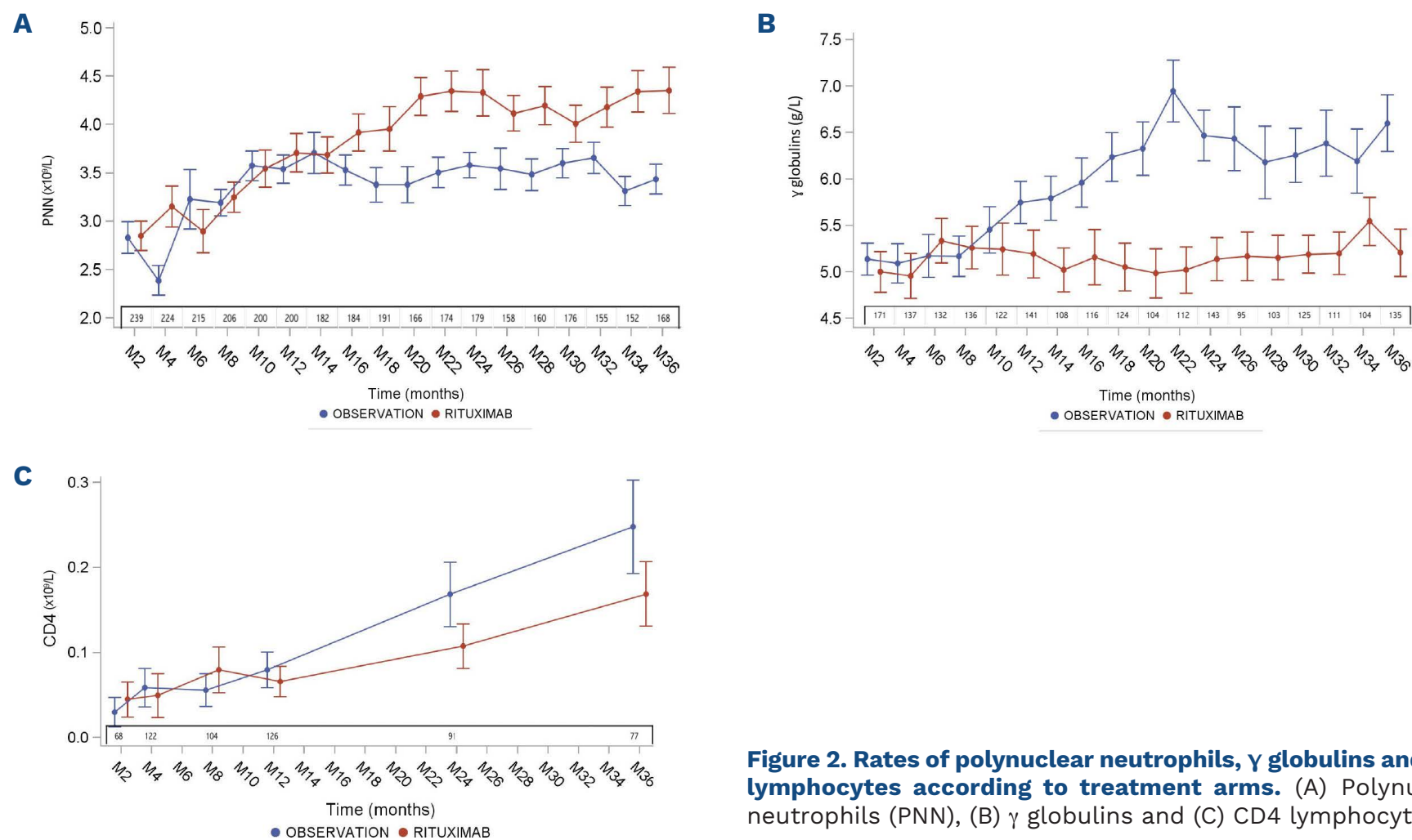


Figure 2. Rates of polynuclear neutrophils, γ globulins and CD4 lymphocytes according to treatment arms. (A) Polynuclear neutrophils (PNN), (B) γ globulins and (C) CD4 lymphocytes.

with a 36 months PFS of 90% versus 73.2%, $P=0.003$ in the whole cohort (HR adjusted on treatment arm =0.562, 95% CI: 0.324-0.975, $P=0.003$; Figure 3C) and a 36 months PFS of 95.7% versus 79.5%, $P=0.03$ in the RM arm (HR=0.384; 95% CI: 0.157-0.941; Figure 3D). In the Obs arm, this was not significant, $P=0.36$. When adjusted on number of rituximab injections, impact of hypogammaglobulinemia on PFS was still significant, with a HR=0.565; 95% CI: 0.334-0.955; $P=0.033$. There was no impact of hypogammaglobulinemia (<6g/L or <4g/L) on OS in the whole cohort ($P=0.45$ and $P=0.48$) or in any arm (Obs arm, $P=0.75$ and $P=0.38$; RM arm, $P=0.22$ and $P=0.22$). Occurrence of CD4 lymphopenia did not impact PFS or OS in the whole cohort (PFS, $P=0.10$ and OS $P=0.95$) nor did it impact PFS or OS in either arm (Obs arm : PFS, $P=0.16$ and OS $P=0.98$; RM arm : PFS, $P=0.38$ and OS $P=0.98$).

Statistical analyses regarding risk of infections and delayed immune restoration

Univariate analysis

Univariate analysis demonstrated that performance status 0 at diagnosis was associated with lower risk of CD4 lymphopenia, $P=0.02$. Receiving more than half of the maintenance program (nine rituximab injections) was associated with an increased risk of infectious episode, $P<0.001$ as well as hypogammaglobulinemia < 6g/L, $P=0.02$ and < 4g/L, $P=0.03$. Neutropenia was not associated with any variable. Univariate analysis is reported in Table 3.

Multivariate analysis

In multivariate analysis, patients presenting with a classic morphologic variant at diagnosis had less risk of hypogammaglobulinemia < 6g/L (odds ratio [OR]=0.278, 95% CI: 0.086-0.899, $P=0.033$). Performance status 0 at diagnosis appeared to be a protective factor for occurrence of CD4 lymphopenia (OR=0.423, 95% CI: 0.220-0.812, $P=0.01$). Complete response after induction increased the risk factor of hypogammaglobulinemia < 6 g/L, (OR=2.972, 95% CI: 1.263-6.994, $P=0.013$). Patients who received more than nine rituximab injections had more infectious episodes; (OR=11.17, 95% CI: 2.482-50.263, $P=0.002$) and increased occurrence of hypogammaglobulinemia < 6 g/L; (OR=4.278, 95% CI: 1.393-13.141, $P=0.01$) and < 4 g/L, (OR=2.882, 95% CI: 1.131-73.45, $P=0.03$). No risk or protective factor was identified for neutropenia occurrence. Multivariate analysis is represented in Table 4.

Discussion

Our study shows that RM after ASCT increases infectious risk but only as from 12 months post ASCT. This suggests that during the first year post ASCT, infectious risk is related to the ASCT conditioning regimen and not to RM. The most reported infection sites were upper and lower respiratory tracts with a significantly higher proportion of bacterial colitis episodes in RM. Among the biological parameters tested, only 1-year post-ASCT hypogamma-

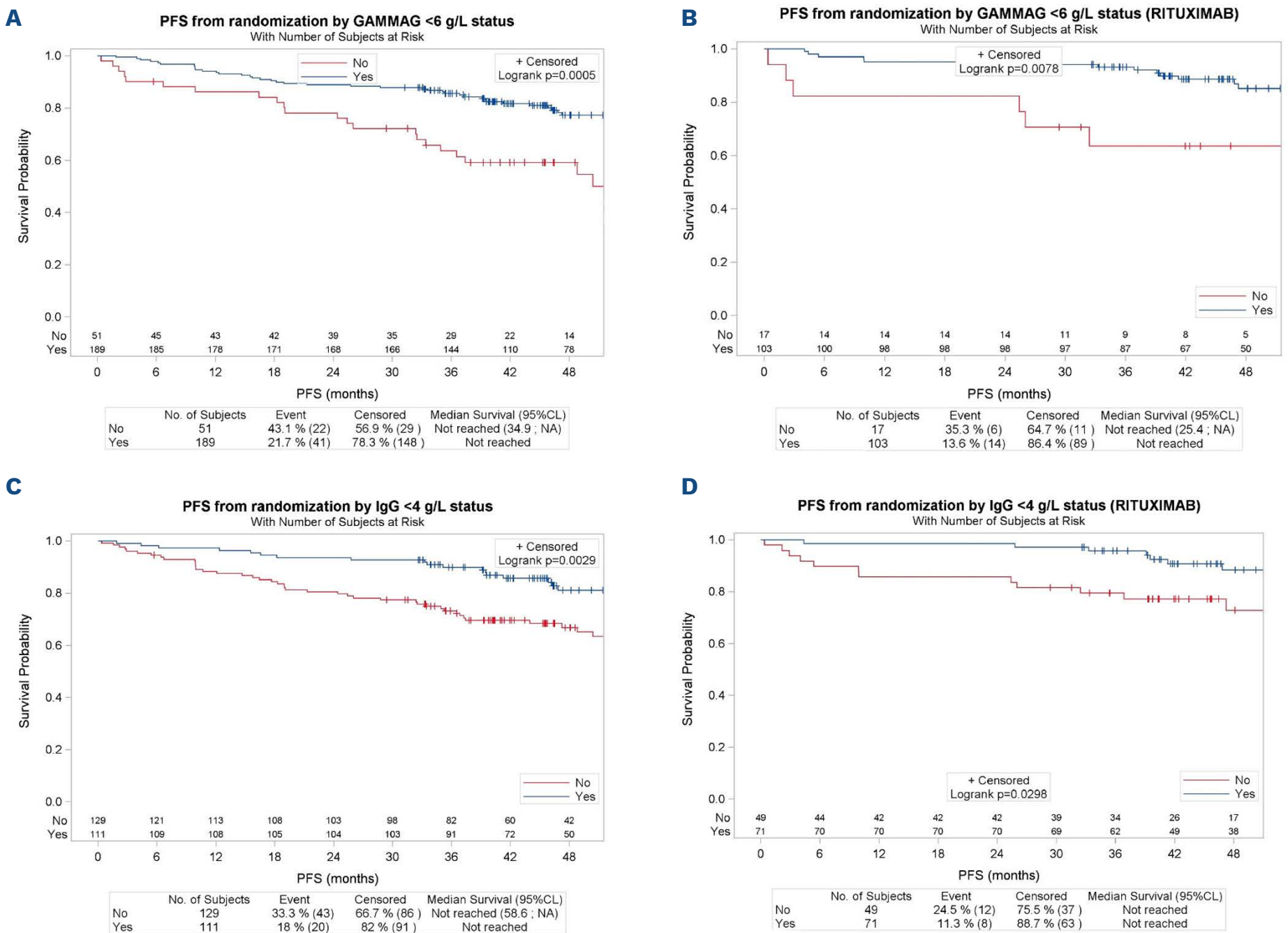


Figure 3. Progression-free survival from randomization according to occurrence of hypogammaglobulinemia <6 g/L and hypogammaglobulinemia <4 g/L. Representation of progression-free survival (PFS) in (A) the whole cohort and in (B) the rituximab maintenance (RM) arm according to γ globulin status <6 g/L and PFS in (C) the whole cohort and in (D) the RM arm according to occurrence of hypogammaglobulinemia <4 g/L. GAMMAG: γ globulin rate.

globulinemia was statistically more frequent in RM. This highlights the side effect of RM on humoral immunity. Multivariate analysis shows that patients who received at least nine rituximab injections, which amounts to half the maintenance program, are more exposed to infectious events and hypogammaglobulinemia. Our work corroborates previously reported findings on the cumulative effect of RM on infectious risk.¹⁰

Although data were collected and monitored prospectively, our study has its limits: microbiological documentations are frequently missing mainly because the vast majority of infections were of low grade in upper and lower respiratory tracts which are not routinely explored by physicians in practice. In addition, the LyMa trial electronic case report form (e-CRF) did not report treatment prophylaxis and use of granulocyte colony-stimulating factor (G-CSF) support but we can presume that, according to international guidelines¹⁶ in this post-ASCT

setting, the patients did receive at least *P.jiroveci* and *herpes simplex virus* prophylaxis and probably G-CSF support when needed. Thus, we can not conclude about these associated measures and treatments. Unfortunately, LyMa e-CRF did not report the vaccination strategy used for patients and thus patients were vaccinated according to local vaccination strategy in each center. We believe that European Society for Blood and Marrow Transplantation recommendations¹⁷ were applied. We also did not investigate the impact of recurring low grade infection consequences on quality of life. However, the higher incidence of infections in the RM arm is offset by its benefits in terms of EFS, PFS and OS. This higher incidence could be explained, to a large extent, by the occurrence of hypogammaglobulinemia after 1 year post transplant, and not by neutropenia or T CD4 depletion. Ig substitution was not recommended in the LyMa trial and was left to the choice of investigator in

Table 3. Univariate analysis for infectious episode, neutropenia, hypogammaglobulinemia and CD4 lymphopenia.

	Infectious episode (%)		Neutropenia (%)		Hypogammaglobulinemia < 6X10 ⁹ /L (%)		CD4 lymphopenia (%)	
Sex								
Male N=189	32.3	0.25	11.1	1.0	78.8	0.70	21.2	0.70
Female N=51	41.2		9.8		82.4		17.6	
Age								
<60 y N=172	34.9	0.76	8.7	0.11	78.5	0.60	22.7	0.21
>60 y N=68	32.4		16.2		82.4		14.7	
PS								
0 N=156	35.9	0.27	9.6	0.60	81.4	0.47	16.0	0.02
1 N=74	33.8		13.5		77.0		31.1	
2 N=10	10.0		10.0		70.0		10.0	
Ann arbor								
II N=12	50.0	0.30	8.3	1.0	100	0.22	8.3	0.49
III N=31	25.8		9.7		77.4		25.8	
IV N=196	34.2		11.2		78.6		20.4	
MIPI score								
Low N=133	33.8	0.17	9.8	0.81	80.5	0.33	21.1	0.91
Int N=65	41.5		12.3		73.8		18.5	
High N=42	23.8		11.9		85.7		21.4	
Morphologic variant								
Classic N=134	31.3	0.84	8.2	0.34	76.1	0.11	20.1	0.50
Others N=36	33.3		13.9		88.9		25.0	
Bone marrow involvement								
Yes N=149	36.2	0.46	12.8	0.44	79.9	0.90	20.8	0.87
No N=72	27.8		6.9		79.2		19.4	
PS post R-DHAC								
0 N=163	32.5	0.95	14.1	0.11	78.5	0.83	19.6	0.63
1 N=67	34.3		4.5		80.6		23.9	
2 N=4	25.0		0.0		100		25.0	
PET post R-DHAC								
Pos. N=51	37.3	0.87	9.8	1.0	80.4	1.0	23.5	0.55
Neg. N=175	35.4		11.4		78.9		18.9	
Medullar response post R-DHAC								
Yes N=179	33.0	0.18	10.1	0.42	78.8	0.59	21.2	0.59
No N=5	0.0		20.0		100		0.0	
CT scanner post R-DHAC								
Cr N=115	33.0	0.51	10.4	0.95	83.5	0.07	18.3	0.52
Pr>75% N=97	33.0		11.3		73.2		22.7	
Pr<75% N=22	45.5		9.1		90.0		27.3	
RCHOP salvage								
Yes N=11	36.4	1.0	18.2	0.34	100	0.13	18.2	1.0
No N=229	34.1		10.5		78.6		20.5	
Asct-maintenance delay								
<=2 mth N=91	38.5	0.33	12.1	0.67	82.4	0.42	23.1	0.51
>2 mth N=149	31.5		10.1		77.9		18.8	
Number of CD 34/kg								
<5.106 N=73	35.6	0.17	8.2	0.42	78.1	0.45	17.8	0.86
5-8.106 N=76	26.3		14.5		84.2		21.1	
>8.106 N=90	40.0		8.9		76.7		21.1	
Number of RM injections (in RM group only)								
<=9 inj N=23	8.7	<.001	11.9	0.67	69.6	0.014	19.6	0.75
>9 inj N=97	51.5		9.3		90.7		21.6	

PS: performance status; PET: positron emission tomography; CT: computerized tomography; inj: injections; R-DHAC: rituximab, dexamethasone, cytarabine and platinum derivative; RCHOP: rituximab, cyclophosphamide, doxorubicin, vincristine and prednisolone; RM: rituximab maintenance; ASCT: autologous stem cell transplantation; MIPI: mantle cell lymphoma international prognostic index; mth: months.

Table 4. Multivariate analysis for infectious episode, neutropenia, hypogammaglobulinemia and CD4 lymphopenia.

	Modality	OR	95% CI	P
Infectious episode	>9 ritux inj	11.17	2.482-50.263	0.0017
Neutropenia	-	-	-	-
Hypogammaglobulinemia <6x10 ⁹ /L	Classical morphologic variant	0.278	0.086-0.899	0.033
	Morphologic CR	2.972	1.263-6.994	0.013
	>9 ritux inj	4.278	1.393-13.141	0.011
Hypogammaglobulinemia <4x10 ⁹ /L	>9 ritux inj	2.882	1.131-73.450	0.027
CD4 lymphopenia	PS 0 at diagnosis	0.423	0.220-0.812	0.010

Inj: injection; CR: complete response; PS: performance status; int: interval; OR: odds ratio; CI: confidence interval; ritux: rituximab.

each center. Lack of efficacy of the Ig substitution might suggest that other factors could also be involved or that Ig substitution fails to restore an active humoral immunity. Therefore, our study questions the relevance of Ig substitution which has an added financial cost. In the absence of a prospective randomized study, our study does not call for a systematic use of Ig substitution, including for patients with recurrent infections. Another interesting finding of our work is the relationship between hypogammaglobulinemia and complete response, as well as prolonged duration of response. Although there is a guaranteed time bias as hypogammaglobulinemia can develop only late post transplant, very few patients presented an hypogammaglobulinemia after having recovered an Ig level superior of 6 g/L and the relationship between hypogammaglobulinemia and PFS was still significant when adjusted on the number of rituximab injections. Moreover, we conducted a landmark methodology (every 2 months from M2 to M36) which did not highlight the appropriate and precise time point for monitoring Ig level. This might suggest that rituximab-induced B-cell depletion indirectly reflect the rituximab anti-MCL effect. This hypothesis is supported by the multivariate analysis showing a dose effect relationship between rituximab and hypogammaglobulinemia. However, improved PFS for hypogammaglobulinemic patients does not only reflect a rituximab dose effect, as it is still significant when adjusted on number of rituximab injections. Other parameters such as *FCGR3A* gene polymorphism could also explain discrep-

ancies between patients in terms of rituximab anti-MCL effect.^{18,19}

In conclusion, our work highlights the B-cell and humoral immunodepression induced by RM as from 1-year post transplant in MCL patients. Prior to 1 year, humoral immune status reflects effects of rituximab before the transplant and the transplant procedure itself. RM does neither induce a higher incidence of neutropenia nor T CD4 depletion which are the result of the transplant procedure. Ig substitution remains an open question although it doesn't appear to balance the hypogammaglobulinemia-induced infections. Interestingly, hypogammaglobulinemia could become a surrogate marker for the RM anti-MCL effect.

Disclosures

No conflicts of interest to disclose.

Contributions

LB and SLG performed the research and wrote the manuscript; BT and SB analyzed the data. All other authors gave advice and supervised the writing of the manuscript.

Funding

This work is an ancillary study of The LyMa trial which was funded by Roche SAS.

Data-sharing statement

Data of the present work will be shared upon request to the corresponding author.

References

- Jain P, Wang M. Mantle cell lymphoma: 2019 update on the diagnosis, pathogenesis, prognostication, and management. *Am J Hematol.* 2019;94(6):710-725.
- Dreyling M, Campo E, Hermine O, et al. Newly diagnosed and relapsed mantle cell lymphoma: ESMO Clinical Practice Guidelines for diagnosis, treatment and follow-up. *Ann Oncol.* 2017;28(Suppl 4):S62-71.
- Le Gouill S, Thieblemont C, Oberic L, et al. Rituximab after autologous stem-cell transplantation in mantle-cell lymphoma. *N Engl J Med.* 2017;377(13):1250-1260.

4. Coiffier B. Treatment of non-Hodgkin's lymphoma: a look over the past decade. *Clin Lymphoma Myeloma*. 2006;7 (Suppl 1):S7-13.
5. Forstpointner R, Unterhalt M, Dreyling M, et al. Maintenance therapy with rituximab leads to a significant prolongation of response duration after salvage therapy with a combination of rituximab, fludarabine, cyclophosphamide, and mitoxantrone (R-FCM) in patients with recurring and refractory follicular and mantle cell lymphomas: results of a prospective randomized study of the German Low Grade Lymphoma Study Group (GLSG). *Blood*. 2006;108(13):4003-4008.
6. van Oers MHJ, Van Glabbeke M, Giurgea L, et al. Rituximab maintenance treatment of relapsed/resistant follicular non-Hodgkin's lymphoma: long-term outcome of the EORTC 20981 phase III randomized Intergroup Study. *J Clin Oncol*. 2010;28(17):2853-2858.
7. Vidal L, Gafter-Gvili A, Salles G, et al. Rituximab maintenance improves overall survival of patients with follicular lymphoma- Individual patient data meta-analysis. *Eur J Cancer*. 2017;76:216-225.
8. Salles G, Seymour JF, Offner F, et al. Rituximab maintenance for 2 years in patients with high tumour burden follicular lymphoma responding to rituximab plus chemotherapy (PRIMA): a phase 3, randomised controlled trial. *Lancet*. 2011;377(9759):42-51.
9. Pettengell R, Uddin R, Boumendil A, et al. Durable benefit of rituximab maintenance post-autograft in patients with relapsed follicular lymphoma: 12-year follow-up of the EBMT lymphoma working party Lym1 trial. *Bone Marrow Transplant*. 2021;56(6):1413-1421.
10. Casulo C, Maragulia J, Zelenetz AD. Incidence of hypogammaglobulinemia in patients receiving rituximab and the use of intravenous immunoglobulin for recurrent infections. *Clin Lymphoma Myeloma Leuk*. 2013;13(2):106-111.
11. Stamatopoulos K, Papadaki T, Pontikoglou C, et al. Lymphocyte subpopulation imbalances, bone marrow hematopoiesis and histopathology in rituximab-treated lymphoma patients with late-onset neutropenia. *Leukemia*. 2008;22(7):1446-1449.
12. Dunleavy K. B-cell recovery following rituximab-based therapy is associated with perturbations in stromal derived factor-1 and granulocyte homeostasis. *Blood*. 2005;106(3):795-802.
13. Aksoy S, Dizdar Ö, Hayran M, Harputluoglu H. Infectious complications of rituximab in patients with lymphoma during maintenance therapy: a systematic review and meta-analysis. *Leuk Lymphoma*. 2009;50(3):357-365.
14. Jiang X, Mei X, Feng D, Wang X, Tanowitz H. Prophylaxis and treatment of pneumocystis jiroveci pneumonia in lymphoma patients subjected to rituximab-contained therapy: a systemic review and meta-analysis. *Tanowitz HB, éditeur. PLoS One*. 2015;10(4):e0122171.
15. Carson KR, Evens AM, Richey EA, et al. Progressive multifocal leukoencephalopathy after rituximab therapy in HIV-negative patients: a report of 57 cases from the Research on Adverse Drug Events and Reports project. *Blood*. 2009;113(20):4834-4840.
16. Taplitz RA, Kennedy EB, Bow EJ, et al. Antimicrobial prophylaxis for adult patients with cancer-related immunosuppression: ASCO and IDSA clinical practice guideline update. *J Clin Oncol*. 2018;36(30):3043-3054.
17. Ljungman P, Cordonnier C, Einsele H, et al. Vaccination of hematopoietic cell transplant recipients. *Bone Marrow Transplant*. 2009;44(8):521-526.
18. Cartron G, Dacheux L, Salles G, et al. Therapeutic activity of humanized anti-CD20 monoclonal antibody and polymorphism in IgG Fc receptor FcγRIIIa gene. *Blood*. 2002;99(3):754-758.
19. Kim DH, Jung HD, Kim JG, et al. FCGR3A gene polymorphisms may correlate with response to frontline R-CHOP therapy for diffuse large B-cell lymphoma. *Blood*. 2006;108(8):2720-2725.

Rituximab in addition to LMB-based chemotherapy regimen in children and adolescents with primary mediastinal large B-cell lymphoma: results of the French LMB2001 prospective study

Marie Emilie Dourthe,^{1,2} Aurélie Phulpin,³ Anne Auperin,⁴ Jacques Bosq,⁵ Marie-Laure Couec,⁶ Peggy Dartigues,⁵ Stéphane Ducassou,⁷ Nathalie Garnier,⁸ Stéphanie Haouy,⁹ Thierry Leblanc,² Amaury Leruste,¹⁰ Catherine Paillard,¹¹ Charlotte Rigaud,¹² Mathieu Simonin,^{2,13} Catherine Patte¹² and Véronique Minard-Colin^{12,14}

¹Department of Pediatric Hematology and Immunology, Robert Debré University Hospital, AP-HP and University de Paris, Paris; ²Université de Paris, Institut Necker-Enfants Malades (INEM), Institut National de la Santé et de la Recherche Médicale, INSERM U1151, and Laboratory of Onco-Hematology, Assistance Publique-Hôpitaux de Paris, Hôpital Necker Enfants-Malades, Paris; ³Pediatric Oncology and Hematology Department, University Hospital of Nancy (CHRU Nancy), Nancy; ⁴Service de Biostatistique et d'Epidémiologie, Gustave Roussy Cancer Campus, INSERM U1018, CESP, Université Paris-Sud, Université Paris-Saclay, Villejuif; ⁵Department of Biopathology, Morphology Unit, Gustave Roussy, Université Paris Saclay, Villejuif; ⁶Department of Pediatric Hematology and Oncology, University Hospital of Nantes, Nantes; ⁷Department of Pediatric Oncology and Hematology, University Hospital of Bordeaux, Bordeaux; ⁸Institut d'Hématologie et d'Oncologie Pédiatrique, Hospices Civils de Lyon, Lyon; ⁹Department of Pediatric Oncology and Hematology, University Hospital of Montpellier, Montpellier; ¹⁰SIREDO Oncology Center, Institute Curie, PSL Research University, Paris; ¹¹Department of Pediatric Hematology Oncology, University Hospital of Strasbourg, INSERM UMRS 1109, Strasbourg; ¹²Department of Pediatric and Adolescent Oncology, Gustave Roussy, Université Paris-Saclay, Villejuif; ¹³Pediatric Hematology Oncology Department, Sorbonne Université/Trousseau Hospital, AP-HP, Paris and ¹⁴Gustave Roussy and Paris-Saclay University, INSERM 1015, Paris, France

Correspondence:

M-E. Dourthe
marie-emilie.dourthe@aphp.fr

V. Minard-Colin
veronique.minard@gustaveroussy.fr

Received: October 27, 2021.
Accepted: February 23, 2022.
Prepublished: March 3, 2022.

<https://doi.org/10.3324/haematol.2021.280257>

©2022 Ferrata Storti Foundation

Published under a CC BY-NC license



Abstract

Primary mediastinal large B-cell lymphoma (PMLBL) is a rare entity predominantly affecting adolescents and young adults. Recently, an international phase II trial in pediatric patients using dose-adjusted etoposide, doxorubicin, and cyclophosphamide with vincristine and prednisone plus rituximab (DA-EPOCH-R) failed to reproduce excellent survival reported in some adult studies. The optimal therapy regimen needs to be determined in this disease. The French prospective LMB2001 trial included all patients ≤ 18 years with mature B-cell lymphoma treated in French centers. For patients with PMLBL, treatment included four to eight courses of Lymphomes Malins B (LMB)-based chemotherapy without radiotherapy. From 2008, rituximab was added before each chemotherapy course. From 09/2001 to 03/2012, 42 patients with PMLBL were registered. The median age was 15 years (range, 8-18). Twenty-one patients were treated with chemotherapy plus rituximab. The median follow-up was 7.1 years (interquartile range, 5.8-11.1). Five-year event-free and overall survival were 88.1% (95% confidence interval (CI): 75.0-94.8) and 95.2% (95% CI: 84.0-98.7) for the whole population. The 5-year EFS was 81.0% (95% CI: 60.0-92.3) and 95.2% (95% CI: 77.3-99.2) (hazard ratio =0.24; 95% CI: 0.03-2.2) and 5-year overall survival was 90.5% (95% CI: 71.1-97.3) and 100% for patients treated without and with rituximab, respectively. Only one of 21 patients treated with rituximab and LMB-based chemotherapy had local early treatment failure but achieved prolonged complete remission with second-line chemotherapy and radiotherapy. Intensive LMB-based chemotherapy with rituximab achieved excellent survival in children/adolescents with PMLBL. Further international prospective studies are required to confirm these results in this population.

Introduction

Primary mediastinal (thymic) large B-cell lymphoma

(PMLBL) is a distinct pathogenetic subtype of mature B-cell neoplasms.¹ It is a rare entity representing 2-4% of adult and pediatric non-Hodgkin lymphoma.^{2,3} PMLBL

most commonly presents in female adolescents and young adults with signs and symptoms of bulky mediastinal disease. It is biologically related to nodular sclerosing Hodgkin lymphoma on pathology and gene expression profiling although some phenotype markers (MUM1, MAL),⁴ as well as lactate dehydrogenase (LDH) levels and 18fluorodeoxyglucose-positron emission tomography/computed tomography (18F-FDG PET/CT) findings help discriminate mediastinal Hodgkin lymphoma from PMLBL.⁵ In adults with PMLBL, although there is a lack of consensus about the optimal therapeutic strategy for newly diagnosed patients, highly curative strategies, including rituximab, cyclophosphamide, doxorubicin, vincristine and prednisone (R-CHOP) and dose-adjusted etoposide, doxorubicin, and cyclophosphamide with vincristine and prednisone plus rituximab (DA-EPOCH-R) are mainly recommended.⁶ However, significant cumulative doses of chemotherapy are achieved with both chemotherapy regimens and a substantial rate of patients still need radiation therapy (RT), especially with R-CHOP.

In children and adolescents, the first prospective international phase II study of DA-EPOCH-R regimen⁷ failed to reproduce the outstanding survival reported with this regimen in some adults studies. Treatment strategies originally designed for Burkitt lymphoma are successfully used for children with diffuse large B-cell lymphoma (DLBCL)^{8,9} but patients with PMLBL presented more aggressive disease and specific approaches were needed.^{10,11} Herein, we reported the experience of the prospective French LMB 2001 study with 42 PMLBL patients treated with intensive LMB-based chemotherapy between 09/2001 and 03/2012, with the addition of rituximab from 2008.

Methods

Diagnosis, classification and staging

The French LMB 2001 prospective study included patients less or equal to 18 years old, with mature B-cell lymphoma including PMLBL. Patients with known pre-existing immunodeficiency were not included. For the purpose of this analysis, pathology was planned to be reviewed by national experts for diagnosis as PMLBL. The LMB2001 study has been approved by the SFCE Scientific Committee and National Ethics Committee. Parents/legal guardians provided written informed consent for the inclusion of their children in the studies in accordance with the Declaration of Helsinki. Minimal work-up included clinical examination, chest x-ray, abdominal ultrasound or CT, two bone marrow (BM) aspirates and biopsies, cerebrospinal fluid (CSF) cytology, and standard blood analysis including LDH level (\leq or $>2N$ the upper limit of the institution's normal range). PET/CT was recommended but staging was not based on its result only. Other imaging was performed

as clinically indicated. Staging was based according to the St Jude's/Murphy's and Ann Arbor classifications.

Study therapy

LMB2001 was a FAB (French-American-British)/LMB 96-based protocol. Treatment was based on St Jude's/Murphy's stage. Therapeutic groups were defined as in previous LMB studies.⁹ All patients received a pre-phase of low-dose cyclophosphamide, vincristine, and prednisone (COP). Group B patients (stage III and non-CNS stage IV with marrow involvement $<25\%$) received therapy similar to Group B on FAB/LMB96 with four cycles of chemotherapy. For all Group C patients, Group C1 patients (stage IV disease with marrow involvement $\geq 25\%$ without CNS-positive disease) received high-dose methotrexate (HD MTX) (8 g/m^2) as previously given over 4 hours, whereas Group C3 patients (central nervous system [CNS]-positive) received HD MTX (8 g/m^2) over 24 hours.¹² Consecutive courses were given as soon as blood counts recovered and the patient's condition allowed, except for the maintenance courses, which were given at 28-day intervals.

From 2008, it was recommended to add rituximab (R) as an intravenous (IV) infusion (375 mg/m^2) on day 1 of each chemotherapy course. Additionally, based on an unpublished prognostic analysis, patients with bulky mediastinal mass ($>10 \text{ cm}$) and/or high LDH serum level ($> 2N$ on the Institution upper limit value), and/or lombo-aortic nodes were assigned to Group C1 regimen. Lastly, in 2010, the LMB-modified B/C chemotherapy with rituximab (total 6 doses) was recommended for all patients, consisting of two courses of RCOPADM Group B (cyclophosphamide, vincristine, prednisone, adriamycin, HD MTX 3 g/m^2) followed by two courses of RCYVE Group C (with high-dose cytarabine, and etoposide) and two courses of maintenance therapy with rituximab. Patients received two double intrathecal (DIT) only at day 2 of each COPADM course (Table 1).

Remission assessment was performed after the first consolidation course for Group B and after the second consolidation course for Group C and B/C. In patients with a residual mass by radiographic evaluation, an excision or biopsy for pathology review was recommended. However, as residual mass is frequent in PMLBL, if the therapy response was adequate and a biopsy was not performed, the patients were to remain on assigned treatment, and remission re-evaluated at the end of therapy. For Group B patients, if viable tumor cells were identified, the therapy was switched to the more intensive Group C1 regimen. Patients with biopsy-proven viable tumor cells after the second consolidation course ((R)CYVE2) were considered to have primary refractory disease and evaluated as an event. No-treatment decisions were based on 18F-FDG PET/CT results only, and 18F-FDG PET/CT were not reviewed for the purpose of this analysis. Patients with per-

Table 1. Outline of the LMB 2001 protocol for PMLBL patients

	Prephase	Course 1	Course 2	Course 3	Course 4	Course 5	Course 6	Course 7	Course 8	Cumulative dose
B	COP* Cy 300 mg/m ² D1 VCR 2 mg/m ² D1 IT (MTX HSHC) D1 pred 60 mg/m ² /D D1-7	COPADM VCR 2 mg/m ² D1 MTX 3 g/m ² D1 Cy 250 mg/m ² / 12 h D2-4 Adriamycin 60 mg/m ² D2 IT (MTX HSHC) D2;6 pred 60 mg/m ² D1-5	COPADM VCR 2 mg/m ² D1 MTX 3 g/m ² D1 Cy 250 mg/m ² / 12 h D2-4 Adriamycin 60 mg/m ² D2 IT (MTX HSHC) D2;6 pred 60 mg/m ² D1-5	CYM MTX 3 g/m ² D1 cytarabine 100 mg/m ² D2-6 IVC 24h IT (MTX HSHC) D2; HSHC araC D7)	CYM MTX 3 g/m ² D1 cytarabine 100 mg/m ² D2-6 IVC 24 h IT (MTX HSHC) D2; HSHC araC D7)					Cyclophosphamide 3,300 mg/m ² Adriamycin 120 mg/m ² IT=8*
C1	COP* Cy 300 mg/m ² D1 VCR 2 mg/m ² D1 IT (MTX HSHC) araC) D1, D3, D5 pred 60 mg/m ² D1-7	COPADM VCR 2 mg/m ² D1 MTX 8 g/m ² D1 Cy 250 mg/m ² / 12 h D2-4 Adriamycin 60 mg/m ² D2 IT (MTX HSHC) 60 mg/m ² D2 AraC) D2, 4, 6 pred 60 mg/m ² D1-5	COPADM VCR 2 mg/m ² D1 MTX 8 g/m ² D1 Cy 500 mg/m ² / 12 h D2-4 Adriamycin 60 mg/m ² D2 IT (MTX HSHC) AraC) D2, 4, 6 pred 60 mg/m ² D1-5	CYVE cytarabine 50 mg/m ² IVC 12 h D1-5 Cytarabine 3 g/m ² D2-5 VP16 200 mg/m ² D2-5	CYVE cytarabine 50 mg/m ² IVC 12 h D1-5 Cytarabine 3 g/m ² D2-5 VP16 200 mg/m ² D2-5	Seq1 VCR 2 mg/m ² D1 MTX 8 g/m ² D1 Cy 500 mg/m ² D2-3 Adriamycin 60 mg/m ² D2 IT (MTX HSHC) AraC) D2 pred 60 mg/m ² D1-5	Seq2 Cytarabine 50 mg/m ² /12 h D1-5 VP16 150 mg/m ² D1-3	Seq3 VCR 2 mg/m ² D1 Cy 500 mg/m ² D1-2 Adriamycin 60 mg/m ² D1 pred 60 mg/m ² D1-5	Seq4 Cytarabine 50 mg/m ² /12 h D1-5 VP16 150 mg/m ² D1-3	Cyclophosphamide 6,800 mg/m ² Adriamycin 240 mg/m ² IT=7*

Continued on following page.

C3	COP*	COPADM	COPADM	CYVE	CYVE	CYVE	Seq1	Seq2	Seq3	Seq4	Cyclophosphamide
	Cy 300 mg/m ² VCR 2 mg/m ² IT (MTX HSHC) araC) D1, D3, D5 pred 60 mg/m ² /D D1-7	VCR 2 mg/m ² D1 MTX 8 g/m ² D1 Cy 250 mg/m ² m ² /12 h D2-4 Adriamycin 60 mg/m ² D2 IT (MTX HSHC) AraC) D2, 4, 6 pred 60 mg/m ² D1-5	VCR 2 mg/m ² D1 D1 cytarabine 50 mg/m ² IVC 12 h D1-5 Cytarabine 3 g/m ² D2-5 VP16 200 mg/m ² D2-5 MTX 8 g/m ² D18 IT (MTX HSHC) AraC) D2	IT (MTX +HSHC) D1 cytarabine 50 mg/m ² IVC 12 h D1-5 Cytarabine 3 g/m ² D2-5 VP16 200 mg/m ² D2-5	VCR 2 mg/m ² D1 MTX 8 g/m ² D1 Cy 500 mg/m ² D2-3 Adriamycin 60 mg/m ² D2 IT (MTX HSHC) AraC) D2 pred 60 mg/m ² /D D1-5	Cytarabine 50 mg/m ² /12 h VP16 150 mg/m ² D1-3 D1-5	VCR 2 mg/m ² D1 Cy 500 mg/m ² D1-5 D1-2 Adriamycin 60 mg/m ² D1 pred 60 mg/m ²	Cytarabine 50 mg/m ² /12 h D1-5 VP16 150 mg/m ² D1-3 D1-5	VCR 2 mg/m ² D1 Cy 500 mg/m ² D1-5 D1-2 Adriamycin 60 mg/m ² D1 pred 60 mg/m ²	Cytarabine 50 mg/m ² /12 h D1-5 VP16 150 mg/m ² D1-3 D1-5	Cyclophosphamide 6,800 mg/m ² Adriamycin 240mg/m ² IT=10*
B-C (after 2010)	COP* Cy 300 mg/m ² D1 VCR 2 mg/m ² D1 IT (MTX HSHC) D1, pred 60 mg/m ² D1-7	VCR 2 mg/m ² D1 MTX 3 g/m ² D1 Cy 250 mg/m ² /12 h D2-4 Adriamycin 60 mg/m ² D2 IT (MTX HSHC) D2 pred 60 mg/m ² D1-5	VCR 2 mg/m ² D1 D1 cytarabine 50 mg/m ² IVC 12 h D1-5 Cytarabine 3 g/m ² D2-5 VP16 200 mg/m ² D2-5	cytarabine 50 mg/m ² IVC 12 h D1-5 Cytarabine 3 g/m ² D2-5 VP16 200 mg/m ² D2-5	VCR 2 mg/m ² D1 MTX 3 g/m ² D1 Cy 250 mg/m ² / 12 h D2-4 Adriamycin 60 mg/m ² D2 IT (MTX HSHC) D2 pred 60 mg/m ² D1-5	Cytarabine 50 mg/m ² IVC 12 h D1-5 Cytarabine 3 g/m ² D2-5 VP16 200 mg/m ² D2-5	VCR 2 mg/m ² D1 Cy 500 mg/m ² D1-2 Adriamycin 60 mg/m ² D1 pred 60 mg/m ² D1-5	VCR 2 mg/m ² D1 Cy 500 mg/m ² D1-2 Adriamycin 60 mg/m ² D1 pred 60 mg/m ² D1-5	VCR 2 mg/m ² D1 Cy 500 mg/m ² D1-2 Adriamycin 60 mg/m ² D1 pred 60 mg/m ² D1-5	Cytarabine 50 mg/m ² /12 h D1-5 VP16 150 mg/m ² D1-3 D1-5	Cyclophosphamide 5,300 mg/m ² Adriamycin 240 mg/m ² IT= 2*
Rituximab (after 2008)		375 mg/m ² D1	375 mg/m ² D1	375 mg/m ² D1	375 mg/m ² D1	375 mg/m ² D1	375 mg/m ² D1	375 mg/m ² D1	375 mg/m ² D1	375 mg/m ² D1	

ADM: adriamycin, doxorubicin; AraC: aracytine; VCR: vincristine; MTX: methotrexate; Cy: cyclophosphamide; pred: prednisolone; IT: intrathecal; RA: remission assessment. *A COP prephase is not mandatory but may be required one week prior to commencement of course 1 for patients requiring urgent treatment whilst awaiting histological confirmation. In case of COP prephase more intrathecal are administered. #remission assessment was required after 4 or 6 courses of chemotherapy. At the end of therapy, if PET-CT is positive, or a large residual tumor remains, then biopsy/removal of the residual mass is recommended. No treatment decisions were to be based on PET-CT results only.

sistent disease after the end of treatment received different therapies, including additional RT, second-line chemotherapy, and consolidation with high-dose chemotherapy and autologous stem cell transplantation.

Statistical analysis

The primary efficacy endpoint was event-free survival (EFS), defined as the time from the start of chemotherapy to the first of the following events: biopsy-positive residual disease following (R)CYVE number 2 or at the end of therapy, progressive disease, relapse, second malignant neoplasm, and death of any cause. Patients without any of these events were censored at the date of the last follow-up. The secondary efficacy endpoint was overall survival (OS), defined as the time from the start of chemotherapy to death from any cause, or to the date of the last follow-up for alive patients. EFS and overall survival (OS) were estimated with the Kaplan-Meier method.¹³ The 95% confidence intervals (95% CI) of the survival rates were calculated with the Rothman method.¹⁴

Results

Baseline characteristics

Between 09/2001 and 03/2012, 42 of the 773 patients (5.4%) with newly diagnosed B-NHL were registered as LBL with mediastinum as primary site in the prospective French LMB2001 study. Baseline characteristics are summarized in Table 2. The median age at diagnosis was 15 years (range, 8.4-18). There were 24 females (57%). Thirty-three patients (79%) had large mediastinal masses of 10 cm or more, 18 patients (43%) had elevated LDH levels (> twice the institutional upper limit of the adult normal value), one patient had BM involvement and two patients were considered with CNS disease (one had facial paresthesia with normal magnetic resonance imaging but CSF could not be explored; one had asymptomatic epidural mass). No patient had positive CSF. In total, initial staging confirmed Ann Arbor stage II disease in 19 patients (45%), stage III in one patient (2%), and stage IV in 22 patients (52%).

Table 2. Baseline characteristics of the patients.

	All patients N=42	Patients treated without rituximab N=21	Patients treated with rituximab N=21
Female, N (%)	24 (57)	12 (57)	12 (57)
Age in years			
Median (range)	15 (8-18)	14 (8-17)	15 (10-18)
Distribution, N (%)			
≥ 8 - < 12 years	4 (10)	3 (14)	1 (5)
≥ 12 - < 15 years	17 (40)	9 (43)	8 (38)
≥ 15 - ≤ 18 years	21 (50)	9 (43)	12 (57)
Ann Arbor stage, N (%)			
II	19 (45)	10 (48)	9 (43)
III	1 (2)	0 (0)	1 (5)
IV	22 (52)	11 (52)	11 (52)
Mediastinal tumor ≥ 10 cm diameter, N (%)	33 (79)	17 (81)	16 (76)
Sites of involvement, N (%)			
Sub-diaphragmatic	11 (26)	4 (19)	7 (33)
Bone marrow involvement	1 (2)	0 (0)	1 (5)
Central nervous system	2* (5)	0 (0)	2 (10)
LDH >2, N (%)	18 (43)	10 (48)	8 (38)
Initial therapeutic group			
Group B	19	16	3
Group B/C or C	23	5	18

*Central nervous system involvement consisted in: facial paresthesia with normal magnetic resonance imaging but the cerebrospinal fluid (CSF) could not be explored=1; asymptomatic epidural mass=1. LDH: lactate dehydrogenase.

Figure 3. Events.

Patient identification number	First line therapy	Site of progression/relapse	Time from inclusion	2 nd line chemotherapy	Radiation therapy	High dose chemotherapy	Patient status at last news
PMLBL1	Group B, R-	mediastinum	Progression after CYVE1 3.4 months*	R-DHAP (3): progression R-ICE (2): progression	No	No	DOD, 23 months
PMLBL2	Group B, R-	mediastinum	Progression after CYM 3.5 months ¹	R-ICE (2): progression R-EPOCH (2): progression	No	No	DOD, 9.3 months
PMLBL3	Group B, R-	mediastinum	Viable cells in residual mass after CYVE2 5.2 months	R-ICE (2)	Yes	BEAM and ASCT	CR, 6.9 years
PMLBL4	Group B, R-	mediastinum	Local relapse 9.9 months	CYVE (2) R (4)	No	No	CR2, 6.7 years
PMLBL5	Group B switched to C after COP, R+	mediastinum	Progression after R-COPADM1 0.6 months	R-ICE (3)	Yes	BEAM and ASCT	CR, 11 years

R: rituximab; BEAM: carmustine, etoposide, cytarabine, melphalan; DHAP: dexamethasone, high dose aracytin, cisplatin; ICE: ifosfamide, etoposide, carboplatin; EPOCH: etoposide, prednisone, vincristine, cyclophosphamide, doxorubicin; ASCT: autologous stem cell transplantation; CR: complete remission; DOD: died of disease. *Candidemia after prolonged aplasia followed by disease progression.

Histological characteristics

The national pathological review was done for 36 of 42 patients (86%) and PMLBL diagnosis was confirmed for all except one case. For one case, a consensus diagnosis was not reached (differential diagnosis between PMLBL and grey zone lymphoma). The remaining six patients had a local pathological report compatible with the diagnosis of PMLBL.

All cases expressed B-cell marker CD20 and were negative for CD3. CD10, BCL6, MUM1, BCL2, CD23 expression were evaluated for 12 cases and showed staining in 21%, 73%, 55%, 42%, and 46% of cases, respectively. CD30 staining was weak and patchy found in 66% of cases. PDL1 expression was observed on tumor cells in 85% of cases. Finally, only one of 23 cases tested had EBER positivity by *in situ* hybridization.

Treatment and response

All patients received LMB-based chemotherapy: 19 patients were treated in Group B, 18 in Group C, and five with LMB-modified B/C. Twenty-one patients received rituximab (R+) (after 2008) while 21 did not (R-). Of the 40 (95%) patients who were received COP therapy, 33 had at least a 20% response. Two patients were transferred to Group C after COP therapy (1 R- ; 1 R+). Three patients had disease progression during therapy (2 R-, 1 R+). Among the

39 other patients, at remission assessment, two patients were in complete response (CR) while 37 had a residual mass on imaging, with a median size of 50 mm (range, 17-135; data available for 30 patients). In total, 26 of 37 had biopsies, excisions or partial excisions: one had viable tumor cells (R-; tumor size: 68 mm after CYM1 vs. 108 mm at baseline) and for all other patients, the histology revealed complete necrosis. Thirty-eight patients (90%, 95% CI: 77-97) were considered to have achieved CR (2 CR, 25 complete necrosis, and 11 residual mass not explored). Thirty-seven patients (88%) had 18F-FDG PET/CT at remission assessment after a median of four chemotherapy courses (range, 3-6) of whom 26 (70%) were considered positive according to current Cheson criteria.¹⁵ Among these 26 patients, four had further treatment failure, including one with histology positive residual disease, one with complete necrosis on biopsy, and two not biopsied (predictive positive value =15%; 95% CI: 4-35). Among the 11 patients with negative 18F-FDG PET/CT, none had treatment failure (predictive negative value =100%; 95% CI: 72-100).

Outcome

The median follow-up was 7.1 years (interquartile range, 5.8-11.1), 10.6 years for patients treated without rituximab, and 6.4 years for patients treated with rituximab. There

were a total of five events (all local failures) (Table 3) with one insufficient response and viable cells in the residual mass (R-, patient obtained and remained in CR after R-ICE and BEAM, ASCT and radiotherapy), three disease progressions during treatment (2 R-, 1 R+) and one relapse (R-, patient obtained and remained in CR2). There was no second malignancy. Two of the three patients who progressed during treatment died of disease despite second-line therapy. The third one (R+) was switched to Group C after COP because of insufficient response and had disease progression after RCOPADM1 but remained in continuous first CR after two courses of RICE, high-dose BEAM chemotherapy (carmustine, etoposide, cytarabine, and melphalan) and radiotherapy. In total, there were two deaths, the two following disease progression during therapy in R- patients. The probability of 5-year EFS was 88.1% (95% CI: 75.0-94.8) in the whole cohort and 81.0% (95% CI :60.0-92.3) in R- patients and 95.2% (95% CI: 77.3-99.2) in R+ patients corresponding to a hazard ratio of 0.24 (95% CI: 0.03-2.2) (Figures 1 and 2A). The probability of 5-year OS was 95.2% (95% CI: 84.0-98.7) in the whole cohort and 90.5% (95% CI: 71.1-97.3) in R- patients) and 100% in R+ patients (Figures 1 and 2B).

Discussion

In this prospective multicentric French LMB2001 study with intensive LMB chemotherapy in addition to rituximab since 2008, pediatric and adolescent patients with PMLBL achieved excellent survivals. Five-year EFS and OS were 88.1% (95% CI: 75.0-94.8) and 95.2% (95% CI: 84.0-98.7) for the whole population. The previous FAB/LMB 96 study in children and adolescents with PMLBL treated with Group B LMB chemotherapy reported a 5-year EFS and OS of 66 % (95% CI: 49-78) and 73% (95% CI: 56-84).¹⁰ By comparison, in the current series, 21 patients with PMLBL

were treated without rituximab (16 therapeutic Group B; 5 Group B/C or C) with 5-year EFS of 81.0% (95% CI: 60.0-92.3). Thus, these current results without rituximab compare favorably with previous FAB/LMB 96 (although not statistically different). Although there is no easy explanation, we cannot exclude that more intense chemotherapy may be more effective (all events except one in the current series occurred in patients treated in Group B and percentage of patients initially treated with Group C or B/C is higher in the current series). It has been distinctly demonstrated in adult patients with PMLBL that the addition of rituximab improves the outcome (HR for events 0.3; 95% CI: 0.1-0.8).¹⁶ In the French LMB2001 study, the assessment of rituximab addition to LMB-based chemotherapy, which was not based on a randomized comparison but on a comparison of two periods, showed a similar HR (HR for events 0.24; 95% CI: 0.03-2.2) with 5-year EFS of 81.0% (95% CI: 60.0-92.3) without rituximab and 95.2% (95% CI: 77.3-99.2) with rituximab.

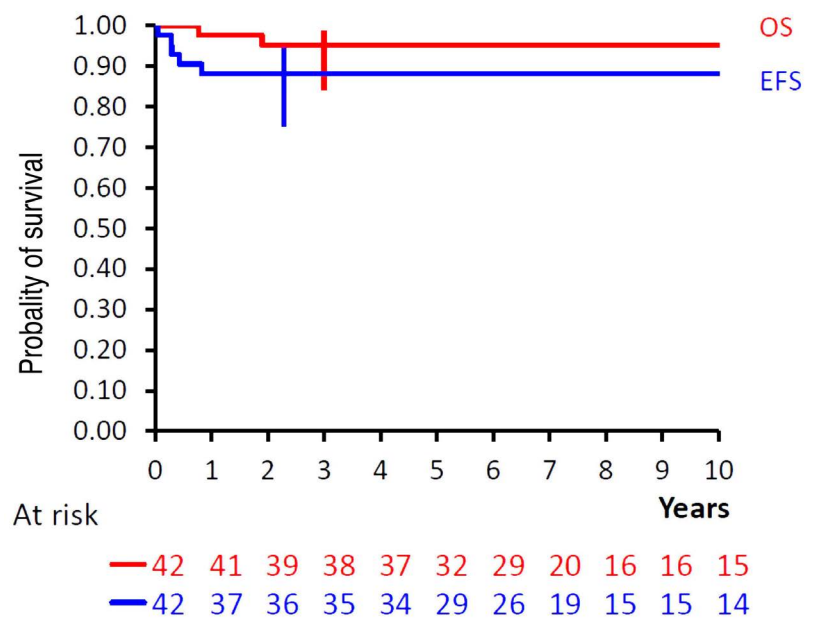


Figure 1. Kaplan Meier estimates of overall survival and event-free survival. Vertical lines represent the Rothman 95% confidence interval. EFS: event-free survival; OS: overall survival.

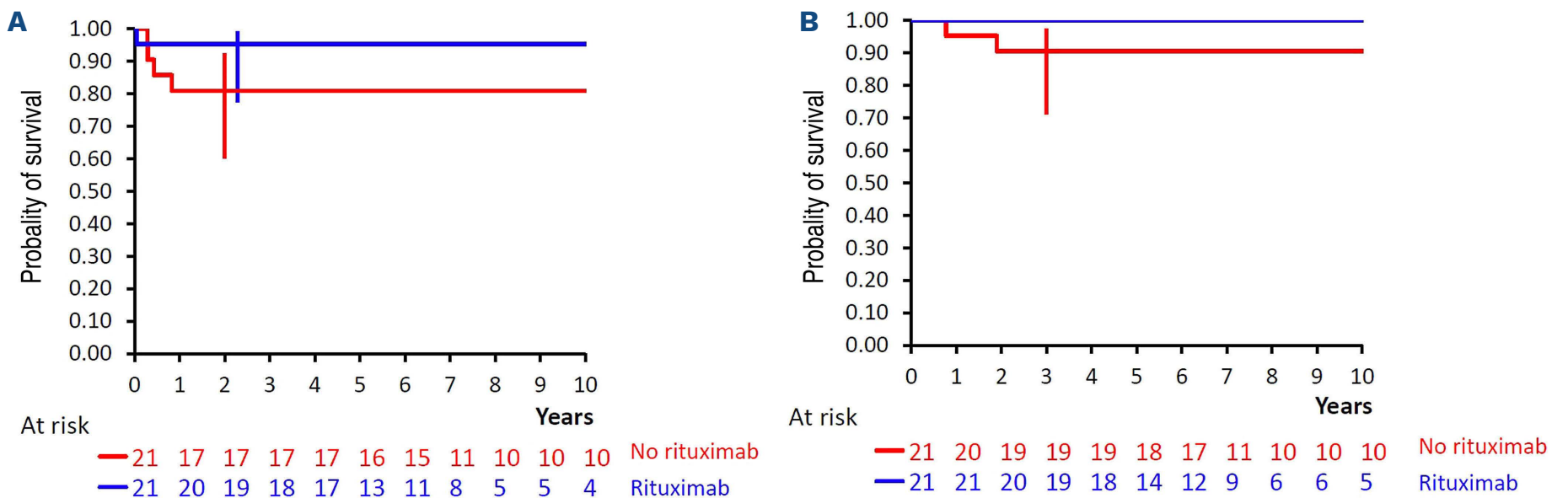


Figure 2. Kaplan Meier estimates of event-free survival and overall survival according to rituximab administration. (A) Event-free survival. (B) Overall survival. Vertical lines represent the Rothman 95% confidence interval.

These excellent results contrast with the results recently published with DA-EPOCH-R in 46 children and adolescents included in the international phase II Inter B-NHL-ritux 2010 study⁷ (Table 4). Although the characteristics of the patients included in this study do not differ from those of the phase II Inter B-NHL-ritux 2010, 12 disease-related events were observed in the phase II, with 4-year EFS and OS of 69.6% (95% CI: 55.2-80.9) and 84.8% (95% CI: 71.8-92.4), respectively, and three (6.5%) parenchymal central nervous system relapses. All five disease-related events in the French LMB2001 study were local/mediastinal with no CNS relapses. Thus, CNS-directed therapy may be important in PMLBL and explains why we recommended since 2008 LMB B/C-modified regimen with rituximab, with some intrathecal therapy but also HD MTX and high-dose cytarabine (AraC). Recently, a real-world study from the French LYSA group also reinforces the benefit of dose intense immuno-chemotherapy regimens in PMLBL¹⁷: patients treated with R-ACVBP or R-CHOP14 achieved a better outcome than those treated with R-CHOP21 (progression-free survival of 89.4% vs. 74.7%). R-ACVBP also included some CNS-directed therapies such as HD MTX and intrathecal in the majority of patients and CNS relapse rate was low (2.9%) in this series.

By contrast with the pediatric phase II Inter-B-NHL ritux 2010 trial, outstanding survival for adult patients with PMLBL has been reported with DA-EPOCH-R in a single-institution, non-randomized phase II study, of 51 patients with EFS of 93% (95% CI: 81-98) and OS of 97% (95% CI: 81-99).¹⁸ In the same way, a large multicenter retrospective analysis reported on the outcome of pediatric and adult patients treated with DA-EPOCH-R for PMLBL.¹⁹ Survivals were not statistically different between pediatric and adult patients for both EFS (81.0% vs. 87.4%, $P=0.338$) and OS (90.7% vs. 97.1%, $P=0.170$).

Clinically and pathologically, PMLBL disease in the pediatric population is indistinguishable from that seen in adult patients. Thus, the difference in outcome between

the two main DA-EPOCH-R studies is therefore hard to explain although the methodology of these studies is very different (i.e., international vs. single-institution). Other registry-based or retrospective studies of children and adolescents with PMLBL treated with DA-EPOCH-R have been also reported. The BFM NHL group reported their multicentric experience between 2004 and 2019 with modified DA-EPOCH-R (addition of at least one intrathecal triple therapy and a cumulative doxorubicin dose limit at 360 mg/m²) (n=67 patients) or intensified chemotherapy B-NHL BMF04 (n=29 patients) and compared it retrospectively to the treatment regimen in the B-NHL BMF95 trial (n=20 patients), both without rituximab.²⁰ For patients treated with DA-EPOCH-R, the 5-year EFS and OS were 84% (95% CI: 72-91) and 90% (95% CI: 79-95), respectively. These results are intermediate between the outstanding results obtained in the phase II study in adult patients and the phase II Inter-B-NHL ritux 2010 in children (Table 4). However, despite the use of triple intrathecal, at relapse four of 11 patients treated with DA-EPOCH-R had parenchymal CNS disease, strengthening the fact that it is necessary to improve CNS disease control in this pathology.

Pediatric-type B-NHL regimens, such as LMB and others, have higher acute toxicity when compared with DA-EPOCH-R regimen. The DA-EPOCH-R phase II Inter-B-NHL ritux 2010 study in pediatric patients reported febrile neutropenia in 11% of courses and 46% of patients, infections grade ≥ 3 in 4% of courses and 17% of patients and stomatitis grade ≥ 3 in 3% of courses and 15% of patients. Although we did not register toxicity in the prospective French LMB2001 trial (but no toxic death occurred), other LMB-based chemotherapy trials with rituximab reported febrile neutropenia, infection grade ≥ 3 and stomatitis grade ≥ 3 , in 92.6%, 58.6%, and 79.6% of patients, respectively.²¹ However, management of long-term toxicity is also very important in this young population. The risks for significant long-term sequelae are relatively modest using

Table 4. Summary of R-DA-EPOCH studies and the LMB 2001 study.

Study	Regimen	Type of study	Population	N of patients	Median FU	N of events (CNS relapse)	EFS, % (95% CI)	OS, % (95% CI)
NCI ¹⁸	DA-EPOCH-R	Phase 2, monocentric	Adults	51	5 years	3 (0)	93 (81-98)	97 (81-99)
BFM ¹⁹	DA-EPOCH-R	Registry, multicentric	Child/ado	67	4 years	11 (4)	84 (72-91)	90 (79-95)
Inter B-NHL ritux 2010 ⁷	DA-EPOCH-R	Phase 2, multicentric	Child/ado	46	5 years	14 (3)	70 (55-81)	85 (72-92)
LMB 2001	R-LMB	Registry, multicentric	Child/ado	21	6 years	1 (0)	95 (77-99)	100
LMB 2001	LMB	Registry, multicentric	Child/ado	21	10 years	4 (0)	81 (60-92)	90 (71-97)

Child/ado: children/adolescents; CI: confidence interval; EFS: event-free survival; FU: follow-up; OS: overall survival; DA-EPOCH-R: dose-adjusted etoposide, doxorubicin, and cyclophosphamide with vincristine and prednisone plus rituximab.

LMB chemotherapy backbone²² and the total cumulative dose of doxorubicin is limited and of 240 mg/m² with the LMB B/C-modified combination (favorably compared with the DA-EPOCH-R in the Inter-B-NHL ritux 2010 study where 72% of patients received ≥ 300 mg/m² doxorubicin and 24% ≥ 350 mg/m²)⁷.

Although our study has some limitations, i.e., i) relative small series of 42 patients but it compares well with other published reports in this rare disease, ii) pathology review for only 85% of cases, iii) no randomized comparison between LMB chemotherapy only and LMB chemotherapy with rituximab, and iv) some differences during the study duration in terms of chemotherapy group recommendations, this was a prospective multicentric study, and we believe that these excellent results are important for the medical community of pediatric, adolescents, and young adults oncologists. Further prospective and international trials are required to confirm these results and define optimal treatment for patients with PMLBL (all ages included). Novel agents (e.g., NF- κ B pathway inhibitors or anti-PD1 therapies combined or not with brentuximab-vedotin) may be required next to reduce chemotherapy intensity and improve outcome in this population.²³

Disclosures

No conflicts of interest to disclose.

Contributions

CP, AA, MED, and VM-C conceived the study and oversaw the project; AP, NG, NA, JM, SH, CP, JL-P, TL, CS, CP and VM-C recruited patients; AP, VM-C, AA, CP, JB and MED collected and assembled data; AA performed statistical analysis; MED, AP, AA, JB, CP, VM-C analyzed and interpreted data; MED, AP and VM-C wrote the manuscript. All authors approved the manuscript.

Acknowledgments

The authors thank Yasmina Oubouzar for data management. We thank all patients and their families for participating in the studies. We thank our colleagues in the hospitals and reference institutions who contributed to this study, for their care for the children and families, and the supplied data.

Data-sharing statement

The data that support the findings of this study are available on request from the corresponding author.

References

1. Swerdlow SH, Campo E, Pileri SA, et al. The 2016 revision of the World Health Organization classification of lymphoid neoplasms. *Blood*. 2016;127(20):2375-2390.
2. Burkhardt B, Zimmermann M, Oschlies I, et al. The impact of age and gender on biology, clinical features and treatment outcome of non-Hodgkin lymphoma in childhood and adolescence. *Br J Haematol*. 2005;131(1):39-49.
3. Martelli M, Di Rocco A, Russo E, Perrone S, Foà R. Primary mediastinal lymphoma: diagnosis and treatment options. *Expert Rev Hematol*. 2015;8(2):173-186.
4. Copie-Bergman C, Plonquet A, Alonso MA, et al. MAL expression in lymphoid cells: further evidence for MAL as a distinct molecular marker of primary mediastinal large B-cell lymphomas. *Mod Pathol*. 2002;15(11):1172-1180.
5. Alkhawtani RHM, Noordzij W, Glaudemans AWJM, et al. Lactate dehydrogenase levels and 18F-FDG PET/CT metrics differentiate between mediastinal Hodgkin's lymphoma and primary mediastinal B-cell lymphoma. *Nucl Med Commun*. 2018;39(6):572-578.
6. Melani C, Wilson WH, Roschewski M. What is the standard of care for primary mediastinal b-cell lymphoma; R-CHOP or DA-EPOCH-R? *Br J Haematol*. 2019;184(5):836-838.
7. Burke GAA, Minard-Colin V, Auperin A, et al. Dose-adjusted etoposide, doxorubicin, and cyclophosphamide with vincristine and prednisone plus rituximab therapy in children and adolescents with primary mediastinal B-cell lymphoma: a multicenter phase II trial. *J Clin Oncol*. 2021;39(33):3716-3724.
8. Patte C, Auperin A, Michon J, et al. The Société Française d'Oncologie Pédiatrique LMB89 protocol: highly effective multiagent chemotherapy tailored to the tumor burden and initial response in 561 unselected children with B-cell lymphomas and L3 leukemia. *Blood*. 2001;97(11):3370-3379.
9. Patte C, Auperin A, Gerrard M, et al. Results of the randomized international FAB/LMB96 trial for intermediate risk B-cell non-Hodgkin lymphoma in children and adolescents: it is possible to reduce treatment for the early responding patients. *Blood*. 2007;109(7):2773-2780.
10. Gerrard M, Waxman IM, Sposto R, et al. Outcome and pathologic classification of children and adolescents with mediastinal large B-cell lymphoma treated with FAB/LMB96 mature B-NHL therapy. *Blood*. 2013;121(2):278-285.
11. Seidemann K, Tiemann M, Lauterbach I, et al. Primary mediastinal large B-cell lymphoma with sclerosis in pediatric and adolescent patients: treatment and results from three therapeutic studies of the Berlin-Frankfurt-Münster Group. *J Clin Oncol*. 2003;21(9):1782-1789.
12. Cairo MS, Gerrard M, Sposto R, et al. Results of a randomized international study of high-risk central nervous system B non-Hodgkin lymphoma and B acute lymphoblastic leukemia in children and adolescents. *Blood*. 2007;109(7):2736-2743.
13. Kaplan EL, Meier P. Nonparametric estimation from incomplete observations. *J Am Stat Assoc*. 1958;53(282):457-481.
14. Rothman KJ. Estimation of confidence limits for the cumulative probability of survival in life table analysis. *J Chronic Dis*. 1978;31(8):557-560.
15. Cheson BD, Fisher RI, Barrington SF, et al. Recommendations for initial evaluation, staging, and response assessment of Hodgkin and non-Hodgkin lymphoma: the Lugano classification. *J Clin Oncol*. 2014;32(27):3059-3068.
16. Rieger M, Osterborg A, Pettengell R, et al. Primary mediastinal B-cell lymphoma treated with CHOP-like chemotherapy with or without rituximab: results of the Mabthera International Trial Group study. *Ann Oncol*. 2011;22(3):664-670.
17. Camus V, Rossi C, Sesques P, et al. Outcomes after first-line

- immunochemotherapy for primary mediastinal B cell lymphoma patients: a LYSA study. *Blood Adv.* 2021;5(19):3862-3872.
18. Dunleavy K, Pittaluga S, Maeda LS, et al. Dose-adjusted EPOCH-rituximab therapy in primary mediastinal B-cell lymphoma. *N Engl J Med.* 2013;368(15):1408-1416.
 19. Giulino-Roth L, O'Donohue T, Chen Z, et al. Outcomes of adults and children with primary mediastinal B-cell lymphoma treated with dose-adjusted EPOCH-R. *Br J Haematol.* 2017;179(5):739-747.
 20. Knörr F, Zimmermann M, Attarbaschi A, et al. Dose-adjusted EPOCH-Rituximab or intensified B-NHL therapy for pediatric primary mediastinal large B-cell lymphoma. *Haematologica.* 2021;106(12):3232-3235.
 21. Minard-Colin V, Aupérin A, Pillon M, et al. Rituximab for high-risk, mature B-cell non-Hodgkin's lymphoma in children. *N Engl J Med.* 2020;382(23):2207-2219.
 22. Ehrhardt MJ, Chen Y, Sandlund JT, et al. Late health outcomes after contemporary Lymphome Malin de Burkitt therapy for mature B-cell non-Hodgkin lymphoma: a report from the Childhood Cancer Survivor Study. *J Clin Oncol.* 2019;37(28):2556-2570.
 23. Armand P, Rodig S, Melnichenko V, et al. Pembrolizumab in relapsed or refractory primary mediastinal large B-cell lymphoma. *J Clin Oncol.* 2019;37(34):3291-3299.

Extracellular vesicles mediate the communication between multiple myeloma and bone marrow microenvironment in a NOTCH dependent way

Domenica Giannandrea,¹ Natalia Platonova,¹ Michela Colombo,¹ Mara Mazzola,² Valentina Citro,¹ Raffaella Adami,¹ Filippo Maltoni,¹ Silvia Ancona,¹ Vincenza Dolo,³ Iaria Giusti,³ Andrea Basile,⁴ Anna Pistocchi,² Laura Cantone,⁵ Valentina Bollati,⁵ Lavinia Casati,¹ Elisabetta Calzavara,⁶ Mauro Turrini,⁶ Elena Lesma¹ and Raffaella Chiamonte¹

¹Department of Health Sciences, Università degli Studi di Milano, Milano; ²Department of Medical Biotechnology and Translational Medicine, Università degli Studi di Milano, Milano; ³Department of Life, Health and Environment Sciences, Università degli Studi dell'Aquila, L'Aquila; ⁴Department of Oncology and Hematology-Oncology, Università degli Studi di Milano, Milano; ⁵Department of Clinical Sciences and Community Health, Università degli Studi di Milano, Milano and ⁶Division of Hematology, Valduce Hospital, Como, Italy

Correspondence: R. Chiamonte
raffaella.chiamonte@unimi.it

Received: August 11, 2021.

Accepted: March 2, 2022.

Prepublished: March 10, 2022.

<https://doi.org/10.3324/haematol.2021.279716>

©2022 Ferrata Storti Foundation

Published under a CC BY-NC license



Abstract

Multiple myeloma (MM) is an incurable hematologic neoplasm, whose poor prognosis is deeply affected by the propensity of tumor cells to localize in the bone marrow (BM) and induce the protumorigenic activity of normal BM cells, leading to events associated with tumor progression, including tumor angiogenesis, osteoclastogenesis, and the spread of osteolytic bone lesions. The interplay between MM cells and the BM niche does not only rely on direct cell-cell interaction, but a crucial role is also played by MM-derived extracellular vesicles (MM-EV). Here, we demonstrated that the oncogenic NOTCH receptors are part of MM-EV cargo and play a key role in EV protumorigenic ability. We used *in vitro* and *in vivo* models to investigate the role of EV-derived NOTCH2 in stimulating the protumorigenic behavior of endothelial cells and osteoclast progenitors. Importantly, MM-EV can transfer NOTCH2 between distant cells and increase NOTCH signaling in target cells. MM-EV stimulation increases endothelial cell angiogenic ability and osteoclast differentiation in a NOTCH2-dependent way. Indeed, interfering with NOTCH2 expression in MM cells may decrease the amount of NOTCH2 also in MM-EV and affect their angiogenic and osteoclastogenic potential. Finally, we demonstrated that the pharmacologic blockade of NOTCH activation by γ -secretase inhibitors may hamper the biological effect of EV derived by MM cell lines and by the BM of MM patients. These results provide the first evidence that targeting the NOTCH pathway may be a valid therapeutic strategy to hamper the protumorigenic role of EV in MM as well as other tumors.

Introduction

Multiple myeloma (MM) is a clonal plasma cell neoplasm representing alone 13% of all hematological malignancies.¹ Despite the development of new therapies, MM still remains incurable,² mainly due to MM cell ability to shape the bone marrow (BM) niche sustaining tumor progression. Upon the localization in the BM, MM cells establish anomalous signaling loops with the neighboring cells and "educate" BM-residing non-tumor cells to support different steps of MM progression, including tumor cell growth, survival, angiogenesis, and bone osteolysis.³

In this complex picture, extracellular vesicles (EV) are new key players recently come to light. EV include a heterogeneous group of cell-derived membranous structures classified into two main subtypes according to their ori-

gin. Exosomes, the smaller ones, originate from the endosomal system, while the larger vesicles are shed from the plasma cell membrane. Due to the difficulty to distinguish these subtypes based on their origin, a recent position statement of the International Society for Extracellular Vesicles has suggested a distinction based on their size: i.e., small EV <200 nm and large EV >200 nm.⁴

EV are key mediators in the communication between tumor and stroma due to their ability to transport proteins and RNA.⁵ Circulating EV from MM patients display characteristic size distribution and concentration,^{6,7} and their microRNA (miRNA) cargo is prognostic in MM.⁸⁻¹⁰ Recent evidence indicates that MM cell-derived EV (MM-EV) modulate the BM niche, promoting angiogenesis, immunosuppression,¹¹ and bone disease.¹² Additionally, several

features of MM-EV may contribute to MM dissemination at distant sites, thereby favoring skeletal metastasis formation, progression and bone disease.¹³

This work elucidates how MM cells exploit the aberrantly expressed *NOTCH2* oncogene to shape the BM niche via MM-EV, specifically focusing on tumor angiogenesis and osteoclastogenesis.

NOTCH is a family of transmembrane receptors (NOTCH1-4) activated by the interaction with five different membrane-bound ligands (JAGGED1-2 and DLL1-3-4) present on the adjacent cells. The consequence of this interaction is the activation of cleavage by γ -secretase, which releases the active form of NOTCH (NOTCH-IC) from the cell membrane and allows its translocation to the nucleus and the activation of the CSL transcription factor.¹⁴

NOTCH deregulation in MM cells is due to the aberrant expression of NOTCH receptors and/or ligands.¹⁵ High levels of NOTCH pathway activity are associated with increased myeloma cell infiltration in BM biopsies of MM patients.¹⁶ Other studies suggest that MM cell skeletal infiltration may be due to events promoted by NOTCH, including MM cell recruitment at the BM,¹⁷ mitogenic or anti-apoptotic effect¹⁷⁻¹⁹ or MM stem cell self-renewal.²⁰ Additionally, MM infiltration of BM niche is also associated with the activation of NOTCH signaling in the tumor niche, which promotes angiogenesis,^{16,21} osteoclastogenesis,²²⁻²⁴ and bone marrow stromal cell (BMSC)-mediated release of cytokines involved in these events (IL-6, VEGF, IGF-1, SDF-1, RANKL, etc.).^{16,18,19,25}

Up to now, the increased activation of NOTCH signaling in the tumor microenvironment has been attributed to the presence of high levels of MM cell-derived JAGGED ligands. Here, we demonstrate that MM cells may trigger tumor angiogenesis and osteoclastogenesis by transferring NOTCH2 receptor via EV. Moreover, we provide evidence that targeting the NOTCH pathway may represent a suitable strategy to hamper the MM-EV-mediated pathological communication with the BM niche.

Methods

Extracellular vesicles isolation from human multiple myeloma cell line and multiple myeloma patients' bone marrow aspirates

EV were obtained from supernatants of RPMI8226 and OPM2 cells cultured for 48 hours (h) in RPMI1640 medium depleted of fetal bovine serum-derived bovine EV or from the plasma obtained by BM aspirates of monoclonal gammopathy of undetermined significance (MGUS) (MGUS-BM-EV) and MM patients (MM-BM-EV). The Institutional Review Board of Insubria Italy approved the design of this study (approval n. 1 on 27th February 2018). Written informed consent was obtained in accordance with the

Declaration of Helsinki. Clinical information of patients is reported in the *Online Supplementary Table S1*.

EV pellets were resuspended in the appropriate buffer/medium for subsequent studies. Further details are reported in *Online Supplementary Appendix*.

Production of viral supernatants and NOTCH2 knockdown

Viral supernatants were generated by calcium phosphate-DNA transfection of HEK293T cells with the Dharmacon Trans-lentiviral packaging kit containing pTRIPZ vector carrying a doxycycline-inducible system (Tet-on) expressing short hairpin RNA (shRNA) against NOTCH2, or the corresponding scrambled shRNA (Horizon Discovery, United Kingdom). A pilot experiment on HEK293T cells was carried out by transient transfection of four shRNA for NOTCH2 to select the more effective NOTCH2 shRNA (Cat.ID RHS5087-EG4853 - mature antisense sequence: ATGTCACAAGAGACATTGG). Lentiviral supernatants were used to infect and generate stable clones of RPMI8226 and OPM2 cells. shRNA expression was induced by treatment with 1 μ g/mL doxycycline (Sigma Aldrich, Italy).

In vivo experiments

In vivo experiments were carried out on transgenic zebrafish (*Danio rerio*) embryos obtained by crossing *Tg(T2KTp1bglob:hmgb1-mCherry)* with *Tg(fli1a:EGFP)* obtained from the Wilson lab, University College London, UK. Zebrafish embryos were raised and maintained under standard conditions and national guidelines (Italian decree 4th March 2014, n. 26). All experiments have been conducted within 5 days post fertilization (dpf). EV were injected into the duct of Cuvier of embryos at 48 hours post fertilization (hpf) with a manual microinjector (Eppendorf, Germany) using glass microinjection needles. Further details on the above procedures and information concerning cell cultures, transmission electron microscopy, *in vitro* uptake, western blot, EV-derived NOTCH2 tracking system, viral particle production, luciferase reporter assay, *in vivo* experiments, osteoclastogenesis and angiogenesis assays, *ex vivo* experiments and statistical analyses are reported in the *Online Supplementary Appendix*.

Results

Multiple myeloma-derived extracellular vesicles are uptaken by bone marrow cell populations

EV produced by two different human MM cell lines (HMCL), RPMI8226 and OPM2, were isolated by ultracentrifugation and fully characterized. Particle size distribution assessed by nanoparticle tracking analysis (NTA) revealed that the EV populations produced by the two

HMCL were characterized by the presence of both small (30-200 nm) and large (200-1,000 nm) vesicles (Figure 1A). The shape and integrity of MM-EV was assessed by transmission electronic microscopy (TEM), showing the presence of whole, undamaged small and large EV (Figure 1B). We assessed the ability of MM-EV to transfer their content to two key BM cell populations crucial in supporting MM progression, osteoclasts (OCL) and endothelial cells (EC). The uptake was assessed in a quantitative (Figure 2A and 2) and qualitative way (Figure 2C). EV isolated by a 48 hours (h) culture of RPMI8226 cells were stained with the fluorescent lipophilic dye CM-DIL and put in contact with a monolayer of OCL progenitors (Raw264.7 cells) and EC (primary human pulmonary arterial cells [HPAEC]) for 4 h at 37°C. The negative control was maintained at 4°C to inhibit the uptake. In Figure 2A and B, MM-EV uptake was quantified through flow cytometry by measuring the CM-DIL fluorescent signal in receiving cells. The dot plot analysis clearly shows that the two different cell types

take up MM-EV with a similar efficiency. The graph in the *Online Supplementary Figure S1* summarizes the mean values and the statistical analysis of flow cytometry detection. These results were confirmed by fluorescence microscopy analysis. Stack projection images (Figure 2C) and z-stack videos (*Online Supplementary Videos*) show the presence of high levels of fluorescent signal in Raw264.7 cells (*Online Supplementary Videos S1*) and HPAEC (*Online Supplementary Videos S2*) treated with MM-EV at 37°C, indicating that MM-EV may be internalized by these cells. As expected, internalization is blocked when cells are kept at 4°C, suggesting that an active process is involved.

Multiple myeloma-derived extracellular vesicles carry NOTCH2

Due to the important role of NOTCH in the interplay between MM and the BM microenvironment, we wondered if MM-EV contribute to NOTCH activation in BM cells by

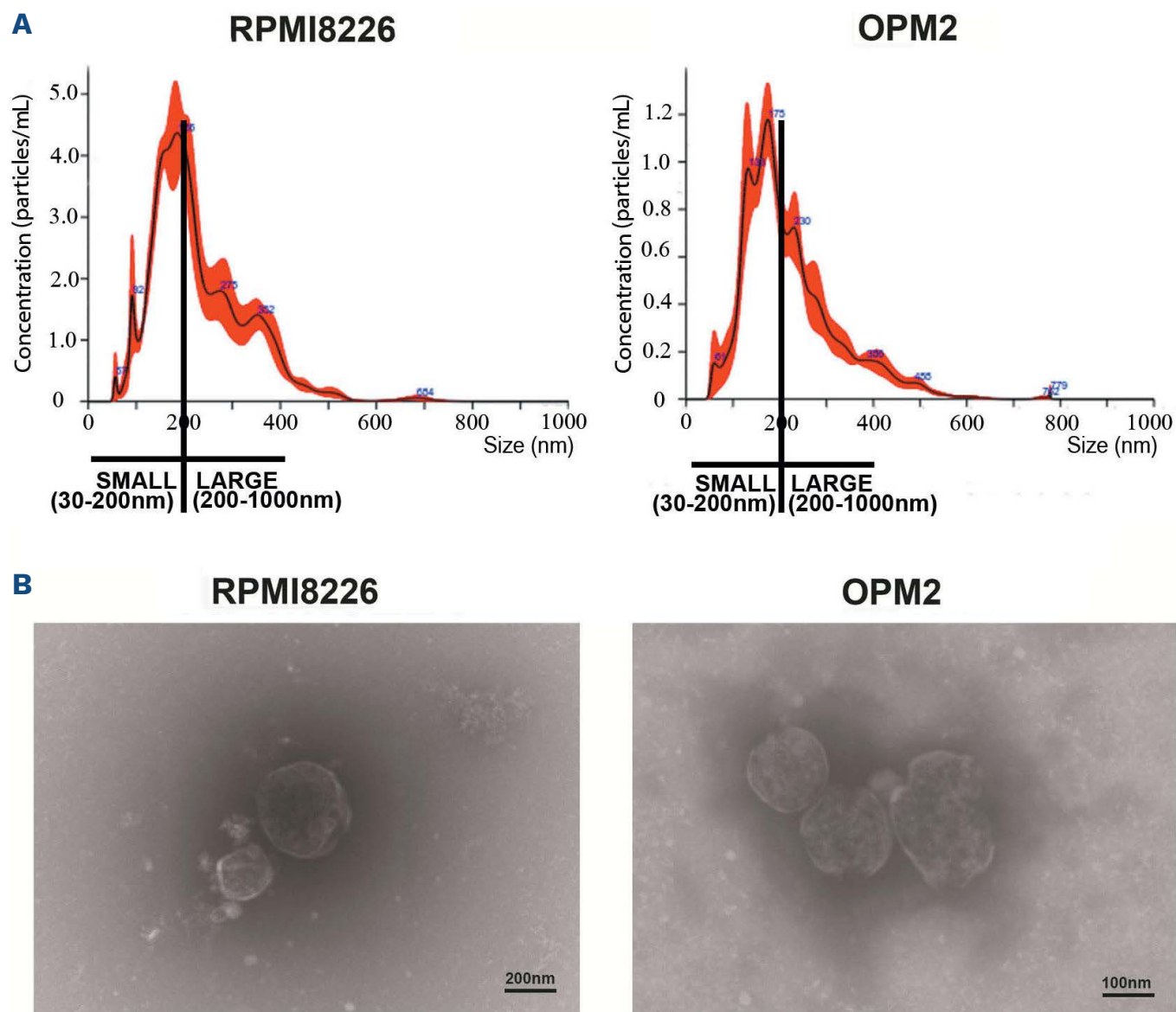


Figure 1. Characterization of multiple myeloma cell-released extracellular vesicles. Extracellular vesicles (EV) from multiple myeloma cell lines (HMCL) RPMI8226 and OPM2 cells (MM-EV), were isolated by ultracentrifugation and analyzed by (A) nanotrack particle analysis (NTA) and (B) electron transmission microscopy (TEM). (A) NTA analysis reveals the presence of small (30-200 nm) and large (200-1,000 nm) vesicles. Size and concentration of EV were determined by NanoSight NS300 system (Malvern Panalytical Ltd, Malvern, UK). A camera level of 12 and 5 30-second recordings were used for the acquisition of each sample of 3 independent EV isolations and one representative image is shown. (B) TEM analysis confirms the isolation of intact small and large vesicles.

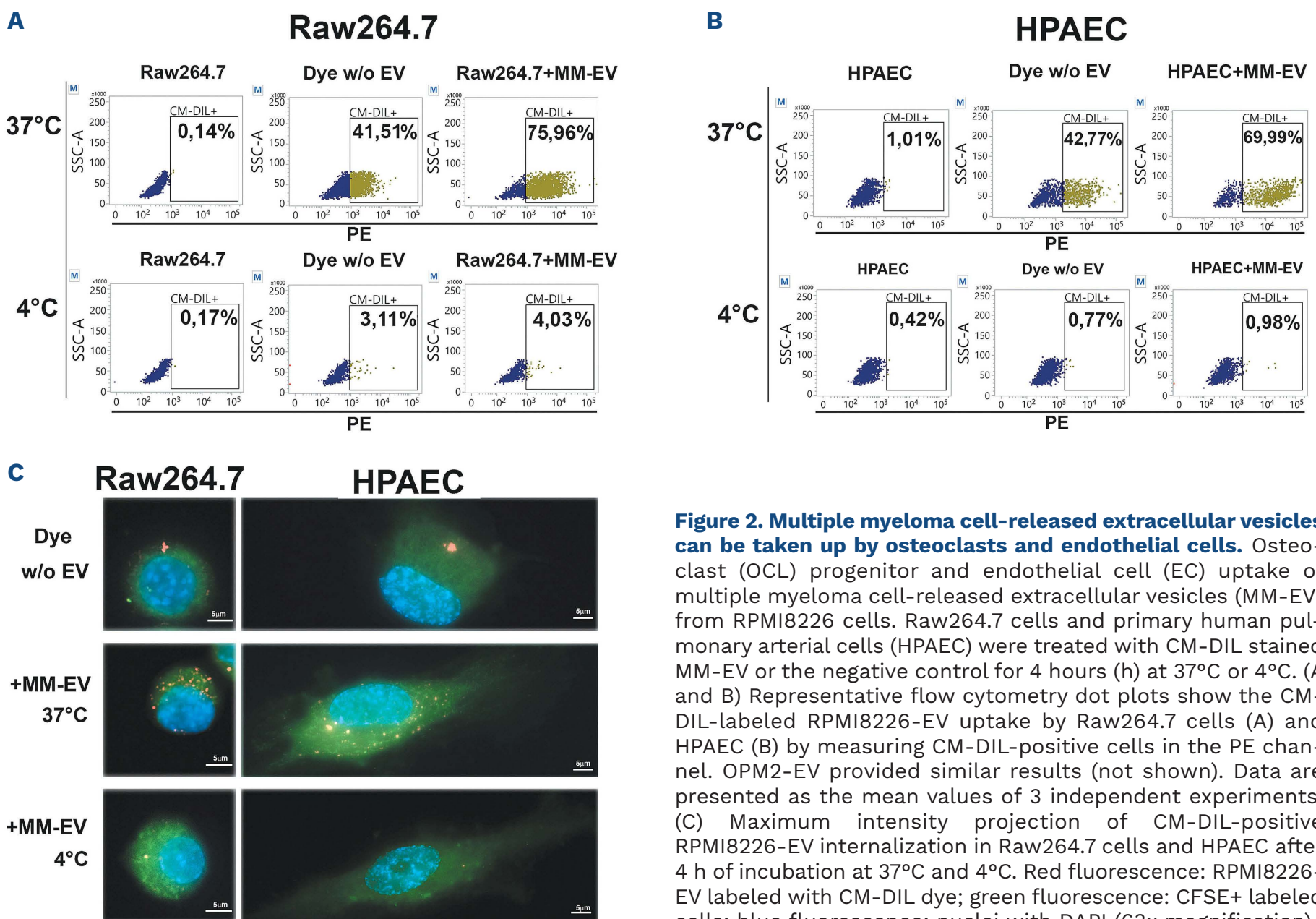


Figure 2. Multiple myeloma cell-released extracellular vesicles can be taken up by osteoclasts and endothelial cells. Osteoclast (OCL) progenitor and endothelial cell (EC) uptake of multiple myeloma cell-released extracellular vesicles (MM-EV) from RPMI8226 cells. Raw264.7 cells and primary human pulmonary arterial cells (HPAEC) were treated with CM-DIL stained MM-EV or the negative control for 4 hours (h) at 37°C or 4°C. (A and B) Representative flow cytometry dot plots show the CM-DIL-labeled RPMI8226-EV uptake by Raw264.7 cells (A) and HPAEC (B) by measuring CM-DIL-positive cells in the PE channel. OPM2-EV provided similar results (not shown). Data are presented as the mean values of 3 independent experiments. (C) Maximum intensity projection of CM-DIL-positive RPMI8226-EV internalization in Raw264.7 cells and HPAEC after 4 h of incubation at 37°C and 4°C. Red fluorescence: RPMI8226-EV labeled with CM-DIL dye; green fluorescence: CFSE+ labeled cells; blue fluorescence: nuclei with DAPI (63x magnification).

carrying NOTCH receptors and, in particular the over-expressed receptor NOTCH2,²⁶ as part of their cargo. By western blot analysis, we compared NOTCH2 expression in protein extracts from seven HMCL, namely AMO1, JJN3, H929, RPMI8226, LP1, KMS12, OPM2, and EV isolated from HMCL conditioned media (CM). Figure 3A shows that MM-EV are able to carry NOTCH2, whose relative amount reflects that expressed in the different protein extracts of the HMCL. The analysis of the different forms of NOTCH2 indicated that MM-EV could carry not only the transmembrane NOTCH2 (NOTCH2-TM) but also the full-length un-cleaved NOTCH2 (NOTCH2-FL). Since the cleavage operated by γ -secretase on the intracellular portion of NOTCH takes place inside the endocytic bodies²⁷ and exosomes arise from late endosomes,²⁸ we investigated whether the active cleaved intracellular NOTCH2-IC may be included in MM-EV cargo by using a specific antibody. Results in Figure 3A indicate that MM-EV cargo also carries NOTCH2-IC. *Online Supplementary Figure S2* shows that also NOTCH1 is widely represented in MM-EV, while the presence of other two isoforms in MM-EV is less noticeable.

In order to assess which EV fraction expresses NOTCH2,

we performed a western blot analysis on large and small vesicles collected from the HMCL CM by sequential ultracentrifugation at 20,000 g (20 K) and 110,000 g (110 K). We found that NOTCH2-TM and NOTCH2-IC were present both in large and small vesicles (Figure 3B). Interestingly, NOTCH2-IC level was increased in 110K MM-EV fraction. EV allow distant cells to communicate between each other, thus modifying their behavior. In order to demonstrate that NOTCH2 may be involved in these processes and can be transferred to distant cells *via* EV, we developed a model system of HEK293 donor and receiving cells (Figure 3C). The first were forced to constitutively express NOTCH2 tagged with HA at the C-terminus (NOTCH2-HA)²⁹ to distinguish it from the endogenous NOTCH2. In addition, the position of the HA-tag at the C-terminus of NOTCH2 enabled us to detect NOTCH2-FL, the NOTCH2-TM portion of the heterodimeric NOTCH2 form, matured in the trans-Golgi network upon the cleavage by a furin-like convertase,³⁰ and the mature NOTCH2-IC, due to homotypic activation mediated by ADAM10 and the γ -secretase.²⁹ EV-donor cells were added to the culture medium of receiving HEK293 cells. Figure 3C shows a western blot analysis performed with an anti-HA antibody, confirming

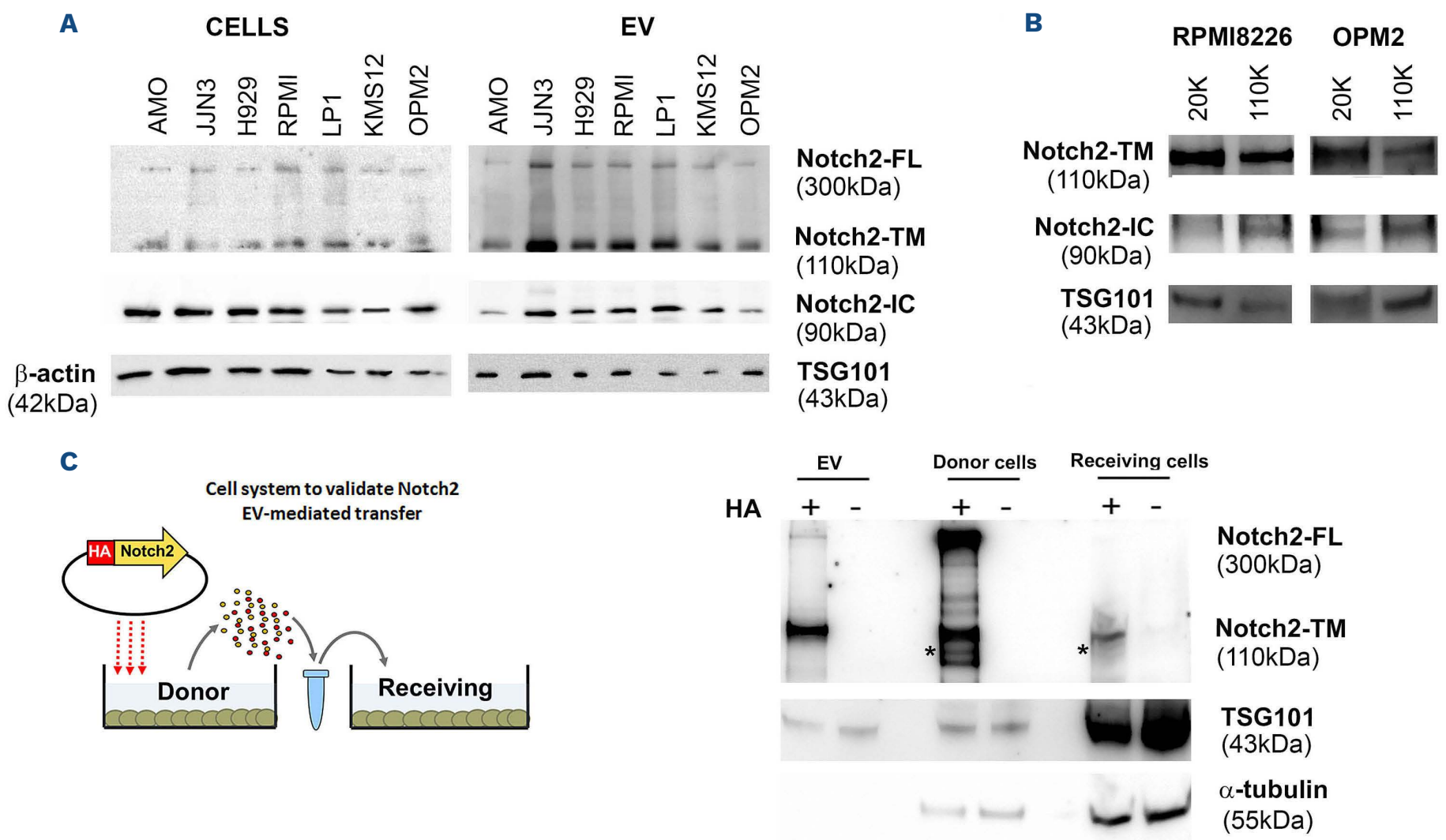


Figure 3. NOTCH receptors and ligands in extracellular vesicles. (A) Western blot analysis for NOTCH2-FL (full length), NOTCH2-TM (transmembrane form), and NOTCH2-IC (active intracellular NOTCH2) expressed in 7 different human multiple myeloma cell lines (HMCL) and the respective produced extracellular vesicles (EV). β -actin and TSG101 were used as loading controls for cells and vesicle protein extracts, respectively. In order to perform all the hybridizations, two western blots were performed with cell and EV extracts loaded with an identical amount of protein. (B) Western blot analysis shows the expression of NOTCH2-TM and NOTCH2-IC in EV populations of different sizes. Large and small EV were isolated from RPMI8226 and OPM2 cells by sequential ultracentrifugation at 20,000 g (20K) and 110,000 g (110K), and the expression of the two NOTCH2 forms was separately assessed by western blot analyses using specific antibodies for NOTCH2 and NOTCH2-IC; TSG101 was used as control for vesicle protein extracts. (C) EV-mediated cell-to-cell transfer of NOTCH2: the donor HEK293 cell line was forced to express HA-tagged NOTCH2 carried by pCDNA3.1 or the corresponding empty vector (negative control); EV secreted by donor cells were collected by ultracentrifugation and used to treat receiving HEK293 cells for 24 hours. Cell and EV protein extracts were analyzed by western blot using a specific primary antibody anti-HA. α -tubulin and TSG101 were used to normalize cellular and vesicular protein extract loading, respectively. NOTCH2-IC identified by rehybridization of the same membrane with anti-NOTCH-IC (see the *Online Supplementary Figure S3*) is indicated by an asterisk.

the presence of the HA-signal in donor cells carrying NOTCH2-HA, isolated EV, and receiving cells. This demonstrates that EV can transfer NOTCH2 between distant cells. In this model system, the EV cargo include NOTCH2-TM and NOTCH2-FL, while both donor and receiving cells show also the presence of NOTCH2-IC. The absence of NOTCH2-IC in HEK293-derived EV might be due to a lower level of NOTCH activation in HEK293 cells in comparison to HMCL.

Multiple myeloma-derived extracellular vesicles activate NOTCH signaling in receiving cells

In order to address if the variation of NOTCH2 levels in MM cells may affect MM-EV-mediated communication, we studied the effect of NOTCH2 silencing in RPMI8226 and OPM2 cells. These cells were transduced with the pTRIPZ lentiviral vector conditionally expressing shRNA for NOTCH2

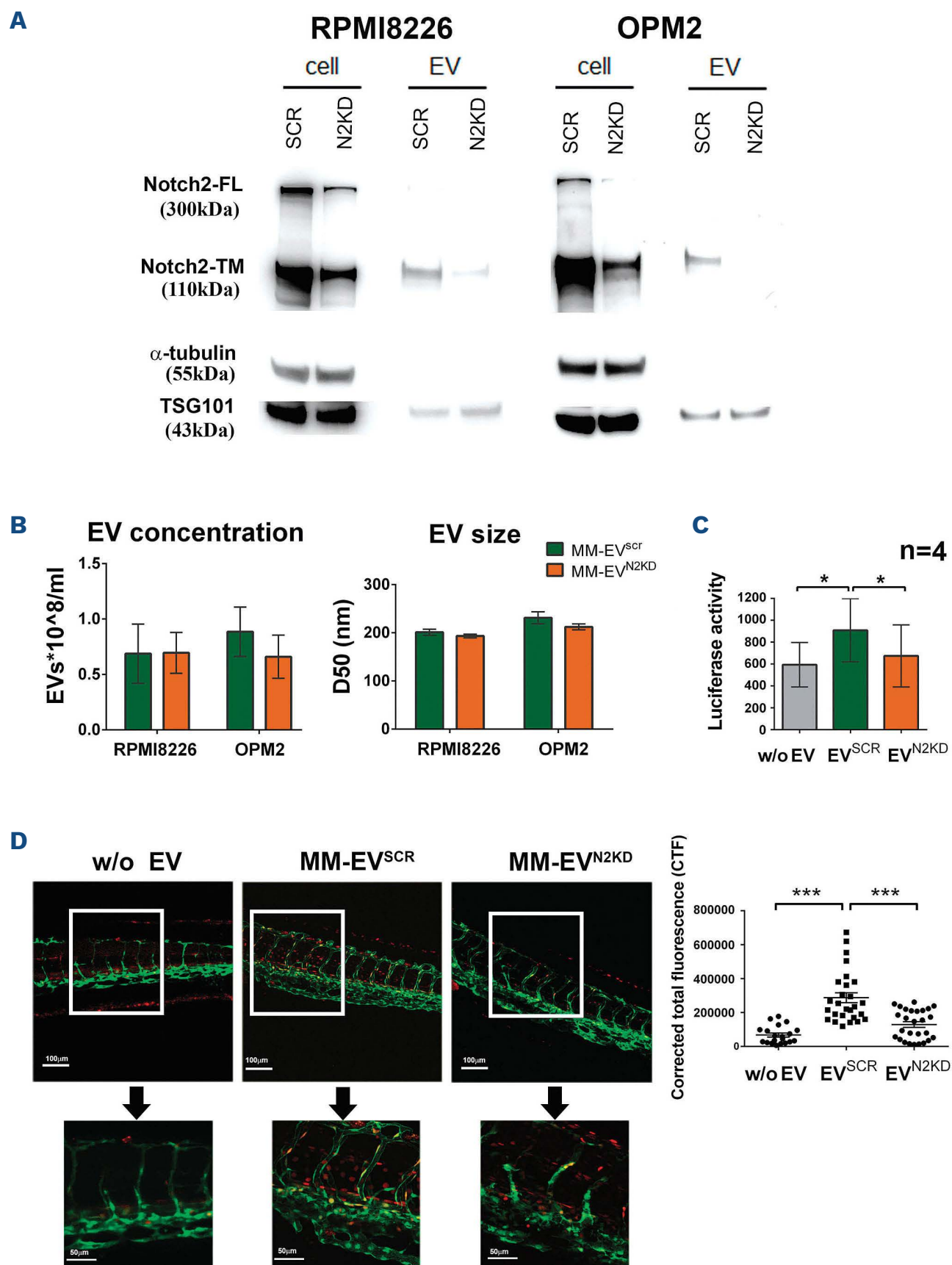
(HMCL^{N2KD}) or the scrambled sequence (HMCL^{SCR}) and single cell clones were isolated. Figure 4A confirms that RPMI8226 and OPM2 cells are knocked down (KD) for NOTCH2 and clearly shows that also the produced MM-EV displayed a reduced level of NOTCH2. Also NOTCH2-IC decreased in OPM2 cells with a corresponding decrease in the shed EV, while NOTCH2-IC decrease in EV release from RPMI8226 was less evident (*Online Supplementary Figure S4*). Through alignment search tool BlastN (USA National Center for Biotechnology Information) we excluded regions of local similarities between the used shRNA and the sequences of other NOTCH receptors and ligands (E values range between 1 and 15). However, the high sequence homology between the four NOTCH receptors prompted us to analyze by western blot the expression of the other NOTCH receptor isoforms. The *Online Supple-*

mentary Figure S5 shows that NOTCH2 KD did not affect the expression of NOTCH1, 3 and 4 in protein extracts from cells and MM-EV. The outcome of NOTCH2 KD on EV size and concentration evaluated by NTA showed no significant effect on MM-EV size and concentration (Figure 4B).

In order to assess if the NOTCH2 protein carried by MM-EV is functionally active and is able to trigger NOTCH signaling in receiving cells, we tested the effect of EV isolated from HMCL^{N2KD} (MM-EV^{N2KD}) or HMCL^{SCR} (MM-EV^{SCR}) through a NOTCH responsive luciferase reporter assay. This assay was carried out in HeLa cells, which is a highly-

transfectable cell line characterized by a low level of NOTCH signaling activation (not shown). Figure 4C shows that MM-EV^{SCR} can activate the NOTCH signaling pathway in the receiving HeLa cells, while this ability is significantly reduced for MM-EV^{N2KD}.

The ability of MM-EV to activate NOTCH signaling was also validated in an *in vivo* NOTCH reporter zebrafish embryo obtained by crossing *Tg(T2KTp1bglob:hmgb1-mCherry)* with *Tg(fli1a:EGFP)* that carry EGFP+ endothelial cells (green) and express the mCherry protein (red) under the control of a NOTCH-responsive element. EV isolated from RPMI8226 cells were injected in the duct of Cuvier of 48 hpf



Continued on following page.

Figure 4. Molecular effects of NOTCH2 modulation on multiple myeloma cell-released extracellular vesicles. (A) Western blot analysis confirms the knockdown (KD) efficacy on NOTCH2-TM levels in human multiple myeloma cell lines (HMCL) and the produced multiple myeloma extracellular vesicles (MM-EV). α -tubulin and TSG101 were used as loading controls for cell and vesicle protein extracts, respectively. (B) Nanoparticle tracking analysis (NTA) on MM-EV^{SCR} and MM-EV^{N2KD} from HMCL does not show significant changes in concentration and size; D50=size point below which 50% of the extracellular vesicles (EV) are contained. Data are expressed as mean value \pm standard error of the mean of at least 4 experiments (RPMI8226 n=4; OPM2 n=6). Statistics by two-tailed *t*-test did not show any significant difference. (C) MM-derived EV activate NOTCH signaling in receiving cells: a NOTCH reporter assay was carried out on HeLa cells stimulated with MM-EV^{SCR} and MM-EV^{N2KD} from HMCL (EV derived from OPM2 cells), or control fresh medium (w/o EV). Luciferase activity is expressed as the ratio between Nano/Firefly luciferase luminescence units. Data are expressed as mean value \pm standard error of 4 experiments. Statistics by ANOVA and Tukey post-test: **P*<0.05. (D) Activation of NOTCH signaling in the trunk of *Tg(T2KTp1bglob:hmgb1-mCherry)* zebrafish embryos (zf) 4 hours after the injection of MM-EV^{SCR} and MM-EV^{N2KD} (EV derived from RPMI8226 cells), or control fresh medium (w/o EV). Representative pictures of each condition are reported on the left (20x and 60x magnification, the upper and the lower respectively); a graph on the right represents the mean value \pm standard error of the mean of the corrected total fluorescence (CTF) measured in caudal hematopoietic tissue (CHT). In particular four *in vivo* experiments involved zf embryos injected with negative control (n=20) or MM-EV^{SCR} (n=27) and MM-EV^{N2KD} (n=27). Statistics by ANOVA and Tukey post-test excluding outliers identified through the ROUT method (Q=1%): *** *P*<0.001.

transgenic zebrafish embryos. Images were acquired 4 h postinjection. Figure 4D shows MM-EV^{SCR} mediated NOTCH activation in the intersegmental vessels (Se), caudal artery (CA), and in the area of the caudal hematopoietic tissue (CHT), while MM-EV^{N2KD} induces a barely visible stimulation.

NOTCH2 carried by multiple myeloma-derived extracellular vesicles contributes to the education of bone marrow cell populations

We and other groups previously reported that MM cells affect the surrounding BM microenvironment inducing osteoclastogenesis²²⁻²⁴ and tumor angiogenesis^{16,21} in a NOTCH-dependent way. Moreover, recent evidence indicates that MM-EV stimulate osteoclastogenesis,^{13,31-33} angiogenesis and carry pro-angiogenic proteins.^{11,34} Therefore, we verified the osteoclastogenic potential of MM-EV^{SCR} and MM-EV^{N2KD} by treating the monocyte cell line Raw264.7 in the presence of the osteoclastogenic chemokine RANKL (30 ng/mL). We used MM-EV released by the RPMI8226 cell line due to the ability of these cells to induce osteoclastogenesis, differently from OPM2 cells.²² After 7 days of treatment with MM-EV, OCL count showed that MM-EV^{SCR} induced Raw264.7 cell differentiation, while MM-EV^{N2KD} lost this ability (Figure 5A).

We assessed MM-EV^{N2KD} angiogenic potential using a tube formation assay with HPAEC seeded on a Matrigel layer. Results in Figure 5B show that MM-EV^{SCR} promotes tube organization of HPAEC, while treatment with MM-EV^{N2KD} reduces this effect. In conclusion, this specific RNA interference approach unequivocally demonstrated that NOTCH2 KD affects the MM-EV mediated osteoclastogenesis and angiogenesis.

Targeting NOTCH signaling blocks the pathological communication mediated by multiple myeloma-derived extracellular vesicles

In order to provide a higher translational potential to our findings, we exploited the strategy illustrated in Figure 6A. We used γ -secretase inhibitors (50 μ M DAPT), used in research works and clinics to inhibit pan-Notch signaling¹⁵ to

block NOTCH activation in EC and OCL induced by MM-EV. Figure 6B and C clearly show that MM-EV induce angiogenesis and osteoclastogenesis in a NOTCH-dependent way. In consideration of the well known osteoclastogenic and angiogenic roles of NOTCH signaling,^{16,21-24} we planned our experiments to distinguish the effect of the endogenous and vesicular NOTCH. Indeed, if we compare the effect of DAPT on osteoclastogenesis (Figure 6B) in the absence of EV and suboptimal concentration of RANKL, we can see that it abrogates OCL differentiation with a non-statistically significant decrease, while DAPT abrogates much higher levels of osteoclastogenesis induced by MM-EV (+250%) in a statistically significant way, indicating that the greater effect of MM-EV is NOTCH dependent.

The effect of DAPT on MM-EV-induced angiogenesis was analogous. The high increase of HPAEC tube organization upon the administration of MM-EV from RPMI8226 and OPM2 cells was completely abrogated by DAPT, showing a statistically significant reduction in areas and nodes (ranging from 29,5% to 51,3%). This effect was clearly higher than the slight inhibitory trend observed on basal angiogenesis upon DAPT administration (Figure 6C). We also ruled out that the obtained results could be due to the toxic effect of DAPT on OCL and EC (*Online Supplementary Figure S6*).

Overall, these results confirm that the studied biological effects of EV are NOTCH mediated and can be blocked by treatment with γ -secretase inhibitors.

Finally, in order to strengthen the translational potential of our *in vitro* findings, we reasoned that the BM of MM patients does not contain only MM-derived EV, but EV derived from the whole MM-educated BM cell populations. Therefore, in order to confirm the NOTCH-dependent role of EV in the pathological communication occurring in the BM of MM patients, we got advantage of EV from BM aspirates of patients with the benign MGUS (MGUS-BM-EV) or MM (MM-BM-EV) (*Online Supplementary Table S1*), which may recapitulate the complexity of the BM microenvironment. We compared the angiogenic potential of HPAEC untreated or treated with MGUS-BM-EV or MM-BM-EV. Fig-

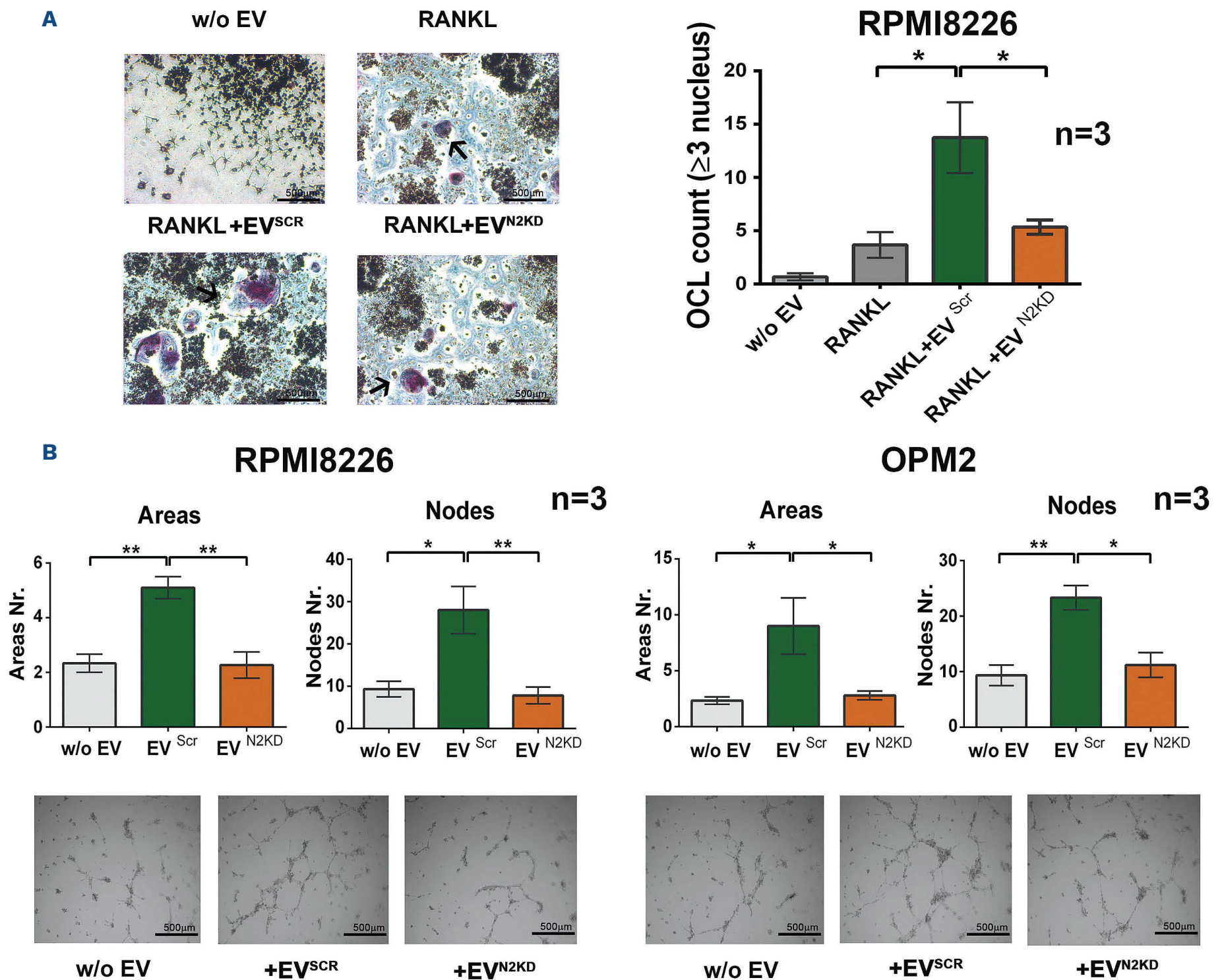


Figure 5. NOTCH2 contributes to the protumorigenic communication of multiple myeloma cell-released extracellular vesicles toward osteoclasts and endothelial cells. (A) The effect of MM-EV^{SCR} and MM-EV^{N2KD} collected from the osteoclastogenic cell line RPMI8226. The Raw264.7 cell line was treated with or without the osteoclastogenic RANKL (30 ng/mL), multiple myeloma cell-released extracellular vesicles (MM-EV) or control fresh medium (w/o EV). After 7 days TRAP-positive multinucleated cells (≥3 nuclei) were enumerated (TRAP-positive multinucleated cells are indicated by an arrow). Representative images are shown for each condition on the left (4x magnification); a graph on the right represents the mean value of the absolute number of TRAP+ multinucleated cells +/- standard error of the mean. Statistical analysis by a one-way ANOVA with Tukey post-test; **P*<0.05. (B) Tumor angiogenesis induced by MM-EV^{SCR} and MM-EV^{N2KD}. Tube formation assay performed for 13 hours with primary human pulmonary arterial cells (HPAEC) laid on a matrigel-coated support stimulated with MM-EV^{SCR} and MM-EV^{N2KD} collected from RPMI8226 and OPM2 cells or control fresh medium (w/o EV). The graphs show the mean values of areas and nodes (branch points) enumerated in four quadrant of the well +/- standard error of the mean. Statistical analysis was performed by ANOVA and Tukey post-test; **P*<0.05, ***P*<0.01. Representative images are shown below for each condition (4x magnification).

ure 6D shows that MM-BM-EV boost the angiogenic potential of HPAEC while MGUS-BM-EV showed a non-statistically significant increasing trend. Importantly, the inhibitory effect of DAPT is statistically significant when added to HPAEC treated with MM-BM-EV. These results confirm the increasing angiogenic potential of EV released in the BM during MM progression, the role played by NOTCH delivered via MM-BM-EV and strengthen the po-

tential of a NOTCH-directed therapeutic approach to block the support of MM microenvironment to the disease progression.

Discussion

The pathological interplay between malignant cells and

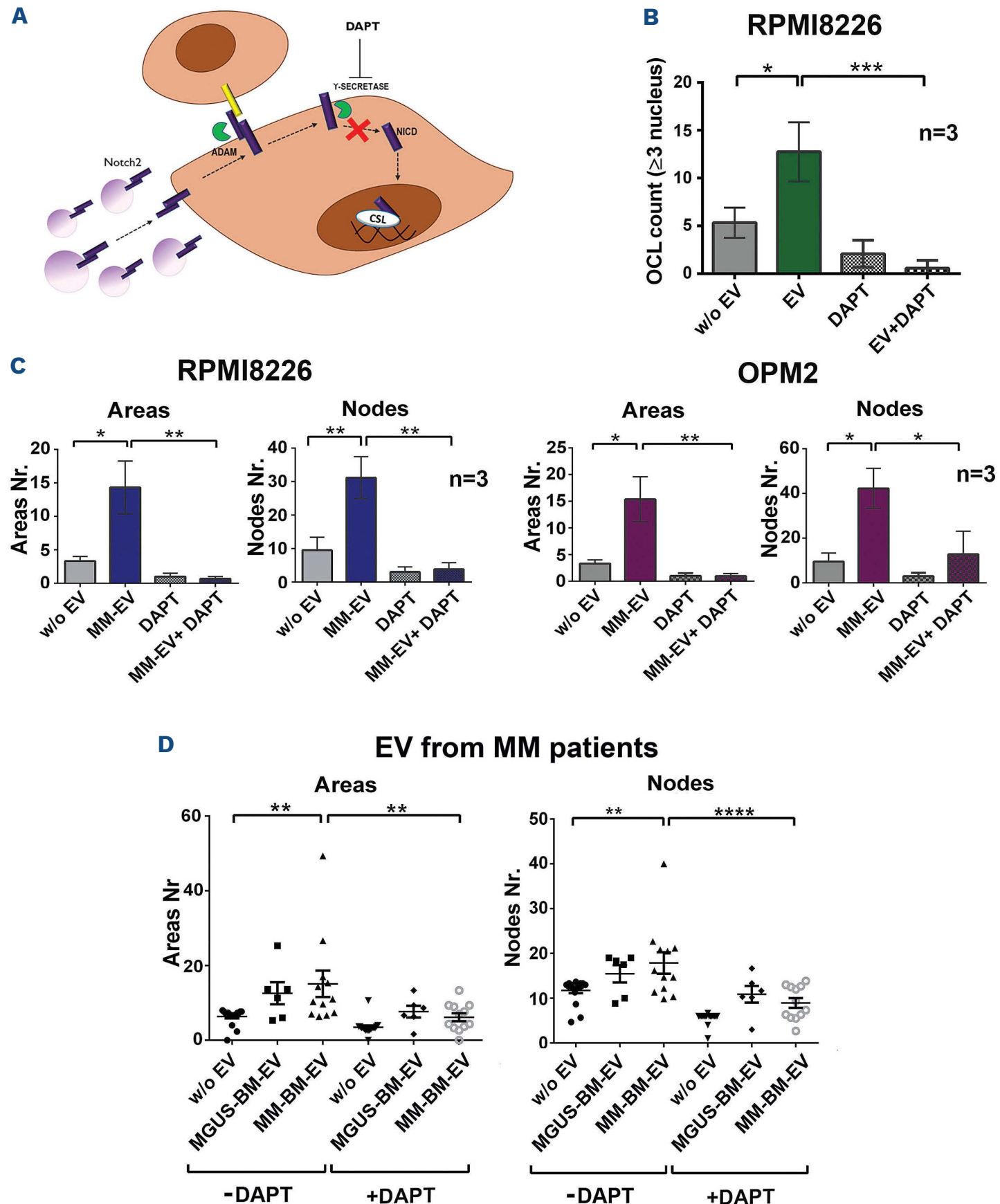


Figure 6. γ -secretase blockade of NOTCH2 activation inhibits the effect of multiple myeloma cell-released extracellular vesicles on osteoclastogenesis and angiogenesis. (A) Experimental rationale. Multiple myeloma cell-released extracellular vesicles (MM-EV) derived NOTCH2 may increase NOTCH signaling activation on target cells (osteoclast [OCL] progenitors and endothelial cells [EC]) that may be blocked by DAPT administration. (B) Raw267.4 cells induced to differentiate into OCL in the presence of 30 ng/mL RANKL were treated with MM-EV collected from the osteoclastogenic cell line RPMI8226 or the control fresh medium (w/o EV) and in the presence or absence of DAPT to inhibit NOTCH signaling activation. For each condition a negative control cultured in the absence of RANKL was carried out. After 7 days TRAP+ multinucleated cells (≥ 3 nuclei) were enumerated. The graph shows the mean values of TRAP+ multinucleated cells obtained in the different conditions for RANKL treated cells. Given the large number of conditions, to make the graph simpler and easier to understand, each value was subtracted of the respective control without RANKL (+/- standard error of the mean [SEM]). Statistical analysis was performed by a one-way ANOVA with Tukey post-test; * $P < 0.05$; *** $P < 0.001$. (C) Tube formation assay on primary human pulmonary arterial cells (HPAEC) was performed for 13 hours (h) with MM-EV collected from RPMI8226 and OPM2 cells or control fresh medium (w/o EV) in the presence or the absence of DAPT. The graphs show the mean values of areas and nodes enumerated in four quadrant of the well +/- SEM. Statistical analysis was performed by ANOVA and Tukey post-test; * $P < 0.05$, ** $P < 0.01$. (D) Tube formation assay on HPAEC treated for 13 h with EV collected from the bone marrow of MGUS patients or MM patients in the presence or the absence of DAPT. The graphs show the mean values of areas and nodes enumerated in 4 quadrant of the well (+/- SEM). Statistical analysis was performed by ANOVA and Tukey post-test; ** $P < 0.01$, **** $P < 0.0001$. The characteristics and number of MM patients are reported in the *Online Supplementary Table S1*.

the surrounding non-tumoral BM cells promotes neoplastic cell growth and survival as well as key events of tumor progression including bone disease and angiogenesis. These lines of evidence suggest that an effective therapeutic approach should not be focused merely on the MM cells, but it should target their interaction with the surrounding BM niche.

Recently, EV have been reported as critical players in the communication between MM cells and the nearby BM cells and leading to MM progression. Indeed, MM-EV promote different events associated with MM progression, including angiogenesis^{11,13,34,35} and osteoclastogenesis.^{13,31-33} Here, we contribute to elucidate the molecular mechanisms involved in MM-EV pathological communication with the BM microenvironment, strengthening the role of the EV pathological communication as a promising therapeutic target in MM.

The evidence that NOTCH signaling activation, mediated by MM cell heterotypic interaction with the surrounding BM cells, plays a key role in tumor angiogenesis^{16,21} and osteoclastogenesis²²⁻²⁴ prompted us to investigate whether NOTCH signaling contributes to determine the impact of MM-EV on these processes.

Our analysis on a panel of HMCL and the respective shed EV indicate that NOTCH receptors were present in MM-EV cargo with high levels of NOTCH2 and slightly lower levels of NOTCH1, consistently with evidence from EV released by other cell types.³⁶ We focused on NOTCH2 receptor, widely expressed in MM cell lines and in primary MM cells, particularly from high-risk patients.^{18,26} In details, we found that MM-EV carried the mature heterodimeric form of NOTCH2 (since we detected the NOTCH2-TM portion), the immature NOTCH2-FL and the activated NOTCH2-IC, that upon delivering to target cells might directly activate the transcription of the NOTCH target genes without requiring the interaction with ligands and the activation by ADAM protease and γ -secretase.

The expression of NOTCH receptors has been reported in exosomes³⁷ but also in microvesicles.³⁸ Thereby, we wondered which of the two subpopulations of EV hosted NOTCH2. We separated large and small vesicles and found the presence of NOTCH2-TM both in large and small particles, while NOTCH2-IC level was higher in 110K small EV fraction. Although it is impossible to distinguish exosome and microvesicles only on the basis of their dimension, we presume that small vesicles are enriched with exosomes respect to large vesicles. Therefore our results suggest the presence of NOTCH2-IC within exosomes consistently with its presence in the endosomal compartment from which exosomes take origin.

Before validating the hypothesis that vesicular NOTCH2 contributes to molecular and biological effects on relevant BM cell populations as OCL and EC, we monitored if these cells uptake MM-EV, using respectively Raw264.7

cells and HPAEC. Flow cytometry detection showed a quick (4 h) uptake of MM-EV by the majority of cells in both models, confirmed by a Z-stack analysis in confocal microscopy.

Additionally, we unequivocally assessed that NOTCH signaling members could be transferred via EV from one cell to another using an experimental system model based on HEK293 cells forced to express NOTCH2 tagged with HA. This model system allowed us to assess that NOTCH2-HA could be released within EV and be transferred to distant cells. In this system, we have confirmed that EV carried high levels of NOTCH2-TM form and NOTCH2-FL, even if at much lower level. On the contrary, although the NOTCH2-IC form was present in MM-EV shed by HMCL, we could not detect it in HEK293-derived EV, possibly due to a lower level of NOTCH2 activation in HEK293 cells in comparison to HMCL. Receiving cells clearly took up the transmembrane form of NOTCH2-HA, but also showed a very faint band corresponding to NOTCH2-IC, consistently with a slight NOTCH2 activation after EV uptake. This result provided a first indication that EV carrying NOTCH2 may activate NOTCH signaling in receiving cells.

Using a selective RNA interference of NOTCH2 in RPMI8226 and OPM2 cells, we confirmed that NOTCH2 KD in HMCL impacted the levels of vesicular NOTCH2-TM, NOTCH2-FL and NOTCH2-IC, although the decrease of the activated form was evident only in OPM2 cells. On the contrary, NOTCH2 KD did not significantly affect MM-EV size and concentration.

In order to confirm that MM-EV might activate the oncogenic NOTCH signaling in receiving cells, we tested MM-EV^{SCR} or MM-EV^{N2KD} in *in vitro* and *in vivo* NOTCH reporter systems. The first *in vitro* cellular model transfected with a Nanoluc-based NOTCH reporter vector, indicated that MM-EV^{SCR} might activate a NOTCH-dependent gene reporter, while MM-EV^{N2KD} induced a significantly lower activation. This result was confirmed by a second reporter *in vivo* system recapitulating the complexity of a whole organism. The injection of MM-EV^{SCR} or MM-EV^{N2KD} in transgenic zebrafish embryo reporter for NOTCH not only confirmed the observed MM-EV-mediated NOTCH signaling activation but also provided evidence of MM-EV ability to induce NOTCH signaling activation at distant sites through the circulation. Indeed, MM-EV injected in the duct of Cuvier may be transported through the circulation and activate NOTCH signaling in the caudal hematopoietic tissue which represents the main hematopoietic organ in zebrafish embryo, analogous to the human BM.³⁹ In contrast, NOTCH signaling activation mediated by MM-EV^{N2KD} was significantly lower. MM-EV effectiveness in inducing NOTCH signaling activation at distant sites in zebrafish embryos carried by the blood stream suggests that MM-EV could also play an important role in the metastatic process, as reported for pancreatic cancer.⁴⁰

For instance they may help preparing the premetastatic niche through the formation of new permeable vessels for the extravasation of tumor cells, and the destruction of the bone matrix to make space for metastatic cells.

Taken as a whole, the *in vitro* and *in vivo* NOTCH reporter assays confirmed that NOTCH activity in target cells was due to NOTCH2 delivered by the injected MM-EV.

This evidence and the acknowledged effect of NOTCH signaling on OCL and EC, prompted us to verify if NOTCH2 delivery by MM-EV could affect the biology of these cells. Through the same specific RNA interference approach on two different HMCL, we provided an unequivocal demonstration that vesicular NOTCH2 participates in MM-induced OCL differentiation and angiogenesis, assessed by a tube formation assay. The dependency of these processes on NOTCH signaling was clearly demonstrated by the fact that MM-EV^{N2KD} impact was significantly lower. The presence of other NOTCH receptors in MM-EV cargo, even if at a lower level, (i.e. NOTCH1) suggests that they may also provide a contribution.

In order to strengthen the translational potential of our results we used a dual approach: i) the outcome of an anti-NOTCH therapeutic approach already tested in clinics was assessed *in vitro* and *ex vivo*; ii) *ex vivo* experiments were carried out with EV released in the BM of MM patients, taking into account that a systemic treatment is expected to affect the communication of MM-EV, as well as that of EV from all the BM cell populations. In the first case, we showed that γ -secretase inhibitors (GSI), already used in clinics,¹⁵ greatly affected MM-EV ability to inhibit angiogenesis and osteoclastogenesis *in vitro*. Concerning the second point, EV collected from the BM of MM patients, but not MGUS patients, displayed a clear pro-angiogenic effect that could be hampered by GSI.

In conclusion, the RNA interfering approach specific for NOTCH2 on HMCL, complemented by a pan-NOTCH chemical inhibition on HMCL- and MM patients' BM-derived EV, provides a new important evidence of the effect of NOTCH signaling pathway on EV-mediated pathological communication in myelomatous BM. The important inhibitory effect of GSI suggests that the form of the NOTCH2 oncogene which mostly contributes to MM-EV mediated education is NOTCH2-TM and not NOTCH2-IC whose activity is GSI resistant. Although, the presence of

NOTCH2-IC in MM-EV cargo is much intriguing since it may deliver an active oncogenic signal, we believe that vesicular NOTCH-IC might be more relevant in tumor that expresses the constitutively active form of NOTCH, such as T-cell acute lymphoblastic leukemia.

In conclusion, our results strengthen the rationale for therapeutic approaches directed to inhibit NOTCH activation mediated by MM-EV, suggesting that they have the potential of interfering with the pathological communication of the MM cells mediated by EV in the short and potentially in the long range and, thereby, they may influence the cross-talk with the surrounding microenvironment and the dissemination of the disease at distant skeletal sites.

Disclosures

No conflicts of interest to disclose.

Contributions

DG, NP and MC designed and performed experiments, acquire data and wrote the manuscript; MM, VC, RA, FM, SA, EL performed experiments and acquired data; VD and IG performed TEM morphologic analysis; MC, MM, AP performed the in vivo zebrafish experiment; DG, LCan and VB analyzed data; MT and EC collected patients' samples and clinical information, performed patients' sample first processing; DG, MT, AB and LCas performed statistical analysis; DG, MT, AB, AP, EL, VB and LCas revised the manuscript; LCas acquired data; RC, DG, AB and MT interpreted data; RC set up the experiment design and supervised the research, interpreted data and statistical analysis, drafted, wrote and critical revised the manuscript.

Funding

This study was supported by grants from Associazione Italiana Ricerca sul Cancro, Investigator Grant to RC (20614), My First Grant to AP (18714); Fondazione Italiana per la Ricerca sul Cancro to MC (post-doctoral fellowship 18013); Università degli Studi di Milano to RC (Linea 2B-2017 - Dept. Health Sciences), to NP (postdoctoral fellowship type A) and DG (PhD fellowship in experimental medicine).

Data-sharing statement

For any question, please contact the corresponding author.

References

- Kyle RA, Rajkumar SV. Multiple myeloma. *Blood*. 2008;111(6):2962-2972.
- Cowan AJ, Allen C, Barac A, et al. Global burden of multiple myeloma: a systematic analysis for the global burden of disease study 2016. *JAMA Oncol*. 2018;4(9):1221-1227.
- Manier S, Sacco A, Leleu X, Ghobrial IM, Roccato AM. Bone marrow microenvironment in multiple myeloma progression. *J Biomed Biotechnol*. 2012;2012:157496.
- Thery C, Witwer KW, Aikawa E, et al. Minimal information for studies of extracellular vesicles 2018 (MISEV2018): a position statement of the International Society for Extracellular Vesicles and update of the MISEV2014 guidelines. *J Extracell Vesicles*. 2018;7(1):1535750.
- Webber J, Yeung V, Clayton A. Extracellular vesicles as modula-

- tors of the cancer microenvironment. *Semin Cell Dev Biol.* 2015;40:27-34.
6. Caivano A, Laurenzana I, De Luca L, et al. High serum levels of extracellular vesicles expressing malignancy-related markers are released in patients with various types of hematological neoplastic disorders. *Tumour Biol.* 2015;36(12):9739-9752.
 7. Krishnan SR, Luk F, Brown RD, et al. Isolation of human CD138(+) microparticles from the plasma of patients with multiple myeloma. *Neoplasia.* 2016;18(1):25-32.
 8. Manier S, Liu CJ, Avet-Loiseau H, et al. Prognostic role of circulating exosomal miRNAs in multiple myeloma. *Blood.* 2017;129(17):2429-2436.
 9. Caivano A, La Rocca F, Simeon V, et al. MicroRNA-155 in serum-derived extracellular vesicles as a potential biomarker for hematologic malignancies - a short report. *Cell Oncol (Dordr).* 2017;40(1):97-103.
 10. Rajeev Krishnan S, De Rubis G, Suen H, et al. A liquid biopsy to detect multidrug resistance and disease burden in multiple myeloma. *Blood Cancer J.* 2020;10(3):37.
 11. Wang J, De Veirman K, Faict S, et al. Multiple myeloma exosomes establish a favourable bone marrow microenvironment with enhanced angiogenesis and immunosuppression. *J Pathol.* 2016;239(2):162-173.
 12. Zhang L, Lei Q, Wang H, et al. Tumor-derived extracellular vesicles inhibit osteogenesis and exacerbate myeloma bone disease. *Theranostics.* 2019;9(1):196-209.
 13. Colombo M, Giannandrea D, Lesma E, Basile A, Chiaramonte R. Extracellular vesicles enhance multiple myeloma metastatic dissemination. *Int J Mol Sci.* 2019;20(13):3236.
 14. Colombo M, Mirandola L, Platonova N, et al. Notch-directed microenvironment reprogramming in myeloma: a single path to multiple outcomes. *Leukemia.* 2013;27(5):1009-1018.
 15. Colombo M, Galletti S, Garavelli S, et al. Notch signaling deregulation in multiple myeloma: a rational molecular target. *Oncotarget.* 2015;6(29):26826-26840.
 16. Palano MT, Giannandrea D, Platonova N, et al. Jagged ligands enhance the pro-angiogenic activity of multiple myeloma cells. *Cancers (Basel).* 2020;12(9):2600.
 17. Mirandola L, Apicella L, Colombo M, et al. Anti-Notch treatment prevents multiple myeloma cells localization to the bone marrow via the chemokine system CXCR4/SDF-1. *Leukemia.* 2013;27(7):1558-1566.
 18. Colombo M, Galletti S, Bulfamante G, et al. Multiple myeloma-derived Jagged ligands increases autocrine and paracrine interleukin-6 expression in bone marrow niche. *Oncotarget.* 2016;7(35):56013-56029.
 19. Colombo M, Garavelli S, Mazzola M, et al. Multiple myeloma exploits Jagged1 and Jagged2 to promote intrinsic and bone marrow-dependent drug resistance. *Haematologica.* 2020;105(7):1925-1936.
 20. Chiron D, Maiga S, Descamps G, et al. Critical role of the NOTCH ligand JAG2 in self-renewal of myeloma cells. *Blood Cells Mol Dis.* 2012;48(4):247-253.
 21. Saltarella I, Frassanito MA, Lamanuzzi A, et al. Homotypic and heterotypic activation of the Notch pathway in multiple myeloma-enhanced angiogenesis: a novel therapeutic target? *Neoplasia.* 2019;21(1):93-105.
 22. Colombo M, Thummler K, Mirandola L, et al. Notch signaling drives multiple myeloma induced osteoclastogenesis. *Oncotarget.* 2014;5(21):10393-10406.
 23. Schwarzer R, Kaiser M, Acikgoez O, et al. Notch inhibition blocks multiple myeloma cell-induced osteoclast activation. *Leukemia.* 2008;22(12):2273-2277.
 24. Schwarzer R, Nickel N, Godau J, et al. Notch pathway inhibition controls myeloma bone disease in the murine MOPC315.BM model. *Blood Cancer J.* 2014;4:e217.
 25. Houde C, Li Y, Song L, et al. Overexpression of the NOTCH ligand JAG2 in malignant plasma cells from multiple myeloma patients and cell lines. *Blood.* 2004;104(12):3697-3704.
 26. van Stralen E, van de Wetering M, Agnelli L, et al. Identification of primary MAFB target genes in multiple myeloma. *Exp Hematol.* 2009;37(1):78-86.
 27. Chastagner P, Brou C. Tracking trafficking of Notch and its ligands in mammalian cells. *Methods Mol Biol.* 2014;1187:87-100.
 28. Rajagopal C, Harikumar KB. The origin and functions of exosomes in cancer. *Front Oncol.* 2018;8:66.
 29. Groot AJ, Habets R, Yahyanejad S, et al. Regulated proteolysis of NOTCH2 and NOTCH3 receptors by ADAM10 and presenilins. *Mol Cell Biol.* 2014;34(15):2822-2832.
 30. Blaumueller CM, Qi H, Zagouras P, Artavanis-Tsakonas S. Intracellular cleavage of Notch leads to a heterodimeric receptor on the plasma membrane. *Cell.* 1997;90(2):281-291.
 31. Raimondi L, De Luca A, Fontana S, et al. Multiple myeloma-derived extracellular vesicles induce osteoclastogenesis through the activation of the XBP1/IRE1 α axis. *Cancers (Basel).* 2020;12(8):2167.
 32. Raimondo S, Saieva L, Vicario E, et al. Multiple myeloma-derived exosomes are enriched of amphiregulin (AREG) and activate the epidermal growth factor pathway in the bone microenvironment leading to osteoclastogenesis. *J Hematol Oncol.* 2019;12(1):2.
 33. Faict S, Muller J, De Veirman K, et al. Exosomes play a role in multiple myeloma bone disease and tumor development by targeting osteoclasts and osteoblasts. *Blood Cancer J.* 2018;8(11):105.
 34. Umezumi T, Tadokoro H, Azuma K, et al. Exosomal miR-135b shed from hypoxic multiple myeloma cells enhances angiogenesis by targeting factor-inhibiting HIF-1. *Blood.* 2014;124(25):3748-3757.
 35. Liu Y, Zhu XJ, Zeng C, et al. Microvesicles secreted from human multiple myeloma cells promote angiogenesis. *Acta Pharmacol Sin.* 2014;35(2):230-238.
 36. Wang Q, Lu Q. Plasma membrane-derived extracellular microvesicles mediate non-canonical intercellular NOTCH signaling. *Nat Commun.* 2017;8(1):709.
 37. Patel B, Patel J, Cho JH, et al. Exosomes mediate the acquisition of the disease phenotypes by cells with normal genome in tuberous sclerosis complex. *Oncogene.* 2016;35(23):3027-3036.
 38. Suwakulsiri W, Rai A, Xu R, et al. Proteomic profiling reveals key cancer progression modulators in shed microvesicles released from isogenic human primary and metastatic colorectal cancer cell lines. *Biochim Biophys Acta Proteins Proteom.* 2019;1867(12):140171.
 39. Sacco A, Roccaro AM, Ma D, et al. Cancer cell dissemination and homing to the bone marrow in a Zebrafish model. *Cancer Res.* 2016;76(2):463-471.
 40. Ogawa K, Lin Q, Li L, et al. Prometastatic secretome trafficking via exosomes initiates pancreatic cancer pulmonary metastasis. *Cancer Lett.* 2020;481:63-75.

Antiplatelet antibody predicts platelet desialylation and apoptosis in immune thrombocytopenia

Shiyong Silvia Zheng,^{1,2} Zohra Ahmadi,¹ Halina Hoi Laam Leung,¹ Rose Wong,^{1,2} Feng Yan,^{1,2} José Sail Perdomo^{1#} and Beng Hock Chong^{1,2#}

¹Hematology Research Unit, St. George and Sutherland Clinical School, University of New South Wales, Sydney and ²Department of Hematology, St. George Hospital, Kogarah, New South Wales, Australia

#JSP and BHC contributed equally as co-senior authors.

Correspondence: S. S. Zheng
silvia.zheng@health.nsw.gov.au

Received: August 5, 2021.

Accepted: February 18, 2021.

Prepublished: February 24, 2022.

<https://doi.org/10.3324/haematol.2021.279751>

©2022 Ferrata Storti Foundation

Published under a CC BY-NC license



Abstract

Immune thrombocytopenia (ITP) is a bleeding disorder caused by dysregulated B- and T- cell functions, which lead to platelet destruction. A well-recognized mechanism of ITP pathogenesis involves anti-platelet and anti-megakaryocyte antibodies recognizing membrane glycoprotein (GP) complexes, mainly GPIb/IX and GPIIb/IIIa. In addition to the current view of phagocytosis of the opsonised platelets by splenic and hepatic macrophages via their Fc γ receptors, antibody-induced platelet desialylation and apoptosis have also been reported to contribute to ITP pathogenesis. Nevertheless, the relationship between the specific thrombocytopenic mechanisms and various types of anti-platelet antibodies has not been established. In order to ascertain such association, we used sera from 61 ITP patients and assessed the capacity of anti-platelet antibodies to induce neuraminidase 1 (NEU1) surface expression, RCA-1 lectin binding and loss of mitochondrial inner membrane potential on donors' platelets. Sera from ITP patients with detectable antibodies caused significant platelet desialylation and apoptosis. Anti-GPIIb/IIIa antibodies appeared more capable of causing NEU1 surface translocation while anti-GPIb/IX complex antibodies resulted in a higher degree of platelet apoptosis. In ITP patients with anti-GPIIb/IIIa antibodies, both desialylation and apoptosis were dependent on Fc γ R1a signaling rather than platelet activation. Finally, we confirmed in a murine model of ITP that destruction of human platelets induced by anti-GPIIb/IIIa antibodies can be prevented with the NEU1 inhibitor oseltamivir. A collaborative clinical trial is warranted to investigate the utility of oseltamivir in the treatment of ITP.

Introduction

Immune thrombocytopenia (ITP) is an acquired autoimmune disease characterized by enhanced platelet destruction and impaired platelet production from megakaryocytes.¹ ITP patients can present with no predisposing condition (hence, primary ITP) or with a variety of associated disorders (secondary ITP),² such as autoimmune diseases (especially systemic lupus erythematosus),³ infections (notably Hepatitis C virus and HIV)⁴ as well as malignancies.⁵ Primary ITP is estimated to represent approximately 80% of all adult ITP.⁴ Regarding the incidence of ITP, studies from Europe have estimated that to be 2.9–3.9/100,000 annually in adults,^{6–9} with an overall incidence slightly higher in females than males. The prevalence is approximately 9.5–23.6/100,000.^{6,7,10} The pathogenesis of ITP involves antibodies recognizing

membrane glycoprotein (GP) complexes.^{2,9} The seminal Harrington-Hollingsworth experiment of self-infusion of ITP plasma led to the discovery of a humoral factor accountable for platelet destruction in ITP.^{11,12} Subsequently, Shulman identified that this factor could be adsorbed by platelets and was associated with immunoglobulin G (IgG).¹³ Currently, the widely-accepted mechanism is that antibody-coated platelets are phagocytosed by splenic and/or hepatic macrophages of the reticuloendothelial system, via their Fc γ receptors (Fc γ R), resulting in accelerated platelet clearance.^{1,9,14} Equally important in the pathogenesis of ITP is the dysfunction of T cells.¹⁵ Both CD4⁺ T-regulatory cells reduction^{16–18} and CD8⁺ T-cell-mediated cytotoxicity^{19–21} have been reported in ITP.^{2,9,15} In addition, CD8⁺ T-regulatory cells' immunosuppressive role in ITP has been recognized.²² This further highlights the significant role of T cells in immune dysregulation and ITP.²³

Antibody-mediated platelet apoptosis has also been suggested in ITP. In 2006, Leytin and colleagues reported in the mouse model that monoclonal anti-GPIIb antibody injection induced thrombocytopenia, caspase-3 activation, enhanced phosphatidylserine (PS) exposure and mitochondrial inner transmembrane potential ($\Delta\Psi_m$) depolarisation.²⁴ In 2012, Winkler *et al.* demonstrated similar findings in pediatric patients with ITP.²⁵ More recently, platelet apoptosis was also confirmed in adult ITP patients by Goette and colleagues.²⁶ However, the relationship between platelet apoptosis and ITP antibody specificity was unclear, as only one patient carried sole anti-GPIb/IX antibodies in this study.

Another ITP pathway that has also been previously²⁷ and recently²⁸ described is Fc-independent platelet clearance. Li and co-workers reported platelet desialylation through antibody-induced platelet activation by treating donor platelets with monoclonal anti-GPIb/IX antibodies and ITP sera.²⁸ Using a murine model of ITP secondary to monoclonal anti-GPIb α antibodies, the group demonstrated evidence of platelet removal via Ashwell-Morell receptors on hepatocytes, and the use of sialidase inhibitors to attenuate thrombocytopenia.²⁸ Although the model is not directly relevant to human disease due to the absence of platelet surface Fc γ RIIA on mouse platelets and the polyclonal nature of primary ITP,^{9,29} these findings still have potential therapeutic implications: patients with anti-GPIb/IX antibodies may respond to sialidase inhibitors while patients with anti-GPIIb/IIIa antibodies were considered unlikely to respond to this novel treatment. Conversely, patients who harbor anti-GPIIb/IIIa antibodies possibly respond to IVIg therapy better than those with sole anti-GPIb/IX antibodies, because anti-GPIIb/IIIa antibodies could drive ITP in an Fc-dependent fashion.^{23,30-32} Similarly, splenectomy may be ineffective in patients with only anti-GPIb/IX autoantibodies as desialylated platelets are removed by the liver.²⁸ This differential effect and, therefore, determining antibody specificity, may influence treatment decision and ultimately patient outcomes. Nevertheless, these views have been recently challenged by Cantoni *et al.*, who studied 93 ITP patients and found no predictability of anti-platelet antibody (APA)-specificity on the site of platelet clearance.³³ Thus, ongoing investigations to determine whether antibody specificity predicts therapeutic response is vital.

The true extent to which platelet desialylation and/or platelet apoptosis are involved in ITP pathology remains unclear. Notably, both desialylated and apoptotic platelets were reported to be removed by the liver.^{28,34,35} Yet, platelet apoptosis was observed in a murine ITP model induced by monoclonal anti-GPIIb antibodies,²⁴ but desialylation has been demonstrated in ITP patients with anti-GPIb α ²⁸ and anti-GPIIb/IIIa antibodies.^{36,37} Whether there is a link between platelet desialylation and platelet intrinsic apop-

osis in ITP caused by these two antibodies is still not defined. In addition, the possibility of using neuraminidase inhibitors in the treatment of ITP is also to be investigated. We recently examined the sera from 61 ITP patients for the presence of APA and their specificities.³⁸ Here, we further scrutinize the sera's capability to induce platelet desialylation and apoptosis, and studied these two potential thrombocytopenic mechanisms' relationship with the antibody subtypes. Additionally, we established a mouse model to elucidate the therapeutic effect of neuraminidase inhibitor in preserving human platelet number in the presence of patients' antibody and provide *in vivo* data on the feasibility of this agent in the treatment of ITP.

Methods

Patient sample collection

The study was approved by the Human Research and Animal Care Ethics Committees of the University of New South Wales (Sydney, Australia). Sera were obtained from 61 adult ITP patients (aged between 18-90 years) and 21 healthy controls with written informed consent. All 61 patients were diagnosed with ITP according to the international working group's criteria,³⁹ which was also consistent with the 2019 updated consensus report.⁴⁰ Whole blood was centrifuged at 860xg for 10 minutes (min). The sera and plasma were stored in aliquots at -80°C until required for analysis. In some experiments, IgG fraction, purified using Protein G affinity chromatography (Sigma-Aldrich, USA), was used. The purity was over 95% as determined by gel densitometry (ImageJ, Version 2.1.0/1.53c).

Anti-platelet antibody detection and specificity determination

The indirect detection of APA and the determination of antibody specificities in this cohort of patients have recently been published.³⁸ Briefly, venous blood was collected into 3.2% trisodium citrate. Platelet pellets were washed with wash buffer (pH 6.0) containing 140 mM NaCl, 5 mM KCl, 12 mM trisodium citrate, 10 mM glucose, 12.5 mM sucrose, followed by resuspension in buffer (pH 7.4) containing 140 mM NaCl, 3 mM KCl, 0.5 mM MgCl₂, 5 mM NaHCO₃, 10 mM glucose and 10 mM HEPES. Washed platelets (1x10⁶) were incubated with patients' samples at various dilutions for 30 min at 37°C, washed twice, incubated with Alexa Fluor 488 or 647-labeled anti-human IgG (Invitrogen, 1:100), washed and analyzed by flow cytometry (LSRFortessa™ X-20 [BD, USA]).

For antibody specificity determination, monoclonal antibody immobilization of platelet specific antigens assay (MAIPA) was performed as previously described.^{38,41} Donor platelets were incubated with sera, followed by washing

and incubation with antibodies against GPIIb/IIIa complex (AP2; Beckman Coulter, USA), GPIX (FMC25, Millipore, USA) or GPV (G-11, Santa Cruz Biotechnology, Inc. USA). The platelets were washed, solubilized and incubated in goat anti-mouse IgG Fc fragment-specific antibody (Jackson ImmunoResearch, USA) precoated microtiter plates (ThermoFisher, USA). The reactions were washed and further incubated with goat anti-human IgG Fc fragment-specific-horseradish peroxidase-conjugated antibody (Sigma-Aldrich, USA). SureBlue™ TMB-microwell peroxidase substrate (KPL Inc. USA) was then added and stopped at 10 min with 0.18 M sulphuric acid. The absorbance was read at dual wavelength (450 nm and 492 nm).

Platelet neuraminidase expression, desialylation and activation

In order to examine sera-induced platelet neuraminidase expression, 1×10^6 washed donor platelets were incubated with patient or control sera (1:25) for 30 min at 37°C followed by washing and incubation with anti-NEU1 mouse monoclonal antibody (1:25, Santa Cruz Biotechnology, Inc. USA) for 20 min at room temperature and washing. Similarly, for platelet desialylation, the washed sera-donor platelet reactions were incubated with FITC-labeled *Ricinus communis* lectin (RCA-1, Vector Laboratories, USA, 0.5 µg/mL). In order to determine the effect of patients' IgG, control experiments were performed using purified IgG from healthy donors and ITP patients (50 µg/mL). Platelet activation was assessed by flow cytometry with anti-P-selectin monoclonal antibody APC (1:5, eBioscience™, Germany).

Platelet apoptosis

In order to evaluate ITP patient sera's effect on platelet mitochondrial inner membrane depolarization potential, 1×10^6 washed donor platelets in phosphate-buffered saline containing 1 mM MgCl₂, 5.6 mM glucose, 10 mM HEPES and 0.1% bovine serum albumin were incubated with patients' or controls' sera (1:10) for 30 min at 37°C, followed by washing and incubation with 100 nM DiOC₆ (Molecular Probes) for 15 min in the dark. In order to examine the role of FcγR in platelet apoptosis, platelets were pre-incubated with anti-FcγRIIIa antibody (clone IV.3, 2.5 µg/mL) for 10 min at 37°C prior to treatment with patients' sera. In order to determine the effect of patients' IgG on platelet apoptosis, experiments were performed using 50 µg/mL of IgG, followed by washing and incubation with 50 nM DiOC₆.

NOD/SCID mouse model of immune thrombocytopenia

Human platelets (450×10^6) were transfused via the tail vein into the non-obese diabetic/severe combined immunodeficient (NOD/SCID) mice and allowed to stabilize for 2.5 hours (h). Forty µg/g of patients' or controls' IgG was then administered intravenously.⁴² Oseltamivir-treated mice re-

ceived intraperitoneal (IP) injection of 10 µg/g oseltamivir immediately prior to human platelet infusion and again, immediately before IgG injection. Mouse blood was collected at time 0 (prior to IgG injection), 2, 4 and 6 h following IgG injection. Human platelets were identified using anti-human CD41a V450 (BD Biosciences, USA) by flow cytometry. The percentage of human platelets at time 0 was set at 100%.

Statistical analysis

Flow cytometry data were processed with FlowJo software (LCC, USA). Data were analyzed with GraphPad Prism version 8 (GraphPad Software, USA). The significance level was set at less than 0.05. Kruskal-Wallis test with Dunn's multiple comparison was carried out for *in vitro* desialylation and apoptosis experiments. Linear mixed model was used to examine the effect of neuraminidase inhibitor on platelet survival *in vivo*. Mann Whitney test was applied in other analyses.

Results

Patient characteristics

Of the 61 patients (aged between 18-90 years old) included in this study, 61% were female. The majority (84%) had primary ITP. Thirty-five patients (57%) had detectable APA in their sera as determined by flow cytometry. MAIPA demonstrated that nine patients had sole anti-GPIIb/IIIa antibodies, five patients had sole anti-GPIb/IX antibodies while seven other patients had antibodies against both complexes. The rest (14 patients, 23%) had no detectable anti-GPIIb/IIIa or anti-GPIb/IX antibodies by MAIPA (Figure 1A).³⁸ Compared to the direct testing,⁴³ the lower detection rate of dual antibody positive patients may reflect the lower sensitivity in antibody determination using indirect method, which is consistent with a prior MAIPA report.⁴¹ Recent work demonstrated that GPV is an important target of APA in ITP.^{44,45} We additionally interrogated patient samples with positive indirect APA (sera from 31 patients were available) for the presence of anti-GPV antibodies. Using a cutoff of 3 standard deviations (SD) over the mean of 20 normal controls, 21 patients were positive for antibodies against GPIIb/IIIa, GPIb/IX and/or GPV (Table 1). Seven were found to have anti-GPV antibodies in their sera. However, two patients have co-existing anti-GPIIb/IIIa antibodies, two others have co-existing anti-GPIb/IX antibodies, and one patient had all three antibodies (Table 1; Figure 1B).

Anti-platelet antibodies predict platelet desialylation

In order to determine whether ITP patients' sera can induce desialylation, we treated donor platelets with ITP or control sera and measured NEU1 expression by flow cyto-

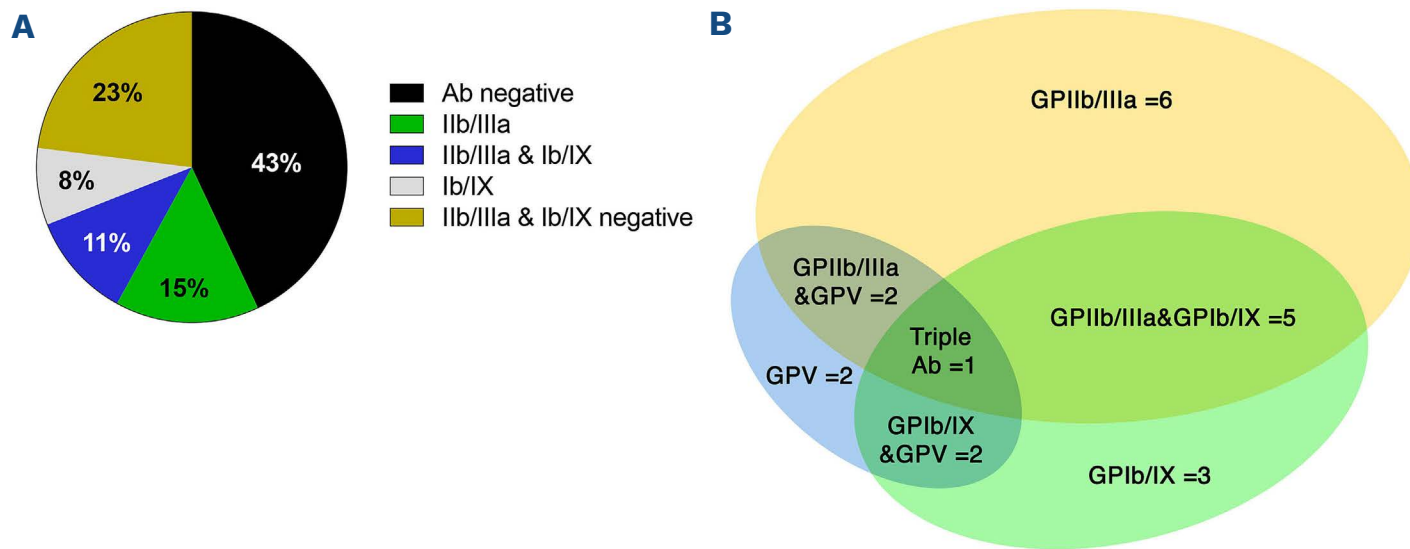


Figure 1. Antibody pattern by indirect flow cytometry and monoclonal antibody immobilization of platelet-specific antigen assay. (A) Focusing on GPIIb/IIIa and GPIb/IX in 61 immune thrombocytopenia (ITP) patients, 43% had no detectable antibodies by flow cytometry (Ab negative); of the 35 patients with positive antibody by flow cytometry, 15% had antibodies against GPIIb/IIIa (IIb/IIIa); 8% against GPIb/IX (Ib/IX); 11% had antibodies against both complexes (IIb/IIIa & Ib/IX). (B) Examination of anti-GPV antibody by monoclonal antibody immobilization of platelet-specific antigen assay (MAIPA) in 31 patients with available sera, in relation to anti GPIIb/IIIa and GPIb/IX antibodies. GP: glycoprotein.

metry. NEU1 expression was significantly increased in ITP sera-treated platelets compared to controls (Figure 2A). Further scrutiny of the patient subgroups, determined by the antibody status, demonstrated that NEU1 translocation was significantly different from controls only in platelets treated with sera from patients with detectable APA (Figure 2B). Indeed, when we examined the level of platelet desialylation, as assessed by RCA-1 binding, we found that only antibody-positive sera could induce detectable desialylation (Figure 2C). Of note, a significant difference in RCA-1 binding was not detected when comparing the whole ITP group (antibody-positive and -negative sera) to normal controls (Figure 2D). This is likely due to the weak binding of lectins (such as RCA-1) to their target sugars.⁴⁶

We further examined whether the IgG fraction was responsible for platelet desialylation. We used purified IgG

Table 1. Summary of anti-platelet antibodies found in sera as determined by monoclonal antibody immobilization of platelet-specific antigens assay.

	Patient N	Patient %
GPIIb/IIIa	6	28.6
GPIb/IX	3	14.3
GPV	2	9.5
GPIIb/IIIa+GPIb/IX	5	23.8
GPIIb/IIIa+GPV	2	9.5
GPIb/IX+GPV	2	9.5
GPIIb/IIIa+GPIb/IX+GPV	1	4.8
Total	21	100.00

GP: glycoprotein.

from two ITP patients containing anti-GPIIb/IIIa antibodies to treat donor's platelets. Figure 2E shows that the IgG fraction causes significant platelet desialylation. This result confirmed the findings by Marini and colleagues, that ITP patients' IgG leads to cleavage of platelets' sialic acid and hence, platelet desialylation.³⁶ Together, these data show that ITP autoantibodies induce NEU1 translocation and platelet desialylation.

Given the previous observation of platelet activation by monoclonal antibodies against GPIb α causing platelet desialylation,²⁸ we examined the ability for ITP patients' sera to induce P-selectin externalization. Compared to the control group, there was no enhanced anti-CD62P binding to treated platelets (Figure 2F). Unlike NEU1 expression and desialylation, no difference in platelet activation was noted between sera from patients with or without detectable APA (Figure 2G). Interestingly, the three sera with the highest P-selectin expression were all from secondary ITP patients (systemic lupus erythematosus [SLE], anti-phospholipid syndrome [APS] and B-cell lymphoma), raising the likelihood of distinct disease biology in secondary ITP. Finally, no difference was seen when patients with GPIIb/IIIa APA were compared with those with anti-GPIb/IX antibodies (Figure 2H).

Anti-platelet antibodies predict platelet apoptosis

In order to determine the role of ITP auto-antibodies in platelet apoptosis, washed platelets were treated with either ITP or control sera. Like NEU1 expression, upon treatment with patients' sera, platelets showed significantly reduced DiOC₆ fluorescence compared to the control (Figure 3A). This denotes the loss of mitochondrial inner membrane potential, $\Delta\Psi_m$, indicating the presence of platelet apoptosis. Consistent with the observations for

desialylation, when compared to the controls, antibody positive patients' sera disrupted mitochondrial $\Delta\Psi_m$ more effectively than the antibody negative group (Figure 3B). Importantly, these changes are induced by the IgG fraction of ITP sera (Figure 3C). Therefore, the presence of APA in ITP sera induces platelet apoptosis as determined by changes in mitochondrial $\Delta\Psi_m$.

Anti-GPIIb/IIIa antiplatelet antibodies induce platelet apoptosis via Fc γ receptor

Prior literature demonstrated that the platelet desialylating capacity of anti-GPIb α antibody was Fc γ R-independent.²⁸ However, in the case of anti-GPIIb/IIIa antibodies induced ITP, we and others have shown that Fc γ R is the driver of antibody-mediated platelet desialylation.^{36,37} Also

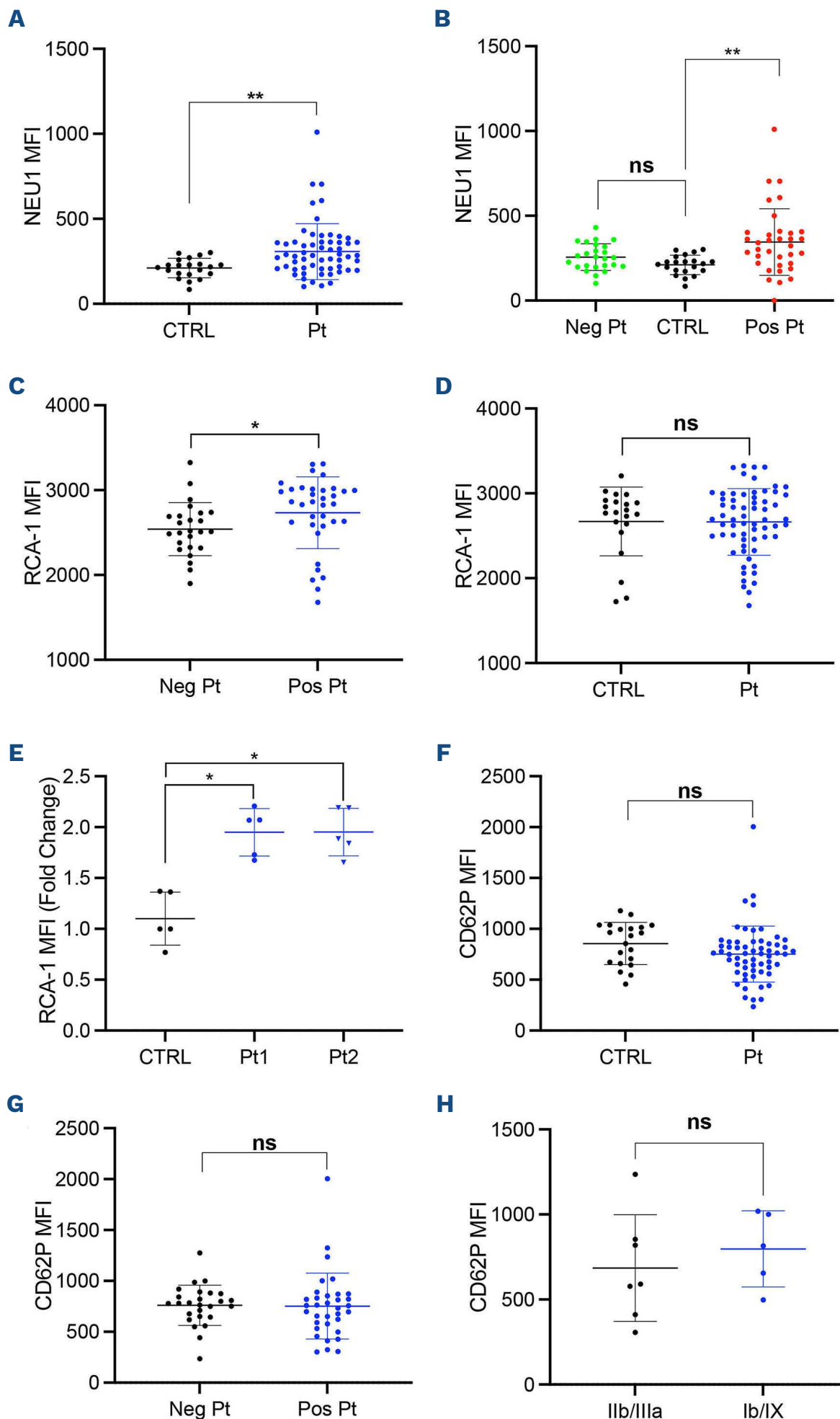


Figure 2. Effect of immune thrombocytopenia patient sera on platelet desialylation and activation. (A and B) NEU1 surface translocation and (C and D), RCA-1 lectin binding comparing patient subgroups and controls. (E) Effect of purified immune thrombocytopenia (ITP) immunoglobulin G (IgG) (50 μ g/mL) on RCA-1 lectin binding. (F and G) P-selectin expression on control and patient sera treated platelets. (H) P-selectin expression on platelets treated with GPIIb/IIIa or GPIb/IX antibodies. CTRL: control; Pt: patient; Neg: antibody-negative; Pos: antibody-positive; MFI: mean fluorescence intensity. Data shown as mean \pm standard deviation. Levels of significance are expressed as *P*-values. ns: non-significant, **P*<0.05, ***P*<0.01. Mann Whitney and Kruskal-Wallis test with Dunn's multiple comparison.

clinically relevant is that, anti-GPIIb/IIIa auto-antibodies account for the majority of antibody positive cases in our patient population (Figure 1B), which is consistent with a recent report.⁴³ Therefore, further examination into the pathogenesis of anti-GPIIb/IIIa antibody driven ITP is of clinical significance.

In order to establish the relationship amongst anti-GPIIb/IIIa antibodies, platelet Fc γ R and platelet apoptosis in ITP, we evaluated the impact of Fc γ RIIA inhibition with the monoclonal antibody IV.3 on platelet apoptosis. Platelets were treated with patient sera with or without the presence of IV.3, and the effect on platelet $\Delta\Psi$ m was examined. In the presence of Fc γ RIIA inhibitor, APA' ability to induce loss of $\Delta\Psi$ m was impaired (Figure 3D). The rise in $\Delta\Psi$ m in platelets pretreated with IV.3 was quantified and is shown in Figure 3E. This observation indicates that the anti-GPIIb/IIIa auto-antibodies signal via Fc γ RIIA to initiate platelet apoptosis pathway.

Anti-platelet antibodies have differential effects on the thrombocytopenic pathway

We further examined the differential effects of the most

common APA's on platelet desialylation and apoptosis. Although only nine sera contained anti-GPIIb/IIIa without the presence of anti-GPIb/IX antibodies, six of these antibodies induced NEU1 translocation (defined as mean fluorescence intensity [MFI] greater than 2SD of the controls). In contrast, only one of the five sera with anti-GPIb/IX antibodies, without anti-GPIIb/IIIa, was able to do so (Figure 4A, table 2). To our surprise, four of these five anti-GPIb/IX sera led to platelet apoptosis as reflected by significant loss of $\Delta\Psi$ m (defined as MFI lower than 2SD of the controls) while only three of the nine anti-GPIIb/IIIa sera induced this change (Figure 4B; Table 2). Together, these novel findings indicate that APA specificity is an important determinant of platelet fate in ITP and the missing link between the previously unobserved relationship between platelet desialylation and apoptosis.³⁶

Two patient sera were found to have sole anti-GPV antibodies. Repeated experiments using these two sera did not show evidence of desialylation on donor platelets (Figure 5A). However, treatment of donor platelets using one of the two patients' sera produced significant reduction of DiOC6 fluorescence (Figure 5B). The second

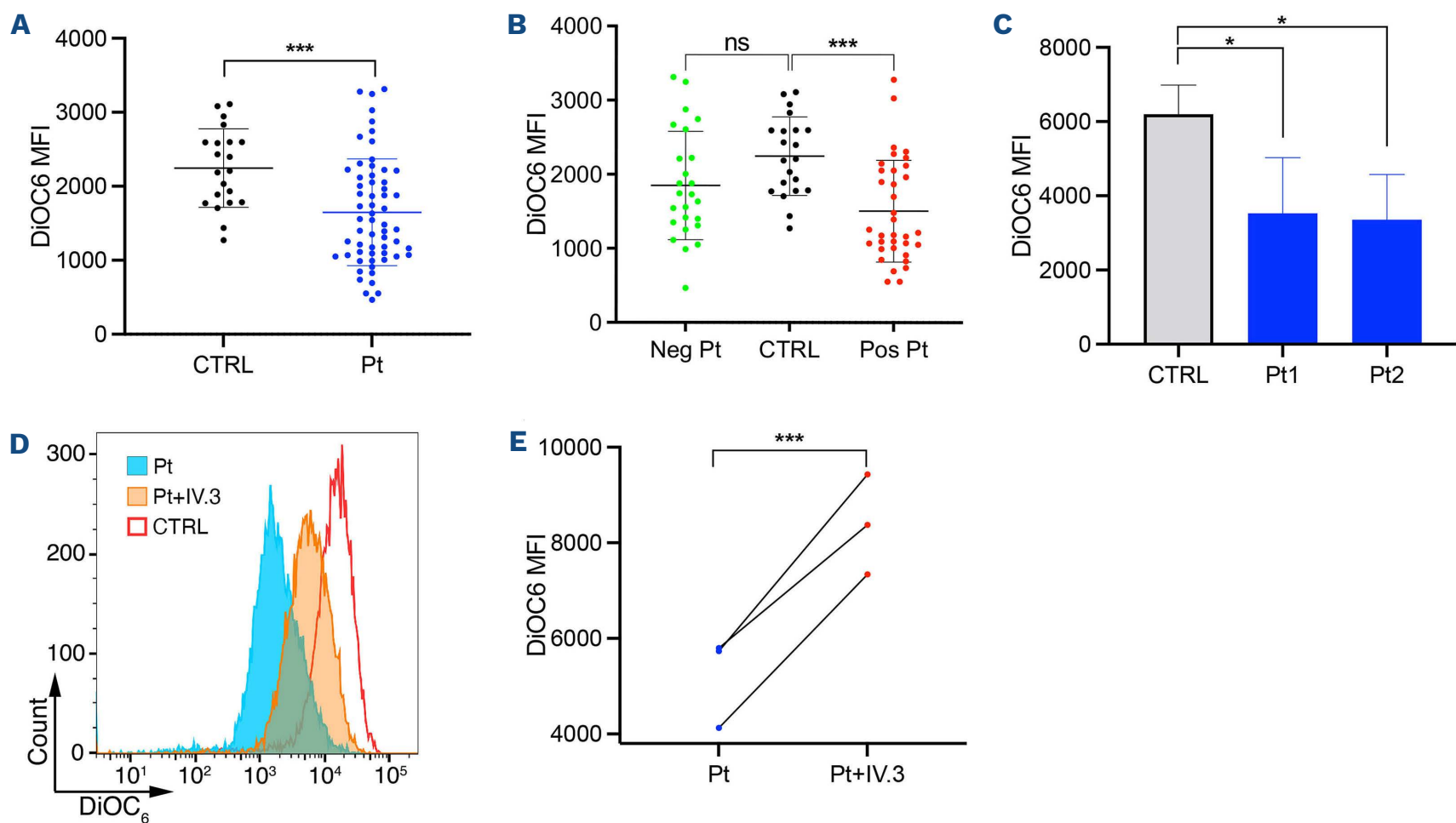


Figure 3. Effect of immune thrombocytopenia sera on platelet apoptosis. Loss of mitochondrial inner transmembrane potential ($\Delta\Psi$ m) as measured by DiOC₆ in platelets treated by (A) immune thrombocytopenia (ITP) patients' (Pt) and controls' sera (CTRL), as well as (B) antibody-positive (Pos) and antibody-negative (Neg) patients' sera. (C) Effect of purified ITP immunoglobulin G (IgG) (50 μ g/mL) on washed platelets. (D) Histogram representing the effect of anti-Fc γ RIIA antibody IV.3 on $\Delta\Psi$ m despite the presence of patient sera. (E) Effect of anti-Fc γ RIIA antibody IV.3 on $\Delta\Psi$ m of 3 patients; data point represents the mean of 3 experiments. MFI: mean fluorescence intensity. Data shown as mean \pm standard deviation. Levels of significance are expressed as *P*-values. ns: non-significant, **P*<0.05, ****P*<0.001. Mann Whitney and Kruskal-Wallis test with Dunn's multiple comparison. Repeated measures ANOVA used in 3E.

Table 2. Relative effects of anti-GPIIb/IIIa and anti-GPIb/IX antibodies on platelet desialylation and apoptosis.

Effect	Anti-GPIIb/IIIa sera	Anti-GPIb/IX sera
Positive NEU1 translocation	67%	20%
Significant loss of $\Delta\Psi_m$	33%	80%

GP: glycoprotein; $\Delta\Psi_m$: mitochondrial inner transmembrane potential.

sample also led to decreased $\Delta\Psi_m$ compared to controls but was not statistically significant ($P=0.15$; Kruskal Wallis with Dunn's multiple comparison), indicating that anti-GPV APA possibly lead to platelet apoptosis. A larger sample size with sole anti-GPV antibody is needed to assess its functional effect on platelets.

Oseltamivir protects platelets from GPIIb/IIIa antibody mediated destruction *in vivo*

Neuraminidase inhibitor oseltamivir has been previously reported to protect platelets from anti-GPIb α monoclonal antibody driven platelet destruction in murine studies.²⁸ More recently, we demonstrated oseltamivir's effect on platelet number preservation in the presence of polyclonal human anti-GPII/IIIa antibody from a patient with acquired Glanzmann Thrombasthenia.³⁷ Following our findings that anti-GPIIb/IIIa antibodies induce desialylation (Figure 4A), we extended our *in vivo* experiments to examine other ITP patients with sole anti-GPIIb/IIIa antibodies. In order to test whether destruction of human platelets could be prevented *in vivo*, we treated recipient mice with oseltamivir. As shown in Figure 6, oseltamivir protected human platelets from anti-GPIIb/IIIa antibody-mediated destruction. Therefore, the protective effect of desialylation inhibitors could be generalized to patients with anti-GPIIb/IIIa antibodies. Oseltamivir reduces platelet destruction in ITP and is potentially an efficacious

treatment for a larger proportion of ITP patients as anti-GPIIb/IIIa antibody is a more common antibody than anti-GPIb α antibody.

Discussion

ITP is a heterogenous disease with multiple proposed mechanisms. Potential therapeutic advances require more detailed understanding of the means that lead to platelet destruction. As such, we sought to examine platelet desialylation and apoptosis as contributors to thrombocytopenia in ITP. We studied 61 ITP patient sera and examined the presence of APA as a predictor for these two processes. Antibody specificity was interrogated, specifically, anti-GPIb/IX, anti-GPIIb/IIIa and GPV antibodies. GPIa was not examined as isolated anti-GPIa/IIa antibody positivity has not been reported in recent literature.^{43,47} We demonstrated that the presence of APA in ITP patients' sera is associated with platelet desialylation in our patient population. Although desialylation was initially thought to be induced by anti-GPIb/IX antibodies in ITP,²⁸ here we found that enhanced neuraminidase expression was observed in the majority of our patient cohort with detectable APA. This supports recent studies which reported that the loss of sialic acid is a more frequent finding in ITP than previously thought.^{36,48} Furthermore, in a murine model of ITP utilising patients' anti-GPIIb/IIIa antibodies and human platelets, we found solid and reproducible³⁶ evidence to support the use of neuraminidase inhibitors as potential new therapeutics for ITP.

The status of whether the patients have detectable ITP antibodies also influences the degree of platelet apoptosis. Sera with ITP antibodies induced significantly greater loss of $\Delta\Psi_m$ compared to the controls, which was not observed in the antibody-negative group. As we and others have found that desialylation depends on FcR activity in

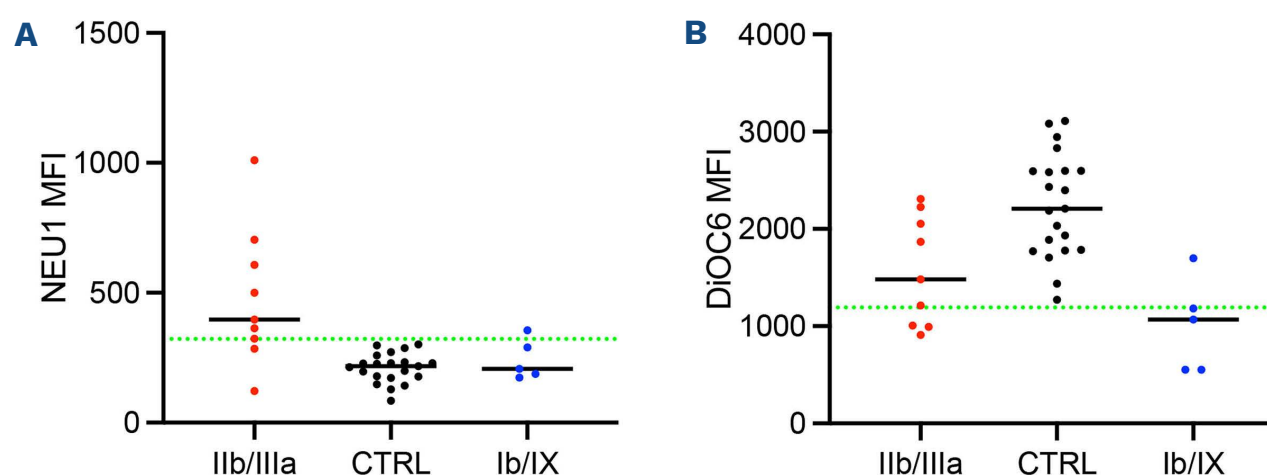


Figure 4. Differential effect of anti-GPIIb/IIIa and anti-GPIb/IX antibodies on NEU1 surface translocation and mitochondrial inner transmembrane potential. (A) Effect on NEU1 surface translocation and (B) on mitochondrial inner transmembrane potential ($\Delta\Psi_m$). CTRL: control. Black horizontal lines represent the means for each group. Green horizontal lines indicate the cutoff for positive samples (2SD over [for NEU1] and under [for DiOC₆] the average of controls). Two patients in the anti-GPIIb/IIIa antibody subgroup and 2 patients in the anti-GPIb/IX subgroup had concomitant anti-GPV antibodies. MFI: mean fluorescence intensity.

anti-GPIIb/IIIa antibody-driven ITP,^{36,37} we further examined the relationship between platelet FcγR and the downstream signaling of these ITP antibodies in platelet apoptosis. FcγRIIa inhibitor IV.3 effectively suppressed antibody-induced platelet loss of ΔΨm, indicating that anti-GPIIb/IIIa antibodies may signal through FcγR to initiate platelet apoptosis.

In addition to the ability to predict desialylation and apoptosis, antibody specificity appears to have an impact on the predominant thrombocytopenic mechanism in ITP. Unlike a prior report,²⁸ we found that anti-GPIIb/IIIa antibodies resulted in higher degree of NEU1 translocation. On the other hand, anti-GPIb/IX antibodies appeared to cause more platelet apoptosis. A recent systematic study examined antibody specificity and platelet/megakaryocyte desialylation.³⁶ The report described no association between antibody-induced desialylation and platelet apoptosis in

ITP.³⁶ However, this study did not report the relationship between antibody specificity and the induction of either desialylation or apoptosis. In our study, the finding of differential effects with respect to the antibody specificity provides a potential new dimension to the understanding of ITP pathogenesis.

The small number of patients containing sole anti-GPV antibodies precludes definite conclusions on its effect on the subsequent platelet events, but it is notable that sera from both patients did not induce desialylation. Interestingly, this result is consistent with the finding by Amini and colleagues, who recently reported the lack of hepatic uptake of Indium-111 labeled platelet in patients with anti-GPV antibodies.⁴⁹ Of note, serum from one anti-GPV positive patient induced significant loss of platelet ΔΨm, indicating anti-GPV may drive ITP via platelet apoptosis. While APA testing is available in specialized platelet lab-

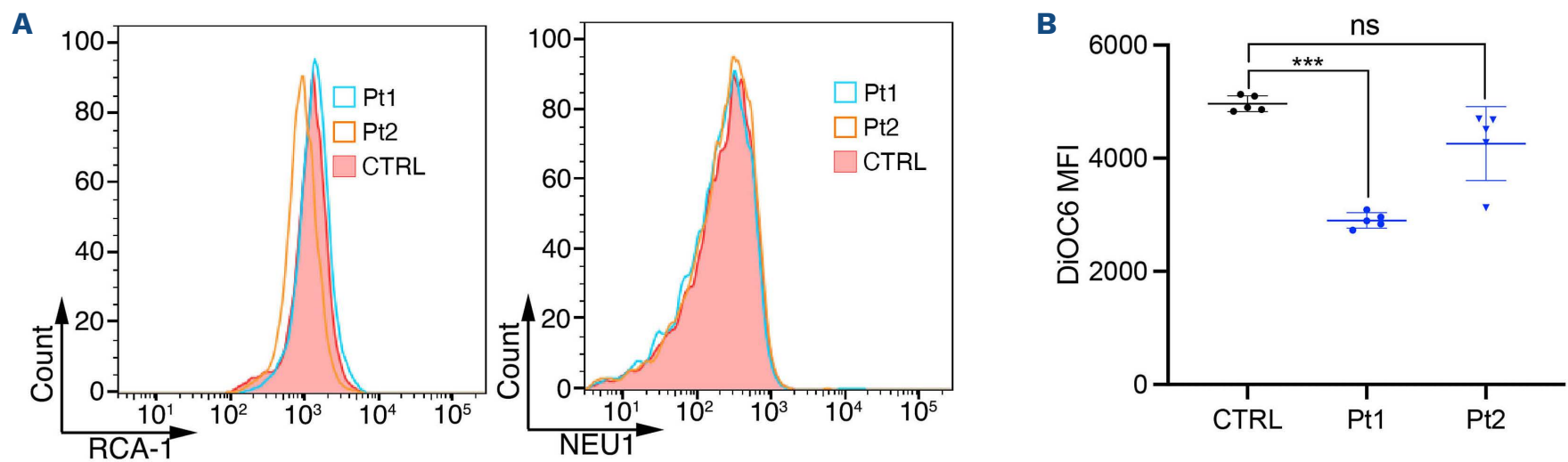


Figure 5. Effect of anti-GPV antibodies on platelet desialylation and apoptosis. (A) Effect on desialylation and (B) on apoptosis. CTRL: control; Pt: patient. Data shown as mean ± standard deviation. ns: non-significant, ****P*<0.001. Kruskal-Wallis test with Dunn’s multiple comparison. MFI: mean fluorescence intensity.

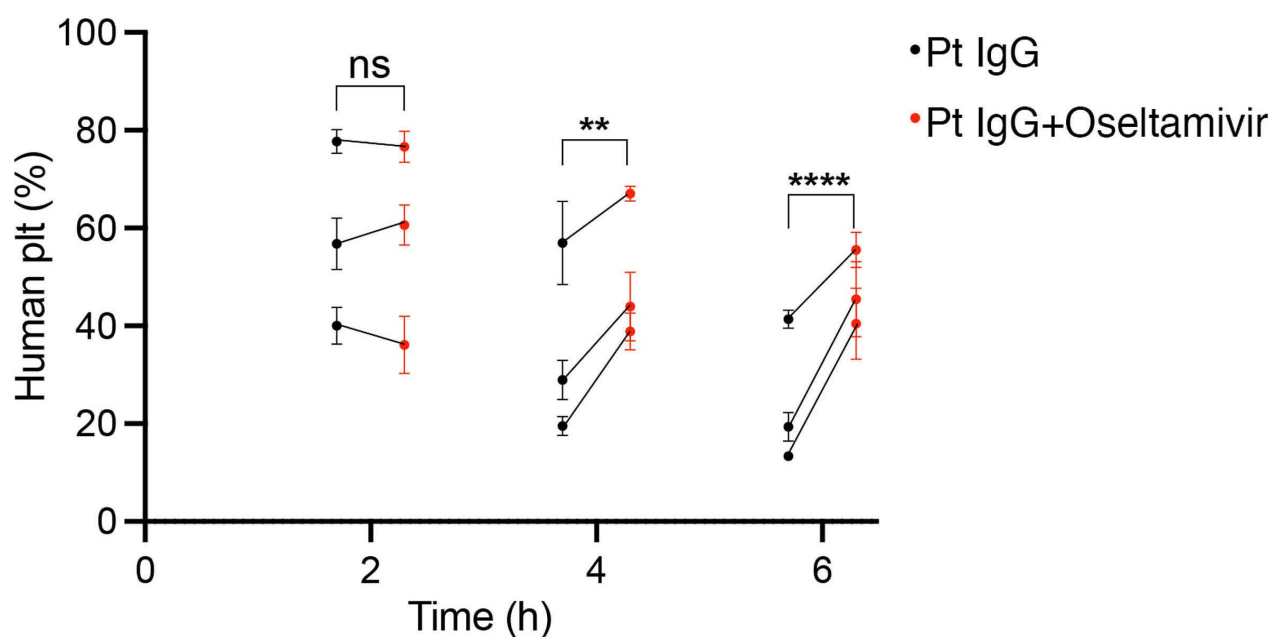


Figure 6. Murine model of immune thrombocytopenia with anti-GPIIb/IIIa antibodies. Effect of 3 immune thrombocytopenia (ITP) patients’ (Pt) immunoglobulin G (IgG) (black dots) and oseltamivir treatment (red dots) in the presence of patient IgG, on human platelet (plt) survival in NOD/SCID mice (n=5 for each patient group) measured as human platelet percentage at 2, 4, and 6 hours after IgG injection. Data shown as mean ± standard error of the mean. Levels of significance are expressed as *P*-values. ns: non-significant, ***P*<0.01, *****P*<0.0001. Linear mixed model. NOD/SCID: non-obese diabetic/severe combined immunodeficient.

oratories, routine testing has not been recommended, and ITP remains a disease without any confirmatory investigation or a “gold standard” test. Given the additional important information provided by a positive result, which is the ability of patients’ antibodies to induce platelet desialylation and apoptosis, we suggest ITP antibody testing to be incorporated into ITP management algorithm. It may provide new insight into ITP pathology and could guide treatment individualization.

The main weakness of our study is that it was performed on stored patient samples. Prospective evaluation of pathological ITP sera would allow us to correlate the sera’s ability to induce desialylation and apoptosis with patients’ treatment and disease response. Another significant limitation in using stored samples is the lack of direct testing on patient platelets. Direct glycoprotein-specific APA assays will improve testing sensitivity^{43,50} and is the recommended test by the International Society of Thrombosis and Hemostasis (ISTH).⁵¹ Nevertheless, indirect examination allowed us to determine the impact of APA present in the patient serum on donor platelets and compared such effect of different patient samples as well as with controls.

Another limitation is the small number of patients with single APA specificity. Larger sample size is desirable to capture the difference between each antibody type and the associated downstream effect on platelet survival more accurately, which may ultimately lead to ITP treatment individualization. An additional challenge is the difficulties in performing platelet antibody testing outside specialized laboratories. In agreement with the ISTH recommendation, we recommend referral of platelet immunology tests to a centralized laboratory, where staff are adequately trained in specialized methods to minimize laboratory variability.⁵¹

In conclusion, we report the predictive capability of APA in relation to the potential underlying ITP mechanisms, specifically platelet desialylation and apoptosis. We showed the differential effects of antibody subtypes on these two ITP pathogenesis pathways and the role of FcγR on anti-GPIIb/IIIa antibodies induced platelet apoptosis.

We also demonstrated the therapeutic effect of neuraminidase inhibitor in platelet preservation despite the presence of anti-GPIIb/IIIa antibodies. Hence, such treatment can potentially be applied to most ITP patients since it is likely that both anti-GPIIb/IIIa antibodies (this study) and anti-GPIb/IX antibodies²⁸ lead to platelet desialylation. Further collaboration is required to investigate the treatment potential using neuraminidase and/or apoptosis inhibitors in prospective randomized ITP clinical trials.

Disclosures

No conflicts of interest to disclose.

Contributions

SSZ designed and performed experiments, collected, and analyzed the data, and wrote the manuscript; ZA, HLL, RW, FY performed the experiments; JSP and BHC contributed equally, provided project supervision, and reviewed the manuscript. All authors read and approved the manuscript.

Acknowledgements

The authors thank Dr. Zhixin Liu (Stats Central, UNSW) for her statistical expertise.

Funding

This work was supported by the National Health and Medical Research Council project grant to BHC (GNT 1012409) as well as St. George and Sutherland Medical Research Foundation Grant to JSP. SSZ received NSW Ministry of Health PhD Scholarship. In Vivo data presented in this work was acquired at the Mark Wainright Analytical Centre (MWAC) of UNSW Sydney, which is in part funded by the Research Infrastructure Program of UNSW.

Data-sharing statement

Data that support the findings of this study are available from the corresponding author upon reasonable request. All data generated or analysed are included in this published article.

References

1. Johnsen J. Pathogenesis in immune thrombocytopenia: new insights. *Hematology Am Soc Hematol Educ Program*. 2012;2012:306-312.
2. Zufferey A, Kapur R, Semple JW. Pathogenesis and therapeutic mechanisms in immune thrombocytopenia (ITP). *J Clin Med*. 2017;6(2):16.
3. Arkfeld DG, Weitz IC. Immune thrombocytopenia in patients with connective tissue disorders and the antiphospholipid antibody syndrome. *Hematol Oncol Clin North Am*. 2009;23(6):1239-1249.
4. Cines DB BJ, Liebman HA, Luning Prak ET. The ITP syndrome: pathogenic and clinical diversity. *Blood*. 2009;113(26):6511-6521.
5. Krauth MT, Puthenpambil J, Lechner K. Paraneoplastic autoimmune thrombocytopenia in solid tumors. *Crit Rev Oncol Hematol*. 2012;81(1):75-81.
6. Abrahamson PE, Hall SA, Feudjo-Tepie M, Mitrani-Gold FS, Logie J. The incidence of idiopathic thrombocytopenic purpura among adults: a population-based study and literature review. *Eur J Haematol*. 2009;83(2):83-89.
7. Schoonen WM, Kucera G, Coalson J, et al. Epidemiology of im-

- immune thrombocytopenic purpura in the General Practice Research Database. *Br J Haematol.* 2009;145(2):235-244.
8. Moulis G, Palmaro A, Montastruc JL, Godeau B, Lapeyre-Mestre M, Sailler L. Epidemiology of incident immune thrombocytopenia: a nationwide population-based study in France. *Blood.* 2014;124(22):3308-3315.
 9. Audia S, Mahévas M, Nivet M, Ouandji S, Ciudad M, Bonnotte B. Immune thrombocytopenia: recent advances in pathogenesis and treatments. *Hemasphere.* 2021;5(6):e574-e574.
 10. Segal JB, Powe NR. Prevalence of immune thrombocytopenia: analyses of administrative data. *J Thromb Haemost.* 2006;4(11):2377-2383.
 11. Harrington WJ, Minnich V, Hollingsworth JW, Moore CV. Demonstration of a thrombocytopenic factor in the blood of patients with thrombocytopenic purpura. *J Lab Clin Med.* 1951;38(1):1-10.
 12. Schwartz RS. Immune thrombocytopenic purpura--from agony to agonist. *N Engl J Med.* 2007;357(22):2299-2301.
 13. Shulman NR, Marder VJ, Weinrach RS. Similarities between known antiplatelet antibodies and the factor responsible for thrombocytopenia in idiopathic purpura. Physiologic, serologic and isotopic studies. *Ann N Y Acad Sci.* 1965;124(2):499-542.
 14. Cines DB, Cuker A, Semple JW. Pathogenesis of immune thrombocytopenia. *Presse Med.* 2014;43(4P2):e49-e59.
 15. Semple JW, Rebetz J, Maouia A, Kapur R. An update on the pathophysiology of immune thrombocytopenia. *Curr Opin Hematol.* 2020;27(6):423-429.
 16. Stasi R, Cooper N, Del Poeta G, et al. Analysis of regulatory T-cell changes in patients with idiopathic thrombocytopenic purpura receiving B cell-depleting therapy with rituximab. *Blood.* 2008;112(4):1147-1150.
 17. Liu B, Zhao H, Poon MC, et al. Abnormality of CD4(+)CD25(+) regulatory T cells in idiopathic thrombocytopenic purpura. *Eur J Haematol.* 2007;78(2):139-143.
 18. Ling Y, Cao X, Yu Z, Ruan C. Circulating dendritic cells subsets and CD4+Foxp3+ regulatory T cells in adult patients with chronic ITP before and after treatment with high-dose dexamethasone. *Eur J Haematol.* 2007;79(4):310-316.
 19. Olsson B, Andersson PO, Jernas M, et al. T-cell-mediated cytotoxicity toward platelets in chronic idiopathic thrombocytopenic purpura. *Nat Med.* 2003;9(9):1123-1124.
 20. Zhang F, Chu X, Wang L, et al. Cell-mediated lysis of autologous platelets in chronic idiopathic thrombocytopenic purpura. *Eur J Haematol.* 2006;76(5):427-431.
 21. Zhao C, Li X, Zhang F, Wang L, Peng J, Hou M. Increased cytotoxic T-lymphocyte-mediated cytotoxicity predominant in patients with idiopathic thrombocytopenic purpura without platelet autoantibodies. *Haematologica.* 2008;93(9):1428-1430.
 22. Ma L, Simpson E, Li J, et al. CD8⁺ T cells are predominantly protective and required for effective steroid therapy in murine models of immune thrombocytopenia. *Blood.* 2015;126(2):247-256.
 23. Swinkels M, Rijkers M, Voorberg J, Vidarsson G, Leebeek FWG, Jansen AJG. Emerging concepts in immune thrombocytopenia. *Front Immunol.* 2018;9:880.
 24. Leytin V, Mykhalov S, Starkey AF, et al. Intravenous immunoglobulin inhibits anti-glycoprotein IIb-induced platelet apoptosis in a murine model of immune thrombocytopenia. *Br J Haematol.* 2006;133(1):78-82.
 25. Winkler J, Kroiss S, Rand ML, et al. Platelet apoptosis in paediatric immune thrombocytopenia is ameliorated by intravenous immunoglobulin. *Br J Haematol.* 2012;156(4):508-515.
 26. Goette NP, Glembotsky AC, Lev PR, et al. Platelet apoptosis in adult immune thrombocytopenia: insights into the mechanism of damage triggered by auto-antibodies. *PLoS One.* 2016;11(8):e0160563.
 27. Nieswandt B, Bergmeier W, Rackebrandt K, Gessner JE, Zirngibl H. Identification of critical antigen-specific mechanisms in the development of immune thrombocytopenic purpura in mice. *Blood.* 2000;96(7):2520-2527.
 28. Li J, Van Der Wal DE, Zhu G, et al. Desialylation is a mechanism of Fc-independent platelet clearance and a therapeutic target in immune thrombocytopenia. *Nat Commun.* 2015;6:7737.
 29. Chan H, Moore JC, Finch CN, Warkentin TE, Kelton JG. The IgG subclasses of platelet-associated autoantibodies directed against platelet glycoproteins IIb/IIIa in patients with idiopathic thrombocytopenic purpura. *Br J Haematol.* 2003;122(5):818-824.
 30. Webster ML, Sayeh E, Crow M, et al. Relative efficacy of intravenous immunoglobulin G in ameliorating thrombocytopenia induced by antiplatelet GPIIb/IIIa versus GPIIb/IIIa antibodies. *Blood.* 2006;108(3):943-946.
 31. Go RS, Johnston KL, Bruden KC. The association between platelet autoantibody specificity and response to intravenous immunoglobulin G in the treatment of patients with immune thrombocytopenia. *Haematologica.* 2007;92(2):283-284.
 32. Peng J, Ma SH, Liu J, et al. Association of autoantibody specificity and response to intravenous immunoglobulin G therapy in immune thrombocytopenia: a multicenter cohort study. *J Thromb Haemost.* 2014;12(4):497-504.
 33. Cantoni S, Carpenedo M, Nichelatti M, et al. Clinical relevance of antiplatelet antibodies and the hepatic clearance of platelets in patients with immune thrombocytopenia. *Blood.* 2016;128(17):2183-2185.
 34. Rumjantseva V, Grewal PK, Wandall HH, et al. Dual roles for hepatic lectin receptors in the clearance of chilled platelets. *Nat Med.* 2009;15(11):1273-1280.
 35. Zhang H, Nimmer PM, Tahir SK, et al. Bcl-2 family proteins are essential for platelet survival. *Cell Death Differ.* 2007;14(5):943-951.
 36. Marini I, Zlamal J, Faul C, et al. Autoantibody-mediated desialylation impairs human thrombopoiesis and platelet lifespan. *Haematologica.* 2021;106(1):196-207.
 37. Zheng SS, Perdomo JS, Leung HHL, Yan F, Chong BH. Acquired Glanzmann thrombasthenia associated with platelet desialylation. *J Thromb Haemost.* 2020;18(3):714-721.
 38. Zheng SS, Perdomo JS, Ahmadi Z, Chong BH. Indirect detection of anti-platelet antibodies in immune thrombocytopenia. *Pathology.* 2021;53(6):759-762.
 39. Rodeghiero F, Stasi R, Gernsheimer T, et al. Standardization of terminology, definitions and outcome criteria in immune thrombocytopenic purpura of adults and children: report from an international working group. *Blood.* 2009;113(11):2386-2393.
 40. Provan D, Arnold DM, Bussel JB, et al. Updated international consensus report on the investigation and management of primary immune thrombocytopenia. *Blood Adv.* 2019;3(22):3780-3817.
 41. Brighton TA, Evans S, Castaldi PA, Chesterman CN, Chong BH. Prospective evaluation of the clinical usefulness of an antigen-specific assay (MAIPA) in idiopathic thrombocytopenic purpura and other immune thrombocytopenias. *Blood.* 1996;88(1):194-201.
 42. Liang SX, Pinkevych M, Khachigian LM, Parish CR, Davenport MP, Chong BH. Drug-induced thrombocytopenia: development of a novel NOD/SCID mouse model to evaluate clearance of circulating platelets by drug-dependent antibodies and the efficacy of IVIG. *Blood.* 2010;116(11):1958-1960.
 43. Al-Samkari H, Rosovsky RP, Karp Leaf RS, et al. A modern reassessment of glycoprotein-specific direct platelet autoantibody testing in immune thrombocytopenia. *Blood Adv.* 2019;4(1):9-18.

44. Vollenberg R, Jouni R, Norris PAA, et al. Glycoprotein V is a relevant immune target in patients with immune thrombocytopenia. *Haematologica*. 2019;104(6):1237-1243.
45. Porcelijn L, Schmidt DE, van der Schoot CE, Vidarsson G, de Haas M, Kapur R. Anti-glycoprotein Ib α autoantibodies do not impair circulating thrombopoietin levels in immune thrombocytopenia patients. *Haematologica*. 2020;105(4):e172-e174.
46. Yamamoto K, Kawasaki N. Chapter Eleven - Detection of Weak-Binding Sugar Activity Using Membrane-Based Carbohydrates. In: Fukuda M, ed. *Methods in Enzymology*: Academic Press. 2010:233-240.
47. Porcelijn L, Huiskes E, Oldert G, Schipperus M, Zwaginga JJ, de Haas M. Detection of platelet autoantibodies to identify immune thrombocytopenia: state of the art. *Br J Haematol*. 2018;182(3):423-426.
48. Grodzielski M, Goette NP, Glembotsky AC, et al. Multiple concomitant mechanisms contribute to low platelet count in patients with immune thrombocytopenia. *Sci Rep*. 2019;9(1):2208.
49. Amini SN, Porcelijn L, Sobels A, et al. Anti-glycoprotein antibodies and sequestration pattern of indium labeled platelets in immune thrombocytopenia. *Blood Adv*. 2022;6(6):1797-1803
50. Vrbensky JR, Moore JE, Arnold DM, Smith JW, Kelton JG, Nazy I. The sensitivity and specificity of platelet autoantibody testing in immune thrombocytopenia: a systematic review and meta-analysis of a diagnostic test. *J Thromb Haemost*. 2019;17(5):787-794.
51. Arnold DM, Santoso S, Greinacher A. Platelet Immunology Scientific Subcommittee of the ISTH. Recommendations for the implementation of platelet autoantibody testing in clinical trials of immune thrombocytopenia. *J Thromb Haemost*. 2012;10(4):695-697.

Specific inhibition of the transporter MRP4/ABCC4 affects multiple signaling pathways and thrombus formation in human platelets

Robert Wolf,^{1,2} Sophie Grammbauer,¹ Raghavendra Palankar,³ Céline Tolksdorf,^{1,4} Eileen Moritz,^{1,2} Andreas Böhm,¹ Mahmoud Hasan,¹ Annika Hafkemeyer,¹ Andreas Greinacher,³ Mladen V. Tzvetkov,¹ Bernhard H. Rauch^{1,2,4#} and Gabriele Jedlitschky^{1#}

¹Department of General Pharmacology, Center of Drug Absorption and Transport (C_DAT), University Medicine Greifswald, Greifswald; ²German Center for Cardiovascular Research (DZHK), Partner Site Greifswald; ³Department of Immunology and Transfusion Medicine, University Medicine Greifswald, Greifswald and ⁴Department of Human Medicine, Section of Pharmacology and Toxicology, Carl von Ossietzky University of Oldenburg, Oldenburg, Germany

[#]BHR and GJ contributed equally as co-senior authors.

Correspondence: G. Jedlitschky
gabriele.jedlitschky@med.uni-greifswald.de

Received: August 4, 2021.

Accepted: March 9, 2022.

Prepublished: March 17, 2022.

<https://doi.org/10.3324/haematol.2021.279761>

©2022 Ferrata Storti Foundation

Published under a CC BY-NC license



Abstract

The multidrug resistance protein 4 (MRP4) is highly expressed in platelets and several lines of evidence point to an impact on platelet function. MRP4 represents a transporter for cyclic nucleotides as well as for certain lipid mediators. The aim of the present study was to comprehensively characterize the effect of a short-time specific pharmacological inhibition of MRP4 on signaling pathways in platelets. Transport assays in isolated membrane vesicles showed a concentration-dependent inhibition of MRP4-mediated transport of cyclic nucleotides, thromboxane (Tx)B2 and fluorescein (FITC)-labeled sphingosine-1-phosphate (S1P) by the selective MRP4 inhibitor Ceefourin-1. In *ex vivo* aggregometry studies in human platelets, Ceefourin-1 significantly inhibited platelet aggregation by about 30-50% when ADP or collagen was used as activating agents, respectively. Ceefourin-1 significantly lowered the ADP-induced activation of integrin α IIb β 3, indicated by binding of FITC-fibrinogen (about 50% reduction at 50 μ M Ceefourin-1), and reduced calcium influx. Furthermore, pre-incubation with Ceefourin-1 significantly increased PGE₁- and cinaciguat-induced vasodilator-stimulated phosphoprotein (VASP) phosphorylation, indicating increased cytosolic cAMP as well as cGMP concentrations, respectively. The release of TxB2 from activated human platelets was also attenuated. Finally, selective MRP4 inhibition significantly reduced both the total area covered by thrombi and the average thrombus size by about 40% in a flow chamber model. In conclusion, selective MRP4 inhibition causes reduced platelet adhesion and thrombus formation under flow conditions. This finding is mechanistically supported by inhibition of integrin α IIb β 3 activation, elevated VASP phosphorylation and reduced calcium influx, based on inhibited cyclic nucleotide and thromboxane transport as well as possible further mechanisms.

Introduction

The multidrug resistance protein 4 (MRP4) (ABCC4) is a member of the MRP/CFTR subfamily (C-branch) of the ATP-binding cassette (ABC) transporters, a family of proteins that mediate an ATP-driven transmembrane transport of compounds. It represents a very versatile transporter, which is expressed in several tissues with high amounts in platelets.¹⁻⁴ Its substrate spectrum covers several drugs, namely nucleoside-based antiviral and anti-cancer agents but interestingly also a number of endogenous signaling molecules. These include primarily the cyclic nucleotides cAMP and cGMP.^{5,6} MRP4 has been established as an inde-

pendent regulator of intracellular cAMP levels and of cell proliferation and differentiation in several cell types, including vascular smooth muscle cells as well as hematopoietic cells.^{7,8} Furthermore, cyclic nucleotides play a major role in platelet activation and regulation. In MRP4-deficient mice, dysregulation of platelet cAMP homeostasis was observed.⁹⁻¹¹ This dysregulation may be due to reduced cAMP efflux and/or intracellular sequestration since the exact localization of MRP4 in resting platelets has yet to be clarified. There is evidence for plasma membrane localization,¹⁰ but also for a partial intracellular localization of MRP4 in association with the dense granule markers.^{1-3,11} In addition, Cheepala *et al.* reported a reduced plasma membrane lo-

calization of the major collagen receptor GPVI and inhibition of collagen-induced platelet aggregation in their knockout mouse model.¹⁰ While the role of MRP4 in cAMP signaling is well established, its role in platelet cGMP homeostasis and other cAMP-independent pathways is less clear. MRP4 also transports lipid mediators such as eicosanoids and may directly mediate the export of thromboxane from platelets.^{12,13} In addition, we showed that MRP4 is also involved in the release of sphingosine-1-phosphate (S1P), a potent pro-inflammatory mediator, from platelets.¹⁴ Thus, MRP4 appears to be an essential factor in the paracrine function of platelets. Based on these findings, the transporter has emerged as a potential target to interfere with platelet function.^{1,3,6,9-11,14} MRP4 inhibitors may complement the currently used aggregation inhibitors, whereby especially platelet hyperreactivity as well as platelet-induced inflammatory processes may be reduced. Enhanced platelet reactivity has been linked to MRP4 overexpression in cases of aspirin resistance^{3,15,16} as well as in patients infected with the human immunodeficiency virus (HIV).¹⁷ The present study aimed to comprehensively characterize the effect of a selective MRP4 inhibitor on different mediators and signaling pathways in platelets, thereby evaluating the impact of a short-term pharmacological MRP4 inhibition on the function of human platelets. In previous studies, often rather unspecific inhibitors such as the leukotriene receptor antagonist MK571¹⁸ were used to inhibit MRP4.^{19,20} Meanwhile, more selective inhibitors of MRP4, namely Ceefourin-1,²¹ have become available. Effects on thrombus formation were also studied in a microfluidic flow chamber model to mimic physiological shear stress in both whole human blood and in samples from MRP4-deficient compared to control mice.

Methods

More details are provided in the *Online Supplementary Appendix*.

Human blood samples and animals

Human venous blood was taken from healthy volunteers after written informed consent according to the Declaration of Helsinki and approval from the Institutional Ethics Committee. Mrp4-deficient (Mrp4 (-/-)) mice were kindly provided by the late Dr. Gary D. Kruh (Cancer Center, University of Illinois, Chicago, IL, USA) and were maintained and backcrossed to C57BL/6 wild-type (WT) animals at the animal facility of the University Medicine Greifswald. Murine blood was obtained by right ventricular heart puncture.

Light transmission aggregometry and platelet thromboxane release

For aggregometry, platelet-rich plasma (PRP) was pre-

pared from human citrate blood as described¹⁴ and pre-incubated with Ceefourin-1, aspirin or cinaciguat as stated in the figure legends. For measurement of thromboxane release, washed platelets were pre-incubated with Ceefourin-1 and activated with collagen-related peptide CRP-XL and thrombin receptor-activating peptide PAR1-AP (15 minutes [min]). Concentrations of TxB2 in separated platelets and supernatants were determined by liquid chromatography-tandem mass spectrometry (LC-MS/MS).

Flow cytometric analyses

Fibrinogen binding to integrin $\alpha IIb\beta 3$ - PRP was diluted in HEPES-buffered saline (HBS), pre-incubated with Ceefourin-1 (10-50 μ M) (15 min) and stimulated with either CRP-XL or ADP (10 min), before FITC-labeled human fibrinogen and R-phycoerythrin anti-human-CD62P were added (for supplier see the *Online Supplementary Appendix*). After 20 min, samples were fixed in 0.2% formaldehyde and subjected to flow cytometric acquisition.

VASP phosphorylation - Washed platelets were resuspended in HBS and pre-incubated with either Ceefourin-1 (50 μ M) alone or with Ceefourin-1 added to PGE₁ or cinaciguat (0.5-1 μ M). Platelets were fixed with formaldehyde and permeabilized with Triton-X100. Phospho-specific antibodies either against serine residue 157 or serine residue 239 of vasodilator-stimulated phosphoprotein (VASP) and the respective Alexa Fluor 488-conjugated secondary antibodies were added for flow cytometric analysis.

Calcium measurements

Washed platelets were incubated with Fura-2 AM and subjected to ratiometric calcium analysis using a fluorescence spectrophotometer (excitation 340/380 nm, emission 510 nm).

Flow chamber experiments

Parallel channel flow chambers (ibidi μ -slide VI 0.1, Gräfelting, Germany) were coated with Horm collagen (Takeda Pharmaceutical, Berlin, Germany). Human or murine blood was anticoagulated with hirudin (525 ATU/mL) and heparin (5 IU/mL) or with PPACK (Cayman Chemical, Ann Arbor, MI, USA) (400 μ M) and hirudin, respectively. Platelet specific antibodies (FITC-labeled anti-human CD42a or DyLight 488-conjugated anti-mouse GPIIb β) (for supplier see the *Online Supplementary Appendix*) were added and blood was incubated with Ceefourin-1 or the respective solvent at 37°C. Blood was perfused through the microchannels under high arterial shear conditions (1,800⁻¹) for 5 min. After completion of the experiment, two images at the beginning, two at the end and one in the center of the channel were obtained, using a confocal laser scanning microscope (Carl Zeiss LSM 780, Oberkochen, Germany) (40x objective). Size of thrombi and surface area coverage

were analyzed with ImageJ²² software. Image segmentation was performed in Bitplane Imaris version 7.65. (Oxford Instruments, Abingdon, UK) using the surfaces creation wizard algorithm.²³ All flow experiments were performed according to International Society on Thrombosis and Hemostasis Scientific and Standardization Committee (ISTH SSC) recommendations.²⁴

Results

Ceefourin-1 effectively inhibits MRP4-mediated transport of several signaling compounds *in vitro*

In order to evaluate how effectively Ceefourin-1 interferes with the direct ATP-dependent transport of several signaling compounds, transport assays using inside-out membrane vesicles containing recombinant human MRP4 were performed. ATP-dependent transport of ³H-labeled cGMP was inhibited with a half maximal inhibitory concentration (IC₅₀) value of 5.7 μM, indicating that the transport of cyclic nucleotides is affected by Ceefourin-1 with high affinity (*Online Supplementary Figure S1A*). Also the more lipophilic substrates TxB2 and S1P were actively transported by MRP4, confirming previous studies.^{13,14} TxB2 transport could be blocked by Ceefourin-1 with nearly the same *in vitro* potency (IC₅₀: 3.6 μM) as cGMP transport (*Online Supplementary Figure S1B*). However, higher concentrations of Ceefourin-1 were required to interfere with S1P transport (IC₅₀ of about 50 μM) (*Online Supplementary Figure S1C*).

MRP4 inhibition reduces the release of thromboxane from human platelets

Since the ATP-dependent TxB2 transport was potently inhibited by Ceefourin-1 in the membrane vesicle assay, the impact of MRP4 inhibition on thromboxane release by stimulated human platelets *ex vivo* was further investigated. For this, incubation of the platelets with Ceefourin-1 was performed prior to the addition of CRP-XL or PAR1-AP, which activate collagen or thrombin receptors, respectively. Subsequently, concentrations of TxB2 (the stable metabolite of TxA2) were measured in platelet supernatants and the respective pellets by LC-MS/MS. In order to validate the results, we compared this method with an established enzyme-linked immunosorbent assay (ELISA) and found only a negligible inter-method variability (*Online Supplementary Figure S2*). Basal TxB2 release in control platelets was 2.27±0.39 pg/10⁶ platelets and increased strongly upon stimulation with CRP-XL (1 μg/mL) and PAR1-AP (50 μM) to 5.96±1.56 pg/10⁶ and 5.91±1.64 pg/10⁶ platelets, respectively. In comparison, pre-treatment with Ceefourin-1 led to a significant decrease in basal as well as CRP-XL- and PAR1-AP-induced TxB2 release (Figure 1A). In addition, also the total amount of TxB2 (supernatant and pellet combined) was significantly re-

duced by Ceefourin-1 in CRP-XL- and PAR1-AP-treated samples (Figure 1B). This indicates that TxB2 formation is also affected by MRP4 inhibition. However, further analyses of our data revealed that the relative TxB2 release, which was calculated from the fraction released divided by the total amount, was still significantly diminished. In platelets stimulated with CRP-XL (1 μg/mL) 35.8±3.3% were released in the presence of Ceefourin-1 (vs. control: 45.0±1.5%) and with PAR1-AP (50 μM) 36.4±4.7% (vs. control: 48.0±7.8%) (Figure 1C). This suggests that Ceefourin-1 attenuates platelet TxB2 release via a diminished TxB2 synthesis during activation combined with a direct effect on the TxB2 transport across the plasma membrane.

Ceefourin-1 treatment impairs platelet aggregation in human and murine PRP

Light transmission aggregometry with different stimuli was performed to investigate, whether short-time exposure of PRP to Ceefourin-1 leads to impaired platelet aggregation. MRP4 inhibition resulted in a reduction of maximum platelet aggregation, with the most prominent effect (about 50% inhibition at 10 μM Ceefourin-1) being observed with the strong agonist collagen (5 μg/mL) (38.3±10.3% aggregation vs. 77.3±4.0% for the solvent control) (Figure 2). Although less pronounced, a significant effect on aggregation was also observed in ADP- and PAR1-AP-stimulated platelets (27% and 13% reduction at 10 μM Ceefourin-1, respectively), while the synthetic thromboxane analog U46619 had no significant effect. In comparison, aspirin was used to block thromboxane synthesis, leading, as expected, to a reduced aggregation with the most pronounced effect also with collagen-induced activation (63% at 30 μM aspirin). When both compounds were combined, only a tendency towards an additive effect was observed, which, however, was not statistically significant. These results further substantiate the finding of MRP4 being involved in the release of thromboxane, not excluding its potential role in intrinsically controlling platelet activation and, therefore, thromboxane production.

Since several MRP4-inhibiting compounds show significant off-target effects, we performed platelet aggregation experiments with PRP from WT and *Mrp4*-deficient mice to verify the selectivity of Ceefourin-1. In line with previous studies,^{9,10} the *Mrp4* knockout led to an impaired aggregation response to collagen stimulation (30.7±5.7% vs. 46.7±3.8% aggregation with 10 μg/mL collagen) (Figure 2C). A similar reduction was achieved by the treatment with Ceefourin-1 in WT platelets (31.3±3.9% vs. 46.7±3.8%). However, Ceefourin-1 resulted in no further attenuation of aggregation in the *Mrp4*-deficient platelets, indicating that the effect of Ceefourin-1 on platelet function is only due to MRP4 inhibition. Ceefourin-1 also reduced platelet aggregation after stimulation with ADP only in the WT platelets (*Online Supplementary Figure S3*).

In addition, we evaluated the effect of Ceefourin-1 on platelet viability using an assay based on the intracellular calcein accumulation as described in the *Online Supplementary Appendix*. Ceefourin-1 in concentrations of up to 50 μM had no significant effect on platelet viability compared to the solvent control (*Online Supplementary Figure S4*).

Platelet fibrinogen binding and calcium influx is inhibited by Ceefourin-1

The impact of Ceefourin-1 on different sub-aspects of platelet activation, like integrin $\alpha\text{IIb}\beta\text{3}$ activation and α -granule release were assessed by flow cytometric analyses of fluorescence-labeled fibrinogen and anti-CD62P antibody binding. Fibrinogen binding was significantly reduced by Ceefourin-1 ($80.9\pm 4.9\%$ and $75.3\pm 4.0\%$ of control with 30 μM and 50 μM Ceefourin-1, respectively) at a sub-maximal concentration of CRP-XL (Figure 3A). ADP-induced fibrinogen binding was also markedly abrogated to $47.1\pm 7.3\%$ of control with 50 μM Ceefourin-1 (Figure 3B). Higher concentrations of the agonists led to a less pronounced effect of MRP4 inhibition, which disappeared completely at the highest concentrations used. Additionally, we found CD62P surface exposure to be significantly reduced upon stimulation with ADP but not with CRP-XL (Figure 3C and D).

Since calcium is essential for the change in conformation of integrin $\alpha\text{IIb}\beta\text{3}$, allowing it to bind fibrinogen, we measured the increase of free cytosolic calcium in Fura-2-loaded human platelets (Figure 4A to C). In order to discriminate between calcium influx and mobilization from intracellular stores, platelets were activated in the presence (left panels) or absence (right panels) of external calcium. Blocking MRP4 entails a reduction in the area under the fluorescence curve (area under the curve [AUC]) upon stimulation with ADP, resulting predominantly from an impaired calcium influx (8.0 ± 0.5 vs. 11.4 ± 0.8 R(340/380)*s in calcium-containing medium). The signal in calcium-free medium, reflecting mobilization from intracellular stores, was markedly lower. However, there was also a trend towards reduced AUC values after incubation with Ceefourin-1 for the calcium mobilization, which became statistically significant when the decrease was calculated relative to the respective solvent control of each blood sample donor (separate experiment) (Figure 4C).

Ceefourin-1 enhances VASP phosphorylation and cyclic nucleotide-dependent platelet inhibition

The cyclic nucleotides cGMP and cAMP are important second messengers involved in platelet inhibition, especially by endothelium-derived factors, such as nitric oxide (NO) or prostacyclin (PGI₂). Both cGMP and cAMP are able to activate protein kinases (PK), leading to the phosphorylation and inhibition of proteins, which are involved in the signaling for platelet activation. In order to

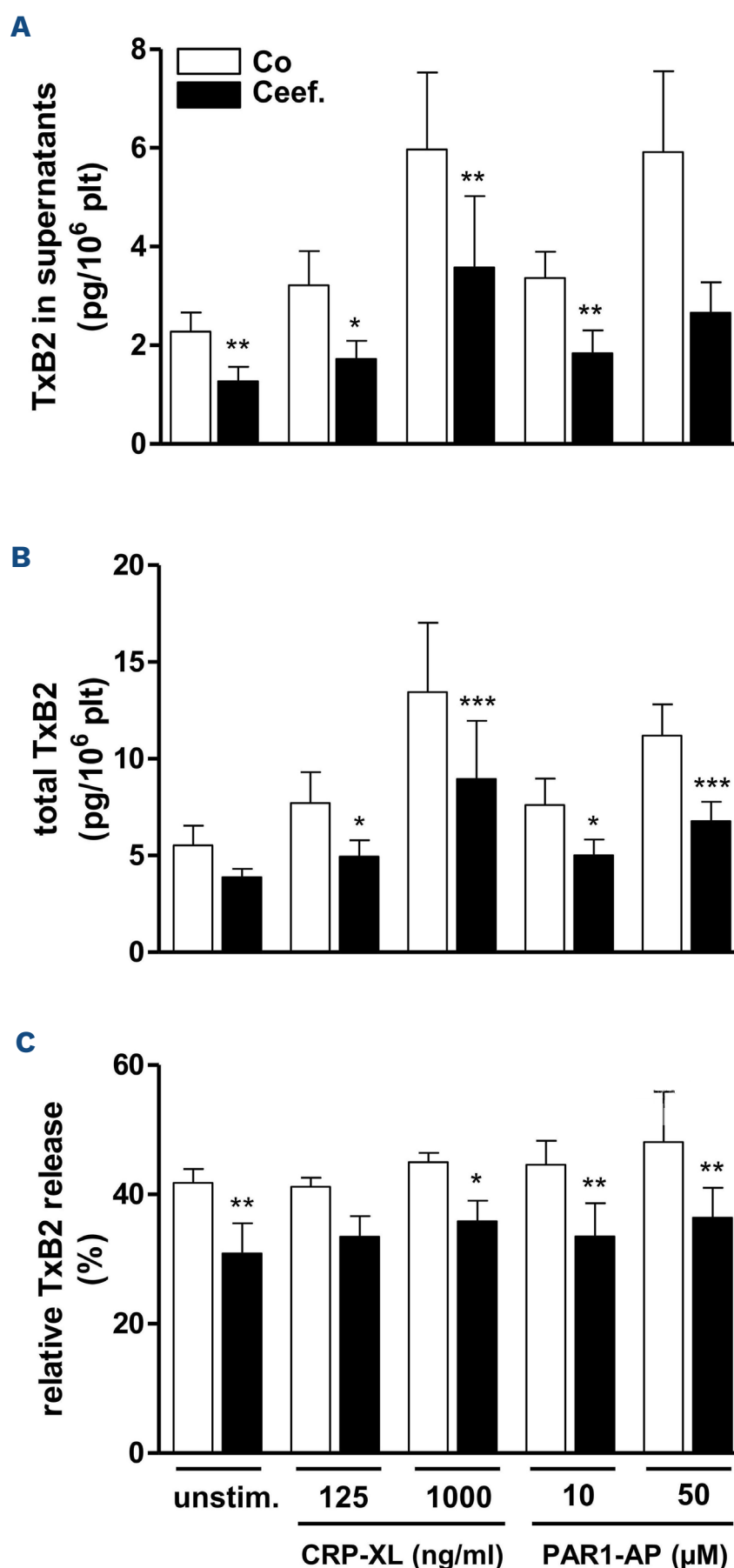


Figure 1. Inhibition of TxB2 release from human platelets by Ceefourin-1. Washed platelets were incubated for 15 minutes at 37°C with Ceefourin-1 (Ceef., 50 μM , black bars) or the respective solvent control (Co, 0.5% dimethyl sulfoxide [DMSO], white bars) and then either left unstimulated (unstim.) or activated with collagen-related peptide CRP-XL (125 ng/mL and 1,000 ng/mL) and the thrombin receptor-activating peptide PAR1-AP (10 μM and 50 μM). After 15 min, the platelets were pelleted and TxB2 was analyzed by liquid chromatography-tandem mass spectrometry (LC-MS/MS) in the supernatants and pellets. (A and B) Absolute TxB2 concentrations in platelet supernatants (A) and in platelet pellets (B) in pg/1x10⁶ platelets (plt). (C) Platelet TxB2 release in % of the total amount formed. Values represent means + standard error of the mean from n=6 different donors. *P<0.05; **P<0.01 vs. the respective solvent control.

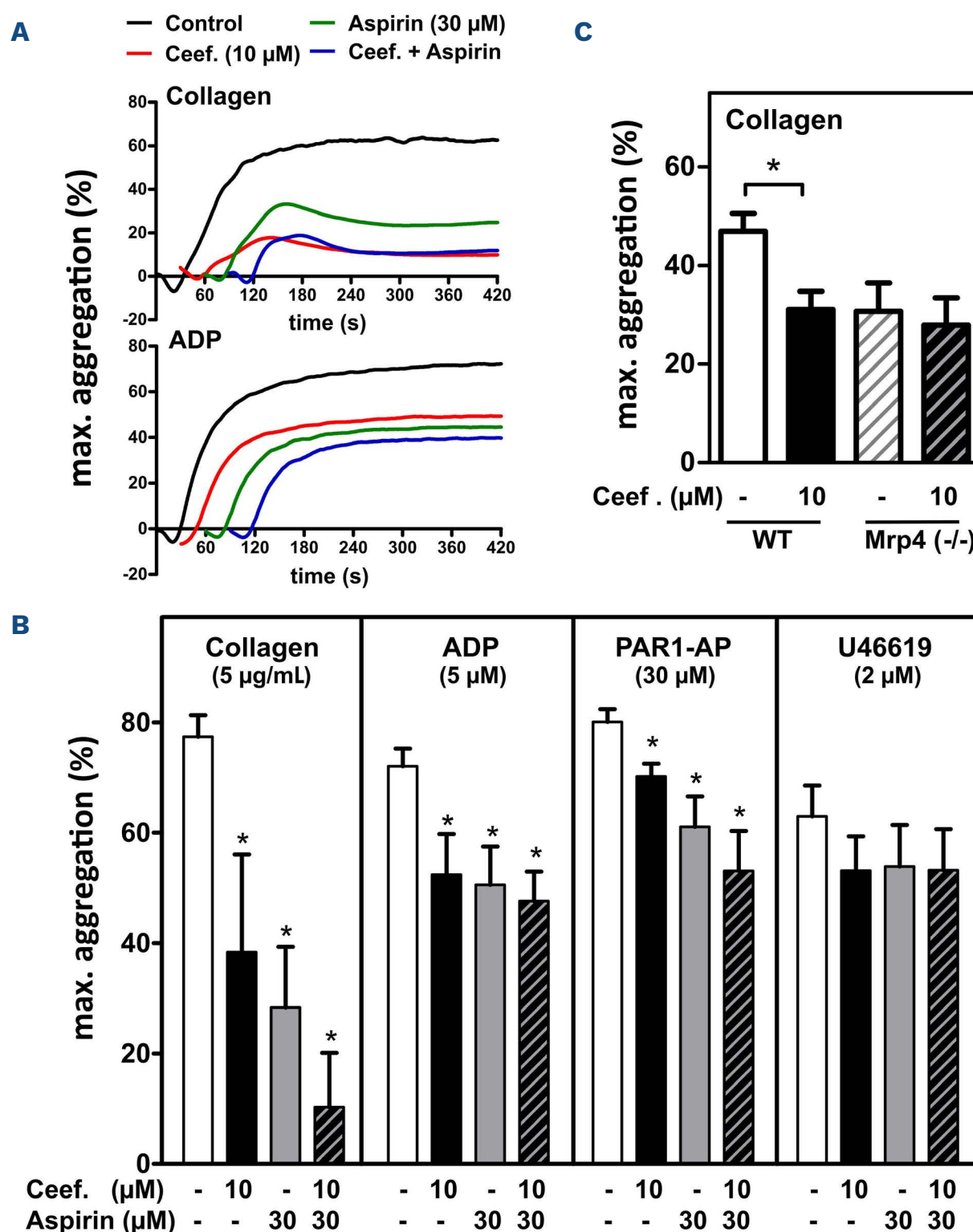


Figure 2. Effect of Ceefourin-1 on platelet aggregation ex vivo. (A and B) Human platelet-rich plasma (PRP) was pretreated with either only the solvent (control, (-)), or Ceefourin-1 (Ceef.; 10 μM for 20 minutes), or aspirin (30 μM ; for 5 minutes), or the combination of both, and then stimulated with the following agonists: collagen (5 $\mu\text{g}/\text{mL}$), ADP (5 μM), PAR1-AP (30 μM) or U46619 (2 μM). Platelet aggregation was determined by light transmission aggregometry. Representative curves of platelet aggregation stimulated by collagen and ADP are given in (A). The inhibition of the maximal aggregation is summarized in (B) (means + standard error of the mean [SEM]; $n=6-11$; $*P<0.05$ vs. control). (C) PRP (diluted 1:2 with Tyrode's buffer) from age- and sex-matched wild-type (WT) or Mrp4-deficient (Mrp4 $^{-/-}$) mice was pretreated with either only the solvent (control, (-)) or Ceefourin-1 (Ceef.; 10 μM) and then stimulated with collagen (10 $\mu\text{g}/\text{mL}$). Aggregation curves were monitored and the maximal extent of aggregation (%) was calculated (mean + SEM; $n=5-7$). Ceefourin-1 led to a significant reduction of the aggregation only in WT platelets ($*P<0.05$).

determine cytosolic cyclic nucleotide levels in human platelets, we measured the phosphorylation of VASP at two different serine residues (ser-157 and ser-239) by flow cytometry. The cAMP-elevating agent PGE₁ profoundly increased VASP phosphorylation at ser-157, the preferred phosphorylation site of PKA. Pre-incubation with Ceefourin-1 (50 μM) significantly increased this effect (310.4 \pm 25.3% vs. 211.3 \pm 14.7% with 1 μM PGE₁) (Figure 5A, left panel). Note that Ceefourin-1 alone only tends to

elevate background VASP phosphorylation. The phosphorylation of ser-239, the preferred substrate of PKG, is similarly elevated in the presence of cinaciguat, an activator of soluble guanylate cyclase. As shown in Figure 5A, right panel, the specific inhibition of MRP4 resulted in a 1.8-fold increase in the cinaciguat-stimulated VASP phosphorylation.

In order to investigate whether MRP4 inhibition can enhance cGMP-mediated effects in platelets, we measured

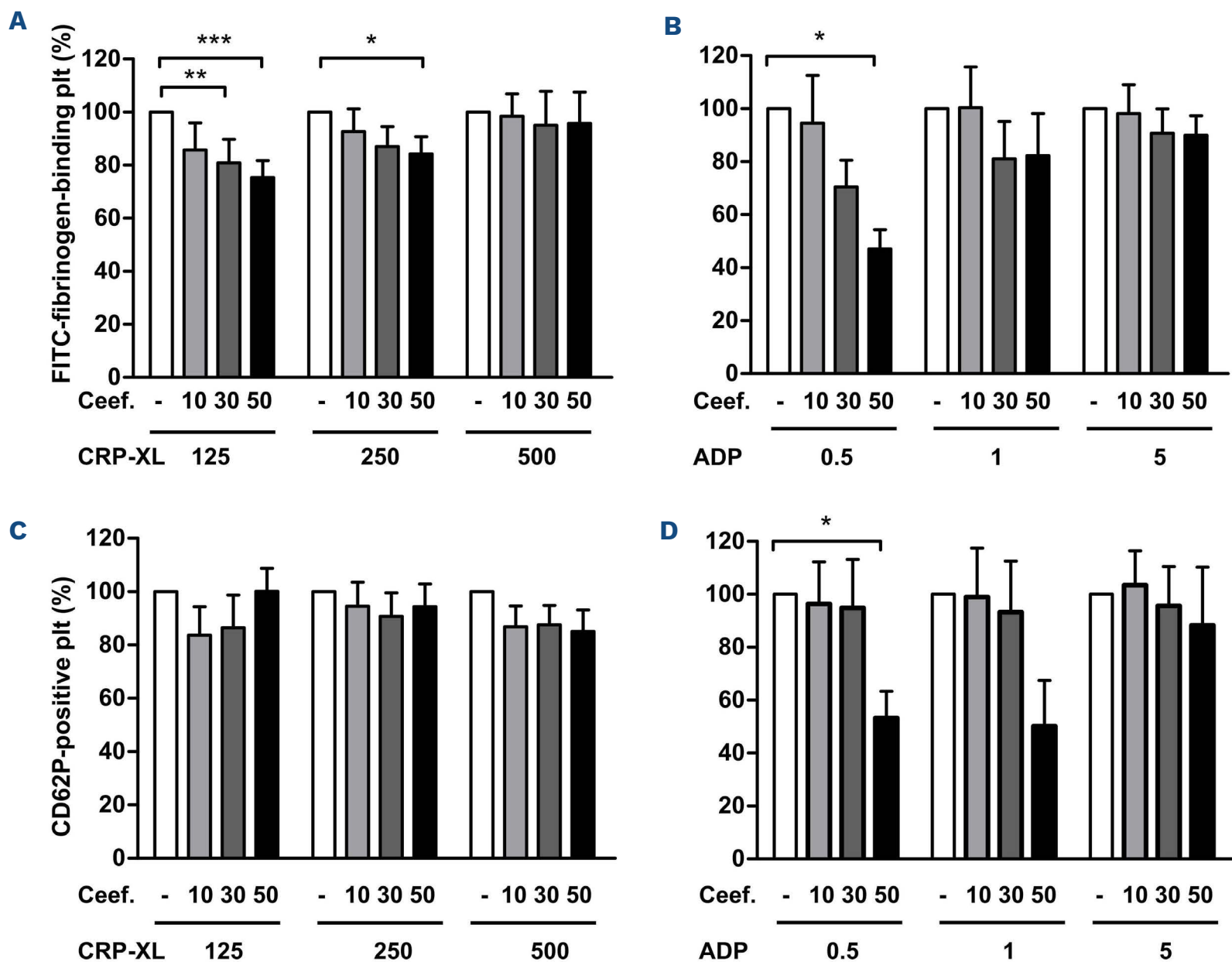


Figure 3. Effect of MRP4 inhibition on platelet fibrinogen binding and CD62P surface exposure. Binding of FITC-labeled fibrinogen (A and B) and R-phycoerythrin-labeled anti-CD62P antibody (C and D) to platelets (plt) was assessed by flow cytometry as a measure for integrin $\alpha\text{IIb}\beta\text{3}$ activation and α -granule release, respectively. Platelet-rich plasma was preincubated with Ceefourin-1 (Ceef.) (10–50 μM) or the solvent control (0.5% dimethyl sulfoxide [DMSO]) for 15 minutes (min) and then stimulated with the collagen-related peptide CRP-XL (125–500 ng/mL) (A and C) or ADP (0.5–5 μM) (B and D) for 10 min before FITC-fibrinogen or anti-CD62P antibody were added. After fixation in formaldehyde the samples were subjected to flow cytometric analysis. Data are given in % of the respective solvent control (means + standard error of the mean, $n=4-6$ platelet-rich plasma samples of different donors, performed in duplicates). Significant differences with $*P<0.05$, $**P<0.01$, and $***P<0.005$ vs. the respective solvent control.

platelet aggregation in the presence of cinaciguat (0.1 μM) and Ceefourin-1 (50 μM). A 3-minute pre-incubation with either substance alone led to only a modest reduction of maximum platelet aggregation as well as aggregation slope (Figure 5B). However, both substances combined significantly decreased the magnitude and slope of platelet aggregation to 37% and 46% of control, respectively.

Specific inhibition of MRP4 reduces platelet adhesion and thrombus formation under flow

In order to investigate whether the effect of Ceefourin-1 on platelet aggregation is also relevant under shear conditions, whole blood with FITC-anti-CD42a-labeled platelets was perfused through collagen-coated microchannels under high arterial shear conditions. Platelet

adhesion and thrombus formation were analyzed. Spiking whole blood with Ceefourin-1 (50 μM) resulted in a significant reduction in the area of platelet thrombi ($29.9\pm 1.4 \mu\text{m}^2$ vs. $18.4\pm 0.8 \mu\text{m}^2$) as well as in the total area of the channel, which was covered by thrombi (Figure 6A and B). We verified the selectivity of Ceefourin-1 again in this assay by conducting perfusion experiments with freshly taken samples of whole blood from *Mrp4*-deficient and WT control mice. As shown in Figure 6C and D, the average area of thrombi was reduced in blood from *Mrp4* (-/-) mice by about 45% as well as after incubation of blood from WT animals with Ceefourin-1 *ex vivo* as compared to control (WT without Ceefourin-1). Strikingly, no inhibitory effect on thrombus formation was seen with Ceefourin-1 in blood from *Mrp4*-deficient mice.

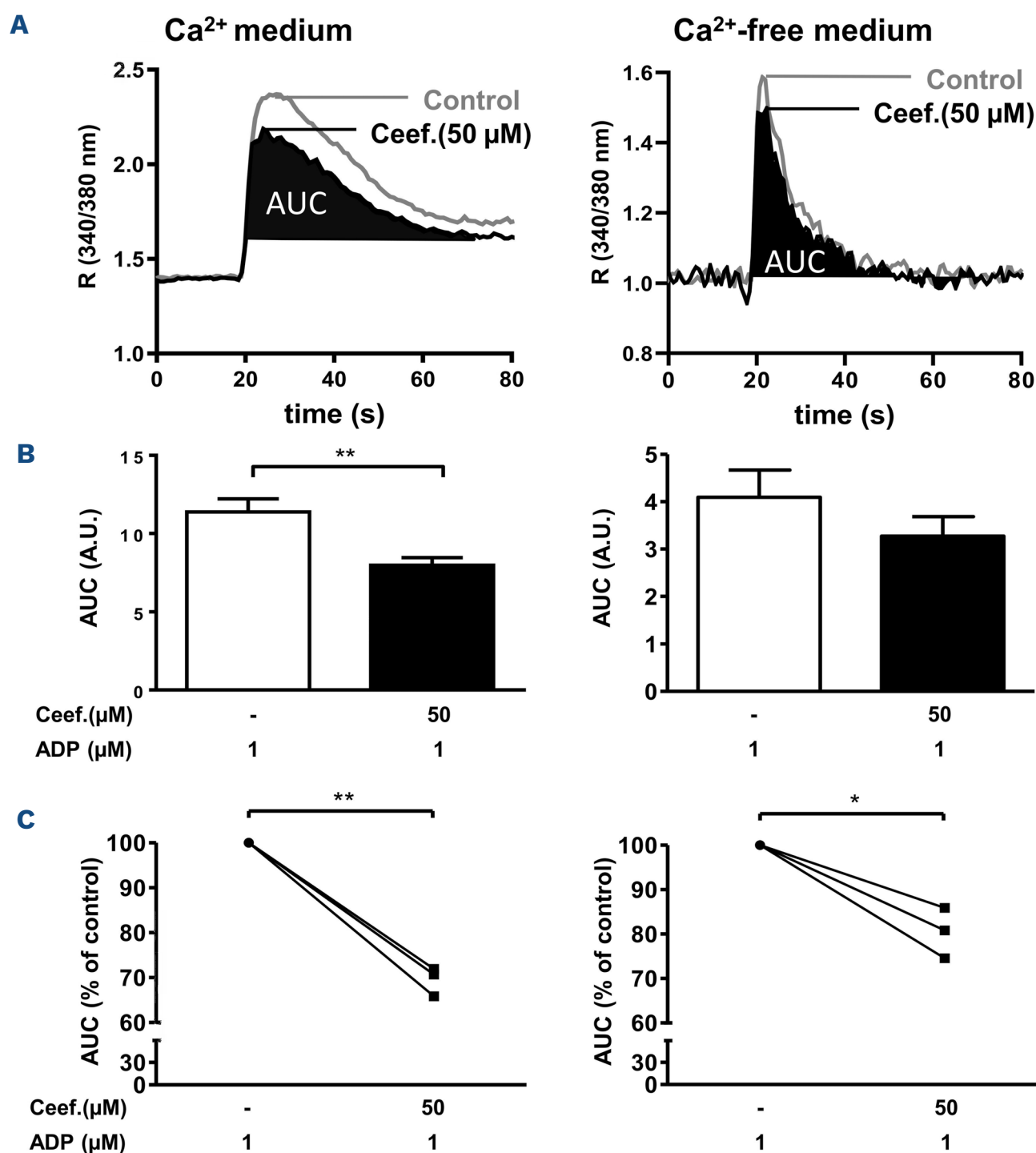


Figure 4. Effect of MRP4 inhibition on intracellular calcium levels in platelets. Cytosolic free calcium was measured spectrophotofluorometrically in Fura-2-loaded washed platelets. Measurements were performed either in Ca²⁺ medium (Tyrode's buffer with 2 mM CaCl₂) (left panels) or Ca²⁺-free medium (Tyrode's buffer with 0.2 mM EGTA) (right panels). In (A) the time-dependent increase in cytosolic calcium (indicated by R (340/380 nm)) after stimulation with ADP (1 μM) and the effect of Ceefourin-1 (50 μM) in representative experiments are depicted. In (B) the area under the fluorescence curve (area under the curve [AUC]) as a measure for the total change in calcium concentration was calculated (means + standard error of the mean from n=3 different donors, each measured in duplicates or quadruplicates). The reduction after Ceefourin-1 treatment is also given in % of the respective solvent control for each donor (each separate experiment) in (C) (significant differences with **P*<0.05, and ***P*<0.01).

Discussion

An impact of MRP4 on platelet function is indicated by several lines of evidence, including studies in *Mrp4* knockout mice^{9,10} and recent data from human individuals with a defect in the *ABCC4/MRP4* gene.⁴ MRP4 may affect different signaling pathways in human platelets through the transport of several compounds. In the present study, we used Ceefourin-1, which has been described as a selective MRP4 inhibitor²¹ to comprehensively characterize the effects on the function of human platelets that could be anticipated when applying a short-time pharmacological

inhibition of MRP4. It has been shown that Ceefourin-1 is highly selective for MRP4 over several ABC transporters, including other members of the MRP family such as MRP1 and MRP3 (ABCC1 and ABCC3), which are also expressed in platelets.² However, this does not exclude off-target effects of Ceefourin-1 on other structures in platelets. Therefore, we compared the effect of the compound in WT and *Mrp4*-deficient mice in the classic aggregometry studies and in the flow chamber experiments and observed significant effects on platelet function only when MRP4 is expressed. Possible unspecific effects of Ceefourin-1 on platelet viability were also tested and ruled

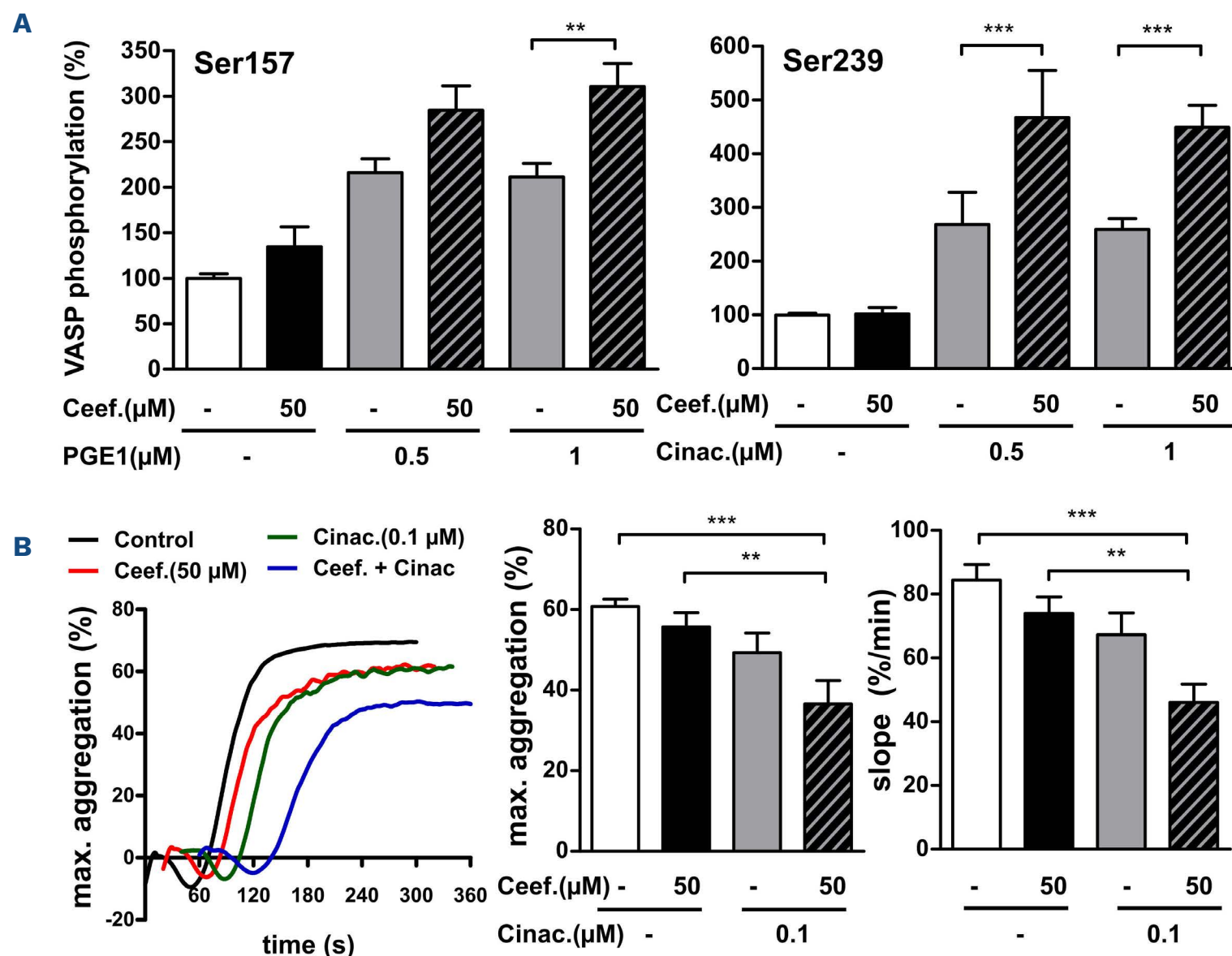


Figure 5. Effect of Ceefourin-1 on VASP phosphorylation (A) and cyclic nucleotide-dependent platelet inhibition (B). The phosphorylation of VASP at two different serine residues, serine-157 (the preferred substrate of PKA) (A, left panel) and serine-239 (the preferred substrate of PKG) (A, right panel) was determined by flow cytometry in human platelets as a measure for the cytosolic levels of cAMP and cGMP, respectively. Ceefourin-1 (Ceef., 50 μM) significantly amplified cAMP- and cGMP-dependent VASP phosphorylation, induced by PGE1 (1 μM) and cinaciguat (Cinac., 0.5 and 1 μM), respectively (means + standard error of the mean, n=6). (B) Platelet aggregation in the presence of cinaciguat (Cinac., 0.1 μM) and Ceefourin-1 (Ceef., 50 μM) was measured by light transmission aggregometry, to confirm the enhancement of cGMP-mediated effects by MRP4 inhibition. The aggregation was here stimulated by 1.25 μg/mL collagen. The left panel shows the aggregation curves of a representative experiment. Maximum platelet aggregation (middle panel) and the slope of platelet aggregation (right panel) were markedly decreased when both compounds were combined (means + standard error of the mean; n=20 measurements with platelet-rich plasma from 4 different donors).

out for the used concentrations. We further examined if there are substrate-dependent differences in the potency of Ceefourin-1 to inhibit the direct MRP4-mediated transport measured in inside-out membrane vesicles. Here, we observed that the MRP4-mediated transport of TxB2 is inhibited by Ceefourin-1 with a similar IC_{50} value as the transport of the cyclic nucleotide cGMP, although the structure of Ceefourin-1²¹ is more analogous to cyclic nucleotides than to eicosanoids. However, for inhibition of S1P transport, higher concentrations were required. This may indicate that the binding pocket for this substrate may be slightly different and Ceefourin-1 may not be the best compound to specifically interfere with the export or sequestration of this mediator. It should also be noted that the IC_{50} values determined in the inside-out membrane vesicles cannot directly be compared with the concentrations that are necessary to detect effects in intact

platelets. This is because only the proportion of the externally added Ceefourin-1 that has been taken up into the cells can inhibit the transporter at the cytosolic substrate binding site.

Thromboxane A2 (TxA2) is produced *de novo* upon activation of the platelets and amplifies the platelet response to a variety of stimulating agents. After its release, it is rapidly degraded to TxB2. Thromboxane has been supposed to diffuse through the platelet plasma membrane. However, *in vitro* assays in isolated membrane vesicles indicate that the presence of an ATP-dependent export pump is required for an effective export.¹³ Therefore, we investigated the impact of MRP4 inhibition on thromboxane release by stimulated human platelets in more detail. Ceefourin-1 pretreatment significantly reduced the thromboxane release from platelets after stimulation of the collagen or thrombin receptor. Thereby, the reduction in

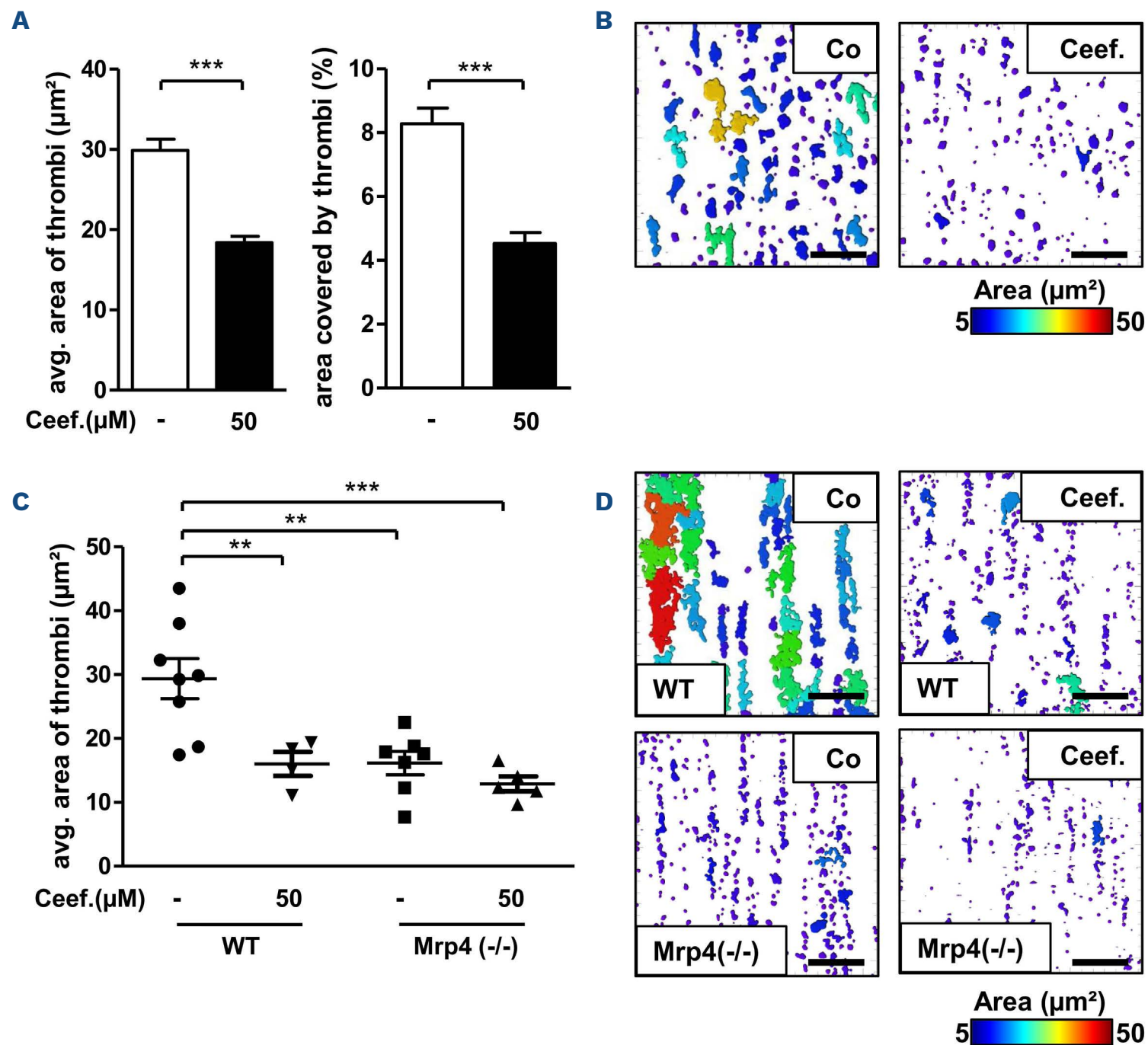


Figure 6. Role of MRP4 in platelet adhesion and thrombus formation under flow. (A and B) Whole human blood with FITC-anti-CD42a-labeled platelets (from $n=3$ different donors) was pre-incubated with Ceefourin-1 (Ceef., $50 \mu\text{M}$) or the respective solvent (Co, 0.5% dimethyl sulfoxide [DMSO]) and perfused through collagen-coated microchannels under high arterial shear conditions ($1,800\text{-}^{-1}$) for 5 minutes. Micrographs were taken at the beginning, the end, and in the center of the channel using a confocal laser scanning microscope (Zeiss LSM 780) with a $40\times$ objective. The average thrombus area (A, left panel) and surface area coverage by thrombi (A, right panel; means + standard error of the mean [SEM]) were analyzed with the ImageJ software. In (B) representative images are shown. (C and D) The effect of Ceefourin-1 was also evaluated in perfusions performed with whole blood from age- and sex-matched wild-type (WT) or $\text{Mrp4}(-/-)$ mice (with X488-labeled platelets). The average thrombus area (C, means \pm SEM and values of individual animals; $n=4-8$) was markedly reduced in $\text{Mrp4}(-/-)$ and Ceefourin-1-treated WT mice with no significant additional Ceefourin-1 effect in $\text{Mrp4}(-/-)$ animals. (D) Representative micrographs. Scale bars correspond to $50 \mu\text{m}$.

thromboxane release seems to be a combined effect of a diminished thromboxane synthesis during activation and a direct impact on the transport across the plasma membrane, since not only the total amount of this mediator but also the relative percentage that was released, was reduced. The fact that we observed no significant effect of Ceefourin-1 on the aggregation induced by the synthetic thromboxane analog U46619 and only a tendency towards an additive effect with aspirin is in agreement with this assumption. However, the effect of Ceefourin-1 to reduce thromboxane release was rather small compared with the potent ability of aspirin to prevent thromboxane forma-

tion, which is required to effectively inhibit thromboxane-dependent platelet activation.²⁵ Therefore, this effect of Ceefourin-1 can be an additional factor but is unlikely to fully account for the observed inhibition of platelet activation in response to agonists such as ADP and collagen. We studied platelet aggregation after short-time exposure to Ceefourin-1 with different stimuli because the published aggregometry data are also inconsistent. While Cheepala *et al.*¹⁰ reported that diminished aggregation of platelets from Mrp4 knockout mice is specific for collagen and $\text{Mrp4}(-/-)$ platelets did not have any defect in aggregation with either ADP or thrombin, Decouture *et al.*⁹ ob-

served a significant decrease in ADP- and PAR-4-activating peptide-induced aggregation in their knockout model. In human platelets, an impact of MRP4 inhibition was reported mainly on collagen-induced platelet aggregation.^{10,15,16} However, in ABCC4/MRP4-negative individuals a significant decrease in platelet aggregation was not observed with collagen and ADP at high concentration (10 μ M), but at lower ADP concentrations of 2.5 μ M and 5 μ M.⁴ With Ceefourin-1, we observed a significant effect on aggregation when collagen (5 μ g/mL) was used, but also with ADP (5 μ M) or PAR1-AP (30 μ M). Detection of fibrinogen binding to the platelets as a measure for integrin α IIb β 3 activation affirmed the observation that MRP4 inhibition affects platelet reactivity most effectively when the activating stimuli were used at a low submaximal dose, while it does not interfere at maximal activating conditions. At low ADP concentrations, an effect on degranulation was also observed indicated by the reduced surface exposure of P-selectin (CD62P).

Inconsistent observations regarding the role of cGMP in the context of MRP4-mediated effects on platelet function have been reported. ATP-dependent transmembrane transport and export of cGMP in platelets were shown to be affected by MRP4 inhibitors.^{1,19} However, Decouture et al.⁹ reported that MRP4 appears not to interfere with platelet cGMP homeostasis in their murine model since they observed no difference in total and secreted cGMP in WT or Mrp4-deficient platelets pre-incubated with sodium nitroprusside and stimulated by a PAR4-activating peptide. A rise in platelet cGMP levels, e.g., induced by NO-mediated activation of the soluble guanylate cyclase, results in a downregulation of platelet-activating signaling pathways. In this study, we used the phosphorylation of VASP at ser-239 as an indicator of platelet cytosolic cGMP levels and cinaciguat²⁶ as an activator of the soluble guanylate cyclase. Here, Ceefourin-1 was able to significantly increase the cinaciguat-stimulated VASP phosphorylation as well as to enhance markedly the cinaciguat-induced inhibitory effects on platelet aggregation. Ceefourin-1 analogously increased the phosphorylation at ser-157 induced by the cAMP-elevating agent PGE₁. These results indicate that MRP4 inhibition can intensify both cAMP- and cGMP-mediated effects in platelets and thus the response to several endothelium-derived vasodilators such as cAMP-elevating prosta-glandins as well as the cGMP-elevating nitric oxide, even though Ceefourin-1 alone only slightly elevated the background levels of these mediators. VASP phosphorylation is one key factor in the inhibition of platelet aggregation, while G α i signaling leads to activation. Ca²⁺-dependent signaling pathways synergize with the G α i signaling in the activation of integrin α IIb β 3 and also play a key role in granule secretion from activated platelets. Therefore, we examined the effect of Ceefourin-1 on the free calcium

concentrations in platelets, both in the presence and the absence of extracellular calcium, to discriminate between calcium entry across the plasma membrane and release from intracellular stores in the dense tubular system. The results indicate that blocking MRP4 mainly affects the agonist-induced calcium influx but also to some extent the intracellular calcium mobilization through direct or indirect mechanisms.

It was also the question if these relatively moderate effects of a short-time pharmacological MRP4 inhibition on platelet activation are sufficient to affect platelet adhesion and thrombus formation under blood flow. Therefore, we also tested the impact of Ceefourin-1 in a microfluidic flow chamber model and perfused whole blood through collagen-coated microchannels under high arterial shear conditions. Such devices have been recognized as a valuable tool to mimic the anatomy of healthy and stenotic blood vessels.^{27,28} Here, we could also demonstrate that spiking human or WT murine blood with the MRP4 inhibitor significantly reduced the average thrombus size and the surface area covered by thrombi.

In conclusion, pharmacological inhibition of MRP4 affects several signaling pathways in platelets mechanistically based on the transport inhibition not only of cAMP but also cGMP as well as of the lipid mediators thromboxane and S1P. However, additional direct effects on alternative biochemical pathways cannot be excluded. MRP4-selective platelet inhibitors may perspective prove advantageous, especially in cases of platelet hyperreactivity that may be associated with MRP4 overexpression. Besides Ceefourin-1, other effective MRP4-inhibiting compounds have been recently published.²⁹ These were developed primarily for the reversal of drug resistance in MRP4-overexpressing cancer cells. Since tumors are often associated with thrombosis and aspirin has been recently recognized as a promising cancer-preventive agent probably based on anti-platelet-mediated effects,³⁰ one may speculate that MRP4 inhibitors may provide dual benefits in some tumor patients. Other compounds such as the phosphodiesterase-3 and MRP4 inhibitor cilostazol may affect platelet reactivity by a dual-action.^{10,16} Further studies are required to evaluate which MRP4 inhibitors may be best suitable for an *in vivo* application.

Disclosures

No conflicts of interests to disclose.

Contributions

RW and SG conducted and designed the main experiments and data analyses. RP, CT, EM, AB, MH, and AH provided additional analyses and methodological expertise. AG and MVT contributed to the study design, BHR and GJ designed and supervised the study. RW and GJ drafted and all authors edited the manuscript.

Acknowledgments

The authors thank Edita Kaliwe and Sarah Polster for their expert technical assistance. *Mrp4*-deficient (*Mrp4* (-/-)) mice were kindly provided by the late Dr. Gary D. Kruh, Cancer Center, University of Illinois, Chicago, USA.

Funding

This study was supported by grants from the Deutsche Forschungsgemeinschaft to GJ (DFG, JE 234/4-1) and to BHR (DFG, RA 1714/1-2). RW has received a doctoral scholarship

from the DZHK (Deutsches Zentrum für Herz-Kreislauf-Forschung e.V., grant 81X3400103). RP and AG receive support from Deutsche Forschungsgemeinschaft, grant/award number: 374031971-TRR 240. We also acknowledge support for the Article Processing Charge from the DFG and the Open Access Publication Fund of the University of Greifswald.

Data-sharing statement

All original data and protocols can be made available to other investigators upon request.

References

- Jedlitschky G, Tirschmann K, Lubenow LE, et al. The nucleotide transporter MRP4 (ABCC4) is highly expressed in human platelets and present in dense granules, indicating a role in mediator storage. *Blood*. 2004;104(12):3603-3610.
- Niessen J, Jedlitschky G, Grube M, et al. Expression of ABC-type transport proteins in human platelets. *Pharmacogenet Genomics*. 2010;20(6):396-400.
- Mattiello T, Guerriero R, Lotti LV, et al. Aspirin extrusion from human platelets through multidrug resistance protein-4-mediated transport: evidence of a reduced drug action in patients after coronary artery bypass grafting. *J Am Coll Cardiol*. 2011;58(7):752-761.
- Azouzi S, Mikdar M, Hermand P, et al. Lack of the multidrug transporter MRP4/ABCC4 defines the PEL-negative blood group and impairs platelet aggregation. *Blood*. 2020; 6;135(6):441-448.
- Ritter CA, Jedlitschky G, Meyer zu Schwabedissen H, et al. Cellular export of drugs and signaling molecules by the ATP-binding cassette transporters MRP4 (ABCC4) and MRP5 (ABCC5). *Drug Metab Rev*. 2005;37(1):253-278.
- Jedlitschky G, Greinacher A, Kroemer HK. Transporters in human platelets: physiologic function and impact for pharmacotherapy. *Blood*. 2012;119(15):3394-3402.
- Sassi Y, Lipskaia L, Vandecasteele G, et al. Multidrug resistance-associated protein 4 regulates cAMP-dependent signaling pathways and controls human and rat SMC proliferation. *J Clin Invest*. 2008;118(8):2747-2757.
- Coepsel S, Garcia C, Diez F, et al. Multidrug resistance protein 4 (MRP4/ABCC4) regulates cAMP cellular levels and controls human leukemia cell proliferation and differentiation. *J Biol Chem*. 2011;286(9):6979-698.
- Decouture B, Dreano E, Belleville-Rolland T, et al. Impaired platelet activation and cAMP homeostasis in MRP4-deficient mice. *Blood*. 2015;126(15):1823-1830.
- Cheepala SB, Pitre A, Fukuda Y, et al. The ABCC4 membrane transporter modulates platelet aggregation. *Blood*. 2015;126(20):2307-2319.
- Belleville-Rolland T, Sassi Y, Decouture B, et al. MRP4 (ABCC4) as a potential pharmacologic target for cardiovascular disease. *Pharmacol Res*. 2016;107:381-389.
- Reid G, Wielinga P, Zelcer N, et al. The human multidrug resistance protein MRP4 functions as a prostaglandin efflux transporter and is inhibited by nonsteroidal antiinflammatory drugs. *Proc Natl Acad Sci U S A*. 2003;100(16):9244-9249.
- Rius M, Hummel-Eisenbeiss J, Keppler D. ATP-dependent transport of leukotrienes B4 and C4 by the multidrug resistance protein ABCC4 (MRP4). *J Pharmacol Exp Ther*. 2008;324(1):86-94.
- Vogt K, Mahajan-Thakur S, Wolf R, et al. Release of platelet-derived sphingosine-1-phosphate involves multidrug resistance protein 4 (MRP4/ABCC4) and is inhibited by statins. *Thromb Haemost*. 2018;118(1):132-142.
- Massimi I, Lotti LV, Temperilli F, et al. Enhanced platelet MRP4 expression and correlation with platelet function in patients under chronic aspirin treatment. *Thromb Haemost*. 2016;116(6):1100-1110.
- Alemanno L, Massimi I, Klaus V et al. Impact of multidrug resistance protein-4 inhibitors on modulating platelet function and high on-aspirin treatment platelet reactivity. *Thromb Haemost*. 2018;118(3):490-501.
- Marcantoni E, Allen N, Cambria MR, et al. Platelet transcriptome profiling in HIV and ATP-binding cassette subfamily C member 4 (ABCC4) as a mediator of platelet activity. *JACC Basic Transl Sci* 2018;3(1):9-22.
- Keppler D, Jedlitschky G, Leier I. Transport function and substrate specificity of multidrug resistance protein. *Methods Enzymol*. 1998;292:607-616.
- Borgognone A, Pulcinelli FM. Reduction of cAMP and cGMP inhibitory effects in human platelets by MRP4-mediated transport. *Thromb Haemost*. 2012;108(5):955-962.
- Lien LM, Chen ZC, Chung CL, et al. Multidrug resistance protein 4 (MRP4/ABCC4) regulates thrombus formation in vitro and in vivo. *Eur J Pharmacol*. 2014;737:159-167.
- Cheung L, Flemming CL, Watt F, et al. High-throughput screening identifies Ceefourin 1 and Ceefourin 2 as highly selective inhibitors of multidrug resistance protein 4 (MRP4). *Biochem Pharmacol*. 2014; 91(1):97-108.
- Schneider CA, Rasband WS, Eliceiri KW. NIH Image to ImageJ: 25 years of image analysis. *Nat Methods*. 2012;9(7):671-675.
- Jahn K, Handtke S, Palankar R, et al. Pneumolysin induces platelet destruction, not platelet activation, which can be prevented by immunoglobulin preparations in vitro. *Blood Adv*. 2020;4(24):6315-6326.
- Mangin PH, Gardiner EE, Nesbitt WS, et al. In vitro flow based systems to study platelet function and thrombus formation: recommendations for standardization: communication from the SSC on Biorheology of the ISTH. *J Thromb Haemost*. 2020;18(3):748-752.
- Schrör K, Rauch BH. Aspirin and lipid mediators in the cardiovascular system. *Prostaglandins Other Lipid Mediat*. 2015;121(Pt A):17-23.
- Tamargo J, Duarte J, Caballero R, Delpón E. Cinaciguat, a soluble guanylate cyclase activator for the potential treatment of acute heart failure. *Curr Opin Investig Drugs*. 2010;11(9):1039-1047.

27. Westein E, deWitt S, Lamers M, Cosemans JM, Heemskerk JW. Monitoring in vitro thrombus formation with novel microfluidic devices. *Platelets*. 2012;23(7):501-509.
28. Scavone M, Bozzi S, Mencarini T, Podda G, Cattaneo M, Redaelli A. Platelet adhesion and thrombus formation in microchannels: the effect of assay-dependent variables. *Int J Mol Sci*. 2020;21(3):750.
29. Döring H, Kreutzer D, Ritter C, Hilgeroth A. Discovery of novel symmetrical 1,4-dihydropyridines as inhibitors of multidrug-resistant protein (MRP4) efflux pump for anticancer therapy. *Molecules*. 2021;26(1):18.
30. Xu XR, Yousef GM, Ni H. Cancer and platelet crosstalk: opportunities and challenges for aspirin and other antiplatelet agents. *Blood*. 2018;131(16):1777-1789.

Deregulated JAK3 mediates growth advantage and hemophagocytosis in extranodal nasal-type natural killer/T-cell lymphoma

Advanced extranodal, nasal-type natural killer/T-cell lymphoma (NKTCL) is an aggressive malignancy with dismal prognosis, typically associated with hemophagocytic syndrome that worsens the prognosis.^{1,2} Hemophagocytic syndrome results from excessive production of interferon- γ , although the mechanisms leading to interferon- γ overproduction in NKTCL cells remain unclear. A deregulation of Janus kinase 3 (JAK3) protein is a general oncogenic event in NKTCL, with up to 80% of patients harboring constitutive phosphorylation in the activating Y980 residue, and 7%–35% of patients displaying acquired activating mutations, mainly in the pseudokinase domain, which account for its constitutive activation.^{3–6} Here we demonstrate that constitutively activated JAK3 confers natural killer (NK) cell hypersensitivity to interleukin-2 (IL-2), leading to growth advantage and excessive production of interferon- γ through activation of downstream substrates. We also show that the expression of constitutively activated JAK3^{A573V} in hematopoietic progenitors leads to NK-cell expansion in mice. Finally, using an original *in vivo* murine model based on the expression of JAK3^{A573V} in primary NK cells from *Rag2*^{-/-} mice, we observed that transplanted wild-type recipients reproduce the typical features of NKTCL including NK-cell expansion and hemophagocytic syndrome.

To get insights into the role of JAK3 in NKTCL pathophysiology, we hypothesized that JAK3 deregulation could lead to an excessive sensitivity to cytokines. In preliminary experiments, we treated control NK cells and the NK-cell line MEC04, derived from a NKTCL (harboring the JAK3^{A573V} mutation), and NKL and KHYG-1 cell lines, derived from NK-cell leukemias, all harboring a constitutively phosphorylated JAK3 on Y980 residue,³ with recombinant IL-2 (rIL-2) as a representative cytokine that stimulates a receptor involving the common γ c/JAK3 axis. Cells were exposed to 100 U/mL of rIL-2 for 2 days and counted daily using the trypan blue exclusion assay. A rapid and significant increase in the number of viable cells was observed throughout time when compared to control NK cells isolated from healthy donors or to MEC04 cells cultured without rIL-2 (*Online Supplementary Figure S1A*). After 2 days of culture, there was a more than 4-fold increase in the number of MEC04 cells in comparison with normal NK cells ($P < 0.0001$). Similar results were observed for NKL and KHYG1 cells (*Online Supplementary Figure S1*). Strikingly, this proliferative effect observed after exposure to

rIL-2 was totally abrogated when cells were exposed to the JAK3 inhibitor CP-690550 (*Online Supplementary Figure S1A*), providing further evidence that JAK3 signaling is important in NKTCL oncogenesis.

To confirm the importance of JAK3 signaling in NKTCL, MEC04 cells were stimulated with rIL-2 for 30 minutes and subjected to western-blot analysis for the phosphorylation of the tyrosine 705 (Y705) residue of Signal transducer and activator of transcription 3 (STAT3) oncogene.^{3,7} We found that before stimulation with rIL-2, Y705-STAT3 showed constitutive baseline phosphorylation in MEC04 cells when compared to control NK cells. After stimulation with rIL-2, Y705-STAT3 phosphorylation was increased in MEC04 cells. This phenomenon was abrogated when cells were exposed to CP-690550 before rIL-2 stimulation (*Online Supplementary Figure S1B*). Collectively, these results provide evidence for a synergistic role between JAK3 deregulation and IL-2 signaling in the growth of NK-cell lines.

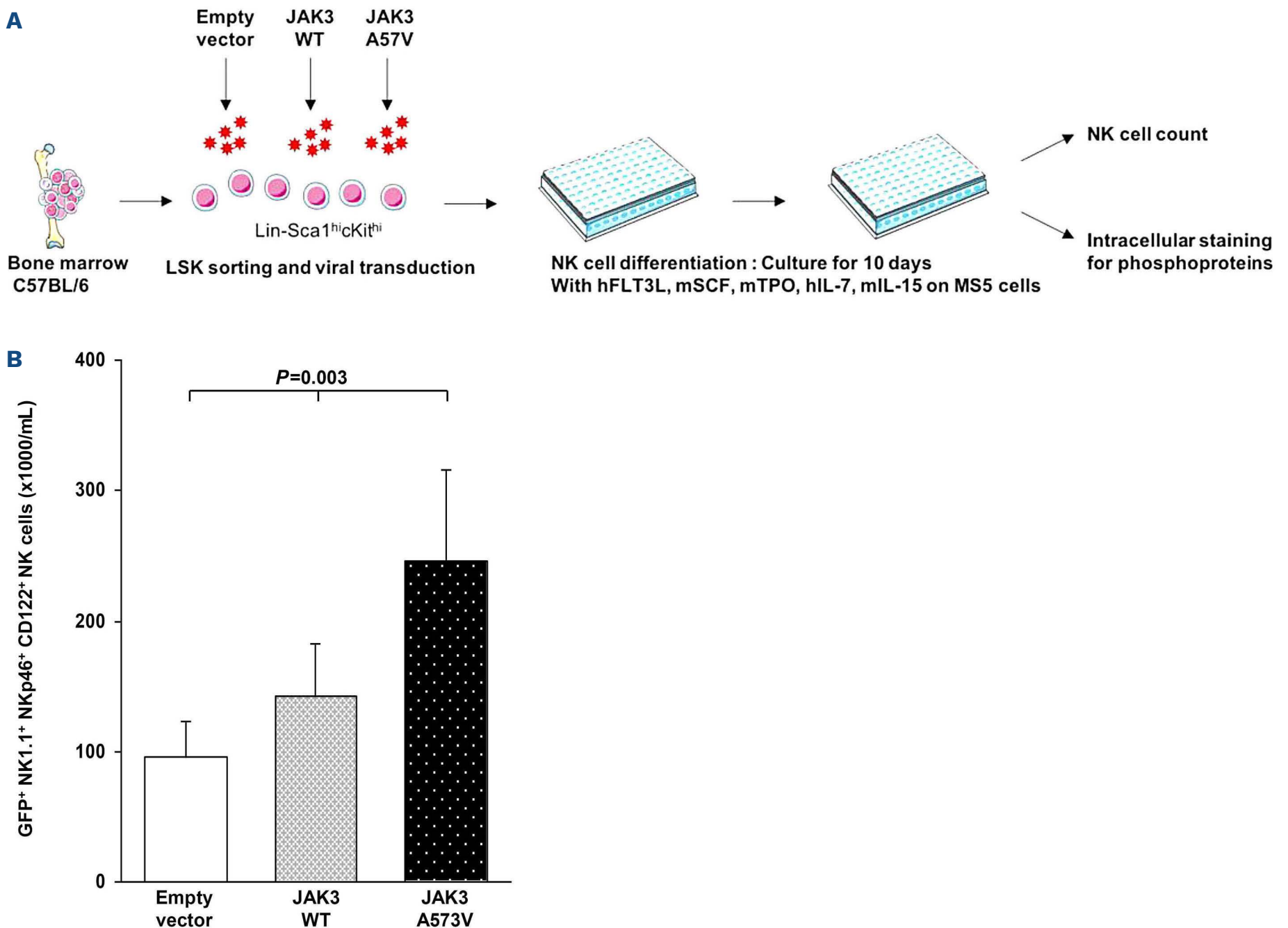
To explore the involvement of deregulated JAK3 in the hypersecretion of interferon- γ , we used NKL and KHYG-1 cells as they produce the highest amounts of interferon- γ . Cells were cultured in the presence or absence of rIL-2, and interferon- γ in the supernatant was measured after 48 h of culture. The two cell lines spontaneously secrete low levels of interferon- γ in the absence of rIL-2. In the presence of rIL-2, the amount of secreted interferon- γ /10⁶ viable cultured cells increased dramatically. This effect was almost completely abrogated when cells were concomitantly cultured with CP-690550 (*Online Supplementary Table S1*). Accordingly, the phosphorylation of target proteins STAT3, AKT and ERK1/2 was decreased in the presence of JAK3 inhibitors (*Online Supplementary Figure S1C*). To confirm further the role of JAK3 signaling in interferon- γ secretion, we selectively knocked-down JAK3 in NKL cells using specific siRNA. The decreased expression of JAK3 induced a rapid decrease in cell viability (*Online Supplementary Figure S1D*), with dephosphorylation of target proteins (*Online Supplementary Figure S1E*), as well as a major decrease in interferon- γ secretion after 2 days of cell culture (27 \pm 2.1 pg/mL/10⁶ viable cells in the presence of JAK3-targeting siRNA vs. 127 \pm 3.4 pg/mL/10⁶ viable cells in the presence of scrambled siRNA, $P < 0.001$). Furthermore, the phosphorylation of AKT and ERK, two substrates downstream of JAK3, was inhibited by GDC-0941 and UO126, respectively, as assessed after culture

for 48 h in the presence of rIL-2 (*Online Supplementary Figure S1F*). We found that both inhibitors were able to inhibit mostly (UO126) or completely (GDC-0941) the secretion of interferon- γ after 48 h of culture (*Online Supplementary Table 1*). Taken together, these results provide evidence that deregulated JAK3 and its corresponding downstream substrates are involved in the excessive secretion of interferon- γ in NKTCL.

To provide further evidence that deregulated JAK3 is oncogenic in NKTCL, we cultured mouse NK cells expressing the JAK3^{A573V} oncogenic protein. For this, Lin⁻, Sca^{hi}, Kit^{hi} (LSK) progenitors obtained from C57Bl/6 mice were transduced with retroviral vectors encoding the wild-type form of human JAK3 (JAK3^{WT}) or JAK3^{A573V}, as well as with an empty vector.⁸ Transduced cells were cultured on MS5 stromal cells in the presence of mouse stem cell factor, mouse thrombopoietin, human Fms-like tyrosine kinase 3-ligand (hFlt3-L), human IL-7, and mouse IL-15 for NK-cell differentiation (Figure 1A). After 10 days, we observed a three-fold increase in the number of NK cells expressing JAK3^{A573V} as compared to cells transduced with empty

vector, and an intermediate number of cells transduced with JAK3^{WT} vector (Figure 1B), consistent with the view that deregulated JAK3 confers a growth advantage to NK cells. Accordingly, we found maximal phosphorylation of the JAK3 substrates Y705-STAT3, Y594-STAT5, Y202/204-ERK1/2 and S473-AKT by flow cytometry in NK cells harboring JAK3^{A573V} (Figure 1C).

JAK3 activating mutations have been shown to induce a rapid-onset T-cell lymphoproliferation in mouse bone marrow transplantation assays.⁹ Since NK cells represent a minor lymphoid population, we hypothesized that T-cell proliferation either masked or inhibited the development of a NK-cell disorder. Hence, we assessed the transforming ability of JAK3^{A573V} in a T-cell deficient bone marrow transplantation assay by using donor *Rag2*^{-/-} mice (Figure 2A). Transplantation of JAK3^{A573V}-transduced bone marrow cells from *Rag2*^{-/-} mice into wild-type C57Bl/6 recipients resulted in a lymphoproliferative disease characterized by an expansion of eGFP⁺ CD3⁻ NK1.1⁺ NK cells in blood (Figure 2B) leading to the death of all animals within 7 months. Conversely, mice transplanted with empty vector



Continued on following page.

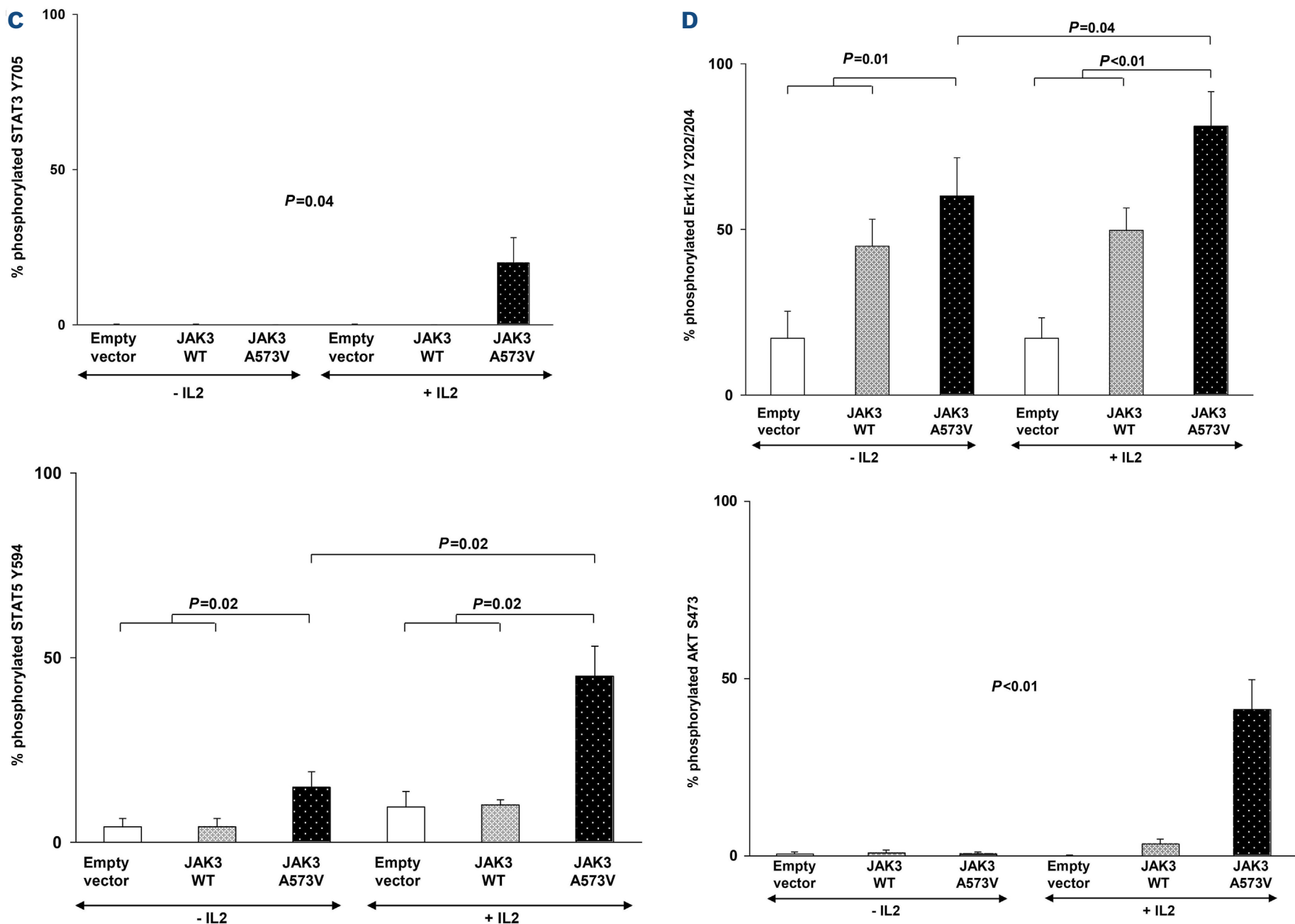


Figure 1. Generation of murine natural killer cells from LSK progenitors. (A) Experimental procedure. Five 6- to 10-week-old C57BL/6H mice were pooled in each experiment. Freshly isolated bone marrow cells were treated with Fc-block (CD16/CD32) and stained with biotin-conjugated lineage antibodies (CD3 [145-2C11], Gr-1 [RB6-8C5], B220 [B-220], and TER-119 [TER-119]). Lineage-positive cells were first depleted by magnetic-activated cell separation using Streptavidin Microbeads (BD Biosciences, Le Pont de Claix, France). Cells were then stained with anti-CD3-APC/Cy7, anti-Gr1-APC/Cy7, anti-B220-APC/Cy7, anti-TER119-APC/Cy7, anti-Sca1-FITC (E13-161.7), and anti-c-Kit-PerCP/Cy5.5 (2B8) and LSK cells were sorted with a Beckton Dickinson FAC-SInflux. All antibodies were purchased from Ozyme (Saint Quentin en Yvelines, France), except for biotin-conjugated lineage antibodies and the anti TER119-APC/Cy7, which were purchased from BD Biosciences (Le Pont de Claix, France). LSK cells were then transduced with JAK3^{A573V}, JAK3^{WT} or empty vector as previously described^{8,9} and cultured in 96-well plates on MS5 stromal cells for 10 days in Dulbecco modified Eagle medium with murine stem cell factor (25 ng/mL), murine thrombopoietin (10 ng/mL), human interleukin-7 (10 ng/mL), murine interleukin-15 (50 ng/mL) (all from PeproTech, Rocky Hill, NJ, USA) and human Fms-like tyrosine kinase 3-ligand (10 ng/mL) (Celldex Therapeutics, Inc., Needham, MA, USA), for natural killer (NK)-cell differentiation. Cells were then stained with anti-CD3-APC, anti-NK1.1-PerCp/Cy5.5, anti-NKp46-PECy7, as well as intracellular Alexa Fluor[®] 647 fluorochrome-conjugated antibodies for PY-STAT3 (Y705), PY-STAT5 (Y594) or PY-ERK 1/2 (Y202/204) or phospho-AKT (S473) after permeabilization with Perifix expose purchased from Beckman Coulter (Villepinte, France), according to the manufacturer's instructions. (B) The bar chart shows that the number of mature murine NK cells (CD3⁻, NK1.1⁺, NKp46⁺) obtained from 10⁴ LSK cells transduced with JAK3^{A573V}, JAK3^{WT} or empty vector, after 10 days of culture. Results are the mean \pm standard deviation of three independent experiments. The statistical significance was calculated by a Kruskal-Wallis test. (C) Analysis of intracellular staining for Y705-STAT3, Y594-STAT5, Y202/204-ERK1/2, and S573-AKT. Results are provided in percentages from CD3⁻ NK1.1⁺ NKp46⁺ NK cells. LSK: Lin⁻, Sca^{hi}, Kit^{hi}; WT: wild-type; mSCF: murine stem cell factor; mIL-3: murine interleukin-3; hFlt3-L: human Fms-like tyrosine kinase 3-ligand; hIL-7: human interleukin-7; mIL-15: murine interleukin-15; hIL-2: human interleukin-2; NK: natural killer; GFP: green fluorescent protein.

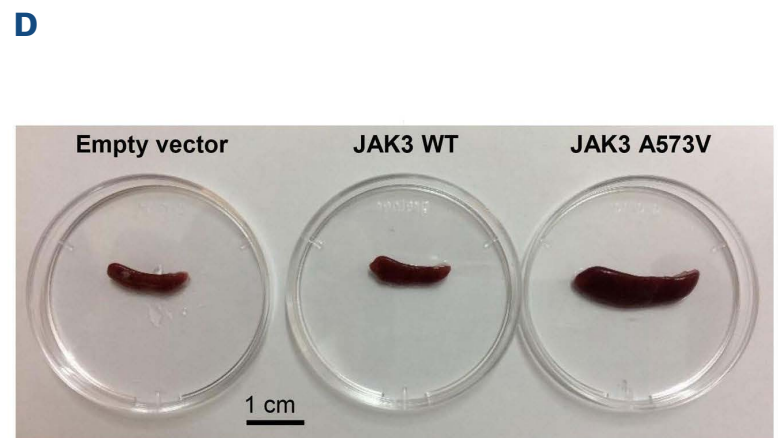
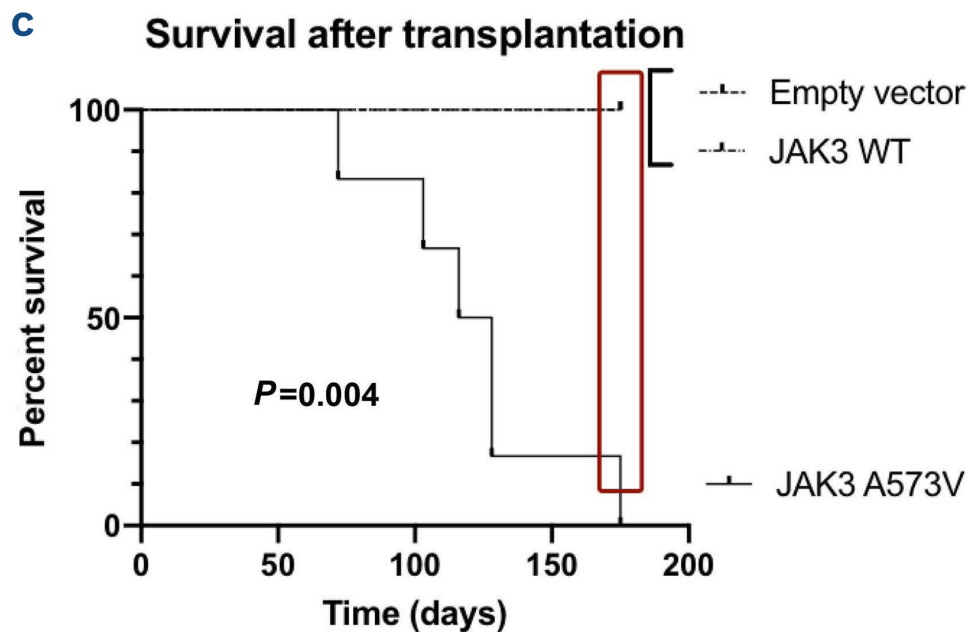
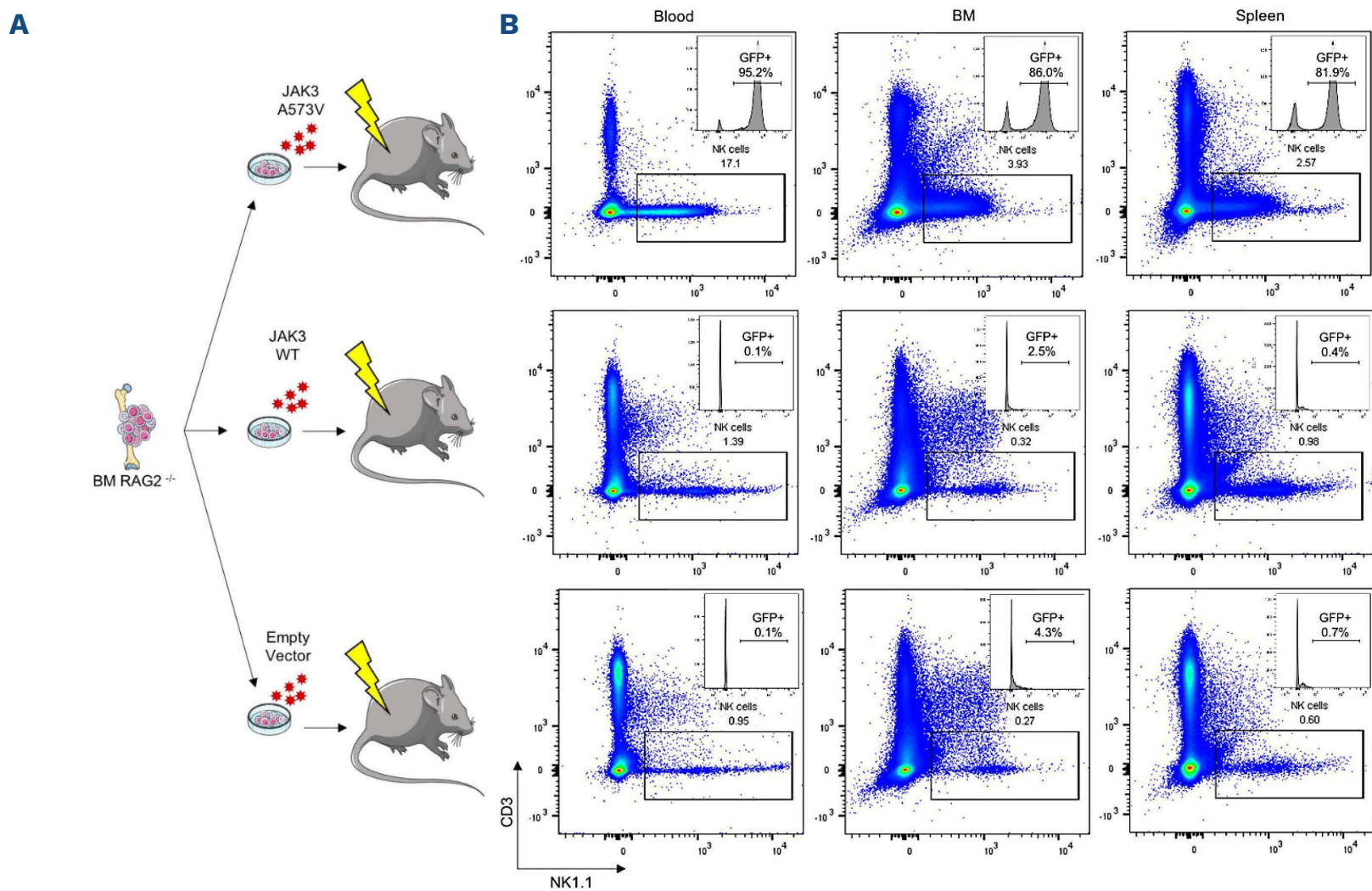
or JAK3^{WT} remained alive and disease-free (log-rank test, $P=0.004$) (Figure 2C). Moreover, the blood cell count of two sick JAK3^{A573V} mice before autopsy showed pancytopenia, with the lymphopenia and thrombocytopenia being par-

ticularly pronounced (Online Supplementary Table S2), a hallmark of hemophagocytic syndrome.¹⁰ Autopsy of these two mice was remarkable for the spleen enlargement (492 \pm 285 mg vs. 86 \pm 9 mg and 82 \pm 9 mg in mice trans-

planted with bone marrow cells transduced with JAK3^{WT} and with empty vector, respectively) (Figure 2D). Histopathological analysis of the spleen, liver, bone marrow and lung showed massive and destructive infiltration by malignant cells (Figure 2E). Immunostaining performed on spleen and lung, which were the most massively infiltrated tissues, was positive for NK1.1 and for cytoplasmic CD3 ϵ , consistent with a NK-cell proliferation. We verified that JAK3 is constitutively phosphorylated in the activating Y980 residue in these tumors. In contrast, we found no tumoral infiltration in empty vector- and JAK3^{WT}-transplanted mice. In liver biopsies, shown as illustrative tis-

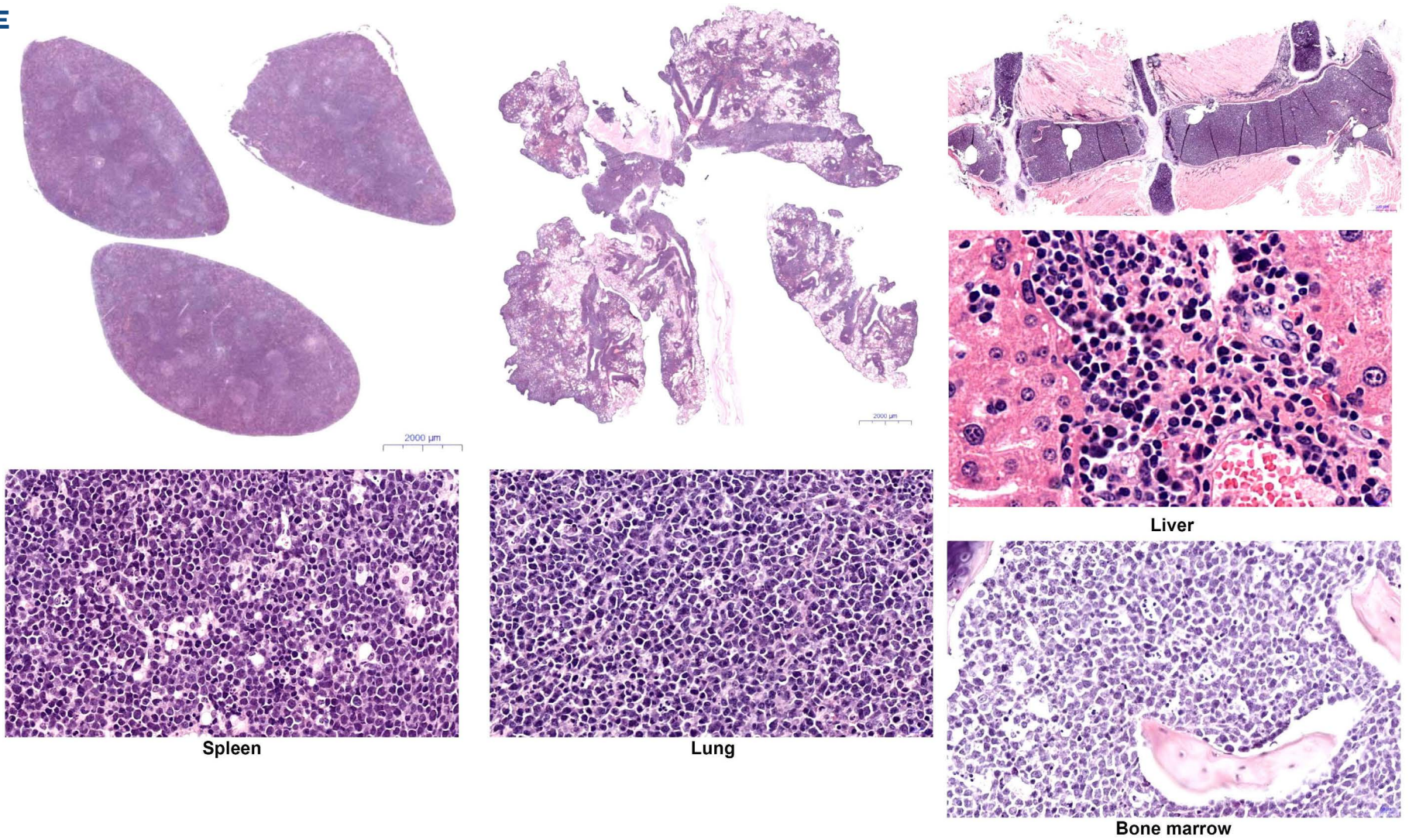
sues, we only observed small non-tumoral (probably autologous) CD3⁺ lymphocytes on portal tracts, suggesting mild inflammation (Figure 2F).

Lastly, multiple images of hemophagocytosis were recognizable on both spleen and lung samples (Figure 3A) and were unequivocally detected in the cytoplasm of CD68⁺ activated macrophages (Figure 3B). Malignant cells expressed interferon- γ (Figure 3C), whereas macrophages expressed tumor necrosis factor- α (Figure 3D), consistent with the histopathological pictures of hemophagocytosis. Here we took advantage of the identification of JAK3^{A573V} mutation as a model of JAK3 deregulation to explore the

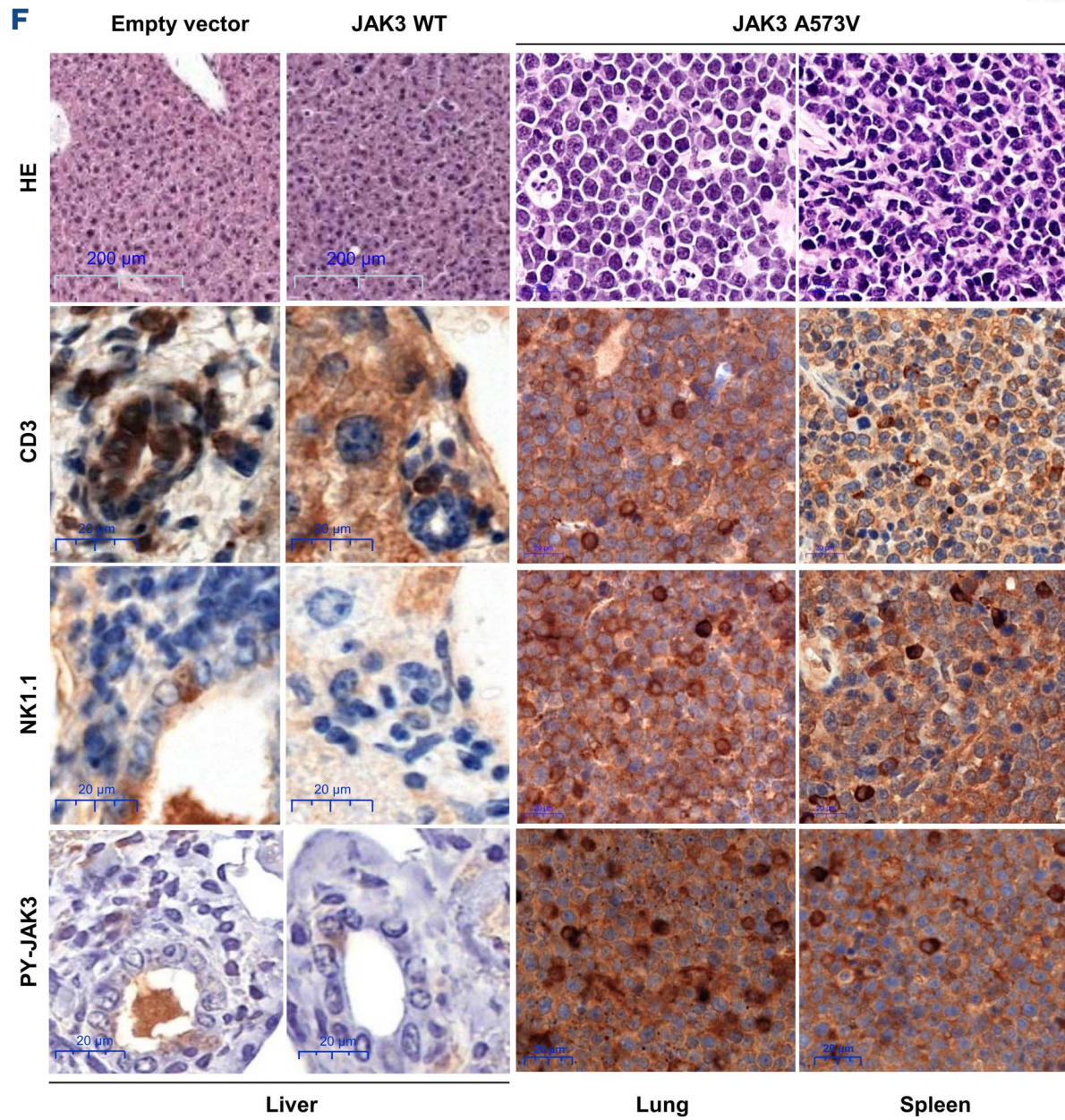


Continued on following page.

E



F



Continued on following page.

Figure 2. Natural killer cells expressing $JAK3^{A573V}$ generate a massive lymphoproliferative disease in mice. (A) Eight- to 10-week-old $Rag2^{-/-}$ donor mice were injected intraperitoneally with 150 mg/kg 5-fluorouracil (5-FU; Sigma-Aldrich, St Louis, MO, USA) 5 days prior to bone marrow collection from iliac bones, femora and tibiae. Bone marrow cells transduced with $JAK3^{A573V}$, $JAK3^{WT}$ or empty vector were administered intravenously to sublethally irradiated C57BL/6 recipient mice (N=6 for each condition). (B) $NK1.1^+/CD3^-eGFP^+$ cells from the peripheral blood, bone marrow or spleen of mice. Cells were harvested at the time of autopsy. (C) Survival of wild-type C57BL/6 mice transplanted with $JAK3^{A573V-}$, $JAK3^{WT-}$ and empty vector-transduced bone marrow cells from $Rag2^{-/-}$ mice. The red box represents the time of cell harvesting for immunophenotyping analysis and autopsy of the last diseased $JAK3^{A573V-}$ -transplanted mouse as well as healthy $JAK3^{WT-}$ and empty vector-transplanted mice. Log-rank empty vector or $JAK3^{WT}$ vs. $JAK3^{A573V}$, $P=0.004$. (D) Comparison of spleen size between conditions. (E) Hematoxylin & eosin staining showing the infiltration of spleen, lung, bone marrow (sternum), and liver in peri-portal spaces. (F) Hematoxylin & eosin staining and immunostaining with CD3 ϵ (primary antibody: clone SP7, ThermoFisher Scientific SAS, Illkirch, France), NK1.1 (clone PK136, ThermoFisher Scientific SAS, Illkirch, France) and PY-JAK3 (D44E3, Cell Signaling Technology, Danvers, MA, USA) of spleen, lung and liver tissue. Specimens were counterstained with the corresponding secondary antibodies. BM: bone marrow; eGFP: enhanced green fluorescent protein. $Rag2$: recombination activating gene 2; LSK: Lin^- , Sca^{hi} , Kit^{hi} . HE: hematoxylin & eosin; PY-JAK3: phosphorylated JAK3.

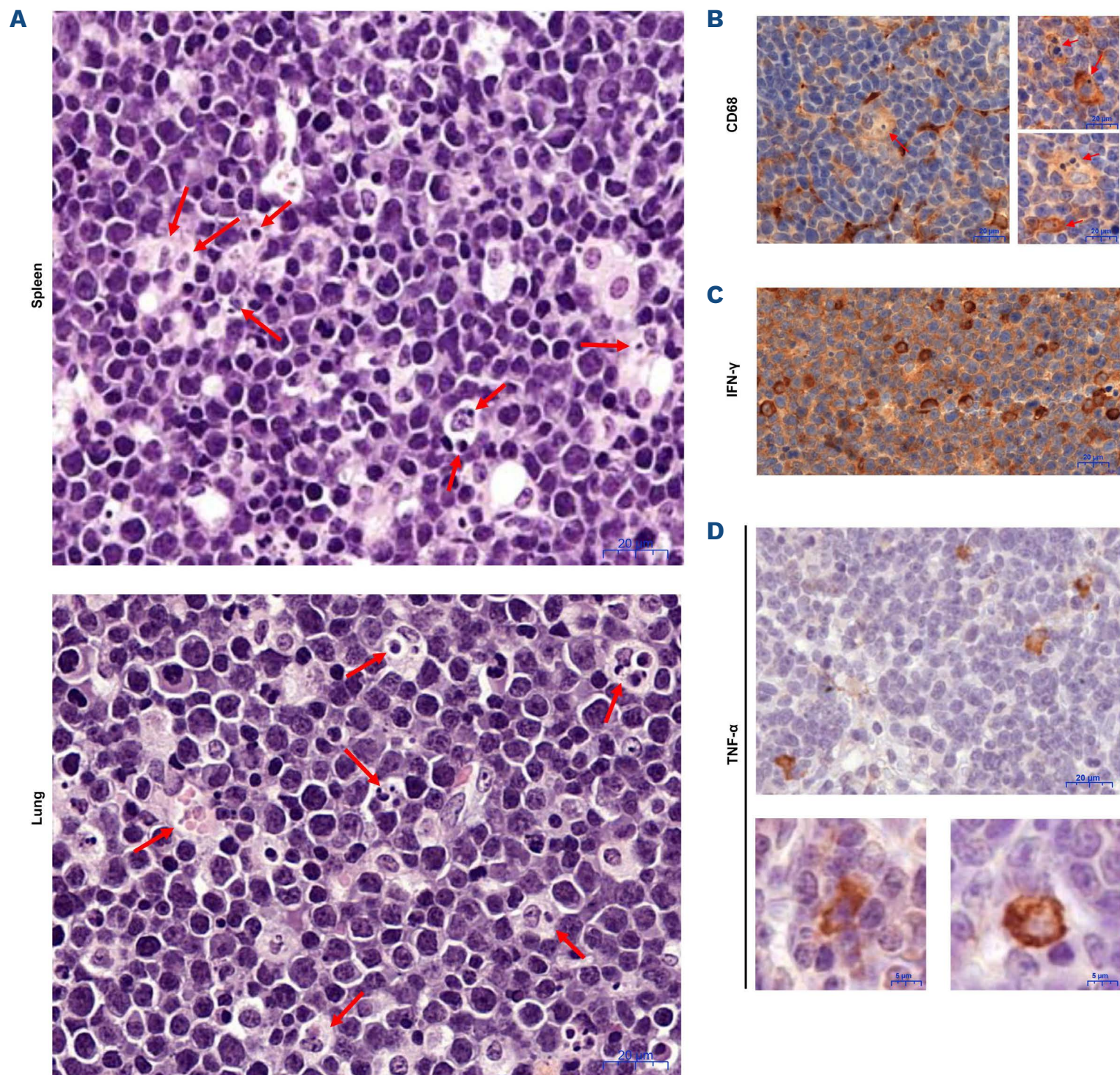


Figure 3. Mice with $JAK3^{A573V}$ -induced lymphoproliferative disease develop hemophagocytosis. (A) Macrophages phagocytosing cells (red arrows) in spleen and lung tissue. (B) CD68 stain (clone 514H12, Leica Biosystems, Nanterre, France) shows numerous macrophages as large, irregularly shaped CD68 $^+$ cells. Detail of CD68 stain shows active phagocytosis by CD68 $^+$ macrophages of lymphocytes (red arrows). (C) Interferon- γ stain (clone ab216642, Abcam, Paris, France) shows interferon- γ production by malignant cells. (D) Tumor necrosis factor- α (TNF- α) stain (AF410-NA, R&D System, Minneapolis, MN, USA) shows TNF- α production by macrophages, identified as large irregularly shaped cells with an abundant cytoplasm. A detailed morphology of TNF- α -secreting macrophages is provided. HE: hematoxylin & eosin; IFN- γ : interferon- γ . TNF- α : tumor necrosis factor- α .

consequences of a constitutively activated JAK3 in NK-cell neoplasms, and its role in the occurrence of hemophagocytic syndrome. By reproducing an animal model of aggressive NKTCL with the features of hemophagocytic syndrome, we found evidence that JAK3 deregulation in NKTCL provides a growth advantage to malignant cells,^{3,4} but also leads to an excessive production of interferon- γ , accounting for the systemic manifestations associated with NKTCL, such as hemophagocytic syndrome.^{11,12} Given that deregulated JAK3 is a common feature in NKTCL, our findings provide an explanation for the high prevalence of hemophagocytic syndrome reported in advanced NKTCL.¹³ Notably, the physiological regulation of interferon- γ secretion was related to multiple signaling proteins, including those in the STAT family and PI3-kinase and MAP-kinase pathways,^{14,15} and their constitutive activation in the presence of deregulated JAK3 is in accordance with our model. An excessive production of interferon- γ , in turn, activates macrophages that release tumor necrosis factor- α . The conjunction of both cytokines accounts for the usual features of hemophagocytic syndrome, including fever and wasting, acute cytopenia, hyperferritinemia, hypertriglyceridemia, hyponatremia and hypofibrinogenemia.¹⁰ The crucial role of deregulated JAK3 in the pathophysiology of NKTCL, accounting for both growth advantage and excessive interferon- γ secretion, but also invasiveness through an amoeboid, matrix metalloproteinase-independent mechanism,³ makes this oncogenic protein targetable with specific inhibitors already approved for the treatment of inflammatory diseases.

Authors

Adrien Picod,^{1*} Suella Martino,^{1*} Pascale Cervera,^{2*} Gregory Manuceau,¹ Marc Arca,¹ Monica Wittner,¹ YanYan Zhang,¹ He Liang,¹ Florian Beghi,¹ Eric Solary,¹ Fawzia Louache^{1,3,4} and Paul Coppo^{1,5}

¹Inserm U1287, Gustave Roussy Institute, Villejuif; ²Service d'Anatomopathologie, Assistance Publique - Hôpitaux de Paris (AP-HP), Sorbonne Université, Paris; ³Université Paris-Sud, Orsay;

⁴French National Center for Scientific Research (CNRS) Research

Group (GDR) 3697 MicroNiT and ⁵Centre de Référence des Microangiopathies Thrombotiques (CNR-MAT), Service d'Hématologie, AP-HP - Sorbonne Université, Paris, France.

*AP, SM and PC contributed equally as co-first authors.

Correspondence:

P. COPPO - paul.coppo@aphp.fr

<https://doi.org/10.3324/haematol.2021.280349>

Received: November 15, 2021.

Accepted: April 22, 2022.

Prepublished: May 5, 2022.

©2022 Ferrata Storti Foundation

Published under a CC BY-NC license 

Disclosures

No conflicts of interest to disclose.

Contributions

AP performed experiments on mice and wrote the first version of the manuscript. SM, GM and MA performed experiments *in vitro*. MW, YZ, HL and FB performed experiments on mice. PCe performed histopathological analyses. ES, FL and PCo designed experiments and supervised the work.

Acknowledgments

The authors would like to thank Sébastien Malinge and Thomas Mercher, who provided JAK3^{WT} and JAK3^{A573V} retroviral vectors, and Sophie Ezine who provided *Rag2*^{-/-} mice. Figures describing protocols were created using Servier Medical Art (smart.servier.com).

Funding

This work was funded in part by grants from the following institutions: Fondation pour la Recherche Médicale (FRM), Association pour la Recherche contre le Cancer, and Société d'Hématologie et d'Immunologie Pédiatrique (SHIP).

Data-sharing statement

Data from the current work are available on request.

References

1. Bigenwald C, Fardet L, Coppo P, et al. A comprehensive analysis of lymphoma-associated haemophagocytic syndrome in a large French multicentre cohort detects some clues to improve prognosis. *Br J Haematol*. 2018;183(1):68-75.
2. Wang H, Fu BB, Gale RP, Liang Y. NK-/T-cell lymphomas. *Leukemia*. 2021;35(9):2460-2468.
3. Bouchekioua A, Scourzic L, de Wever O, et al. JAK3 deregulation by activating mutations confers invasive growth advantage in extranodal nasal-type natural killer cell lymphoma. *Leukemia*. 2014;28(2):338-348.
4. Koo GC, Tan SY, Tang T, et al. Janus kinase 3-activating mutations identified in natural killer/T-cell lymphoma. *Cancer Discov*. 2012;2(7):591-597.
5. Lee S, Park HY, Kang SY, et al. Genetic alterations of JAK/STAT cascade and histone modification in extranodal NK/T-cell lymphoma nasal type. *Oncotarget*. 2015;6(19):17764-17776.

6. Sim SH, Kim S, Kim TM, et al. Novel JAK3-activating mutations in extranodal NK/T-cell lymphoma, nasal type. *Am J Pathol.* 2017;187(5):980-986.
7. Coppo P, Gouilleux-Gruart V, Huang Y, et al. STAT3 transcription factor is constitutively activated and is oncogenic in nasal-type NK/T-cell lymphoma. *Leukemia.* 2009;23(9):1667-1678.
8. Malinge S, Ragu C, Della-Valle V, et al. Activating mutations in human acute megakaryoblastic leukemia. *Blood.* 2008;112(10):4220-4226.
9. Cornejo MG, Kharas MG, Werneck MB, et al. Constitutive JAK3 activation induces lymphoproliferative syndromes in murine bone marrow transplantation models. *Blood.* 2009;113(12):2746-2754.
10. Fardet L, Galicier L, Lambotte O, et al. Development and validation of the HScore, a score for the diagnosis of reactive hemophagocytic syndrome. *Arthritis Rheumatol.* 2014;66(9):2613-2620.
11. Jordan MB, Hildeman D, Kappler J, Marrack P. An animal model of hemophagocytic lymphohistiocytosis (HLH): CD8+ T cells and interferon gamma are essential for the disorder. *Blood.* 2004;104(3):735-743.
12. Zoller EE, Lykens JE, Terrell CE, et al. Hemophagocytosis causes a consumptive anemia of inflammation. *J Exp Med.* 2011;208(6):1203-1214.
13. Jia J, Song Y, Lin N, et al. Clinical features and survival of extranodal natural killer/T cell lymphoma with and without hemophagocytic syndrome. *Ann Hematol.* 2016;95(12):2023-2031.
14. Schoenborn JR, Wilson CB. Regulation of interferon-gamma during innate and adaptive immune responses. *Adv Immunol.* 2007;96:41-101.
15. Souza-Fonseca-Guimaraes F, Parlato M, de Oliveira RB, et al. Interferon-gamma and granulocyte/monocyte colony-stimulating factor production by natural killer cells involves different signaling pathways and the adaptor stimulator of interferon genes (STING). *J Biol Chem.* 2013;288(15):10715-10721.

β adrenergic signaling regulates hematopoietic stem and progenitor cell commitment and therapy sensitivity in multiple myeloma

Multiple myeloma (MM) development is dependent upon critical interactions with the bone marrow (BM) niche.¹ The contribution of catecholamines and adrenergic signaling from the highly innervated BM niche² to MM development is under-explored. MM patients demonstrate an elevated conserved transcriptional response to adversity (CTRA), indicative of stress that correlates with poor survival.³ A retrospective study evaluating the effects of the non-selective β adrenergic receptor (AR) blocker propranolol in immunomodulatory drug-treated MM found propranolol to improve progression-free survival (PFS) and overall survival (OS).⁴ MM patients exhibit reduced megakaryocyte-erythrocyte progenitors (MEP) and increased monocytic myeloid-derived suppressor cells (MDSC) (CD14⁺HLADR^{low}) in the BM, suggestive of increased myeloid bias.⁵ Introduction of MM precursor monoclonal gammopathy of undetermined significance (MGUS) cells into humanized IL-6 MIS(KI)TRG6 mice promotes progression to MM, suggesting the sufficiency of extrinsic BM niche elements in fostering MM development.⁶ Consistent with this, administration of propranolol in MM patients undergoing hematopoietic stem cell transplant (HSCT) demonstrates a significant reduction of not only the CTRA response, but also marked reductions in myeloid lineage bias.³ How targeting adrenergic signaling regulates hematopoietic stem and progenitor cell (HSPC) commitment in MM remains poorly understood. Our study provides mechanistic rationale for the application of propranolol to resolve both microenvironmental and MM-specific tumor promoting biology.

For this study, samples from MM patients, ranging from newly diagnosed to those with relapsed refractory MM were analyzed, exhibiting a range of reduced hemoglobin (Hgb) levels (characteristics in the *Online Supplementary Table S1*) and anemia. BM aspirates were obtained from consenting patients following an Emory University Institutional Review Board-approved protocol. Research was conducted in accordance with the Declaration of Helsinki. Ficoll gradient isolated mononuclear cells were cultured for phase I expansion in serum-free expansion medium (SFEM) containing granulocyte macrophage colony-stimulating factor (GM-CSF), stem cell factor (SCF), interleukin 3 (IL-3 – pluripotent hematopoietic colony-stimulating factor) or further expanded in phase II (day 6–16) by culture in SCF, HT (holo-transferrin), EPO (erythropoietin), and SFEM for all assays involving progenitor cells as previously described.^{7,8} Cell death/viability were assessed by

AnnexinV/DAPI flow cytometry. The CoMMpass MM trial (clinicaltrials.gov. Identifier: NCT0145429) data was downloaded from Genomic Data Commons. All other assays are as previously reported.^{8,9}

Analysis of the proportion of granulocyte-monocyte-progenitors (GMP) (Lin^{neg} CD34⁺CD38⁺CD123⁻CD45RA⁺) versus MEP (Lin^{neg} CD34⁺CD38⁺CD123⁻CD45RA⁻) reconfirmed the significantly reduced number of MEP¹⁰ and importantly for the first time, identified a higher proportion of GMP in MM BM (n=10) versus control bone marrow (CBM) (Figure 1A). Myeloid-biased hematopoiesis contributes to anemia and a protumorigenic BM marrow niche in MM. Strategies targeting the myeloid lineage skew can potentially prevent MM progression and development of fatal refractory disease. V-maf avian musculoaponeurotic fibrosarcoma oncogene homolog B transcription factor (MAFB) and globin transcription factor 1 (GATA1) are central regulators of myeloid versus erythroid lineage commitment. We previously showed that the development of anemia in human burn patients and scald burn mice is driven by high MAFB versus GATA1 expression in CMP. Similarly, we found CMP from MM BM (n=10) expressed significantly higher MAFB and reduced GATA1 expression compared to CMP from CBM (Figure 1B), which inversely correlated with the percentage of MEP. Notably, both reduced MEP/GMP ratio and elevated MAFB/GATA1 expression in MM CMP were maintained after phase I expansion of HSPC, suggesting that the skew in lineage specification is intrinsically driven (*Online Supplementary Figure S1A and B*). Genetic suppression of MAFB expression reduced GMP and increased MEP in the MM BM samples (n=4) (Figure 1C), suggesting that reduction of MAFB was sufficient to block the myeloid bias detected in MM.

Concordant with reduced MM MEP specification, MM BM also exhibited significantly lower total erythroblasts compared to CBM (Figure 1D). Although variability in early erythroblast (EEB) numbers were noticed, late erythroblasts (LEB) were uniformly lower in all MM BM samples (n=10), indicating erythropoietic arrest in MM (Figure 1D).

We have previously shown in human burn patients and scald burn mice that conditions resulting in high catecholamines instigate myelo-erythroid reprioritization and anemia.⁸ As stress and catecholamines are known to modulate the BM microenvironment in MM,¹¹ we investigated whether adrenergic signaling regulated MEP/GMP specification in MM BM.

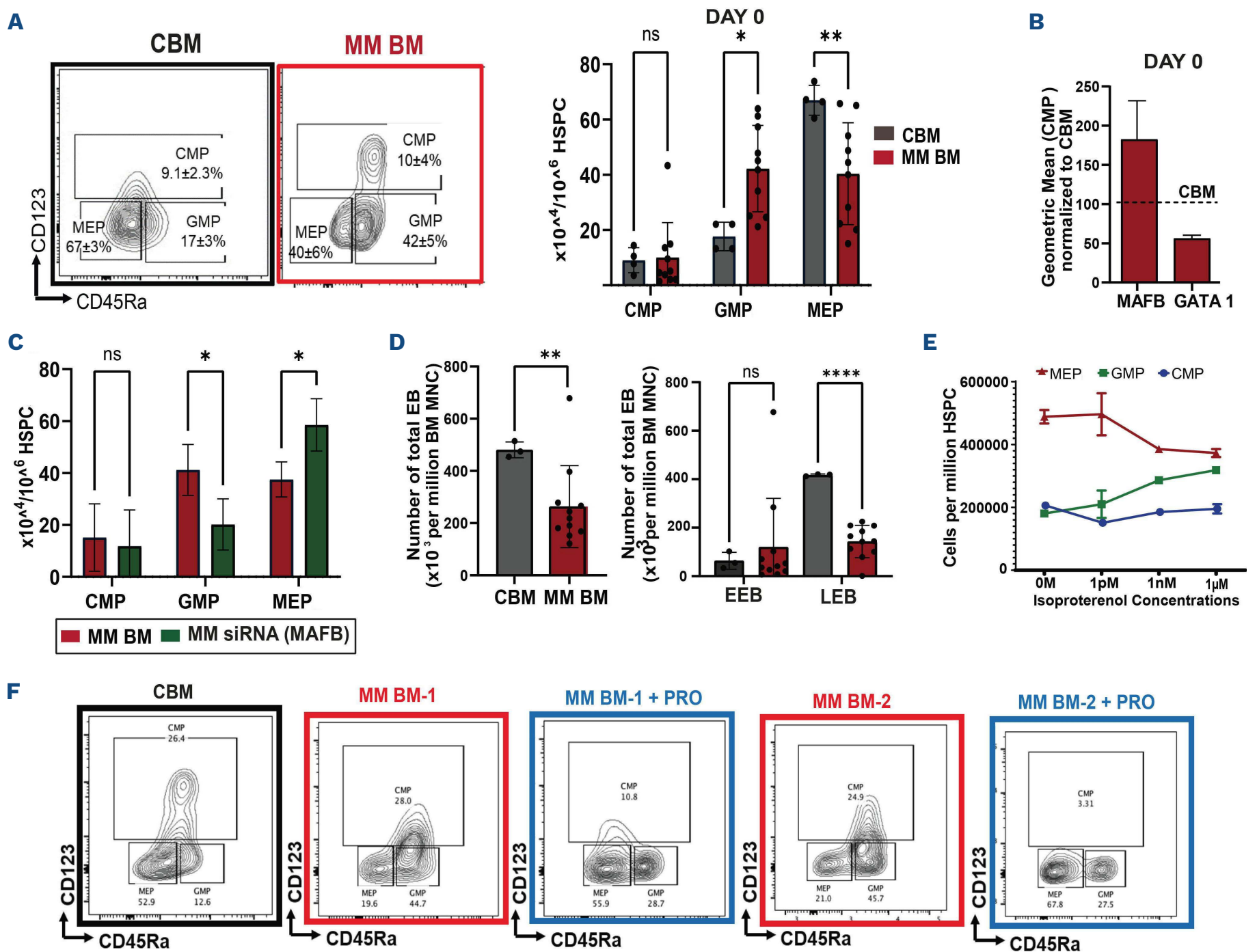


Figure 1. Multiple myeloma patient samples exhibit reduced megakaryocyte-erythrocyte progenitors, elevated MAFB/GATA1 and reduced late erythroblast development that is reversed with propranolol treatment. (A) Representative contour plots of control bone marrow (CBM) and multiple myeloma (MM) sample mononuclear cells in forward vs. side scatter (left panel), from flow cytometry day 0 CBM and MM BM evaluated for common myeloid progenitors (CMP)/ granulocyte-monocyte-progenitors (GMP)/megakaryocyte-erythrocyte progenitors (MEP) frequencies (n=10) (right panel). (B) Mean fluorescence intensity (MFI) of MAFB and GATA1 expression in CMP from 10 MM patients at day 0, evaluated by flow cytometry. (C) Introduction of non-targeting and MAFB-directed small interfering RNA (siRNA) in MM BM samples (n=4). Frequencies of CMP, GMP and MEP in MM vs. MM siRNA-transfected samples are shown. (D) Evaluation of total erythroblasts (EB) (CD71⁺CD235a⁺) in MM vs. CBM $P < 0.001$ (n=10) (left panel). Late erythroblasts (LEB) (CD71⁺CD235a⁺) are significantly decreased ($P < 0.0001$) compared to early erythroblasts (EEB) (CD71⁺CD235a⁻) suggesting erythropoietic arrest in MM (right panel). (E) MEP, GMP and CMP quantified in hematopoietic stem and progenitor cell (HSPC) in phase 1 cultures treated with increasing doses of isoproterenol (ISO). (F) CMP, GMP and MEP frequencies quantified in CBM and MM treated ex vivo with propranolol (PRO).

We first evaluated basal expression levels of the α and β AR by flow cytometry. HSPC of MM BM and CBM were found to exhibit similar expression of both α (α_1 , α_2) and β (β_1 , β_2 , β_3) AR (data not shown). Stimulation of CBM HSPC with increasing concentrations of isoproterenol, a specific agonist of β AR, increased GMP with a corresponding reduction of MEPs (Figure 1E). Isoproterenol, importantly, increased MAFB expression in CMP and GMP and reduced GATA1 expression in CMP, GMP and MEP (Online Supplementary Figure S1C and D). Phenylephrine, an α AR spe-

cific agonist, had no effect on HSPC specification towards GMP versus MEP (n=4) or on MAFB/GATA1 expression, suggesting β adrenergic stimulation specifically regulates myeloid bias (Online Supplementary Figure S1E). Inhibition of β AR with propranolol suppressed MAFB expression in CMP (Online Supplementary Figure S1C). Importantly, β AR inhibition with propranolol was also able to reverse the low MEP:GMP ratio in MM BM (Figure 1F). These results, in sum, demonstrate that in MM, i) β adrenergic signaling can regulate HSPC specification; ii) propranolol reverses the

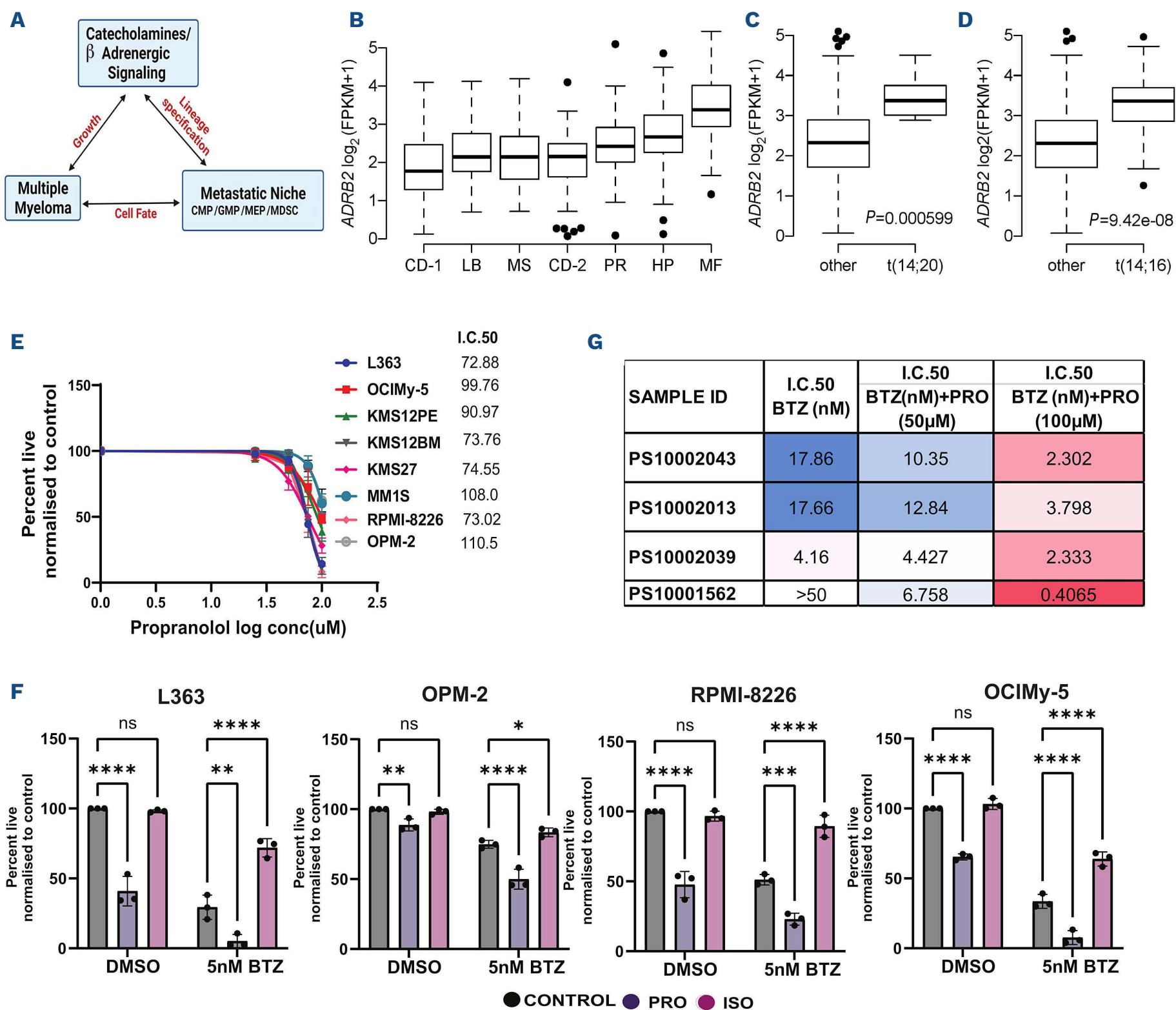


Figure 2. Isoproterenol and propranolol regulate multiple myeloma sensitivity to the proteasome inhibitor bortezomib. (A) Model of how β adrenergic signaling establishes a tumor promoting triad between multiple myeloma (MM) and the skewed common myeloid lineage specification in the BM (bone marrow) niche. (B) *ADRB2* expression in MM gene expression subtypes from the CoMMpass study (IA17). CD-1: Cyclin D1; LB: low bone disease; MS: MMSET; CD-2: Cyclin D1 and CD20; PR: proliferation; HP: hyperdiploid; MF: MAF. (C) *ADRB2* expression in patients with t(14;20) (IGH-MAFB) (D) and t(14;16) (IGH-MAF) translocations. *P*-values were determined by two-sided *t*-test. (E) MM lines treated with dose range of propranolol (PRO) for 24 hours (h) assessed for viability using Annexin V/DAPI flow cytometric staining. (F) Cell lines treated with 75 μ M PRO or isoproterenol (ISO) as indicated for 24 h assessed for viability using Annexin V/DAPI flow cytometric staining. (G) MM patient BM mononuclear cells treated with 50 or 100 μ M PRO in combination with bortezomib (BTZ) assessed for BTZ half maximal inhibitory concentration (I.C.50) using AnnexinV/DAPI flow cytometric staining.

effects of β agonist-stimulated elevation in GMP and lastly; iii) propranolol regulates MAFB/GATA1 expression to restore MEP commitment in MM (Figure 2A).

Ectopic MAFB expression in mouse HSC promotes acquisition of a tumoral plasma cell fate without induction of MAF in tumor cells.¹² MAF also has a role in promoting MM growth and its expression correlates with poor OS.¹³ MAF thus has both cell extrinsic and intrinsic roles in

shaping myeloma genesis, warranting development of strategies to target MAF for MM therapy. Evaluation of RNA sequencing in primary MM samples from the CoMMpass trial¹⁴ (clinical trials gov. Identifier: NCT0145429) indicated *ADRB2* was significantly higher in the MAF (MF) gene expression subtype (Figure 2B). Consistent with this, *ADRB2* expression was elevated in MM samples harboring the high risk-associated t(14;20) or t(14;16) translocations that

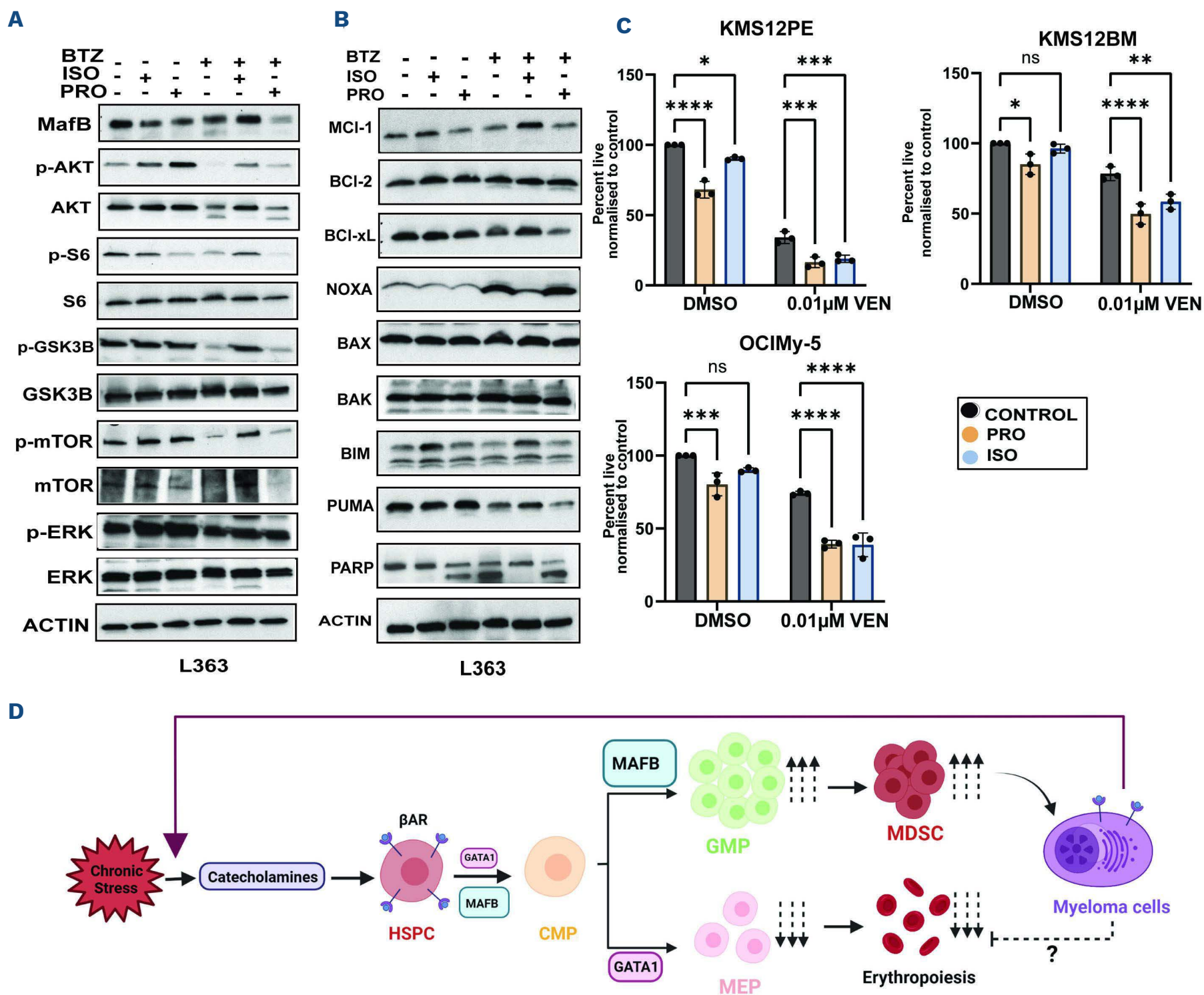


Figure 3. Propranolol increases sensitivity to the BCL-2 antagonist venetoclax. (A and B) L363 cells treated with bortezomib (BTZ) and/or isoproterenol (ISO)/propranolol (PRO) as indicated for 18 hours (h), assessed for indicated proteins by immunoblot analyses. (C) Cell lines treated with 75 μM PRO or 75 μM ISO in combination with 0.01 μM venetoclax (VEN) for 24 h assessed for viability. All cell death/viability assessed by AnnexinV/DAPI flow cytometry. (D) Model: β adrenergic signaling elevates MAFB vs. GATA1 expression in common myeloid progenitors (CMP) leading to increased granulocyte monocyte progenitor (GMP) vs. megakaryocyte erythrocyte progenitor (MEP) specification in multiple myeloma, establishing a feed forward loop. Model is created in BioRender.com. MDSC: myeloid-derived suppressor cells; HSPC: hematopoietic stem and progenitor cells; βAR: β adrenergic receptor.

juxtapose the IgH enhancer to drive elevated levels of *MAFB* and *MAF* expression, respectively (Figure 2C and D). *ADRB1* and *ADRB3* expression was low to undetectable in most MM samples (*data not shown*). Additionally, *ADRB2* was detected in all MM cell lines tested (*Online Supplementary Figure S1F*). These observations prompted us to examine the effects of propranolol on MM cells.

Propranolol has potent anti-cancer effects attributed to both tumor intrinsic and extrinsic effects.¹⁵ We found propranolol to elicit cytotoxicity in MM cell lines (Figure 2E). Proteasome inhibitors (PI) like bortezomib (BTZ) are backbone MM therapeutics, however, most MM patients be-

come refractory to PI. We found treatment of MM cell lines with lower doses of propranolol enhanced, while isoproterenol reversed, sensitivity to BTZ, irrespective of *MAFB* expression status (Figure 2F). In order to clinically validate our observations, we tested the effects of isoproterenol, propranolol and BTZ treatments in MM patient samples (n=4). As seen in cell lines, isoproterenol promoted resistance to BTZ, while isoproterenol increased sensitivity to BTZ in the MM primary cells (Figure 2G). We found isoproterenol in the context of BTZ treatment to elevate *MAFB*, *pAKT*, *p-S6* and *pmTORC1* (Figure 3A). While treatment with BTZ is known to stabilize *MAFB* expression,¹⁶ propra-

nolol significantly reduced MAFB expression in BTZ treated cells, underscoring the utility of using propranolol to target MAFB and overcome β adrenergic-stimulated activation of the AKT-mTOR axis (Figure 3A).

Since most chemo-resistance occurs because of impaired ability to execute apoptosis consequent to reduced “priming” i.e., suboptimal quantities of BH3 activators bound to anti-apoptotics,^{9,17,18} we evaluated the expression of the major BCL-2 family proteins (Figure 3B). BTZ cytotoxicity is dependent upon increased NOXA expression that, upon binding MCL-1, allows for pro-apoptotic BIM release. Interestingly, we found BTZ-induced elevation of NOXA and reduction of MCL-1 and BCL-xL is suppressed by isoproterenol (Figure 3A). Co-treatment with propranolol and BTZ maintains NOXA induction, MCL-1 suppression, and PARP cleavage with further reduction of BCL-xL and PUMA. Lastly, we found propranolol increases sensitivity to the BCL-2 antagonist venetoclax (VEN) and importantly, isoproterenol stimulation did not reverse propranolol-induced sensitivity to VEN (Figure 3C).

In conclusion, our results suggest neurotransmitters elevate MAFB in MM CMP to augment pro-tumorigenic GMP-MDSC commitment, as summarized in the schematic (Figure 3D), that can be reversed with propranolol, restricting myelopoiesis in MM. Additionally, we show that β adrenergic stimuli selectively increase resistance to proteasome inhibitors, while targeting β adrenergic signaling with propranolol increases sensitivity to BTZ and VEN. We acknowledge the limited patient sample size for the current study and the need for greater mechanistic understanding of how β adrenergic signals regulate intra- and inter-cellular signaling to promote niche remodeling and drug sensitivity. Our results, in sum, underscore the importance of further interrogation of early application of propranolol and other β blockers in MM therapy.

Authors

Remya Nair,^{1*} Vimal Subramaniam,^{2*} Benjamin G. Barwick,¹ Vikas A. Gupta,¹ Shannon M. Matulis,¹ Sagar Lonial,¹ Lawrence H. Boise,¹ Ajay K. Nooka,¹ Kuzhali Muthumalaiappan^{2#} and Mala Shanmugam^{1#}

¹Department of Hematology and Medical Oncology, Winship Cancer Institute, School of Medicine, Emory University, Atlanta, GA and

²Department of Surgery, Loyola University Medical Center, Maywood, Illinois and Burn and Shock Trauma Research Institute, Loyola University Chicago, Chicago, IL, USA

**RN and VS contributed equally as co-first authors.*

#KM and MS contributed equally as co-senior authors.

Correspondence:

M. SHANMUGAM - mala.shan@emory.edu

<https://doi.org/10.3324/haematol.2022.280907>

Received: February 23, 2022.

Accepted: April 26, 2022.

Prepublished: May 5, 2022.

©2022 Ferrata Storti Foundation

Published under a CC BY-NC license 

Disclosures

AKN has significant financial interest in Janssen Pharmaceuticals and has participated on advisory boards and received honoraria from Janssen, Takeda, Amgen, BMS/Celgene, Glaxo SmithKline, Sanofi, Oncopeptides, BeyondSpring, Karyopharm, SecuraBio, and Adaptive Technologies. SL is a consultant for Takeda, Celgene, Novartis, BMS, Amgen, ABBVIE, and Janssen and on the Board of directors with stock for TG therapeutics. LHB receives research funding from AstraZeneca (2019), consultancy, and honoraria from AstraZeneca; and performs consultancy for Genentech (2019) and Abbvie. All other authors declare no competing financial interests.

Contributions

RN, VS, KM, MS conceived and designed the research; RN and VS performed all experimentation; Bioinformatic analyses were performed by BGB. SMM and VAG assisted with patient sample purification; AKN, SL oversaw myeloma patient sample collection; LHB, BGB, VAG, AKN, SKM and KM provided helpful critique; KM provided edits to the manuscript; RN and MS wrote the manuscript.

Acknowledgments

We would like to thank Anthea Hammond, Ph.D., Emory University for editorial assistance.

Funding

This study was supported in part by NIH/NCI R01 CA208328 to MS, Leukemia Lymphoma Society TRP Award #6573-19 to MS and NIH/NIDDK 2R56DK097760 to KM and the Winship's Cancer Center Support Grant (P30CA138292) awarded by the National Cancer Institute of the National Institutes of Health.

Data-sharing statement

All technical information pertaining to the experimentation performed is available on request.

References

1. Ghobrial IM, Detappe A, Anderson KC, Steensma DP. The bone-marrow niche in MDS and MGUS: implications for AML and MM. *Nat Rev Clin Oncol*. 2018;15(4):219-233.
2. Kuntz A, Richins CA. Innervation of the bone marrow. *J Comp Neurol*. 1945;83:213-222.
3. Knight JM, Rizzo JD, Hari P, et al. Propranolol inhibits molecular risk markers in HCT recipients: a phase 2 randomized controlled biomarker trial. *Blood Adv*. 2020;4(3):467-476.
4. Hwa YL, Shi Q, Kumar SK, et al. Beta-blockers improve survival outcomes in patients with multiple myeloma: a retrospective evaluation. *Am J Hematol*. 2017;92(1):50-55.
5. Brimnes MK, Vangstedt AJ, Knudsen LM, et al. Increased level of both CD4+FOXP3+ regulatory T cells and CD14+HLA-DR(-)/low myeloid-derived suppressor cells and decreased level of dendritic cells in patients with multiple myeloma. *Scand J Immunol*. 2010;72(6):540-547.
6. Das R, Strowig T, Verma R, et al. Microenvironment-dependent growth of preneoplastic and malignant plasma cells in humanized mice. *Nat Med*. 2016;22(11):1351-1357.
7. Walczak J, Bunn C, Saini P, Liu YM, Baldea AJ, Muthumalaiappan K. Transient improvement in erythropoiesis is achieved via the chaperone AHSP with early administration of propranolol in burn patients. *J Burn Care Res*. 2020;42(2):311-322.
8. Hasan S, Johnson NB, Mosier MJ, et al. Myelo-erythroid commitment after burn injury is under β -adrenergic control via MafB regulation. *Am J Physiol Cell Physiol*. 2017;312(3):C286-C301.
9. Bajpai R, Sharma A, Achreja A, et al. Electron transport chain activity is a predictor and target for venetoclax sensitivity in multiple myeloma. *Nat Commun*. 2020;11(1):1228.
10. Liu L, Yu Z, Cheng H, et al. Multiple myeloma hinders erythropoiesis and causes anaemia owing to high levels of CCL3 in the bone marrow microenvironment. *Sci Rep*. 2020;10(1):20508.
11. Cheng Y, Sun F, D'Souza A, et al. Autonomic nervous system control of multiple myeloma. *Blood Rev*. 2021;46:100741.
12. Vicente-Dueñas C, Romero-Camarero I, González-Herrero I, et al. A novel molecular mechanism involved in multiple myeloma development revealed by targeting MafB to haematopoietic progenitors. *EMBO J*. 2012;31(18):3704-3717.
13. Qiang YW, Ye S, Chen Y, et al. MAF protein mediates innate resistance to proteasome inhibition therapy in multiple myeloma. *Blood*. 2016;128(25):2919-2930.
14. Barwick BG, Neri P, Bahlis NJ, et al. Multiple myeloma immunoglobulin lambda translocations portend poor prognosis. *Nat Commun*. 2019;10(1):1911.
15. Pantziarka P, Bouche G, Sukhatme V, Meheus L, Rooman I, Sukhatme VP. Repurposing Drugs in Oncology (ReDO)-Propranolol as an anti-cancer agent. *Ecancermedicallscience*. 2016;10:680.
16. Qiang Y-W, Ye S, Huang Y, et al. MAFb protein confers intrinsic resistance to proteasome inhibitors in multiple myeloma. *BMC Cancer*. 2018;18(1):724.
17. Ni Chonghaile T, Sarosiek KA, Vo TT, et al. Pretreatment mitochondrial priming correlates with clinical response to cytotoxic chemotherapy. *Science*. 2011;334(6059):1129-1133.
18. Montero J, Sarosiek KA, DeAngelo JD, et al. Drug-induced death signaling strategy rapidly predicts cancer response to chemotherapy. *Cell*. 2015;160(5):977-989.

Pure erythroid leukemia is characterized by biallelic *TP53* inactivation and abnormal p53 expression patterns in *de novo* and secondary cases

Pure erythroid leukemia (PEL) is a rare type of acute myeloid leukemia (AML) characterized by a neoplastic proliferation of immature erythroblasts associated with a complex karyotype and a poor prognosis.¹⁻³ PEL can arise *de novo*, but more frequently occurs as a therapy-related neoplasm or transformation from myelodysplastic syndromes (MDS).^{4,5} To date, the potential differences between *de novo* and secondary (therapy-related or MDS-derived) PEL have not been well explored. Recent studies have shown that *TP53* mutations are common in PEL^{1,5} and that p53 overexpression is also frequent.⁶ Strong p53 expression shown by immunohistochemistry has become an important clue in the initial workup of PEL. However, we have observed some PEL cases lacking p53 expression despite the presence of *TP53* mutations. We conducted the current study to investigate *TP53* mutation characteristics and p53 protein expression in PEL and to examine whether secondary PEL cases differ from *de novo* disease. Another aim of this study was to address PEL as an entity that should be histopathologically and genetically defined, *versus* classifying these cases following the current classification scheme in which a history of prior chemoradiation therapy or MDS is relatively more emphasized.

We collected 22 cases of PEL, defined by a predominant proliferation of neoplastic erythroblasts that formed sheets in bone marrow, of which 30% or more were pronormoblasts. The clinical characteristics of our patients are summarized in Table 1. There were 14 men and eight women with a median age of 69 years (range, 37-81). Eleven (50%) patients had a history of chemotherapy for other malignancies (therapy-related), five (23%) had MDS, one (4%) had primary myelofibrosis (PMF), and five (23%) occurred *de novo*. Among 21 patients with treatment information available, five (24%) did not receive any therapy due to poor performance status or poor response to prior treatments for MDS. The remaining 16 patients received treatments after the diagnosis of PEL (Table 1). Four (25%) patients achieved a complete response with incomplete hematologic recovery; the response in three patients (#3, 12, 20) was transient and one patient (#22) remained in complete response with incomplete hematologic recovery at last follow-up, 4.7 months after diagnosis. None of the patients was eligible for stem cell transplantation. Twenty-one patients had clinical follow-up: 20 had died at last follow-up and one patient (#22) was alive. The

median survival time for this entire cohort was 2.8 months (range, 0.2-7.3); 2.3 months (range, 0.2-7.3) for therapy-related, 2.6 months (range, 0.4-4.9) for patients with a history of MDS, and 3.9 months (range, 2.2-5.5) for *de novo* PEL.

Targeted next generation sequencing (NGS) with panels composed of genes commonly mutated in myeloid neoplasms was performed on bone marrow samples from 20 patients (19 using an 81-gene panel and 1 using a 28-gene panel) at the time of PEL diagnosis as previously described.⁷ One case was tested for *TP53* mutation using Sanger sequencing. In total, 21 cases were tested and all patients had *TP53* mutation(s) (Table 2). A total of 25 *TP53* mutations were detected: 18 patients had one *TP53* mutation, two patients (#15 and 17) had two mutations, and one (#5) patient had three mutations. Twenty-two (88%) mutations occurred in the DNA binding domain (exons 5-8), including 12 in exon 5, one in exon 6, four in exon 7, and five in exon 8. The remaining three mutations occurred in exon 4, exon 10, and a splice site, respectively. The types of *TP53* mutations included 19 (76%) missense, 1 (4%) nonsense, 1 (4%) splice site, and 4 (16%) small deletion. Among the four cases with small deletion mutations, three caused frameshift. The median variant allele frequency (VAF) of *TP53* mutations was 35% (range, 1-92.3%). One patient (#13) was not assessed for *TP53* mutation, but immunohistochemistry showed strong and diffuse p53 expression, suggestive of *TP53* mutations. The detailed *TP53* mutational profiles are summarized in Table 2. Among the 16 patients who received treatment, 11 (#3, 4, 7, 8, 11, 15, 17, 18, 20-22) had repeat *TP53* mutation analysis by NGS after treatment and all showed persistent *TP53* mutations. Among the 20 cases tested by NGS, additional gene mutations were detected in nine (45%) patients (*Online Supplementary Table S1*), including *DNMT3A* (n=3; VAF 10.3-29.3%), *NRAS* (n=2; VAF 5% and 26.6%), *TET2* (n=1; VAF <3%), *FLT3* (n=1; VAF 1.7%), *PRPF40B* (n=1; VAF 40.8%), *KMT2A* (n=1; VAF 15.2%) and *GATA2* (n=1; VAF 1.8%). Patient #22 had a history of PMF that was positive for *JAK2* V617F (VAF 32%) and negative for *TP53*. At the time of progression to PEL, *JAK2* V617F was detected with a VAF of 1%, and *TP53* mutation was acquired (VAF 80.6%).

Twenty cases underwent conventional karyotyping at the time of PEL diagnosis and all (100%) had complex karyotypes (*Online Supplementary Table S1*). Among 19 cases with karyotype data available, 12 (63%) had -5/5q-, 12

Table 1. Clinical characteristics of pure erythroid leukemia.

Case #	Sex	Age years	F/U months	Treatment	Response	Status at F/U	History
1	M	77	2.8	None	N/A	Dead	Therapy-related (B-ALL and DLBCL)
2	M	66	0.2	None	N/A	Dead	Therapy-related (PCN)
3	F	68	7.3	Decitabine + Venetoclax, 4 cycles Azacitidine + Hu5F9-G4, 1 cycle	Transient CRi, 2.1 months	Dead	Therapy-related (ovarian cancer)
4	M	55	1.4	CLIA + Venetoclax, 1 cycle	No	Dead	Therapy-related (DLBCL)
5	F	70	1.7	Decitabine + Venetoclax, 1 cycle	No	Dead	Therapy-related (PCN)
6	M	48	2.3	Fludarabine + AraC + Idarubicin, 1 cycle	No	Dead	Therapy-related (AML)
7	F	54	4.8	Cytarabine + Daunorubicine, 1 cycle Decitabine + Venetoclax, 2 cycles	No	Dead	Therapy-related (breast cancer)
8	M	66	6.3	Azacitidine, 4 cycles	No	Dead	Therapy-related (PCN)
9	F	81	0.8	None	N/A	Dead	Therapy-related (DLBCL)
10	M	69	2.1	Low dose Cytarabine + Venetoclax, 1 cycle	No	Dead	Therapy-related (lung cancer)
11	M	56	4.4	ASTX660 + ASTX727, 1 cycle	No	Dead	Therapy-related (PCN)
12	M	76	4.9	Sapacitabine, 3 cycles	Transient CRi, 2 months	Dead	MDS
13	F	37	0.4	None	N/A	Dead	MDS
14	M	78	2.6	Low dose Cytarabine + Venetoclax, 2 cycles	No	Dead	MDS
15	M	79	3.6	FF1101 (BET inhibitor), 2 cycles	No	Dead	MDS
16	M	60	1.3	None	N/A	Dead	MDS
17	F	78	2.2	Azacitidine + Nivolumab, 2 cycles	No	Dead	De novo
18	M	59	5.5	Azacitidine, 3 cycles FIA + Venetoclax, 1 cycle	No	Dead	De novo
19	F	78	N/A	N/K	N/K	N/K	De novo
20	M	65	5.0	Azacitidine + Venetoclax, 2 cycles	Transient CRi, 2.6 months	Dead	De novo
21	M	72	2.8	Decitabine + Venetoclax, 1 cycle	No	Dead	De novo
22	F	73	4.7	Azacitidine + Venclexta + Magrolimab, 3 cycles	CRi at the last F/U, 3 months	Alive	PMF

AML: acute myeloid leukemia; B-ALL: B-acute lymphoblastic leukemia; BET: bromodomain and extra-terminal; CLIA: cladribine, idarubicin, and cytarabine; CRi: complete response with incomplete hematologic recovery; DLBCL: diffuse large B-cell lymphoma; FIA: fludarabine, idarubicin, cytarabine; F/U: follow up; MDS: myelodysplastic syndrome; N/A: not applicable; N/K: not known; PCN: plasma cell neoplasm; PMF: primary myelofibrosis.

(63%) had -7/7q-, and nine (47%) had concomitant -5/5q- and -7/7q-. The status of 17p/TP53 was assessed by conventional karyotyping and/or fluorescence *in situ* hybridization (FISH) in 17 cases: deletion of 17p and/or TP53 was detected in 13 (76%) cases (Table 2). The remaining four patients were negative but three (cases # 5, 15, and

17, Table 2) had more than one TP53 mutation by NGS, raising the possibility that both alleles were affected by TP53 mutations. In one patient (#12), the status of 17p/TP53 was unknown, but the VAF of TP53 mutation was 92.3%, consistent with the loss of wild-type TP53. We performed p53 immunohistochemistry on 21 cases

and correlated the results with *TP53* mutation types (Table 2). Sixteen (76%) cases of PEL were strongly and uniformly positive for p53; 15 had missense mutations and one had a deletion mutation but no frameshift (#3). In the remaining five (24%) cases, p53 expression was completely absent in the neoplastic cells (null pattern). In cases negative for p53 expression, three (#6, 16, 21) had *TP53* frameshift mutations, one (#18) had a nonsense mutation, and one (#1) had a splice site mutation. Representative cases of PEL with p53 overexpression and completely absence of p53 expression are shown in Figure 1A and B. In this study, two patients (cases #3 and 14) had a single *TP53* mutation with a VAF less than 15%. In both cases, erythroblasts formed sheets in the core biopsy and

were diffusely and strongly positive for p53 by immunohistochemistry. These findings suggest that most of the erythroblasts had mutated *TP53* and the low VAF of *TP53* mutation may be due to hemodiluted specimen submitted for molecular analysis. However, we also cannot exclude the possibility that only a subclone of leukemic cells had *TP53* mutation.

These data demonstrate that PEL is characterized by biallelic *TP53* alterations, frequently present as a mutation in one allele and deletion in another allele. In cases with no *TP53* deletion, two or more mutations were often detected. Mutations frequently seen in other myeloid neoplasms are less common in PEL, indicating that biallelic loss of *TP53* function is a feature of PEL and may play a

Table 2. *TP53* mutational profiles and p53 protein expression in pure erythroid leukemia.

Case #	Monosomy 17 or <i>TP53</i> Deletion (karyotype or FISH)*	Number of <i>TP53</i> Mutation	Biallelic <i>TP53</i> Inactivation	<i>TP53</i> Mutation (Ref: NM_000546.5)	Type of Mutation	VAF %	Exon(s)	IHC-p53
1	yes	1	yes	c.673-2A>T	splice site	74.9	splice site	negative
2	yes	1	yes	c.405C>G p.C135W	missense	42.1	5	positive
3	yes	1	yes	c.534_536del p.H179del	deletion, no frameshift	11.9	5	positive
4	yes	1	yes	c.818G>A p.R273H	missense	59.6	8	positive
5	no	3	likely yes	c.715A>G p.N239D c.401T>G p.F134C c.329G>T p.R110L	missense missense missense	1 29.3 32	4,5,7	positive
6	N/K	1	N/K	c.501del p.Q167fs	deletion, frameshift	62.6	5	negative
7	N/K	1	N/K	c.524G>A p.R175H	missense	37.2	5	positive
8	yes	1	yes	c.377A>C p.Y126S	missense	23.0	5	positive
9	N/K	1	N/K	c.715A>G p.N239D	missense	42.6	7	positive
10	yes	1	yes	c.818G>C p.R273P	missense	27.2	8	positive
11	yes	1	yes	c.488A>G p.Y163C	missense	48.0	5	positive
12	N/K	1	likely yes	c.797G>A p.G266E	missense	92.3	8	positive
13	N/K	N/D	N/K	N/D	N/D	N/D	N/D	positive
14	yes	1	yes	c.745A>G p.R249G	missense	8.4	7	positive
15	no	2	likely yes	c.434T>G p.L145R c.1010G>C p.R337P	missense missense	20.4 18.5	5,10	N/D
16	yes	1	yes	c.455del p.P152fs	deletion, frameshift	70.1%	5	negative
17	no	2	likely yes	c.844C>T p.R282W c.734G>T p.G245V	missense missense	35.1 14.4	7,8	positive
18	yes	1	yes	c.493C>T p.Q165*	nonsense	39.1	5	negative
19	no	1	probably no	c.476C>T p.A159V	missense	16.0	5	positive
20	yes	1	yes	c.590T>G p.V197G	missense	15.1	6	positive
21	yes	1	yes	c.558del p.D186fs	deletion, frameshift	47.1	5	negative
22	yes	1	yes	c.824G>T p.C275F	missense	80.6	8	positive

IHC: immunohistochemistry; N/D: not done; N/K: not known; VAF: variant allele frequency; FISH: fluorescence *in situ* hybridization. *Detailed karyotype and FISH findings are listed in the *Online Supplementary Table S1*.

critical role in the development of PEL. Of note, biallelic *TP53* alteration is not specific to PEL and can be seen in other myeloid neoplasms, such as AML⁸ and therapy-related MDS.⁹ Thus, *TP53* mutations alone may not be sufficient to block the differentiation of erythroid lineage and drive pronormoblast proliferation, a pathognomonic feature of PEL. Alterations of other genes (not covered in our mutation panels) or pathways involved in erythroid differentiation likely also play a role in PEL development. As mutational analysis often takes time, checking p53 expression status by immunohistochemistry has been used

as a surrogate to predict the presence of *TP53* mutations.^{6,10,11} One caveat is that *TP53* mutations do not always correlate with p53 overexpression. In the current study, approximately one quarter of PEL cases showed a null pattern by immunohistochemistry. In these cases, *TP53* mutations were either frameshift, nonsense, or involved a splice site. Of note, the null pattern of p53 expression can usually be distinguished from the “negative” wild-type pattern which often shows variable p53 expression in a subset of cells and the staining intensity ranges from weak to moderate (Figure 1C). In some cases, however, as-

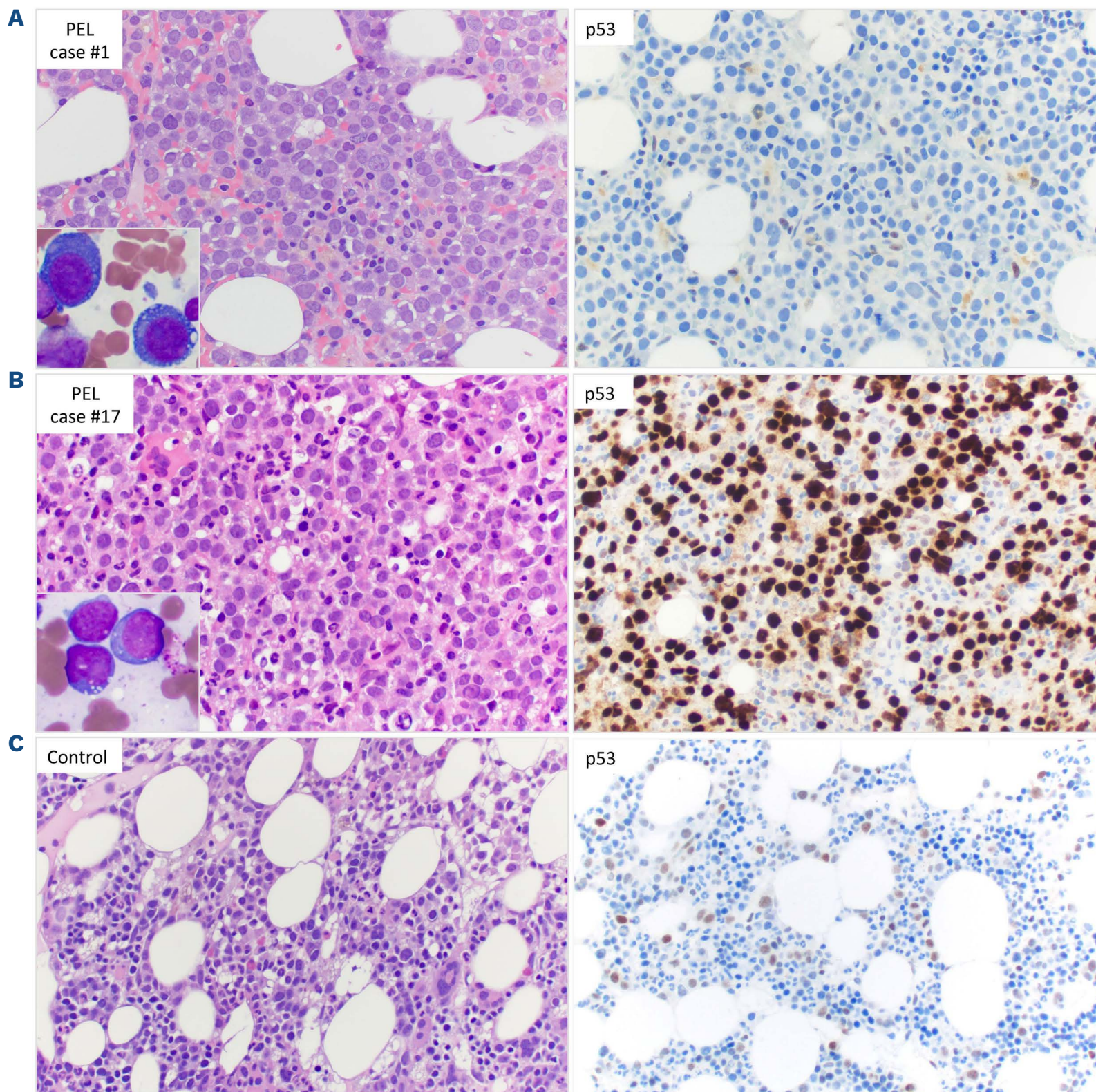


Figure 1. The expression pattern of p53 by immunohistochemistry in pure erythroid leukemia. Immunohistochemistry shows two patterns of p53 expression: complete absence of p53 expression (case #1, upper panel) and uniform and strong overexpression (case #17, middle panel). Of note, in the case with absence of p53 expression in tumor cells (case #1, upper panel), there were scattered reactive cells in the background variably positive for p53, serving as positive controls. A normal bone marrow and its p53 expression by immunohistochemistry is illustrated in the lower panel, in which p53 is variably expressed in a subset of cells with weak to moderate intensity.

assessment of p53 using immunohistochemistry can be challenging, especially in cases where PEL is mixed with residual normal hematopoietic cells in the background which have a wild-type p53 staining pattern.

Lastly, we suggest that the category of PEL should be preserved, despite the fact that some cases also can be classified as therapy-related AML/MDS or AML with myelodysplasia-related changes (AML-MRC) using the current World Health Organization (WHO) criteria. We believe classifying these cases as something other than PEL does not fully capture the distinctive features of this disease. The rationale for this proposal includes: i) PEL cases, irrespective of their origin (*de novo* or secondary), share similar clinicopathological features including poor response to treatment, dismal prognosis, complex karyotype, and biallelic *TP53* alterations. By contrast, the WHO-defined categories of therapy-related AML/MDS or AML-MRC are highly heterogeneous at the molecular level, and are associated with highly variable prognoses for different patient subsets.^{12,13} We believe that the distinctive clinicopathologic and molecular features of PEL may be obscured when these neoplasms are placed in the therapy-related AML/MDS or AML-MRC WHO categories; ii) the survival of PEL patients with a history of receiving cytotoxic therapy or MDS is similar to *de novo* PEL patients but is worse than patients with therapy-related AML¹² and AML-MRC,¹³ respectively; iii) all PEL cases, whether they are *de novo* or secondary, share distinctive morphologic features with prominent pronormoblast proliferation. Pronormoblasts have been shown to play an important role in treatment resistance and increased pronormoblasts have contributed to a poorer prognosis in AML patients.^{14,15} By keeping secondary PEL cases in the category of PEL, these cases can be studied together to explore therapeutic strategies targeting the neoplastic pronormoblasts. Of note, the number of *de novo* PEL cases in our study is relatively small and future studies to include more cases will be valuable.

In summary, we show that PEL is characterized by biallelic *TP53* loss-of-function, a complex karyotype, poor response to AML or MDS directed therapy, and a very dismal prognosis. These unique features are the same for *de novo* or secondary cases of PEL, and therefore we advocate for keeping them under the entity of PEL to facilitate further studies and drug discovery. Immunohistochemistry for p53 can be used as a preliminary screening tool to assess *TP53*; strong p53 expression correlates with missense mutations of *TP53* and a null p53 pattern is often associated with frameshift, nonsense, or *TP53* mutations involving splice sites.

Authors

Hong Fang,¹ Sa A. Wang,¹ Joseph D. Khoury,¹ Siba El Hussein,¹ Do Hwan Kim,¹ Mehrnoosh Tashakori,¹ Zhenya Tang,¹ Shaoying Li,¹ Zhihong Hu,² Fatima Zahra Jelloul,¹ Keyur P. Patel,¹ Timothy J. McDonnell,¹ Tapan Kadia,³ L. Jeffrey Medeiros¹ and Wei Wang¹

¹Department of Hematopathology, The University of Texas MD Anderson Cancer Center; ²Department of Pathology, The University of Texas Health Science Center at Houston and ³Department of Leukemia, The University of Texas MD Anderson Cancer Center, Houston, TX, USA

Correspondence:

W. WANG - wwang13@mdanderson.org

<https://doi.org/10.3324/haematol.2021.280487>

Received: December 16, 2021.

Accepted: April 28, 2022.

Prepublished: May 5, 2022.

©2022 Ferrata Storti Foundation

Published under a CC BY-NC license 

Disclosures

No conflicts of interest to disclose.

Contributions

HF had substantial contributions to the design of the work, drafting the work, revising it, and the acquisition, analysis, interpretation of data for the work. WW had substantial contributions to the conception and design of the work, revising it critically for important intellectual content, and analysis, interpretation of data for the work. SAW and LJM had substantial contributions to the conception and design of the work and revising it critically for important intellectual content. JDK, SE, DHK, MT, ZT, SL, ZH, FZJ, KPP, TJM, and TK had contributions to the acquisition, analysis of data for the work and revising it critically for important intellectual content. All authors had final approval of the version to be published and an agreement to be accountable for all aspects of the work in ensuring that questions related to the accuracy or integrity of any part of the work are appropriately investigated and resolved.

Data-sharing statement

All data are available for sharing upon request to the corresponding author.

References

1. Wang W, Wang SA, Medeiros LJ, Khoury JD. Pure erythroid leukemia. *Am J Hematol.* 2017;92(3):292-296.

2. Reinig EF, Greipp PT, Chiu A, Howard MT, Reichard KK. De novo pure erythroid leukemia: refining the clinicopathologic and

- cytogenetic characteristics of a rare entity. *Mod Pathol.* 2018;31(5):705-717.
3. Wang SA, Hasserjian RP. Acute erythroleukemias, acute megakaryoblastic leukemias, and reactive mimics: a guide to a number of perplexing entities. *Am J Clin Pathol.* 2015;144(1):44-60.
 4. Liu W, Hasserjian RP, Hu Y, et al. Pure erythroid leukemia: a reassessment of the entity using the 2008 World Health Organization classification. *Mod Pathol.* 2011;24(3):375-383.
 5. Montalban-Bravo G, Benton CB, Wang SA, et al. More than 1 TP53 abnormality is a dominant characteristic of pure erythroid leukemia. *Blood.* 2017;129(18):2584-2587.
 6. Alexandres C, Basha B, King RL, Howard MT, Reichard KK. p53 immunohistochemistry discriminates between pure erythroid leukemia and reactive erythroid hyperplasia. *J Hematop.* 2021;14(1):15-22.
 7. Fang H, Yabe M, Zhang X, et al. Myelodysplastic syndrome with t(6;9)(p22;q34.1)/DEK-NUP214 better classified as acute myeloid leukemia? A multicenter study of 107 cases. *Mod Pathol.* 2021;34(6):1143-1152.
 8. Tashakori M, Kadia TM, Loghavi S, et al. TP53 copy number and protein expression inform mutation status across risk categories in acute myeloid leukemia. *Blood.* 2022;140(1):58-72.
 9. Bernard E, Nannya Y, Hasserjian RP, et al. Implications of TP53 allelic state for genome stability, clinical presentation and outcomes in myelodysplastic syndromes. *Nat Med.* 2020;26(10):1549-1556.
 10. Murnyak B, Hortobagyi T. Immunohistochemical correlates of TP53 somatic mutations in cancer. *Oncotarget.* 2016;7(40):64910-64920.
 11. Ruzinova MB, Lee YS, Duncavage EJ, Welch JS. TP53 immunohistochemistry correlates with TP53 mutation status and clearance in decitabine-treated patients with myeloid malignancies. *Haematologica.* 2019;104(8):e345-e348.
 12. Kern W, Haferlach T, Schnittger S, Hiddemann W, Schoch C. Prognosis in therapy-related acute myeloid leukemia and impact of karyotype. *J Clin Oncol.* 2004;22(12):2510-2511.
 13. Montalban-Bravo G, Kanagal-Shamanna R, Class CA, et al. Outcomes of acute myeloid leukemia with myelodysplasia related changes depend on diagnostic criteria and therapy. *Am J Hematol.* 2020;95(6):612-622.
 14. Mazzella FM, Smith D, Horn P, et al. Prognostic significance of pronormoblasts in erythrocyte predominant myelodysplastic patients. *Am J Hematol.* 2006;81(7):484-491.
 15. Kowal-Vern A, Cotelingam J, Schumacher HR. The prognostic significance of proerythroblasts in acute erythroleukemia. *Am J Clin Pathol.* 1992;98(1):34-40.

The gut microbiome in patients with chronic lymphocytic leukemia

The gut microbiome, an ecosystem formed by commensal, symbiotic, and pathogenic microorganisms colonizing the gastrointestinal tract, may impact both immune function and carcinogenesis. The host immune system plays a vital role in the maintenance of gut microbiome homeostasis by establishing a balance between eliminating invading pathogens and promoting the growth of beneficial microbes. When this balance is disturbed, a state of dysbiosis arises in the microbial ecosystem. Conditions found to be associated with gut dysbiosis include, but are not limited to, inflammatory disorders including inflammatory bowel diseases (IBD),¹ diabetes,² as well as obesity,³ and asthma.⁴ The gut microbiome also seems to influence cancer susceptibility, and to correlate with tumorigenesis and progression.⁵ Within the area of hematological malignancies, studies focusing on acute leukemias, lymphoproliferative disorders, and multiple myeloma, have found microbiome dysbiosis and decreased microbiome diversity to be related to microenvironmental alterations induced by the disease itself, chemotherapy, and/or antibiotics.⁶

To our knowledge, no previous studies have investigated the gut microbiome in patients with chronic lymphocytic leukemia (CLL). As CLL represents an antigen-driven malignancy with immune dysfunction,⁷ the gut microbiome could both be implicated in the pathogenesis of CLL through antigenic drive, and contribute to the distortion of the immune system. However, the CLL microbiome itself may also be impacted by the immune dysfunction as well as reflect the increased prescription of antimicrobials for this patient group. Thus, our study focusing on the fecal microbiome in patients with CLL aimed to describe perturbations in the gut microbial composition, and to characterize potential signature for CLL-related gut dysbiosis.

We included fecal samples from ten patients enrolled during regular out-patient visits. Control cohorts were selected from an array of previously published cohorts^{8,9} and matched to the CLL cohort on criteria including mean age, residency, year of sampling, and sampling methods. Using shotgun metagenomic sequencing and taxonomical profiling, we assessed fecal microbiome composition, diversity, and dynamics. Bioinformatic analyses were performed following the state-of-the-art methods as well as using innovative tailor-made approaches.

Ten patients diagnosed with CLL delivered 12 stool samples between January 2016 and October 2018. Sampling was prior to treatment for eight patients and after

treatment for four patients, thus, two patients, were sampled both before and after treatment. No patients received antibiotics within 4 months prior to sample collection. For an overview of patient and control baseline characteristics, and patient treatment see the *Online Supplementary Figure S1A* to *C*. Changes in relative abundance of ten major bacterial genera in patients sampled both before and after treatment are demonstrated in the *Online Supplementary Figure S1D*.

We observed high intra-variability among the CLL microbiomes (Figure 1A). At the genus level, *Bacteroides* was the most abundant genus in six of the 12 CLL samples. Additionally, there was a trend of *Bacteroides* acquiring bacterial dominance (>30% relative abundance) in five of 12 samples. Several other bacterial genera such as *Parabacteroides*, *Prevotella*, and *Acinetobacter* also acquired bacterial dominance among CLL patients. We next assessed microbiome diversity in CLL patients and healthy controls. Richness (the observed number of species) was lowest for patients with CLL and was significantly different compared to each of the two control cohorts (Observed: CLL vs. C1: median, 53 vs. 69; $P=0.00057$; CLL vs. C2: median, 53 vs. 73; $P=6.8e-05$; Figure 1B). Patients with CLL also showed lower α diversity compared to the control groups when assessed by Shannon index (CLL vs. C1: median, 1.90 vs. 2.90; $P=2.1e-05$; CLL vs. C2: median, 1.90 vs. 2.75; $P=0.00057$) and InvSimpson index (CLL vs. C1: median, 4.18 vs. 11.94; $P=4.3e-05$; CLL vs. C2: median, 4.18 vs. 10.05; $P=0.00057$; Figure 1B). The two control cohorts also demonstrated a significant difference in diversity between one another (C1 vs. C2: Shannon: median, 2.90 vs. 2.75; $P=0.00057$; InvSimpson: median, 11.94 vs. 10.05; $P=0.017$). In addition to reduced diversity, a difference in the specific microbial composition between the CLL cohort and the two control cohorts was observed: at the phylum level, we focused on the differences in *Bacteroidetes*, *Firmicutes*, *Proteobacteria* and *Actinobacteria* as they comprised 95% of the total bacterial content in CLL patients, on average. The distribution of these four phylotypes across each cohort highlights a significantly higher abundance of *Bacteroidetes* and *Proteobacteria* relative to the controls (Figure 1C). In contrast, both control groups showed greater proportions of *Firmicutes* and *Actinobacteria*.

At the family level, *Bacteroidaceae*, *Prevotellaceae*, *Clostridiaceae*, *Lachnospiraceae* and *Ruminococcaceae* were the most abundant five families among both CLL patients and controls (Figure 2A). *Bacteroidaceae* were present in

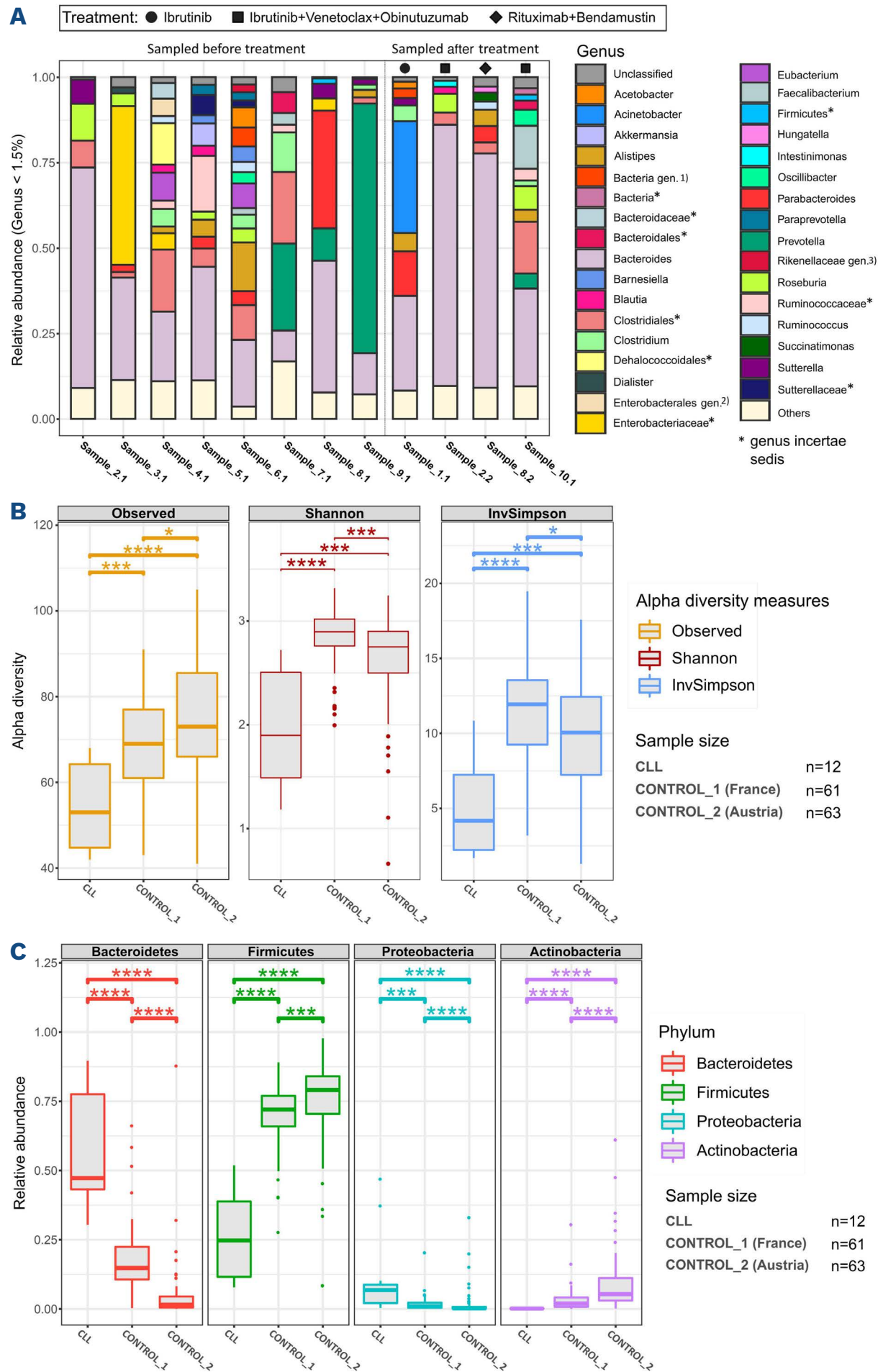


Figure 1. Gut microbiome composition and diversity in chronic lymphocytic leukemia patients and controls. (A) The relative abundance of bacterial genera in all 10 chronic lymphocytic leukemia (CLL) patients (12 samples). Bacterial genera whose abundance was <1.5% in a sample were grouped as 'Others'. Sequences that could not be assigned to a genus were grouped as 'Unclassified'. Taxa having zero counts across all samples were removed prior to all analyses. If the sample was taken after treatment, the treatment regimen is indicated by a corresponding shape on the top of each bar and described in the legend. Bacterial abundance was visualized using stacked barplots from R package *ggplot2*. Unambiguously assigned genera: 1) [*Rhodospirillum/Lactobacillus/Azospirillum*]; 2) [*Enterobacter/Escherichia/Klebsiella/Serratia*]; 3) [*Tidjanibacter/Alistipes*]. (B) Fecal diversity in CLL samples and healthy samples at genus level (α diversity measures: observed number of genera, Shannon and Inverse Simpson indexes). In box plots, box edges represent the 25th and 75th percentiles, the center line shows the median and whiskers extend from the box edges to the most extreme data point. Data beyond the end of the whiskers are plotted individually as dots. The *P*-values (adjusted for multiple testing with the Benjamini-Hochberg [BH]) obtained upon Wilcoxon rank-sum tests are indicated, values <0.05 were considered significant. Not significant (Ns) $P>0.05$; * $P<0.05$; ** $P<0.01$; *** $P<0.001$; **** $P<0.0001$. (C) Relative abundance of 4 major bacterial phyla forming the microbiota in the CLL cohort. Box plots are constructed as described in (B).

high proportions in the CLL cohort. Interestingly, a major difference was also observed between the samples from patients with CLL and the healthy controls with lower relative abundance of *Lachnospiraceae* and *Ruminococcaceae* taxa, while the dissimilarities between the control groups were small. We further aimed to identify groups of bacterial taxa differentially abundant between patients with CLL and controls. Analyzing the composition of microbiomes based on the abundance at the genus level, we detected *Bacteroides*, *Sutterella* and *Parabacteroides*,

to be overrepresented in CLL relative to the average microbiome (abundance of a taxon across all CLL and healthy samples). In contrast, we identified a group of taxa including *Bifidobacterium*, *Anaerostipes*, and nine other bacterial genera to be underrepresented among patients with CLL as compared to controls (Figure 2B). Bearing in mind the complexity of bacterial communities, we also sought to characterize groups of bacteria co-occurring across all CLL and healthy samples. We calculated proportional co-occurrence coefficient for all pairs of bacter-

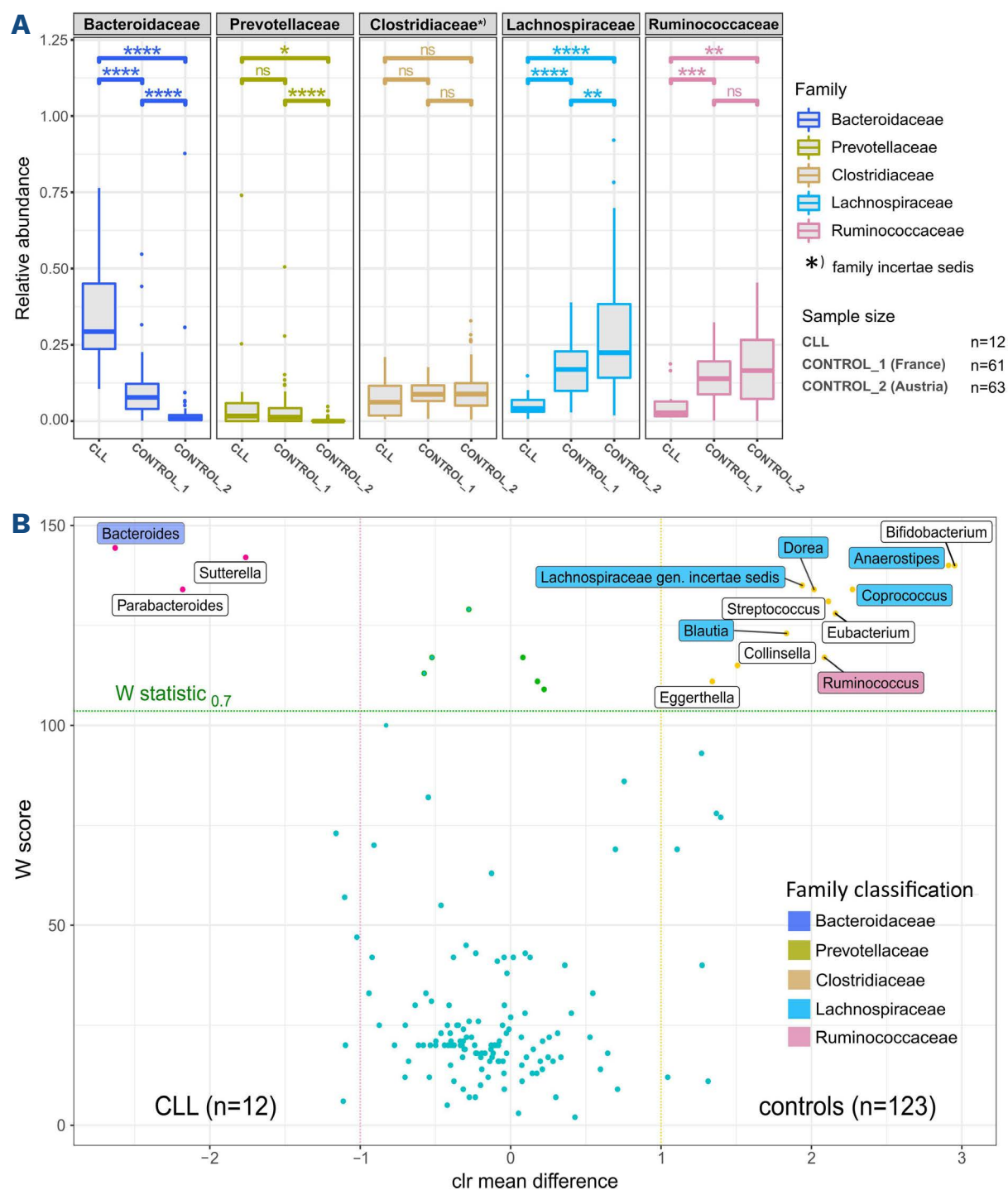


Figure 2. Relative and differential abundance of bacterial families and genera. (A) Relative abundance of five most abundant bacterial families in chronic lymphocytic leukemia (CLL) and healthy feces samples. Box plots are constructed as described in Figure 1(B). Not significant (Ns) $P>0.05$; * $P<0.05$; ** $P<0.01$; *** $P<0.001$; **** $P<0.0001$. (B) Differential abundance of bacterial genera between CLL and the merged control cohorts. Bacterial genera are color coded according to its higher taxonomic rank - family. The y-axis W value represents number of times the null hypothesis (H_0 : the average abundance of a given taxon is equal across cohorts) was rejected for a given taxon. The x-axis value represents the centered log-ratio (clr)-transformed mean difference in abundance of a given taxon between the CLL and healthy groups with respect to average abundance of a given taxon. Positive value at the x-axis indicates bacterial genera being differentially abundant in controls, negative value indicates bacterial genera being differentially abundant in CLL cohort. Only bacterial genera with null hypothesis rejected in $>70\%$ of cases and clr mean difference $-/+ 1$ are labeled. The analysis and volcano plot visualization were done in R by implementation of Analysis of Compositions of Microbiomes (ANCOM).

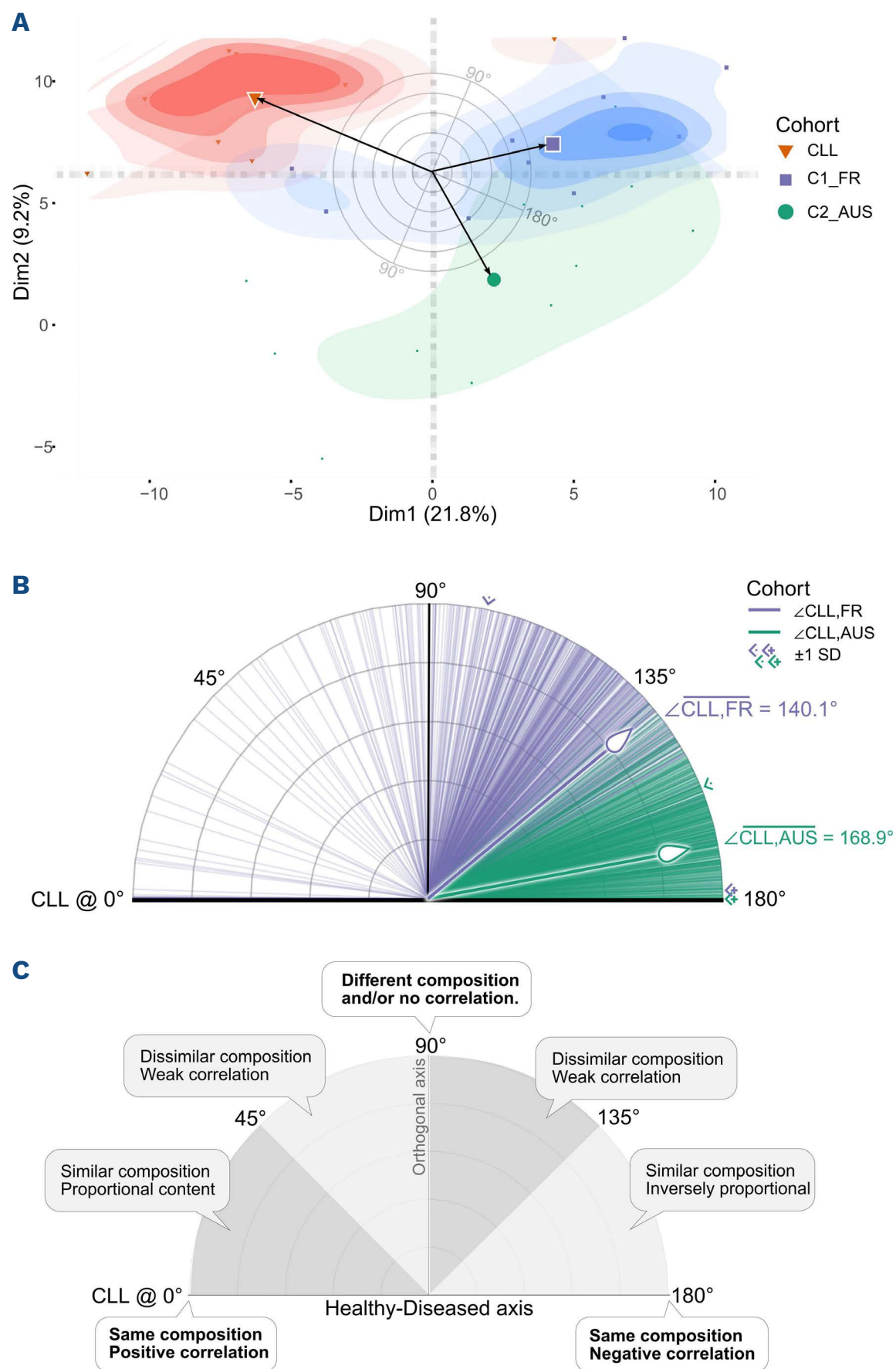


Figure 3. Analysis of covariance by principal component analysis. In order to assess similarity between the chronic lymphocytic leukemia (CLL) microbiome and the control microbiome in a multidimensional space, a principal component analysis (PCA) was performed. (A) The biplot illustrates the distance between the CLL cohort and the 2 control cohorts in terms of a 2-dimensional representative plot of 1,000 iterations run on the original dataset ($n=12$ per cohort totaling 36 cases per cohort per iteration), delimited by principal component (PC) 1 and PC2. The large symbols (centroids) represent the mean PC score from each cohort. The PC score for each individual is plotted relative to their position along each of the PC. The biplot shows vectors (black) pointing to the centroid of each cohort, as well as the individuals of each cohort (CLL – red triangles, C1_FR – purple squares, C2_AUS – green circles). Colored contour maps represent the density and distribution of individuals grouped by cohorts. The biplot is overlaid with a protractor-like plot displaying degrees from 0 to 180°. The angles between 2 cohorts were calculated as the angles between vectors pointing to centroids of individual cohorts ($\cos\theta = \frac{a \cdot b}{(|a| |b|)}$), with CLL being always positioned at 0°. Although C1_FR show certain overlap with CLL, note that the patients with CLL are distinctly clustered from both healthy control cohorts. (B) The protractor-like plot represents all angles identified over the 1,000 iterations between CLL-C1_FR and CLL-C2_AUS. The mean of all centroid vectors per cohort is drawn as a thick line with a white symbol at its end. The standard deviation (SD) is visualized by arrows of a color corresponding to the cohort, on the outside of the plot. (C) The protractor-like plot provides interpretation of the angles on healthy-diseased axis. An angle between vectors is interpreted as an approximation of the correlation and the similarity between the cohorts' variables; i.e., the C1_FR cohort has a dissimilar composition with weaker correlation with the CLL cohort, whereas the C2_AUS control cohort is inversely correlated to the CLL cohort.

ial genera across the CLL and healthy cohorts. When we visualized the relationships between the 23 most strongly proportional taxa, three clusters were formed (*Online Supplementary Figure S2A*). Abundance/depletion of the proportional bacterial taxa across all samples revealed clear discrimination between CLL patients and healthy controls (*Online Supplementary Figure S2B; Online Supplementary Table S1*). An overlap of the two analytical methodologies indicated lack of bacteria mainly from *Lachnospiraceae* and *Ruminococcaceae* families among the CLL samples. In particular, lower abundances of *Anaerostipes*, *Bifidobacterium*, *Blautia*, *Coprococcus*, *Dorea*, *Eubacterium*, *Ruminococcus*, and *Streptococcus* were observed in CLL samples when compared to controls. The two approaches also indicated higher abundances of *Bacteroides* and *Parabacteroides* in CLL compared to controls.

While canonical metrics have revealed statistically significant differences between CLL and healthy cohorts, we note that controls are also significantly different from one another across several metrics. Thus, we set out to answer whether there exists a healthy-diseased axis such that healthy patients from both control cohorts co-vary and are distinct from CLL patients. In order to do this we characterized the structure of covariance in each cohort by their centroids in PCA-space (Figure 3A). We assessed the similarity between cohorts by calculating the angles between their centroids within this reduced multidimensional space (interpretation of angles in Figure 3C). On average, CLL gut profiles were inversely proportional, i.e., dissimilar, to C1 & C2 cohorts ($\angle_{\text{CLL,C1}} = 140.1 \pm 38.5^\circ$, purple; $\angle_{\text{CLL,C2}} = 168.9 \pm 11^\circ$, green; Figure 3B). We also observed an acute relationship, i.e., similarity, between healthy cohorts ($\angle_{\text{C1,C2}} = 51 \pm 43.9^\circ$). These results highlight the presence of a strong inverse axis between diseased and healthy states that is defined by the angles between centroids of the CLL and the two control groups.

The lower fecal diversity observed in the CLL cohort is in line with previous findings of reduced bacterial diversity in other inflammatory conditions including IBD, type 1 and 2 diabetes, and obesity,^{10,11} as well as hematologic malignancies.^{6,12} We suggest that the decreased diversity/increase in *Bacteroidetes* and *Proteobacteria* observed in the CLL cohort could imply a general loss of bacteria, but may also indicate a loss of complexity for the remaining microbiome.

Most of the bacterial genera in the microbial signature depleted in patients with CLL belonged to *Lachnospiraceae* and *Ruminococcaceae* family. Members of the *Lachnospiraceae* and *Ruminococcaceae* families are among the main producers of short chain fatty acids, which are known to modulate the surrounding microbial environment and to directly interact with the host immune system.¹³ Interestingly, *Blautia* (*Lachnospiraceae* family) and *Ruminococcus* (*Ruminococcaceae* family) were also identified with higher

abundance among controls than among patients with CLL. High abundance of intestinal *Blautia* has been associated with improved survival upon graft-versus-host disease,¹⁴ and is together with *Ruminococcus* often underrepresented in feces samples from patients with colorectal cancer.¹⁵

In conclusion, despite low sample size, the CLL microbiome demonstrated lower microbiome diversity and lower enrichment of short chain fatty acid-producing bacterial taxa when compared to healthy controls. We hypothesize that the overabundance of bacteria from the *Bacteroidetes* phylum together with depletion of *Lachnospiraceae* and *Ruminococcaceae* family bacteria might play a role in – or is observed due to – immune dysfunction among CLL patients. This microbiome signature is warranting validation and refinement in larger CLL cohorts including patients needing treatment, patients assigned to watch and wait, patients with other hematological malignancies, as well as other healthy cohorts. This as a focus of ours in a follow-up study will hopefully lay foundation for defining microbiome characteristics of hematological malignancies and microbiome signatures discriminating subgroups of patients with CLL.

Authors

Tereza Faitová,¹ Rebecka Svanberg,¹ Caspar da Cunha-Bang,¹ Emma E. Ilett,² Mette Jørgensen,² Marc Noguera-Julian,^{3,4} Roger Paredes,^{3,5} Cameron R. MacPherson² and Carsten U. Niemann^{1,6}

¹Department of Hematology, Rigshospitalet, Copenhagen, Denmark;

²PERSIMUNE Center of Excellence, Rigshospitalet, Copenhagen, Denmark;

³Institut de Recerca de la Sida-IrsiCaixa, Hospital Universitari Germans Trias i Pujol, Badalona, Catalonia, Spain;

⁴University of Vic-Central University of Catalonia, Barcelona, Spain;

⁵Infectious Diseases Department, Hospital Universitari Germans Trias i Pujol, Badalona, Catalonia, Spain and ⁶Department of Clinical Medicine, University of Copenhagen, Copenhagen, Denmark

Correspondence:

C. U. NIEMANN - carsten.utoft.niemann@regionh.dk

<https://doi.org/10.3324/haematol.2021.280455>

Received: December 1, 2021.

Accepted: May 5, 2022.

Prepublished: May 12, 2022.

©2022 Ferrata Storti Foundation

Published under a CC BY-NC license 

Disclosures

CUN received research funding and/or consultancy fees from

Abbvie, AstraZeneca, CSL Behring, Janssen, Octapharma, Roche and Takeda outside this work. MNJ is founder and shareholder of Nano1Health S.L.

Contributions

CUN, RS, and TF designed the study; EI, CC and CUN were responsible for sample collection and inclusion of patients; MNJ and RP performed the sequencing; TF, MJ, and CRM performed the bioinformatic and statistical analyses; TF and CUN wrote the first version of the manuscript. All authors read, contributed and approved the final version of the manuscript.

Acknowledgments

The authors would like to express sincere thanks to the patients providing samples for the study and making this kind of research possible. This research would not have been possible without our collaborator, PERSIMUNE Center of Excellence, which provided the infrastructure as well as financial support and exceptional expertise. The staff at the Hematology Department and at the PERSIMUNE biobank at Rigshospitalet were essential for this study as they organized and collected the samples for our research.

Computerome team provided computational platform and technical support.

Funding

The study was funded by the Danish Cancer Society (grant R269-A15924) and the Novo Nordisk Foundation (grant NNF16OC0019302). The infrastructure for sampling and analyses was within the Danish National Research Foundation funded PERSIMUNE project (grant 126). The work was also supported by the CLL-CLUE project funded by the European Union.

Data-sharing statement

The datasets generated and analyzed during this study are derived from patients treated in Denmark. The datasets contain sensitive patient data governed by GDPR and Danish law. Due to Danish legislation (Act No. 502 of 23 May 2018) and approvals granted by the Danish Data Protection Agency, it is not possible to upload raw data to a publicly available database. However, access to these data can be made available from the corresponding author on reasonable request, provided a data transfer agreement is entered into according to current regulations.

References

1. Alam MT, Amos GCA, Murphy ARJ, Murch S, Wellington EMH, Arasaradnam RP. Microbial imbalance in inflammatory bowel disease patients at different taxonomic levels. *Gut Pathog.* 2020;12:1.
2. Larsen N, Vogensen FK, van den Berg FWJ, et al. Gut microbiota in human adults with type 2 diabetes differs from non-diabetic adults. *PloS One.* 2010;5(2):e9085.
3. Turnbaugh PJ, Hamady M, Yatsunencko T, et al. A core gut microbiome in obese and lean twins. *Nature.* 2009;457(7228):480-484.
4. Abrahamsson TR, Jakobsson HE, Andersson AF, Björkstén B, Engstrand L, Jenmalm MC. Low gut microbiota diversity in early infancy precedes asthma at school age. *Clin Exp Allergy.* 2014;44(6):842-850.
5. Zitvogel L, Galluzzi L, Viaud S, et al. Cancer and the gut microbiota: an unexpected link. *Sci Transl Med.* 2015;7(271):271ps1.
6. Uribe-Herranz M, Klein-González N, Rodríguez-Lobato LG, Juan M, de Larrea CF. Gut Microbiota influence in hematological malignancies: from genesis to cure. *Int J M Sci.* 2021;22(3):1026.
7. Svanberg R, Janum S, Patten PEM, Ramsay AG, Niemann CU. Targeting the tumor microenvironment in chronic lymphocytic leukemia. *Haematologica.* 2021;106(9):2312-2324.
8. Zeller G, Tap J, Voigt AY, et al. Potential of fecal microbiota for early-stage detection of colorectal cancer. *Mol Syst Biol.* 2014;10(11):766.
9. Feng Q, Liang S, Jia H, et al. Gut microbiome development along the colorectal adenoma–carcinoma sequence. *Nat Commun.* 2015;6(1):6528.
10. Valdes AM, Walter J, Segal E, Spector TD. Role of the gut microbiota in nutrition and health. *BMJ.* 2018;361:k2179.
11. Wilkins LJ, Monga M, Miller AW. Defining dysbiosis for a cluster of chronic diseases. *Sci Rep.* 2019;9(1):12918.
12. Cozen W, Yu G, Gail MH, et al. Fecal microbiota diversity in survivors of adolescent/young adult Hodgkin lymphoma: a study of twins. *Br J Cancer.* 2013;108(5):1163-1167.
13. Yoo JY, Groer M, Dutra SVO, Sarkar A, McSkimming DI. Gut Microbiota and immune system interactions. *Microorganisms.* 2020;8(10):1587.
14. Ilett EE, Jørgensen M, Noguera-Julian M, et al. Associations of the gut microbiome and clinical factors with acute GVHD in allogeneic HSCT recipients. *Blood Adv.* 2020;4(22):5797-5809.
15. Weir TL, Manter DK, Sheflin AM, Barnett BA, Heuberger AL, Ryan EP. Stool microbiome and metabolome differences between colorectal cancer patients and healthy adults. *PloS One.* 2013;8(8):e70803.

A validated clinical-genetic score for assessing the risk of thrombosis in patients with COVID-19 receiving thromboprophylaxis

Venous thromboembolic events (VTE) have emerged as a common complication among patients hospitalized for COVID-19 with an estimated incidence of 14–31%, increasing disease severity and mortality.¹ The incidence is even higher in critically ill patients admitted to intensive care units (ICU),^{1,2} including those provided thromboprophylaxis at the moment of hospital admission.² Therefore, the effectiveness of anticoagulant prophylaxis is actually unclear due to no significant reduction in thrombotic complications despite prophylactic therapy.^{2,3} These studies, however, face a major limitation: the lack of tools for assessing the risk of VTE. Many variables affect the appearance of a VTE, both clinical and genetic.⁴ With this in mind, the present work examines whether the Thrombo inCode (TiC) score, which combines genetic and clinical risk variables and has shown the capacity to predict VTE in different populations,^{5,6,7} is of use in predicting VTE in patients with COVID-19 who were administered prophylactic anticoagulation therapy at the time of hospital admission.

The PRECIS_COVID19 cohort consists of 734 patients; all aged over 18 years, with a confirmed diagnosis of COVID-19, all of whom were admitted to the *Hospital de la Santa Creu i Sant Pau* (Barcelona, Spain) between April and July 2020. COVID-19 was confirmed by real-time reverse-transcription polymerase chain reaction (PCR) assays using nasal and pharyngeal swabs. All patients were administered standard thromboprophylactic treatment at the time of their admission to hospital following international recommendations.⁸

A total of 279 patients had a D-Dimer value below 1,000 ng/mL (validated threshold to rule out VTE)⁹ and were thus considered as non-VTE (control) patients. Of the remainder, 382 patients had D-Dimer levels of >1,000 ng/mL and were excluded from further analyses, and 73 suffered a VTE event during hospitalization (either a deep venous thrombosis or a pulmonary embolism). Diagnoses were confirmed using Doppler ultrasonography, magnetic resonance, arteriography, phlebography, pulmonary gammagraphy and computed tomography pulmonary angiography. The total number of subjects in the study was therefore $n=352$ (279 controls plus 73 cases). A total of five models were therefore compared, the details of which are described below:

1. Genetic risk score (GRS)

The twelve genetic variants reported by Soria et al.⁵, in-

cluding the variants rs6025, rs118203905, rs118203906, rs1799963, rs121909548 (chr1:173873176:C:A, *SERPINC1*), rs1801020 (chr5:176836532:A:G, *F12*), rs5985 (chr6:6318795:C:A, *F13*), rs2232698 (chr14:94756669:G:A, *SERPINE10*) and four variants providing the ABO:A1 haplotype (additive effect of A1 allele).

2. Clinical risk score (CRS)

Five clinical variables were assessed: age, sex, obesity, smoking habit, and diabetes. These variables have been shown to be associated with VTE and have been reported to be useful in estimating VTE risk.⁷ Smoking habit was codified as a dichotomic variable (smoker/non-smoker); obesity was defined as body mass index >30.

3. Thrombo inCode model (TiC)

A combination of the variables in both the genetic risk score (GRS) and the clinical risk score (CRS) described in the models 1 and 2. The original Thrombo inCode (TiC) model also includes family history, oral contraceptive use and pregnancy, but were not evaluated, as they were difficult to obtain in the COVID19 context.

4. Factor V Leiden plus prothrombin score

The classic genetic thrombophilia model based on the Factor V Leiden (FVL) (rs6025; chr1:169519049:T:C, *F5*) and prothrombin (PT) G20210A (rs1799963; chr11:46761055:G:A, *F2*) mutations.

5. Factor V Leiden plus prothrombin plus clinical risk score

Combination of the variables in the FVL+PT and the CRS models explained before.

A descriptive analysis of both the genetic and clinical variables was performed, and the relationship with VTE assessed by the Chi-squared test for bivariate associations. The same method was used to evaluate the association between ICU admission and mortality rates (at 30 and 90 days after hospital admission), as well as the association between VTE and mortality rates and ICU admission. Significance was set at $P<0.05$.

All risk models were constructed by including the corresponding variables as additive linear predictors of VTE using logistic regression. The predictive capacity of the different models was examined using receiver operating curves (ROC), employing the optimal cut-off based on the Youden index.¹¹ The significance of the predictive capacity of each score was measured by comparing with a random model (area under the ROC curve [AUC] of 0.5), using the DeLong test.¹³ In addition to determining test sensitivity

and specificity, the negative and positive predictive values (NPV and PPV) of each model were determined as well as the odds ratio (OR). All calculations were performed using SPSS v.26.0 software (Released 2019) (IBM Corp., Armonk, NY, USA).

Table 1 provides the descriptive analysis of the clinical and genetic variables of all 352 patients. The associations between VTE and four clinical variables (age, sex, obesity and smoking habit) and the genetic variants rs121909548 in *SERPINC1* and rs5985 in *F13* were significant ($P < 0.05$). We found no carriers of the variants rs118203906 and rs118203905, corresponding to FV_Cambridge and FV_Hong Kong, respectively, in our cohort.

It is important to note that a significant association was detected between the suffering of a VTE and 30 and 90 days mortality (13.7% cases vs. 5% controls, $P = 0.06$; 14% cases vs. 5.7% controls, $P < 0.001$; respectively), as well as admission to an ICU (61.6% cases vs. 4.3% controls, $P < 0.001$), highlighting the impact of VTE on the progression and severity of COVID-19. These results are in agreement with previous reports,^{1,2} and reinforce the need to improve prophylactic strategies. In this context, some authors have examined predictive models that take into account clinical and laboratory variables related to VTE.¹² However, to our knowledge, and despite the strong gen-

etic component of VTE,⁴ no previous study has examined the genetic risk of COVID-19 patients suffering a VTE event.

Table 2 shows the predictive capacity of each of the five models tested. Only the FVL+PT model showed no predictive capacity at all (AUC 0.506, $P = 0.86$). While these two genetic mutations imply a higher risk of VTE, their low frequency in the general population render them poor markers for predicting such events. Similar results have been reported previously.^{5,7} The TiC score, in contrast, showed the best and an excellent predictive capacity, with an AUC of 0.78 (95% confidence interval [CI]: 0.72-0.84), a sensitivity of 68.5%, and a specificity of 76.7%. Patients identified as being at high risk of suffering a VTE by the TiC score had an associated OR of 7.16. The accuracy measures shown in Table 2 for this model reveal a number needed to treat (NNT) of 2.3.

It is important to note that the genetic risk variants included in the TiC score have known functional consequences on the coagulation pathway,⁵ and the link between these variants and VTE has been established in different genome-wide association studies.¹³ In addition, the useful predictive capacity of the GRS included in the TiC score has been validated in independent populations.^{5,6,7} Furthermore, it should be noted that one of the

Table 1. Descriptive analysis of the clinical and genetic variables in the PRECIS_COVID19 cohort.

		PRECIS_COVID19 (N=352)	Patients with VTE (N=73)	Non-VTE Controls (N=279)	P-value
Age in years, mean (SD)		59.0 (15.0)	64.9 (11.5)	57.5 (15.4)	<0.001
Female, N (%)		158 (44.9)	25 (34.2)	133 (47.7)	0.040
Obesity, N (%)		38 (10.8)	21 (28.8)	17 (6.1)	<0.001
Smoking, N (%)		24 (6.8)	15 (20.5)	9 (3.2)	<0.001
Diabetes, N (%)		47 (13.4)	14 (19.2)	33 (11.8)	0.100
ABO:A1, N (%)	0	221 (62.8)	43 (58.9)	178 (63.8)	0.411
	1/2	131 (37.2)	30 (41.1)	101 (36.2)	
rs6025 F5, N (%)	0	344 (97.7)	71 (97.3)	273 (97.8)	1.000
	1	8 (2.3)	2 (2.7)	6 (2.2)	
rs1799963 F2, N (%)	0	349 (99.3)	72 (98.6)	277 (99.3)	1.000
	1	3 (0.7)	1 (1.4)	2 (0.7)	
rs121909548 <i>SERPINC1</i> , N (%)	0	344 (98)	68 (93.2)	276 (98.9)	0.011
	1	8 (2.0)	5 (6.8)	3 (1.1)	
rs1801020 F12, N (%)	0	204 (58.0)	46 (63.0)	158 (56.6)	0.325
	1/2	148 (42.0)	27 (37.0)	121 (43.4)	
rs5985 F13, N (%)	0	200 (56.8)	34 (46.6)	166 (59.5)	0.047
	1/2	152 (43.2)	39 (53.4)	113 (40.5)	
rs2232698 <i>SERPINE10</i> , N (%)	0	348 (98.9)	72 (98.6)	276 (98.9)	1.000
	1	4 (1.1)	1 (1.4)	3 (1.1)	

Frequency and distribution of clinical variables, and frequencies of both reference and risk alleles for the 12 genetic variants. The P-value (P) refers to the association with venous thromboembolic events (VTE) (bivariate analysis). SD: standard deviation.

Table 2. Capacity of the tested models to predict venous thromboembolic events.

	TiC	GRS	CRS	FVL+PT	FVL+PT+CRS
AUC	0.781 (0.72-0.84)	0.615 (0.54-0.69)	0.756 (0.70-0.82)	0.506 (0.43-0.58)	0.757 (0.70-0.82)
P	<0.001	0.002	<0.001	0.869	<0.001
Sensitivity	68.5 (56.6-78.9) 50/73	52.1 (40.0-63.9) 38/73	71.2 (59.4-81.2) 52/73	-	65.8 (53.7-76.5) 48/73
Specificity	76.7 (71.3-81.5) 214/279	72.0 (66.4-72.2) 201/279	62.7 (56.8-68.4) 175/279	-	74.9 (69.4-79.9) 209/279
PPV	43.5 (34.3-53.0) 50/115	32.8 (24.3-42.1) 38/116	33.3 (26.0-41.3) 52/156	-	40.7 (31.7-50.1) 48/118
NPV	90.3 (85.8-93.7) 214/237	85.2 (80.0-89.5) 201/236	89.3 (84.1-93.2) 175/196	-	89.3 (84.6-93.0) 209/234
LR+	2.94	1.87	1.91	-	2.63
LR-	0.41	0.67	0.46	-	0.46
OR	7.16 (4.06-12.61)	2.80 (1.65-4.75)	4.17 (2.38-7.31)	-	5.73 (3.29-9.79)

'P' refers to the significance against a random model of area under the ROC curve (AUC) of 0.5. Numbers (in parentheses) are 95% confidence intervals. TiC: thrombo inCode score; GRS: genetic risk score; CRS: clinical risk score; FVL+PT: Factor V Leiden and prothrombin mutations; FVL+PT +CRS: Factor V Leiden and prothrombin mutations plus clinical risk score; PPV: positive predictive value; NPV: negative predictive value; LR: likelihood ratio; OR: odds ratio.

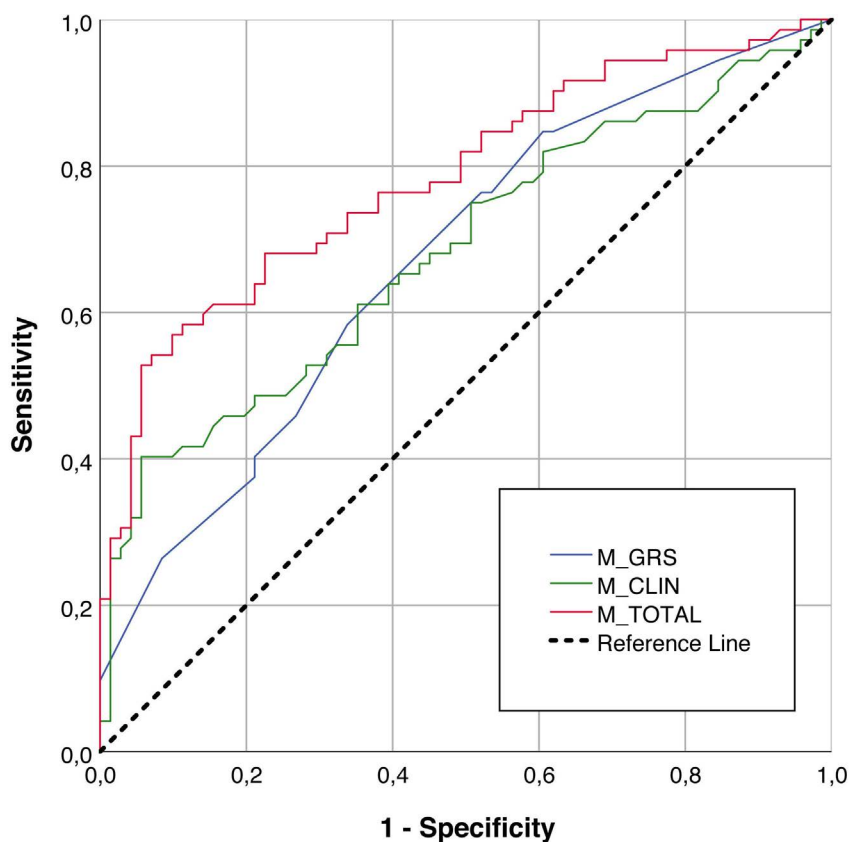


Figure 1. Predictive capacity of the different models. ROC curves are shown for each model: model with clinical variables only (M_CLIN); model with genetic variables only (M_GRS); and the combination of both models (M_TOTAL or TiC).

risk variants assessed is the A1 allele or haplotype for ABO blood type; the risk of VTE for A1 allele carriers is estimated to be increased by ~1.8 fold,⁵ and has also been significantly associated with different indicators of COVID-19 severity.¹⁴

Certain clinical variables are associated with an increased risk of VTE, and different studies report a better capacity

to predict VTE when genetic and clinical variables are combined.⁸ In agreement with this, the present results show that the best predictive capacity was obtained when taking both into account - i.e., when using the TiC score (Figure 1). The results also show that the correlation between the risk estimates provided by the CRS and GRS models alone was not significant ($\beta=0.039$; $P=0.6$). These

models may, therefore, reflect different sources of risk. The importance of thrombosis risk assessment in COVID-19 patients at hospital admission has been highlighted by a recent large observational study,¹⁵ where they determine that there is a profoundly increased rate of VTE within the first week following positive COVID-19 testing. With an AUC of 0.78 and good predictive values, the TiC score is an excellent predictor of VTE risk at the time of hospital admission. In fact, although all patients included in this cohort were receiving prophylactic treatment, the TiC model showed that 68.5% of patients that ended up having a VTE event may have benefited from more intense prophylaxis than they received. In addition, it should also be underscored that the TiC model is easy to use; it takes into account only 12 genetic variants plus clinical variables usually included in patient's records.

The present work suffers from the limitation of a relatively small sample size (n=352). Also, the absence of VTE in the control patients was not confirmed diagnostically, although a validated D-Dimer threshold was used to identify them. Finally, all patients were admitted to the same hospital; the results need to be confirmed at other centers that treat other populations (although the TiC score has been validated for use in a number of other populations).^{5,6,7}

In conclusion, the present work shows that the TiC score is useful in identifying patients with COVID-19 at high risk of VTE. It could therefore guide clinical decisions regarding the optimal intensity of anticoagulation treatment at hospital admission. Such personalized therapy could have a substantial impact on the morbidity and mortality of patients with COVID-19.

Authors

José Manuel Soria,^{1*} Sergi Mojal,² Angel Martinez-Perez,¹ Francisco René Acosta,² Sonia López,¹ Sara Miqueleiz,³ Diana Rodriguez,³ Maria Angeles Quijada,^{4,5} Antonio Cardenas,¹ Francisco Vidal,⁶ Angel Remacha,⁷ Rosa Maria Antonijoan^{4,5} and Juan Carlos Souto²

¹Genomics of Complex Diseases Unit, Research Institute of Hospital de la Santa Creu i Sant Pau, IIB Sant Pau; ²Hemostasis and Thrombosis Unit, Hospital de la Santa Creu i Sant Pau, IIB

Sant Pau; ³Clinical Trials Unit (AGDAC), Hematology Service, Hospital de la Santa Creu i Sant Pau, IIB Sant Pau; ⁴Clinical Pharmacology Service, Hospital de la Santa Creu i Sant Pau, IIB Sant Pau; ⁵Drug Research Center, Institut d'Investigació Biomèdica Sant Pau, IIB-Sant Pau; ⁶Blood and Tissue Bank (BST) and ⁷Hematology Service, Hospital de la Santa Creu i Sant Pau, IIB Sant Pau, Barcelona, Spain

Correspondence:

J.M. SORIA - jsoria@santpau.cat

<https://doi.org/10.3324/haematol.2022.281068>

Received: March 22, 2022.

Accepted: May 5, 2022.

Prepublished: May 12, 2022.

©2022 Ferrata Storti Foundation

Published under a CC BY-NC license 

Disclosures

No conflicts of interest to disclose.

Contributions

JMS and JCS supervised the study, wrote the paper, obtained funds; Sergi M performed analyses; AMP performed analyses and cleaned the database; FRA analyzed and cleaned the database; SL analysed samples; Sara M and DM designed the study design and collected data; MAQ and AR collected data; AC analyzed samples and collected data; FV and MRA designed and supervised the study.

Acknowledgments

The authors thanks GENinCode Plc (Oxford, UK) for providing the Thrombo inCode kit and reagents used in sample genotyping.

Funding

This work was funded by the Regional Government of Catalonia under grants SGR_1736 (to JMS), the CERCA Program, and the non-profit association Activa' TT por la Salud.

Data-sharing statement

PRECIS_project data are deposited in a national repository and can be shared on demand and with the corresponding approval of the IIB Sant Pau Ethics Committee.

References

1. Porfidia A, Valeriani E, Pola R, et al. Venous thromboembolism in patients with COVID-19: Systematic review and meta-analysis. *Thromb Res.* 2020;196:67-74.
2. Chi G, Lee JJ, Jamil A, et al. Venous thromboembolism among hospitalized patients with COVID-19 undergoing thromboprophylaxis: a systematic review and meta-analysis. *J Clin Med.* 2020;9(8):2489.
3. Sadeghipour P, Talasaz AH, Rashidi F, et al. Effect of intermediate-dose vs standard-dose prophylactic anticoagulation on thrombotic events, extracorporeal membrane oxygenation treatment, or mortality among patients with COVID-19 admitted to the intensive care unit: the INSPIRATION randomized Clin. *JAMA.* 2021;325(16):1620-1630.
4. Souto JC, Almasy L, Borrell M, et al. Genetic susceptibility to

- thrombosis and its relationship to physiological risk factors: the GAIT study. *Genetic Analysis of Idiopathic Thrombophilia*. *Am J Hum Genet*. 2000;67(6):1452-1459.
5. Soria JM, Morange PE, Vila J, et al. Multilocus genetic risk scores for venous thromboembolism risk assessment. *J Am Heart Assoc*. 2014;3(5):1-10.
 6. McInnes G, Daneshjou R, Katsonis P, et al. Predicting venous thromboembolism risk from exomes in the Critical Assessment of Genome Interpretation (CAGI) challenges. *Hum Mutat*. 2019;40(9):1314-1320.
 7. Salas E, Farm M, Pich S, et al. Predictive ability of a clinical-genetic risk score for venous thromboembolism in northern and southern european populations. *TH Open*. 2021;5(3):e303-e311.
 8. Spyropoulos AC, Levy JH, Ageno W, et al. Scientific and standardization committee communication: clinical guidance on the diagnosis, prevention, and treatment of venous thromboembolism in hospitalized patients with COVID-19. *J Thromb Haemost*. 2020;18(8):1859-1865.
 9. Choi JJ, Wehmeyer GT, Li HA, et al. D-dimer cut-off points and risk of venous thromboembolism in adult hospitalized patients with COVID-19. *Thromb Res*. 2020;196:318-321.
 10. Ruopp MD, Perkins NJ, Whitcomb BW, Schisterman EF. Youden Index and optimal cut-point estimated from observations affected by a lower limit of detection. *Biom J*. 2008;50(3):419-430.
 11. DeLong ER, DeLong DM, Clarke-Pearson DL. Comparing the areas under two or more correlated receiver operating characteristic curves: a nonparametric approach. *Biometrics*. 1988;44(3):837-845.
 12. Dujardin RWG, Hilderink BN, Haksteen WE, et al. Biomarkers for the prediction of venous thromboembolism in critically ill COVID-19 patients. *Thromb Res*. 2020;196:308-312.
 13. Lindström S, Wang L, Smith EN, et al. Genomic and transcriptomic association studies identify 16 novel susceptibility loci for venous thromboembolism. *Blood*. 2019;134(19):1645-1657.
 14. Hoiland RL, Fergusson NA, Mitra AR, et al. The association of ABO blood group with indices of disease severity and multiorgan dysfunction in COVID-19. *Blood Adv*. 2020;4(20):4981-4989.
 15. Pasha AK, McBane RD, Chaudhary R, et al. Timing of venous thromboembolism diagnosis in hospitalized and non-hospitalized patients with COVID-19. *Thromb Res*. 2021;207:150-157.

ETV6-related thrombocytopenia: dominant negative effect of mutations as common pathogenic mechanism

Inherited thrombocytopenias are a group of rare diseases characterized by low platelet count and variable bleeding tendency. In some forms, patients might develop additional phenotypes during life, such as myeloid neoplasms as in ETV6-related thrombocytopenia (ETV6-RT). ETV6-RT is caused by germline heterozygous mutations of *ETV6*, a gene encoding a master hematopoietic transcriptional repressor structured in three functional domains: the N-terminal pointed (PNT), the central regulatory domain (CRD) and C-terminal DNA-binding (ETS).¹

To our knowledge, at least 15 different ETV6 variants, mainly amino acid substitutions, have been associated with thrombocytopenia,²⁻⁹ though their pathogenic role has not always been clarified. Moreover, whereas ETV6 is well known as a tumor suppressor in chromosomal translocations associated to childhood leukemia,¹⁰ the molecular mechanism responsible for ETV6-RT remains to be elucidated.^{2,3} Understanding the molecular mechanisms involved in ETV6-RT pathogenesis is important in order to clarify the role of ETV6 in megakaryopoiesis and leukemia, to identify a possible therapeutic approach able to correct platelet biogenesis and to prevent the onset of leukemia. For these reasons we have studied seven ETV6 missense variants identified in patients with thrombocytopenia, demonstrating that five of them reduce the repression activity of ETV6 preventing its localization into the nucleus, as confirmed by inhibition of the nuclear export by leptomycin B. Moreover, we have demonstrated that the mutations act through a dominant negative effect, which results in accumulation of the wild-type (WT) protein in the cytoplasm likely due to formation of WT-mutant dimer of ETV6.

Individuals with suspicion of inherited thrombocytopenia due to their low platelet count were referred to our Institution for molecular diagnostic purpose. A next generation sequencing (NGS) approach allowed us to identify seven missense variants in *ETV6* gene, some of which were previously reported in patients with thrombocytopenia or leukemia (*Online Supplementary Table S1*).^{5-7,9}

All the variants are clustered within the ETS domain except for the S22N, that hits the PNT domain, and the H224Q, which is located in the CRD as the control mutation P214L. The ETS domain is a critical site for the binding of ETV6 to the DNA, suggesting that its impairment can lead to a loss or an alteration in transcriptional repression. Accordingly, different bioinformatic tools suggest a higher impact on the protein functions for the five variants that reside in the ETS domain, while H224Q and S22N were

predicted as likely benign substitutions. The pathogenic role of these five variants clustered within the ETS domain is supported also by structural analysis revealing a potential effect not only of R369W and W380R⁶ but also of the novel Q347P and R396G variants on protein stability and folding (*Online Supplementary Figure S1A*). Moreover, since structural analysis of ETS bound to a specific DNA sequence revealed that R396 and R399 are involved in electrostatic interactions with its DNA cognate (*Online Supplementary Figure S1B*), R396G and R399H substitutions are likely to prevent the binding of the mutant forms of ETV6 to its targets.

Notably, two germline disease causing mutations, c.1106G>A and c.1195C>T involving R369 and R399, respectively, but with a different amino acid substitution have been previously reported.^{3,9}

In order to verify the predictions obtained from *in silico* analyses, we tested the activity of reporter luciferase gene under the control of the Stromelysin-1 (MMP3) promoter, a validated target of ETV6.¹¹ In HEK293T cells, overexpression of the WT form of ETV6 resulted in a repression of luciferase activity to 44.3±8.6% compared to the empty vector. On the contrary, transfecting the Q347P, R369W, W380R, R396G and R399H mutant (M-ETV6) forms, as well as P214L used as control,^{2,3} we observed significantly higher luciferase activity (*Online Supplementary Figure S2*).

These results highlight the loss of the repression ability of these ETV6 variants on the MMP3 promoter, confirming their pathogenicity. On the contrary, the repressive activity was maintained by S22N and H224Q fully comparable to the WT, suggesting the absence of any pathogenic role, according to the *in silico* predictions.

In order to determine whether the loss of repression activity of the M-ETV6 forms could be explained also with a reduced nuclear localization of the protein, as observed for other mutations,^{2,3} we performed immunofluorescence assays in HeLa cells. Whereas the WT, S22N and H224Q forms are mainly detected in the nucleus, the other mutant proteins are prevalently cytoplasmatic (Figure 1A and B). The aberrant localization of the Q347P, R369W, W380R, R396G and R399H mutants was confirmed by western blot assays of cellular fractions. While the WT protein detected in the nucleus is 69.9±16.5%, the nuclear fractions of mutant proteins account for 5,7±4,1%, 28,3±9.7%, 7,7±5.8%, 30,8±15.3% and 23,2±8.8%, respectively (Figure 1C and D).

We next investigated the mechanisms retaining the M-

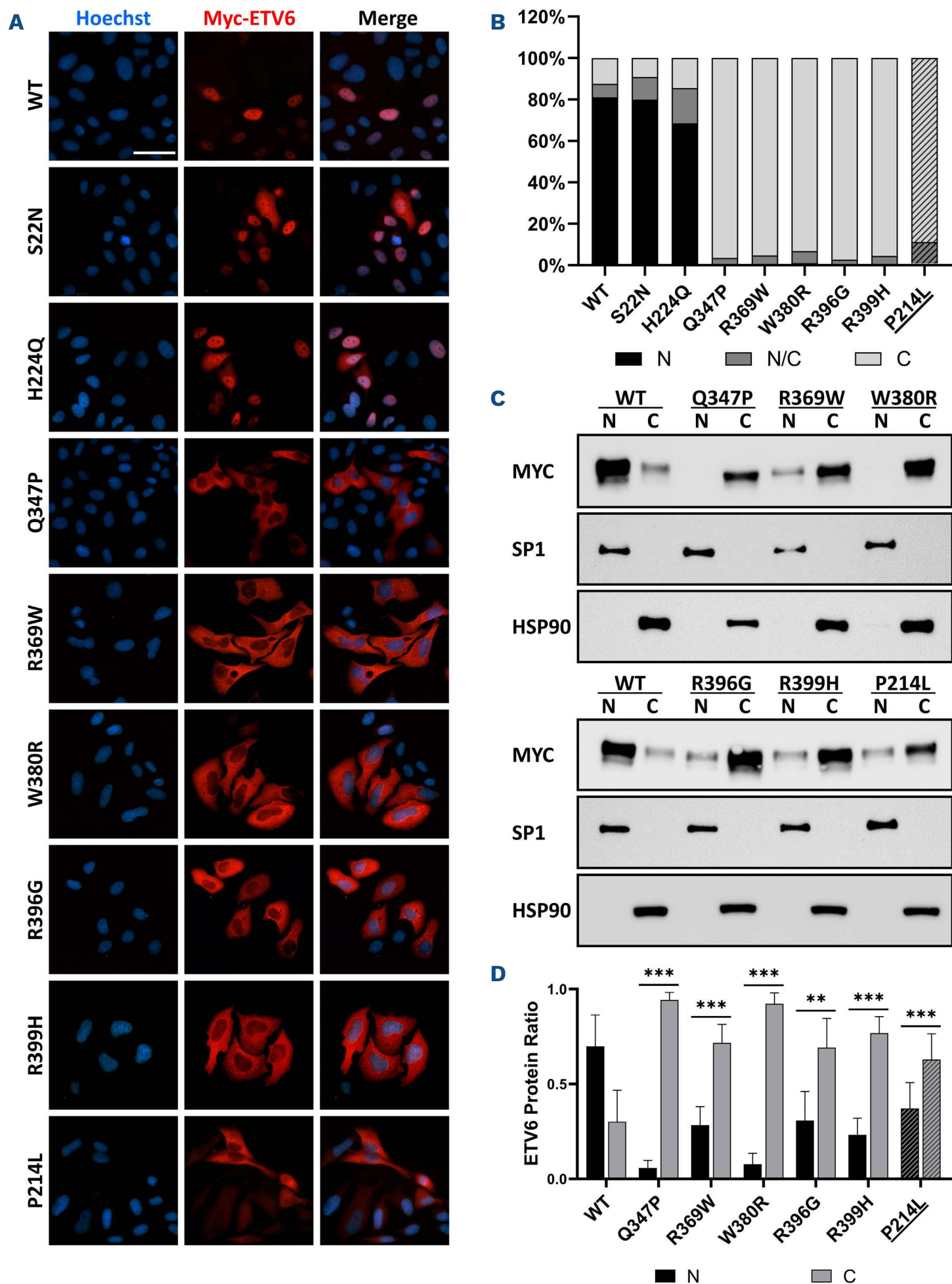


Figure 1. Altered protein distribution caused by ETV6 mutation. (A) Immunofluorescence analysis in HeLa cells after transfection of wild-type (WT) or mutated *ETV6* cDNA cloned into pcDNA3.1-Myc tagged expression vector. P214L was used as control mutation. ETV6-Myc forms were detected using anti-Myc antibody (red), nuclei were marked with Hoechst staining (blue). Images were obtained with a Zeiss Axioplan 2 epifluorescence imaging microscope and acquired with a Zeiss Axiocam 506 color using a 40X Plan-NEOFLUAR objective. Images were processed using Zeiss ZEN 3.1 (blue edition), while brightness and contrast were adjusted using Adobe Photoshop 2020. Scale bar =50 μ m. (B). Histogram represents cell fraction with nuclear (N), cytoplasmatic (C) or both (N/C) ETV6 staining. Striped column represents control mutation. (C) Western blot (WB) analysis of nuclear and cytoplasmatic fraction of HEK293T cells 48 hours after transfection with *ETV6* Myc-tagged. Hsp90 and SP1 were used as cytoplasmatic and nuclear markers, respectively. (D) WB semi-quantitative analysis performed using ImageJ 1.53e (National Institutes of Health). Histogram shows the protein ratio of nuclear (N) and cytoplasmatic (C) fraction. All data reported are representative of at least 3 independent experiments. Error bars represent standard deviation (SD). ** $P < 0.01$, *** $P < 0.001$, vs. ETV6-WT protein ratio, Student's *t*-test.

ETV6 in the cytoplasm to understand whether mutations prevent ETV6 from entering the nucleus or whether the non-functional proteins rapidly re-localize to the cytoplasm. Since the nuclear export of ETV6 is inhibited by leptomycin B,¹² we treated cells overexpressing Q347P- and R399H-ETV6, whose substitutions are predicted to affect the folding and the DNA binding, respectively (*Online Supplementary Figure S1*). In addition, we analyzed also the W380R mutation which has previously been demonstrated to have a strong impact on protein folding.⁶ The leptomycin B treatment resulted in an increase of cells with WT-ETV6 nuclear localization, suggesting that the portion of protein that enter into the nucleus is no longer able to be exported, as observed also for the p65 subunit of NF- κ B used as control.¹³ In contrast, Q347P-, W380R-

and R399H-ETV6 maintained their cytoplasmic localization, indicating that M-ETV6 forms, independently of the extent of the defect caused by mutations on folding or DNA binding, do not enter the nucleus (Figure 2).

Since mutations fail to correctly localize in the nucleus and ETV6 exerts its function after homodimerization mediated by its PNT domain,¹⁴ the pathogenetic mechanism in ETV6-RT could be mediated by a dominant negative mechanism leading to the accumulation not only of the mutated but also of the WT forms of ETV6 in the cytoplasmic compartment.

Co-transfection of HEK293T cells with WT- and M-ETV6 differentially tagged allowed us to confirm that both WT-ETV6-Myc and WT-ETV6-Flag proteins gather in the nucleus. On the contrary, when the WT-ETV6-Flag is

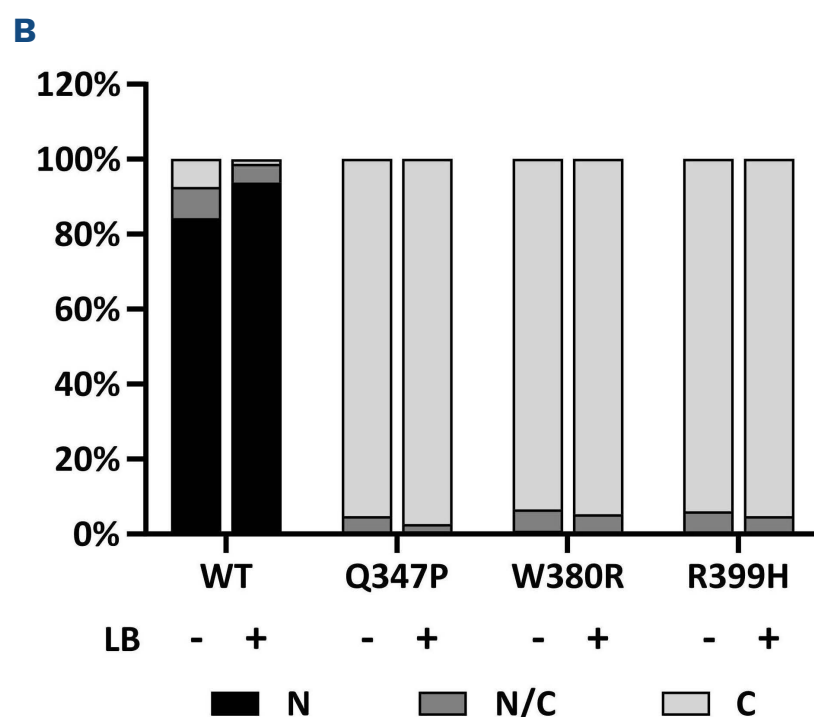
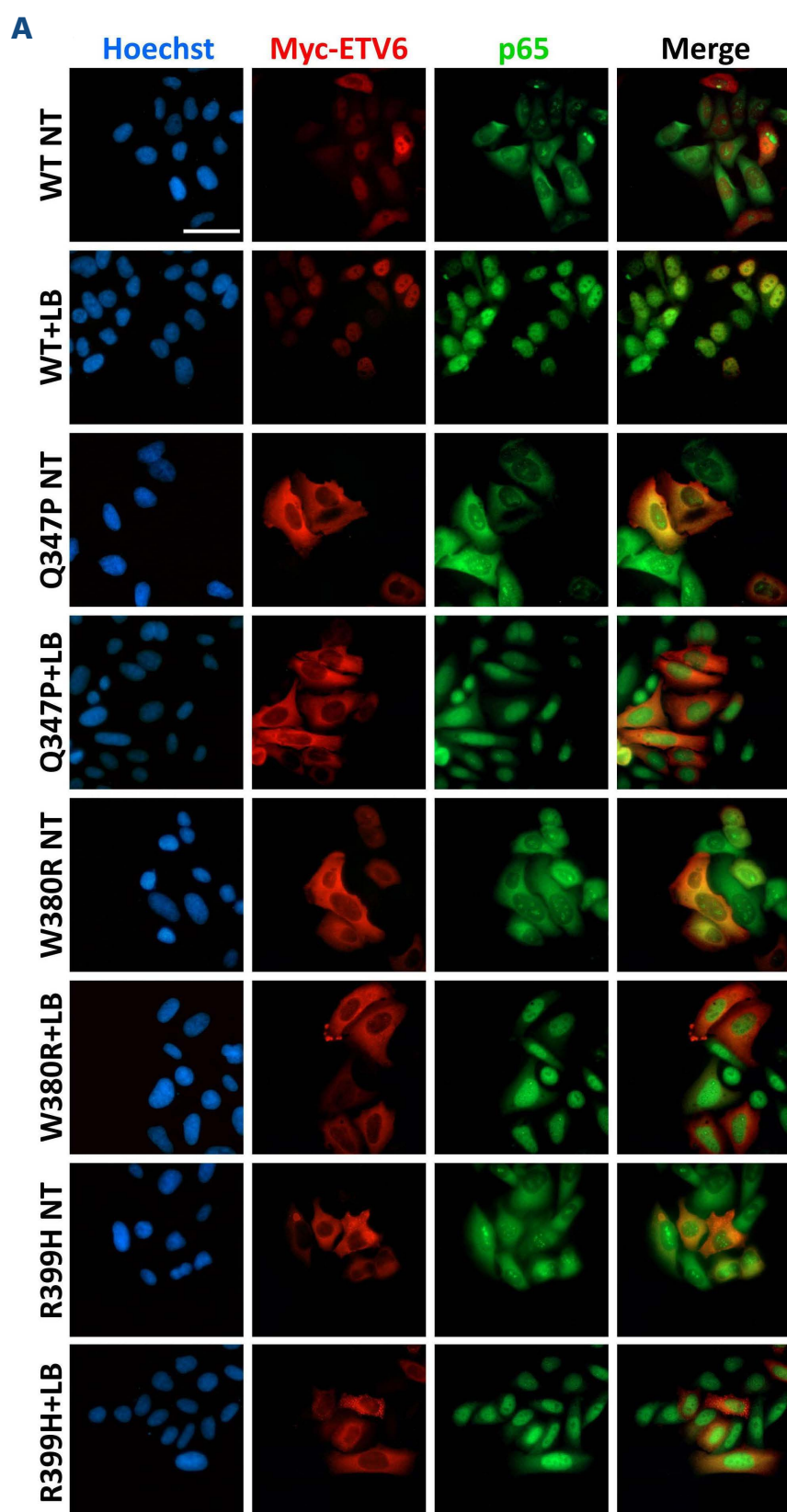


Figure 2. ETV6 mutations impair its ability to enter into the nucleus. (A) ETV6 immunostaining in HeLa cells after 4 hours of Leptomycin B (LB) treatment (50 nM). Subcellular localization of Q347P, W380R and R399H mutation (red) and p65 (green) before (NT) and after LB treatment. Nuclei were marked with Hoechst staining (blue). Images were obtained with a Zeiss Axioplan 2 epifluorescence imaging microscope and acquired with a Zeiss AxioCam 506 color using a 40X Plan-NEOFLUAR objective. Images were processed using Zeiss ZEN 3.1 (blue edition), while brightness and contrast were adjusted using Adobe Photoshop 2020. (B) Cell counts basing on ETV6 subcellular localization before and after treatment with LB. Histogram represents cell fraction with nuclear (N), cytoplasmic (C) or both (N/C) staining, confirming the intracellular distribution variation of ETV6 variants after LB treatment. All data reported are representative of at least 3 independent experiments.

co-expressed with M-ETV6-Myc, both proteins were mainly detected in the cytoplasm (Figure 3A). A significant shift of WT-ETV6-Flag from nucleus to cytoplasm was confirmed also by quantitative analysis which detected $37.0 \pm 16.4\%$ of the WT protein in the cytoplasm when co-expressed with WT-ETV6-Myc, while when transfected in combination with all M-ETV6 tested the protein amount reached a value of up to $81.1 \pm 10.8\%$ (Figure 3B), supporting our hypothesis that the mutated forms act through a dominant negative effect on WT protein, retaining this

form in the cytoplasm and consequently affecting its functions.

In order to further support the dominant negative effect, we tested the transcriptional activity using the luciferase assay. As above (*Online Supplementary Figure S2*), expression of WT-ETV6 alone represses the luciferase activity whereas expression of M-ETV6 abolishes the inhibition. Consistent with a dominant negative effect, co-expressing the WT- with the M-ETV6, we did not detect any significant difference in comparison with the effect of

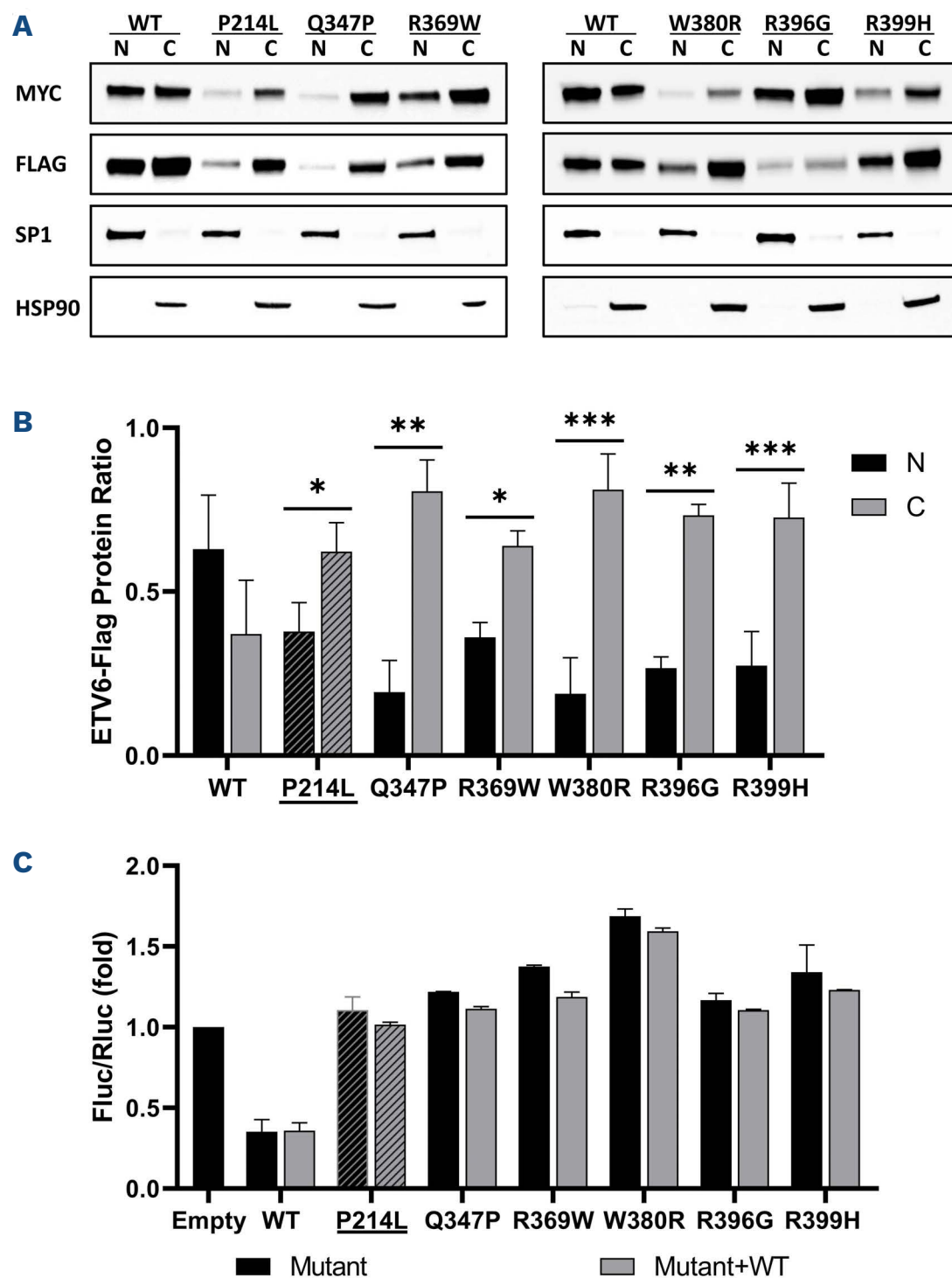


Figure 3. Alteration of wild-type function and intracellular distribution after co-transfection with mutant forms. (A) Western blot analysis performed in HEK293T 48 hours after transfection. Mutant forms and control wild-type (WT) are Myc-tagged, instead the co-transfected WT form is Flag-tagged. Hsp90 and SP1 were used as cytoplasmatic and nuclear markers, respectively. (B) Semi-quantitative analysis of WT-ETV6 Flag-tagged protein ratio was obtained using ImageJ. Histogram shows nuclear (N) and cytoplasmatic (C) ratios of respective variant. Error bars represent standard deviation of 3 independent experiments. * $P < 0.05$, ** $P < 0.01$, *** $P < 0.001$, vs. WT-ETV6, Student's *t*-test. (C) Luciferase assay performed on HEK293T 48 hours after single transfection (black) or co-transfection (grey) of respective variant with WT form to analyse functional loss of WT form due to the presence of mutated forms. Firefly luciferase cloned downstream MMP3 promoter was used as reporter and *Renilla* luciferase under the control of CMV promoter as normalizer. The experiment shows co-transfection cause only a partial reduction of firefly/*renilla* ratio, accordingly to the dominant negative hypothesis. P214L used as control mutation (striped column). Error bars represent standard deviation of 3 independent experiments.

mutants alone (Figure 3C), confirming that M-ETV6 antagonizes the repression activity of WT-ETV6. For all the mutations tested, we observed a slight increment of the repression activity, which could be explained by formation of WT/WT functionally active homodimers.

In summary, we show that all but two of the variants identified are pathogenic. Indeed, their respective mutant transcription factors do not enter the nucleus to exert their repressive activity. Moreover, inhibiting the protein nuclear export, we fully demonstrated that there is no trafficking of the mutant transcription factor between cytoplasm and nucleus, further supporting the hypothesis that M-ETV6 are unable to translocate to the nucleus.

In addition, we demonstrate and extend the dominant negative effect of ETV6 mutations described to date^{2,3,9} to other mutations (Q347P, W380R and R396G), suggesting that this is a common pathogenic mechanism of the disease.

These results increase our knowledge on the molecular basis of ETV6-RT and allow us to correctly classify variants to provide a definitive molecular diagnosis to patients and their families.

Since ETV6-RT is associated with an increased risk to develop hematological malignancies as supported also by identification of ETV6 germline mutations in patients affected by leukemia,^{3-5,9} correct molecular diagnosis would allow us to better understand this disease and to evaluate additional risks for patients. Moreover, improving our knowledge on pathogenic mechanisms is of fundamental importance to develop therapeutic strategies. Since M-ETV6 is unable to enter the nucleus, as fully demonstrated by the leptomycin B treatment, we should develop approaches leading to "release" the WT form of ETV6, for instance silencing the mutated transcript and/or preventing the dimerization of the WT and mutated forms of the transcription factor.

Authors

Michela Faleschini,¹ Daniele Ammeti,¹ Nicole Papa,² Caterina Alfano,³ Roberta Bottega,¹ Giorgia Fontana,¹ Valeria Capaci,² Melania E. Zanchetta,¹ Federico Pozzani,⁴ Francesca Montanari,⁵ Valeria Petroni,⁶ Paola Giordano,⁷ Patrizia Noris,⁸ Fiorina Giona⁹ and Anna Savoia^{1,2}

¹Istituto for Maternal and Child Health – IRCCS Burlo Garofolo, Trieste; ²Department of Medical Sciences, University of Trieste,

Trieste; ³Structural Biology and Biophysics Unit, Fondazione Ri.MED, Palermo; ⁴Department of Life Sciences, University of Trieste, Trieste; ⁵Sant'Orsola-Malpighi University Hospital, Medical Genetics Unit, Bologna; ⁶SOSD Pediatric Oncohematology, University Hospital "Ospedali Riuniti", Ancona; ⁷Interdisciplinary department of Medicine, Pediatric Unit, University "A.Moro" of Bari, Bari; ⁸Department of Internal Medicine, IRCCS Policlinico San Matteo Foundation, University of Pavia, Pavia and ⁹Department of Translational and Precision Medicine, Sapienza University of Rome, Rome, Italy

Correspondence:

A. SAVOIA - anna.savoia@burlo.trieste.it.

<https://doi.org/10.3324/haematol.2022.280729>

Received: February 4, 2022.

Accepted: May 10, 2022.

Prepublished: May 19, 2022.

©2022 Ferrata Storti Foundation

Published under a CC BY-NC license 

Disclosures

No conflicts of interest to disclose.

Contributions

MF and AS designed the study; MF and DA performed research and analysed data; NP and FP performed luciferase assays; AC performed structural analysis; RB and GF performed mutational screenings; VC and MEZ performed immunofluorescence assays; FM, VP, PG, PN and FG enrolled the patients; FM, DA and AS wrote the manuscript. All authors read and approved the manuscript.

Acknowledgments

We thank Professor Walter H.A. Khar for providing the lentiviral vector from which we cloned the wild-type full-length *ETV6* cDNA.

Funding

This study was supported by IRCCS "Burlo Garofolo" (Ricerca Corrente 01/2018), AIRC Grant IG-21974 and IRCCS Policlinico San Matteo Foundation (Ricerca corrente 2018 intramural research grant to NP).

Data-sharing statement

All data relevant to the study are included in the manuscript and are available upon request to the corresponding author.

References

- Galera P, Dulau-Florea A, Calvo KR. Inherited thrombocytopenia and platelet disorders with germline predisposition to myeloid neoplasia. *Int Lab Hematol.* 2019;41(S1):131-141.
- Noetzi L, Lo RW, Lee-Sherick AB, et al. Germline mutations in

- ETV6 are associated with thrombocytopenia, red cell macrocytosis and predisposition to lymphoblastic leukemia. *Nat Genet.* 2015;47(5):535-538.
3. Zhang MY, Churpek JE, Keel SB, et al. Germline ETV6 mutations in familial thrombocytopenia and hematologic malignancy. *Nat Genet.* 2015;47(2):180-185.
 4. Topka S, Vijai J, Walsh MF, et al. Germline ETV6 mutations confer susceptibility to acute lymphoblastic leukemia and thrombocytopenia. *PLoS Genet.* 2015;11(6):1-14.
 5. Moriyama T, Metzger ML, Wu G, et al. Germline genetic variation in ETV6 and risk of childhood acute lymphoblastic leukaemia: A systematic genetic study. *Lancet Oncol.* 2015;16(16):1659-1666.
 6. Melazzini F, Palombo F, Balduini A, et al. Clinical and pathogenic features of ETV6-related thrombocytopenia with predisposition to acute lymphoblastic leukemia. *Haematologica.* 2016;101(11):1333-1342.
 7. Poggi M, Canault M, Favier M, et al. Germline variants in ETV6 underlie reduced platelet formation, platelet dysfunction and increased levels of circulating CD34+ progenitors. *Haematologica.* 2017;102(2):282-294.
 8. Karastaneva A, Nebral K, Schlagenhaut A, et al. Novel phenotypes observed in patients with ETV6 -linked leukaemia/familial thrombocytopenia syndrome and a biallelic ARID5B risk allele as leukaemogenic cofactor. *J Med Genet.* 2020;57(6):427-433.
 9. Nishii R, Baskin-Doerfler R, Yang W, et al. Molecular basis of ETV6-mediated predisposition to childhood acute lymphoblastic leukemia. *Blood.* 2021;137(3):364-373.
 10. Rubnitz JE, Pui CH, Downing JR. The role of TEL fusion genes in pediatric leukemias. *Leukemia.* 1999;13(1):6-13.
 11. Fenrick R, Wang L, Nip J, et al. TEL, a putative tumor suppressor, modulates cell growth and cell morphology of Ras-transformed cells while repressing the transcription of stromelysin-1. *Mol Cell Biol.* 2000;20(16):5828-5839.
 12. Wood LD, Irvin BJ, Nucifora G, Nellide AH, Luce KS, Hiebert SW. Small ubiquitin-like modifier conjugation regulates nuclear export of TEL, a putative tumor suppressor. *Proc Natl Acad Sci U S A.* 2003;100(6):3257-3262.
 13. Benko S, Magalhaes JG, Philpott DJ, Girardin SE. NLRC5 limits the activation of inflammatory pathways. *J Immunol.* 2010;185(3):1681-1691.
 14. Green SM, Coyne HJ, McIntosh HP, Benet N, Graves BJ. DNA binding by the ETS protein TEL (ETV6) is regulated by autoinhibition and self-association. *J Biol Chem.* 2010;285(24):18496-18504.

Profound and sustained response with next-generation ALK inhibitors in patients with relapsed or progressive ALK-positive anaplastic large cell lymphoma with central nervous system involvement

Anaplastic large cell lymphoma (ALCL) is a rare disease accounting for less than 15% of all non-Hodgkin lymphomas in childhood. In children and adolescents, more than 90% of cases of ALCL harbor a translocation involving the anaplastic lymphoma kinase (ALK) gene, leading to constitutive activation of the ALK-kinase.¹ Outcome is good in most patients with a 5-year overall survival reaching 90% according to recent reports.² Involvement of the central nervous system (CNS) at diagnosis or at relapse/progression is uncommon with a 5-year cumulative risk of 4%.³ ALK inhibitors have now been used for several years in patients with relapsed ALK-positive ALCL with response rates ranging from 53% to 90%.⁴⁻⁶ Most previous trials were based on the first-generation ALK inhibitor, crizotinib, which is known to have poor CNS penetration. By contrast, next-generation ALK inhibitors, which have been developed for lung cancer and brain metastases, have good CNS penetration and could therefore be of great interest for treating patients with ALK-positive ALCL and CNS involvement. We prospectively collected data on all French patients <22 years old treated between 2017 and 2020 with next-generation ALK inhibitors for a CNS relapse/progression of ALK-positive ALCL.

Ten patients, suffering from 11 CNS relapses/progression, were identified. Data for each individual and details of each CNS relapse/progression are available in Tables 1 and 2 and *Online Supplementary Table S1*.

One patient only had CNS involvement at diagnosis. Of note, all patients underwent a diagnostic cerebrospinal fluid evaluation as routine staging. CNS imaging was only performed in cases of clinical suspicion. Three patients had a leukemic presentation or bone marrow involvement at diagnosis and six had no particular clinical risk factor for CNS evolution (Table 1). Of note, at frontline therapy, all patients at diagnosis, except for one, were at high risk of relapse or progression with minimal disseminated disease and minimal residual disease after one course of treatment. Five patients experienced disease progression while on frontline therapy. For the five others who achieved complete remission and completed the frontline therapy schedule, the time from end of treatment to the first relapse ranged from 0.6 to 2.1 months.

CNS disease was diagnosed during frontline treatment in one patient, at the first relapse in five and after the sec-

ond or further relapse in four. The median age at CNS relapse/progression was 11 years (range, 1.8-19). The median delay between diagnosis and CNS relapse/progression in the nine patients free of CNS involvement at diagnosis was 9 months (range, 1.6-54). Before the initiation of treatment with next-generation ALK inhibitors, all patients had received one to three previous treatment lines and four of them had received crizotinib (*Online Supplementary Table S1*). Interestingly, nine patients had positive minimal residual disease while on the treatment line preceding CNS relapse/progression although eight were in complete clinical and radiological remission. Of note, six patients had CNS relapse while on treatment, with either vinblastine (n=3) or crizotinib (n=3). At the time of CNS progression/relapse, four patients had only CNS involvement and the six others also had systemic disease. CNS involvement was restricted to the presence of tumor cells on cytological examination in the cerebrospinal fluid in three patients, while seven had intracranial masses, associated with cerebrospinal fluid positivity on cytological examination in three of the five in whom the cerebrospinal fluid could be examined.

Among the 11 episodes of CNS relapse/progression reported here, the next-generation ALK inhibitor used was ceritinib (n=3), lorlatinib (n=3) or alectinib (n=5). The median duration of the treatment with a next-generation ALK inhibitor was 11.3 months (range, 1.2- 27.2). Regarding response to these ALK inhibitors, we report ten responses in the 11 episodes of CNS relapse/progression. One progression of disease occurred on ceritinib in patient #5 who finally achieved complete remission after being switched to high-dose methotrexate followed by alectinib. The median time to best response was 1.5 months (range, 0.5-6) (Figure 1). Only one patient experienced systemic and CNS disease relapse after achieving complete remission on alectinib (patient #9). This progression was not well documented either on a molecular level (i.e., resistance mutation) or on a pharmacokinetic level. Alectinib was stopped and this patient benefited from CNS-directed chemotherapy and finally achieved third complete remission. She unfortunately died while in this third complete remission in the context of an invasive mucormycosis infection.

Regarding the nine patients with prolonged complete re-

Table 1. Patients' initial diagnosis and relapse characteristics.

Patient (age at diagnosis in years)	Disease characteristics at diagnosis					Characteristics of CNS relapse treated with a next-generation ALK inhibitors					
	Initial CNS status	Other clinical risk factors for CNS at diagnosis*	MDD/ early MRD status in frontline	Histological pattern (SC/LH component vs. common)	Time from EOT to first relapse (months)	Interval between initial diagnosis and CNS involvement (months)	Number of relapse/ progression (type)	Last treatment before CNS relapse	Peripheral blood MRD status on previous treatment line	Type of relapse	Type of CNS involvement
1 (16)	negative	no	positive/positive	common	0.7	54	3, relapse	vinblastine	positive	systemic and CNS	CNS mass (CSF nd)
2 (6)	negative	leukemic presentation (blood circulating cells on cytology)	positive/positive	SC/LH	on therapy	4.9	3, progression	vinblastine	positive	systemic (including uncontrolled leukemic form) and CNS	multiple CNS masses + CSF positive
3 (19)	positive	na	nd	common	on therapy	na	1, progression	radio-therapy	positive	systemic and CNS	CNS mass (CSF nd)
4 (11)	negative	biopsy of choroid plexus papilloma at treatment initiation.	positive/positive	common	on therapy	4.1	1, relapse (on biopsy route while on vinblastine for recovery post CNS biopsy)	vinblastine	positive	CNS only	multiple CNS masses
5 (9)	negative	no	positive/positive	SC/LH	2.1	10.1	1, relapse	ALCL99	negative at EOT with ALCL99	systemic and CNS	CSF positive only
6 (1.8)	negative	BM involvement (diagnosed on cytology)	positive/positive	SC/LH	on therapy	1.6	1, relapse	ALCL99	positive	systemic (including BM) and CNS	CSF positive only
7 (11)	negative	no	positive/positive	nd	on therapy	9	2, relapse	crizotinib	positive	CNS only	CNS mass + CSF positive
8 (13)	negative	no	positive/positive	nd	1.5	5.8	1, relapse	ALCL99	positive at EOT with ALCL99	systemic and CNS	CSF positive only
9 (4)	negative	BM involvement (diagnosed on cytology), severe HLH	positive/positive	SC/LH	1.9	15.8	2, relapse	crizotinib	positive	CNS only	CNS mass
10 (19)	negative	no	positive/positive	SC/LH	0.6	14.8	2, relapse	crizotinib	positive	CNS only	multiple CNS masses + CSF positive

*Leukemic presentation, bone marrow involvement, central nervous system involvement at diagnosis. CNS: central nervous system; MDD: minimal disseminated disease; early MRD: early measurement (after one chemotherapy course) of minimal residual disease; SC: small cell component; LH: lymphohistiocytic component; EOT: end of treatment; CSF: cerebrospinal fluid; nd: not done; na: not applicable; BM: bone marrow; HLH: hemophagocytic lymphohistiocytosis.

mission, four patients were still on ALK inhibitors at the date of the last follow-up visit. The treatment had been discontinued in the other five patients for various reasons: one patient (#8) underwent allogeneic hematopoietic

stem cell transplantation after complete remission; one patient (#3) stopped ceritinib because of grade 3 toxicity and was switched to weekly vinblastine for 3 months and received no further treatment after vinblastine, with a fol-

low-up time off lymphoma therapy of 42 months; two patients (#1 and #6) were included in the NIVOALCL trial (NCT03703050) and received nivolumab while still in complete remission; and one patient (#5) definitively stopped the next-generation ALK inhibitor and received no further therapy, with more than 10 months off treatment at the date of last follow-up considered for the study.

Overall, nine out of ten patients were alive in complete remission at the date of last visit. The median duration of the follow-up from the initiation of ALK inhibitor treatment in these nine patients was 24.2 months (range, 11.3-

48.1).

Of note, next-generation ALK inhibitors could be helpful in critically ill patients as clinical improvements occurred very fast; for example, patient #3 was in a coma at treatment initiation and regained normal consciousness. Response on imaging was also impressive for the patients with intracranial masses (*Online Supplementary Figure S1*). Regarding tolerance of next-generation ALK inhibitors, we reported notable adverse events of grade 3 or higher in eight patients, including weight gain in three patients, neuropsychological manifestations in three patients and

Table 2. Response to next-generation ALK inhibitors and patients' outcome.

Patient	Name of ALKi	Type of CNS involvement	Best response	Time to best response (months)	Treatment duration (months)	Next treatment after ALKi	Notable adverse events	Current outcome and disease status (FU from ALKi initiation, in months)
1	lorlatinib	CNS mass (CSF nd)	CR	6	7	other investigational treatment in CR for consolidation	hallucinations, anxiety grade 3	alive in CR (30.2)
2	alectinib	multiple CNS masses + CSF positive	CR	1.6	14.5	na	weight gain grade 3	alive in CR (14.5)
3	ceritinib	CNS mass (CSF n.d.)	CR	0.5	3	vinblastine 3 months then no further treatment	GI toxicity grade 3	alive in CR (48.1)
4	lorlatinib	multiple CNS masses	CR	1	27.2	na	weight gain grade 3	alive in CR (27.2)
5	ceritinib	CSF positive	PD	1.2	1.2	na	hepatic toxicity grade 3	alive in CR
5 (2 nd episode treated with ALKi)	alectinib	CSF positive	CR	n.a.(CR obtained with 2 courses of HD MTX)	26	no further treatment	weight gain grade 3	alive in CR (36.5)
6	ceritinib	CSF positive	CR	1.3	16.9	other investigational treatment in CR for consolidation	GI and hepatic toxicity grade 3	alive in CR (40.8)
7	lorlatinib	CNS mass + CSF positive	CR	1.6	21	na	irritability and aggression grade 2	alive in CR (21.0)
8	alectinib	CSF positive	CR	2.5	2.9	allogeneic transplant in CR	none	alive in CR (19.1)
9	alectinib	CNS mass	CR	1.4	2.5	CNS-directed chemotherapy for CNS disease progression	none	died, in CR3 in context of mucormycosis infection (9.4)
10	alectinib	multiple CNS masses + CSF positive	CR	3.6	11.3	na	acute delirium Grade 3	alive in CR (11.3)

ALKi: ALK inhibitors; CNS: central nervous system; FU: follow-up; CSF: cerebrospinal fluid; nd: not done; CR: complete response; na: not applicable; GI: gastrointestinal; PD: progressive disease; HD-MTX: high-dose methotrexate; CR3: third complete response.

grade 3 gastrointestinal and/or hepatic adverse events in three patients.

In contrast to the overall population of patients with ALK-positive ALCL, patients with CNS involvement any time during the course of their disease are known to have a dismal outcome.^{7,8} This was recently confirmed in a report from the European Inter-Group for Childhood Non-Hodgkin Lymphoma, in which the 3-year overall survival of patients after CNS relapse was less than 50%, and the median time to death after CNS relapse was 3.5 months in the 4% of patients experiencing such relapses.³

The range of therapeutic options for relapsed/refractory ALK-positive ALCL has increased significantly during the past decades. Besides conventional chemotherapy, several targeted therapies such as brentuximab vedotin and ALK inhibitors are now widely used to treat patients with ALCL at relapse.^{4,9} However, there is no evidence that vinblastine and the antibody-drug conjugate brentuximab vedotin cross the blood-brain barrier,¹⁰ and several cases of CNS relapses occurring in ALCL patients treated with vinblastine or brentuximab for systemic disease have been reported.^{11,12}

ALK inhibitors have been used for several years now, with some success. The first-in-class, crizotinib, showed quite good results in relapsed/refractory ALK-positive ALCL.⁴⁻⁶ However, it might not be efficient for CNS prophylaxis. Indeed, CNS progression during crizotinib treatment is one

of the common modes of failure in patients treated for ALK-rearranged non-small cell lung cancer, accounting for nearly 70% of the treatment failures in some studies.¹³ This might be attributed to poor CNS penetration of crizotinib, with a concentration in cerebrospinal fluid almost 400-fold lower than that in the serum.¹⁴ This lack of ALCL CNS disease control with crizotinib was also evidenced in a brief report by Ruf and colleague in 2018.¹¹ To overcome this problem, next-generation ALK inhibitors were designed to cross the blood-brain barrier more efficiently, thus achieving a higher concentration in the cerebrospinal fluid. As a result these molecules, which include ceritinib, alectinib, brigatinib and lorlatinib, demonstrated a prominent ability to control CNS disease in ALK-rearranged non-small cell lung cancer.¹⁵

We report here 11 neuro-meningeal relapses or progressions in ten patients with ALK-positive ALCL treated with next-generation ALK inhibitors. We first want to emphasize that this number is quite high as we report here ten patients with CNS relapses in 3 years compared to the previous 25 CNS relapses in nearly 20 years reported in the already mentioned European Inter-Group for Childhood Non-Hodgkin Lymphoma report.³ This could be caused by some changes in our practices such as the wider use of vinblastine and the introduction of prolonged crizotinib treatment in a relapse setting, especially in patients with high-risk disease and in those who are positive

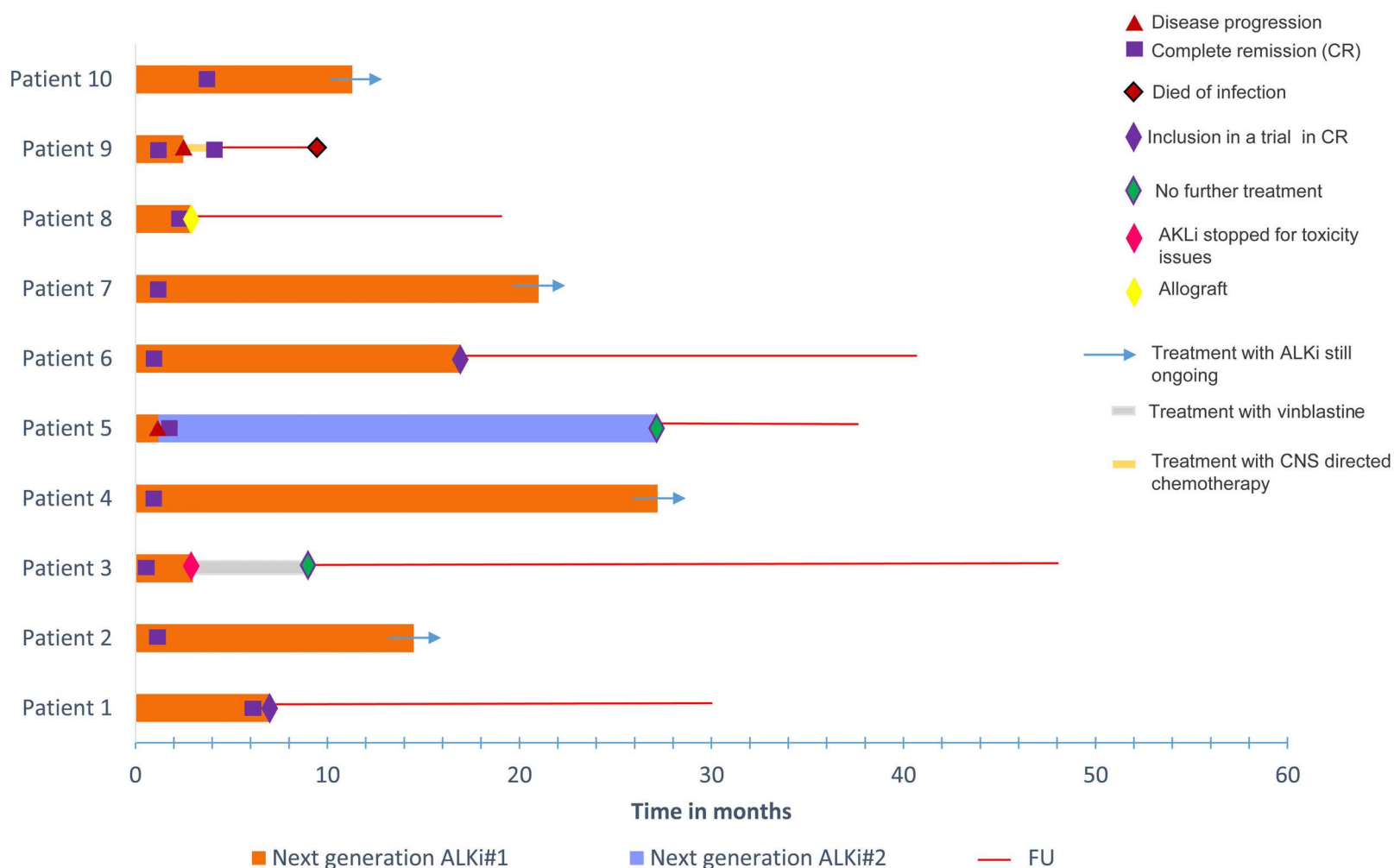


Figure 1. Swimmer-plot of French pediatric patients treated with next-generation ALK inhibitors for central nervous system relapse or progression of ALK-positive anaplastic large cell lymphoma. ALKi: ALK inhibitor; CNS: central nervous system; FU: follow-up.

for minimal residual disease. Of note, six of our patients relapsed on vinblastine or crizotinib. In this report of 11 CNS relapses treated with next-generation ALK inhibitors, a rapid, profound response was observed in all ten patients. Only one patient experienced secondary progression while on a next-generation ALK inhibitor whereas nine patients were still alive in complete remission at the last follow-up. Even though this series is small, the response rate and general outcome appears far better than that for relapsed/refractory ALK-positive ALCL with CNS involvement previously reported in the literature.³

The optimal duration of treatment with next-generation ALK inhibitors has not been assessed yet. Of note, although the majority of the patients achieved durable complete remissions, they may not be cured since abrupt relapses have been reported after the discontinuation of ALK inhibitors, even after several years of treatment.¹⁶ In this series, one patient is still in complete remission after having stopped his treatment with an ALK inhibitor for nearly 1 year, with no further treatment.

In conclusion, despite the small number of cases, this report suggests a promising activity of next generation ALK inhibitors in patients with ALK-positive ALCL and CNS involvement at relapse. It also suggests that we should be more careful regarding the CNS prophylaxis of high-risk and relapsed ALK-positive ALCL and next-generation ALK inhibitors should be considered as part of CNS prophylaxis.

Authors

Charlotte Rigaud,¹ Samuel Abbou,¹ Stéphane Ducasso,² Mathieu Simonin,³ Lou Le Mouel,⁴ Victor Pereira,⁵ Stéphanie Gourdon,⁶ Anne Lambilliotte,⁷ Birgit Georger,¹ Véronique Minard-Colin¹ and Laurence Brugières¹

References

- Lamant L, Meggetto F, al Saati T, et al. High incidence of the t(2;5)(p23;q35) translocation in anaplastic large cell lymphoma and its lack of detection in Hodgkin's disease. Comparison of cytogenetic analysis, reverse transcriptase-polymerase chain reaction, and P-80 immunostaining. *Blood*. 1996;87(1):284-291.
- Mussolin L, Le Deley M-C, Carraro E, et al. Prognostic factors in childhood anaplastic large cell lymphoma: long term results of the international ALCL99 trial. *Cancers*. 2020;12(10):E2747.
- Del Baldo G, Abbas R, Woessmann W, et al. Neuro-meningeal relapse in anaplastic large-cell lymphoma: incidence, risk factors and prognosis – a report from the European Intergroup for Childhood Non-Hodgkin Lymphoma. *Br J Haematol*. 2021;192(6):1039-1048.
- Mossé YP, Lim MS, Voss SD, et al. Safety and activity of crizotinib for paediatric patients with refractory solid tumours or anaplastic large-cell lymphoma: a Children's Oncology Group phase 1 consortium study. *Lancet Oncol*. 2013;14(6):472-480.
- Brugières L, Houot R, Cozic N, et al. Crizotinib in advanced ALK+ anaplastic large cell lymphoma in children and adults: results of the Acs© phase II trial. *Blood*. 2017;130(Suppl 1):2831.
- Gambacorti-Passerini C, Orlov S, Zhang L, et al. Long-term effects of crizotinib in ALK-positive tumors (excluding NSCLC): a phase 1b open-label study. *Am J Hematol*. 2018;93(5):607-614.
- Brugières L, Le Deley M-C, Rosolen A, et al. Impact of the methotrexate administration dose on the need for intrathecal treatment in children and adolescents with anaplastic large-cell lymphoma: results of a randomized trial of the EICNHL Group. *J Clin Oncol*. 2009;27(6):897-903.
- Woessmann W, Zimmermann M, Lenhard M, et al. Relapsed or refractory anaplastic large-cell lymphoma in children and adolescents after Berlin-Frankfurt-Muenster (BFM)-type first-line therapy: a BFM-group study. *J Clin Oncol*.

¹Department of Children and Adolescents Oncology, Gustave Roussy Cancer Center, Paris-Saclay University, Villejuif; ²Department of Pediatric Oncology and Hematology, Bordeaux University Hospital, Bordeaux; ³Department of Pediatric Oncology and Hematology, Armand Trousseau Hospital- APHP, Paris; ⁴Department of Pediatric Hematology, Robert Debré Hospital- APHP, Paris; ⁵Department of Pediatric Oncology and Hematology, Besançon University Hospital, Besançon; ⁶Department of Pediatric Oncology and Hematology, Saint-Denis de la Réunion University Hospital, La Réunion and ⁷Department of Pediatric Hematology, Lille University Hospital, Lille, France.

Correspondence:

CHARLOTTE RIGAUD - charlotte.rigaud@gustaveroussy.fr

<https://doi.org/10.3324/haematol.2021.280081>

Received: November 10, 2021.

Accepted: May 11, 2022.

Prepublished: May 19, 2022.

©2022 Ferrata Storti Foundation

Published under a CC BY-NC license 

Disclosures

No conflicts of interest to disclose.

Contributions

LB and CR planned the study. CR wrote the first draft of the manuscript. All the authors contributed to data control and to writing and revising the manuscript.

Data-sharing statement

The data that support the findings of this study are available on request from the corresponding author. The data are not publicly available due to privacy or ethical restrictions.

- 2011;29(22):3065-3071.
9. Pro B, Advani R, Brice P, et al. Five-year results of brentuximab vedotin in patients with relapsed or refractory systemic anaplastic large cell lymphoma. *Blood*. 2017;130(25):2709-2717.
 10. Ginsberg S, Kirshner J, Reich S, et al. Systemic chemotherapy for a primary germ cell tumor of the brain: a pharmacokinetic study. *Cancer Treat Rep*. 1981;65(5-6):477-483.
 11. Ruf S, Hebart H, Hjalgrim LL, et al. CNS progression during vinblastine or targeted therapies for high-risk relapsed ALK-positive anaplastic large cell lymphoma: a case series. *Pediatr Blood Cancer*. 2018;65(6):e27003.
 12. Abid MB, Wang S, Loi HY, Poon LM. ALK-negative anaplastic large cell lymphoma with CNS involvement needs more than just brentuximab vedotin. *Ann Hematol*. 2016;95(10):1725-1726.
 13. Solomon BJ, Cappuzzo F, Felip E, et al. Intracranial efficacy of crizotinib versus chemotherapy in patients with advanced ALK-positive non-small-cell lung cancer: results from PROFILE 1014. *J Clin Oncol*. 2016;34(24):2858-2865.
 14. Costa DB, Kobayashi S, Pandya SS, et al. CSF concentration of the anaplastic lymphoma kinase inhibitor crizotinib. *J Clin Oncol*. 2011;29(15):e443-445.
 15. Gadgeel SM, Gandhi L, Riely GJ, et al. Safety and activity of alectinib against systemic disease and brain metastases in patients with crizotinib-resistant ALK-rearranged non-small-cell lung cancer (AF-002JG): results from the dose-finding portion of a phase 1/2 study. *Lancet Oncol*. 2014;15(10):1119-1128.
 16. Gambacorti-Passerini C, Mussolin L, Brugieres L. Abrupt relapse of ALK-positive lymphoma after discontinuation of crizotinib. *N Engl J Med*. 2016;374(1):95-96.

Autologous stem cell transplantation in an older adult population

Over the past decade there has been a remarkable progress in the treatment of multiple myeloma (MM) and non-Hodgkin lymphoma (NHL). Nevertheless, autologous stem cell transplant (ASCT) remains an integral part of the care for patients with MM, and one of few curative options for patients with relapsed/refractory (R/R) NHL. Historically, an arbitrary age of 65 has been used to determine patient's eligibility for ASCT. This stems from the fact that the majority of prospective studies evaluating efficacy of ASCT in MM have excluded patients >65 years old.¹ Currently, nearly half of new diagnoses of MM and NHL are >75 years old.^{2,3} However, the data on safety and efficacy of ASCT patients >75 years remains limited.

Racial minorities remain severely underrepresented in cancer clinical trials, thus limiting the generalizability of clinical cancer research to these populations.⁴ Data on ASCT in elderly minority patients has to our knowledge not yet been reported. In this letter we present results of a retrospective study showing comparable transplant related mortality in minority patients >75 years old as compared to those aged 55-66 years old.

We conducted a retrospective cohort study comparing ASCT outcomes in patients >75 years old and 55-65 years old for the diagnosis of MM or NHL, who were conditioned with either melphalan or BEAM (carmustine, etoposide, cytarabine, melphalan) respectively. Patients were selected from an internal database which has all ASCT performed at our center between 2005-2021. The study group included patients >75 years old. The control group included patients 55-65 years old that were matched to the study group patients by sex and date of transplant. Electronic medical records were reviewed to gather data. The primary outcomes were admission mortality, length of stay, time to white blood cell (WBC) and platelet engraftment, incidence of neutropenic fever, positive blood culture, intensive care unit (ICU) admission, and 30-day rehospitalization rate. Secondary outcome were 1- and 5-year mortality rates. Patients with no follow-up post ASCT and ASCT prior to 1- and 5-year follow-up were excluded from analysis. Admission mortality and long-term survival probability were calculated using log rank test. Continuous data was reported as medians and interquartile ratios (IQR) and analyzed using Wilcoxon rank sum test. Significance was denoted by $\alpha=0.05$.

Between 12/2005 and 3/2021, there were 43 patients >75 years old who underwent ASCT for MM or NHL. Data collection was censored on 4/2/22. Table 1 summarizes patient characteristics at index ASCT. Twenty-four (55.8%)

patients were female. The median age in the study group was 77.1 (range, 76.2-77.9) years old and 61.9 (range, 57.4-63.0) years old in the control group. Both groups predominantly included minority patients: 55.8% and 46.5% were Spanish/Hispanic/Latino and 25.6% and 14.0% were Afri-

Table 1. Patient characteristics.

	Study	Control
N	43	43
Female, N (%)	24 (55.8)	24 (55.8)
Age, median (IQR)	77.1 (76.2-77.9)	61.9 (57.4-63.0)
Performance status, N	28	31
100	5	2
90	14	16
80	5	7
70	3	3
60	1	3
Minority, N (%)		
Spanish/Hispanic/Latino	24 (55.8)	20 (46.5)
African American	11 (25.6)	6 (14.0)
Non-minority*, N (%)	8 (18.6)	17 (39.5)
Medicaid insurance**, N (%)		
Minority	12/33 (36.4)	20/25 (80.0)
Non-minority	0	9/13 (69.2)
Auto-HSCT indication		
Multiple myeloma, N (%)	34 (79.1)	33 (76.7)
Upfront	28 (82.4)	24 (72.7)
Relapsed/refractory	6 (17.6)	9 (27.3)
Melphalan dose, N (%)		
200 mg/m ²	5 (14.7)	28 (84.8)
140 mg/m ²	19 (55.9)	5 (15.6)
100 mg/m ²	9 (26.5)	0
50 mg/m ²	1 (2.9)	0
Lymphoma, N (%) ***	9 (20.9)	10 (23.3)
DLBCL	7 (77.8)	7 (70.0)
Other	2 (22.2)	3 (30.0)
Upfront	4 (44.4)	6 (60.0)
Relapsed/refractory	5 (55.6)	4 (40.0)
Prior auto-HSCT for relapsed disease, N (%)	1 (2.3)	2 (4.6)

Auto-HSCT: autologous hematopoietic stem cell transplant; IQR: interquartile ratio; DLBCL: diffuse large B-cell lymphoma. *Non-minority patients include those with ethnicity other than Spanish/Hispanic/Latino and those without documented Race/Ethnicity. ** In the study group: 1/43 patient had unknown insurance status, 39/42 had Medicare coverage, of 11/39 had dual Medicare/Medicaid coverage, 1/42 patient only had Medicaid coverage and 2/42 had commercial insurance. In the control group: 5 had unknown insurance status, 24/38 had only Medicaid coverage, 5/38 had dual Medicare/Medicaid coverage, 1/38 had only Medicare, 8/38 had commercial insurance. ***All patients with lymphoma received BEAM (carmustine, etoposide, cytarabine, melphalan) conditioning.

can American, in the study and control groups, respectively. MM was the most common indication for auto-HSCT comprising 34 (79.1%) and 33 (76.1%) patients in the study and control groups, respectively.

Table 2 outlines patient outcomes. Admission mortality did not differ significantly between the groups, with only one death in the control group ($P=0.083$). The length of stay was comparable at 18 (range, 17-22) days and 19 (range, 16-20) days ($P=0.2$) for study and control groups, respectively. Time to WBC engraftment in the study group was 12 (range, 11-12) days and 11 (range, 11-12) days in the control group ($P=0.032$). Time to platelet engraftment in the study group was 14 (range, 12-15) days and 12 (range, 11-14) days in the control group ($P=0.014$). Although time to both WBC and platelet engraftment was significantly

longer in the study group, the clinical significance of this finding is questionable, especially as it did not significantly prolong length of stay. There was no significant difference between incidence of neutropenic fever, or between incidence of positive blood cultures in patients with neutropenic fever. There was a non-statistically significant increase in the rate of ICU admissions in the study (4/43) versus control group (0/43) ($P=0.12$). The 30-day re-hospitalization rate was comparable between the two groups ($P=0.68$).

In the study group, two patients died within 1 year of ASCT (day +360 and +133) translating into 1-year mortality of 4.9% (2/41). Five-year survival was 53.8% (14/26). In the control group, one patient died on day +26 of ASCT translating into 1-year mortality of 2.8% (1/36). Five-year sur-

Table 2. Outcomes.

	Study	Control	P value
Admission mortality, N (%)	0	1 (2.3)	0.083
Minority	0	0	
Non-minority	0	1/1	
LOS - days, median (IQR)	18 (17-22)	19 (16-20)	0.2
Minority	18 (16-20.5)	17 (16.3-20)	
Non-minority	19.5 (17.75-28.25)	18 (16-19)	
Days to WBC engraftment, median (IQR)	12 (11-12)	11 (11-12)	0.032
Minority	12 (11-12)	11 (11-12)	
Non-minority	12 (12-12.3)	11 (10-12)	
Days to Plt engraftment, median (IQR)	14 (12-15)	12 (11-14)	0.014
Minority	13.5 (12-15)	13 (11.5-14)	
Non-minority	15 (14-22.8)	12 (11-13)	
Neutropenic fever, N (%)	22 (51.2)	27 (62.8)	0.38
Positive blood culture, N (%*)	7 (31.8)	11 (40.7)	0.56
Minority	17/35	15/26	
Non-minority	5/8	12/1	
ICU admission, N (%)	4 (9.3)	0	0.12
Minority	4/35	0	
Non-minority	0/8	0	
30-day readmission, N (%)	4 (9.3)	2 (4.8)	0.68
Minority	3/35	1/25	
Non-minority	1/8	1/17	
1-year survival, N (%)**	39/41 (95.1)	35/36 (97.2)	1
Minority	32/33	21/22	
Non-minority	7/8	14/14	
5-year survival, N (%)***	14/26 (53.8)	13/24 (54.2)	1
Minority	13/22	9/15	
Non-minority	1/4	4/9	

LOS: length of stay; WBC: white blood cells; Plt: platelets; ICU: intensive care unit; ASCT: autologous stem cell transplant. Minority subgroup includes African American and Spanish/Hispanic/Latino patients. *Percent of those with neutropenic fever. **Only includes patients with transplant >1 year ago and with follow-up after 1 year post-ASCT. Study group: 2 patients were excluded from analysis: 1 patient was lost to follow-up prior to the 1 year mark and 1 patient had ASCT <1 year ago. Control group: 7 patients were excluded from analysis: 5 patients were lost to follow-up prior to the 1 year mark and 2 patients had ASCT <1 year ago. ***Only includes patients with ASCT >5 years ago and with follow-up after 5 years post ASCT. Study group: 17 patients excluded from analysis: 6 patients were lost to follow up prior to the 5 year post ASCT follow-up; 11 patients had ASCT <5 years ago. Control group: 19 patients were excluded from analysis: 8 patients were lost to follow-up prior to the 5 year post ASCT follow up; 11 patients had ASCT <5 years ago.

vival was 54.2% (13/24) (Figure 1).

The treatment landscape for elderly patients with both MM and NHL has dramatically improved in recent years. However, ASCT remains a significant contributor to improved outcomes in the elderly population with MM, and one of the few options for long term disease control for patients with R/R NHL.⁵⁻¹⁰ The main concern related to ASCT in the elderly has historically been transplant-related mortality (TRM). With the improvement of supportive care, TRM rates in elderly patients have been declining. Our finding of 0% TRM is similar to that of prior reports in this age category.^{7,11} Additionally, in our study we observed a comparable 5-year mortality rate for elderly patients and their younger counterparts, despite a 15-year age difference.

In contrast to above-mentioned reports, our elderly cohort includes 80% patients from racial minority groups, predominantly Hispanic or African American. Studies have shown that Hispanics and African Americans are far less likely to undergo ASCT, despite an abundance of data

showing similar or better outcomes.^{12,13} Our study is the first to our knowledge to address the outcomes for elderly minority patients undergoing ASCT. It is worth noting that in the two large reports comparing outcomes of ASCT in minorities and Caucasians with MM, the upper age limit in minority cohorts was 75 years old, while Caucasian cohorts included patients up to age of 80.^{12,14} Similar to patients with MM, favorable outcomes for elderly patients with NHL receiving ASCT with BEAM conditioning have been reported, with no reports in the literature on minority elderly patients.¹⁵ This is of clinical importance as various studies have shown that minority patients with NHL have worse outcomes compared to Caucasians.^{16,17} This data suggests that elderly minority patients have two separate variables contributing to a decreased chance of being offered ASCT. 26.4% of the Bronx's population lives below the poverty line.¹⁸ Montefiore Medical Center is one of the largest providers of Medicaid and Medicare in New York State. Analysis of National Cancer Database (NCDB) showed that ASCT improved survival for MM patients from

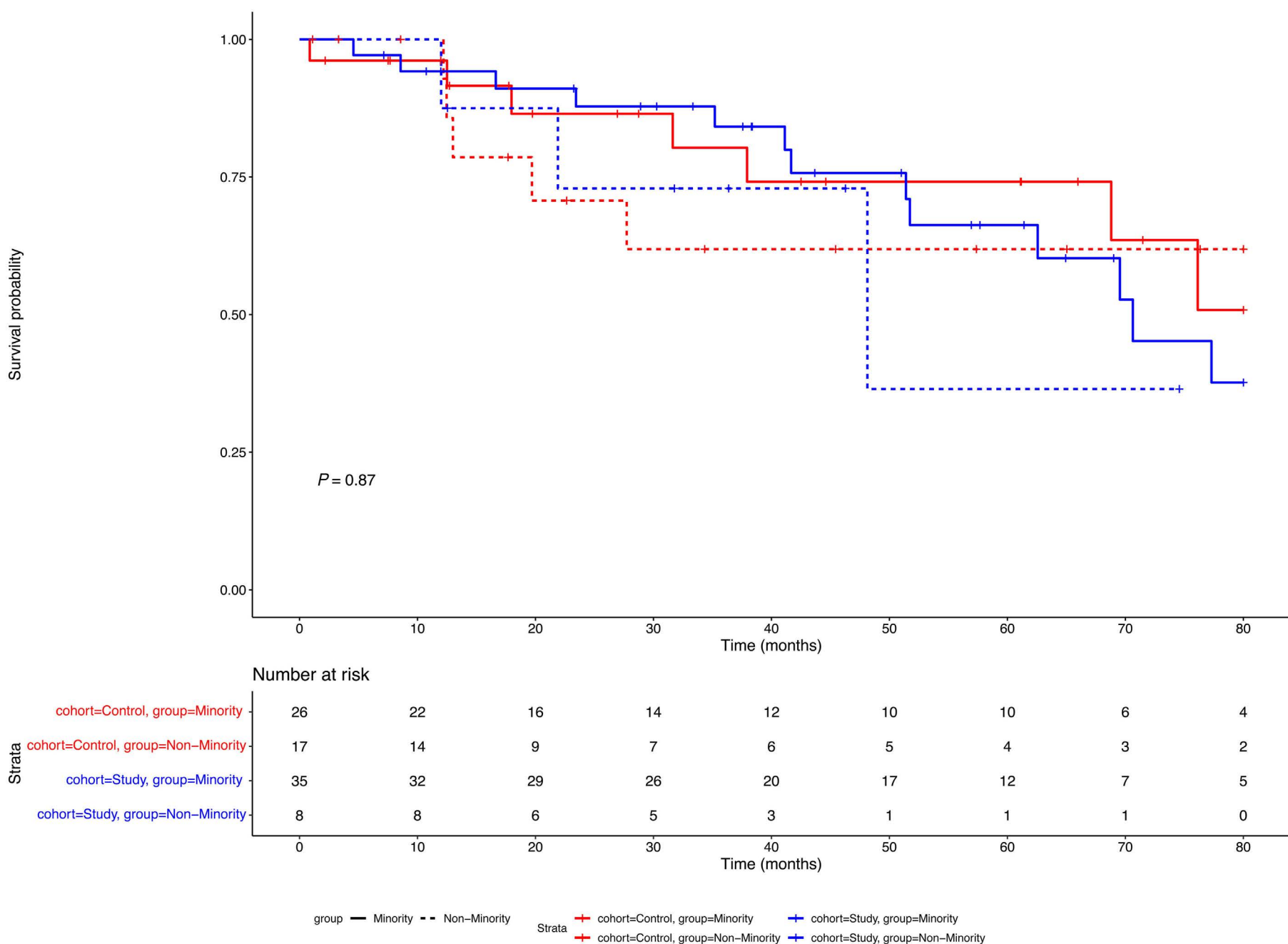


Figure 1. Overall survival. Survival probability of individual patient cohorts was plotted against time with control groups marked in blue and study groups marked in red.

all economic backgrounds, but uninsured patients or those with Medicaid had significantly lower overall survival.¹⁹ Similar trends have been observed with in patients with NHL.²⁰

This study has limitations such as retrospective design, small sample size, variability in minority proportion, and melphalan dosing discrepancy between the groups.

Our study is one of the few to demonstrate the safety of ASCT in patients >75 years old and the only study to evaluate ASCT in a predominantly minority elderly population. We did not find a statistically significant increase in 100-day transplant related mortality in patients > 75 years old compared to patients 55-65 years old. Older patients and those younger than 65 years old appear to have comparable 5-year mortality.

Authors

Kateryna Fedorov,¹ Tanim Jain,² Kith Pradhan,³ Jennat Mustafa,¹ Amanda Lombardo,¹ Fariha Khatun,¹ Felisha Joseph,¹ Kailyn Gillick,¹ Anjali Naik,¹ Richard Elkind,¹ Karen Fehn,¹ Alyssa de Castro,⁴ Roy Browne,⁴ Michelly Abreu,¹ Donika Binakaj,¹ Monika Paroder,⁵ Carlo Palesi,⁵ Kira Gritsman,¹ R. Alejandro Sica,¹ Noah Kornblum,¹ Aditi Shastri,¹ Ioannis Mantzaris,¹ Nishi Shah,¹ Amit Verma,¹ Ira Braunschweig¹ and Mendel Goldfinger¹

¹Department of Oncology; ²Department of Medicine; ³Department of Epidemiology and Population Health; ⁴Department of Pharmacy and ⁵Department of Pathology, Montefiore Medical Center and the Albert Einstein College of Medicine, Bronx, NY, USA

Correspondence:

K. FEDOROV - KateFedorov@gmail.com

M. GOLDFINGER - mgoldfin@montefiore.org

References

1. Attal M, Harousseau JL, Stoppa AM, et al. A prospective, randomized trial of autologous bone marrow transplantation and chemotherapy in multiple myeloma. Intergroupe Francais du Myelome. *N Engl J Med.* 1996;335(2):91-97.
2. Cancer Stat Facts: Myeloma: National Cancer Institute; <https://seer.cancer.gov/statfacts/html/mulmy.html>
3. Cancer Stat Facts: Non-Hodgkin Lymphoma: National Cancer Institute; <https://seer.cancer.gov/statfacts/html/nhl.html>
4. Guerrero S, López-Cortés A, Indacochea A, et al. Analysis of racial/ethnic representation in select basic and applied cancer research studies. *Sci Rep.* 2018;8(1):13978.
5. Ntanasis-Stathopoulos I, Gavriatopoulou M, Kastritis E, Terpos E, Dimopoulos MA. Multiple myeloma: role of autologous transplantation. *Cancer Treat Rev.* 2020;82:101929.
6. Sehn LH, Salles G. Diffuse large B-cell lymphoma. *N Engl J Med.* 2021;384(9):842-858.
7. Vaxman I, Visram A, Kumar S, et al. Autologous stem cell transplantation for multiple myeloma patients aged ≥ 75 treated with novel agents. *Bone Marrow Transplant.* 2021;56(5):1144-1150.
8. Chari A, Vogl DT, Gavriatopoulou M, et al. Oral selinexor-dexamethasone for triple-class refractory multiple myeloma. *N Engl J Med.* 2019;381(8):727-738.
9. Attal M, Richardson PG, Rajkumar SV, et al. Isatuximab plus pomalidomide and low-dose dexamethasone versus pomalidomide and low-dose dexamethasone in patients with relapsed and refractory multiple myeloma (ICARIA-MM): a randomised, multicentre, open-label, phase 3 study. *Lancet.* 2019;394(10214):2096-2107.
10. Usmani SZ, Nahi H, Plesner T, et al. Daratumumab monotherapy in patients with heavily pretreated relapsed or refractory multiple myeloma: final results from the phase 2 GEN501 and

<https://doi.org/10.3324/haematol.2022.281020>

Received: March 14, 2022.

Accepted: May 18, 2022.

Prepublished: May 26, 2022.

©2022 Ferrata Storti Foundation

Published under a CC BY-NC license 

Disclosures

No conflicts of interest to disclose.

Contributions

KF and MG developed the study concept and design; KF and TJ collected data, performed statistical analysis and drafted the manuscript; MG supervised the study and critically revised the manuscript; RE and CP identified study patients; KP performed statistical data analysis; JM, AL, FK, FJ, KG, AN, MA, KF, AdC, RB, DB, MP, CP, KG, RAS, NK, ASi, IM, NS, AV, IB and MG coordinated patient care and follow-up.

Acknowledgments

We would like to acknowledge all the physician assistants and nurses on the bone marrow transplant and cellular therapy unit for their compassionate care for these patients.

Funding

This work was supported by grants from Izzy Englander, Emanuel Chirico, the Jane and Myles Dempsey Family, and Bristol Myers Squibb Foundation Diversity in Clinical Trials Career Development Program.

Data-sharing statement

The data that support the findings of this study are available upon request.

- SIRIUS trials. *Lancet Haematol.* 2020;7(6):e447-e455.
11. Sharma M, Zhang MJ, Zhong X, et al. Older patients with myeloma derive similar benefit from autologous transplantation. *Biol Blood Marrow Transplant.* 2014;20(11):1796-1803.
 12. Hari PN, Majhail NS, Zhang MJ, et al. Race and outcomes of autologous hematopoietic cell transplantation for multiple myeloma. *Biol Blood Marrow Transplant.* 2010;16(3):395-402.
 13. Ailawadhi S, Parikh K, Abouzaid S, et al. Racial disparities in treatment patterns and outcomes among patients with multiple myeloma: a SEER-Medicare analysis. *Blood Adv.* 2019;3(20):2986-2994.
 14. Verma PS, Howard RS, Weiss BM. The impact of race on outcomes of autologous transplantation in patients with multiple myeloma. *Am J Hematol.* 2008;83(5):355-358.
 15. Sun L, Li S, El-Jawahri A, et al. Autologous stem cell transplantation in elderly lymphoma patients in their 70s: outcomes and analysis. *Oncologist.* 2018;23(5):624-630.
 16. Tao L, Foran JM, Clarke CA, Gomez SL, Keegan THM. Socioeconomic disparities in mortality after diffuse large B-cell lymphoma in the modern treatment era. *Blood.* 2014;123(23):3553-3562.
 17. Shenoy PJ, Malik N, Nooka A, et al. Racial differences in the presentation and outcomes of diffuse large B-cell lymphoma in the United States. *Cancer.* 2011;117(11):2530-2540.
 18. Neighborhood Profiles: The Bronx BX: NYU Furman Center; <https://furmancenter.org/neighborhoods/view/the-bronx>
 19. Chamoun K, Firoozmand A, Caimi P, et al. Socioeconomic factors and survival of multiple myeloma patients. *Cancers (Basel).* 2021;13(4):590.
 20. Koroukian SM, Bakaki PM, Raghavan D. Survival disparities by Medicaid status: an analysis of 8 cancers. *Cancer.* 2012;118(17):4271-4279.

Cytomegalovirus proteins, maternal pregnancy cytokines, and their impact on neonatal immune cytokine profiles and acute lymphoblastic leukemogenesis in children

Early cytomegalovirus (CMV) infection and altered cytokine profiles at birth are associated with risk of childhood acute lymphoblastic leukemia (ALL).¹⁻⁵ We examined neonatal cytokine levels and CMV proteins in 130 children who contracted ALL later in life and 460 controls. We assessed the immunodominant viral coat protein (pp65) and CMV proteins that manipulate human immune function (CMV-IL-10, CMV-CXCL-1), which were detectable in most neonatal samples and correlated with specific cytokine levels (IL-10, IL12, TGF- β 1, and TNF α) CMV-IL-10 was positively associated with ALL risk. Neonatal cytokines, analyzed as a principal component loaded by IL-10, IL-12, and TNF α levels, were significantly different between cases and controls. Maternal mid-pregnancy cytokine expression was weakly correlated with cytokines at birth but did not differentiate childhood ALL cases and controls. In sum, the data provide preliminary indications that CMV viral activity during pregnancy may influence the neonatal cytokine profiles linked to risk of childhood ALL.

Maternal mid-pregnancy samples and matched neonatal blood spots from five California counties were obtained from the California Biobank.⁶ The study includes 137 cases born between November 1999 and 2009 and diagnosed with childhood ALL at the age of 0-14 years. Controls were frequency matched to cases on year of birth, sex, and race/ethnicity (non-Hispanic white, non-Hispanic black, Hispanic, Asian/Pacific Islander, or other). Two 4.7-mm blood spot punches were treated to 160 μ L of extraction buffer as described previously.¹ Extracts were randomized to 96-well plates with each plate containing similar proportions of cases and controls and racial/ethnic groups. Twelve cytokines – IL-1 β , IL-2, IL-4, IL-5, IL-6, IL-8, IL-10, IL-12p70, GM-CSF, TNF α , VEGF, and IFN- γ , were measured using a Luminex bead-based assay (R&D Systems) incorporating calibration standards, quality control samples, and blanks. Transforming growth factor (TGF- β 1) and arginase-2 were measured individually.⁷ Whole aqueous maternal sera were analyzed for cytokines by Luminex.

CMV proteins were measured using customized Luminex assays. Three capture antibodies (CMV-IL-10: AF117, R&D systems, Minneapolis, MN;⁸ pp65: OAMA00562, Aviva systems Biology Corp. San Diego, CA; UL146/vCXC1: AF620, R&D systems, Minneapolis, MN) were coupled to Luminex microspheres (Bio-rad kit). CMV protein standards (CMV-

IL-10:117-VL-025, R&D systems; pp65: CV001-1, Virusys Corp; UL146/vCXC1: 620-CM, R&D Systems) and blood spot extracts (10 μ L/sample/test) were incubated with corresponding microspheres (5 μ L/sample) at room temperature using a Curiox wash station, followed by 10 μ L of 1:1,000 diluted biotinylated anti-CMV proteins antibodies (CMV-IL-10: BAF117, R&D systems; pp65: DPATB-H83463, Creative Diagnostics, New York, NY; UL146/vCXC1: BAF620, R&D Systems) and streptavidin-conjugated R-phycoerythrin 1:100 diluted stock (Bio-Rad Laboratories, Inc.). Luminex measurements were converted to concentrations using a standard protein curve, and run in duplicate and averaged. For measurements that were below the level of detection, levels were assigned as one half the lowest level of detection.

Raw data were adjusted for batch, age of the blood spot, and the level of protein extracted. Variance Stabilizing Normalization (VSN)⁹ plus ComBat¹⁰ was used to preprocess and calibrate samples. Seven cases and 40 controls were excluded (due to quality control or technical failure), resulting in 130 cases and 460 controls for the final analysis. Pearson correlation coefficients were calculated among neonatal and maternal cytokines and CMV proteins. Multivariable logistic regression models were utilized to assess associations between neonatal and maternal cytokines, CMV proteins, arginase-2 and risk of childhood ALL.

Most birth characteristics were not significantly different between cases and controls, apart from the frequency of cesarean section which was higher among cases ($P=0.04$; *Online Supplementary Table S1*), compatible with its status as a known risk factor for ALL.¹¹ Cytokines exhibited extensive correlation in children and with CMV proteins (Figure 1). CMV-IL-10 was inversely correlated with human IL-10, as well as IL-12p70, TNF- α , VEGF, arginase-2, and weakly inversely correlated with the other CMV-derived cytokine CMV-CXC-1. CMV-pp65, the coat protein of the CMV virus itself, exhibited similar correlations as CMV-IL-10. CMV-CXC-1 demonstrated significant inverse association with TGF- β 1 which was not observed for the other CMV proteins (Figure 1).

While some correlations between neonatal cytokines approached $\rho=0.6$ (Figure 1), all correlations between maternal cytokines in mid-pregnancy and child cytokines at

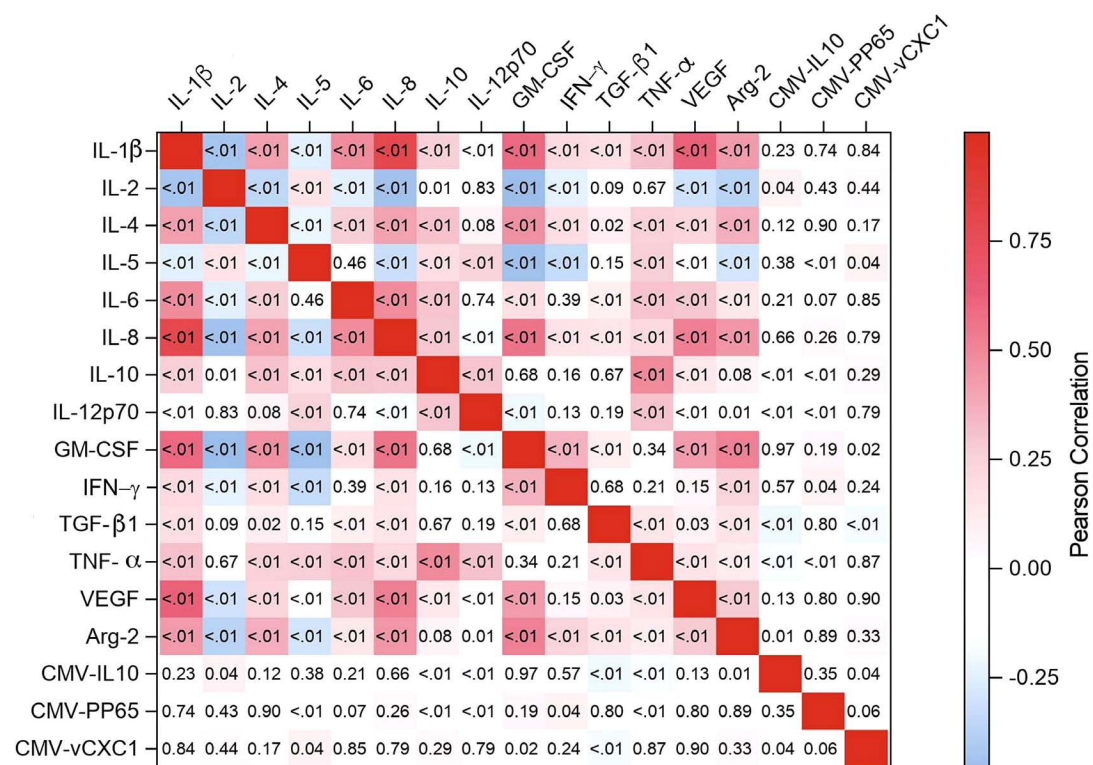


Figure 1. Pearson correlation matrix of cytokines and cytomegalovirus proteins at birth of all neonatal study subjects (n=590: 130 cases and 460 controls). The color of each square is indicative of the coefficient (noted on the scale) and the *P*-value is noted numerically. Correlations were similar among cases and control strata, and the entire sample set is displayed. The color scale is balanced towards positive correlations (red) since strong anti-correlations were less apparent.

birth were lower than absolute value of $\rho=0.21$ (Figure 2). Many maternal-child correlations were significant with some notable differences between cases and controls (Figure 2). For instance, case-only significant positive correlations were apparent between maternal IL-6 and neonatal CMV-pp65, maternal IL-1 β and neonatal CMV-CXC-1, and maternal IFN- γ and neonatal TNF- α ; and inverse correlations between maternal TNF- α and neonatal TNF- α and CMV-CXC1 (Figure 2).

Like prior reports, neonatal cytokine levels were associated with case/control status. When assessed individually, IL-1 β , IL-2, IL-8, and GM-CSF exhibited nominally significant associations, where only GM-CSF remained significant (odds ratio [OR] =2.38, 95% confidence interval [CI]: 1.11-5.13, comparing the third tertile to the first) in the multivariable model. When analyzed as a continuous variable, CMV-IL-10 was significantly associated with case/control status, with higher CMV-IL-10 levels linked to an increased risk of childhood ALL (OR=1.27, 95% CI: 1.01-1.59; *Online Supplementary Table S2*). Because of the high level of correlations between protein markers, we constructed summary independent variables using principal components (PC). About 60% of the variance was explained by five PC (*Online Supplementary Table S3*). The first PC, composed of IL-10, IL-12, and TNF- α , was significantly positively associated with ALL risk (Table 1; *Online Supplementary Table S3*). Principal components that were described by CMV proteins CMV-CXC-1 and pp65 (PC7 and 8) were not associated with ALL risk; however, PC9 which was predominantly loaded with CMV-IL-10 was associated with increased ALL risk (OR=1.24, 95% CI :1.01-1.54; *P*=0.04

as continuous measure, Table 1). Maternal cytokines were not related to case/control status (data not shown). We evaluated whether neonatal cytokines and CMV proteins were associated with birth characteristics, while controlling for year of birth, sex, race/ethnicity, and case-control status. Nominally significant (*P*<0.01) associations (in a positive [+], or inverse [-] direction) were apparent between IL-6 and birthweight (+), IL-1 β , IL-4, and IL-8 and birth order (all -), IL-5 (+) and IFN- γ (-) with male sex, and arginase-2 (+) with cesarean section (data not shown). In this study, cytokines and other immune markers measured at birth are associated with leukemia status later in childhood, a result supported by four previous reports.^{1,3,4,7} In addition, a cytokine produced by CMV, CMV-IL-10, is associated in a positive way with ALL status. This CMV-encoded protein is 27% homologous to human IL-10 and binds with high affinity to the IL-10 receptor.¹² CMV-IL-10 was inversely correlated with human IL-10, suggesting possible feedback control, which is intriguing considering the inverse association between human IL-10 and ALL risk using a more sensitive assay performed in a prior study on a similar California-based population.¹ We found CMV proteins in most (~90%) neonatal samples, including samples from controls. CMV infection is clinically apparent in 1 in 300 in newborns; 90% of CMV-positive neonates are clinically silent.¹³ Our prior study found CMV DNA sequence in 3% of healthy California-born children and 9% in those who later contracted ALL.² Population prevalence of CMV in women of reproductive years is 40-60% in Western countries, and 80-100% in low resource rural areas and developing countries;¹⁴ therefore,

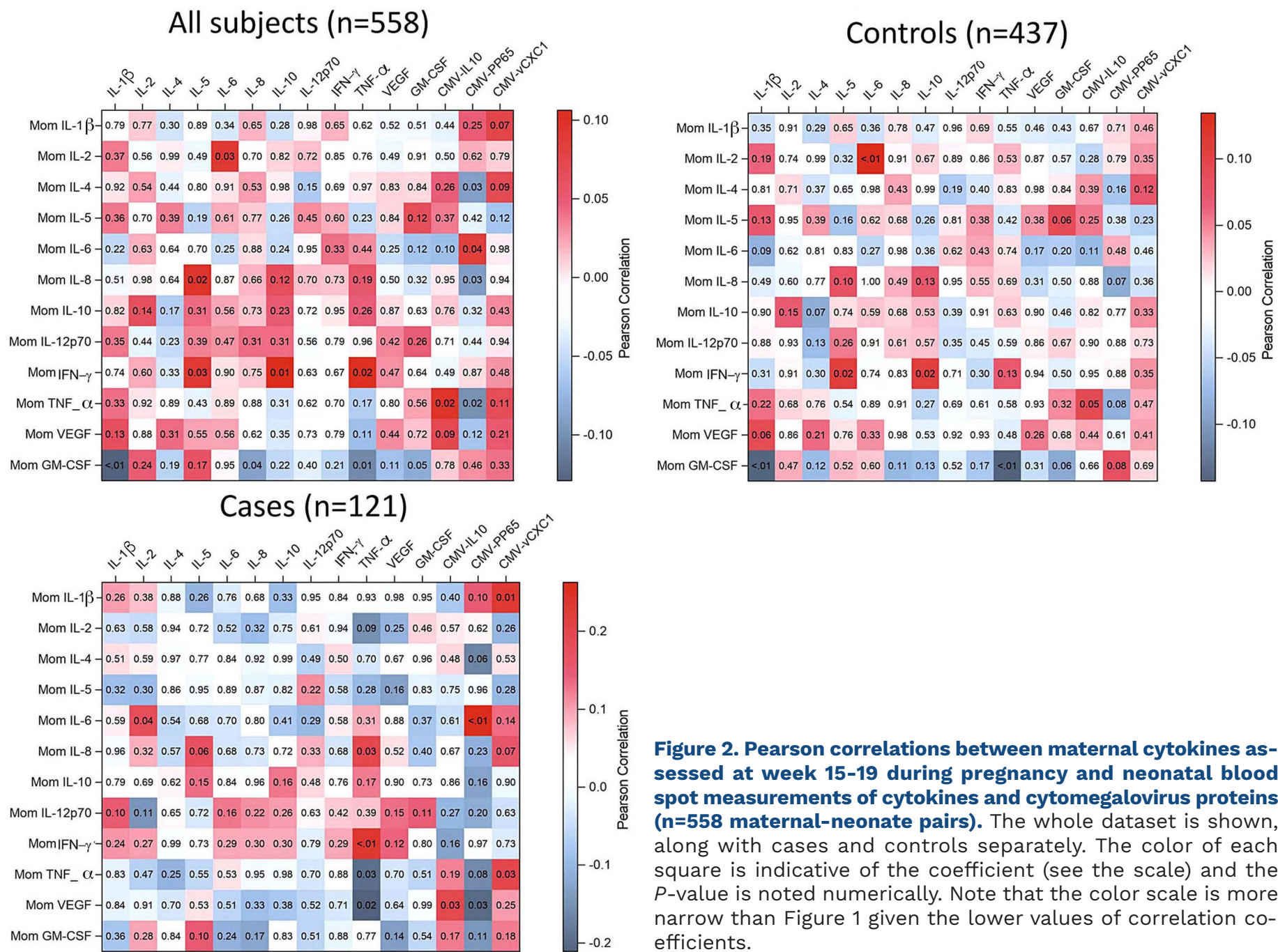


Figure 2. Pearson correlations between maternal cytokines assessed at week 15-19 during pregnancy and neonatal blood spot measurements of cytokines and cytomegalovirus proteins (n=558 maternal-neonate pairs). The whole dataset is shown, along with cases and controls separately. The color of each square is indicative of the coefficient (see the scale) and the P-value is noted numerically. Note that the color scale is more narrow than Figure 1 given the lower values of correlation coefficients.

Table 1. Relationship of cytokine/cytomegalovirus protein derived principal components to risk of childhood acute lymphoblastic leukemia.

PC	Continuous ^a		PC loadings ^b
	OR (95% CI)	P	
PC1	1.25 (1.02-1.54)	0.04	IL-10, IL-12p70, TNF-α
PC2	0.96 (0.77-1.18)	0.68	IL-1b, VEGF
PC3	1.01 (0.82-1.24)	0.96	IL-4, ARG2
PC4	0.94 (0.76-1.16)	0.58	IL-6
PC5	1.04 (0.85-1.28)	0.69	TGF-β
PC6	0.99 (0.81-1.20)	0.89	IFN-γ
PC7	0.99 (0.80-1.23)	0.95	CMV-CXC1
PC8	1.00 (0.82-1.22)	0.97	CMV-p65
PC9	1.24 (1.01-1.53)	0.04	CMV-IL-10
PC10	1.14 (0.92-1.40)	0.23	IL-2

^aOverall risk (OR) for each unit of principal components (PC) increase. All models adjusted for age at collection, year of birth, weight (≥3,500 grams), gestational age (26-26, 27-41, 42-44 weeks, unknown) plurality (single vs. multiple), birth order, mode of delivery (vaginal vs. cesarean), mother's age at delivery (≤24, 25-34, ≥35 years), and mother's birthplace (United States vs. other), and all other PC. ^bImmune factors which contributed most variance to each PC. Factors are listed when they are correlated more than rho=0.6 with each PC noted (see Online Supplementary Table S4).

our detection rate of CMV proteins in the current study mirrors this maternal prevalence rather than the newborn. Proteins cross the placental barrier by active transport as well as passive diffusion, the latter at a rate equivalent to the concentration of the protein.¹⁵

Accepting the source of CMV proteins from the pregnant mother, the correlative structure of proteins assessed here implicate that CMV infection of the mother impacts immune development of the fetus and may be the source of cytokine alterations at birth that distinguish ALL cases from controls in this and prior studies.^{1,3,4,7} Significant correlations between maternal cytokines and neonatal CMV proteins (and neonatal cytokines) suggest direct or indirect manipulation of immune function, even in the absence of primary CMV infection of the neonate. Most notable here is the higher level of CMV-IL-10 found in neonates who grew up to be cases compared to controls who remained healthy. This cytokine interacts directly with the human IL-10 receptor, but is only one of several CMV genes that manipulate the immune system. The presence of CMV-IL-10 protein as a risk factor for ALL requires more analysis to examine whether it is simply a marker of primary CMV infection or is itself the factor that alters neonatal immunity impacting risk of ALL, and therefore pinpoints maternal CMV activity as consequential to ALL risk in the offspring.

To conclude, our results suggest that CMV infection is responsible at least in part for the neonatal cytokine profiles that are associated with risk of childhood ALL. Our results should be considered preliminary as the findings will not meet the more stringent threshold for statistical significance with correction for multiple comparisons, hence the potential for false discovery. CMV is, however, the first specific target for ALL prevention and potentially treatment, and its role in the pathogenesis of childhood ALL and prevention deserves further examination.

Authors

Joseph L. Wiemels,¹ Rong Wang,² Mi Zhou,³ Helen Hansen,³ Rachel Gallant,^{1,4} Junghyun Jung,¹ Nicholas Mancuso,¹ Adam J. de Smith,¹ Catherine Metayer,⁵ Scott C. Kogan³ and Xiaomei Ma²

¹Center for Genetic Epidemiology, Norris Comprehensive Cancer Center, and Department of Population and Public Health Sciences, University of Southern California, Los Angeles, CA; ²Department of Chronic Disease Epidemiology, Yale School of Public Health, Yale University, New Haven, CT; ³School of Medicine; University of California San Francisco, San Francisco, CA; ⁴Children's Hospital Los

Angeles, Los Angeles, CA and ⁵School of Public Health, University of California, Berkeley, Berkeley, CA, USA

Correspondence:

J.L. WIEMELS - wiemels@usc.edu

<https://doi.org/10.3324/haematol.2022.280826>

Received: February 8, 2022.

Accepted: May 27, 2022.

Prepublished: May 31, 2022.

©2022 Ferrata Storti Foundation

Published under a CC BY-NC license 

Disclosures

No conflicts of interest to disclose.

Contributions

JLW and XM designed the research with assistance from CM, obtained the funding, and wrote the manuscript; RW performed the statistical analysis; MZ designed laboratory assays and with HH performed the laboratory measurements; RG, JJ, NM, AJdS, and SCG assisted with analysis and interpretation. All authors reviewed and approved the manuscript.

Acknowledgments

The biospecimens used in this study were obtained from the California Biobank Program, (Screening Information System request number 600), in accordance with Section 6555(b), 17 CCR. The California Department of Public Health (CDPH) is not responsible for the results or conclusions drawn by the authors of this publication. This manuscript is solely the responsibility of the authors and the content does not necessarily represent the official views of the National Institutes of Health. Special thanks to Robin Cooley and Martin Kharrazi (CDPH).

Funding

Research reported in this publication was supported by the National Institutes Health under award numbers R01CA175737 (JLW and XM) and R01CA185058 (JLW and SCK).

Data-sharing statement

We are prohibited by California statutes from publicly sharing data that are derived from biospecimens obtained from the California Biobank. We welcome questions from other investigators or request for additional analyses that are pertinent to the data presented in this Letter, and potential data sharing when permitted by the California Health and Human Services Agency Committee for the Protection of Human Subjects.

References

1. Chang JS, Zhou M, Buffler PA, Chokkalingam AP, Metayer C, Wiemels JL. Profound deficit of IL10 at birth in children who develop childhood acute lymphoblastic leukemia. *Cancer Epidemiol Biomarkers Prev.* 2011;20(8):1736-1740.
2. Francis SS, Wallace AD, Wendt GA, et al. In utero cytomegalovirus infection and development of childhood acute lymphoblastic leukemia. *Blood.* 2017;129(12):1680-1684.
3. Sooregard SH, Rostgaard K, Skogstrand K, Wiemels J, Schmiegelow K, Hjalgrim H. Neonatal inflammatory markers in children later diagnosed with B-cell precursor acute lymphoblastic leukaemia. *Cancer Res.* 2018;78(18):5458-5463.
4. Whitehead TP, Wiemels JL, Zhou M, et al. Cytokine levels at birth in children who developed acute lymphoblastic leukemia. *Cancer Epidemiol Biomarkers Prev.* 2021;30(8):1526-1535.
5. Wiemels JL, Talback M, Francis S, Feychting M. Early infection with cytomegalovirus and risk of childhood hematologic malignancies. *Cancer Epidemiol Biomarkers Prev.* 2019;(6):1024-1027.
6. Kharrazi M, Pearl M, Yang J, et al. California Very Preterm Birth Study: design and characteristics of the population- and biospecimen bank-based nested case-control study. *Paediatr Perinat Epidemiol.* 2012;(3):250-263.
7. Nielsen AB, Zhou M, de Smith AJ, et al. Increased neonatal level of arginase 2 in cases of childhood acute lymphoblastic leukemia implicates immunosuppression in the etiology. *Haematologica.* 2019;104(11):e514-e516.
8. Young VP, Mariano MC, Faure L, Spencer JV. Detection of cytomegalovirus interleukin 10 (cmvIL-10) by enzyme-linked immunosorbent assay (ELISA). *Methods Mol Biol.* 2021;2244:291-299.
9. Huber W, von Heydebreck A, Sultmann H, Poustka A, Vingron M. Variance stabilization applied to microarray data calibration and to the quantification of differential expression. *Bioinformatics.* 2002;18(Suppl 1):S96-104.
10. Johnson WE, Li C, Rabinovic A. Adjusting batch effects in microarray expression data using empirical Bayes methods. *Biostatistics.* 2007; 8(1):118-127.
11. Marcotte EL, Thomopoulos TP, Infante-Rivard C, et al. Caesarean delivery and risk of childhood leukaemia: a pooled analysis from the Childhood Leukemia International Consortium (CLIC). *Lancet Haematol.* 2016;3(4):e176-185.
12. Kotenko SV, Sacconi S, Izotova LS, Mirochnitchenko OV, Pestka S. Human cytomegalovirus harbors its own unique IL-10 homolog (cmvIL-10). *Proc Natl Acad Sci U S A.* 2000;97(4):1695-1700.
13. Manicklal S, Emery VC, Lazzarotto T, Boppana SB, Gupta RK. The "silent" global burden of congenital cytomegalovirus. *Clin Microbiol Rev.* 2013;26(1):86-102.
14. Buxmann H, Hamprecht K, Meyer-Wittkopf M, Friese K. Primary human cytomegalovirus (HCMV) infection in pregnancy. *Dtsch Arztebl Int.* 2017;114(4):45-52.
15. Malek A, Sager R, Schneider H. Transport of proteins across the human placenta. *Am J Reprod Immunol.* 1998;40(5):347-351.

Inducing synthetic lethality for selective targeting of acute myeloid leukemia cells harboring *STAG2* mutations

Acute myeloid leukemia (AML) is a heterogeneous disorder and mostly incurable due to relapse and drug resistance. A key challenge is to target the fraction of more quiescent leukemic cells that are resistant to chemotherapeutic drugs.¹ During recent years, several new small molecule inhibitors have been developed to uniquely target disease-specific molecular events, such as the *FLT3*-ITD mutation. However, such targeted therapies have only met moderate clinical success due to drug resistance and relapse, which is associated with selection and expansion of malignant subclones that are not dependent on the initially targeted mutation.² Thus, additional novel targeted therapeutic strategies are required for leukemia clearance. A particularly attractive approach is to harness specific genetic deficiencies of the tumor cells by targeting synthetic lethal interactions. In this case, a therapeutic effect can be reached even in tumors that are not critically dependent on the mutations that are targeted.

The cohesin protein complex forms a ring-like structure that holds sister chromatids together which is necessary for the proper segregation of chromosomes during mitosis. In addition, cohesin plays an essential role in DNA repair, genome organization and transcriptional regulation.³ The core structure comprises the three proteins RAD21, SMC3 and SMC1A. The fourth subunit consists of either one of two paralogous proteins: STAG1 or STAG2. Whole genome sequencing studies have identified a significant number of somatic mutations in cohesin genes with an accumulated mutation rate between 10% and 15% for AML and myelodysplastic syndrome (MDS).⁴ An even higher rate of cohesin mutations (around 50%) was observed in Down Syndrome associated childhood acute megakaryocytic leukemia (DS-AMKL).⁵ Cohesin mutations have loss-of-function consequences arguing for a tumor suppressor role of cohesin in the context of leukemia.⁴ Since cohesin is necessary for proper chromosomal segregation, mutations were first thought to promote tumor progression via genome instability.⁶ However, the majority of the cohesin-mutated cancers are euploid suggesting that it is rather non-mitotic functions of cohesin such as transcriptional regulation and chromatin organization which are associated with leukemogenesis.⁷ With a mutation frequency of approximately 6% in AML and 18% in DS-AMKL, *STAG2* is the predominantly mutated gene among the cohesin genes.⁴ *STAG2* mutations result in complete loss-of-function in males since these genes are located on the X chromosome.⁸ *STAG2* knockdown promoted the *in vitro* expansion of umbilical cord blood (UCB)-derived hematopoietic stem and progen-

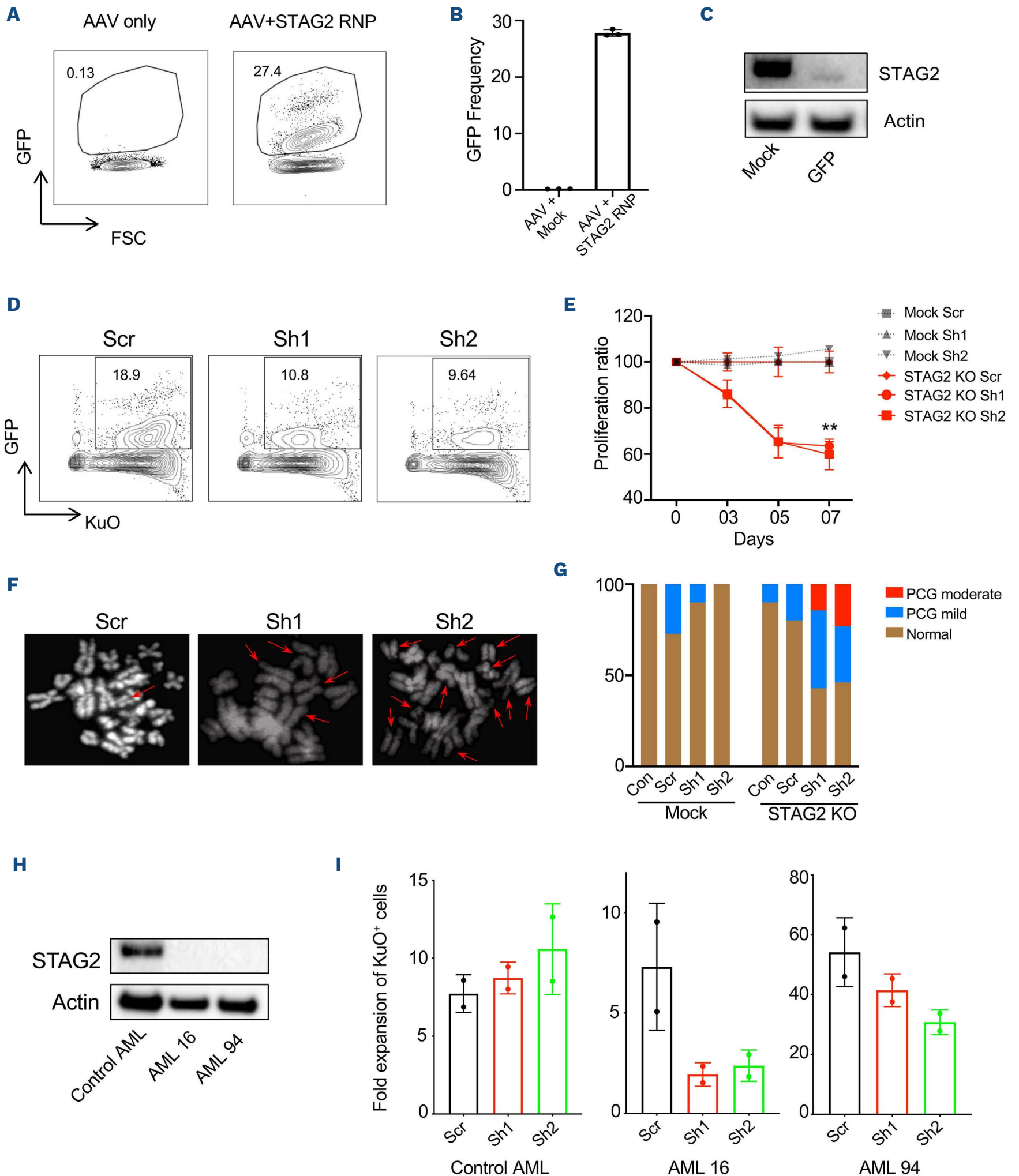
itor cells (HSPC) and enhanced the repopulating activity of human HSPC in xenograft recipients, demonstrating a direct functional association between *STAG2* loss and dysregulated hematopoiesis.⁹ Although *STAG1*- and *STAG2*-containing cohesin complexes might have distinct functions,¹⁰ they are redundant to ensure the chromatid cohesion during mitosis. Hence, *STAG1*-mediated mitotic dependency was observed in *STAG2* knockout (KO) cell lines.^{11,12} Moreover, a recent study in knockout mice showed that the combined loss of *STAG1* and *STAG2*, but not that of each gene alone, resulted in bone marrow aplasia and mortality, further supporting the existence of synthetic lethal interactions between *STAG1* and *STAG2*.¹³ A majority of the cohesin mutations have a high variant allele frequency indicating that they occur relatively early in leukemogenesis.^{4,14} Inducing synthetic lethality in AML harboring *STAG2* mutations should thus eliminate most clones irrespective of any secondary mutations. Though, theoretically possible as a novel therapeutic application to *STAG2* null AML, synthetic lethality from targeting *STAG1* is yet to be demonstrated in primary human leukemic cells. Here, we provide a functional proof-of-concept demonstration for this approach.

First, in order to demonstrate the existence of *STAG1*-mediated mitotic dependency in primary human HSPC, we generated *STAG2* null HSPC derived from UCB utilizing a CRISPR/Cas9 based knockin system. In brief, an early stop codon, followed by an open reading frame encoding enhanced green fluorescent protein (eGFP) was inserted into the targeted *STAG2* locus utilizing homology-directed repair (HDR) (*Online Supplementary Figure S1A*). With this system, successfully edited, eGFP expressing *STAG2* null cells can be distinguished from unedited cells. As *STAG2* is located in the X chromosome, we edited CD34⁺ cells from male donors to achieve successful *STAG2* KO by monoallelic editing. Flow cytometry analysis revealed an eGFP frequency of 27% compared to mock control indicating efficient *STAG2* editing and eGFP integration in HSPCs (Figure 1A and B). Further, Western blotting analysis of the eGFP expressing cells revealed a near complete loss of *STAG2* protein, demonstrating that integration of the eGFP template successfully knocked out *STAG2* expression (Figure 1C). Sanger sequencing of the *STAG2* locus in eGFP-positive cells revealed a successful integration of the donor template at the expected locus (*Online Supplementary Figure S1B*). Altogether we successfully generated *STAG2* KO human HSPC utilizing CRISPR-mediated HDR.

Next, in order to assess *STAG1*-mediated mitotic depend-

ency, we transduced *STAG2* KO human HSPC with two independent short hairpin RNA (shRNA) targeting *STAG1* as well scrambled (Scr) control shRNA. The pLKO shRNA vectors were engineered to express Kusabira orange (KuO) en-

abling tracking of the transduced cells in conjunction with the eGFP marker for *STAG2* null cells. Both *STAG1* shRNA showed successful knockdown of *STAG1* at the mRNA and protein level 72 hours post-transduction (*Online Supple-*



Continued on following page,

Figure 1. STAG1 knockdown perturbs STAG2 null hematopoietic stem and progenitor cells. Umbilical cord blood (UCB) CD34⁺ cells were cultured in serum-free expansion medium (SFEM) added with stem cell factor (SCF), thrombopoietin (TPO) and FMS-like tyrosine kinase 3 ligand (FLT3L) at final concentration of 100 ng/mL each. (A) Flow cytometry analysis of enhanced green fluorescent protein (eGFP) expression in UCB CD34⁺ cells edited with either mock or with single guide RNA (sgRNA) (UCUGGUCCAAACCGAAUGAA) - Cas9 ribonucleoproteins targeting STAG2 along with adeno-associated virus donor template. (B) Quantification of CRISPR/Cas9-mediated eGFP knockin efficiency measurement across 3 replicates. (C) Western blot analysis of STAG2 protein in the mock and eGFP sorted UCB CD34⁺ cells. (D) Day 5 co-transduction analysis of Kusabira orange positive STAG1 small interfering RNA (shRNA) and eGFP-positive STAG2 null cells by flow cytometry. (E) Quantification of STAG1 shRNA-mediated cell proliferation in mock and STAG2 null CD34⁺ cells compared to the scrambled control. Two-way ANOVA, $**P < 0.01$. (F) Fluorescence *in situ* hybridization to analyze the sister chromatid cohesin in STAG2 null cells 3 days after shRNA transduction. (G) Cohesion defects were quantified in around 8-15 cells for each condition. Primary constriction gaps (PCG) measured are the visible gaps between the sister chromatids at the centromeres; PCG mild - defects in 1-4 chromosomes, PCG moderate - defects in 4-19 chromosomes. (H) STAG2 protein expression in a control and 2 STAG2-mutated primary acute myeloid leukemia (AML) samples (AML 16 and 94). (I) The primary AML cells were co-cultured with OP9M2 Stroma and transduced with STAG1 shRNA. Fold expansion of scrambled and STAG1 shRNA transduced cells at day 5 as compared to day 2 is shown. Scr: scrambled shRNA CAACAAGATGAAGAGCACCAA; Sh1: STAG1 shRNA1 CTTCAGCCTTTGGTGTTCAT; Sh2: STAG1 shRNA2 GCCAATGAAAGTTGGAGTTA.

mentary Figure 1C and D). We monitored cell number and frequency of the KuO and GFP-positive population during 1 week of culture and observed that both STAG1 shRNA, but not the control shRNA, induced a significant depletion of STAG2 null HSPC. Moreover, isogenic control cells with intact STAG2 were unaffected by the STAG1 shRNA, demonstrating that the observed cell depletion was highly specific to the combined loss of STAG1 and STAG2 (Figure 1D and E). We reasoned that depletion of both STAG1 and STAG2 in the HSPC model may disrupt cohesin's essential functions of sister chromatid cohesion during cell division and thereby limit cell survival.^{11,12} Indeed, we observed that STAG1 knockdown induced marked sister chromatid cohesion defects in more than 50% of the STAG2 null cells (Figure 1F and G). Later we have also analyzed the effects of STAG1 knockdown in two primary AML samples that lacked STAG2 protein expression due to truncating mutations (Figure 1H; *Online Supplementary Table S1*). STAG1 knockdown induced a 2-5-fold reduction in expansion of STAG2 null AML cells compared to the scrambled control while the STAG2 wild-type (WT) control AML cells were unperturbed (Figure 1I). Overall, these findings demonstrate the existence of a synthetic lethal interaction between STAG1 and STAG2 in primary human HSPC and AML cells.

We then sought to assess whether we could induce synthetic lethality *in vivo* by targeting STAG1 in STAG2-mutated primary AML cells. We chose a primary human AML sample (AML 21) that was readily transplantable in immunodeficient mice and that had been propagated as a patient-derived xenograft (PDX) sample to allow assessment *in vivo*. This sample carried a STAG2 loss-of-function mutation with a variant allele frequency of 89% accompanied with other candidate driver mutations such as IDH2, SRSF2 and NRAS. (*Online Supplementary Table S1*). We analyzed STAG2 protein levels in the PDX sample by western blotting and found a complete lack of STAG2 expression, in line with the sequencing data (Figure 2A). We successfully transduced bulk mononuclear PDX cells with either scrambled or the two independent STAG1 shRNA at frequencies of 30-60% and

transplanted into sub-lethally irradiated NOD-scid IL2Rgnull-3/GM/SF (NSG-S) mice (Figure 2B; *Online Supplementary Figure S2A*). As a reference control, and to assess the effect of STAG1 perturbation on normal HSPC, we also transduced UCB CD34⁺ cells with the same vectors and assayed the cells both *in vitro* and *in vivo* by transplantation to sub-lethally irradiated NOD.Cg-Prkdc^{scid}IL2rg^{tm1Wjl}/SzJ (NSG) mice. Importantly, STAG1 knockdown did not appear to negatively impact the engraftment of UCB CD34⁺ cells (Figure 2C and D). Rather, we observed a moderate increase in the fold expansion of CD34⁺ cells *in vitro*, and a robust contribution of transduced cells *in vivo* that was steadily increasing over time, similar to cells transduced with the scramble control (*Online Supplementary Figure S2B* and C). Altogether this indicates that partial perturbation of STAG1 is well tolerated by human HSPC without a major influence on their repopulation and differentiation properties (*Online Supplementary Figure 2D* to H). By contrast, when we analyzed the bone marrow of NSG-S mice transplanted with transduced PDX-derived AML cells, we found a near complete depletion of cells transduced with either of the two STAG1 shRNA, whereas the mice transplanted with scrambled shRNA transduced cells retained a stable transduced KuO⁺ population (Figure 2E and F). We have also analyzed the PDX material for STAG2 expression to exclude the possibilities of a potential drift of STAG2 null clones and found that the AML cells from scrambled and shRNA transduced conditions maintained STAG2 null clones (*Online Supplementary Figure 2I*). Overall, this suggests that STAG1 knockdown induces a selective impairment of STAG2 null AML cells that is sufficient to eliminate them upon transplantation.

Taken together, we demonstrate that partial perturbation of STAG1 selectively eliminates primary human HSPC and AML cells lacking STAG2, while it is well tolerated by normal HSPC. Developing small molecules such as proteolytic chimeras that selectively degrade STAG1 by recruiting the ubiquitin-proteasomal system would be an ideal way to translate these findings into clinical applications. Moreover,

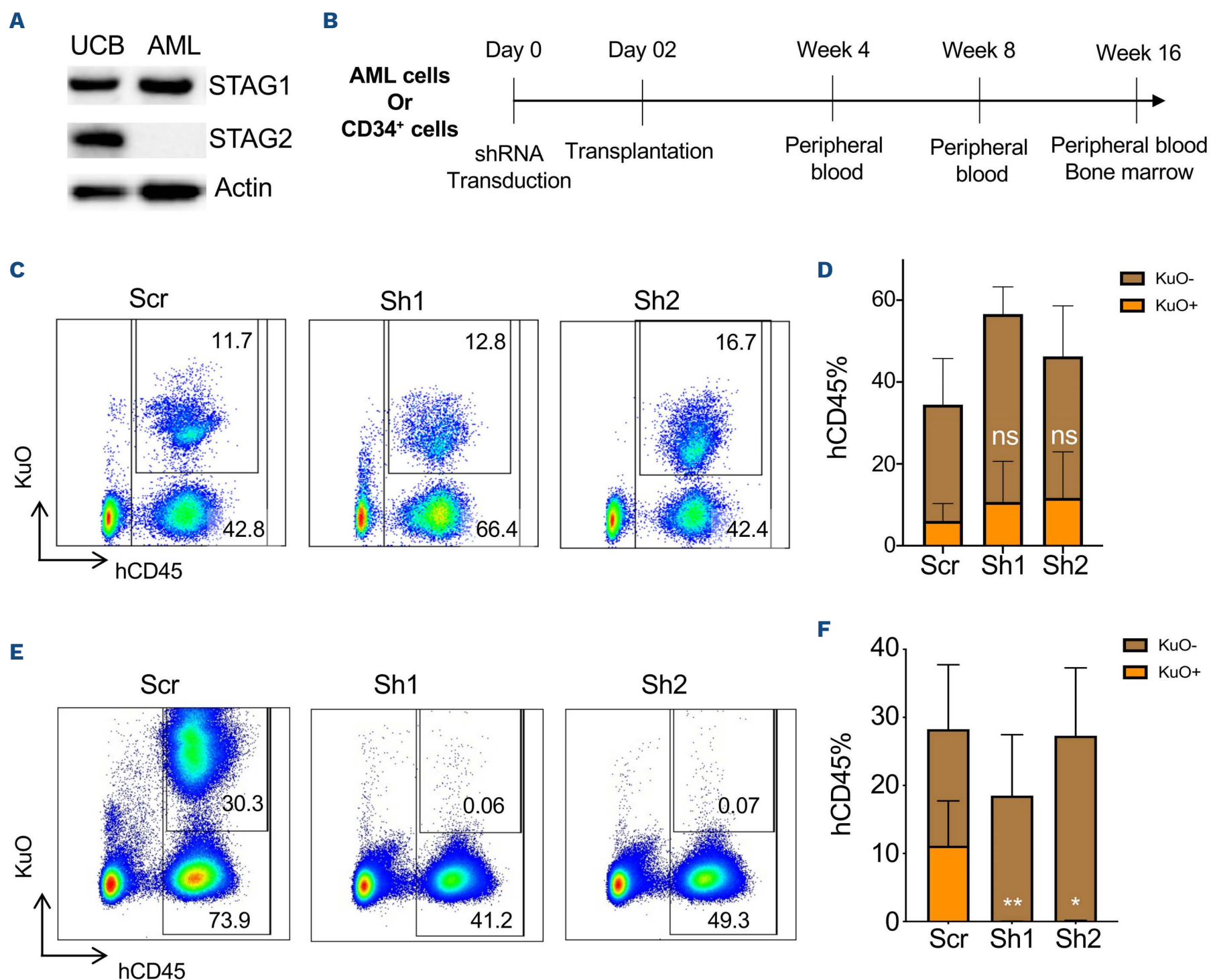


Figure 2. STAG1 knockdown selectively perturbs acute myeloid leukemia cells. (A) STAG1 and STAG2 expression in umbilical cord blood (UCB) and STAG2 null acute myeloid leukemia (AML) 21 cells. (B) UCB and AML cells were transduced with scrambled (Scr) and STAG1 small interfering RNA (shRNA) and transplanted into sub-lethally irradiated NSG and NSG-S mice respectively. Prior to transplantation AML xenograft cells were transduced *in vitro* with lentiviral particles and transferred to a new plate coated with irradiated OP9M2 stroma cells. (C) Fluorescence-activated cell sorting (FACS) plots showing the chimerism of UCB grafts (humanCD45) and frequencies of Kusabira orange-positive shRNA transduced cells at NSG bone marrow 16 weeks post transplantation. (D) Frequency of hCD45 chimerism and the proportion of transduced cells were quantified for each shRNA (n=5). Kruskal-Wallis test with comparison to the scrambled control. ns: not significant. (E) Chimerism of AML grafts (human CD45) and frequencies of Kusabira orange positive shRNA expressing cells in NSG-S bone marrow, analyzed 16 weeks post transplantation. (F) Frequency of AML engraftment and the proportion of transduced cells were quantified for each shRNA (n=4). Kruskal-Wallis test with comparison to the scrambled control. * $P < 0.05$; ** $P < 0.01$. Scr: scrambled shRNA; Sh1: STAG1 shRNA1; Sh2: STAG1 shRNA2.

a recent study by van der Lelij *et al.* identified critical elements of STAG1 that are essential for interaction with the RAD21 protein, thereby opening up another possibility to develop selective STAG1-RAD21 interaction inhibitors.¹⁵ Our study provides a rationale for exploiting synthetic lethality to develop more specific and targeted therapies for tumors with STAG2 mutations, demonstrating a first proof-of-concept within the hematopoietic system.

Authors

Agatheeswaran Subramaniam,¹ Carl Sandén,² Larissa Moura-Castro,² Kristijonas Žemaitis,¹ Ludwig Schmiderer,¹ Aurelie Baudet,¹ Alexandra Bäckström,¹ Elin Arvidsson,¹ Simon Hultmark,¹ Natsumi Miharada,¹ Mattias Magnusson,¹ Kajsa Paulsson,² Thoas Fioretos² and Jonas Larsson¹

¹Molecular Medicine and Gene Therapy, Lund Stem Cell Center and

²Division of Clinical Genetics, Department of Laboratory Medicine, Lund University, Lund, Sweden.

Correspondence:

A. SUBRAMANIAM - agatheeswaran.subramaniam@med.lu.se

J. LARSSON - jonas.larsson@med.lu.se.

doi:10.3324/haematol.2021.280303

Received: November 18, 2021.

Accepted: May 27, 2022.

Prepublished: May 31, 2022.

©2022 Ferrata Storti Foundation

Published under a CC-BY-NC license



Disclosures

No conflicts of interest to disclose.

Contributions

AS, CS, KZ, LS, AuB, AB, EA, SH, and NM performed the experiments and acquired data. LMC and KP helped with the cohesion assay. CS,

TF and MM performed molecular analysis of the AML samples and provided the materials. AS and JL conceived and designed the study, interpreted the results and wrote the manuscript.

Acknowledgements

We would like to thank the staff at animal house and FACS core facilities for their excellent support. We also would like to thank Jenny G. Johansson for helping with the AAV vector production.

Funding

This work was funded to JL by grants from the Swedish Research Council, the Swedish Cancer Foundation, the Swedish Pediatric Cancer Foundation, Knut och Alice Wallenbergs Stiftelse and the European Research Council (ERC) under the European Union's Horizon 2020 research and innovation program (grant agreement No. 648894). AS was supported from the Swedish Cancer Foundation, Royal Physiographic Society of Lund and Lady TATA memorial trust. The work was further supported by the HematoLinné and StemTherapy programs at Lund University.

Data-sharing statement

The datasets generated or analyzed in this study are available upon reasonable request to the corresponding authors (AS and JL).

References

1. Pollyea DA, Gutman JA, Gore L, Smith CA, Jordan CT. Targeting acute myeloid leukemia stem cells: a review and principles for the development of clinical trials. *Haematologica*. 2014;99(8):1277-1284.
2. Kasi PM, Litzow MR, Patnaik MM, Hashmi SK, Gangat N. Clonal evolution of AML on novel FMS-like tyrosine kinase-3 (FLT3) inhibitor therapy with evolving actionable targets. *Leuk Res Rep*. 2016;5:7-10.
3. Losada A. Cohesin in cancer: chromosome segregation and beyond. *Nat Rev Cancer*. 2014;14(6):389-393.
4. Kon A, Shih LY, Minamino M, et al. Recurrent mutations in multiple components of the cohesin complex in myeloid neoplasms. *Nat Genet*. 2013;45(10):1232-1237.
5. Yoshida K, Toki T, Okuno Y, et al. The landscape of somatic mutations in Down syndrome-related myeloid disorders. *Nat Genet*. 2013;45(11):1293-1299.
6. Solomon DA, Kim T, Diaz-Martinez LA, et al. Mutational inactivation of STAG2 causes aneuploidy in human cancer. *Science*. 2011;333(6045):1039-1043.
7. Mazumbar C, Shen Y, Xavy S, et al. Leukemia-associated cohesin mutants dominantly enforce stem cell programs and impair human hematopoietic progenitor differentiation. *Cell Stem Cell*. 2015;17(6):675-688.
8. Thota S, Viny AD, Makishima H, et al. Genetic alterations of the cohesin complex genes in myeloid malignancies. *Blood*. 2014;124(11):1790-1798.
9. Galeev R, Baudet A, Kumar P, et al. Genome-wide RNAi screen identifies cohesin genes as modifiers of renewal and differentiation in human HSCs. *Cell Rep*. 2016;14(12):2988-3000.
10. Kong X, Ball AR, Jr., Pham HX, et al. Distinct functions of human cohesin-SA1 and cohesin-SA2 in double-strand break repair. *Mol Cell Biol*. 2014;34(4):685-698.
11. Benedetti L, Cereda M, Monteverde L, Desai N, Ciccarelli FD. Synthetic lethal interaction between the tumour suppressor STAG2 and its paralog STAG1. *Oncotarget*. 2017;8(23):37619-37632.
12. van der Lelij P, Lieb S, Jude J, et al. Synthetic lethality between the cohesin subunits STAG1 and STAG2 in diverse cancer contexts. *Elife*. 2017;6:e26980.
13. Viny AD, Bowman RL, Liu Y, et al. Cohesin members Stag1 and Stag2 display distinct roles in chromatin accessibility and topological control of HSC self-renewal and differentiation. *Cell Stem Cell*. 2019;25(5):682-696.
14. Corces-Zimmerman MR, Hong WJ, Weissman IL, Medeiros BC, Majeti R. Preleukemic mutations in human acute myeloid leukemia affect epigenetic regulators and persist in remission. *Proc Natl Acad Sci U S A*. 2014;111(7):2548-2553.
15. van der Lelij P, Newman JA, Lieb S, et al. STAG1 vulnerabilities for exploiting cohesin synthetic lethality in STAG2-deficient cancers. *Life Sci Alliance*. 2020;3(7):e202000725.

Prolonged remission with pembrolizumab and radiation therapy in a patient with multisystem Langerhans cell sarcoma

Langerhans cell sarcoma (LCS) is an exceedingly rare hematologic cancer with approximately ten to 12 new cases reported in the United States each year.¹ LCS is a malignant histiocytic neoplasm that frequently involves the reticuloendothelial system (lymph nodes, liver, spleen) and may spread to the skin, lung, bone, or other soft tissues.² Patients with localized or single-system disease are generally treated with surgical resection or radiation therapy and tend to do better than those with multi-system involvement. In patients with multi-system disease, outcomes have been dismal with a 5-year overall survival of only 15%.³ The rarity of this diagnosis has limited our understanding of the disease biology and development of effective treatment. A variety of systemic treatment strategies have been used in LCS, most of them adopted from treatment of aggressive lymphomas, such as anthracycline- and platinum-based regimens.^{3,4} However, the treatment outcomes published in case reports and case series have been disappointing. The identification of mutations in the mitogen-activated protein kinase (MAPK) pathway in other histiocytic neoplasms, especially Langerhans cell histiocytosis (LCH) and Erdheim-Chester disease (ECD) have led to the utilization of targeted therapies. Data on the efficacy of kinase inhibitors and immunotherapy in LCS and other malignant histiocytosis are limited. In this report, we present a case of LCS with exquisite response to the immune checkpoint inhibitor (ICI) pembrolizumab and radiation therapy after disease progression on the MEK inhibitor cobimetinib.

A 33-year-old Caucasian female with no comorbidities presented with a sensation of fullness in her abdomen without any associated pain, nausea, vomiting, or other systemic symptoms. CT scan of the abdomen revealed a lobulated soft tissue mass centered within the mesentery measuring 8.6 cm with additional para-aortic adenopathy. F18-fluorodeoxyglucose positron emission tomography-computed tomography (FDG PET-CT) revealed a large right mesenteric mass with a maximum standardized uptake value (SUV_{max}) of 16.4 along with additional FDG-avid left mesenteric, retroperitoneal, and left supraclavicular lymph nodes. The spleen size was normal but showed mild, diffuse FDG uptake, possibly suggestive of involvement by LCS. Detailed laboratory evaluation at baseline was unremarkable. CT-guided core biopsy of the mesenteric mass showed a diffuse infiltrate of large pleomorphic cells with occasional multinucleation, conspicuous

nucleoli, and abundant pale eosinophilic cytoplasm, intermixed with eosinophils. By immunohistochemistry, the malignant cells were positive for CD68, CD163 (partial), S100, CD1a (partial), and langerin. They did not express BRAF^{V600E} (VE1), B-cell (CD19, CD20, CD79a, PAX5), or T-cell (CD2, CD3, CD43) markers. The morphology and immunophenotypic features were diagnostic of LCS. Additionally, a PD-L1 immunostain (clone 22C3, Dako North America Inc., Carpinteria, CA) showed strong membranous staining in 95% of tumor cells (Figure 1). Multigene next-generation sequencing demonstrated several mutations: *SETD2* p.Q2362* stop gain-loss of function (LOF), variant allele frequency (VAF) 22.4%; *SETD2* c.4715+1G>C splice region variant-LOF, VAF 5.5%; *NRAS* p.Q61L missense variant (exon 3)-gain of function, VAF 14.6%; *TP53* p.R280T missense variant-LOF, VAF 8.5%; *SMARCB1* c.629-1G>c splice region variant- LOF, VAF 5.7%; and *PTPN11* p.E76K missense variant-LOF, VAF 10.6%. Tumor mutational burden (TMB) was 3.3 m/MB. Bone marrow biopsy showed no LCS. Given the presence of the activating *NRAS* mutation, single-agent therapy with a MEK inhibitor (trametinib) was initiated at a dose of 2 mg orally (p.o.) daily. Unfortunately, restaging studies in 2 months demonstrated radiographic progression with new FDG avid lymph nodes in bilateral cervical region along with progression in the dominant right mesenteric mass and a new omental nodule (Figure 2A). Because of the high PD-L1 expression on the tumor specimen, pembrolizumab monotherapy at a dose of 200 mg intravenously (i.v.) every 3 weeks was initiated. Two months after initiation of pembrolizumab therapy, PET-CT demonstrated stable disease in the large right-sided mesenteric mass with normalization of the FDG uptake in the bilateral cervical adenopathy and improvement in the FDG avid omental nodule (Figure 2B). After this initial response, imaging 4 months post pembrolizumab revealed slight increase in size of the right mesenteric mass from 7.5 cm x 5.8 cm x 8.6 cm to 9 cm x 8.7 cm x 10.5 cm, along with increase in the size of the left sided mesenteric nodule with SUV_{max} increasing from 4.8 to 10.5 (Figure 2C). Due to the anatomic and metabolic progression, external beam radiation therapy to the sites of progressive disease (right mesenteric mass and left mesenteric nodule) was completed utilizing four-dimensional CT planning and delivered via intensity modulated radiation therapy with daily cone-beam CT localization for total dose of 3,600 cGy over 18 fractions. She continued pembrolizumab mono-

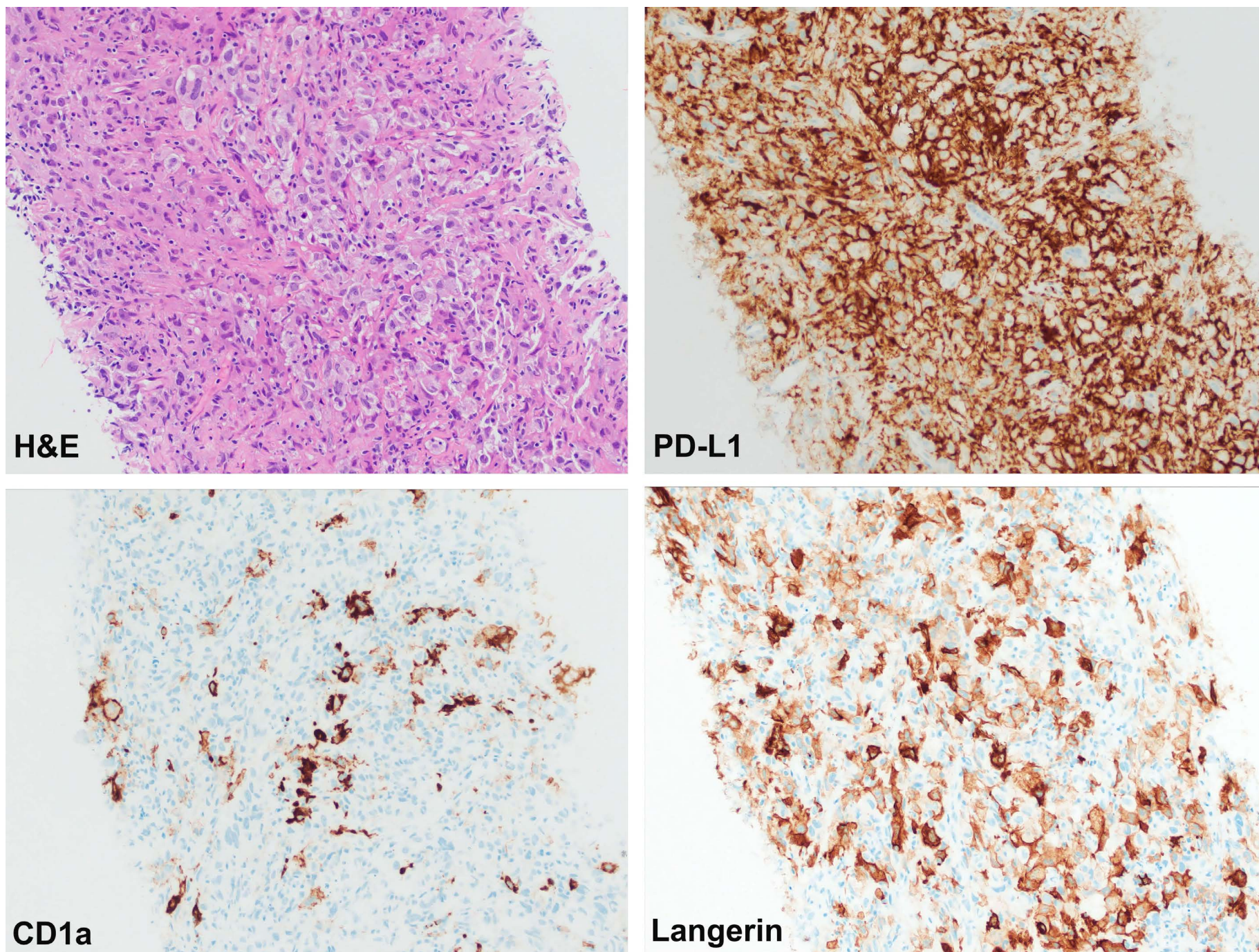


Figure 1. Core biopsy of mesenteric mass involved by Langerhans cell sarcoma characterized by large pleomorphic cells (arrows) with expression of CD1a (partial) and Langerin. PD-L1 immunostain demonstrates membranous positivity in 95% of the tumor cells. H&E: hematoxylin and eosin; magnification x200.

therapy and demonstrated an ongoing reduction in the size and FDG avidity of the of the dominant mesenteric mass (Figure 2D). At 1-year follow-up, her PET-CT demonstrated a significant reduction in size of the mesenteric mass from 9.0 cm x 8.6 cm (SUV_{max} 18.0) to 2.7 cm x 2.4 cm (SUV_{max} 3.2) and resolution of FDG uptake all other sites of disease (Figure 2E). Approximately 18 months into the pembrolizumab therapy, the patient developed grade 2 diarrhea and grade 1 transaminitis that prompted symptomatic treatment and dose reduction to 300 mg i.v. every 6 weeks. At the time of last follow-up, after 36 months of initiation of pembrolizumab, she continued to be in a sustained near complete remission.

Treatment options for multisystem LCS are not well-defined and the use of lymphoma-based chemotherapy regimens have limited success. Therefore, novel approaches are needed in the treatment of these aggressive malignancies. Malignant histiocytic neoplasms demon-

strate occasional presence of mutations in MAPK pathway (like the presence of a *NRAS* mutation in our patient), but limited data currently exist on the role of targeted therapy in these patients. A recent report demonstrated a durable (>2 year) complete response with trametinib in a patient with histiocytic sarcoma (HS) that was noted to have an activating *MAP2K1*^{F53L} mutation.⁵ Similarly, an excellent initial response with vemurafenib was noted in a *BRAF*^{V600E} primary central nervous system HS, but the disease progressed quickly after only 4 months of treatment.⁶

PD-L1 immunohistochemistry and TMB have been used as predictive markers in selecting patients for treatment with ICI in various malignancies (e.g., lung cancer, esophageal cancer, triple negative breast cancer among others).^{7,8} However, limited information exists for PD-L1 staining and TMB in histiocytic neoplasms. A prior study of histiocytic and dendritic cell neoplasms included 14 patients with HS, of which seven were noted to be PD-L1 positive, but

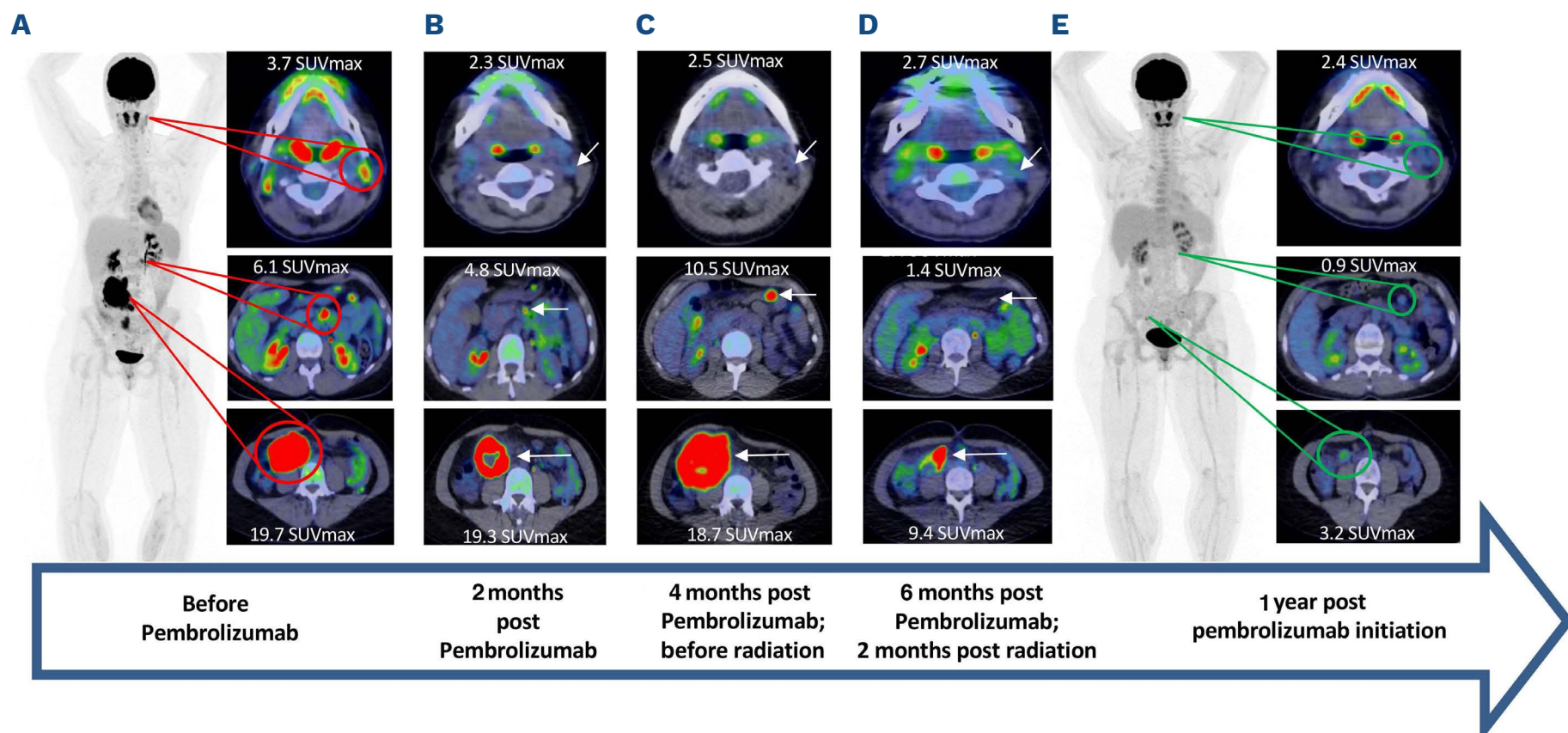


Figure 2. Clinical course of the patient Langerhans cell sarcoma of the mesentery (non-*BRAF*^{V600E} mutated) previously failed treatment with trametinib. A 34 year-old female with biopsy proven Langerhans cell sarcoma (LCS) of the mesentery (non-*BRAF*^{V600E} mutated) previously failed treatment with trametinib. Maximum intensity projection and axial fused F-18 fluorodeoxyglucose positron emission tomography – computed tomography (FDG PET-CT) images demonstrate two intensely FDG avid abdominal masses before (A) and after completion of pembrolizumab with external beam radiation therapy (3,600 centigray) to the abdomen (E). The intervening axial fused FDG PET-CT images reveal response in the cervical adenopathy post initiation of pembrolizumab (B), but subsequent progression in the abdominal masses (C). Post radiation therapy and continuation of pembrolizumab demonstrate eventual near complete response from all sites of LCS (D and E).

there were no patients with LCS in the study population. In this study, staining for PD-L1 was scored as positive if at least 5% of the malignant tumor cells stained positive in a membranous pattern with an intensity of 2+ or 3+.⁹ Another study from our group including 16 patients with histiocytic neoplasms did not have any LCS patients, but the one patient with HS had 5% PD-L1 expression and TMB of 4.27 m/MB.¹⁰ It is important to note that the patient in the current report has a stable/low TMB and a durable response is still demonstrated.

To the best of our knowledge, this represents the first report of prolonged remission using anti-PD1 agent pembrolizumab in combination with radiation therapy in a patient with multisystem LCS. Pembrolizumab or other ICI can be an important therapeutic strategy for these patients who otherwise have a guarded prognosis with limited efficacious options available. A previous report for a patient with HS (PD-L1 expression unknown, TMB intermediate) treated with ipilimumab/nivolumab demonstrated a transient minor response before progression at the 4 month mark,¹¹ somewhat similar to what occurred in our case. Our patient had a focal disease progression approximately 4-months into pembrolizumab, which responded to radiation therapy and continued to demonstrate ongoing systemic remission with maintenance pembrolizumab. In malignant histiocytosis with systemic involvement such as our case, achieving a sustained sys-

temic remission with focal radiation therapy would be unusual. An abscopal effect from the use of radiation therapy could have potentially augmented the response to pembrolizumab, which has been demonstrated in various solid tumors.¹² Utilizing adjunct treatment strategies like focused radiation or surgical resection in appropriate clinical scenarios while continuing ICI may have therapeutic potential. Limited information is available regarding PD-L1 expression in LCS and its implication on response to ICI and these need to be studied further.

Our case highlights that the combination of systemic anti-PD1 agent and focal radiation can be an efficacious treatment option with the potential to provide sustained remissions in LCS. With the lack of treatment options for patients with LCS, further exploration of the role of immune-checkpoint inhibitors in combination with other modalities like radiation therapy is warranted, including correlative biomarker analysis.

Authors

Saurabh Zanwar,¹ Aishwarya Ravindran,² Jithma P. Abeykoon,¹ Jason R. Young,³ Timothy F. Kozelsky,⁴ Karen L. Rech,² Gaurav Goyal^{1,5} and Ronald S. Go¹ on behalf of the Mayo Clinic–University of Alabama at Birmingham Histiocytosis Working Group.

¹Division of Hematology, Mayo Clinic, Rochester, MN; ²Division of Hematopathology, Department of Laboratory Medicine and Pathology, Mayo Clinic, Rochester, MN; ³Department of Radiology, Mayo Clinic, Jacksonville, FL; ⁴Division of Radiation Oncology, Mayo Clinic Health System, Albert Lea, MN and ⁵Division of Hematology-Oncology, University of Alabama at Birmingham, Birmingham, AL, USA

Correspondence:

R. S. Go - go.ronald@mayo.edu

<https://doi.org/10.3324/haematol.2022.280948>

Received: February 27, 2022.

Accepted: May 13, 2022.

Prepublished: May 26, 2022.

©2022 Ferrata Storti Foundation

Published under a CC BY-NC license 

References

1. Tella SH, Kommalapati A, Rech KL, Go RS, Goyal G. Incidence, clinical features, and outcomes of Langerhans cell sarcoma in the United States. *Clin Lymphoma Myeloma Leuk.* 2019;19(7):441-446.
2. Yi W, Chen W-y, Yang T-x, Lan J-p, Liang W-n. Langerhans cell sarcoma arising from antecedent langerhans cell histiocytosis: A case report. *Medicine.* 2019;98(10):e14531.
3. Howard JE, Dwivedi RC, Masterson L, Jani P. Langerhans cell sarcoma: a systematic review. *Cancer Treat Rev.* 2015;41(4):320-331.
4. Alhaj Moustafa M, Jiang L, Tun HW. Langerhans cell sarcoma: the Mayo Clinic experience with an extremely rare disease. *J Clin Oncol.* 2020;38(15_suppl):e19543.
5. Gounder MM, Solit DB, Tap WD. Trametinib in histiocytic sarcoma with an activating MAP2K1 (MEK1) mutation. *N Engl J Med.* 2018;378(20):1945-1947.
6. Idhah A, Mokhtari K, Emile JF, et al. Dramatic response of a BRAF V600E-mutated primary CNS histiocytic sarcoma to vemurafenib. *Neurology.* 2014;83(16):1478-1480.
7. Cortes J, Cescon DW, Rugo HS, et al. Pembrolizumab plus chemotherapy versus placebo plus chemotherapy for previously untreated locally recurrent inoperable or metastatic triple-negative breast cancer (KEYNOTE-355): a randomised, placebo-controlled, double-blind, phase 3 clinical trial. *Lancet.* 2020;396(10265):1817-1828.
8. Gandhi L, Rodríguez-Abreu D, Gadgeel S, et al. Pembrolizumab plus chemotherapy in metastatic non-small-cell lung cancer. *N Engl J Med.* 2018;378(22):2078-2092.
9. Xu J, Sun HH, Fletcher CD, et al. Expression of programmed cell death 1 ligands (PD-L1 and PD-L2) in histiocytic and dendritic cell disorders. *Am J Surg Pathol.* 2016;40(4):443-453.
10. Goyal G, Lau D, Nagle AM, et al. Tumor mutational burden and other predictive immunotherapy markers in histiocytic neoplasms. *Blood.* 2019;133(14):1607-1610.
11. Lee M-y, Bernabe Ramirez C, Ramirez DC, Maki RG. Utility of immune checkpoint inhibitors (ICI) in 3 patients (pts) with sarcomas of antigen presenting cells (follicular dendritic cell sarcoma [FDSC], histiocytic sarcoma [HS]). *J Clin Oncol.* 2020;38(Suppl 15):Se23574.
12. Dagoglu N, Karaman S, Caglar HB, Oral EN. Abscopal effect of radiotherapy in the immunotherapy era: systematic review of reported cases. *Cureus.* 2019;11(2):e4103.

Disclosures

No conflicts of interest to disclose.

Contributions

SZ, AR, GG and RSG conceived, wrote the first draft and modified the final draft; JPA, JRY, TK, KLR critically appraised the manuscript and approved the final draft of the manuscript.

Funding

The study was supported in part by the University of Iowa/Mayo Clinic Lymphoma SPORE CA97274 and the Walter B. Frommeyer, Jr., Fellowship Award in Investigative Medicine, University of Alabama at Birmingham (to GG).

Data-sharing statement

There is no relevant data to disclose.

Hereditary anemia caused by multilocus inheritance of *PIEZO1*, *SLC4A1* and *ABCB6* mutations: a diagnostic and therapeutic challenge

Red blood cell (RBC) membrane disorders encompass a vast group of hemolytic anemias that differ widely in their clinical, morphologic, laboratory, and molecular features. Subtypes include (i) RBC disorders caused by altered membrane structural organization and (ii) RBC disorders caused by altered membrane transport function.¹ The most common anemia among the first group is hereditary spherocytosis (HS), with a prevalence from 1:2000 to 1:5000 births. HS manifests clinically as hemolytic anemia with jaundice, reticulocytosis, splenomegaly, and cholelithiasis.¹ Five genes encoding cytoskeleton and transmembrane proteins are most commonly associated with HS: ankyrin-1 (*ANK1*, 8p11.21), erythrocytic α - and β -spectrin chains (*SPTA1*, 1q21; *SPTB*, 14q23.3), band 3 anion transport protein (*SLC4A1*, 17q21.31), and erythrocyte membrane protein band 4.2 (*EPB42*, 15q15-q21).² Disorders of altered membrane transport function include a wide spectrum of hemolytic disorders in which the erythrocyte membrane cation permeability is altered, with dehydrated hereditary stomatocytosis (DHS) the most frequently encountered. The prevalence of DHS remains uncertain, as this disease is often misdiagnosed.³ DHS exhibits alterations of RBC membrane permeability to monovalent cations Na^+ and K^+ , with consequent alterations of intracellular cation, water content, and cell volume. Patients present with hemolytic anemia, typically macrocytic, with increased mean corpuscular hemoglobin (MCH) and mean corpuscular hemoglobin concentration (MCHC), high reticulocyte count, and jaundice. Blood films may show stomatocytes, usually <10% of total erythrocytes.³ Splenectomy is contraindicated in patients affected by DHS due to the risk of severe thrombotic events.⁴ The two causative genes of DHS are *PIEZO1* (16q24.3) for DHS type 1 (DHS1) and *KCNN4* (19q13.31) for DHS type 2.^{3,5,6} DHS is also frequently associated with iron overload, which frequently leads to hemosiderosis.³ Indeed, recent findings highlight a role for *PIEZO1* in the regulation of iron metabolism.⁷ DHS patients can exhibit hyperferritinemia (and even life-threatening hemosiderosis) accompanied by very low values of plasma hepcidin. Overexpression and pharmacological activation of the R2456H and R2488Q *PIEZO1* gain-of-function (GoF) mutants in hepatoma cell lines induced decreased expression of the hepcidin-encoding gene, *HAMP*.⁷ *PIEZO1* involvement in iron metabolism was further confirmed in constitutive and in macrophage-specific transgenic *PIEZO1* GoF mice. By 1 year of age, these mice develop se-

vere hepatic hemosiderosis with elevated serum ferritin and transferrin saturation, accompanied by increased erythrophagocytosis, erythropoiesis, and erythroferrone expression.⁸

DHS may also present as a syndromic form with pseudohyperkalemia and/or perinatal edema.² Familial pseudohyperkalemia (FP) can also manifest as an isolated autosomal dominant red cell trait characterized by loss of red cell potassium at low temperatures (<37°C).⁵ It is caused by mutations in the *ABCB6* gene (2q35) encoding the *ABCB6* protein, a member of the family of ATP-binding cassette (ABC) solute transporters that translocate many types of metabolites across intra- and extracellular membranes.⁹ The prevalence of FP is probably underestimated, as reflected in the high frequency of certain *ABCB6* missense variants in population databases and in two large cohorts of blood donors.^{5,10}

We describe here a 54-year-old female proband followed for 16 years by our clinical genetics unit for severe anemia and iron overload (Figure 1A). The proband presented at age 24 with moderate anemia (hemoglobin [Hb] 9–11 g/dL), jaundice, gallstones, hepatomegaly, and severe splenomegaly (>18 cm craniocaudal length with weight up to 700 g). Hemoglobinopathies and enzymopathies were excluded. Coombs's test was negative. Blood smear revealed the presence of numerous stomatocytes, target cells, and rare ovalocytes and erythroblasts (Figure 1B). Osmotic fragility was decreased at 2 hours (h) and 24 h post-venesection. Pink and acidified glycerol lysis tests (AGLT) were positive, leading to an initial clinical diagnosis of HS treated by total splenectomy. After surgery, the proband experienced portal vein thrombosis treated with heparin. Worsening anemia to Hb values of 6–7 g/dL required multiple transfusions. Complete red cell count showed macrocytic anemia with MCV between 110 and 147 fL (Table 1). Mean red blood cell (RBC) half-life (measured by *in vitro* calcein fluorescence assay) was 21 days, with probable hepatosplenic destruction of RBC.

At the age of 34 years the proband was diagnosed with severe iron overload and hemosiderosis, and deferoxamine treatment was initiated. At age 38 pulmonary emboli were diagnosed, and she was treated with warfarin. At this time the proband also had hyperkalemia (5.0–6.8 mM). Studies of RBC cation content revealed elevated intracellular [Na] and low intracellular [K], with increased isotopic fluxes at 37°C (Table 2). Temperature-dependence studies

CASE REPORT

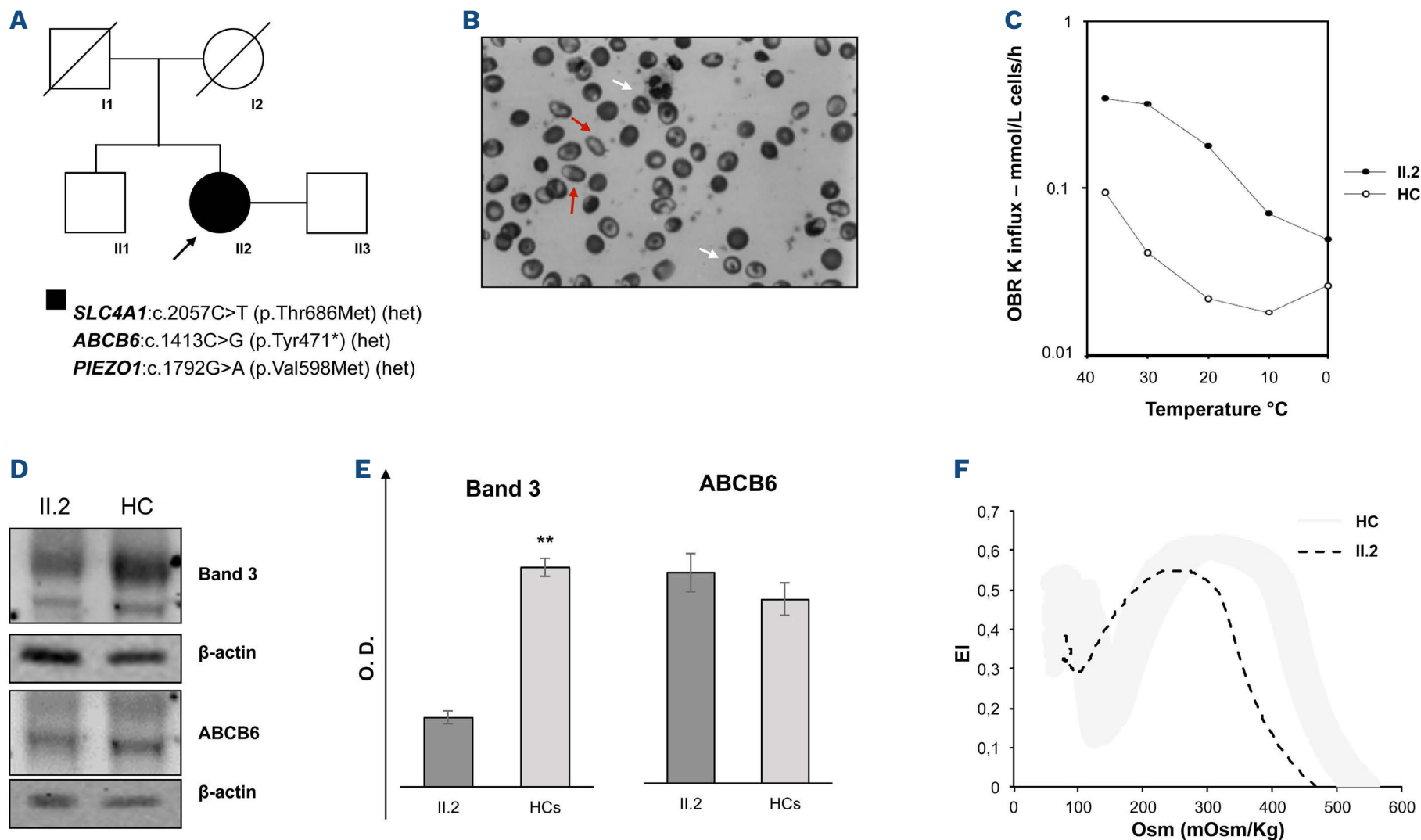


Figure 1. Genetic analysis and functional studies to assess the pathogenicity of the identified variants in the patient here analyzed. (A) Family pedigree of the proband. Squares, males; circles, females; solid symbols, affected patient; arrow indicates the proband. The proband shows three heterozygous variants in three different genes: *SLC4A1*:c.2057C>T (p.Thr686Met), *ABCB6*:c.1413C>G (p.Tyr471*), *PIEZO1*:c.1792G>A (p.Val598Met). (B) Peripheral blood smear (May-Grünwald Giemsa stain 40x) examination of the proband II.2 showing marked anisopoikilocytosis. White arrows indicate stomatocytes; red arrows indicate ovalocytes. (C) Temperature dependence of ‘leak’ K⁺ influx in red blood cells (RBC) of patient II.2 (solid symbols) and control (open symbols). (D) Representative immunoblot showing proband and healthy controls (HC) RBC membrane expression of band 3 (upper) and ABCB6 (lower), normalized to β -actin. (E) Densitometric analysis of immunoblotting shown in panel (D). Data are means \pm standard deviation (SD) of three independent experiments. (***P*-value < 0.001, Student’s *t*-test). O.D.: optical density. (F) The RBC deformability index of RBC from proband II.2 (dashed black curve) and internal healthy controls (light grey lines) was measured as a function of increasing osmolality. Values are means \pm standard error of the mean of 2 independent experiments. EI: elongation index (EI).

performed by flame photometry confirmed the high cation leak flux at 37°C. This cation flux markedly diminished upon cooling of RBC below ~30°C (Figure 1C).¹⁰ The findings were consistent with pseudohyperkalemia.

The 38-year-old proband was referred to our unit and underwent initial genetic testing for HS using a gene-by-gene approach. Sanger sequencing analysis of the *SLC4A1* gene revealed the presence of the heterozygous missense variant NM_000342.4:c.2057C>T (p.Thr686Met) [rs143131877, AF A=0.000088 (12/135994, GnomAD); HGMD ID: CM204624]. This variant in the first nucleotide of exon 17 is predicted to impair exon 16-17 splicing (<https://hsf.genomnis.com/>). Accordingly, it was predicted to be a likely pathogenic variant per current guidelines of the American College of Medical Genetics and Genomics (ACMG). In order to determine the effect of this variant on protein expression, we isolated RBC membrane proteins from the peripheral blood of the patient. Band 3 polypeptide expression in patient RBC mem-

branes was reduced compared to that of healthy controls (HC) by western blotting, confirming the pathogenicity of the identified variant and the diagnosis of HS (Figure 1D and E).

At the age of 54 years, increasing severity of anemia and continued post-splenectomy thrombotic events prompted a re-evaluation of the diagnosis of HS. We extended the molecular analyses by applying a previously described custom gene panel for hereditary anemias.¹¹ Genomic DNA preparation, genetic testing by targeted next-generation sequencing (NGS) for hereditary anemias, and validation of the variant by Sanger sequencing were performed as previously described.^{11,12} We found a novel heterozygous nonsense variant in the *ABCB6* gene (NM_005689.4): c.1413C>G (p.Tyr471*) [rs141029409, AF C=0.00000 (0/14046, ALFA)], predicted as likely pathogenic per ACMG guidelines. We also found the heterozygous missense variant (NM_001142864.4): c.1792G>A (p.Val598Met) [HGMD ID:

CASE REPORT

Table 1. Clinical features of the proband pre- and post-splenectomy.

	Pre-splenectomy	Post-splenectomy		Reference ranges*
		Before iron chelation treatment	After iron chelation treatment	
Blood count				
Age, years	24	25	54	-
RBC x10 ⁶ /mL	3.5	1.5	1.9	3.9-5.6
Hb, g/dL	10.5	6.5	8.8	11.0-16.0
Hct, %	29.0	18.0	25.4	33.0-45.0
MCV, fL	129.0	125.7	128.0	70.0-91.0
MCH, pg	36.0	43.0	44.4	23.0-33.0
Plt x10 ³ /mL	268.0	1,126.0	481.6	150.0-450.0
Retics count x10 ³ /μL	250.0	17.9	11.85	-
Retics, %	7.1	259.6	224.0	0.5-2.0
Hemolytic indices and iron balance				
Total bilirubin, mg/dL	1.6	1.8	1.6	0.2-1.2
Indirect bilirubin, mg/dL	1.3	1.5	1.3	-
LDH, U/L	358.0	380.0	369.0	125.0 – 243.0
Haptoglobin, g/L	0.03	0.02	0.01	0.3-2.0
Iron, g/dL	92.0	130.0	178.0	60.0-180.0
Ferritin, ng/mL	210.00	1,020.0	355.0	22.0-275.0
Transferrin, saturation %	28.0	65.0	-	<45
Hepcidin, nM	-	0.6	-	4.1-8.5

*Reference ranges from AOU Federico II, University of Naples, Italy. RBC: red blood cells; Hb: hemoglobin; Hct: hematocrit; MCV: mean corpuscular volume; MCH: mean corpuscular hemoglobin; Plt: platelets; Retics: reticulocytes; LDH: lactate dehydrogenase.

Table 2. Intracellular erythrocyte [Na⁺] and [K⁺]. Isotopic fluxes at 37°C.

	Storage time/temperature hours/°C	Intracellular [Na ⁺] (mmol/L cells)	Intracellular [K ⁺] (mmol/L cells)
Patient II.2	on arrival	31.98	71.25
Control	on arrival	21.57	86.09
Patient II.2	O.N./ 4°C	35.00	63.58
Control	O.N./ 4°C	24.29	81.01
Reference range	on arrival	5-11	85-105
K⁺ influx at 5 mM external [K⁺] (86Rb⁺ tracer)			
	NaK pump mmol/(L cells.h)	NaK²Cl cotransport mmol/(L cells.h)	Leak mmol/(L cells.h)
	ouabain-sensitive	bumetanide-sensitive	ouabain- + bumetanide-insensitive
Patient II.2	9.695	0.353	0.293
Control	2.163	0.099	0.049
Reference range	1-2	0-1	0.05-0.10

O.N.: over night.

CM1713992] of the *PIEZO1* gene previously described and functionally validated as pathogenic of DHS with hemosiderosis.¹³ We did not perform an inheritance analysis of

all the identified variants, as the proband's parents had already died (for causes not related to anemia).

We further analyzed ABCB6 protein expression in the pa-

tient's erythrocyte membrane proteins to assess if the novel identified variant might cause FP (GoF variants associated with no impairment of the protein expression) or Lan- blood group (loss-of-function variants associated with downregulation or absence of the protein expression).⁵ We demonstrated no alterations of protein expression in the patient compared to healthy controls (Figure 1D and E). Thus, the occurrence of this *ABCB6* pathogenic variant suggested an explanation for the patient's increased serum K values, and functional studies of temperature dependence confirmed the diagnosis of FP.

The presence of the *PIEZO1* variant suggested the diagnosis of DHS.¹⁴ This finding further explained the altered permeability of the RBC, the hemosiderosis, and the post-splenectomy exacerbation of phenotype. The diagnosis of DHS was further confirmed through ektacytometry analysis. Deformability of RBC of the patient and of control subjects was evaluated by osmotic gradient ektacytometry using the laser-assisted optical rotational cell analyzer (LORCA), as previously described.¹⁵ Ektacytometry revealed a left shift of the osmotic curve and a slightly decreased DiMax in the proband compared to healthy controls (Figure 1F). This peculiar curve is typical of multi-locus inheritance caused by the combined presence of HS and DHS, as recently demonstrated.¹⁵

The proband was thus diagnosed, at 54 years of age, with anemia caused by multilocus inheritance (HS, DHS, FP) of mutations in the *SLC4A1*, *PIEZO1*, and *ABCB6* genes. This paradigmatic clinical case underlines the dual importance of correct clinical assessment and genetic diagnosis to guide personalized clinical management of the patient. Earlier diagnosis of DHS would certainly have prevented the splenectomy and ensuing thrombotic complications. This case confirms the importance of NGS-based testing in the diagnostic workflow of hereditary anemias for complete differential diagnosis in both research and clinical settings.

Authors

Barbara Eleni Rosato,^{1,2} Seth L. Alper,³ Giovanna Tomaiuolo,^{2,4} Roberta Russo,^{1,2} Achille Iolascon,^{1,2#} and Immacolata Andolfo^{1,2#}

¹Dipartimento di Medicina Molecolare e Biotecnologie Mediche, Università degli Studi di Napoli 'Federico II', Napoli, Italy; ²CEINGE

Biotecnologie Avanzate, Napoli, Italy; ³Renal Division and Vascular Biology Research Center, Beth Israel Deaconess Medical Center and Department of Medicine, Harvard Medical School, Boston, MA, USA and ⁴Dipartimento di Ingegneria Chimica, dei Materiali e della Produzione Industriale, University of Naples Federico, Naples, Italy.

#AI and IA contributed equally as co-senior authors.

Correspondence:

I. ANDOLFO - immacolata.andolfo@unina.it

R. RUSSO - roberta.russo@unina.it

<https://doi.org/10.3324/haematol.2022.280799>

Received: February 7, 2022.

Accepted: April 8, 2022.

Prepublished: April 21, 2022.

©2022 Ferrata Storti Foundation

Published under a CC BY-NC license 

Disclosures

SLA has received research funding from and consults for to Quest Diagnostics, Inc.

Contributions

IA, AI, and RR designed and conducted the study and prepared the manuscript; RR and IA performed *in silico* design of the NGS panels and interpretation of the genetic variants; BER prepared the initial draft of the manuscript; BER prepared the library enrichment, performed the Sanger sequencing analysis and western blotting analysis; AI cared for the patient; GT performed the ektacytometry analysis; SLA carried out a critical revision of the manuscript.

Acknowledgments

The authors kindly thank Prof. Carlo Brugnara for the critical revision of the manuscript and Prof. G. Stewart for the ion flux measurement.

Funding

This research was funded by an EHA Junior Research Grant to IA (grant number: 3978026), and by Bando Star Linea 1 - Junior Principal Investigator Grants - COINOR, Università degli Studi di Napoli 'Federico II' to RR.

Data-sharing statement

The original data and protocols are available to other investigators upon request.

References

1. Iolascon A, Andolfo I, Russo R. Advances in understanding the pathogenesis of red cell membrane disorders. *Br J Haematol.*

2019;187(1):13-24.

2. Andolfo I, Russo R, Gambale A, Iolascon A. New insights on

- hereditary erythrocyte membrane defects. *Haematologica*. 2016;101(11):1284-1294.
3. Andolfo I, Russo R, Gambale A, Iolascon A. Hereditary stomatocytosis: an underdiagnosed condition. *Am J Hematol*. 2018;93(1):107-121.
 4. Iolascon A, Andolfo I, Barcellini W, et al. Recommendations regarding splenectomy in hereditary hemolytic anemias. *Haematologica*. 2017;102(8):1304-1313.
 5. Andolfo I, Russo R, Manna F, et al. Functional characterization of novel ABCB6 mutations and their clinical implications in familial pseudohyperkalemia. *Haematologica*. 2016;101(8):909-917.
 6. Zarychanski R, Schulz VP, Houston BL, et al. Mutations in the mechanotransduction protein PIEZO1 are associated with hereditary xerocytosis. *Blood*. 2012;120(9):1908-1915.
 7. Andolfo I, Rosato BE, Manna F, et al. Gain-of-function mutations in PIEZO1 directly impair hepatic iron metabolism via the inhibition of the BMP/SMADs pathway. *Am J Hematol*. 2020;95(2):188-197.
 8. Ma S, Dubin AE, Zhang Y, et al. A role of PIEZO1 in iron metabolism in mice and humans. *Cell*. 2021;184(4):969-982 e13.
 9. Andolfo I, Alper SL, Delaunay J, et al. Missense mutations in the ABCB6 transporter cause dominant familial pseudohyperkalemia. *Am J Hematol*. 2013;88(1):66-72.
 10. Bawazir WM, Flatt JF, Wallis JP, et al. Familial pseudohyperkalemia in blood donors: a novel mutation with implications for transfusion practice. *Transfusion*. 2014;54(12):3043-3050.
 11. Russo R, Andolfo I, Manna F, et al. Multi-gene panel testing improves diagnosis and management of patients with hereditary anemias. *Am J Hematol*. 2018;93(5):672-682.
 12. Russo R, Marra R, Rosato BE, Iolascon A, Andolfo I. Genetics and genomics approaches for diagnosis and research into hereditary anemias. *Front Physiol*. 2020;11:613559.
 13. Gnanasambandam R, Rivera A, Vandorpe DH, et al. Increased red cell KCNN4 activity in sporadic hereditary xerocytosis associated with enhanced single channel pressure sensitivity of PIEZO1 mutant V598M. *Hemasphere*. 2018;2(5):e55.
 14. Picard V, Guitton C, Thuret I, et al. Clinical and biological features in PIEZO1-hereditary xerocytosis and Gardos channelopathy: a retrospective series of 126 patients. *Haematologica*. 2019;104(8):1554-1564.
 15. Andolfo I, Martone S, Rosato BE, et al. Complex modes of inheritance in hereditary red blood cell disorders: a case series study of 155 patients. *Genes (Basel)*. 2021;12(7):958.

Reasons for reading



Gold open access journal

Everything published is available, free, for everyone



High scientific value

Everything published has been reviewed by a panel of reviewers and rated as outstanding or excellent by reputed editors



No delay in knowing the most important news in all fields of Hematology

Everything published is visible as 'early view' a few days after acceptance

haematologica

Journal of the Ferrata- Storti Foundation

haematologica

Journal of the Ferrata Storti Foundation 

VOL.

107

SEPTEMBER 2022

